

**smos
pi-mep**

In Situ database Analyses Report

prepared by the Pi-MEP Consortium

June 15, 2023

Contents

1 Overview	11
1.1 <i>In situ</i> datasets	11
1.1.1 Argo	12
1.1.2 Marine mammals	12
1.1.3 Surface drifters	13
1.1.4 Saildrones	13
1.1.5 TSG	13
1.1.6 Moorings	15
1.2 Auxiliary geophysical datasets	15
1.2.1 CMORPH	16
1.2.2 ASCAT	17
1.2.3 ISAS	17
1.2.4 World Ocean Atlas Climatology	17
2 Argo	18
2.1 Introduction	18
2.2 Number of SSS data as a function of time and distance to coast	18
2.3 Histograms of SSS	18
2.4 Distribution of <i>in situ</i> SSS depth measurements	19
2.5 Spatial distribution of SSS	19
2.6 Spatial Maps of the Temporal mean and Std of <i>in situ</i> and ISAS SSS and of the difference (Δ SSS)	20
2.7 Time series of the monthly median and Std of <i>in situ</i> and ISAS SSS and of the difference (Δ SSS)	21
2.8 Zonal mean and Std of <i>in situ</i> and ISAS SSS and of the difference Δ SSS	22
2.9 Scatterplots of ISAS vs <i>in situ</i> SSS by latitudinal bands	23
2.10 Time series of the monthly median and Std of the difference Δ SSS sorted by latitudinal bands	24
2.11 Δ SSS sorted as geophysical conditions	25
2.12 Δ SSS maps and statistics for different geophysical conditions	26
2.13 Summary	28
3 Marine mammals	29
3.1 Introduction	29
3.2 Number of SSS data as a function of time and distance to coast	30
3.3 Histograms of SSS	30
3.4 Distribution of <i>in situ</i> SSS depth measurements	30
3.5 Spatial distribution of SSS	31
3.6 Spatial Maps of the Temporal mean and Std of <i>in situ</i> and ISAS SSS and of the difference (Δ SSS)	31
3.7 Time series of the monthly median and Std of <i>in situ</i> and ISAS SSS and of the difference (Δ SSS)	32
3.8 Zonal mean and Std of <i>in situ</i> and ISAS SSS and of the difference Δ SSS	33
3.9 Scatterplots of ISAS vs <i>in situ</i> SSS by latitudinal bands	34
3.10 Time series of the monthly median and Std of the difference Δ SSS sorted by latitudinal bands	35
3.11 Δ SSS sorted as geophysical conditions	36

3.12	ΔSSS maps and statistics for different geophysical conditions	37
3.13	Summary	39
4	Surface drifters	40
4.1	Introduction	40
4.2	Number of SSS data as a function of time and distance to coast	40
4.3	Histograms of SSS	41
4.4	Distribution of <i>in situ</i> SSS depth measurements	41
4.5	Spatial distribution of SSS	42
4.6	Spatial Maps of the Temporal mean and Std of <i>in situ</i> and ISAS SSS and of the difference (Δ SSS)	42
4.7	Time series of the monthly median and Std of <i>in situ</i> and ISAS SSS and of the difference (Δ SSS)	43
4.8	Zonal mean and Std of <i>in situ</i> and ISAS SSS and of the difference Δ SSS	44
4.9	Scatterplots of ISAS vs <i>in situ</i> SSS by latitudinal bands	45
4.10	Time series of the monthly median and Std of the difference Δ SSS sorted by latitudinal bands	46
4.11	Δ SSS sorted as geophysical conditions	47
4.12	Δ SSS maps and statistics for different geophysical conditions	48
4.13	Summary	50
5	Saildrones	51
5.1	Introduction	51
5.2	Number of SSS data as a function of time and distance to coast	51
5.3	Histograms of SSS	52
5.4	Distribution of <i>in situ</i> SSS depth measurements	52
5.5	Spatial distribution of SSS	53
5.6	Spatial Maps of the Temporal mean and Std of <i>in situ</i> and ISAS SSS and of the difference (Δ SSS)	53
5.7	Time series of the monthly median and Std of <i>in situ</i> and ISAS SSS and of the difference (Δ SSS)	54
5.8	Zonal mean and Std of <i>in situ</i> and ISAS SSS and of the difference Δ SSS	55
5.9	Scatterplots of ISAS vs <i>in situ</i> SSS by latitudinal bands	56
5.10	Time series of the monthly median and Std of the difference Δ SSS sorted by latitudinal bands	57
5.11	Δ SSS sorted as geophysical conditions	58
5.12	Δ SSS maps and statistics for different geophysical conditions	59
5.13	Summary	61
6	TSG	62
6.1	TSG (LEGOS-DM)	63
6.1.1	Introduction	63
6.1.2	Number of SSS data as a function of time and distance to coast	63
6.1.3	Histograms of SSS	63
6.1.4	Distribution of <i>in situ</i> SSS depth measurements	64
6.1.5	Spatial distribution of SSS	64
6.1.6	Spatial Maps of the Temporal mean and Std of <i>in situ</i> and ISAS SSS and of the difference (Δ SSS)	65

6.1.7	Time series of the monthly median and Std of <i>in situ</i> and ISAS SSS and of the difference (Δ SSS)	66
6.1.8	Zonal mean and Std of <i>in situ</i> and ISAS SSS and of the difference Δ SSS	67
6.1.9	Scatterplots of ISAS vs <i>in situ</i> SSS by latitudinal bands	68
6.1.10	Time series of the monthly median and Std of the difference Δ SSS sorted by latitudinal bands	69
6.1.11	Δ SSS sorted as geophysical conditions	70
6.1.12	Δ SSS maps and statistics for different geophysical conditions	71
6.1.13	Summary	73
6.2	TSG (GOSUD-Research-vessel)	74
6.2.1	Introduction	74
6.2.2	Number of SSS data as a function of time and distance to coast	74
6.2.3	Histograms of SSS	75
6.2.4	Distribution of <i>in situ</i> SSS depth measurements	75
6.2.5	Spatial distribution of SSS	76
6.2.6	Spatial Maps of the Temporal mean and Std of <i>in situ</i> and ISAS SSS and of the difference (Δ SSS)	76
6.2.7	Time series of the monthly median and Std of <i>in situ</i> and ISAS SSS and of the difference (Δ SSS)	77
6.2.8	Zonal mean and Std of <i>in situ</i> and ISAS SSS and of the difference Δ SSS	78
6.2.9	Scatterplots of ISAS vs <i>in situ</i> SSS by latitudinal bands	79
6.2.10	Time series of the monthly median and Std of the difference Δ SSS sorted by latitudinal bands	80
6.2.11	Δ SSS sorted as geophysical conditions	81
6.2.12	Δ SSS maps and statistics for different geophysical conditions	82
6.2.13	Summary	84
6.3	TSG (GOSUD-Sailing-ship)	85
6.3.1	Introduction	85
6.3.2	Number of SSS data as a function of time and distance to coast	85
6.3.3	Histograms of SSS	86
6.3.4	Distribution of <i>in situ</i> SSS depth measurements	86
6.3.5	Spatial distribution of SSS	87
6.3.6	Spatial Maps of the Temporal mean and Std of <i>in situ</i> and ISAS SSS and of the difference (Δ SSS)	87
6.3.7	Time series of the monthly median and Std of <i>in situ</i> and ISAS SSS and of the difference (Δ SSS)	88
6.3.8	Zonal mean and Std of <i>in situ</i> and ISAS SSS and of the difference Δ SSS	89
6.3.9	Scatterplots of ISAS vs <i>in situ</i> SSS by latitudinal bands	90
6.3.10	Time series of the monthly median and Std of the difference Δ SSS sorted by latitudinal bands	91
6.3.11	Δ SSS sorted as geophysical conditions	92
6.3.12	Δ SSS maps and statistics for different geophysical conditions	93
6.3.13	Summary	95
6.4	TSG (SAMOS)	96
6.4.1	Introduction	96
6.4.2	Number of SSS data as a function of time and distance to coast	96
6.4.3	Histograms of SSS	97
6.4.4	Distribution of <i>in situ</i> SSS depth measurements	97
6.4.5	Spatial distribution of SSS	98

6.4.6	Spatial Maps of the Temporal mean and Std of <i>in situ</i> and ISAS SSS and of the difference (Δ SSS)	98
6.4.7	Time series of the monthly median and Std of <i>in situ</i> and ISAS SSS and of the difference (Δ SSS)	99
6.4.8	Zonal mean and Std of <i>in situ</i> and ISAS SSS and of the difference Δ SSS	100
6.4.9	Scatterplots of ISAS vs <i>in situ</i> SSS by latitudinal bands	101
6.4.10	Time series of the monthly median and Std of the difference Δ SSS sorted by latitudinal bands	102
6.4.11	Δ SSS sorted as geophysical conditions	103
6.4.12	Δ SSS maps and statistics for different geophysical conditions	104
6.4.13	Summary	106
6.5	TSG (CSIC-UTM)	107
6.5.1	Introduction	107
6.5.2	Number of SSS data as a function of time and distance to coast	107
6.5.3	Histograms of SSS	108
6.5.4	Distribution of <i>in situ</i> SSS depth measurements	108
6.5.5	Spatial distribution of SSS	109
6.5.6	Spatial Maps of the Temporal mean and Std of <i>in situ</i> and ISAS SSS and of the difference (Δ SSS)	109
6.5.7	Time series of the monthly median and Std of <i>in situ</i> and ISAS SSS and of the difference (Δ SSS)	110
6.5.8	Zonal mean and Std of <i>in situ</i> and ISAS SSS and of the difference Δ SSS	111
6.5.9	Scatterplots of ISAS vs <i>in situ</i> SSS by latitudinal bands	112
6.5.10	Time series of the monthly median and Std of the difference Δ SSS sorted by latitudinal bands	113
6.5.11	Δ SSS sorted as geophysical conditions	114
6.5.12	Δ SSS maps and statistics for different geophysical conditions	115
6.5.13	Summary	117
6.6	TSG (Polarstern)	118
6.6.1	Introduction	118
6.6.2	Number of SSS data as a function of time and distance to coast	118
6.6.3	Histograms of SSS	119
6.6.4	Distribution of <i>in situ</i> SSS depth measurements	119
6.6.5	Spatial distribution of SSS	120
6.6.6	Spatial Maps of the Temporal mean and Std of <i>in situ</i> and ISAS SSS and of the difference (Δ SSS)	120
6.6.7	Time series of the monthly median and Std of <i>in situ</i> and ISAS SSS and of the difference (Δ SSS)	121
6.6.8	Zonal mean and Std of <i>in situ</i> and ISAS SSS and of the difference Δ SSS	122
6.6.9	Scatterplots of ISAS vs <i>in situ</i> SSS by latitudinal bands	123
6.6.10	Time series of the monthly median and Std of the difference Δ SSS sorted by latitudinal bands	124
6.6.11	Δ SSS sorted as geophysical conditions	125
6.6.12	Δ SSS maps and statistics for different geophysical conditions	126
6.6.13	Summary	128
6.7	TSG (NCEI-0170743)	129
6.7.1	Introduction	129
6.7.2	Number of SSS data as a function of time and distance to coast	130
6.7.3	Histograms of SSS	130

6.7.4	Distribution of <i>in situ</i> SSS depth measurements	131
6.7.5	Spatial distribution of SSS	131
6.7.6	Spatial Maps of the Temporal mean and Std of <i>in situ</i> and ISAS SSS and of the difference (Δ SSS)	132
6.7.7	Time series of the monthly median and Std of <i>in situ</i> and ISAS SSS and of the difference (Δ SSS)	133
6.7.8	Zonal mean and Std of <i>in situ</i> and ISAS SSS and of the difference Δ SSS . .	134
6.7.9	Scatterplots of ISAS vs <i>in situ</i> SSS by latitudinal bands	135
6.7.10	Time series of the monthly median and Std of the difference Δ SSS sorted by latitudinal bands	136
6.7.11	Δ SSS sorted as geophysical conditions	137
6.7.12	Δ SSS maps and statistics for different geophysical conditions	138
6.7.13	Summary	140
6.8	TSG (LEGOS-Survostral)	141
6.8.1	Introduction	141
6.8.2	Number of SSS data as a function of time and distance to coast	141
6.8.3	Histograms of SSS	142
6.8.4	Distribution of <i>in situ</i> SSS depth measurements	142
6.8.5	Spatial distribution of SSS	143
6.8.6	Spatial Maps of the Temporal mean and Std of <i>in situ</i> and ISAS SSS and of the difference (Δ SSS)	144
6.8.7	Time series of the monthly median and Std of <i>in situ</i> and ISAS SSS and of the difference (Δ SSS)	146
6.8.8	Zonal mean and Std of <i>in situ</i> and ISAS SSS and of the difference Δ SSS . .	146
6.8.9	Scatterplots of ISAS vs <i>in situ</i> SSS by latitudinal bands	147
6.8.10	Time series of the monthly median and Std of the difference Δ SSS sorted by latitudinal bands	149
6.8.11	Δ SSS sorted as geophysical conditions	149
6.8.12	Δ SSS maps and statistics for different geophysical conditions	151
6.8.13	Summary	153
6.9	TSG (LEGOS-Survostral-Adelie)	154
6.9.1	Introduction	154
6.9.2	Number of SSS data as a function of time and distance to coast	154
6.9.3	Histograms of SSS	155
6.9.4	Distribution of <i>in situ</i> SSS depth measurements	155
6.9.5	Spatial distribution of SSS	156
6.9.6	Spatial Maps of the Temporal mean and Std of <i>in situ</i> and ISAS SSS and of the difference (Δ SSS)	157
6.9.7	Time series of the monthly median and Std of <i>in situ</i> and ISAS SSS and of the difference (Δ SSS)	159
6.9.8	Zonal mean and Std of <i>in situ</i> and ISAS SSS and of the difference Δ SSS . .	159
6.9.9	Scatterplots of ISAS vs <i>in situ</i> SSS by latitudinal bands	160
6.9.10	Time series of the monthly median and Std of the difference Δ SSS sorted by latitudinal bands	162
6.9.11	Δ SSS sorted as geophysical conditions	162
6.9.12	Δ SSS maps and statistics for different geophysical conditions	164
6.9.13	Summary	166

7	Moorings	167
7.1	Introduction	167
7.2	Number of SSS data as a function of time and distance to coast	168
7.3	Histogram of SSS	168
7.4	Temporal mean of shallowest salinity	168
7.5	Temporal Std of shallowest salinity	169
7.6	Number of shallowest salinity	169
7.7	Time series of shallowest salinity	170
8	SPURS-2	171
8.1	Salinity Snake	171
8.1.1	Introduction	171
8.1.2	Number of SSS data as a function of time and distance to coast	171
8.1.3	Histograms of SSS	172
8.1.4	Distribution of <i>in situ</i> SSS depth measurements	172
8.1.5	Spatial distribution of SSS	172
8.1.6	Spatial Maps of the Temporal mean and Std of <i>in situ</i> and ISAS SSS and of the difference (Δ SSS)	173
8.1.7	Time series of the monthly median and Std of <i>in situ</i> and ISAS SSS and of the difference (Δ SSS)	175
8.1.8	Zonal mean and Std of <i>in situ</i> and ISAS SSS and of the difference Δ SSS	175
8.1.9	Scatterplots of ISAS vs <i>in situ</i> SSS by latitudinal bands	176
8.1.10	Time series of the monthly median and Std of the difference Δ SSS sorted by latitudinal bands	177
8.1.11	Δ SSS sorted as geophysical conditions	178
8.1.12	Δ SSS maps and statistics for different geophysical conditions	179
8.1.13	Summary	181
8.2	Saildrone	182
8.2.1	Introduction	182
8.2.2	Number of SSS data as a function of time and distance to coast	182
8.2.3	Histograms of SSS	183
8.2.4	Distribution of <i>in situ</i> SSS depth measurements	183
8.2.5	Spatial distribution of SSS	184
8.2.6	Spatial Maps of the Temporal mean and Std of <i>in situ</i> and ISAS SSS and of the difference (Δ SSS)	185
8.2.7	Time series of the monthly median and Std of <i>in situ</i> and ISAS SSS and of the difference (Δ SSS)	187
8.2.8	Zonal mean and Std of <i>in situ</i> and ISAS SSS and of the difference Δ SSS	187
8.2.9	Scatterplots of ISAS vs <i>in situ</i> SSS by latitudinal bands	188
8.2.10	Time series of the monthly median and Std of the difference Δ SSS sorted by latitudinal bands	189
8.2.11	Δ SSS sorted as geophysical conditions	190
8.2.12	Δ SSS maps and statistics for different geophysical conditions	191
8.2.13	Summary	193
8.3	Waveglider	194
8.3.1	Introduction	194
8.3.2	Number of SSS data as a function of time and distance to coast	194
8.3.3	Histograms of SSS	195
8.3.4	Distribution of <i>in situ</i> SSS depth measurements	195

8.3.5	Spatial distribution of SSS	196
8.3.6	Spatial Maps of the Temporal mean and Std of <i>in situ</i> and ISAS SSS and of the difference (Δ SSS)	197
8.3.7	Time series of the monthly median and Std of <i>in situ</i> and ISAS SSS and of the difference (Δ SSS)	199
8.3.8	Zonal mean and Std of <i>in situ</i> and ISAS SSS and of the difference Δ SSS .	199
8.3.9	Scatterplots of ISAS vs <i>in situ</i> SSS by latitudinal bands	200
8.3.10	Time series of the monthly median and Std of the difference Δ SSS sorted by latitudinal bands	201
8.3.11	Δ SSS sorted as geophysical conditions	202
8.3.12	Δ SSS maps and statistics for different geophysical conditions	203
8.3.13	Summary	205
8.4	Seaglider	206
8.4.1	Introduction	206
8.4.2	Number of SSS data as a function of time and distance to coast	206
8.4.3	Histograms of SSS	207
8.4.4	Distribution of <i>in situ</i> SSS depth measurements	207
8.4.5	Spatial distribution of SSS	208
8.4.6	Spatial Maps of the Temporal mean and Std of <i>in situ</i> and ISAS SSS and of the difference (Δ SSS)	209
8.4.7	Time series of the monthly median and Std of <i>in situ</i> and ISAS SSS and of the difference (Δ SSS)	211
8.4.8	Zonal mean and Std of <i>in situ</i> and ISAS SSS and of the difference Δ SSS .	211
8.4.9	Scatterplots of ISAS vs <i>in situ</i> SSS by latitudinal bands	212
8.4.10	Time series of the monthly median and Std of the difference Δ SSS sorted by latitudinal bands	213
8.4.11	Δ SSS sorted as geophysical conditions	214
8.4.12	Δ SSS maps and statistics for different geophysical conditions	215
8.4.13	Summary	217
9	EUREC4A	218
9.1	Introduction	218
9.2	Number of SSS data as a function of time and distance to coast	219
9.3	Histograms of SSS	219
9.4	Distribution of <i>in situ</i> SSS depth measurements	219
9.5	Spatial distribution of SSS	220
9.6	Spatial Maps of the Temporal mean and Std of <i>in situ</i> and ISAS SSS and of the difference (Δ SSS)	221
9.7	Time series of the monthly median and Std of <i>in situ</i> and ISAS SSS and of the difference (Δ SSS)	223
9.8	Zonal mean and Std of <i>in situ</i> and ISAS SSS and of the difference Δ SSS .	223
9.9	Scatterplots of ISAS vs <i>in situ</i> SSS by latitudinal bands	224
9.10	Time series of the monthly median and Std of the difference Δ SSS sorted by latitudinal bands	225
9.11	Δ SSS sorted as geophysical conditions	226
9.12	Δ SSS maps and statistics for different geophysical conditions	227
9.13	Summary	229

10 ICES	230
10.1 Introduction	230
10.2 Number of SSS data as a function of time and distance to coast	230
10.3 Histograms of SSS	231
10.4 Distribution of <i>in situ</i> SSS depth measurements	231
10.5 Spatial distribution of SSS	232
10.6 Spatial Maps of the Temporal mean and Std of <i>in situ</i> and ISAS SSS and of the difference (Δ SSS)	232
10.7 Time series of the monthly median and Std of <i>in situ</i> and ISAS SSS and of the difference (Δ SSS)	233
10.8 Zonal mean and Std of <i>in situ</i> and ISAS SSS and of the difference Δ SSS	234
10.9 Scatterplots of ISAS vs <i>in situ</i> SSS by latitudinal bands	235
10.10 Time series of the monthly median and Std of the difference Δ SSS sorted by latitudinal bands	236
10.11 Δ SSS sorted as geophysical conditions	237
10.12 Δ SSS maps and statistics for different geophysical conditions	238
10.13 Summary	240
11 Summary	241
11.1 Number of SSS data as a function of time	241
11.2 Histogram of SSS	243
11.3 Temporal mean of SSS	245
11.4 Temporal Std of SSS	247
11.5 Spatial density of SSS	249
11.6 Characteristics for each Pi-MEP region	251

Acronym

Aquarius	NASA/CONAE Salinity mission
ASCAT	Advanced Scatterometer
ATBD	Algorithm Theoretical Baseline Document
BLT	Barrier Layer Thickness
CMORPH	CPC MORPHing technique (precipitation analyses)
CPC	Climate Prediction Center
CTD	Instrument used to measure the conductivity, temperature, and pressure of seawater
DM	Delayed Mode
EO	Earth Observation
ESA	European Space Agency
FTP	File Transfer Protocol
GOSUD	Global Ocean Surface Underway Data
GTMBA	The Global Tropical Moored Buoy Array
Ifremer	Institut français de recherche pour l'exploitation de la mer
IPEV	Institut polaire français Paul-Émile Victor
IQR	Interquartile range
ISAS	<i>In Situ</i> Analysis System
Kurt	Kurtosis (fourth central moment divided by fourth power of the standard deviation)
L2	Level 2
LEGO斯	Laboratoire d'Etudes en Géophysique et Océanographie Spatiales
LOCEAN	Laboratoire d'Océanographie et du Climat : Expérimentations et Approches Numériques
LOPS	Laboratoire d'Océanographie Physique et Spatiale
MDB	Match-up Data Base
MEOP	Marine Mammals Exploring the Oceans Pole to Pole
MLD	Mixed Layer Depth
NCEI	National Centers for Environmental Information
NRT	Near Real Time
NTAS	Northwest Tropical Atlantic Station
OI	Optimal interpolation
Pi-MEP	Pilot-Mission Exploitation Platform
PIRATA	Prediction and Researched Moored Array in the Atlantic
QC	Quality control
R_{sat}	Spatial resolution of the satellite SSS product
RAMA	Research Moored Array for African-Asian-Australian Monsoon Analysis and Prediction
r^2	Square of the Pearson correlation coefficient
RMS	Root mean square
RR	Rain rate
SAMOS	Shipboard Automated Meteorological and Oceanographic System
Skew	Skewness (third central moment divided by the cube of the standard deviation)
SMAP	Soil Moisture Active Passive (NASA mission)
SMOS	Soil Moisture and Ocean Salinity (ESA mission)
SPURS	Salinity Processes in the Upper Ocean Regional Study
SSS	Sea Surface Salinity
SSS_{insitu}	<i>In situ</i> SSS data considered for the match-up

SSS_{SAT}	Satellite SSS product considered for the match-up
ΔSSS	Difference between satellite and <i>in situ</i> SSS at colocalized point ($\Delta\text{SSS} = \text{SSS}_{SAT} - \text{SSS}_{insitu}$)
SST	Sea Surface Temperature
Std	Standard deviation
Std*	Robust Standard deviation = $\text{median}(\text{abs}(\text{x}-\text{median}(\text{x}))) / 0.67$ (less affected by outliers than Std)
Stratus	Surface buoy located in the eastern tropical Pacific
Survostral	SURVeillance de l'Océan AuSTRAL (Monitoring the Southern Ocean)
TAO	Tropical Atmosphere Ocean
TSG	ThermoSalinoGraph
WHOI	Woods Hole Oceanographic Institution
WHOTS	WHOI Hawaii Ocean Time-series Station
WOA	World Ocean Atlas

1 Overview

This report presents some characteristics of the 6 major types of *in situ* datasets ([Argo](#), [Marine mammals](#), [Surface drifters](#), [Saildrones](#), [TSG](#), [Moorings](#)) used by the Pi-MEP to validate SMOS, SMAP and Aquarius satellite SSS products. Salinity data from various sensors coming from 2 scientific campaigns [SPURS-2](#) and [EUREC4A](#) have also been added, as well as a compilation of 4 different salinity datasets [ICES](#). For each *in situ* datasets, a series of plots show:

- Number of SSS data as a function of time and distance to coast
- Histogram of shallowest salinity and pressure (if relevant)
- Temporal mean of shallowest salinity pressure measurements (if relevant)
- Spatial density of shallowest salinity
- Spatial Maps of the Time-mean and temporal Std of *in situ* and satellite SSS and of the Δ SSS
- Time series of the monthly median and Std of *in situ* and satellite SSS and of the Δ SSS
- Zonal mean and Std of *in situ* and satellite SSS and of the Δ SSS
- Scatterplots of ISAS vs *in situ* SSS by latitudinal bands
- Time series of the monthly median and Std of the Δ SSS sorted by latitudinal bands
- Δ SSS sorted as function of geophysical parameters
- Δ SSS maps and statistics for different geophysical conditions

1.1 *In situ* datasets

The following table resumes some characteristics (number of points, first and last date, minimum, maximum and mean value of the SSS distribution) of the different *in situ* datasets used by the Pi-MEP.

In situ datasets	#	Time_{min}	Time_{max}	S_{min}	S_{max}	S_{Mean}
Argo	1742042	01/01/2010	01/05/2023	2.14	40.48	34.73
Marine mammals	348682	01/01/2010	19/11/2019	4.07	36.97	33.95
Surface drifters	2215429	01/01/2010	22/09/2020	1.03	44.22	35.62
Saildrone	914382	02/09/2017	07/11/2022	0.00	39.29	33.31
TSG (LEGOS-DM)	8095635	01/01/2010	28/12/2021	0.03	42.74	34.58
TSG (GOSUD-Research-vessel)	5799920	05/01/2010	30/12/2020	0.01	42.00	35.66
TSG (GOSUD-Sailing-ship)	1727960	08/01/2010	28/01/2021	0.01	42.00	34.09
TSG (SAMOS)	31820461	07/01/2010	23/04/2023	5.03	39.80	32.86
TSG (CSIC-UTM)	2869180	05/01/2010	06/12/2022	0.57	40.29	35.60
TSG (Polarstern)	504269	01/01/2010	11/10/2020	20.30	37.75	34.08
TSG (NCEI-0170743)	590389	08/12/2010	02/02/2017	32.41	35.78	34.26
TSG (LEGOS-Survostral)	654661	01/01/2010	02/03/2020	22.67	35.73	34.17
TSG (LEGOS-Surv-Adel)	38903	09/01/2010	25/01/2012	28.14	34.37	34.04
Moorings	7085913	01/01/2010	09/05/2023	27.02	37.81	35.02
Salinity Snake (SPURS 2)	3428541	20/08/2016	13/11/2017	24.04	34.34	33.12
Saildrone (SPURS 2)	9218	16/10/2017	17/11/2017	30.75	33.85	33.29
Waveglider (SPURS 2)	642340	24/08/2016	10/11/2017	27.48	34.47	33.51
Seaglider (SPURS 2)	73542	24/08/2016	07/11/2017	28.99	34.86	33.27
EUREC4A	267680	01/01/2020	30/03/2020	30.20	37.31	35.75
ICES	2257228	06/01/2010	02/12/2022	0.01	39.94	30.10
Total	71086375	01/01/2010	09/05/2023	0.00	44.22	34.05

1.1.1 Argo

Argo is a global array of 3,000 free-drifting profiling floats that measures the temperature and salinity of the upper 2000 m of the ocean. This allows continuous monitoring of the temperature and salinity of the upper ocean, with all data being relayed and made publicly available within hours after collection. The array provides around 100,000 temperature/salinity profiles per year distributed over the global oceans at an average of 3-degree spacing. Only Argo salinity and temperature float data with quality index set to 1 or 2 and data mode set to real time (RT), real time adjusted (RTA) and delayed mode (DM) are considered in the Pi-MEP. Argo floats which may have problems with one or more sensors appearing in the [grey list](#) maintained at the Coriolis/GDACs are discarded. Furthermore, Pi-MEP provides an additional [list](#) of ~1000 "suspicious" argo salinity profiles that are also removed before analysis. The upper ocean salinity and temperature values recorded between 0m and 10m depth are considered as Argo sea surface salinities (SSS) and sea surface temperatures (SST). These data were collected and made freely available by the international Argo project and the national programs that contribute to it ([Argo \(2023\)](#)).

1.1.2 Marine mammals

Instrumentation of southern elephant seals with satellite-linked CTD tags proposes unique temporal and spatial coverage. This includes extensive data from the Antarctic continental slope and shelf regions during the winter months, which is outside the conventional areas of Argo autonomous floats and ship-based studies. The use of elephant seals has been particularly effective to sample the Southern Ocean and the North Pacific. Other seal species have been successfully used in the North Atlantic, such as hooded seals. The marine mammal dataset ([MEOP-CTD database](#)) is quality controlled and calibrated using delayed-mode techniques involving compar-

isons with other existing profiles as well as cross-comparisons similar to established protocols within the Argo community, with a resulting accuracy of ± 0.03 °C in temperature and ± 0.05 in salinity or better (Treasure et al. (2017)). The marine mammal data were collected and made freely available by the International MEOP Consortium and the national programs that contribute to it (<http://www.meop.net>). This dataset is updated once a year and can be downloaded here (Roquet et al. (2021)). A preprocessing stage is applied to the database before being used by the Pi-MEP which consists in keeping only profiles with salinity, temperature and pressure quality flags set to 1 or 2 and if at least one measurement is in the top 10 m depth. Marine mammal SSS corresponds to the top (shallowest) profile salinity data provided that profile depth is 10 m or less.

1.1.3 Surface drifters

The skin depth of the L-band radiometer signal over the ocean is about 1 cm whereas classical surface salinity measured by ships or Argo floats are performed at a few meters depth. In order to improve the knowledge of the SSS variability in the first 50 cm depth, to better document the SSS variability in a satellite pixel and to provide ground-truth as close as possible to the sea surface for validating satellite SSS, the L-band remotely sensed community proposed to deploy numerous surface drifters over various parts of the ocean. Surface drifter data are provided by the LOCEAN (see <https://www.locean-ipsl.upmc.fr/smossdrifters/>). Only validated data are considered with uncertainty order of 0.01 and 0.1.

1.1.4 Saildrones

Saildrone is a state-of-the-art, remotely guided, wind and solar powered unmanned surface vehicle (USV) capable of long distance deployments lasting up to 12 months. It is equipped with a suite of instruments and sensors providing high quality, georeferenced, near real-time, multi-parameter surface ocean and atmospheric observations while transiting at typical speeds of 3-5 knots. All freely available data are included coming from different providers (Saildrone, NOAA/PMEL, ...) and easily accessible via NOAA ERDAP. When 2 different sensors are available, usually from different brands (SeaBird or RBR), the RBR sensor is kept with the exception for the Atlantic to Mediterranean 2019-2020 campaign for which the salinity data from RBR are clearly corrupted. One-minute samples of the original data were resampled every 10 minutes using linear interpolation to reduce the number of point.

1.1.5 TSG

The TSG dataset is subdivided into 9 subdatasets following TSG data providers subdivisions:

- **LEGOS-DM:**

The TSG (LEGOS-DM) dataset corresponds to sea surface salinity delayed mode data derived from voluntary observing ships collected, validated, archived, and made freely available by the French Sea Surface Salinity Observation Service (Alory et al. (2015)). The network is global though more concentrated in the tropical Pacific and North Atlantic oceanic basins. The acquisition system is autonomous with real time transmission and is regularly serviced at harbor calls. The high resolution data retrieved from the acquisition system during ship calls is processed through a dedicated software (freely available) for attribution of data quality flags by visual inspection, and correction of TSG time series by comparison with climatology, onboard daily water samples and collocated Argo data. Adjusted values when available and only collected TSG data that exhibit quality flags=1 and 2 were used.

- **GOSUD-Research-vessel:**

The TSG (GOSUD-Research-vessel) dataset corresponds to French research vessels SSS data that have been collected since the early 2000 as a contribution to the Global Ocean Surface Underway Data (**GOSUD**) program. The set of homogeneous instruments is permanently monitored and regularly calibrated. Water samples are taken on a daily basis by the crew and later analysed in the laboratory. The careful calibration and instrument maintenance, complemented with a rigorous adjustment on water samples, lead to reach an accuracy of a few 10^{-2} PSS in salinity. This delayed mode dataset ([Kolodziejczyk et al. \(2021\)](#)) is updated annually and freely available [here](#). Adjusted values when available and only collected TSG data that exhibit quality flags 1 or 2 were used.

- **GOSUD-Sailing-ship:** The TSG (GOSUD-Sailing-ship) dataset corresponds to observations of sea surface salinity obtained from voluntary sailing ships using medium or small size sensors. They complement the networks installed on research vessels or commercial ships. This delayed mode dataset ([Reynaud et al. \(2021\)](#)) is updated annually as a contribution to GOSUD (<http://www.gosud.org>) and freely available [here](#). Adjusted values when available and only collected TSG data that exhibit quality flags=1 and 2 were used.

- **SAMOS:** The TSG (SAMOS) dataset corresponds to "Research" quality data from the US Shipboard Automated Meteorological and Oceanographic System (SAMOS) initiative ([Smith et al. \(2009\)](#)). Data are available at <http://samos.coaps.fsu.edu/html/>. Adjusted values when available and only collected TSG data that exhibit quality flags=1 and 2 were used. After visual inspection, data from the NANCY FOSTER (ID="WTER", IMO="008993227") with date 2011/03/21 and all data from the ATLANTIS (ID="KAQP", IMO="009105798") for year 2010 have been removed from this dataset. For years, 2013 to 2022, RV Laurence Gould And Nathaniel Palmer data are coming from the "Intermediate" repository.

- **CSIC-UTM:** The TSG (CSIC-UTM) dataset contains sea surface temperature and salinity data collected from 2010 to 2022 mainly in the Atlantic Ocean, Mediterranean Sea and the Southern Ocean from 3 **CSIC-UTM** research vessels (B/O Sarmiento de Gamboa, R/V Hespérides and R/V García del Cid). Measurements have been obtained through thermosalinograph (TSG) during more than 100 cruises. On-board TSG devices have been regularly calibrated and continuously monitored in-between cruises. The data has been gathered through the <http://data.utm.csic.es/portal/> data portal.

- **Polarstern:** The TSG (Polarstern) dataset has been gathered through the <https://www.pangaea.de/> data warehouse utility using the following criteria: basis:"Polarstern", device:"Underway cruise track measurements (CT)", time coverage form 2010/01/01 to present. The result of the query is a collection of 79 different datasets with the following identification numbers: [736345](#), [742729](#), [753224](#), [753225](#), [753226](#), [753227](#), [758080](#), [760120](#), [760121](#), [761277](#), [770034](#), [770035](#), [770828](#), [776596](#), [776597](#), [780004](#), [802809](#), [802810](#), [802811](#), [802812](#), [803431](#), [808835](#), [808836](#), [808838](#), [809727](#), [810678](#), [816055](#), [819831](#), [823259](#), [839406](#), [839407](#), [839408](#), [848615](#), [858879](#), [858880](#), [858881](#), [858882](#), [858883](#), [858884](#), [858885](#), [863228](#), [863229](#), [863230](#), [863231](#), [863232](#), [863234](#), [873145](#), [873147](#), [873151](#), [873153](#), [873155](#), [873156](#), [873158](#), [887767](#), [889444](#), [889513](#), [889515](#), [889516](#), [889517](#), [889535](#), [889542](#), [889548](#), [895578](#), [895579](#), [895581](#), [898225](#), [898233](#), [898266](#), [905555](#), [905562](#), [905608](#), [905610](#), [905734](#), [930022](#), [930023](#), [930024](#), [930026](#), [930027](#), [930028](#).

- **NCEI-0170743:** The TSG (NCEI-0170743) dataset ([Aulicino et al. \(2018\)](#)) contains sea surface temperature and salinity data collected from 2010 to 2017 in the South Atlantic Ocean

and Southern Ocean from S.A. Agulhas and Agulhas-II research vessels, in the framework of South African National Antarctic Programme ([SANAP](#)), South African Department of Environmental Affairs ([DEA](#)) and Italian National Antarctic Research Programme ([PNRA](#)) scientific activities. Measurements have been obtained through thermosalinograph (TSG) during several cruises to both Antarctica and sub-Antarctic islands. On-board TSG devices have been regularly calibrated and continuously monitored in-between cruises; no appreciable sensor drift emerged. Independent water samples taken along the cruises have been used to validate the data; salinity measurement error was a few hundredths of a unit on the practical salinity scale. A careful quality control allowed to discard bad data for each single campaign.

- **LEGOS-Survostral:** The TSG (LEGOS-Survostral) dataset corresponds to delayed mode regional data from TSG installed on the Astrolabe vessel (IPEV) during the round trips between Hobart (Tasmania) and the French Antarctic base at Dumont d'Urville ([Morrow and Kestenare \(2014\)](#)). It is provided by the [Survostral project](#) and available [here](#). Adjusted values when available and only collected TSG data that exhibit quality flags=1 and 2 were used.
- **LEGOS-Survostral-Adélie:** The TSG (LEGOS-Survostral-Adelie) dataset corresponds to delayed mode regional dataset along the Adelie coast provided by the [Survostral project](#) and available via [here](#). Adjusted values when available and only collected TSG data that exhibit quality flags=1 and 2 were used.

1.1.6 Moorings

The Pi-MEP collects data from the Global Tropical Moored Buoy Array ([GTMBA](#)), a multi-national effort to provide data in real-time for climate research and forecasting. Major components include the TAO/TRITON array in the Pacific, PIRATA in the Atlantic, and RAMA in the Indian Ocean. Data collected within TAO/TRITON, PIRATA and RAMA come primarily from ATLAS and TRITON moorings. These two mooring systems are functionally equivalent in terms of sensors, sample rates, and data quality. The data are directly downloaded from [ftp.pmel.noaa.gov](ftp://ftp.pmel.noaa.gov) every day and stored in the Pi-MEP. Only salinity data measured at 1 or 1.5 meter depth with standard (pre-deployment calibration applied) and highest quality (pre/post calibration in agreement) are considered. A careful filtering of suspiciously erroneous mooring salinity data when compared with all satellite data has also been performed (cf. [presentation](#)). The Pi-MEP project acknowledges the GTMBA Project Office of NOAA/PMEL for providing the data. Data from the Ocean Station [PAPA](#) are also added to the Pi-MEP *in situ* database.

From the [Upper Ocean Processes Group](#) at Woods Hole Oceanographic Institution ([WHOI](#)), several moorings data are also included in the Pi-MEP. Namely, delayed mode surface mooring salinity records under the stratus cloud deck in the eastern tropical Pacific ([Stratus](#)), in the trade wind region of the northwest tropical Atlantic ([NTAS](#)), 100 km north of Oahu at the WHOI Hawaii Ocean Time-series Site ([WHOTS](#)), in the salinity maximum region of the subtropical North Atlantic ([SPURS-1](#)) and in the Pacific intertropical convergence zone ([SPURS-2](#)).

1.2 Auxiliary geophysical datasets

Additional EO datasets are used to characterize the geophysical conditions at the *in situ* measurement locations and time, and 10 days prior to the measurements, to get an estimate of the geophysical concomitant condition and history. As discussed in [Boutin et al. \(2016\)](#), the presence of vertical gradients in, and horizontal variability of, sea surface salinity indeed complicates

comparison of satellite and *in situ* measurements. The additional EO data are used here to get a first estimates of conditions for which L-band satellite SSS measured in the first centimeters of the upper ocean within a 50-150 km diameter footprint might differ from pointwise *in situ* measurements performed in general between 10 and 5 m depth below the surface. The spatio-temporal variability of SSS within a satellite footprint (50-150 km) is a major issue for satellite SSS validation in the vicinity of river plumes, frontal zones, and significant precipitation areas, among others. Rainfall can in some cases produce vertical salinity gradients exceeding 1 pss m^{-1} ; consequently, it is recommended that satellite and *in situ* SSS measurements less than 3–6 h after rain events should be considered with care when used in satellite calibration/validation analyses. To identify such situation, the Pi-MEP platform is first using CMORPH products to characterize the local value and history of rain rate and ASCAT gridded data are used to characterize the local surface wind speed and history. For validation purpose, the ISAS monthly SSS *in situ* analysed fields at 5 m depth are collocated and compared with the *in situ* SSS value. The use of ISAS is motivated by the fact that it is used in the SMOS L2 official validation protocol in which systematic comparisons of SMOS L2 retrieved SSS with ISAS are done. In complement to ISAS, annual std climatological field from the World Ocean Atlas (WOA13) at the *in situ* location are also used to have an a priori information of the local SSS variability.

1.2.1 CMORPH

Precipitation are estimated using the CMORPH 3-hourly products at $1/4^\circ$ resolution (Joyce et al. (2004)). CMORPH (CPC MORPHing technique) produces global precipitation analyses at very high spatial and temporal resolution. This technique uses precipitation estimates that have been derived from low orbiter satellite microwave observations exclusively, and whose features are transported via spatial propagation information that is obtained entirely from geostationary satellite IR data. At present NOAA incorporate precipitation estimates derived from the passive microwaves aboard the DMSP 13, 14 and 15 (SSM/I), the NOAA-15, 16, 17 and 18 (AMSU-B), and AMSR-E and TMI aboard NASA's Aqua, TRMM and GPM spacecraft, respectively. These estimates are generated by algorithms of Ferraro (1997) for SSM/I, Ferraro et al. (2000) for AMSU-B and Kummerow et al. (2001) for TMI. Note that this technique is not a precipitation estimation algorithm but a means by which estimates from existing microwave rainfall algorithms can be combined. Therefore, this method is extremely flexible such that any precipitation estimates from any microwave satellite source can be incorporated.

With regard to spatial resolution, although the precipitation estimates are available on a grid with a spacing of 8 km (at the equator), the resolution of the individual satellite-derived estimates is coarser than that - more on the order of 12 x 15 km or so. The finer "resolution" is obtained via interpolation.

In effect, IR data are used as a means to transport the microwave-derived precipitation features during periods when microwave data are not available at a location. Propagation vector matrices are produced by computing spatial lag correlations on successive images of geostationary satellite IR which are then used to propagate the microwave derived precipitation estimates. This process governs the movement of the precipitation features only. At a given location, the shape and intensity of the precipitation features in the intervening half hour periods between microwave scans are determined by performing a time-weighting interpolation between microwave-derived features that have been propagated forward in time from the previous microwave observation and those that have been propagated backward in time from the following microwave scan. NOAA refer to this latter step as "morphing" of the features.

For the present Pi-MEP products, we only considered the 3-hourly products at $1/4$ degree resolution. The entire CMORPH record (December 2002-present) for 3-hourly, $1/4$ de-

gree lat/lon resolution can be found at: ftp://ftp.cpc.ncep.noaa.gov/precip/CMORPH_V1.0/CRT/. CMORPH estimates cover a global belt (-180°W to 180°E) extending from 60°S to 60°N latitude and are available for the complete period of the Pi-MEP core datasets (Jan 2010-now).

1.2.2 ASCAT

Advanced SCATterometer (ASCAT) daily data produced and made available at Ifremer/CERSAT on a 0.25°x0.25° resolution grid ([Bentamy and Fillon \(2012\)](#)) since March 2007 are used to characterize the mean daily wind at the match-up pair location as well as the wind history during the 10-days period preceding the in situ measurement date. These wind fields are calculated based on a geostatistical method with external drift. Remotely sensed data from ASCAT are considered as observations while those from numerical model analysis (ECMWF) are associated with the external drift. The spatial and temporal structure functions for wind speed, zonal and meridional wind components are estimated from ASCAT retrievals. Furthermore, the new procedure includes a temporal interpolation of the retrievals based on the complex empirical orthogonal function (CEOOF) approach, in order to enhance the sampling length of the scatterometer observations. The resulting daily wind fields involves the main known surface wind patterns as well as some variation modes associated with temporal and spatial moving features. The accuracy of the gridded winds was investigated through comparisons with moored buoy data in [Bentamy et al. \(2012\)](#) and resulted in rms differences for wind speed and direction are about 1.50 m.s⁻¹ and 20°.

1.2.3 ISAS

The In Situ Analysis System (ISAS), as described in [Gaillard et al. \(2016\)](#) is a data based re-analysis of temperature and salinity fields over the global ocean 70°N–70°S on a 1/2° grid. It was initially designed to synthesize the temperature and salinity profiles collected by the Argo program. It has been later extended to accommodate all type of vertical profile as well as time series. ISAS gridded fields are entirely based on *in situ* measurements. The methodology and configuration have been conceived to preserve as much as possible the data information content and resolution. ISAS is developed and run in a research laboratory ([LOPS](#)) in close collaboration with Coriolis, one of Argo Global Data Assembly Center and unique data provider for the Mercator operational oceanography system. In Pi-MEP, the products used are the [INSITU_GLO_PHY_TS_OA_MY_013_052](#) for the period 2010 to 2021 and the [INSITU_GLO_PHY_TS_OA_NRT_013_002](#) for the Near-Real Time (2022-2023) derived at the Coriolis data center and provided by the Copernicus Marine Environment Monitoring Service ([CMEMS](#)). The major contribution to the data set is from Argo array of profiling floats, reaching an approximate resolution of one profile every 10-days and every 3-degrees over the satellite SSS period (<http://www.umr-lops.fr/SNO-Argo/Products/ISAS-T-S-fields/>). The ISAS optimal interpolation involves a structure function modeled as the sum of two Gaussian functions, each associated with specific time and space scales, resulting in a smoothing over typically 3 degrees. The smallest scale which can be retrieved with ISAS analysis is not smaller than 300–500 km ([Kolodziejczyk et al. \(2015\)](#)). For validation purpose, the ISAS monthly SSS fields at 5 m depth are collocated and compared with the satellite SSS products and included in the Pi-MEP Match-up files. In addition, the "percentage of variance" fields (PCTVAR) contained in the ISAS analyses provide information on the local variability of *in situ* SSS measurements within 1/2°x1/2° boxes.

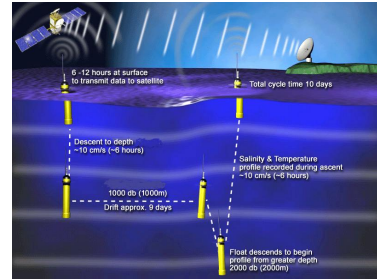
1.2.4 World Ocean Atlas Climatology

The World Ocean Atlas 2013 version 2 ([WOA13 V2](#)) is a set of objectively analyzed (1° grid) climatological fields of *in situ* temperature, salinity and other variables provided at standard depth levels for annual, seasonal, and monthly compositing periods for the World Ocean. It also includes associated statistical fields of observed oceanographic profile data interpolated to standard depth levels on 5° , 1° , and 0.25° grids. We use these fields in complement to ISAS to characterize the climatological fields (annual mean and std) at the match-up pairs location and date.

2 Argo

2.1 Introduction

Argo is a global array of 3,000 free-drifting profiling floats that measures the temperature and salinity of the upper 2000 m of the ocean. This allows continuous monitoring of the temperature and salinity of the upper ocean, with all data being relayed and made publicly available within hours after collection. The array provides around 100,000 temperature/salinity profiles per year distributed over the global oceans at an average of 3-degree spacing. Only Argo salinity and temperature float data with quality index set to 1 or 2 and data mode set to real time (RT), real time adjusted (RTA) and delayed mode (DM) are considered in the Pi-MEP. Argo floats which may have problems with one or more sensors appearing in the [grey list](#) maintained at the Coriolis/GDACs are discarded. Furthermore, Pi-MEP provides an additional [list](#) of ~ 1000 "suspicious" argo salinity profiles that are also removed before analysis. The upper ocean salinity and temperature values recorded between 0m and 10m depth are considered as Argo sea surface salinities (SSS) and sea surface temperatures (SST). These data were collected and made freely available by the international Argo project and the national programs that contribute to it ([Argo \(2023\)](#)).



2.2 Number of SSS data as a function of time and distance to coast

Figure 1 shows the time (a) and distance to coast (b) distributions of the Argo *in situ* dataset.

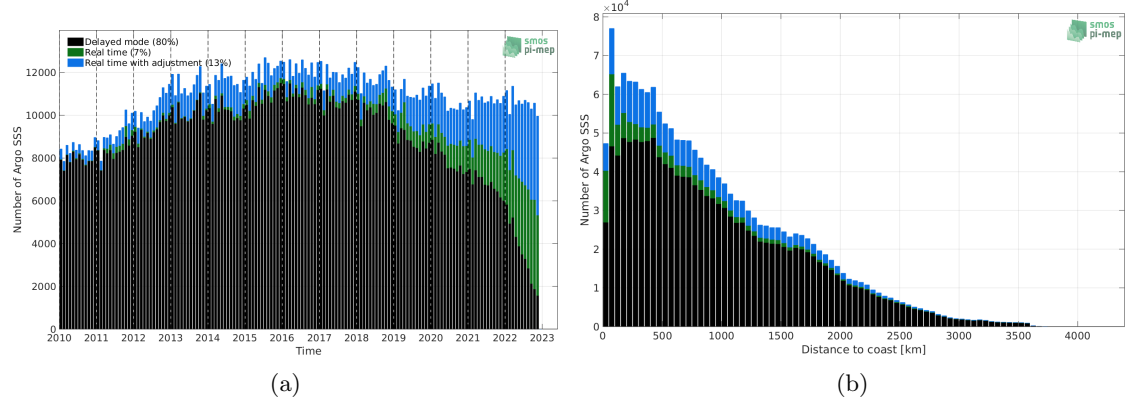


Figure 1: Number of SSS from Argo as a function of time (a) and distance to coast (b).

2.3 Histograms of SSS

Figure 2 shows the SSS distribution of the Argo (a) and colocalized ISAS (b) dataset.

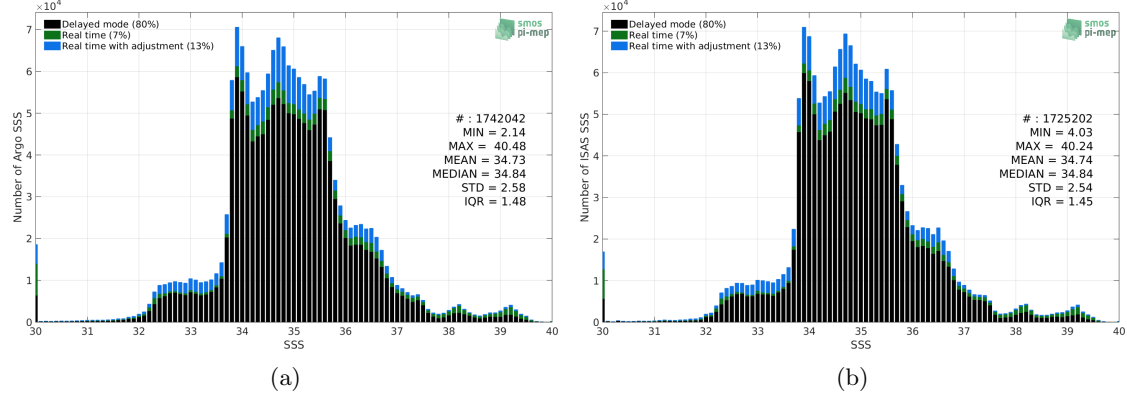


Figure 2: Histograms of SSS from Argo (a) and ISAS (b) per bins of 0.1.

2.4 Distribution of *in situ* SSS depth measurements

In Figure 3, we show the depth distribution of the *in situ* salinity dataset (a) and the spatial distribution of the depth temporal mean in $1^\circ \times 1^\circ$ boxes and considering the full *in situ* dataset period (b).

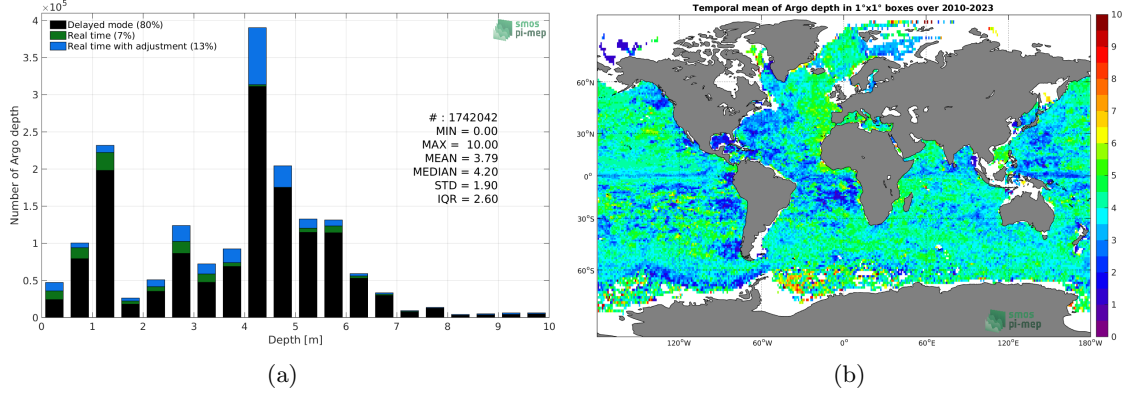


Figure 3: Depth distribution of the upper level SSS measurements from Argo (a) and spatial distribution of the *in situ* SSS depth measurements showing the mean value in $1^\circ \times 1^\circ$ boxes and considering the full *in situ* dataset period (b).

2.5 Spatial distribution of SSS

In Figure 4, the number of Argo SSS measurements in $1^\circ \times 1^\circ$ boxes is shown.

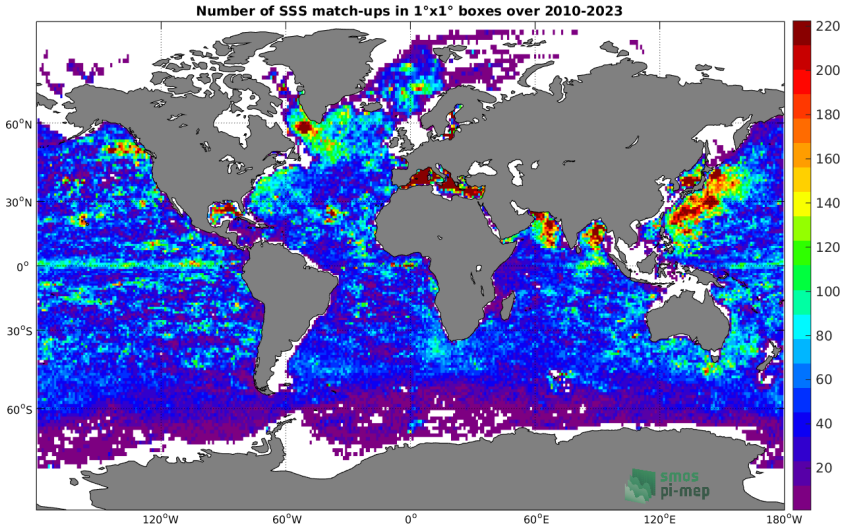


Figure 4: Number of SSS from Argo in $1^\circ \times 1^\circ$ boxes.

2.6 Spatial Maps of the Temporal mean and Std of *in situ* and ISAS SSS and of the difference (Δ SSS)

In Figure 5, maps of temporal mean (left) and standard deviation (right) of ISAS (top), Argo *in situ* dataset (middle) and the difference Δ SSS(ISAS - Argo) (bottom) are shown. The temporal mean and std are calculated using all match-up pairs falling in spatial boxes of size $1^\circ \times 1^\circ$ over the full Argo dataset period.

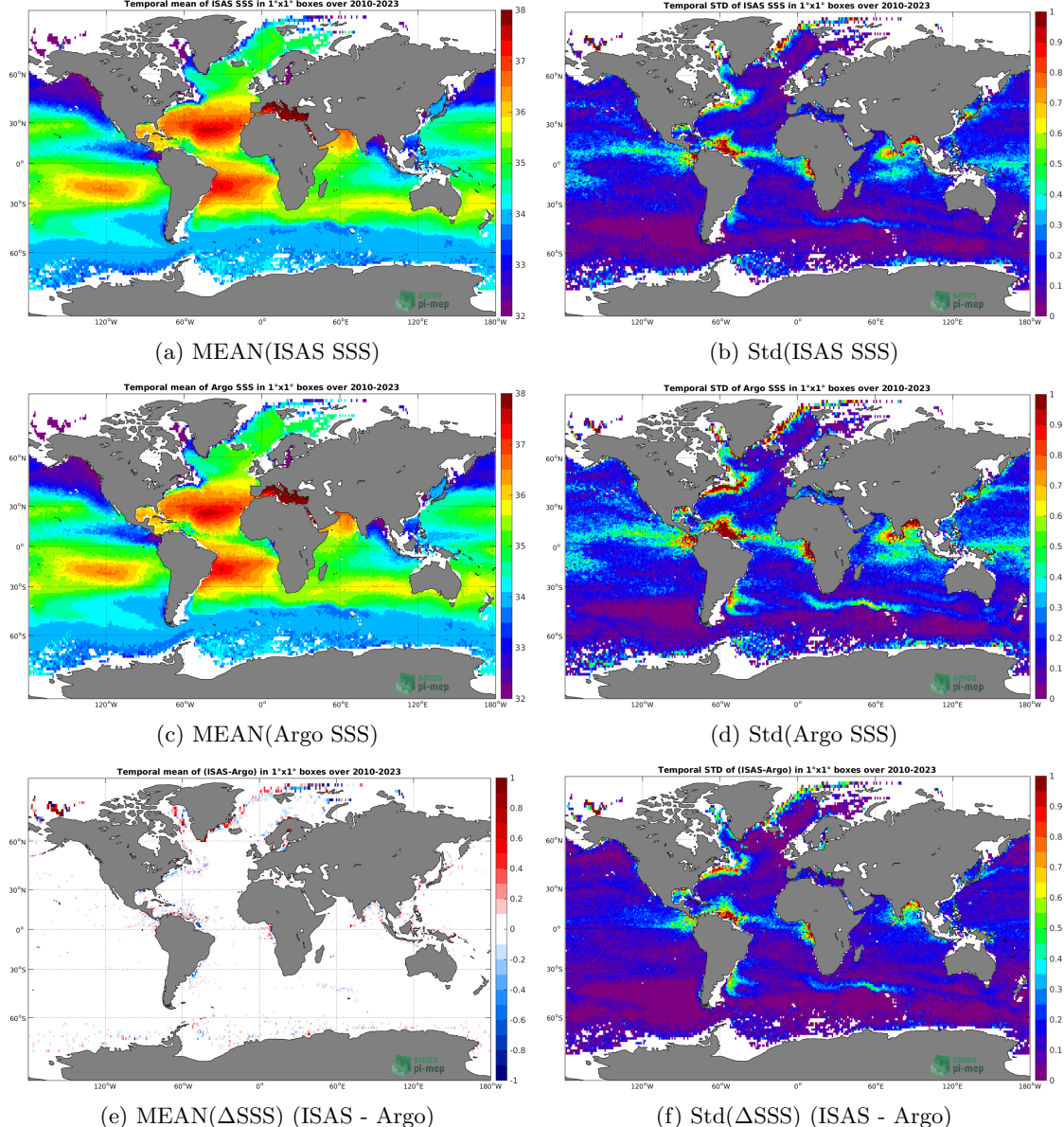


Figure 5: Temporal mean (left) and Std (right) of SSS from ISAS (top), Argo (middle), and of Δ SSS (ISAS - Argo). Only match-up pairs are used to generate these maps.

2.7 Time series of the monthly median and Std of *in situ* and ISAS SSS and of the difference (Δ SSS)

In the top panel of Figure 6, we show the time series of the monthly median SSS estimated for both ISAS SSS product (in black) and the Argo *in situ* dataset (in blue) at the collected Pi-MEP match-up pairs.

In the middle panel of Figure 6, we show the time series of the monthly median of Δ SSS (ISAS - Argo) for the collected Pi-MEP match-up pairs.

In the bottom panel of Figure 6, we show the time series of the monthly standard deviation of the ΔSSS (ISAS - Argo) for the collected Pi-MEP match-up pairs.



Figure 6: Time series of the monthly median SSS (top), median of ΔSSS (ISAS - Argo) and Std of ΔSSS (ISAS - Argo) considering all match-ups collected by the Pi-MEP.

2.8 Zonal mean and Std of *in situ* and ISAS SSS and of the difference ΔSSS

In Figure 7 left panel, we show the zonal mean SSS considering all Pi-MEP match-up pairs for both ISAS SSS product (in black) and the Argo *in situ* dataset (in blue). The full *in situ* dataset period is used to derive the mean.

In the right panel of Figure 7, we show the zonal mean of ΔSSS (ISAS - Argo) for all the collected Pi-MEP match-up pairs estimated over the full *in situ* dataset period.

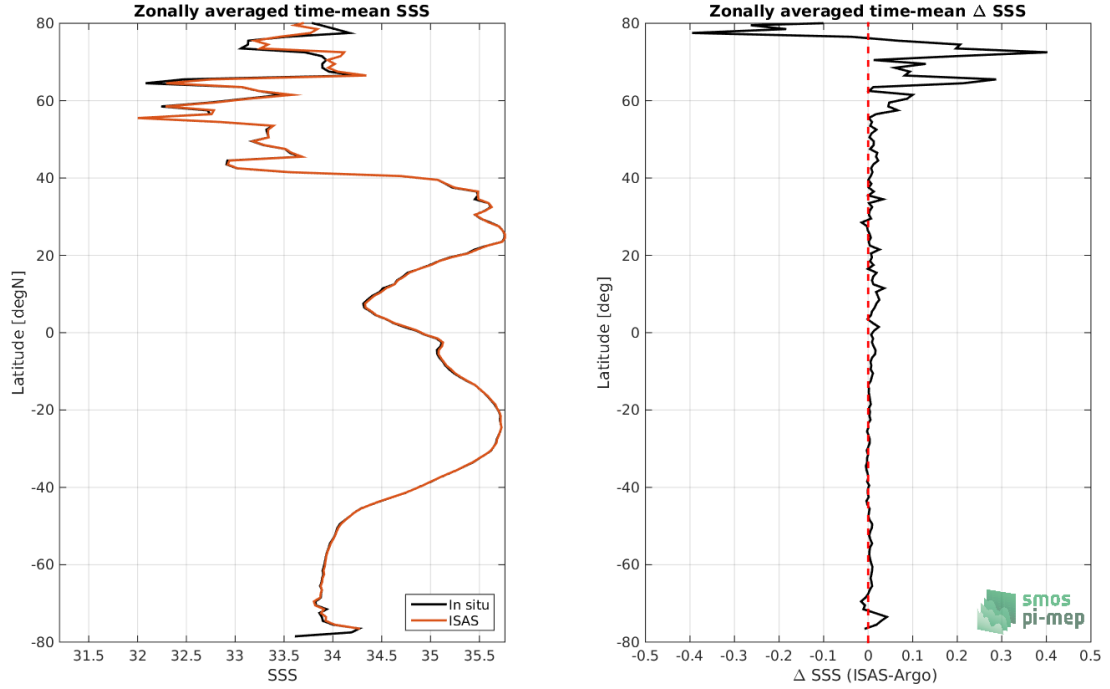


Figure 7: Left panel: Zonal mean SSS from ISAS product (black) and from Argo (blue). Right panel: Zonal mean of Δ SSS (ISAS - Argo) for all the collected Pi-MEP match-up pairs estimated over the full *in situ* dataset period.

2.9 Scatterplots of ISAS vs *in situ* SSS by latitudinal bands

In Figure 8, contour maps of the concentration of ISAS SSS (y-axis) versus Argo SSS (x-axis) at match-up pairs for different latitude bands: (a) 80°S-80°N, (b) 20°S-20°N, (c) 40°S-20°S and 20°N-40°N and (d) 60°S-40°S and 40°N-60°N. For each plot, the red line shows $x=y$. The black thin and dashed lines indicate a linear fit through the data cloud and the $\pm 95\%$ confidence levels, respectively. The number match-up pairs n , the slope and R^2 coefficient of the linear fit, the root mean square (RMS) and the mean bias between ISAS and *in situ* data are indicated for each latitude band in each plots.

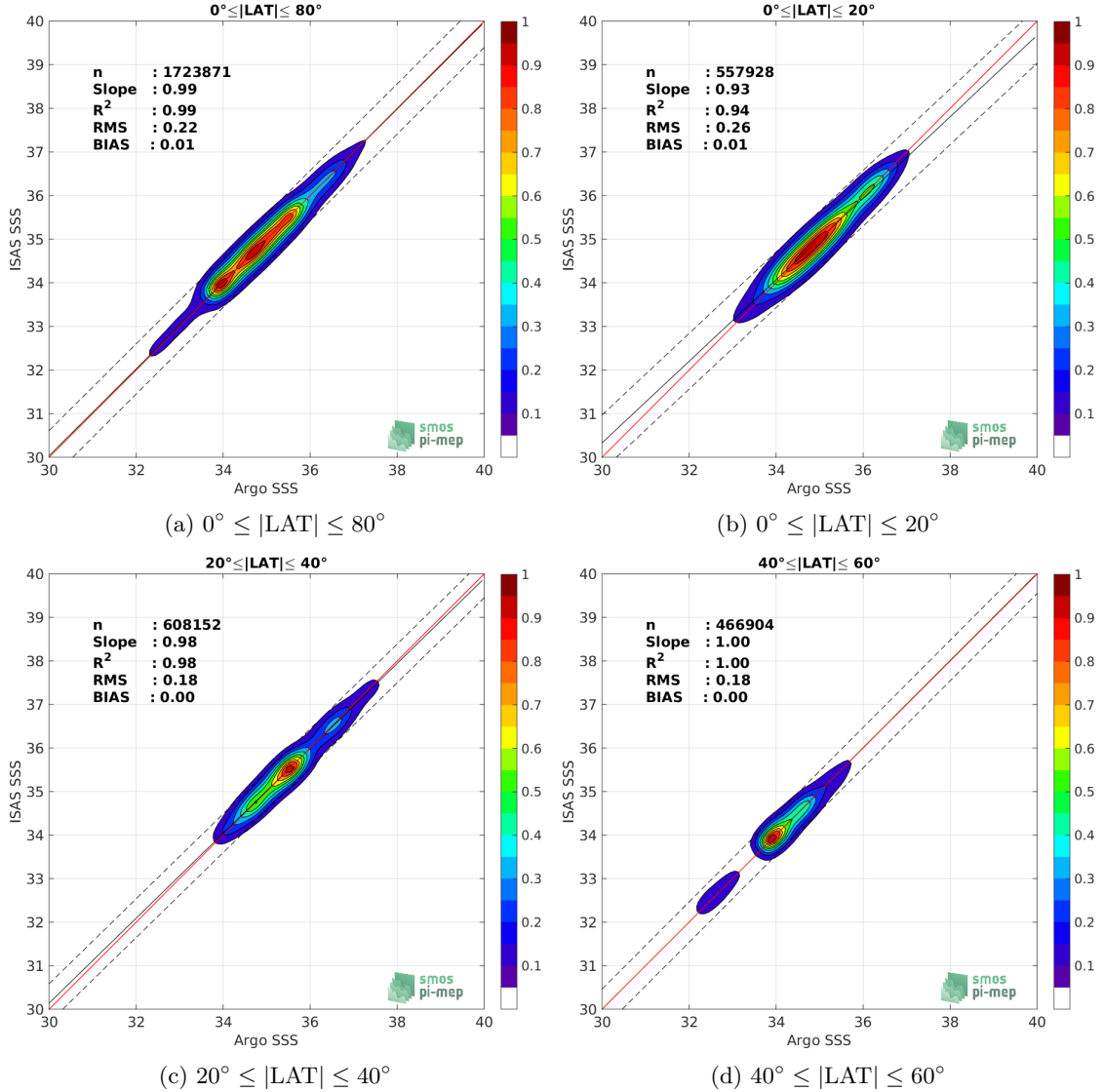


Figure 8: Contour maps of the concentration of ISAS SSS (y-axis) versus Argo SSS (x-axis) at match-up pairs for different latitude bands. For each plot, the red line shows $x=y$. The black thin and dashed lines indicate a linear fit through the data cloud and the $\pm 95\%$ confidence levels, respectively. The number match-up pairs n , the slope and R^2 coefficient of the linear fit, the root mean square (RMS) and the mean bias between ISAS and *in situ* data are indicated for each latitude band in each plots.

2.10 Time series of the monthly median and Std of the difference ΔSSS sorted by latitudinal bands

In Figure 9, time series of the monthly median (red curves) of ΔSSS (ISAS - Argo) and ± 1 Std (black vertical thick bars) as function of time for all the collected Pi-MEP match-up pairs estimated for the full *in situ* dataset period are shown for different latitude bands: (a) $80^\circ\text{S}-80^\circ\text{N}$, (b) $20^\circ\text{S}-20^\circ\text{N}$, (c) $40^\circ\text{S}-20^\circ\text{S}$ and $20^\circ\text{N}-40^\circ\text{N}$ and (d) $60^\circ\text{S}-40^\circ\text{S}$ and $40^\circ\text{N}-60^\circ\text{N}$.

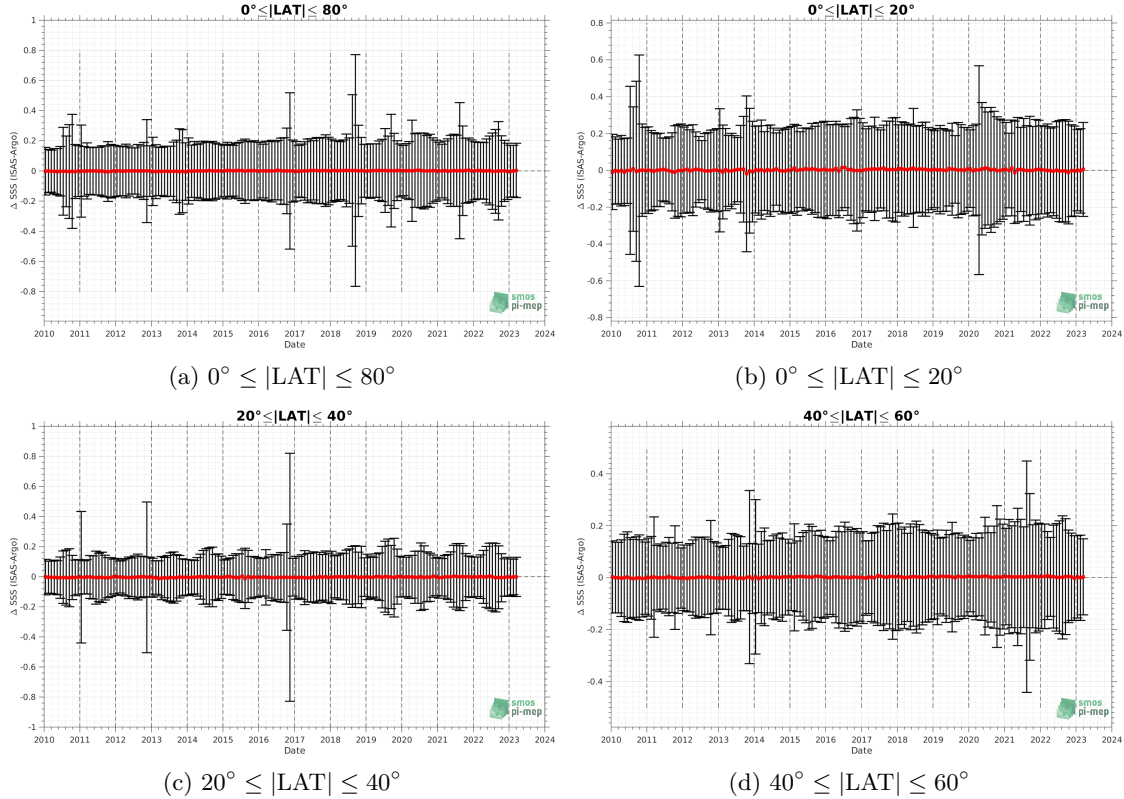


Figure 9: Monthly median (red curves) of ΔSSS (ISAS - Argo) and ± 1 Std (black vertical thick bars) as function of time for all the collected Pi-MEP match-up pairs for the full *in situ* dataset period are shown for different latitude bands: (a) $80^\circ\text{S}-80^\circ\text{N}$, (b) $20^\circ\text{S}-20^\circ\text{N}$, (c) $40^\circ\text{S}-20^\circ\text{S}$ and $20^\circ\text{N}-40^\circ\text{N}$ and (d) $60^\circ\text{S}-40^\circ\text{S}$ and $40^\circ\text{N}-60^\circ\text{N}$.

2.11 ΔSSS sorted as geophysical conditions

In Figure 10, we classify the match-up differences ΔSSS (ISAS - *in situ*) as function of the geophysical conditions at match-up points. The mean and std of ΔSSS (ISAS - Argo) is thus evaluated as function of the

- *in situ* SSS values per bins of width 0.2,
- *in situ* SST values per bins of width 1°C ,
- ASCAT daily wind values per bins of width 1 m/s,
- CMORPH 3-hourly rain rates per bins of width 1 mm/h, and,
- distance to coasts per bins of width 50 km,
- *in situ* measurement depth (if relevant).

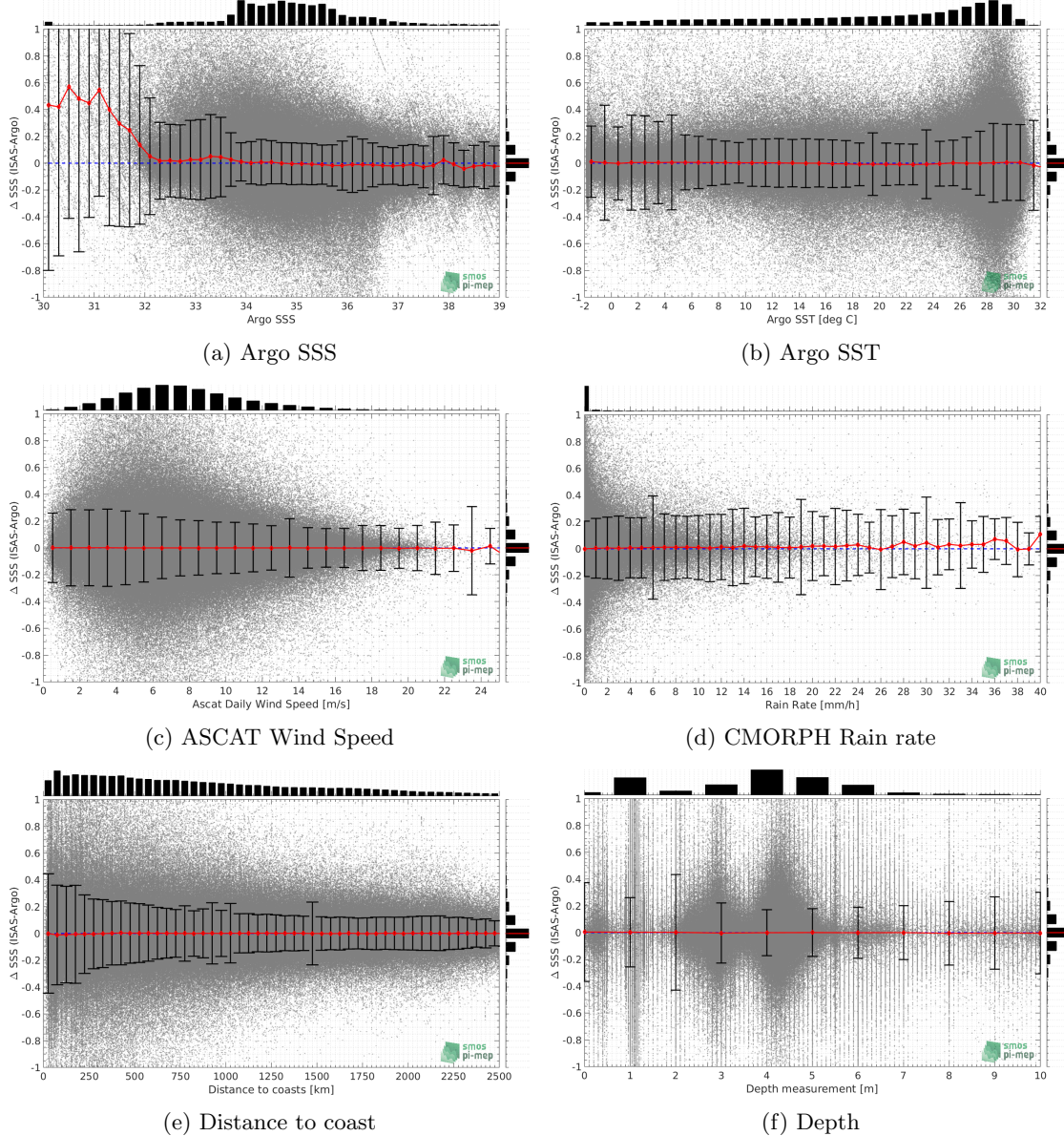


Figure 10: ΔSSS (ISAS - Argo) sorted as geophysical conditions: Argo SSS a), Argo SST b), ASCAT Wind speed c), CMORPH rain rate d), distance to coast (e) and depth measurements (f).

2.12 ΔSSS maps and statistics for different geophysical conditions

In Figures 11 and 12, we focus on sub-datasets of the match-up differences ΔSSS (*ISAS - in situ*) for the following specific geophysical conditions:

- C1: if the local value at *in situ* location of estimated rain rate is zero, mean daily wind is in the range [3, 12] m/s, the SST is $> 5^\circ\text{C}$ and distance to coast is > 800 km.

- **C2:**if the local value at *in situ* location of estimated rain rate is zero, mean daily wind is in the range [3, 12] m/s.
- **C3:**if the local value at *in situ* location of estimated rain rate is high (ie. > 1 mm/h) and mean daily wind is low (ie. < 4 m/s).
- **C4:**if the mixed layer is shallow with depth <20m.
- **C5:**if the *in situ* data is located where the climatological SSS standard deviation is low (ie. above < 0.2).
- **C6:**if the *in situ* data is located where the climatological SSS standard deviation is high (ie. above > 0.2).

For each of these conditions, the temporal mean (gridded over spatial boxes of size $1^\circ \times 1^\circ$) and the histogram of the difference ΔSSS (ISAS - *in situ*) are presented.

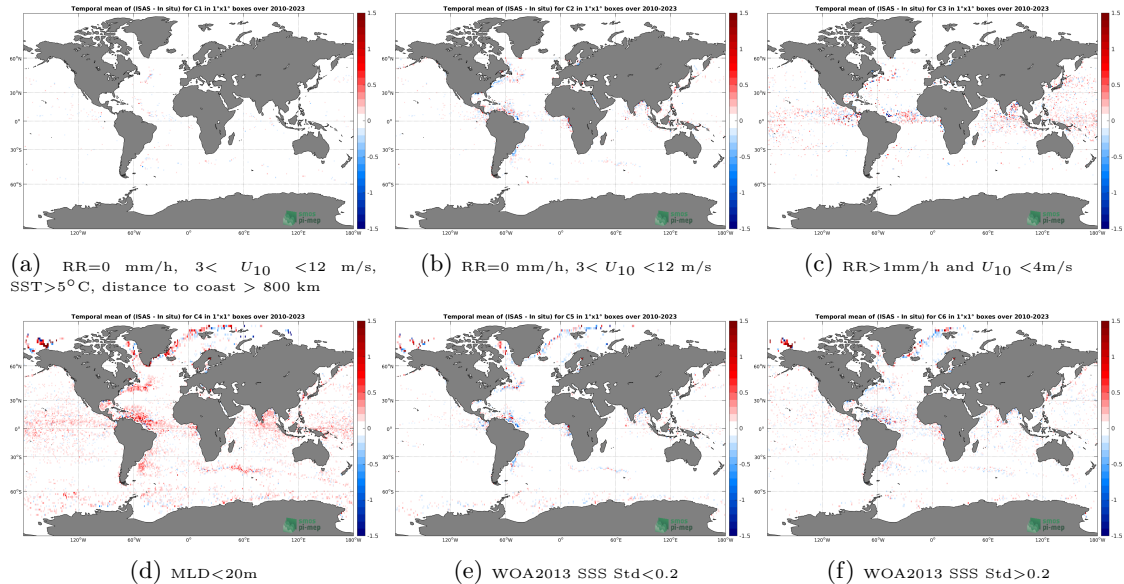


Figure 11: Temporal mean gridded over spatial boxes of size $1^\circ \times 1^\circ$ of ΔSSS (ISAS - Argo) for 6 different subdatasets corresponding to: RR=0 mm/h, $3 < U_{10} < 12$ m/s, SST> 5°C , distance to coast > 800 km (a), RR=0 mm/h, $3 < U_{10} < 12$ m/s (b), RR>1mm/h and $U_{10} < 4$ m/s (c), MLD<20m (d), WOA2013 SSS Std<0.2 (e), WOA2013 SSS Std>0.2 (f).

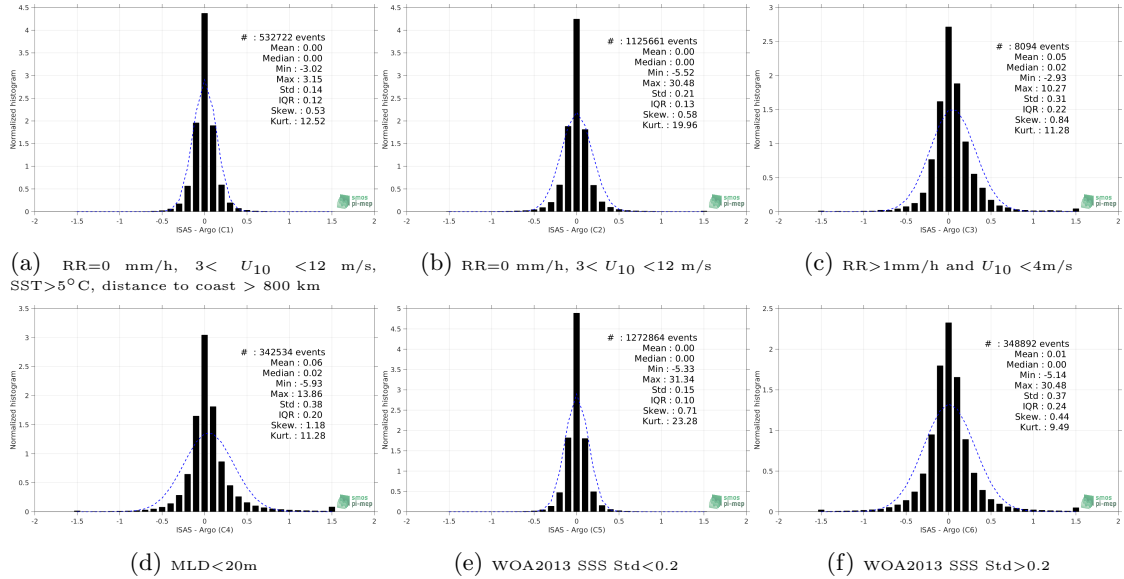


Figure 12: Normalized histogram of ΔSSS (ISAS - Argo) for 6 different subdatasets corresponding to: RR=0 mm/h, $3 < U_{10} < 12$ m/s, SST> 5°C , distance to coast > 800 km (a), RR=0 mm/h, $3 < U_{10} < 12$ m/s (b), RR>1mm/h and $U_{10} < 4$ m/s (c), WOA2013 SSS Std<0.2 (d), WOA2013 SSS Std>0.2 (e).

2.13 Summary

Table 1 shows the mean, median, standard deviation (Std), root mean square (RMS), interquartile range (IQR), correlation coefficient (r^2) and robust standard deviation (Std^*) of the match-up differences ΔSSS (ISAS - Argo) for the following conditions:

- all: All the match-up pairs satellite/in situ SSS are used to derive the statistics
- C1: only pairs where RR=0 mm/h, $3 < U_{10} < 12$ m/s, SST> 5°C , distance to coast > 800 km
- C2: only pairs where RR=0 mm/h, $3 < U_{10} < 12$ m/s
- C3: only pairs where RR>1mm/h and $U_{10} < 4$ m/s
- C4: only pairs where MLD<20m
- C5: only pairs where WOA2013 SSS Std<0.2
- C6: only pairs where WOA2013 SSS Std>0.2
- C7a: only pairs where distance to coast is < 150 km.
- C7b: only pairs where distance to coast is in the range [150, 800] km.
- C7c: only pairs where distance to coast is > 800 km.
- C8a: only pairs where in situ SST is < 5°C .
- C8b: only pairs where in situ SST is in the range [5, 15] $^{\circ}\text{C}$.

- C8c: only pairs where in situ SST is $> 15^{\circ}\text{C}$.
- C9a: only pairs where in situ SSS is < 33 .
- C9b: only pairs where in situ SSS is in the range [33, 37].
- C9c: only pairs where in situ SSS is > 37 .

Table 1: Statistics of ΔSSS (ISAS - Argo)

Condition	#	Median	Mean	Std	RMS	IQR	r^2	Std*
all	1725202	0.00	0.01	0.23	0.23	0.12	0.992	0.09
C1	532722	0.00	0.00	0.14	0.14	0.12	0.979	0.09
C2	1125661	0.00	0.00	0.21	0.21	0.13	0.993	0.09
C3	8094	0.02	0.05	0.31	0.32	0.22	0.979	0.16
C4	342534	0.02	0.06	0.38	0.38	0.20	0.991	0.14
C5	1272864	0.00	0.00	0.15	0.15	0.10	0.994	0.08
C6	348892	0.00	0.01	0.37	0.37	0.24	0.987	0.18
C7a	183547	-0.01	0.02	0.39	0.39	0.17	0.997	0.13
C7b	717972	0.00	0.01	0.25	0.25	0.13	0.965	0.09
C7c	822296	0.00	0.00	0.15	0.15	0.11	0.976	0.08
C8a	167297	0.00	0.03	0.34	0.34	0.07	0.988	0.05
C8b	367276	0.00	0.01	0.18	0.18	0.08	0.997	0.06
C8c	1188794	0.00	0.00	0.22	0.22	0.15	0.987	0.11
C9a	104499	0.02	0.13	0.63	0.64	0.18	0.993	0.12
C9b	1530831	0.00	0.00	0.17	0.17	0.12	0.961	0.09
C9c	89872	-0.02	-0.02	0.15	0.15	0.14	0.963	0.10

Table 1 numerical values can be downloaded as a csv file [here](#).

3 Marine mammals

3.1 Introduction

Instrumentation of southern elephant seals with satellite-linked CTD tags proposes unique temporal and spatial coverage. This includes extensive data from the Antarctic continental slope and shelf regions during the winter months, which is outside the conventional areas of Argo autonomous floats and ship-based studies. The use of elephant seals has been particularly effective to sample the Southern Ocean and the North Pacific. Other seal species have been successfully used in the North Atlantic, such as hooded seals. The marine mammal dataset ([MEOP-CTD database](#)) is quality controlled and calibrated using delayed-mode techniques involving comparisons with other existing profiles as well as cross-comparisons similar to established protocols within the Argo community, with a resulting accuracy of $\pm 0.03^{\circ}\text{C}$ in temperature and ± 0.05 in salinity or better ([Treasure et al. \(2017\)](#)). The marine mammal data were collected and made freely available by the International MEOP Consortium and the national programs that contribute to it (<http://www.meop.net>). This dataset is updated once a year and can be downloaded [here](#) ([Roquet et al. \(2021\)](#)). A preprocessing



stage is applied to the database before being used by the Pi-MEP which consists in keeping only profiles with salinity, temperature and pressure quality flags set to 1 or 2 and if at least one measurement is in the top 10 m depth. Marine mammal SSS corresponds to the top (shallowest) profile salinity data provided that profile depth is 10 m or less.

3.2 Number of SSS data as a function of time and distance to coast

Figure 13 shows the time (a) and distance to coast (b) distributions of the Marine mammals *in situ* dataset.

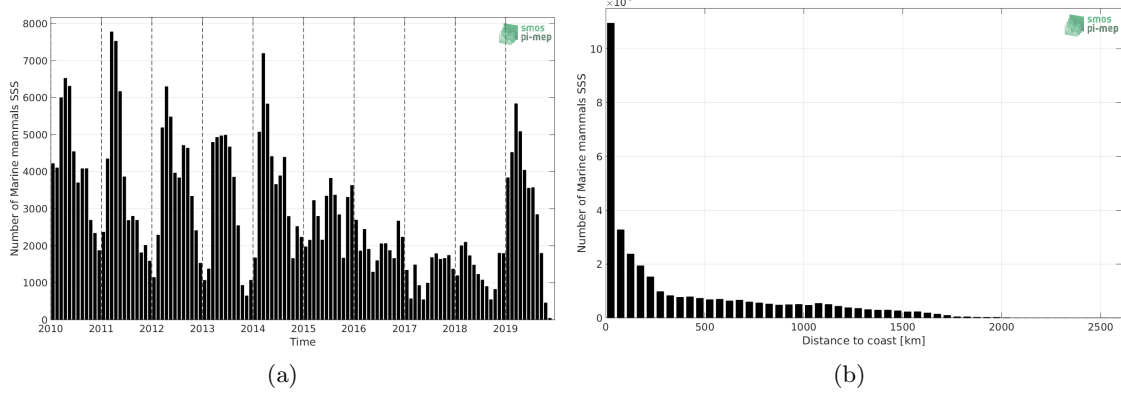


Figure 13: Number of SSS from Marine mammals as a function of time (a) and distance to coast (b).

3.3 Histograms of SSS

Figure 14 shows the SSS distribution of the Marine mammals (a) and colocalized ISAS (b) dataset.

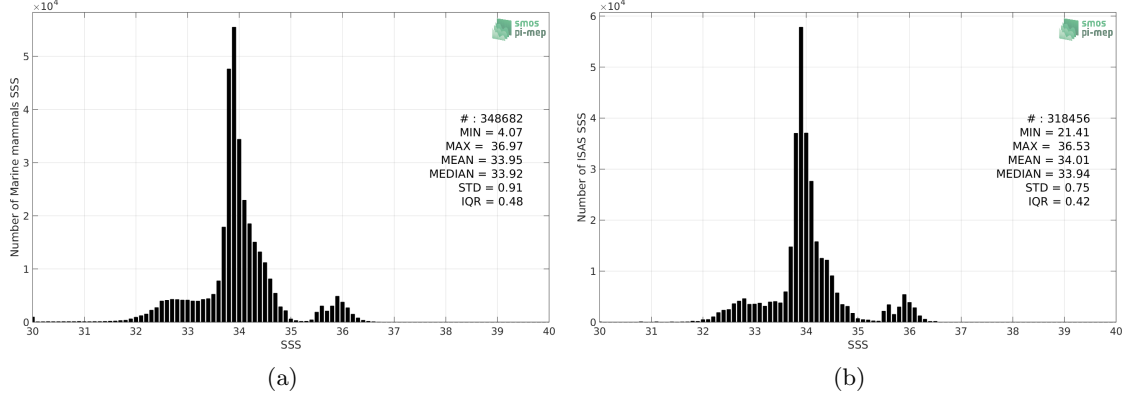


Figure 14: Histograms of SSS from Marine mammals (a) and ISAS (b) per bins of 0.1.

3.4 Distribution of *in situ* SSS depth measurements

In Figure 15, we show the depth distribution of the *in situ* salinity dataset (a) and the spatial distribution of the depth temporal mean in $1^\circ \times 1^\circ$ boxes and considering the full *in situ* dataset period (b).

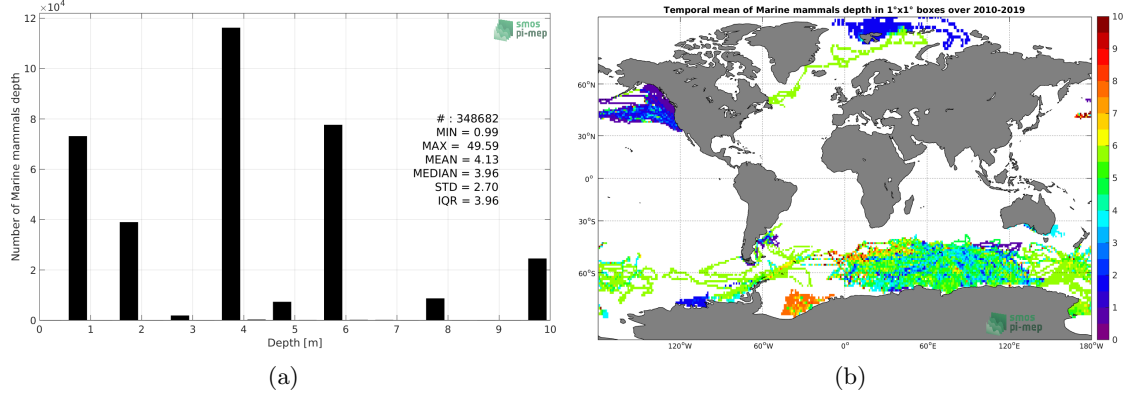


Figure 15: Depth distribution of the upper level SSS measurements from Marine mammals (a) and spatial distribution of the *in situ* SSS depth measurements showing the mean value in $1^\circ \times 1^\circ$ boxes and considering the full *in situ* dataset period (b).

3.5 Spatial distribution of SSS

In Figure 16, the number of Marine mammals SSS measurements in $1^\circ \times 1^\circ$ boxes is shown.

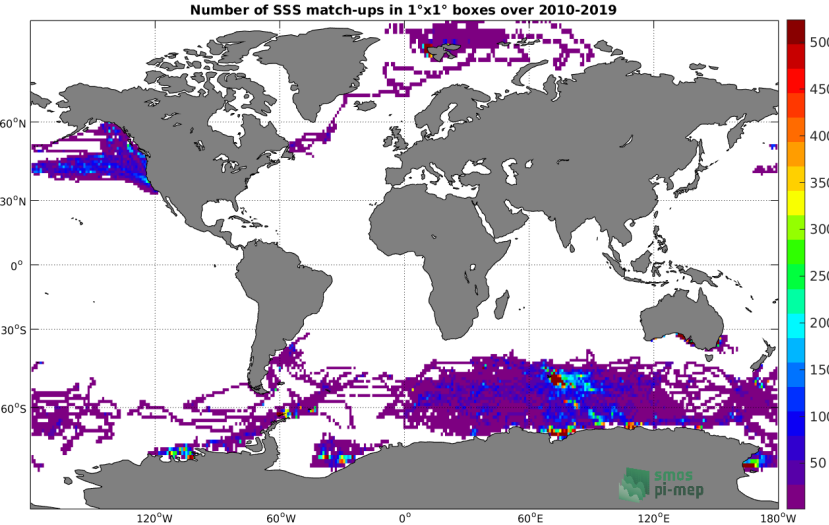


Figure 16: Number of SSS from Marine mammals in $1^\circ \times 1^\circ$ boxes.

3.6 Spatial Maps of the Temporal mean and Std of *in situ* and ISAS SSS and of the difference (Δ SSS)

In Figure 17, maps of temporal mean (left) and standard deviation (right) of ISAS (top), Marine mammals *in situ* dataset (middle) and the difference Δ SSS (ISAS -Marine mammals) (bottom) are shown. The temporal mean and std are calculated using all match-up pairs falling in spatial boxes of size $1^\circ \times 1^\circ$ over the full Marine mammals dataset period.

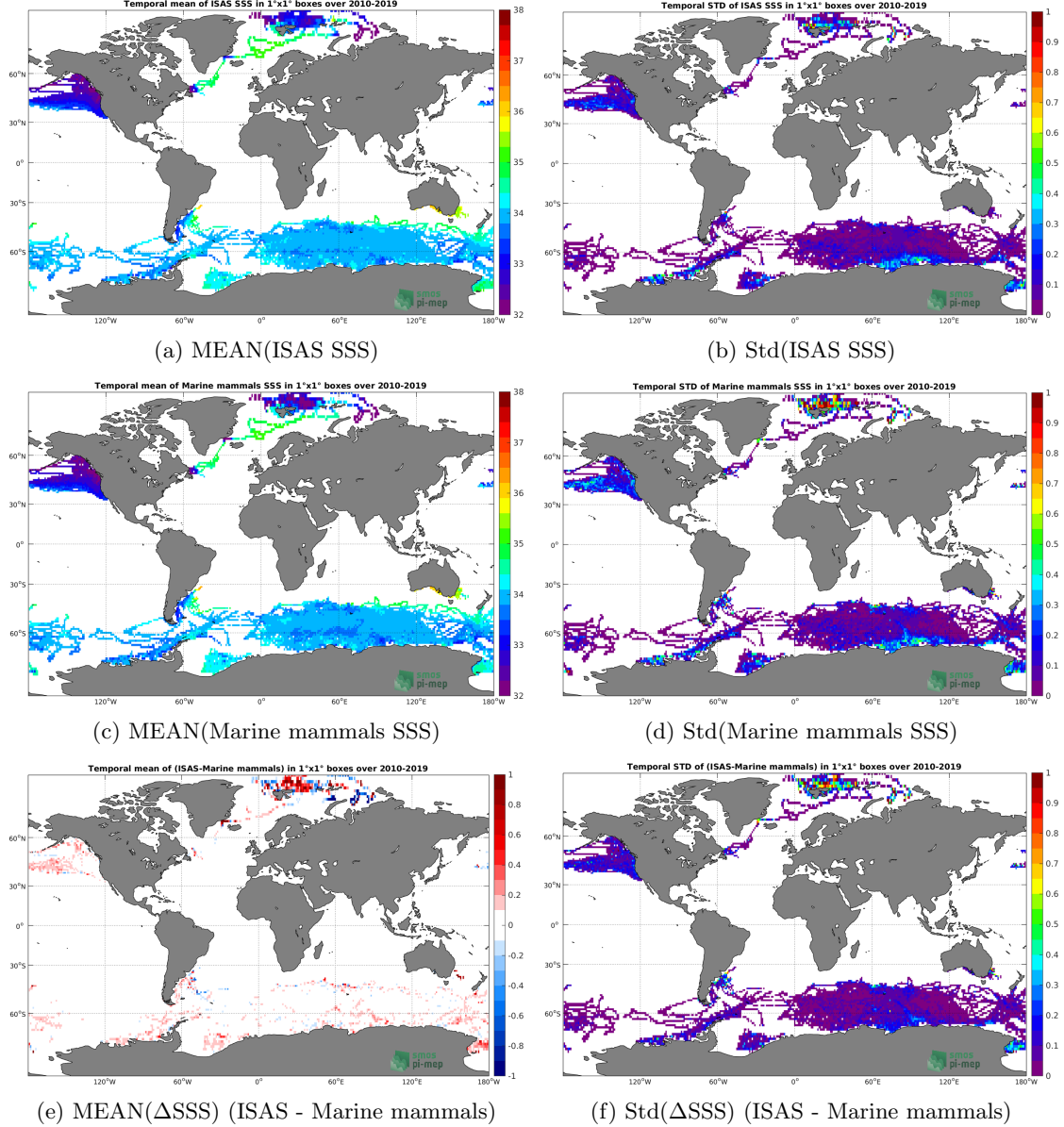


Figure 17: Temporal mean (left) and Std (right) of SSS from ISAS (top), Marine mammals (middle), and of Δ SSS (ISAS - Marine mammals). Only match-up pairs are used to generate these maps.

3.7 Time series of the monthly median and Std of *in situ* and ISAS SSS and of the difference (Δ SSS)

In the top panel of Figure 18, we show the time series of the monthly median SSS estimated for both ISAS SSS product (in black) and the Marine mammals *in situ* dataset (in blue) at the collected Pi-MEP match-up pairs.

In the middle panel of Figure 18, we show the time series of the monthly median of Δ SSS

(ISAS - Marine mammals) for the collected Pi-MEP match-up pairs.

In the bottom panel of Figure 18, we show the time series of the monthly standard deviation of the ΔSSS (ISAS - Marine mammals) for the collected Pi-MEP match-up pairs.

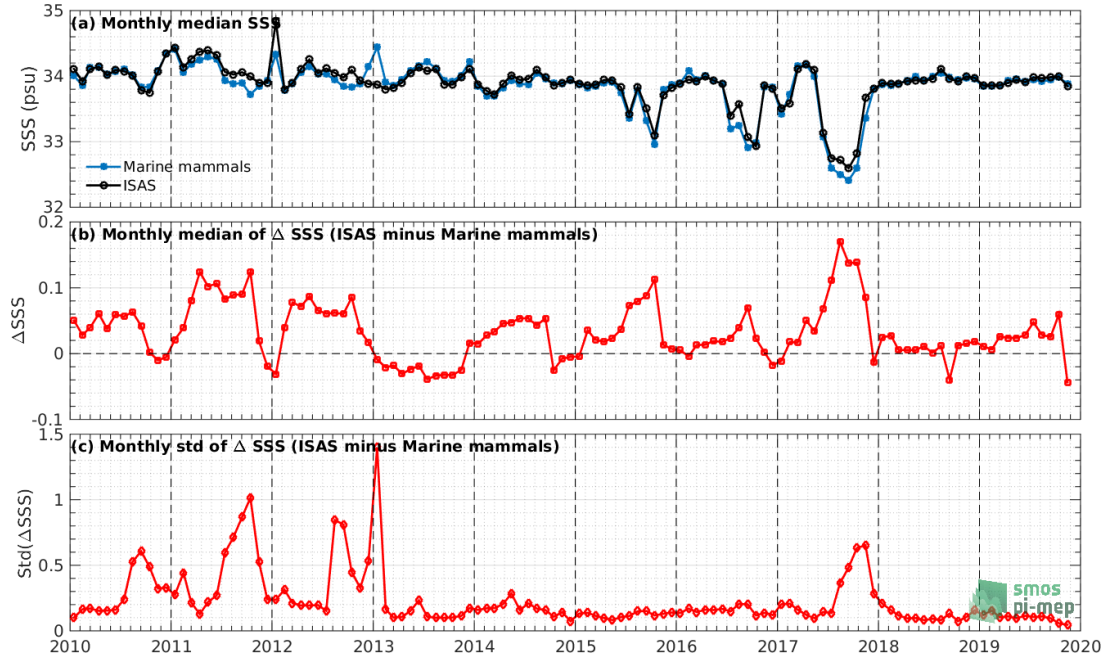


Figure 18: Time series of the monthly median SSS (top), median of ΔSSS (ISAS - Marine mammals) and Std of ΔSSS (ISAS - Marine mammals) considering all match-ups collected by the Pi-MEP.

3.8 Zonal mean and Std of *in situ* and ISAS SSS and of the difference ΔSSS

In Figure 19 left panel, we show the zonal mean SSS considering all Pi-MEP match-up pairs for both ISAS SSS product (in black) and the Marine mammals *in situ* dataset (in blue). The full *in situ* dataset period is used to derive the mean.

In the right panel of Figure 19, we show the zonal mean of ΔSSS (ISAS - Marine mammals) for all the collected Pi-MEP match-up pairs estimated over the full *in situ* dataset period.

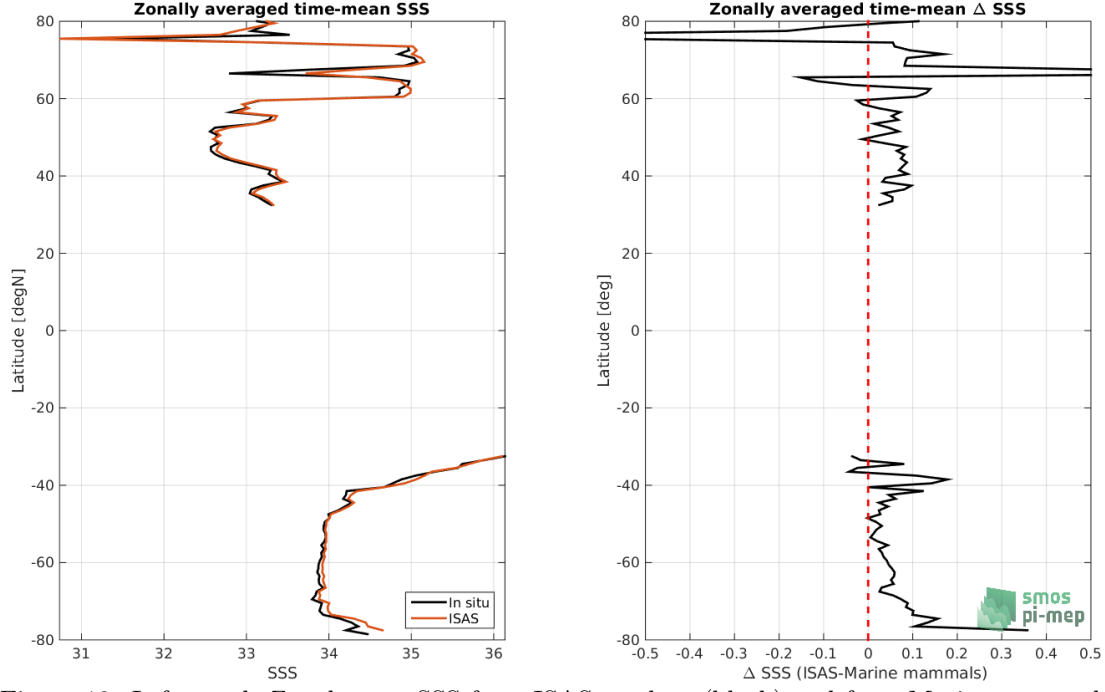


Figure 19: Left panel: Zonal mean SSS from ISAS product (black) and from Marine mammals (blue). Right panel: Zonal mean of Δ SSS (ISAS - Marine mammals) for all the collected Pi-MEP match-up pairs estimated over the full *in situ* dataset period.

3.9 Scatterplots of ISAS vs *in situ* SSS by latitudinal bands

In Figure 20, contour maps of the concentration of ISAS SSS (y-axis) versus Marine mammals SSS (x-axis) at match-up pairs for different latitude bands: (a) 80°S-80°N, (b) 20°S-20°N, (c) 40°S-20°S and 20°N-40°N and (d) 60°S-40°S and 40°N-60°N. For each plot, the red line shows $x=y$. The black thin and dashed lines indicate a linear fit through the data cloud and the $\pm 95\%$ confidence levels, respectively. The number match-up pairs n , the slope and R^2 coefficient of the linear fit, the root mean square (RMS) and the mean bias between ISAS and *in situ* data are indicated for each latitude band in each plots.

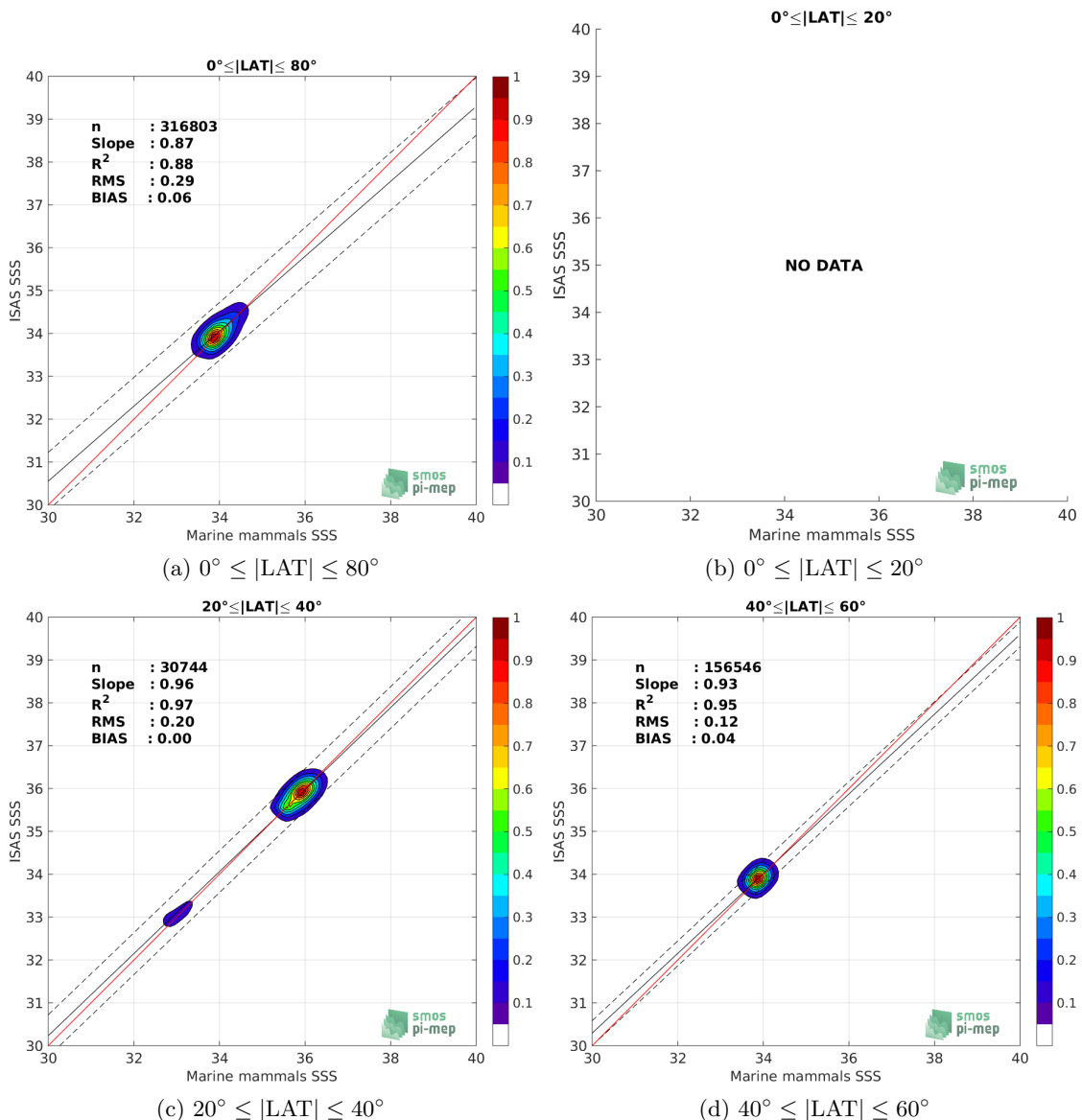


Figure 20: Contour maps of the concentration of ISAS SSS (y-axis) versus Marine mammals SSS (x-axis) at match-up pairs for different latitude bands. For each plot, the red line shows $x=y$. The black thin and dashed lines indicate a linear fit through the data cloud and the $\pm 95\%$ confidence levels, respectively. The number match-up pairs n , the slope and R^2 coefficient of the linear fit, the root mean square (RMS) and the mean bias between ISAS and *in situ* data are indicated for each latitude band in each plots.

3.10 Time series of the monthly median and Std of the difference ΔSSS sorted by latitudinal bands

In Figure 21, time series of the monthly median (red curves) of ΔSSS (ISAS - Marine mammals) and ± 1 Std (black vertical thick bars) as function of time for all the collected Pi-MEP match-up

pairs estimated for the full *in situ* dataset period are shown for different latitude bands: (a) 80°S-80°N, (b) 20°S-20°N, (c) 40°S-20°S and 20°N-40°N and (d) 60°S-40°S and 40°N-60°N.

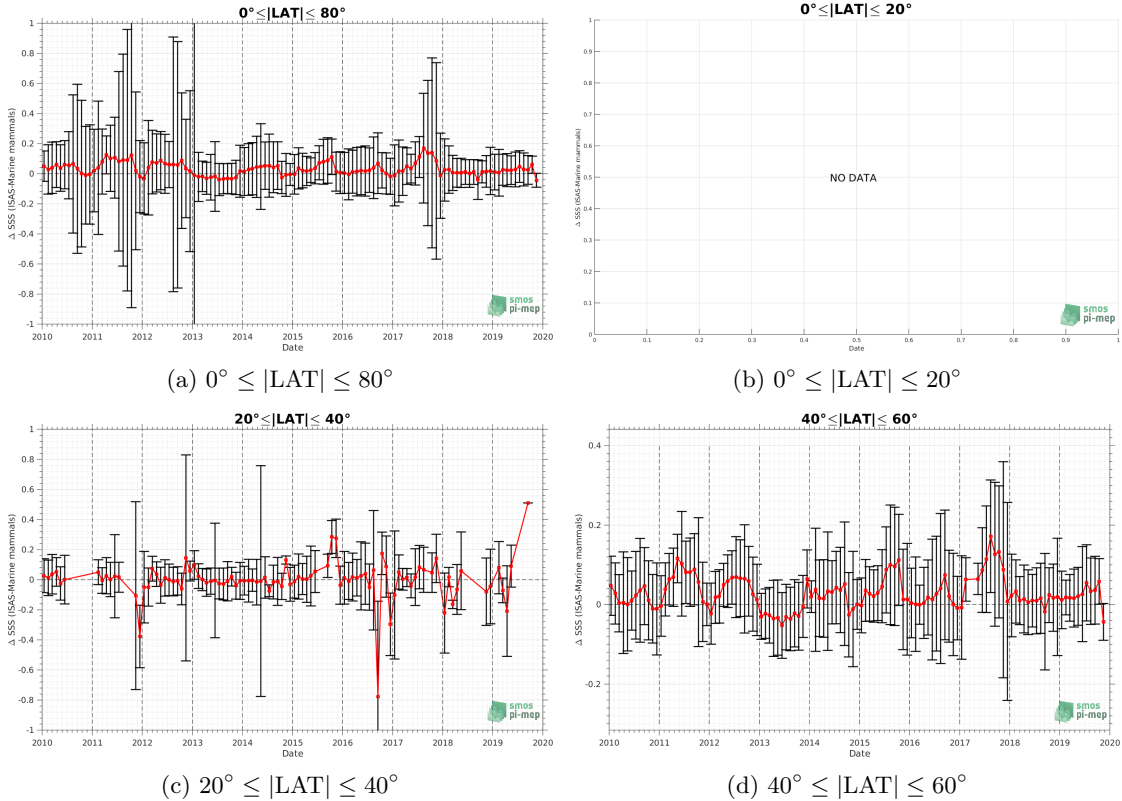


Figure 21: Monthly median (red curves) of ΔSSS (ISAS - Marine mammals) and ± 1 Std (black vertical thick bars) as function of time for all the collected Pi-MEP match-up pairs for the full *in situ* dataset period are shown for different latitude bands: (a) 80°S-80°N, (b) 20°S-20°N, (c) 40°S-20°S and 20°N-40°N and (d) 60°S-40°S and 40°N-60°N.

3.11 ΔSSS sorted as geophysical conditions

In Figure 22, we classify the match-up differences ΔSSS (ISAS - *in situ*) as function of the geophysical conditions at match-up points. The mean and std of ΔSSS (ISAS - Marine mammals) is thus evaluated as function of the

- *in situ* SSS values per bins of width 0.2,
- *in situ* SST values per bins of width 1°C,
- ASCAT daily wind values per bins of width 1 m/s,
- CMORPH 3-hourly rain rates per bins of width 1 mm/h, and,
- distance to coasts per bins of width 50 km,
- *in situ* measurement depth (if relevant).

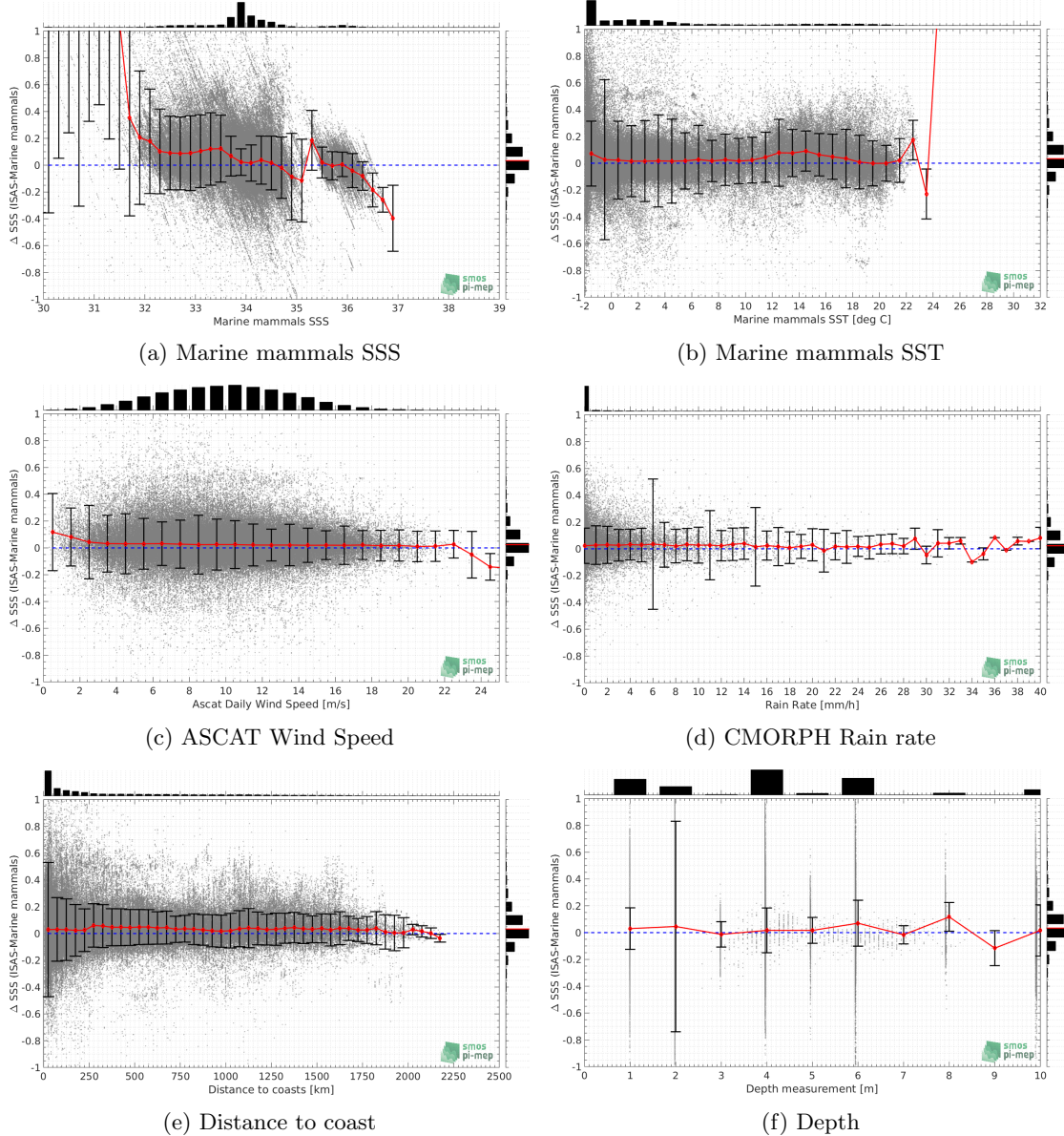


Figure 22: Δ SSS (ISAS - Marine mammals) sorted as geophysical conditions: Marine mammals SSS a), Marine mammals SST b), ASCAT Wind speed c), CMORPH rain rate d), distance to coast (e) and depth measurements (f).

3.12 Δ SSS maps and statistics for different geophysical conditions

In Figures 23 and 24, we focus on sub-datasets of the match-up differences Δ SSS (ISAS - *in situ*) for the following specific geophysical conditions:

- C1: if the local value at *in situ* location of estimated rain rate is zero, mean daily wind is in the range [3, 12] m/s, the SST is $> 5^{\circ}\text{C}$ and distance to coast is > 800 km.

- **C2:** if the local value at *in situ* location of estimated rain rate is zero, mean daily wind is in the range [3, 12] m/s.
- **C3:** if the local value at *in situ* location of estimated rain rate is high (ie. > 1 mm/h) and mean daily wind is low (ie. < 4 m/s).
- **C4:** if the mixed layer is shallow with depth <20m.
- **C5:** if the *in situ* data is located where the climatological SSS standard deviation is low (ie. above < 0.2).
- **C6:** if the *in situ* data is located where the climatological SSS standard deviation is high (ie. above > 0.2).

For each of these conditions, the temporal mean (gridded over spatial boxes of size $1^\circ \times 1^\circ$) and the histogram of the difference ΔSSS (ISAS - *in situ*) are presented.

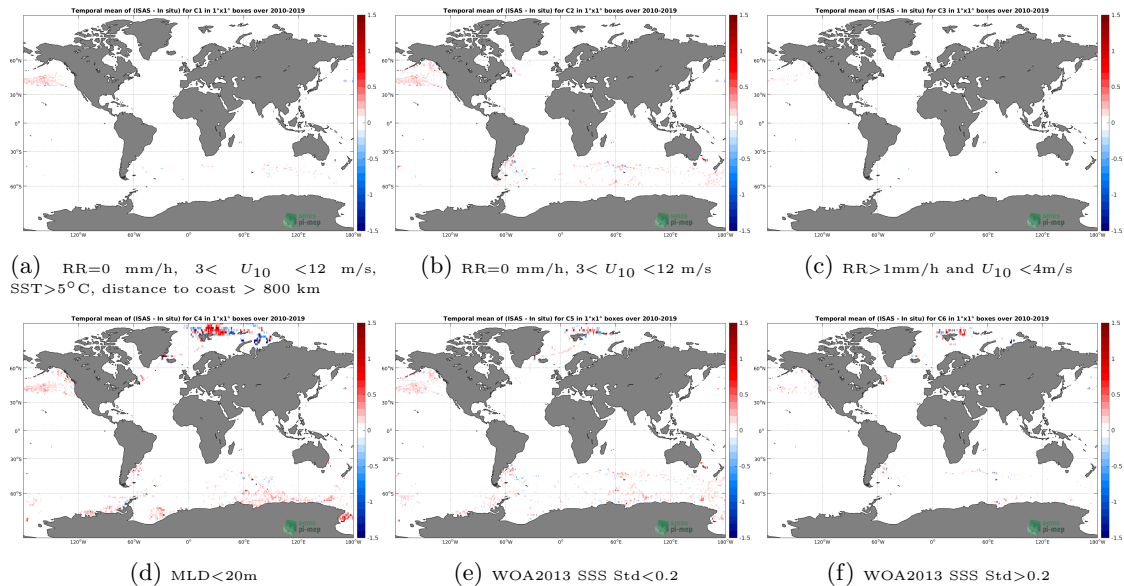


Figure 23: Temporal mean gridded over spatial boxes of size $1^\circ \times 1^\circ$ of ΔSSS (ISAS - Marine mammals) for 6 different subdatasets corresponding to: RR=0 mm/h, $3 < U_{10} < 12$ m/s, SST $>5^\circ\text{C}$, distance to coast > 800 km (a), RR=0 mm/h, $3 < U_{10} < 12$ m/s (b), RR >1 mm/h and $U_{10} < 4$ m/s (c), MLD <20 m (d), WOA2013 SSS Std <0.2 (e), WOA2013 SSS Std >0.2 (f).

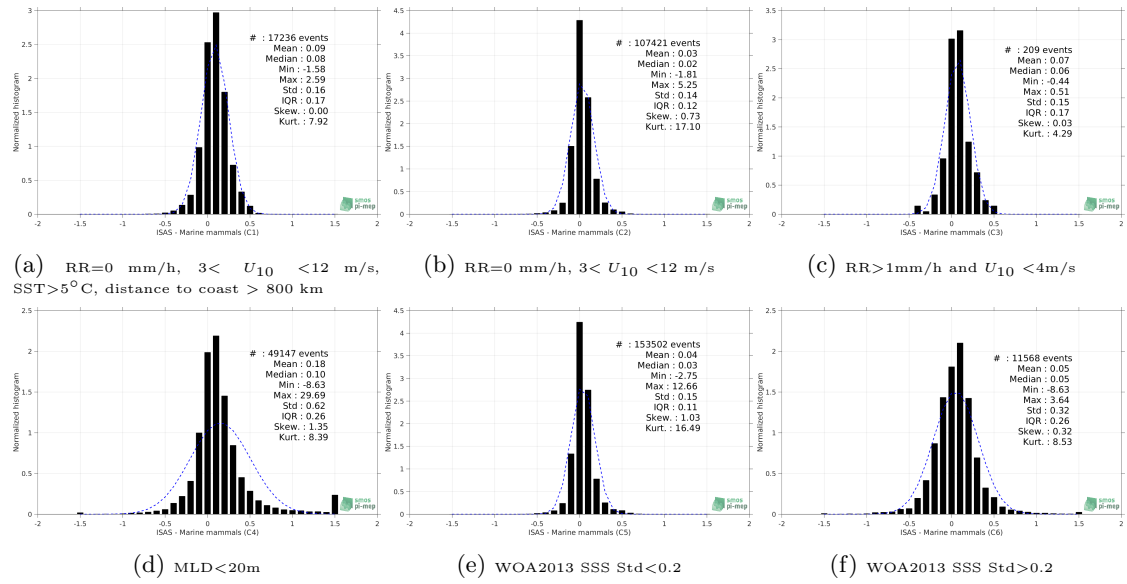


Figure 24: Normalized histogram of ΔSSS (ISAS - Marine mammals) for 6 different subdatasets corresponding to: RR=0 mm/h, $3 < U_{10} < 12$ m/s, SST > 5°C , distance to coast > 800 km (a), RR=0 mm/h, $3 < U_{10} < 12$ m/s (b), RR > 1 mm/h and $U_{10} < 4$ m/s (c), WOA2013 SSS Std < 0.2 (d), WOA2013 SSS Std > 0.2 (e).

3.13 Summary

Table 1 shows the mean, median, standard deviation (Std), root mean square (RMS), interquartile range (IQR), correlation coefficient (r^2) and robust standard deviation (Std*) of the match-up differences ΔSSS (ISAS - Marine mammals) for the following conditions:

- all: All the match-up pairs satellite/in situ SSS are used to derive the statistics
- C1: only pairs where RR=0 mm/h, $3 < U_{10} < 12$ m/s, SST > 5°C , distance to coast > 800 km
- C2: only pairs where RR=0 mm/h, $3 < U_{10} < 12$ m/s
- C3: only pairs where RR > 1 mm/h and $U_{10} < 4$ m/s
- C4: only pairs where MLD < 20 m
- C5: only pairs where WOA2013 SSS Std < 0.2
- C6: only pairs where WOA2013 SSS Std > 0.2
- C7a: only pairs where distance to coast is < 150 km.
- C7b: only pairs where distance to coast is in the range [150, 800] km.
- C7c: only pairs where distance to coast is > 800 km.
- C8a: only pairs where in situ SST is < 5°C .
- C8b: only pairs where in situ SST is in the range [5, 15]°C.

- C8c: only pairs where in situ SST is $> 15^{\circ}\text{C}$.
- C9a: only pairs where in situ SSS is < 33 .
- C9b: only pairs where in situ SSS is in the range [33, 37].
- C9c: only pairs where in situ SSS is > 37 .

Table 1: Statistics of ΔSSS (ISAS - Marine mammals)

Condition	#	Median	Mean	Std	RMS	IQR	r^2	Std*
all	318456	0.03	0.06	0.29	0.29	0.14	0.874	0.10
C1	17236	0.08	0.09	0.16	0.18	0.17	0.932	0.13
C2	107421	0.02	0.03	0.14	0.14	0.12	0.983	0.09
C3	209	0.06	0.07	0.15	0.16	0.17	0.991	0.13
C4	49147	0.10	0.18	0.62	0.64	0.26	0.702	0.19
C5	153502	0.03	0.04	0.15	0.16	0.11	0.958	0.09
C6	11568	0.05	0.05	0.32	0.32	0.26	0.867	0.20
C7a	135832	0.03	0.07	0.41	0.42	0.18	0.826	0.13
C7b	113695	0.04	0.05	0.15	0.16	0.12	0.928	0.09
C7c	68885	0.03	0.05	0.12	0.13	0.11	0.949	0.08
C8a	229750	0.03	0.06	0.32	0.33	0.13	0.575	0.10
C8b	51624	0.04	0.04	0.20	0.20	0.15	0.941	0.11
C8c	37082	0.02	0.04	0.18	0.19	0.16	0.986	0.12
C9a	32192	0.11	0.24	0.75	0.79	0.23	0.170	0.16
C9b	286264	0.03	0.04	0.16	0.16	0.13	0.935	0.10
C9c	0	NaN	NaN	NaN	NaN	NaN	NaN	NaN

Table 1 numerical values can be downloaded as a csv file [here](#).

4 Surface drifters

4.1 Introduction

The skin depth of the L-band radiometer signal over the ocean is about 1 cm whereas classical surface salinity measured by ships or Argo floats are performed at a few meters depth. In order to improve the knowledge of the SSS variability in the first 50 cm depth, to better document the SSS variability in a satellite pixel and to provide ground-truth as close as possible to the sea surface for validating satellite SSS, the L-band remotely sensed community proposed to deploy numerous surface drifters over various parts of the ocean. Surface drifter data are provided by the LOCEAN (see <https://www.locean-ipsl.upmc.fr/smos/drifters/>). Only validated data are considered with uncertainty order of 0.01 and 0.1.

4.2 Number of SSS data as a function of time and distance to coast

Figure 25 shows the time (a) and distance to coast (b) distributions of the Surface drifters *in situ* dataset.

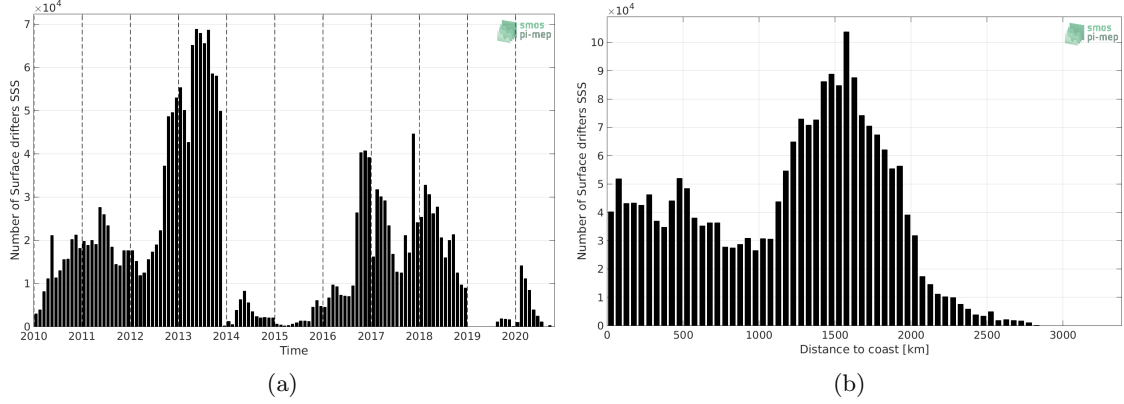


Figure 25: Number of SSS from Surface drifters as a function of time (a) and distance to coast (b).

4.3 Histograms of SSS

Figure 26 shows the SSS distribution of the Surface drifters (a) and colocalized ISAS (b) dataset.

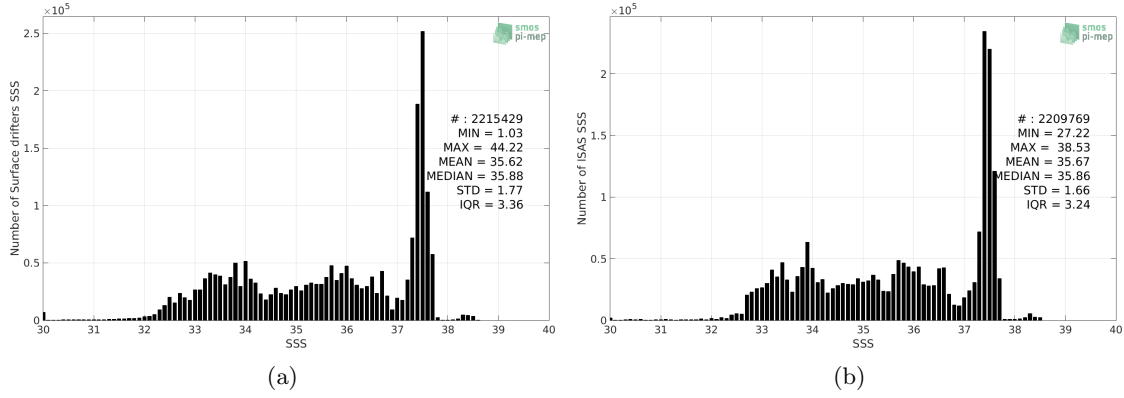


Figure 26: Histograms of SSS from Surface drifters (a) and ISAS (b) per bins of 0.1.

4.4 Distribution of *in situ* SSS depth measurements

In Figure 27, we show the depth distribution of the *in situ* salinity dataset (a) and the spatial distribution of the depth temporal mean in $1^\circ \times 1^\circ$ boxes and considering the full *in situ* dataset period (b).

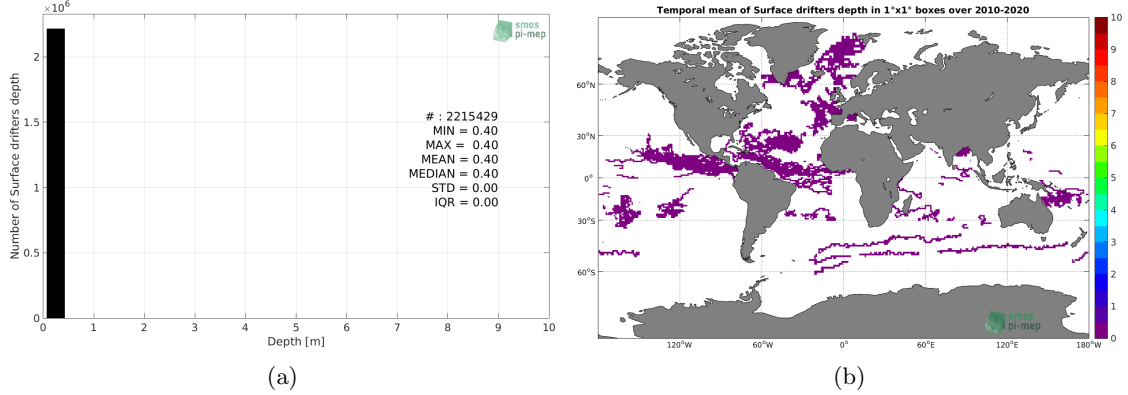


Figure 27: Depth distribution of the upper level SSS measurements from Surface drifters (a) and spatial distribution of the *in situ* SSS depth measurements showing the mean value in $1^\circ \times 1^\circ$ boxes and considering the full *in situ* dataset period (b).

4.5 Spatial distribution of SSS

In Figure 28, the number of Surface drifters SSS measurements in $1^\circ \times 1^\circ$ boxes is shown.

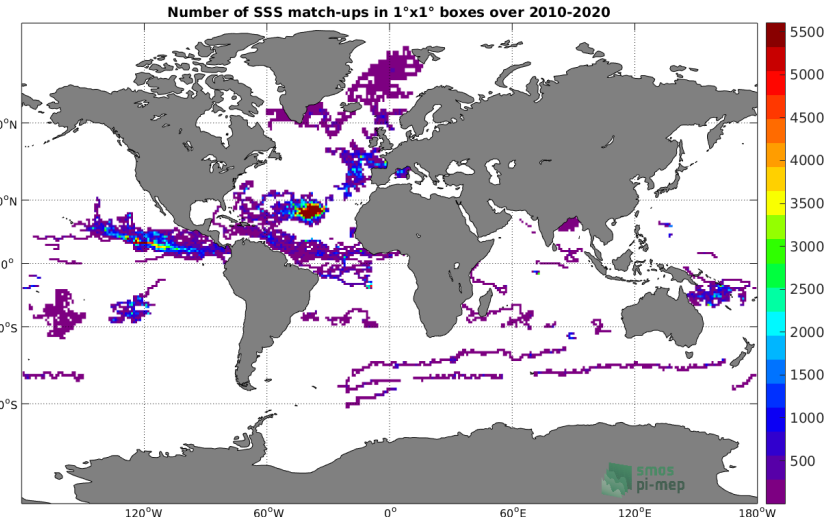


Figure 28: Number of SSS from Surface drifters in $1^\circ \times 1^\circ$ boxes.

4.6 Spatial Maps of the Temporal mean and Std of *in situ* and ISAS SSS and of the difference (Δ SSS)

In Figure 29, maps of temporal mean (left) and standard deviation (right) of ISAS (top), Surface drifters *in situ* dataset (middle) and the difference Δ SSS (ISAS - Surface drifters) (bottom) are shown. The temporal mean and std are calculated using all match-up pairs falling in spatial boxes of size $1^\circ \times 1^\circ$ over the full Surface drifters dataset period.

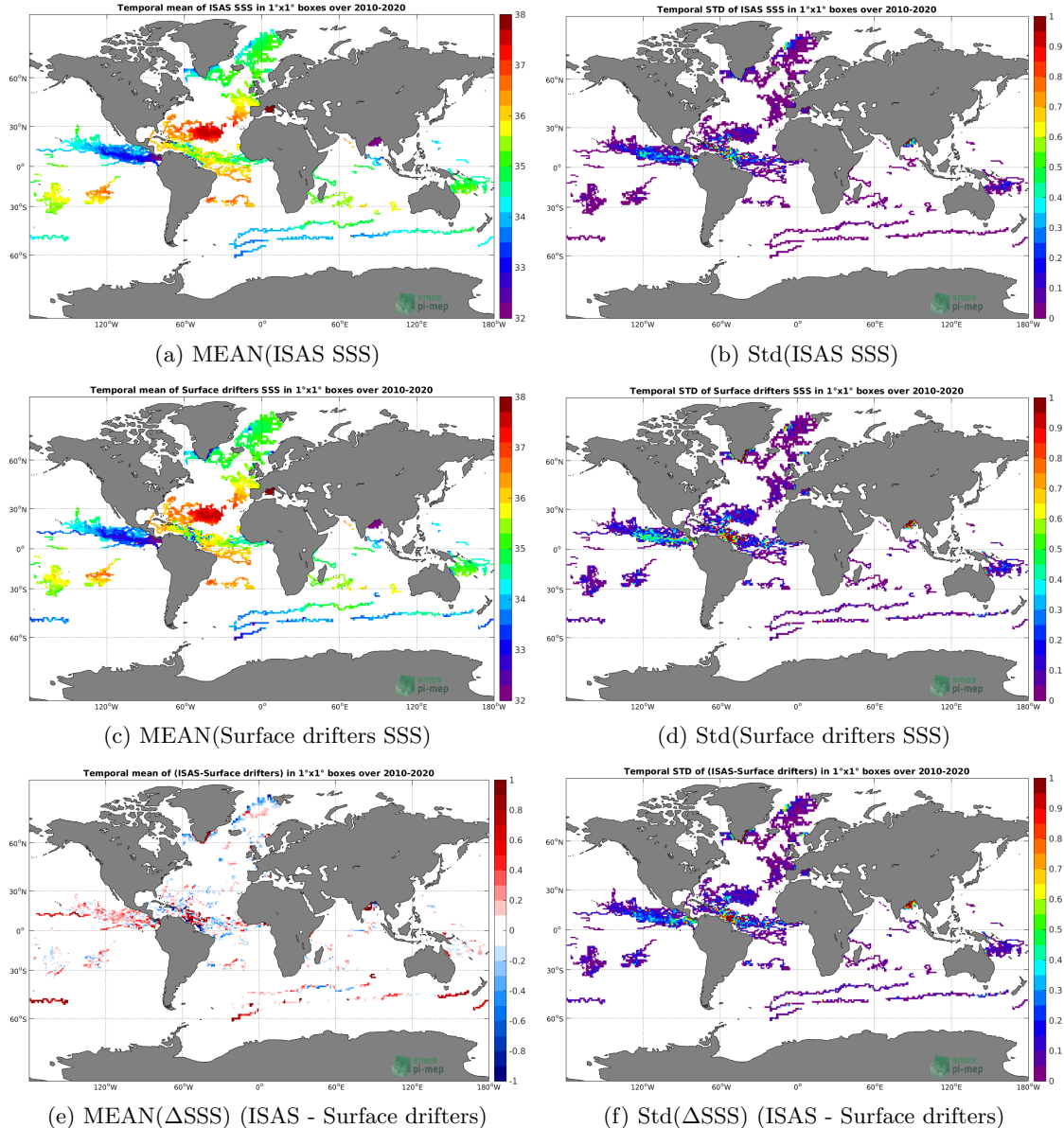


Figure 29: Temporal mean (left) and Std (right) of SSS from ISAS (top), Surface drifters (middle), and of Δ SSS (ISAS - Surface drifters). Only match-up pairs are used to generate these maps.

4.7 Time series of the monthly median and Std of *in situ* and ISAS SSS and of the difference (Δ SSS)

In the top panel of Figure 30, we show the time series of the monthly median SSS estimated for both ISAS SSS product (in black) and the Surface drifters *in situ* dataset (in blue) at the collected Pi-MEP match-up pairs.

In the middle panel of Figure 30, we show the time series of the monthly median of Δ SSS

(ISAS - Surface drifters) for the collected Pi-MEP match-up pairs.

In the bottom panel of Figure 30, we show the time series of the monthly standard deviation of the ΔSSS (ISAS - Surface drifters) for the collected Pi-MEP match-up pairs.

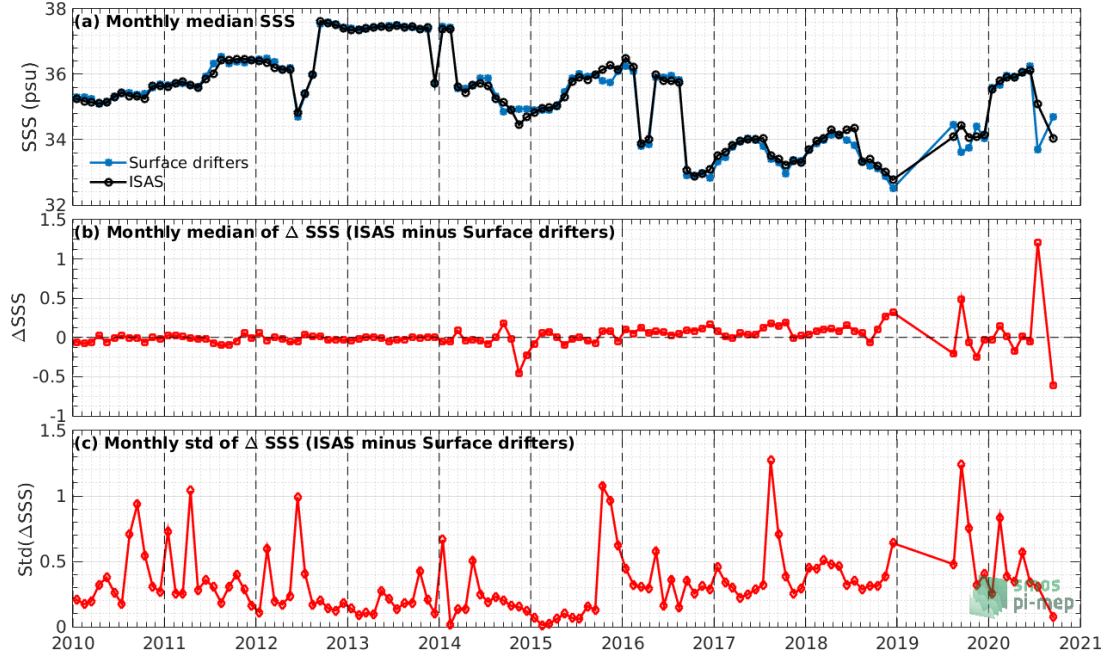


Figure 30: Time series of the monthly median SSS (top), median of ΔSSS (ISAS - Surface drifters) and Std of ΔSSS (ISAS - Surface drifters) considering all match-ups collected by the Pi-MEP.

4.8 Zonal mean and Std of *in situ* and ISAS SSS and of the difference ΔSSS

In Figure 31 left panel, we show the zonal mean SSS considering all Pi-MEP match-up pairs for both ISAS SSS product (in black) and the Surface drifters *in situ* dataset (in blue). The full *in situ* dataset period is used to derive the mean.

In the right panel of Figure 31, we show the zonal mean of ΔSSS (ISAS - Surface drifters) for all the collected Pi-MEP match-up pairs estimated over the full *in situ* dataset period.

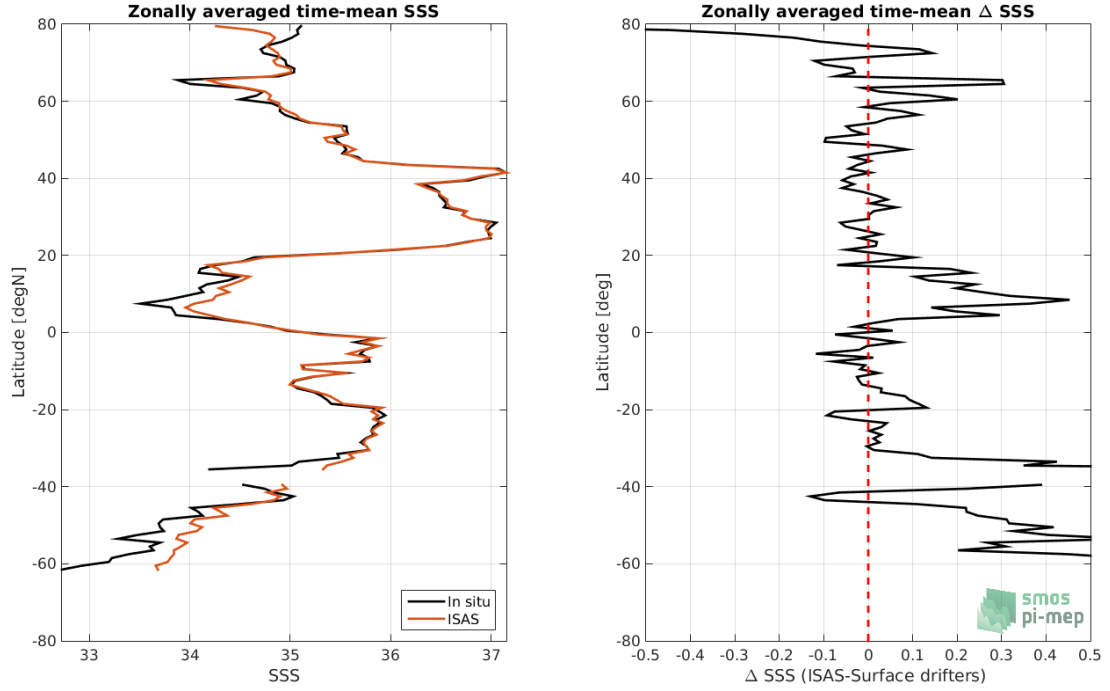


Figure 31: Left panel: Zonal mean SSS from ISAS product (black) and from Surface drifters (blue). Right panel: Zonal mean of Δ SSS (ISAS - Surface drifters) for all the collected Pi-MEP match-up pairs estimated over the full *in situ* dataset period.

4.9 Scatterplots of ISAS vs *in situ* SSS by latitudinal bands

In Figure 32, contour maps of the concentration of ISAS SSS (y-axis) versus Surface drifters SSS (x-axis) at match-up pairs for different latitude bands: (a) 80°S-80°N, (b) 20°S-20°N, (c) 40°S-20°S and 20°N-40°N and (d) 60°S-40°S and 40°N-60°N. For each plot, the red line shows $x=y$. The black thin and dashed lines indicate a linear fit through the data cloud and the ±95% confidence levels, respectively. The number match-up pairs n , the slope and R^2 coefficient of the linear fit, the root mean square (RMS) and the mean bias between ISAS and *in situ* data are indicated for each latitude band in each plots.

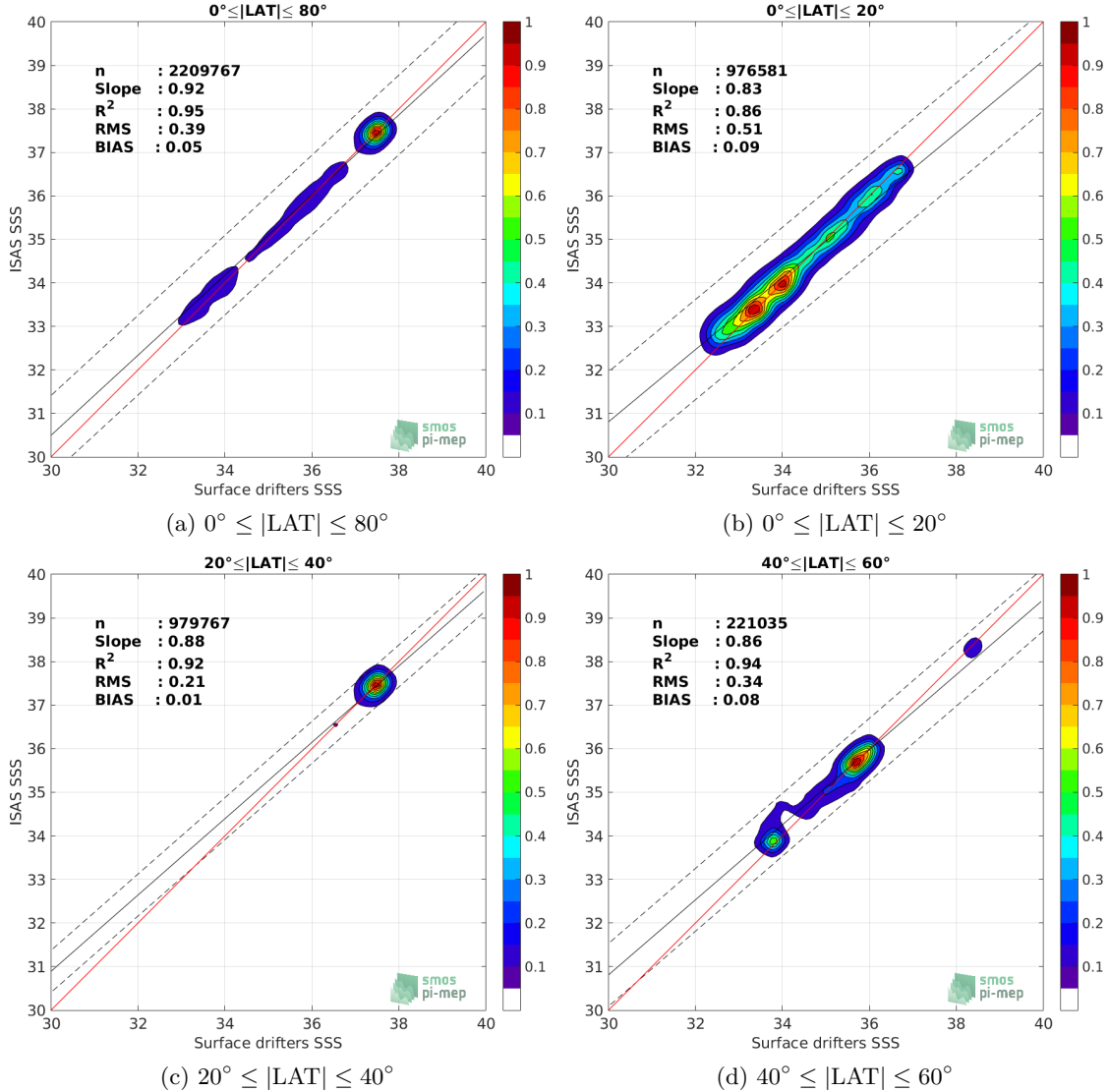


Figure 32: Contour maps of the concentration of ISAS SSS (y-axis) versus Surface drifters SSS (x-axis) at match-up pairs for different latitude bands. For each plot, the red line shows $x=y$. The black thin and dashed lines indicate a linear fit through the data cloud and the $\pm 95\%$ confidence levels, respectively. The number match-up pairs n , the slope and R^2 coefficient of the linear fit, the root mean square (RMS) and the mean bias between ISAS and *in situ* data are indicated for each latitude band in each plots.

4.10 Time series of the monthly median and Std of the difference ΔSSS sorted by latitudinal bands

In Figure 33, time series of the monthly median (red curves) of ΔSSS (ISAS - Surface drifters) and ± 1 Std (black vertical thick bars) as function of time for all the collected Pi-MEP match-up pairs estimated for the full *in situ* dataset period are shown for different latitude bands: (a) $80^\circ\text{S}-80^\circ\text{N}$, (b) $20^\circ\text{S}-20^\circ\text{N}$, (c) $40^\circ\text{S}-20^\circ\text{S}$ and $20^\circ\text{N}-40^\circ\text{N}$ and (d) $60^\circ\text{S}-40^\circ\text{S}$ and $40^\circ\text{N}-60^\circ\text{N}$.

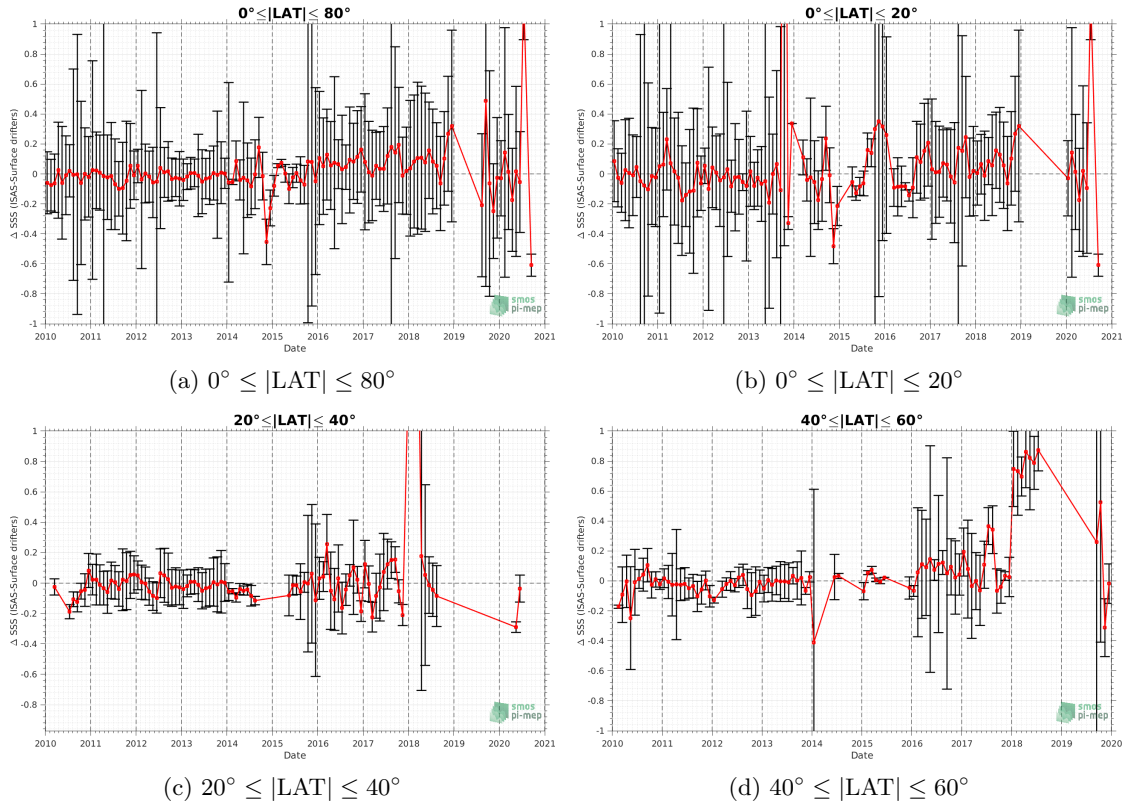


Figure 33: Monthly median (red curves) of ΔSSS (ISAS - Surface drifters) and ± 1 Std (black vertical thick bars) as function of time for all the collected Pi-MEP match-up pairs for the full *in situ* dataset period are shown for different latitude bands: (a) $80^\circ\text{S}-80^\circ\text{N}$, (b) $20^\circ\text{S}-20^\circ\text{N}$, (c) $40^\circ\text{S}-20^\circ\text{S}$ and $20^\circ\text{N}-40^\circ\text{N}$ and (d) $60^\circ\text{S}-40^\circ\text{S}$ and $40^\circ\text{N}-60^\circ\text{N}$.

4.11 ΔSSS sorted as geophysical conditions

In Figure 34, we classify the match-up differences ΔSSS (ISAS - *in situ*) as function of the geophysical conditions at match-up points. The mean and std of ΔSSS (ISAS - Surface drifters) is thus evaluated as function of the

- *in situ* SSS values per bins of width 0.2,
- *in situ* SST values per bins of width 1°C ,
- ASCAT daily wind values per bins of width 1 m/s,
- CMORPH 3-hourly rain rates per bins of width 1 mm/h, and,
- distance to coasts per bins of width 50 km,
- *in situ* measurement depth (if relevant).

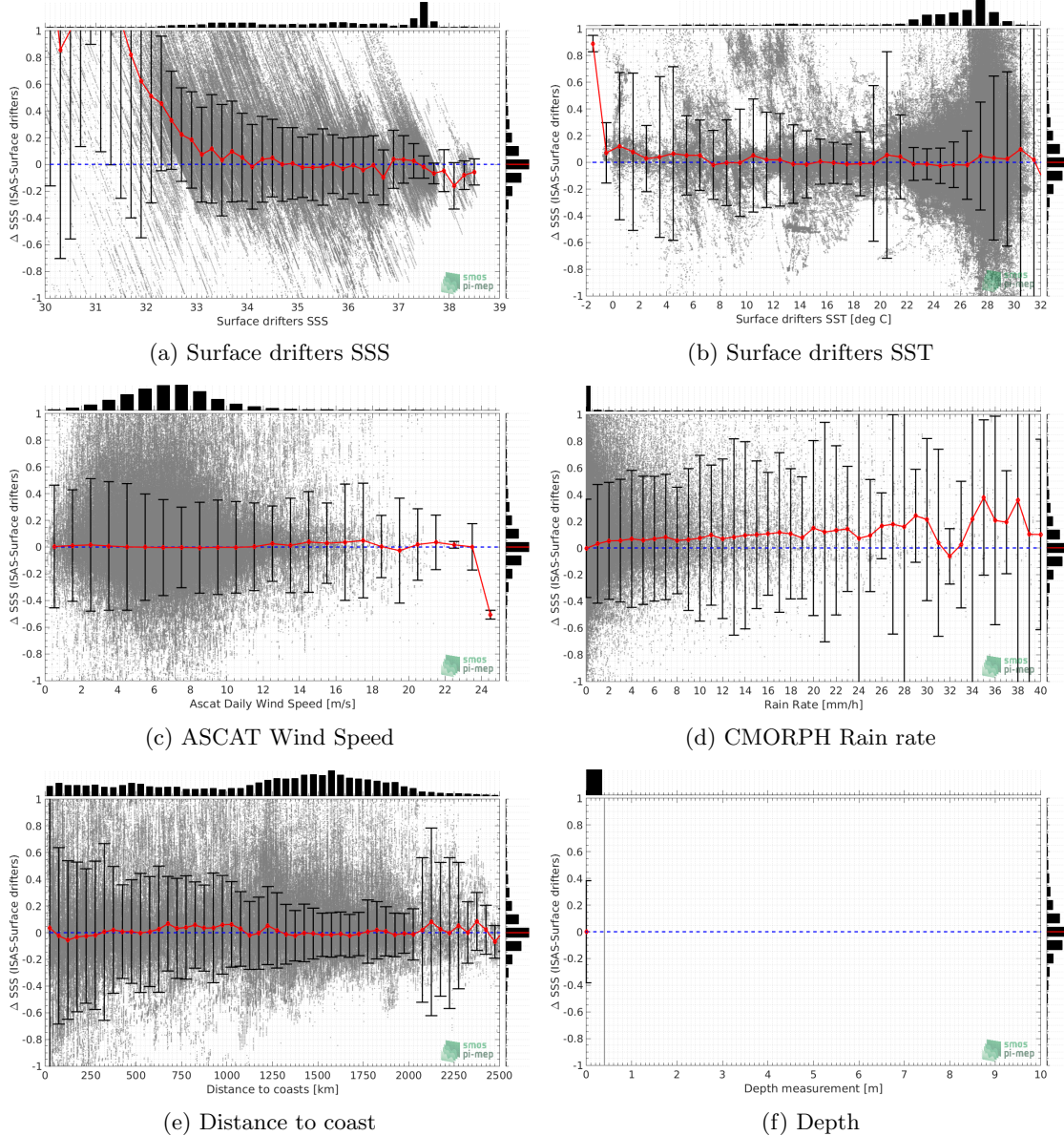


Figure 34: ΔSSS (ISAS - Surface drifters) sorted as geophysical conditions: Surface drifters SSS a), Surface drifters SST b), ASCAT Wind speed c), CMORPH rain rate d), distance to coast (e) and depth measurements (f).

4.12 ΔSSS maps and statistics for different geophysical conditions

In Figures 35 and 36, we focus on sub-datasets of the match-up differences ΔSSS (*ISAS - in situ*) for the following specific geophysical conditions:

- C1: if the local value at *in situ* location of estimated rain rate is zero, mean daily wind is in the range [3, 12] m/s, the SST is $> 5^\circ\text{C}$ and distance to coast is > 800 km.

- **C2:** if the local value at *in situ* location of estimated rain rate is zero, mean daily wind is in the range [3, 12] m/s.
- **C3:** if the local value at *in situ* location of estimated rain rate is high (ie. > 1 mm/h) and mean daily wind is low (ie. < 4 m/s).
- **C5:** if the *in situ* data is located where the climatological SSS standard deviation is low (ie. above < 0.2).
- **C6:** if the *in situ* data is located where the climatological SSS standard deviation is high (ie. above > 0.2).

For each of these conditions, the temporal mean (gridded over spatial boxes of size $1^\circ \times 1^\circ$) and the histogram of the difference ΔSSS (ISAS - *in situ*) are presented.

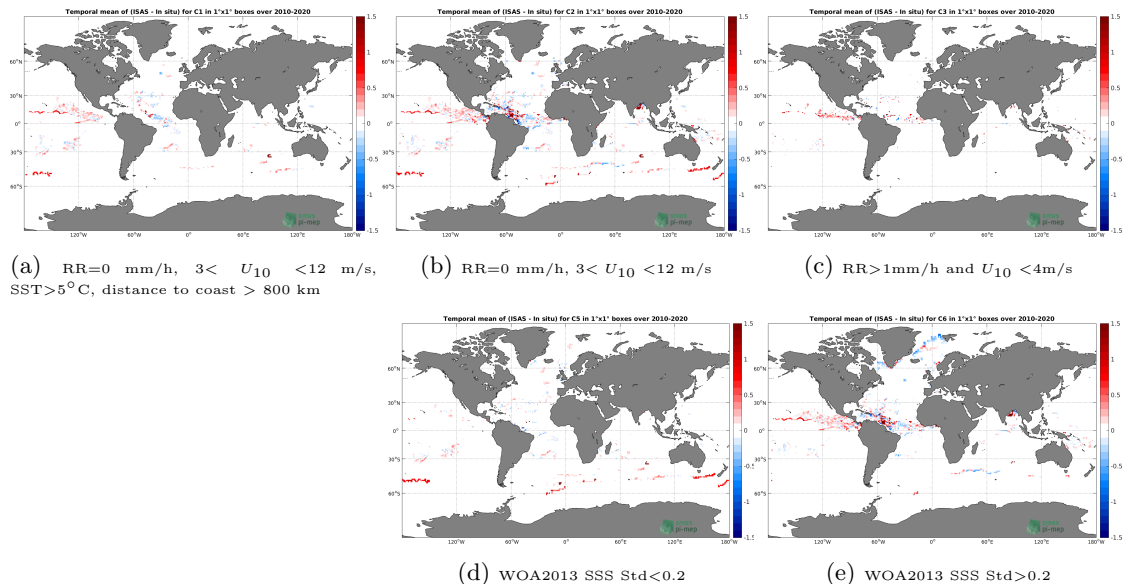


Figure 35: Temporal mean gridded over spatial boxes of size $1^\circ \times 1^\circ$ of ΔSSS (ISAS - Surface drifters) for 5 different subdatasets corresponding to: RR=0 mm/h, $3 < U_{10} < 12$ m/s, SST $>5^\circ\text{C}$, distance to coast > 800 km (a), RR=0 mm/h, $3 < U_{10} < 12$ m/s (b), RR $>1\text{mm/h}$ and $U_{10} < 4\text{m/s}$ (c), WOA2013 SSS Std <0.2 (d), WOA2013 SSS Std >0.2 (e).

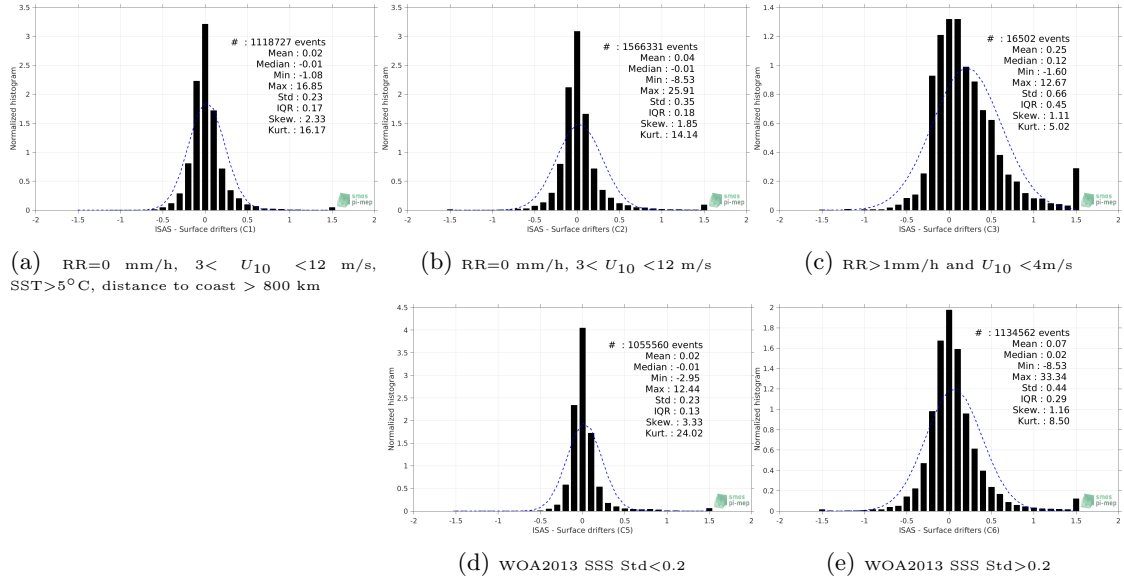


Figure 36: Normalized histogram of ΔSSS (ISAS - Surface drifters) for 5 different subdatasets corresponding to: RR=0 mm/h, $3 < U_{10} < 12$ m/s, SST > 5°C, distance to coast > 800 km (a), RR=0 mm/h, $3 < U_{10} < 12$ m/s (b), RR>1mm/h and $U_{10} < 4$ m/s (c), WOA2013 SSS Std<0.2 (d), WOA2013 SSS Std>0.2 (e).

4.13 Summary

Table 1 shows the mean, median, standard deviation (Std), root mean square (RMS), interquartile range (IQR), correlation coefficient (r^2) and robust standard deviation (Std*) of the match-up differences ΔSSS (ISAS - Surface drifters) for the following conditions:

- all: All the match-up pairs satellite/in situ SSS values are used to derive the statistics
- C1: only pairs where RR=0 mm/h, $3 < U_{10} < 12$ m/s, SST > 5°C, distance to coast > 800 km
- C2: only pairs where RR=0 mm/h, $3 < U_{10} < 12$ m/s
- C3: only pairs where RR>1mm/h and $U_{10} < 4$ m/s
- C5: only pairs where WOA2013 SSS Std<0.2
- C6: only pairs where WOA2013 SSS Std>0.2
- C7a: only pairs with a distance to coast < 150 km.
- C7b: only pairs with a distance to coast in the range [150, 800] km.
- C7c: only pairs with a distance to coast > 800 km.
- C8a: only pairs where SST is < 5°C.
- C8b: only pairs where SST is in the range [5, 15]°C.
- C8c: only pairs where SST is > 15°C.

- C9a: only pairs where SSS is < 33 .
- C9b: only pairs where SSS is in the range [33, 37].
- C9c: only pairs where SSS is > 37 .

Table 1: Statistics of ΔSSS (ISAS - Surface drifters)

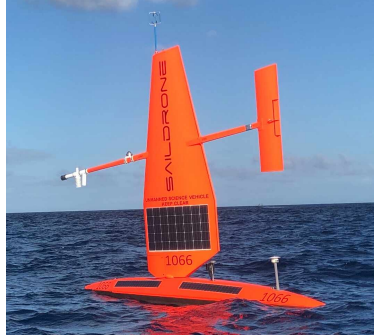
Condition	#	Median	Mean	Std	RMS	IQR	r^2	Std*
all	2209769	0.00	0.05	0.38	0.39	0.19	0.954	0.14
C1	1118727	-0.01	0.02	0.23	0.23	0.17	0.982	0.13
C2	1566331	-0.01	0.04	0.35	0.35	0.18	0.957	0.13
C3	16502	0.12	0.25	0.66	0.71	0.45	0.844	0.32
C5	1055560	-0.01	0.02	0.23	0.23	0.13	0.965	0.10
C6	1134562	0.02	0.07	0.44	0.45	0.29	0.928	0.21
C7a	131297	-0.02	0.13	0.91	0.91	0.30	0.798	0.21
C7b	519947	0.01	0.08	0.47	0.47	0.21	0.871	0.16
C7c	1558469	0.00	0.04	0.25	0.26	0.19	0.981	0.14
C8a	33057	0.07	0.23	0.55	0.60	0.13	0.467	0.09
C8b	144866	0.01	0.08	0.33	0.34	0.16	0.923	0.12
C8c	2026237	0.00	0.05	0.38	0.38	0.20	0.955	0.14
C9a	165932	0.29	0.50	0.97	1.10	0.44	0.153	0.32
C9b	1283786	0.01	0.03	0.31	0.31	0.24	0.929	0.18
C9c	760051	-0.02	-0.02	0.11	0.11	0.11	0.707	0.08

Table 1 numerical values can be downloaded as a csv file [here](#).

5 Saildrones

5.1 Introduction

Saildrone is a state-of-the-art, remotely guided, wind and solar powered unmanned surface vehicle (USV) capable of long distance deployments lasting up to 12 months. It is equipped with a suite of instruments and sensors providing high quality, georeferenced, near real-time, multi-parameter surface ocean and atmospheric observations while transiting at typical speeds of 3-5 knots. All freely available data are included coming from different providers ([Saildrone](#), [NOAA/PMEL](#), ...) and easily accessible via NOAA [ERDAP](#). When 2 different sensors are available, usually from different brands (SeaBird or RBR), the RBR sensor is kept with the exception for the Atlantic to Mediterranean 2019-2020 campaign for which the salinity data from RBR are clearly corrupted. One-minute samples of the original data were resampled every 10 minutes using linear interpolation to reduce the number of point.



5.2 Number of SSS data as a function of time and distance to coast

Figure 37 shows the time (a) and distance to coast (b) distributions of the Saildrones *in situ* dataset.

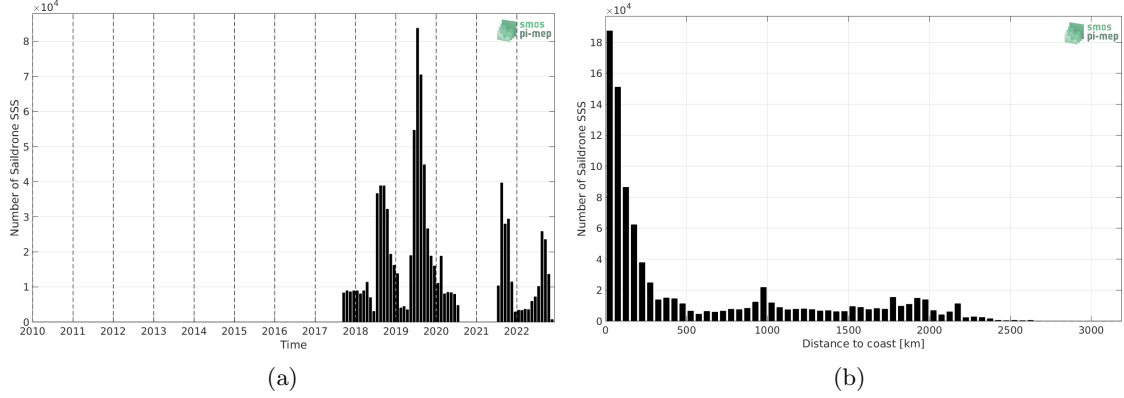


Figure 37: Number of SSS from Saildrones as a function of time (a) and distance to coast (b).

5.3 Histograms of SSS

Figure 38 shows the SSS distribution of the Saildrones (a) and colocalized ISAS (b) dataset.

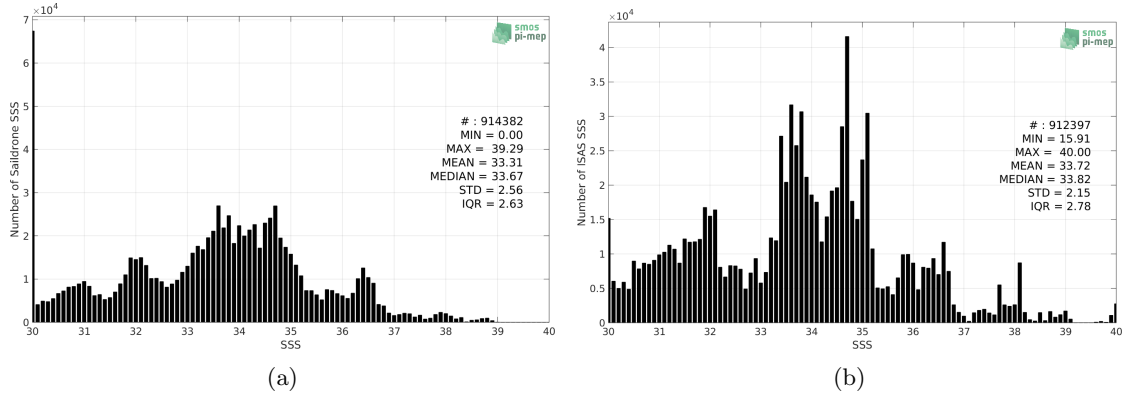


Figure 38: Histograms of SSS from Saildrones (a) and ISAS (b) per bins of 0.1.

5.4 Distribution of *in situ* SSS depth measurements

In Figure 39, we show the depth distribution of the *in situ* salinity dataset (a) and the spatial distribution of the depth temporal mean in $1^\circ \times 1^\circ$ boxes and considering the full *in situ* dataset period (b).

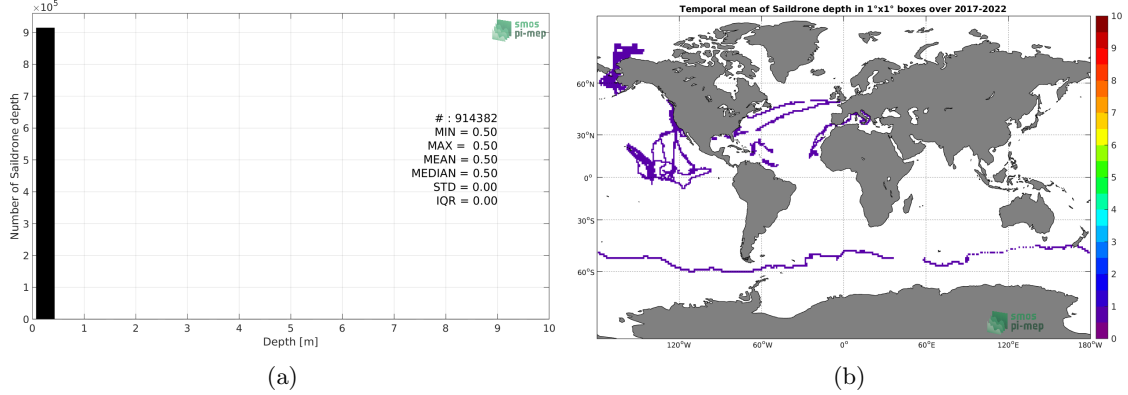


Figure 39: Depth distribution of the upper level SSS measurements from Saildrones (a) and spatial distribution of the *in situ* SSS depth measurements showing the mean value in $1^\circ \times 1^\circ$ boxes and considering the full *in situ* dataset period (b).

5.5 Spatial distribution of SSS

In Figure 40, the number of Saildrones SSS measurements in $1^\circ \times 1^\circ$ boxes is shown.

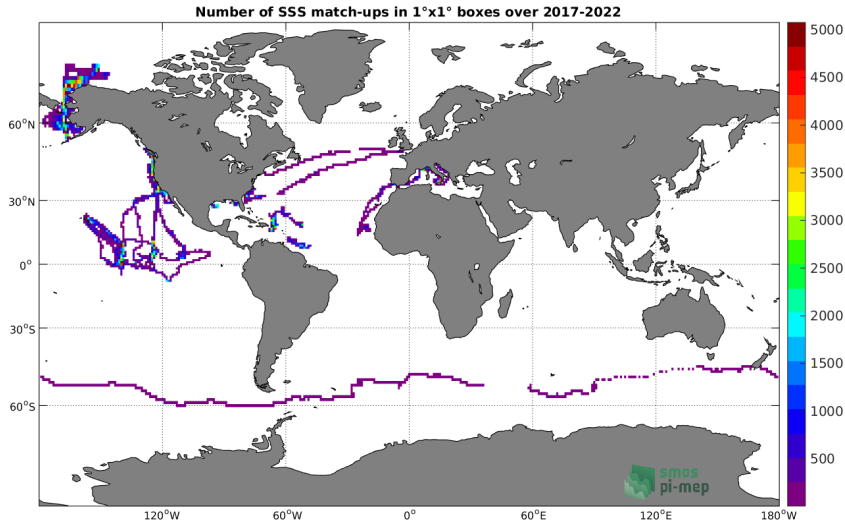


Figure 40: Number of SSS from Saildrones in $1^\circ \times 1^\circ$ boxes.

5.6 Spatial Maps of the Temporal mean and Std of *in situ* and ISAS SSS and of the difference (Δ SSS)

In Figure 41, maps of temporal mean (left) and standard deviation (right) of ISAS (top), Saildrones *in situ* dataset (middle) and the difference Δ SSS(ISAS -Saildrones) (bottom) are shown. The temporal mean and std are calculated using all match-up pairs falling in spatial boxes of size $1^\circ \times 1^\circ$ over the full Saildrones dataset period.

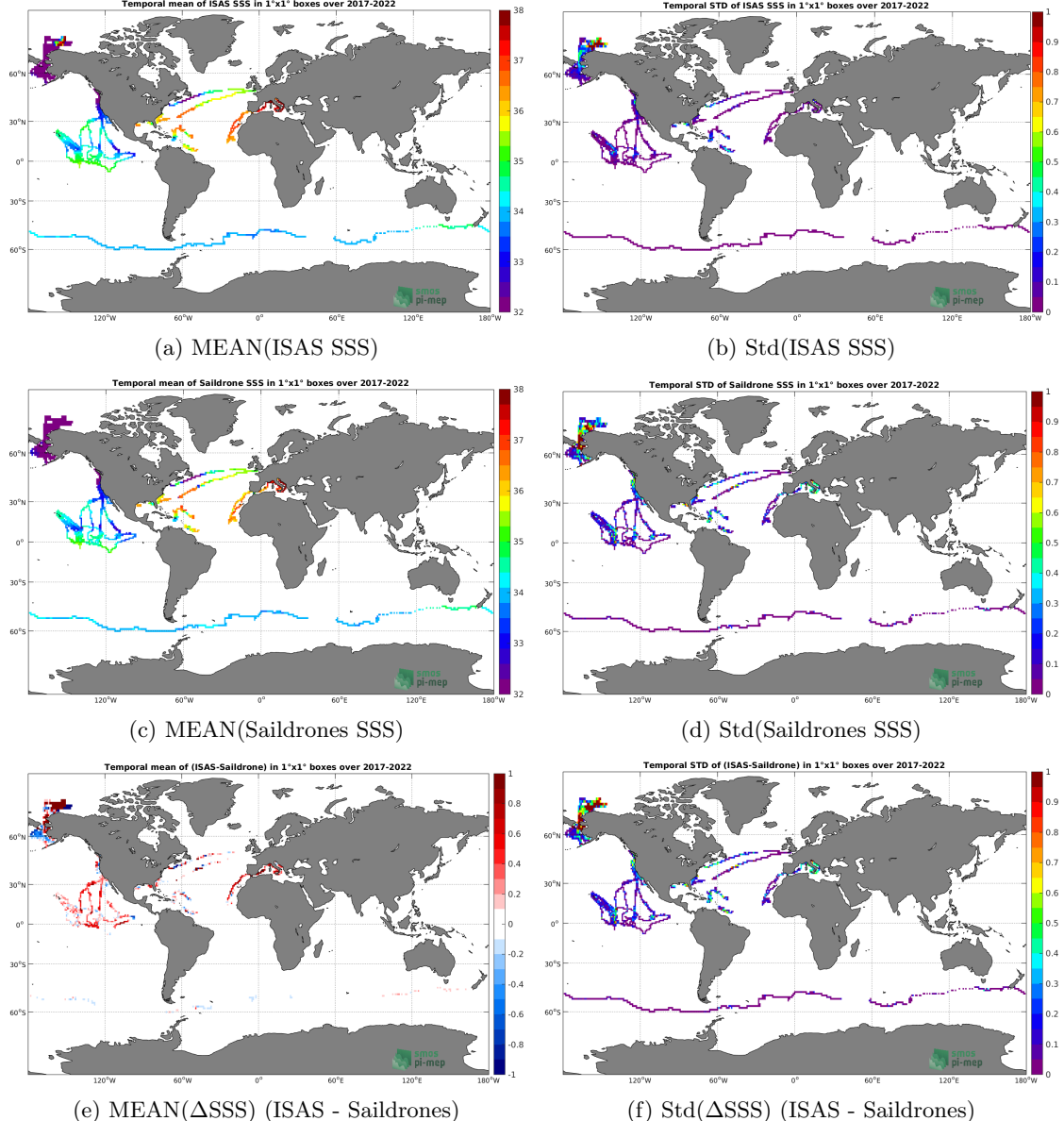


Figure 41: Temporal mean (left) and Std (right) of SSS from ISAS (top), Saildrones (middle), and of Δ SSS (ISAS - Saildrones). Only match-up pairs are used to generate these maps.

5.7 Time series of the monthly median and Std of *in situ* and ISAS SSS and of the difference (Δ SSS)

In the top panel of Figure 42, we show the time series of the monthly median SSS estimated for both ISAS SSS product (in black) and the Saildrones *in situ* dataset (in blue) at the collected Pi-MEP match-up pairs.

In the middle panel of Figure 42, we show the time series of the monthly median of Δ SSS (ISAS - Saildrones) for the collected Pi-MEP match-up pairs.

In the bottom panel of Figure 42, we show the time series of the monthly standard deviation of the Δ SSS (ISAS - Saildrones) for the collected Pi-MEP match-up pairs.

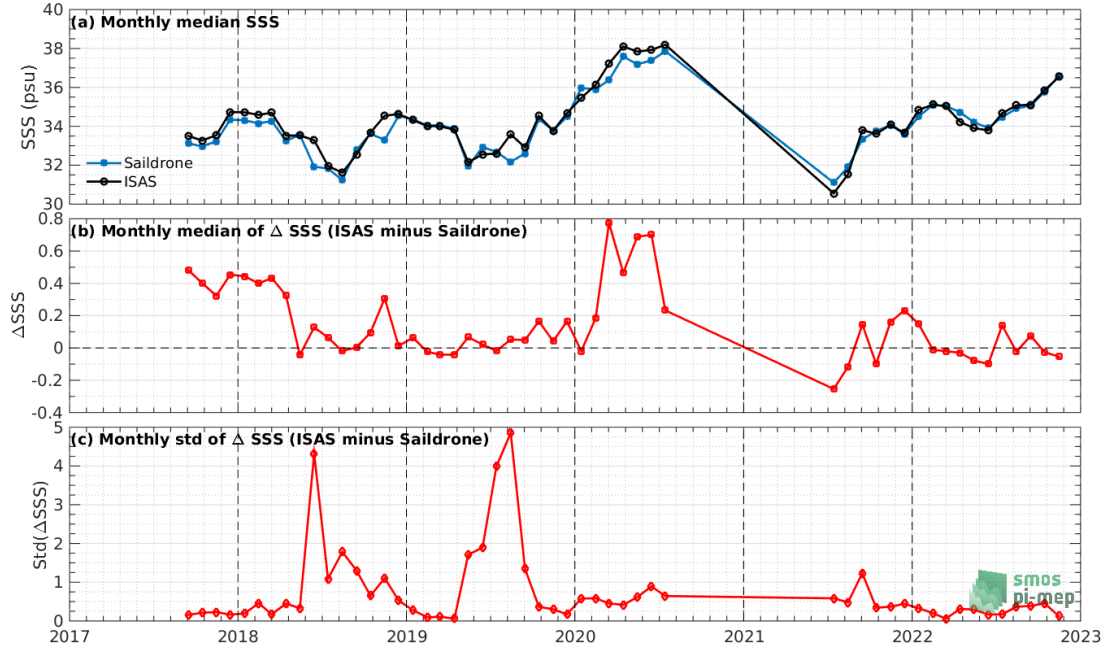


Figure 42: Time series of the monthly median SSS (top), median of Δ SSS (ISAS - Saildrones) and Std of Δ SSS (ISAS - Saildrones) considering all match-ups collected by the Pi-MEP.

5.8 Zonal mean and Std of *in situ* and ISAS SSS and of the difference Δ SSS

In Figure 43 left panel, we show the zonal mean SSS considering all Pi-MEP match-up pairs for both ISAS SSS product (in black) and the Saildrones *in situ* dataset (in blue). The full *in situ* dataset period is used to derive the mean.

In the right panel of Figure 43, we show the zonal mean of Δ SSS (ISAS - Saildrones) for all the collected Pi-MEP match-up pairs estimated over the full *in situ* dataset period.

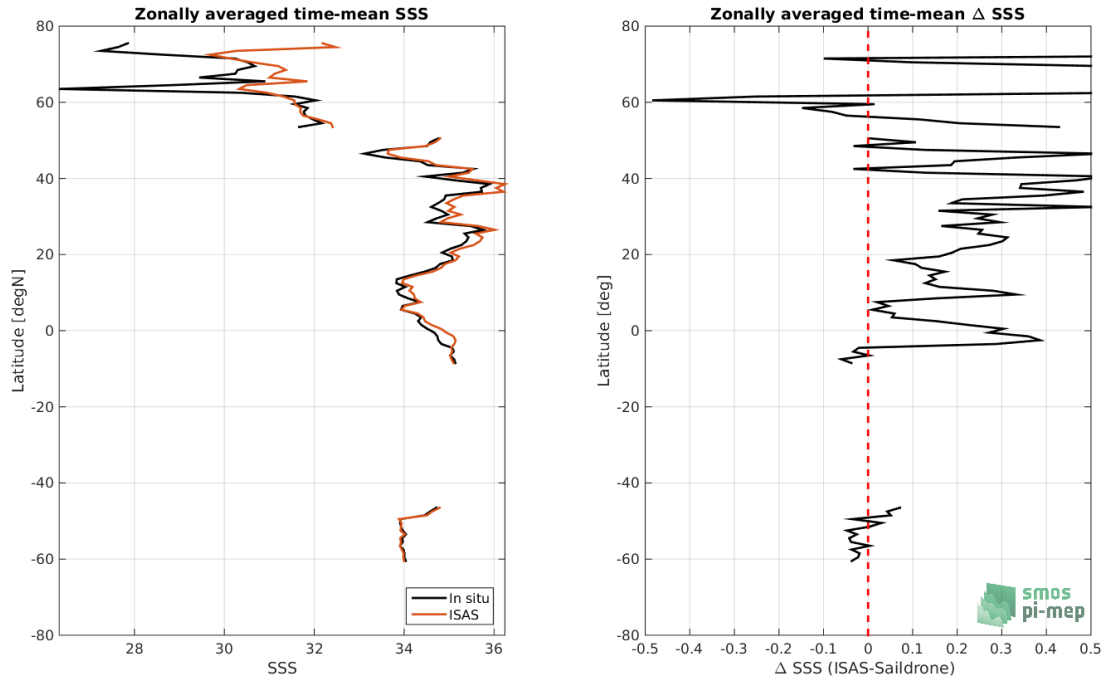


Figure 43: Left panel: Zonal mean SSS from ISAS product (black) and from Saildrones (blue). Right panel: Zonal mean of Δ SSS (ISAS - Saildrones) for all the collected Pi-MEP match-up pairs estimated over the full *in situ* dataset period.

5.9 Scatterplots of ISAS vs *in situ* SSS by latitudinal bands

In Figure 44, contour maps of the concentration of ISAS SSS (y-axis) versus Saildrones SSS (x-axis) at match-up pairs for different latitude bands: (a) 80°S-80°N, (b) 20°S-20°N, (c) 40°S-20°S and 20°N-40°N and (d) 60°S-40°S and 40°N-60°N. For each plot, the red line shows $x=y$. The black thin and dashed lines indicate a linear fit through the data cloud and the $\pm 95\%$ confidence levels, respectively. The number match-up pairs n , the slope and R^2 coefficient of the linear fit, the root mean square (RMS) and the mean bias between ISAS and *in situ* data are indicated for each latitude band in each plots.

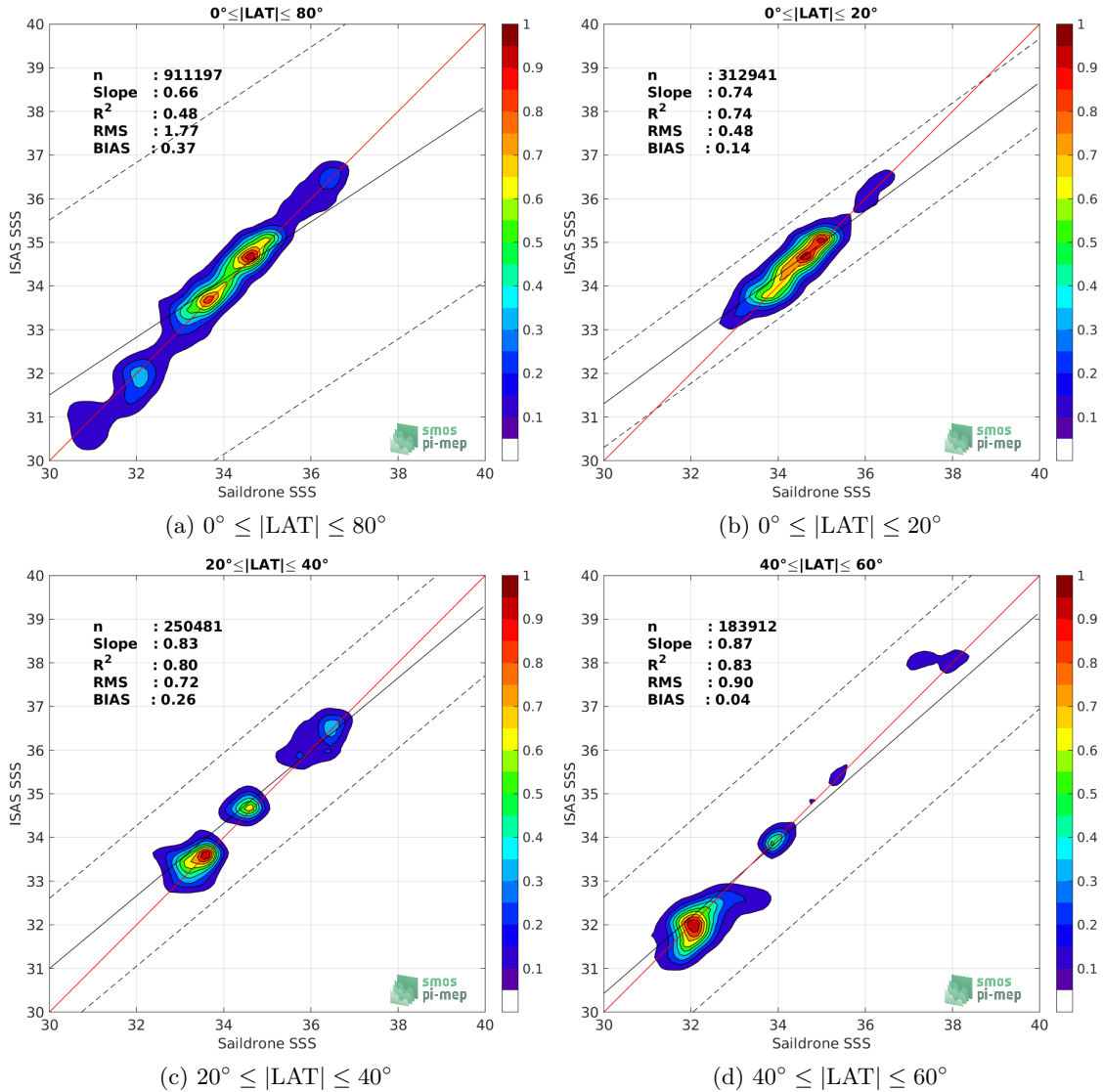


Figure 44: Contour maps of the concentration of ISAS SSS (y-axis) versus Saildrones SSS (x-axis) at match-up pairs for different latitude bands. For each plot, the red line shows $x=y$. The black thin and dashed lines indicate a linear fit through the data cloud and the $\pm 95\%$ confidence levels, respectively. The number match-up pairs n , the slope and R^2 coefficient of the linear fit, the root mean square (RMS) and the mean bias between ISAS and *in situ* data are indicated for each latitude band in each plots.

5.10 Time series of the monthly median and Std of the difference ΔSSS sorted by latitudinal bands

In Figure 45, time series of the monthly median (red curves) of ΔSSS (ISAS - Saildrones) and ± 1 Std (black vertical thick bars) as function of time for all the collected Pi-MEP match-up pairs estimated for the full *in situ* dataset period are shown for different latitude bands: (a) $80^\circ\text{S}-80^\circ\text{N}$, (b) $20^\circ\text{S}-20^\circ\text{N}$, (c) $40^\circ\text{S}-20^\circ\text{S}$ and $20^\circ\text{N}-40^\circ\text{N}$ and (d) $60^\circ\text{S}-40^\circ\text{S}$ and $40^\circ\text{N}-60^\circ\text{N}$.

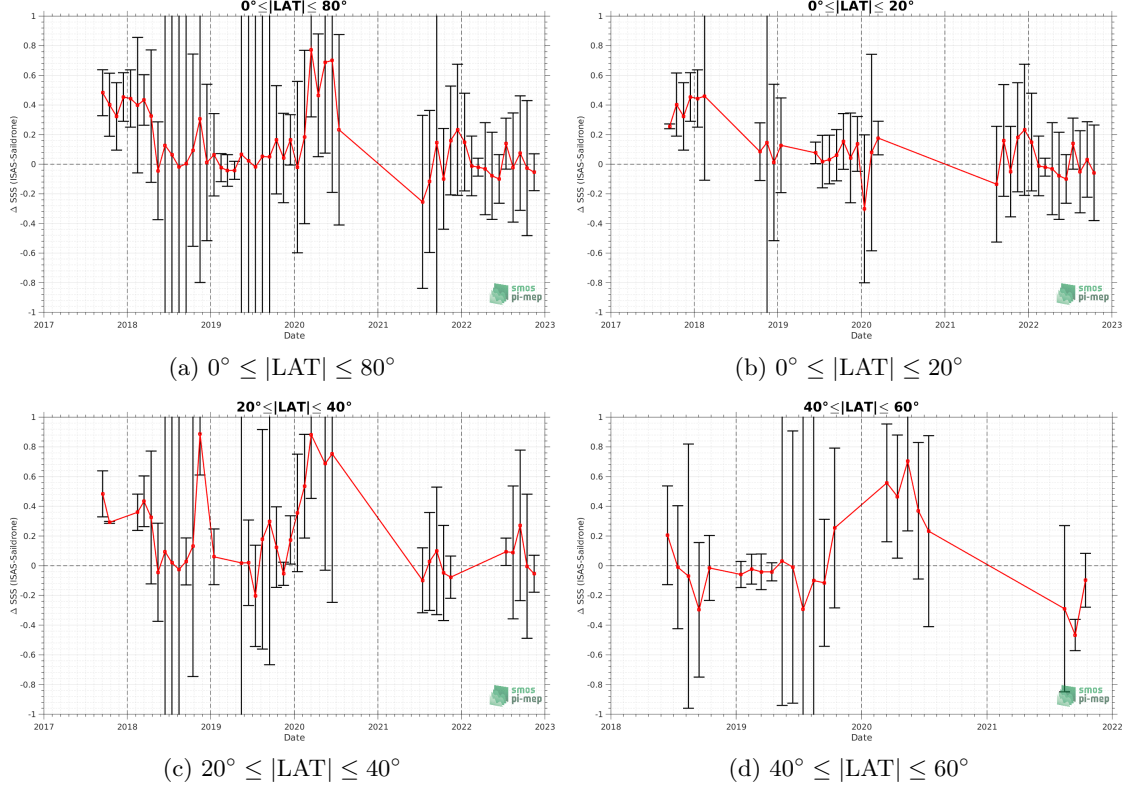


Figure 45: Monthly median (red curves) of ΔSSS (ISAS - Saildrones) and ± 1 Std (black vertical thick bars) as function of time for all the collected Pi-MEP match-up pairs for the full *in situ* dataset period are shown for different latitude bands: (a) $80^\circ\text{S}-80^\circ\text{N}$, (b) $20^\circ\text{S}-20^\circ\text{N}$, (c) $40^\circ\text{S}-20^\circ\text{S}$ and $20^\circ\text{N}-40^\circ\text{N}$ and (d) $60^\circ\text{S}-40^\circ\text{S}$ and $40^\circ\text{N}-60^\circ\text{N}$.

5.11 ΔSSS sorted as geophysical conditions

In Figure 46, we classify the match-up differences ΔSSS (ISAS - *in situ*) as function of the geophysical conditions at match-up points. The mean and std of ΔSSS (ISAS - Saildrones) is thus evaluated as function of the

- *in situ* SSS values per bins of width 0.2,
- *in situ* SST values per bins of width 1°C ,
- ASCAT daily wind values per bins of width 1 m/s,
- CMORPH 3-hourly rain rates per bins of width 1 mm/h, and,
- distance to coasts per bins of width 50 km,
- *in situ* measurement depth (if relevant).

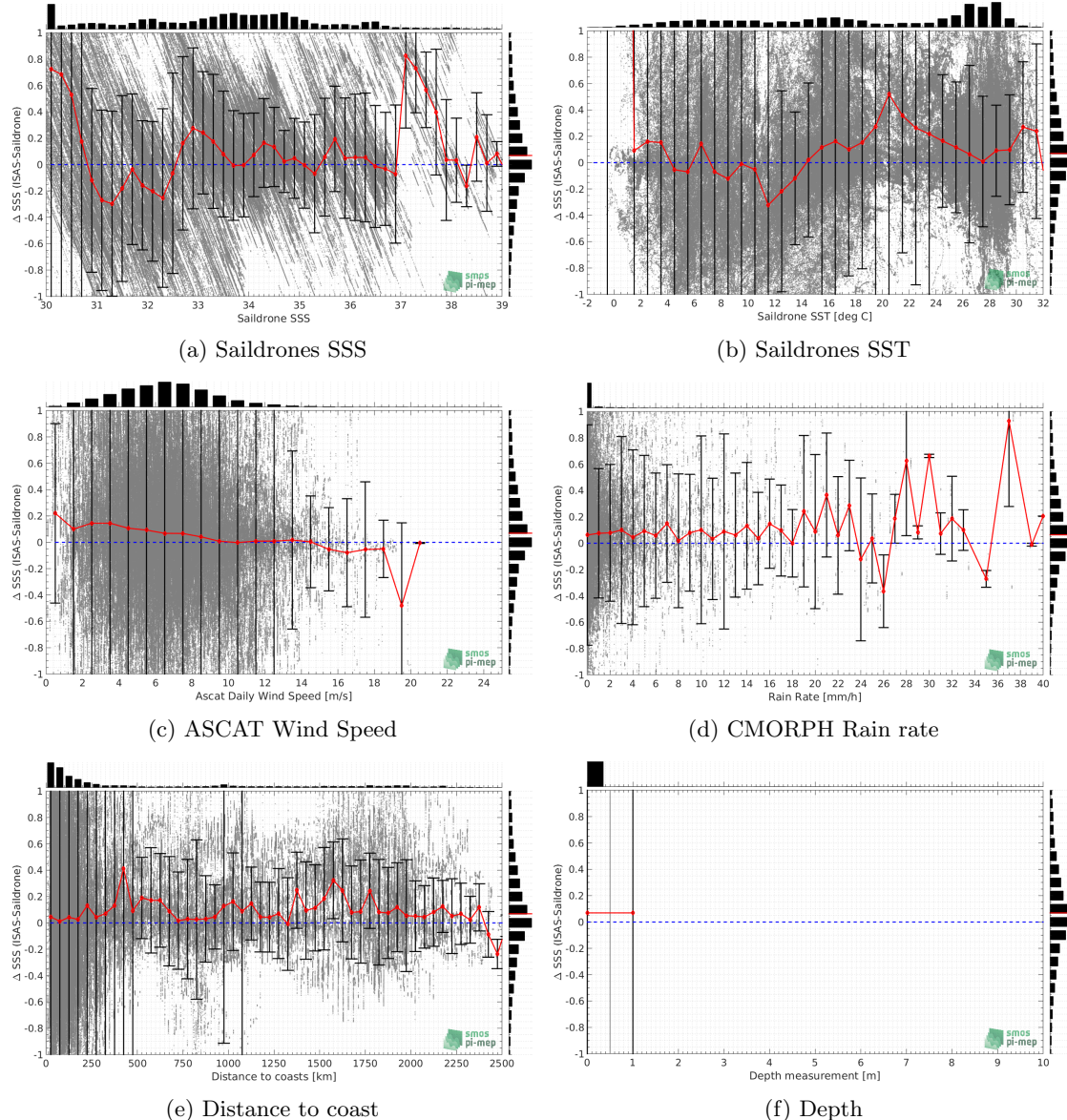


Figure 46: Δ SSS (ISAS - Saildrone) sorted as geophysical conditions: Saildrones SSS a), Saildrones SST b), ASCAT Wind speed c), CMORPH rain rate d), distance to coast (e) and depth measurements (f).

5.12 Δ SSS maps and statistics for different geophysical conditions

In Figures 47 and 48, we focus on sub-datasets of the match-up differences Δ SSS (ISAS - *in situ*) for the following specific geophysical conditions:

- **C1:** if the local value at *in situ* location of estimated rain rate is zero, mean daily wind is in the range [3, 12] m/s, the SST is $> 5^{\circ}\text{C}$ and distance to coast is > 800 km.
- **C2:** if the local value at *in situ* location of estimated rain rate is zero, mean daily wind is

in the range [3, 12] m/s.

- **C3:** if the local value at *in situ* location of estimated rain rate is high (ie. $> 1 \text{ mm/h}$) and mean daily wind is low (ie. $< 4 \text{ m/s}$).
- **C5:** if the *in situ* data is located where the climatological SSS standard deviation is low (ie. above < 0.2).
- **C6:** if the *in situ* data is located where the climatological SSS standard deviation is high (ie. above > 0.2).

For each of these conditions, the temporal mean (gridded over spatial boxes of size $1^\circ \times 1^\circ$) and the histogram of the difference ΔSSS (ISAS - *in situ*) are presented.

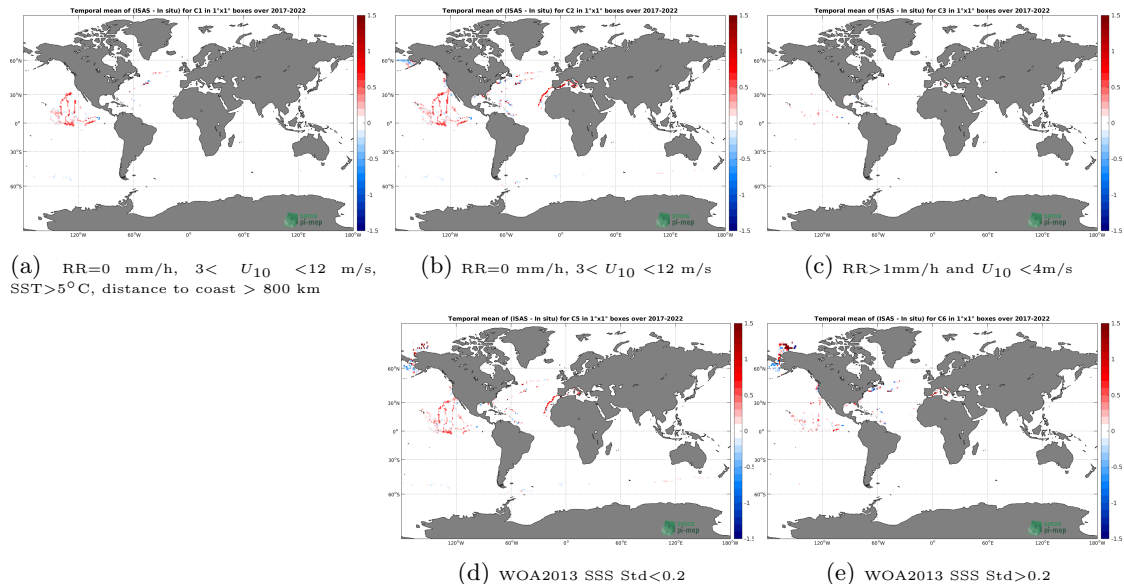


Figure 47: Temporal mean gridded over spatial boxes of size $1^\circ \times 1^\circ$ of ΔSSS (ISAS - Saildrones) for 5 different subdatasets corresponding to: $\text{RR}=0 \text{ mm/h}$, $3 < U_{10} < 12 \text{ m/s}$, $\text{SST} > 5^\circ\text{C}$, distance to coast $> 800 \text{ km}$ (a), $\text{RR}=0 \text{ mm/h}$, $3 < U_{10} < 12 \text{ m/s}$ (b), $\text{RR} > 1\text{mm/h}$ and $U_{10} < 4\text{m/s}$ (c), WOA2013 SSS Std < 0.2 (d), WOA2013 SSS Std > 0.2 (e).

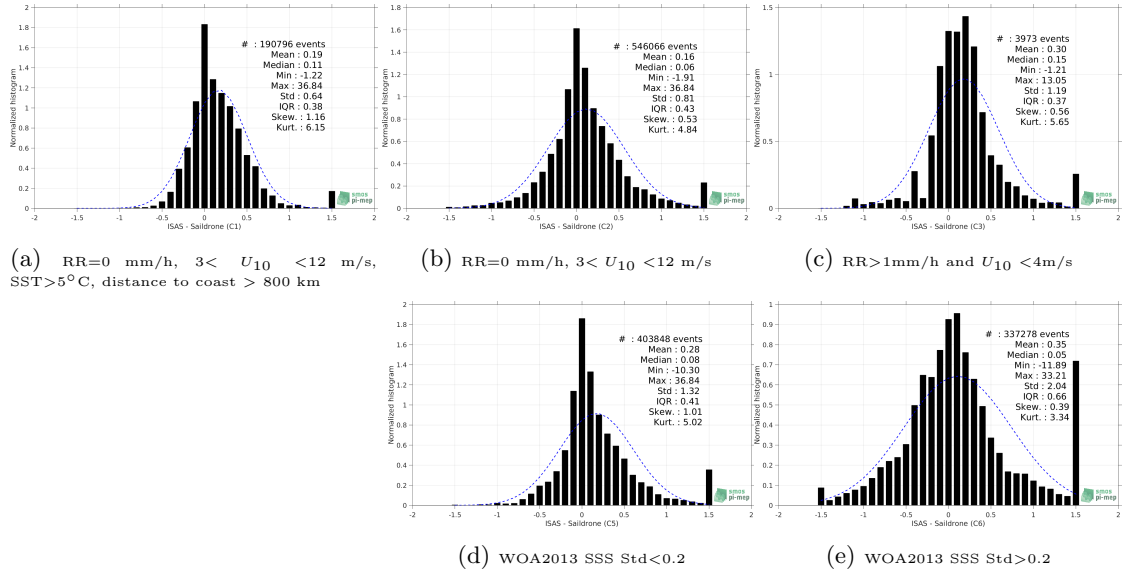


Figure 48: Normalized histogram of ΔSSS (ISAS - Saildrones) for 5 different subdatasets corresponding to: RR=0 mm/h, $3 < U_{10} < 12 \text{ m/s}$, SST > 5°C, distance to coast > 800 km (a), RR=0 mm/h, $3 < U_{10} < 12 \text{ m/s}$ (b), RR > 1 mm/h and $U_{10} < 4 \text{ m/s}$ (c), WOA2013 SSS Std < 0.2 (d), WOA2013 SSS Std > 0.2 (e).

5.13 Summary

Table 1 shows the mean, median, standard deviation (Std), root mean square (RMS), interquartile range (IQR), correlation coefficient (r^2) and robust standard deviation (Std*) of the match-up differences ΔSSS (ISAS - Saildrones) for the following conditions:

- all: All the match-up pairs satellite/in situ SSS values are used to derive the statistics
- C1: only pairs where RR=0 mm/h, $3 < U_{10} < 12 \text{ m/s}$, SST > 5°C, distance to coast > 800 km
- C2: only pairs where RR=0 mm/h, $3 < U_{10} < 12 \text{ m/s}$
- C3: only pairs where RR > 1 mm/h and $U_{10} < 4 \text{ m/s}$
- C5: only pairs where WOA2013 SSS Std < 0.2
- C6: only pairs where WOA2013 SSS Std > 0.2
- C7a: only pairs with a distance to coast < 150 km.
- C7b: only pairs with a distance to coast in the range [150, 800] km.
- C7c: only pairs with a distance to coast > 800 km.
- C8a: only pairs where SST is < 5°C.
- C8b: only pairs where SST is in the range [5, 15]°C.
- C8c: only pairs where SST is > 15°C.

- C9a: only pairs where SSS is < 33.
- C9b: only pairs where SSS is in the range [33, 37].
- C9c: only pairs where SSS is > 37.

Table 1: Statistics of ΔSSS (ISAS - Saildrones)

Condition	#	Median	Mean	Std	RMS	IQR	r^2	Std*
all	912397	0.07	0.41	2.08	2.12	0.53	0.388	0.39
C1	190796	0.11	0.19	0.64	0.66	0.38	0.480	0.27
C2	546066	0.06	0.16	0.81	0.82	0.43	0.760	0.31
C3	3973	0.15	0.30	1.19	1.23	0.37	0.629	0.28
C5	403848	0.08	0.28	1.32	1.35	0.41	0.565	0.28
C6	337278	0.05	0.35	2.04	2.07	0.66	0.452	0.49
C7a	422897	0.03	0.29	1.53	1.56	0.68	0.639	0.50
C7b	216707	0.10	0.94	3.58	3.70	0.63	0.141	0.46
C7c	272778	0.10	0.17	0.57	0.60	0.37	0.588	0.26
C8a	71110	0.07	2.14	5.19	5.62	4.29	0.004	0.97
C8b	244997	-0.06	0.33	2.33	2.36	0.79	0.203	0.58
C8c	589695	0.10	0.23	0.85	0.89	0.42	0.722	0.30
C9a	325944	0.12	0.97	3.36	3.50	1.22	0.000	0.81
C9b	562051	0.06	0.09	0.40	0.41	0.36	0.856	0.27
C9c	24402	0.20	0.31	0.47	0.56	0.79	0.338	0.50

Table 1 numerical values can be downloaded as a csv file [here](#).

6 TSG

The TSG dataset is subdivided into 9 subdatasets following TSG data providers subdivisions.

- [LEGOS-DM](#)
- [GOSUD-Research-vessel](#)
- [GOSUD-Sailing-ship](#)
- [SAMOS](#)
- [CSIC-UTM](#)
- [Polarstern](#)
- [NCEI-0170743](#)
- [LEGOS-Survostral](#)
- [LEGOS-Survostral-Adélie](#)

6.1 TSG (LEGOS-DM)

6.1.1 Introduction

The TSG (LEGOS-DM) dataset corresponds to sea surface salinity delayed mode data derived from voluntary observing ships collected, validated, archived, and made freely available by the French Sea Surface Salinity Observation Service (Alory et al. (2015)). The network is global though more concentrated in the tropical Pacific and North Atlantic oceanic basins. The acquisition system is autonomous with real time transmission and is regularly serviced at harbor calls. The high resolution data retrieved from the acquisition system during ship calls is processed through a dedicated software (freely available) for attribution of data quality flags by visual inspection, and correction of TSG time series by comparison with climatology, onboard daily water samples and collocated Argo data. Adjusted values when available and only collected TSG data that exhibit quality flags=1 and 2 were used.

6.1.2 Number of SSS data as a function of time and distance to coast

Figure 49 shows the time (a) and distance to coast (b) distributions of the TSG (LEGOS-DM) *in situ* dataset.

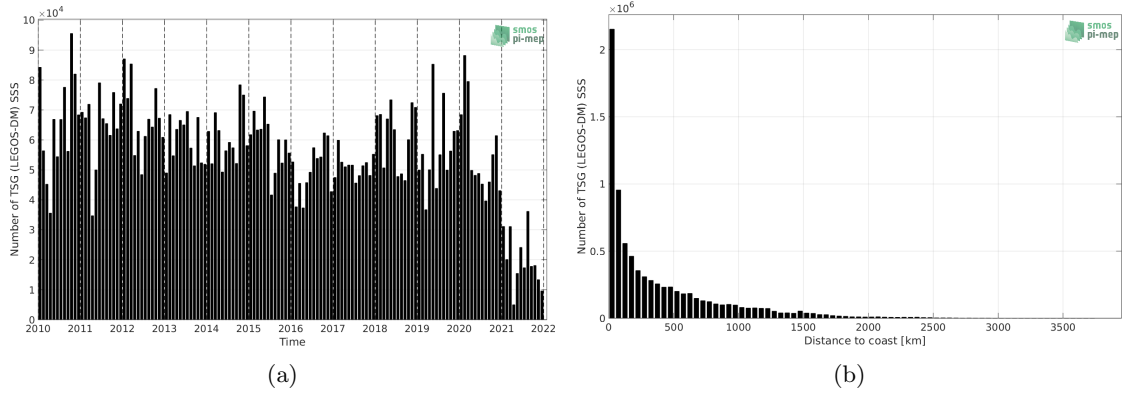


Figure 49: Number of SSS from TSG (LEGOS-DM) as a function of time (a) and distance to coast (b).

6.1.3 Histograms of SSS

Figure 50 shows the SSS distribution of the TSG (LEGOS-DM) (a) and colocalized ISAS (b) dataset.

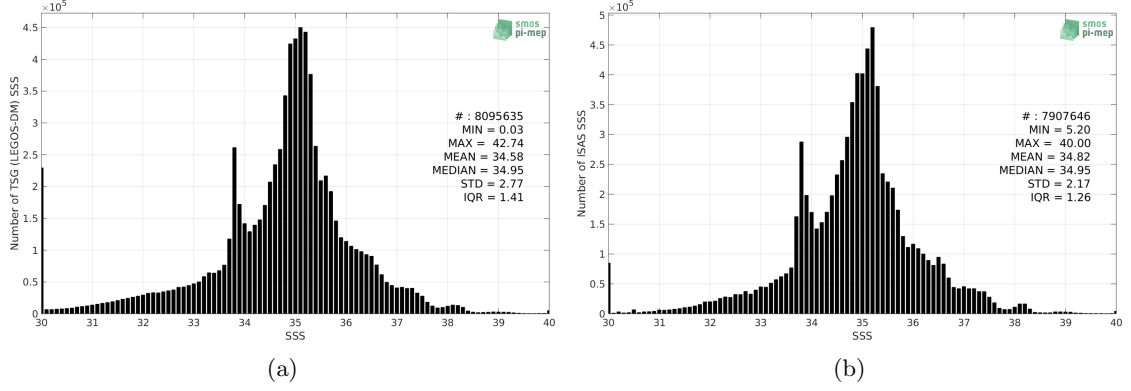


Figure 50: Histograms of SSS from TSG (LEGOS-DM) (a) and ISAS (b) per bins of 0.1.

6.1.4 Distribution of *in situ* SSS depth measurements

In Figure 51, we show the depth distribution of the *in situ* salinity dataset (a) and the spatial distribution of the depth temporal mean in $1^\circ \times 1^\circ$ boxes and considering the full *in situ* dataset period (b).

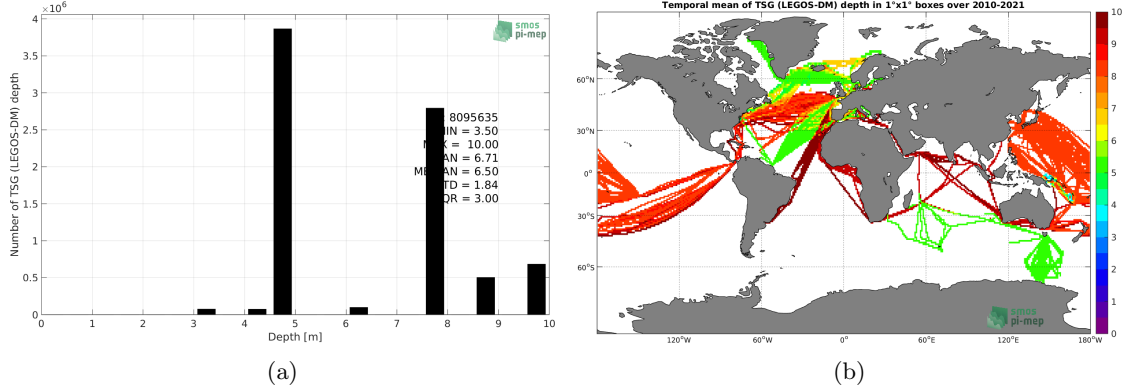


Figure 51: Depth distribution of the upper level SSS measurements from TSG (LEGOS-DM) (a) and spatial distribution of the *in situ* SSS depth measurements showing the mean value in $1^\circ \times 1^\circ$ boxes and considering the full *in situ* dataset period (b).

6.1.5 Spatial distribution of SSS

In Figure 52, the number of TSG (LEGOS-DM) SSS measurements in $1^\circ \times 1^\circ$ boxes is shown.

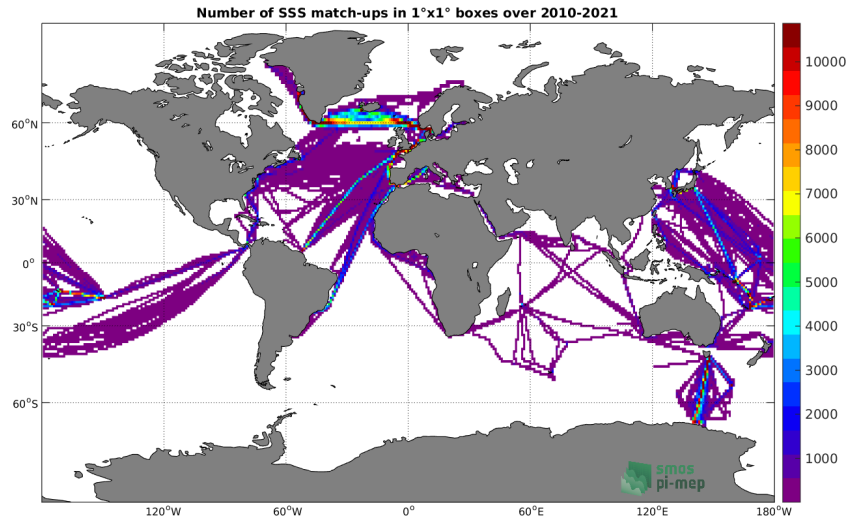


Figure 52: Number of SSS from TSG (LEGOS-DM) in $1^{\circ} \times 1^{\circ}$ boxes.

6.1.6 Spatial Maps of the Temporal mean and Std of *in situ* and ISAS SSS and of the difference (Δ SSS)

In Figure 53, maps of temporal mean (left) and standard deviation (right) of ISAS (top), TSG (LEGOS-DM) *in situ* dataset (middle) and the difference Δ SSS(ISAS -TSG (LEGOS-DM)) (bottom) are shown. The temporal mean and std are calculated using all match-up pairs falling in spatial boxes of size $1^{\circ} \times 1^{\circ}$ over the full TSG (LEGOS-DM) dataset period.

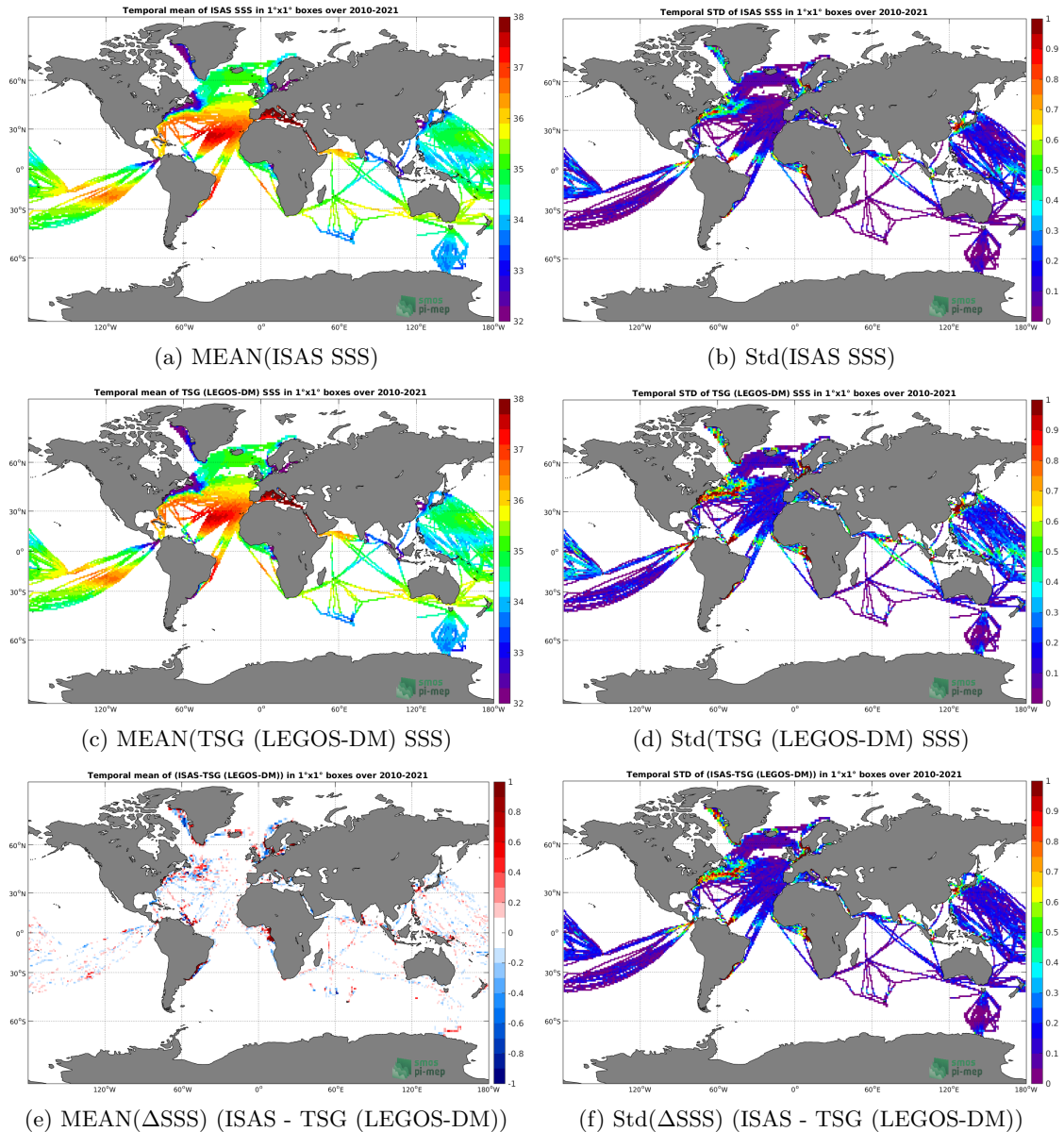


Figure 53: Temporal mean (left) and Std (right) of SSS from ISAS (top), TSG (LEGOS-DM) (middle), and of Δ SSS (ISAS - TSG (LEGOS-DM)). Only match-up pairs are used to generate these maps.

6.1.7 Time series of the monthly median and Std of *in situ* and ISAS SSS and of the difference (Δ SSS)

In the top panel of Figure 54, we show the time series of the monthly median SSS estimated for both ISAS SSS product (in black) and the TSG (LEGOS-DM) *in situ* dataset (in blue) at the collected Pi-MEP match-up pairs.

In the middle panel of Figure 54, we show the time series of the monthly median of Δ SSS

(ISAS - TSG (LEGOS-DM)) for the collected Pi-MEP match-up pairs.

In the bottom panel of Figure 54, we show the time series of the monthly standard deviation of the ΔSSS (ISAS - TSG (LEGOS-DM)) for the collected Pi-MEP match-up pairs.

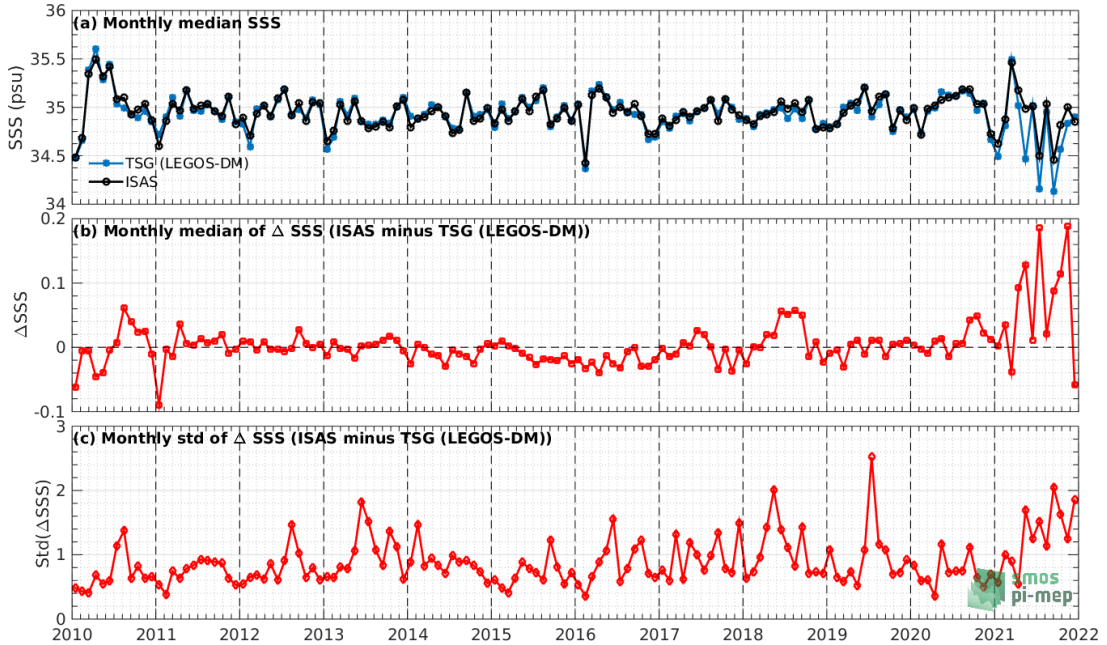


Figure 54: Time series of the monthly median SSS (top), median of ΔSSS (ISAS - TSG (LEGOS-DM)) and Std of ΔSSS (ISAS - TSG (LEGOS-DM)) considering all match-ups collected by the Pi-MEP.

6.1.8 Zonal mean and Std of *in situ* and ISAS SSS and of the difference ΔSSS

In Figure 55 left panel, we show the zonal mean SSS considering all Pi-MEP match-up pairs for both ISAS SSS product (in black) and the TSG (LEGOS-DM) *in situ* dataset (in blue). The full *in situ* dataset period is used to derive the mean.

In the right panel of Figure 55, we show the zonal mean of ΔSSS (ISAS - TSG (LEGOS-DM)) for all the collected Pi-MEP match-up pairs estimated over the full *in situ* dataset period.

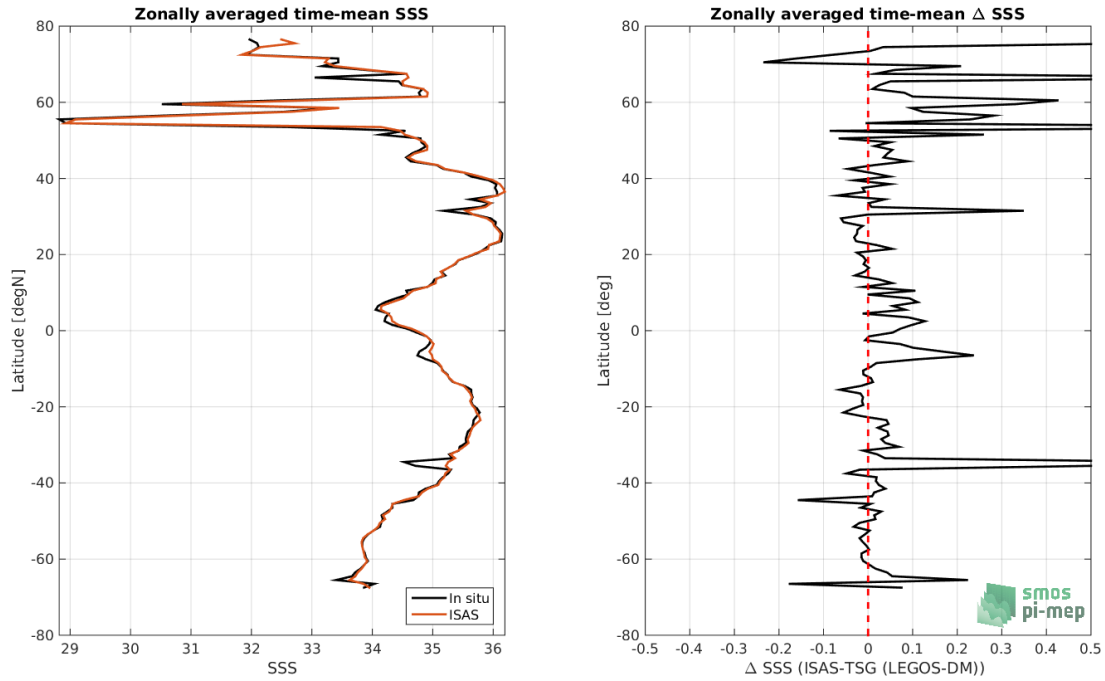


Figure 55: Left panel: Zonal mean SSS from ISAS product (black) and from TSG (LEGOS-DM) (blue). Right panel: Zonal mean of Δ SSS (ISAS - TSG (LEGOS-DM)) for all the collected Pi-MEP match-up pairs estimated over the full *in situ* dataset period.

6.1.9 Scatterplots of ISAS vs *in situ* SSS by latitudinal bands

In Figure 56, contour maps of the concentration of ISAS SSS (y-axis) versus TSG (LEGOS-DM) SSS (x-axis) at match-up pairs for different latitude bands: (a) 80°S-80°N, (b) 20°S-20°N, (c) 40°S-20°S and 20°N-40°N and (d) 60°S-40°S and 40°N-60°N. For each plot, the red line shows $x=y$. The black thin and dashed lines indicate a linear fit through the data cloud and the $\pm 95\%$ confidence levels, respectively. The number match-up pairs n , the slope and R^2 coefficient of the linear fit, the root mean square (RMS) and the mean bias between ISAS and *in situ* data are indicated for each latitude band in each plots.

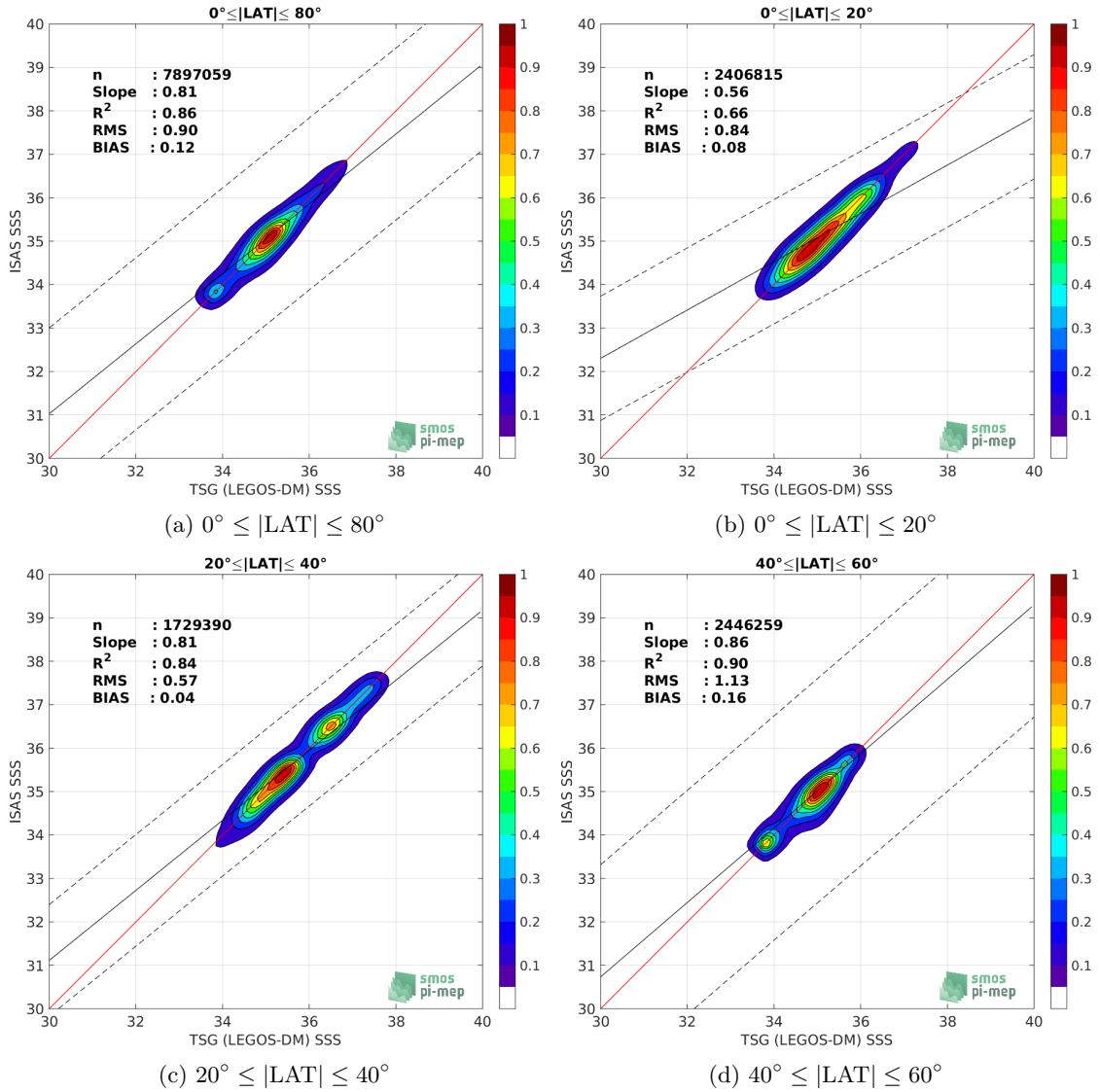


Figure 56: Contour maps of the concentration of ISAS SSS (y-axis) versus TSG (LEGOS-DM) SSS (x-axis) at match-up pairs for different latitude bands. For each plot, the red line shows $x=y$. The black thin and dashed lines indicate a linear fit through the data cloud and the $\pm 95\%$ confidence levels, respectively. The number match-up pairs n , the slope and R^2 coefficient of the linear fit, the root mean square (RMS) and the mean bias between ISAS and *in situ* data are indicated for each latitude band in each plots.

6.1.10 Time series of the monthly median and Std of the difference ΔSSS sorted by latitudinal bands

In Figure 57, time series of the monthly median (red curves) of ΔSSS (ISAS - TSG (LEGOS-DM)) and ± 1 Std (black vertical thick bars) as function of time for all the collected Pi-MEP match-up pairs estimated for the full *in situ* dataset period are shown for different latitude bands: (a) $80^\circ\text{S}-80^\circ\text{N}$, (b) $20^\circ\text{S}-20^\circ\text{N}$, (c) $40^\circ\text{S}-20^\circ\text{S}$ and $20^\circ\text{N}-40^\circ\text{N}$ and (d) $60^\circ\text{S}-40^\circ\text{S}$ and $40^\circ\text{N}-60^\circ\text{N}$.

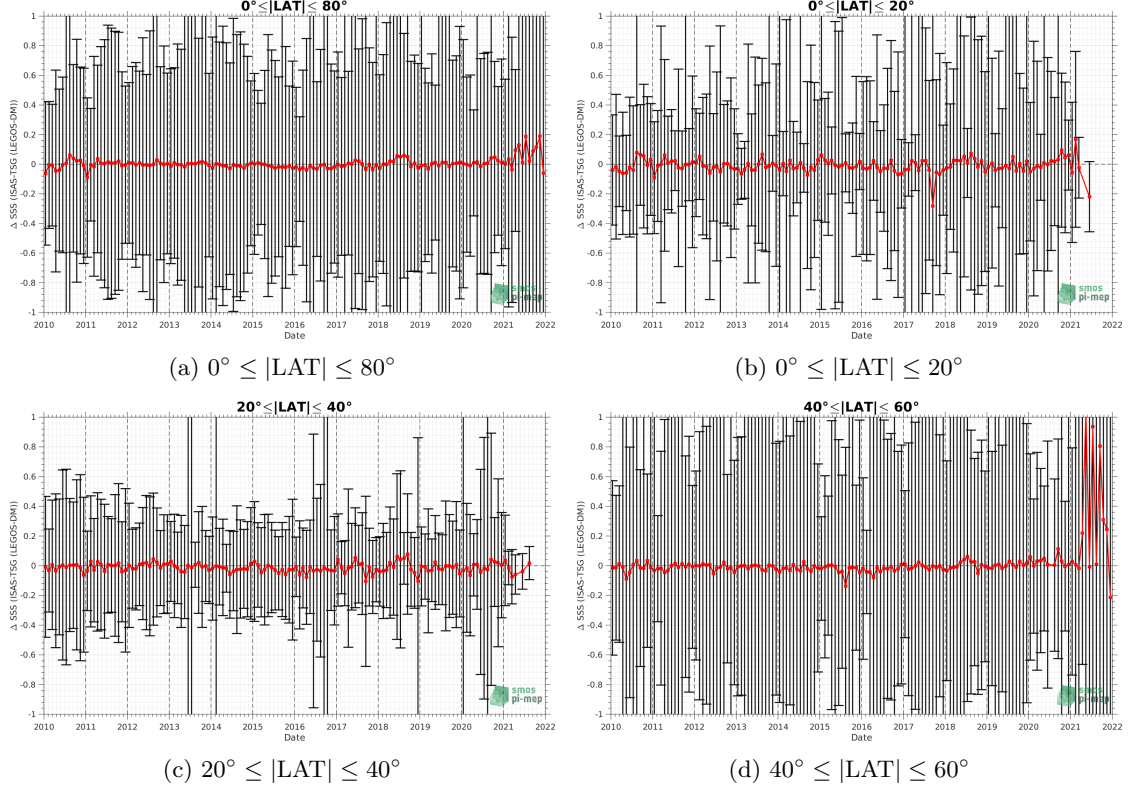


Figure 57: Monthly median (red curves) of ΔSSS (ISAS - TSG (LEGOS-DM)) and ± 1 Std (black vertical thick bars) as function of time for all the collected Pi-MEP match-up pairs for the full *in situ* dataset period are shown for different latitude bands: (a) $80^\circ\text{S}-80^\circ\text{N}$, (b) $20^\circ\text{S}-20^\circ\text{N}$, (c) $40^\circ\text{S}-20^\circ\text{S}$ and $20^\circ\text{N}-40^\circ\text{N}$ and (d) $60^\circ\text{S}-40^\circ\text{S}$ and $40^\circ\text{N}-60^\circ\text{N}$.

6.1.11 ΔSSS sorted as geophysical conditions

In Figure 58, we classify the match-up differences ΔSSS (ISAS - *in situ*) as function of the geophysical conditions at match-up points. The mean and std of ΔSSS (ISAS - TSG (LEGOS-DM)) is thus evaluated as function of the

- *in situ* SSS values per bins of width 0.2,
- *in situ* SST values per bins of width 1°C ,
- ASCAT daily wind values per bins of width 1 m/s,
- CMORPH 3-hourly rain rates per bins of width 1 mm/h, and,
- distance to coasts per bins of width 50 km,
- *in situ* measurement depth (if relevant).

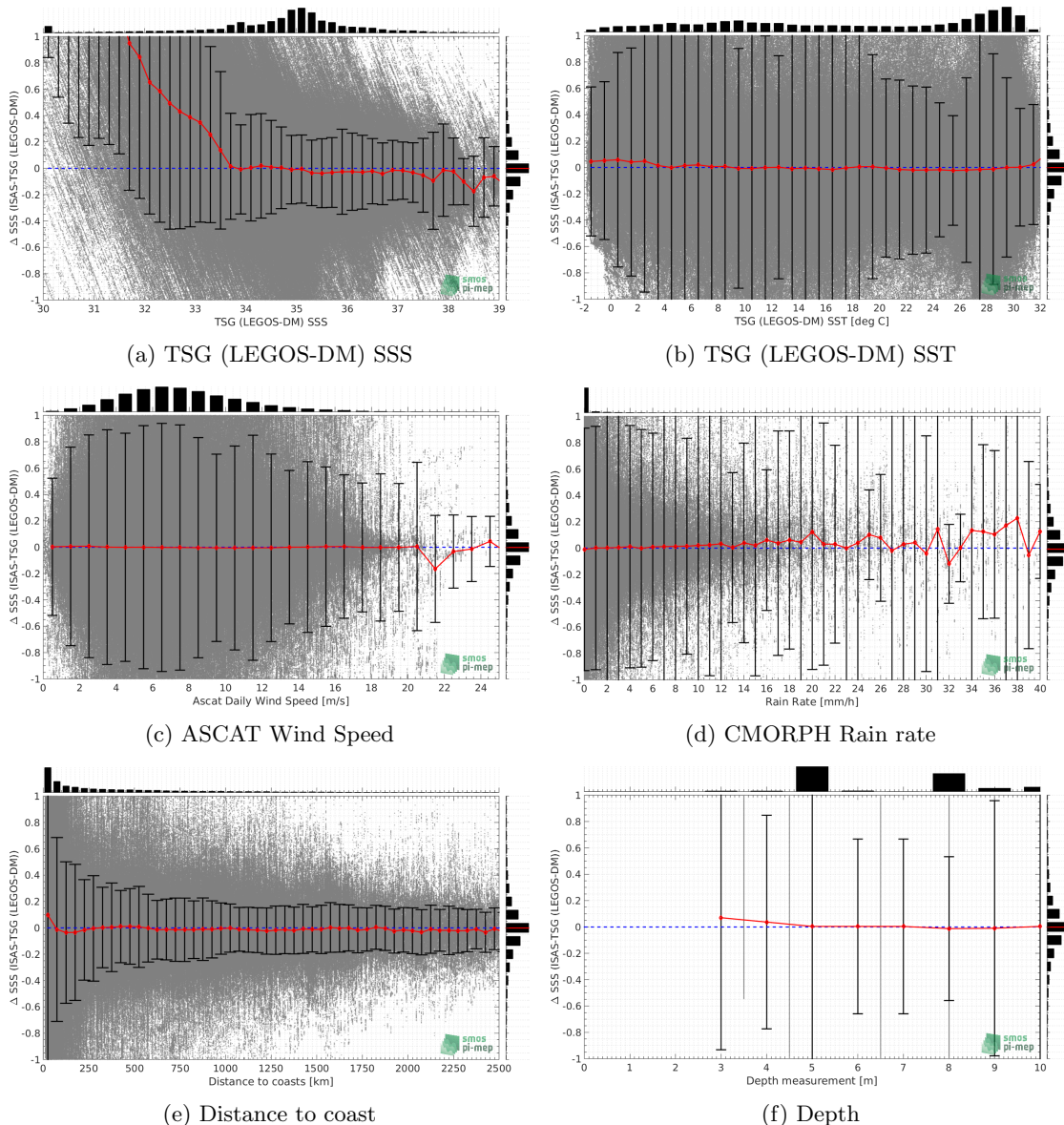


Figure 58: ΔSSS (ISAS - TSG (LEGOS-DM)) sorted as geophysical conditions: TSG (LEGOS-DM) SSS a), TSG (LEGOS-DM) SST b), ASCAT Wind speed c), CMORPH rain rate d), distance to coast (e) and depth measurements (f).

6.1.12 ΔSSS maps and statistics for different geophysical conditions

In Figures 59 and 60, we focus on sub-datasets of the match-up differences ΔSSS (ISAS - *in situ*) for the following specific geophysical conditions:

- **C1:** if the local value at *in situ* location of estimated rain rate is zero, mean daily wind is in the range [3, 12] m/s, the SST is $> 5^\circ\text{C}$ and distance to coast is > 800 km.
- **C2:** if the local value at *in situ* location of estimated rain rate is zero, mean daily wind is

in the range [3, 12] m/s.

- **C3:** if the local value at *in situ* location of estimated rain rate is high (ie. $> 1 \text{ mm/h}$) and mean daily wind is low (ie. $< 4 \text{ m/s}$).
- **C5:** if the *in situ* data is located where the climatological SSS standard deviation is low (ie. above < 0.2).
- **C6:** if the *in situ* data is located where the climatological SSS standard deviation is high (ie. above > 0.2).

For each of these conditions, the temporal mean (gridded over spatial boxes of size $1^\circ \times 1^\circ$) and the histogram of the difference ΔSSS (ISAS - *in situ*) are presented.

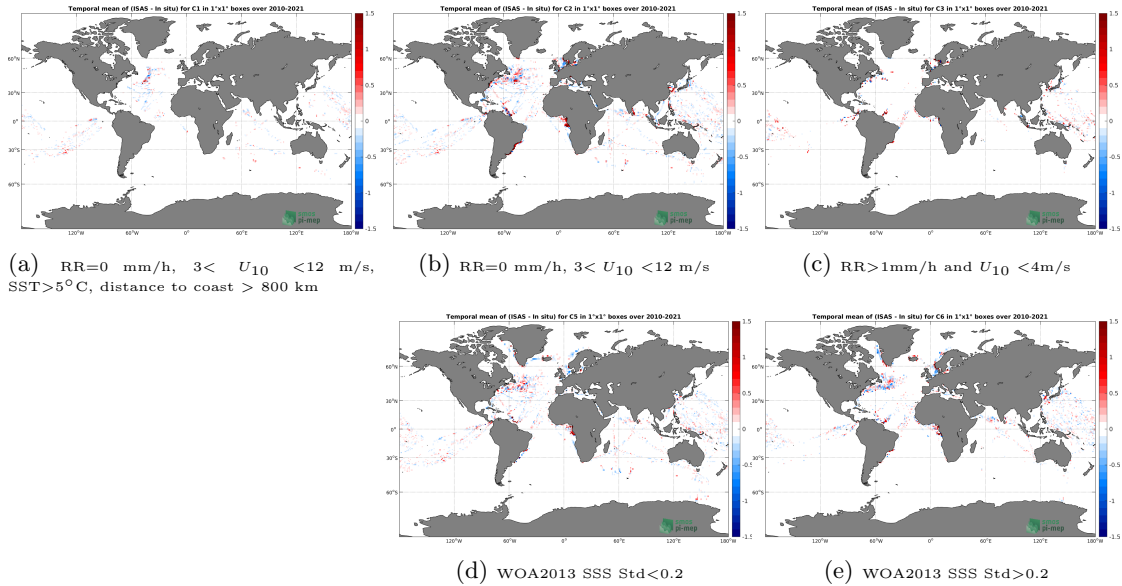


Figure 59: Temporal mean gridded over spatial boxes of size $1^\circ \times 1^\circ$ of ΔSSS (ISAS - TSG (LEGOS-DM)) for 5 different subdatasets corresponding to: $\text{RR}=0 \text{ mm/h}$, $3 < U_{10} < 12 \text{ m/s}$, $\text{SST} > 5^\circ\text{C}$, $\text{distance to coast} > 800 \text{ km}$ (a), $\text{RR}=0 \text{ mm/h}$, $3 < U_{10} < 12 \text{ m/s}$ (b), $\text{RR} > 1\text{mm/h}$ and $U_{10} < 4\text{m/s}$ (c), WOA2013 SSS Std < 0.2 (d), WOA2013 SSS Std > 0.2 (e).

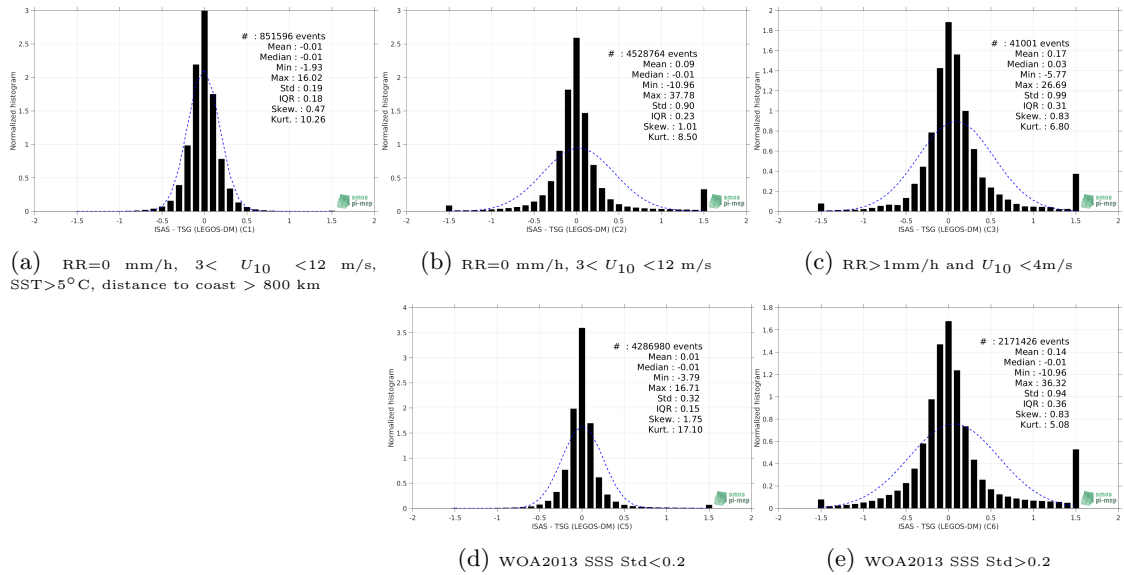


Figure 60: Normalized histogram of ΔSSS (ISAS - TSG (LEGOS-DM)) for 5 different subdatasets corresponding to: $RR=0 \text{ mm/h}$, $3 < U_{10} < 12 \text{ m/s}$, $SST > 5^\circ\text{C}$, distance to coast $> 800 \text{ km}$ (a), $RR=0 \text{ mm/h}$, $3 < U_{10} < 12 \text{ m/s}$ (b), $RR > 1 \text{ mm/h}$ and $U_{10} < 4 \text{ m/s}$ (c), WOA2013 SSS Std < 0.2 (d), WOA2013 SSS Std > 0.2 (e).

6.1.13 Summary

Table 1 shows the mean, median, standard deviation (Std), root mean square (RMS), interquartile range (IQR), correlation coefficient (r^2) and robust standard deviation (Std*) of the match-up differences ΔSSS (ISAS - TSG (LEGOS-DM)) for the following conditions:

- all: All the match-up pairs satellite/in situ SSS values are used to derive the statistics
- C1: only pairs where $RR=0 \text{ mm/h}$, $3 < U_{10} < 12 \text{ m/s}$, $SST > 5^\circ\text{C}$, distance to coast $> 800 \text{ km}$
- C2: only pairs where $RR=0 \text{ mm/h}$, $3 < U_{10} < 12 \text{ m/s}$
- C3: only pairs where $RR > 1 \text{ mm/h}$ and $U_{10} < 4 \text{ m/s}$
- C5: only pairs where WOA2013 SSS Std < 0.2
- C6: only pairs where WOA2013 SSS Std > 0.2
- C7a: only pairs with a distance to coast $< 150 \text{ km}$.
- C7b: only pairs with a distance to coast in the range $[150, 800] \text{ km}$.
- C7c: only pairs with a distance to coast $> 800 \text{ km}$.
- C8a: only pairs where SST is $< 5^\circ\text{C}$.
- C8b: only pairs where SST is in the range $[5, 15]^\circ\text{C}$.
- C8c: only pairs where SST is $> 15^\circ\text{C}$.

- C9a: only pairs where SSS is < 33 .
- C9b: only pairs where SSS is in the range [33, 37].
- C9c: only pairs where SSS is > 37 .

Table 1: Statistics of ΔSSS (ISAS - TSG (LEGOS-DM))

Condition	#	Median	Mean	Std	RMS	IQR	r^2	Std*
all	7907646	0.00	0.13	0.93	0.94	0.23	0.866	0.17
C1	851596	-0.01	-0.01	0.19	0.19	0.18	0.963	0.14
C2	4528764	-0.01	0.09	0.90	0.90	0.23	0.872	0.17
C3	41001	0.03	0.17	0.99	1.01	0.31	0.806	0.23
C5	4286980	-0.01	0.01	0.32	0.32	0.15	0.939	0.11
C6	2171426	-0.01	0.14	0.94	0.95	0.36	0.859	0.27
C7a	3477752	0.02	0.30	1.35	1.38	0.46	0.858	0.32
C7b	3100448	-0.01	0.00	0.35	0.35	0.16	0.861	0.12
C7c	1323778	-0.01	-0.01	0.19	0.19	0.16	0.967	0.12
C8a	1056265	0.02	0.34	0.93	0.99	0.51	0.775	0.24
C8b	2312107	0.00	0.13	1.10	1.11	0.18	0.881	0.13
C8c	4539273	-0.01	0.08	0.83	0.84	0.25	0.844	0.19
C9a	774406	1.03	1.52	2.40	2.84	1.97	0.813	1.39
C9b	6796324	-0.01	-0.02	0.33	0.33	0.20	0.846	0.15
C9c	336916	-0.05	-0.08	0.28	0.29	0.22	0.823	0.16

Table 1 numerical values can be downloaded as a csv file [here](#).

6.2 TSG (GOSUD-Research-vessel)

6.2.1 Introduction

The TSG (GOSUD-Research-vessel) dataset corresponds to French research vessels SSS data that have been collected since the early 2000 as a contribution to the Global Ocean Surface Underway Data ([GOSUD](#)) program. The set of homogeneous instruments is permanently monitored and regularly calibrated. Water samples are taken on a daily basis by the crew and later analysed in the laboratory. The careful calibration and instrument maintenance, complemented with a rigorous adjustment on water samples, lead to reach an accuracy of a few 10^{-2} PSS in salinity. This delayed mode dataset ([Kolodziejczyk et al. \(2021\)](#)) is updated annually and freely available [here](#). Adjusted values when available and only collected TSG data that exhibit quality flags 1 or 2 were used.

6.2.2 Number of SSS data as a function of time and distance to coast

Figure 61 shows the time (a) and distance to coast (b) distributions of the TSG (GOSUD-Research-vessel) *in situ* dataset.

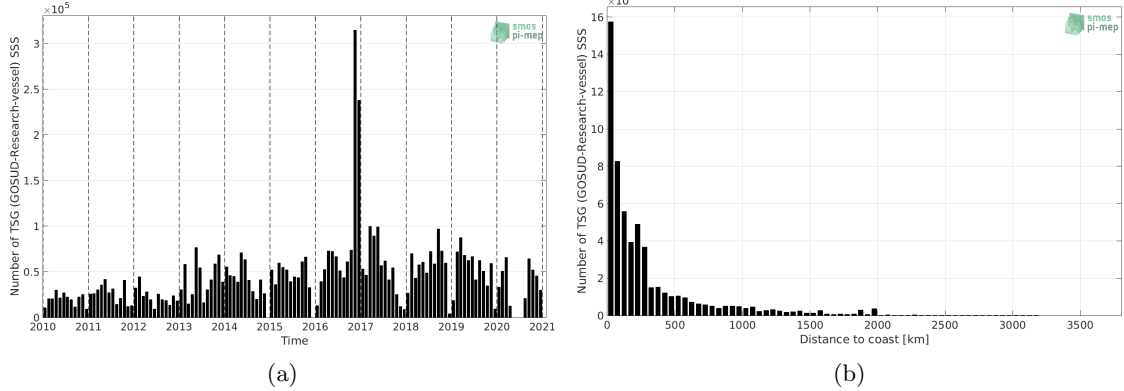


Figure 61: Number of SSS from TSG (GOSUD-Research-vessel) as a function of time (a) and distance to coast (b).

6.2.3 Histograms of SSS

Figure 62 shows the SSS distribution of the TSG (GOSUD-Research-vessel) (a) and colocalized ISAS (b) dataset.

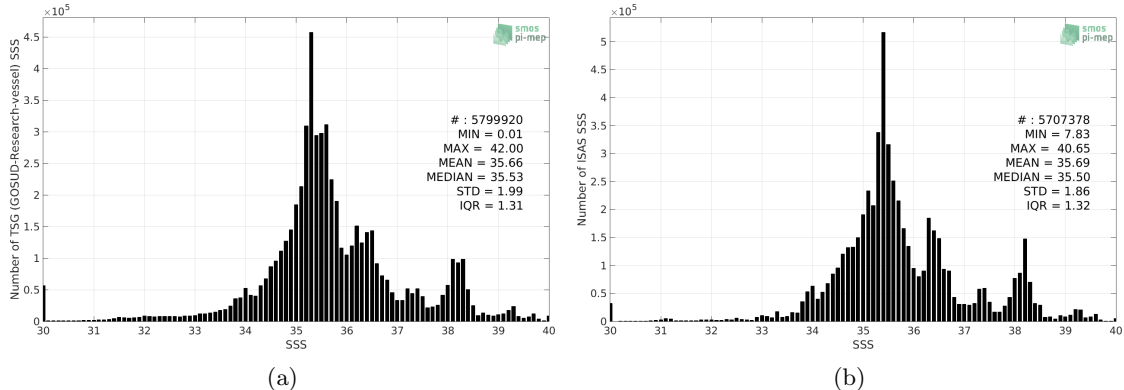


Figure 62: Histograms of SSS from TSG (GOSUD-Research-vessel) (a) and ISAS (b) per bins of 0.1.

6.2.4 Distribution of *in situ* SSS depth measurements

In Figure 63, we show the depth distribution of the *in situ* salinity dataset (a) and the spatial distribution of the depth temporal mean in $1^\circ \times 1^\circ$ boxes and considering the full *in situ* dataset period (b).

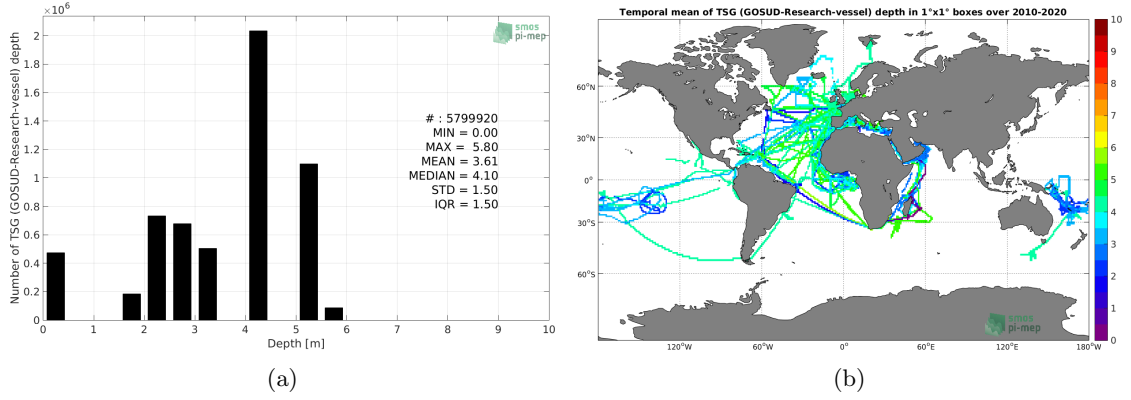


Figure 63: Depth distribution of the upper level SSS measurements from TSG (GOSUD-Research-vessel) (a) and spatial distribution of the *in situ* SSS depth measurements showing the mean value in $1^\circ \times 1^\circ$ boxes and considering the full *in situ* dataset period (b).

6.2.5 Spatial distribution of SSS

In Figure 64, the number of TSG (GOSUD-Research-vessel) SSS measurements in $1^\circ \times 1^\circ$ boxes is shown.

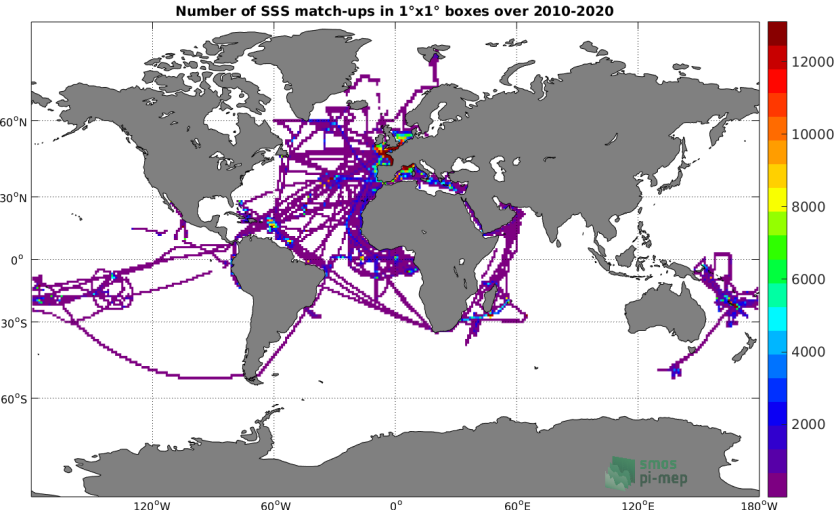


Figure 64: Number of SSS from TSG (GOSUD-Research-vessel) in $1^\circ \times 1^\circ$ boxes.

6.2.6 Spatial Maps of the Temporal mean and Std of *in situ* and ISAS SSS and of the difference (Δ SSS)

In Figure 65, maps of temporal mean (left) and standard deviation (right) of ISAS (top), TSG (GOSUD-Research-vessel) *in situ* dataset (middle) and the difference Δ SSS(ISAS -TSG (GOSUD-Research-vessel)) (bottom) are shown. The temporal mean and std are calculated using all match-up pairs falling in spatial boxes of size $1^\circ \times 1^\circ$ over the full TSG (GOSUD-Research-vessel) dataset period.

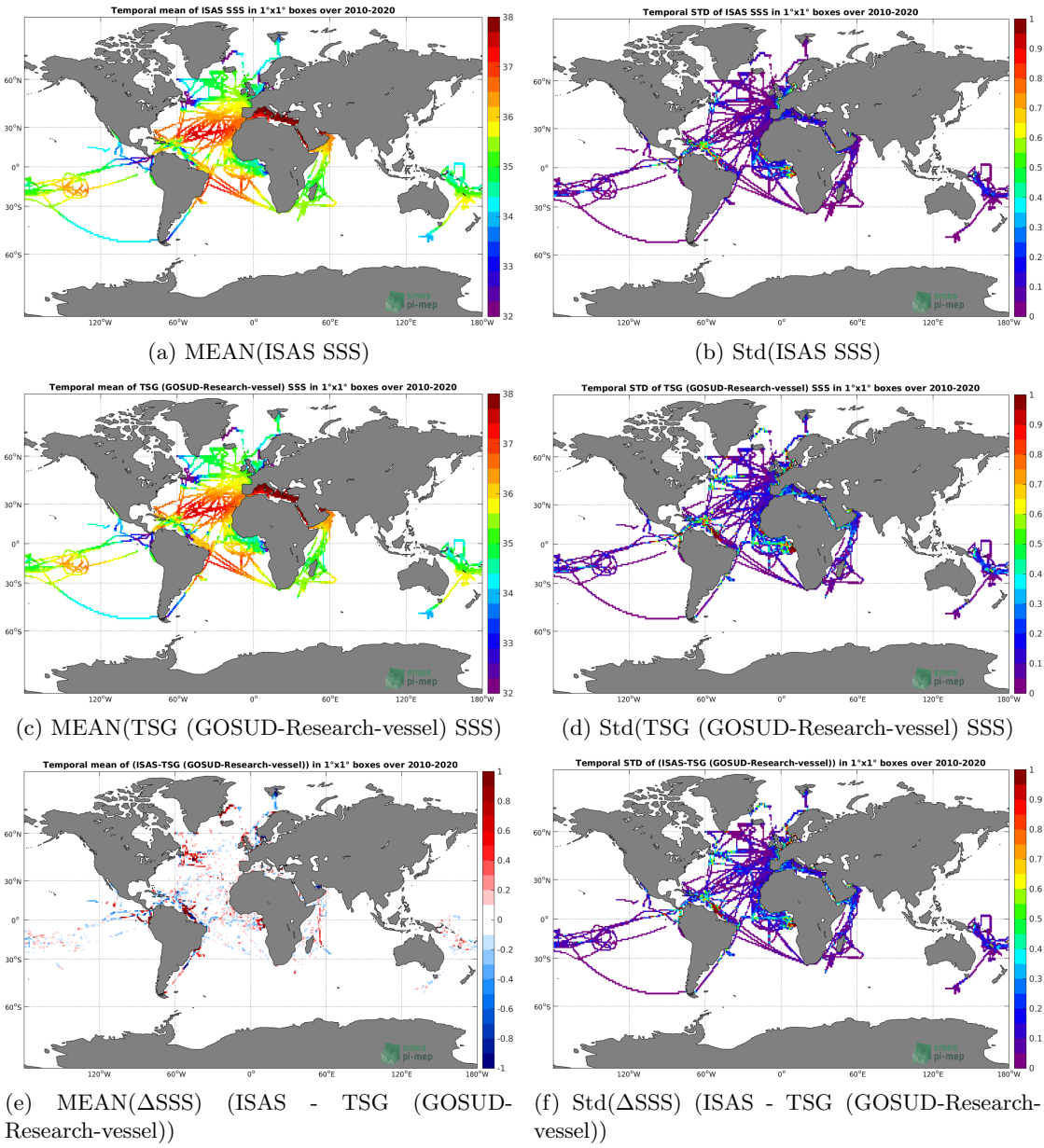


Figure 65: Temporal mean (left) and Std (right) of SSS from ISAS (top), TSG (GOSUD-Research-vessel) (middle), and of Δ SSS (ISAS - TSG (GOSUD-Research-vessel)). Only match-up pairs are used to generate these maps.

6.2.7 Time series of the monthly median and Std of *in situ* and ISAS SSS and of the difference (Δ SSS)

In the top panel of Figure 66, we show the time series of the monthly median SSS estimated for both ISAS SSS product (in black) and the TSG (GOSUD-Research-vessel) *in situ* dataset (in blue) at the collected Pi-MEP match-up pairs.

In the middle panel of Figure 66, we show the time series of the monthly median of Δ SSS

(ISAS - TSG (GOSUD-Research-vessel)) for the collected Pi-MEP match-up pairs.

In the bottom panel of Figure 66, we show the time series of the monthly standard deviation of the ΔSSS (ISAS - TSG (GOSUD-Research-vessel)) for the collected Pi-MEP match-up pairs.

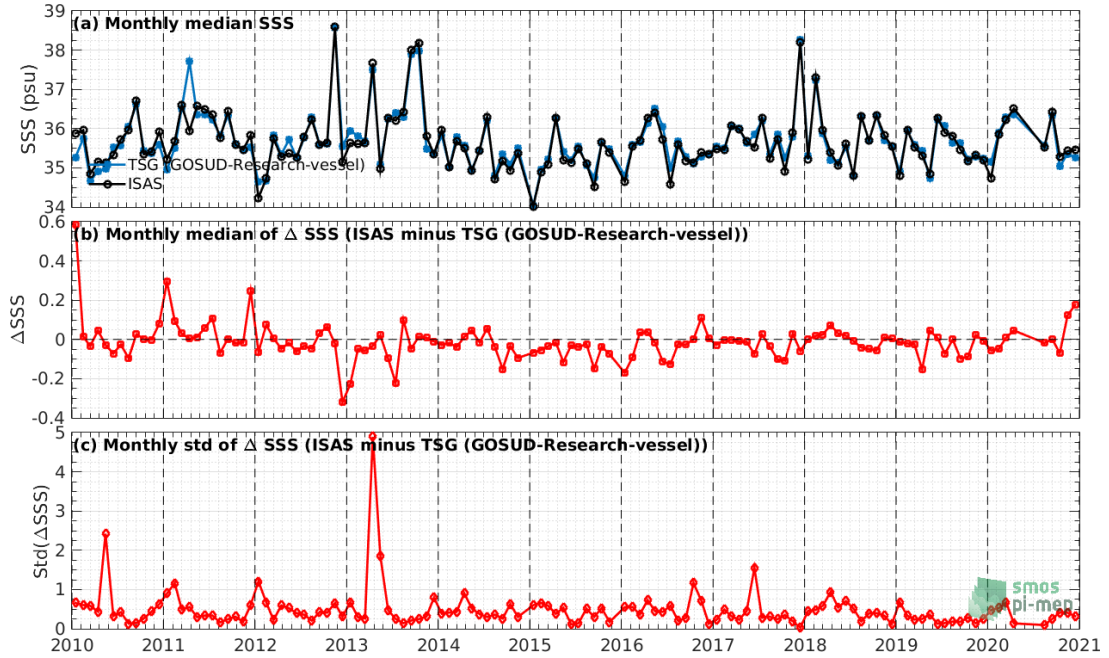


Figure 66: Time series of the monthly median SSS (top), median of ΔSSS (ISAS - TSG (GOSUD-Research-vessel)) and Std of ΔSSS (ISAS - TSG (GOSUD-Research-vessel)) considering all match-ups collected by the Pi-MEP.

6.2.8 Zonal mean and Std of *in situ* and ISAS SSS and of the difference ΔSSS

In Figure 67 left panel, we show the zonal mean SSS considering all Pi-MEP match-up pairs for both ISAS SSS product (in black) and the TSG (GOSUD-Research-vessel) *in situ* dataset (in blue). The full *in situ* dataset period is used to derive the mean.

In the right panel of Figure 67, we show the zonal mean of ΔSSS (ISAS - TSG (GOSUD-Research-vessel)) for all the collected Pi-MEP match-up pairs estimated over the full *in situ* dataset period.

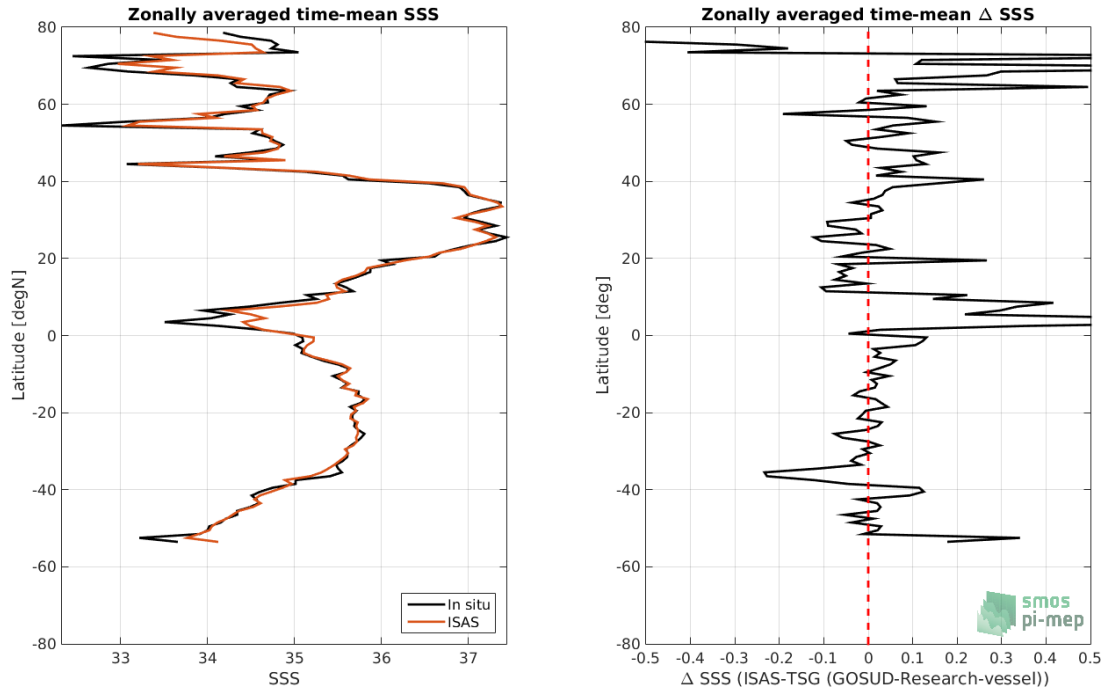


Figure 67: Left panel: Zonal mean SSS from ISAS product (black) and from TSG (GOSUD-Research-vessel) (blue). Right panel: Zonal mean of Δ SSS (ISAS - TSG (GOSUD-Research-vessel)) for all the collected Pi-MEP match-up pairs estimated over the full *in situ* dataset period.

6.2.9 Scatterplots of ISAS vs *in situ* SSS by latitudinal bands

In Figure 68, contour maps of the concentration of ISAS SSS (y-axis) versus TSG (GOSUD-Research-vessel) SSS (x-axis) at match-up pairs for different latitude bands: (a) 80°S-80°N, (b) 20°S-20°N, (c) 40°S-20°S and 20°N-40°N and (d) 60°S-40°S and 40°N-60°N. For each plot, the red line shows $x=y$. The black thin and dashed lines indicate a linear fit through the data cloud and the $\pm 95\%$ confidence levels, respectively. The number match-up pairs n , the slope and R^2 coefficient of the linear fit, the root mean square (RMS) and the mean bias between ISAS and *in situ* data are indicated for each latitude band in each plots.

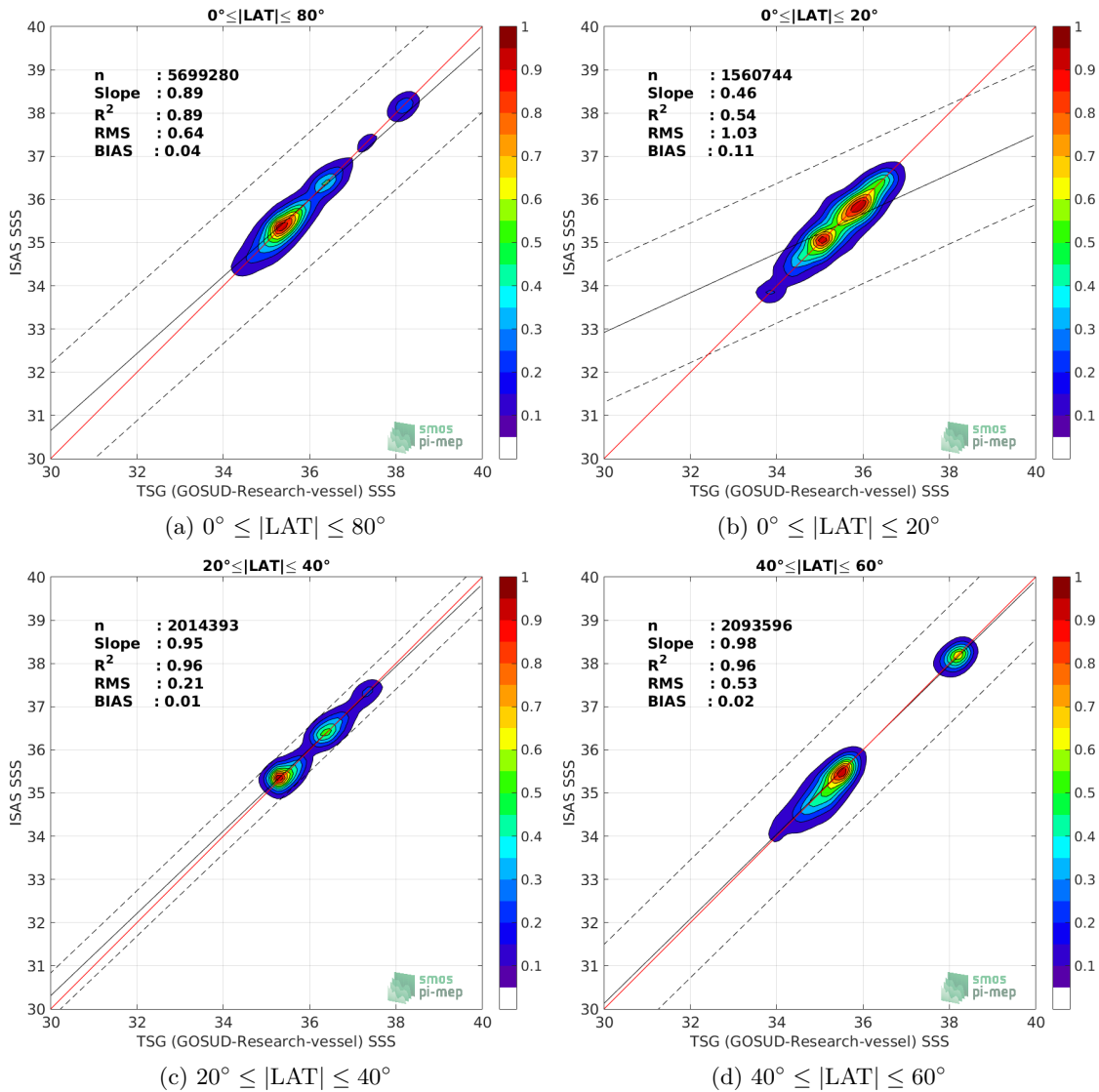


Figure 68: Contour maps of the concentration of ISAS SSS (y-axis) versus TSG (GOSUD-Research-vessel) SSS (x-axis) at match-up pairs for different latitude bands. For each plot, the red line shows $x=y$. The black thin and dashed lines indicate a linear fit through the data cloud and the $\pm 95\%$ confidence levels, respectively. The number match-up pairs n , the slope and R^2 coefficient of the linear fit, the root mean square (RMS) and the mean bias between ISAS and *in situ* data are indicated for each latitude band in each plots.

6.2.10 Time series of the monthly median and Std of the difference ΔSSS sorted by latitudinal bands

In Figure 69, time series of the monthly median (red curves) of ΔSSS (ISAS - TSG (GOSUD-Research-vessel)) and ± 1 Std (black vertical thick bars) as function of time for all the collected Pi-MEP match-up pairs estimated for the full *in situ* dataset period are shown for different latitude bands: (a) $80^\circ\text{S}-80^\circ\text{N}$, (b) $20^\circ\text{S}-20^\circ\text{N}$, (c) $40^\circ\text{S}-20^\circ\text{S}$ and $20^\circ\text{N}-40^\circ\text{N}$ and (d) $60^\circ\text{S}-40^\circ\text{S}$

and 40°N-60°N.

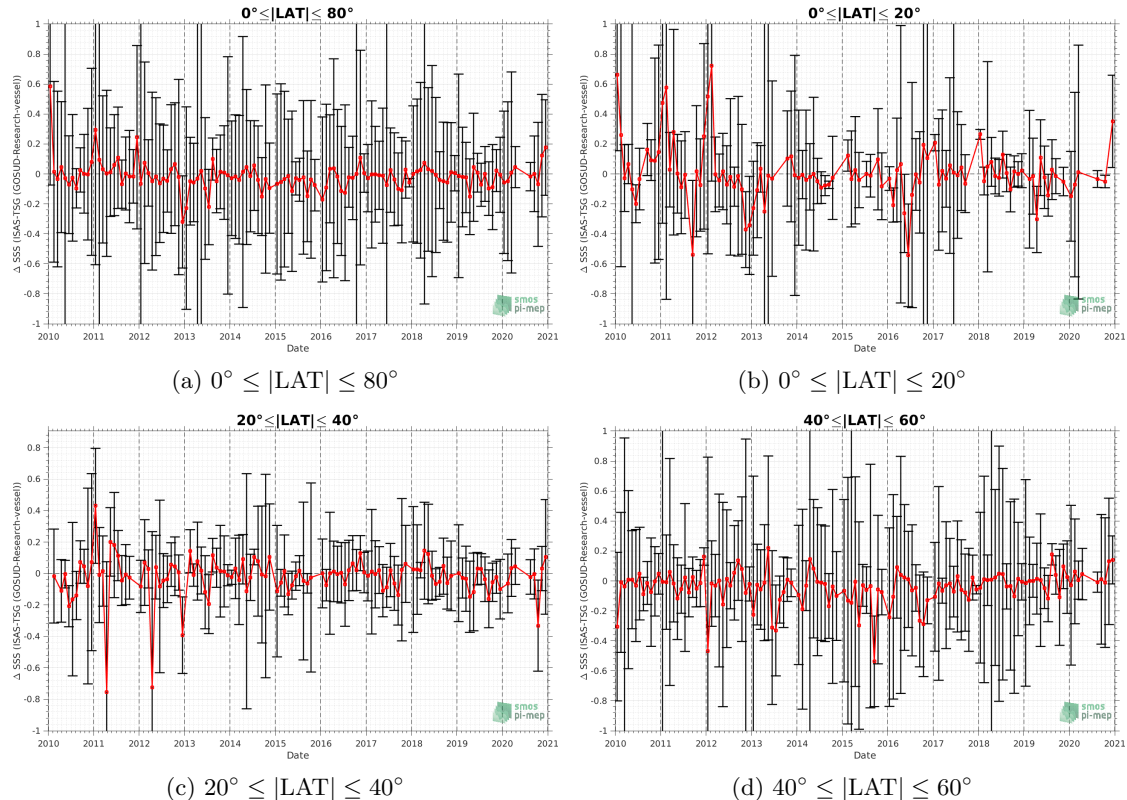


Figure 69: Monthly median (red curves) of ΔSSS (ISAS - TSG (GOSUD-Research-vessel)) and $\pm 1 \text{ Std}$ (black vertical thick bars) as function of time for all the collected Pi-MEP match-up pairs for the full *in situ* dataset period are shown for different latitude bands: (a) $80^\circ\text{S}-80^\circ\text{N}$, (b) $20^\circ\text{S}-20^\circ\text{N}$, (c) $40^\circ\text{S}-20^\circ\text{S}$ and $20^\circ\text{N}-40^\circ\text{N}$ and (d) $60^\circ\text{S}-40^\circ\text{S}$ and $40^\circ\text{N}-60^\circ\text{N}$.

6.2.11 ΔSSS sorted as geophysical conditions

In Figure 70, we classify the match-up differences ΔSSS (ISAS - *in situ*) as function of the geophysical conditions at match-up points. The mean and std of ΔSSS (ISAS - TSG (GOSUD-Research-vessel)) is thus evaluated as function of the

- *in situ* SSS values per bins of width 0.2,
- *in situ* SST values per bins of width 1°C ,
- ASCAT daily wind values per bins of width 1 m/s,
- CMORPH 3-hourly rain rates per bins of width 1 mm/h, and,
- distance to coasts per bins of width 50 km,
- *in situ* measurement depth (if relevant).

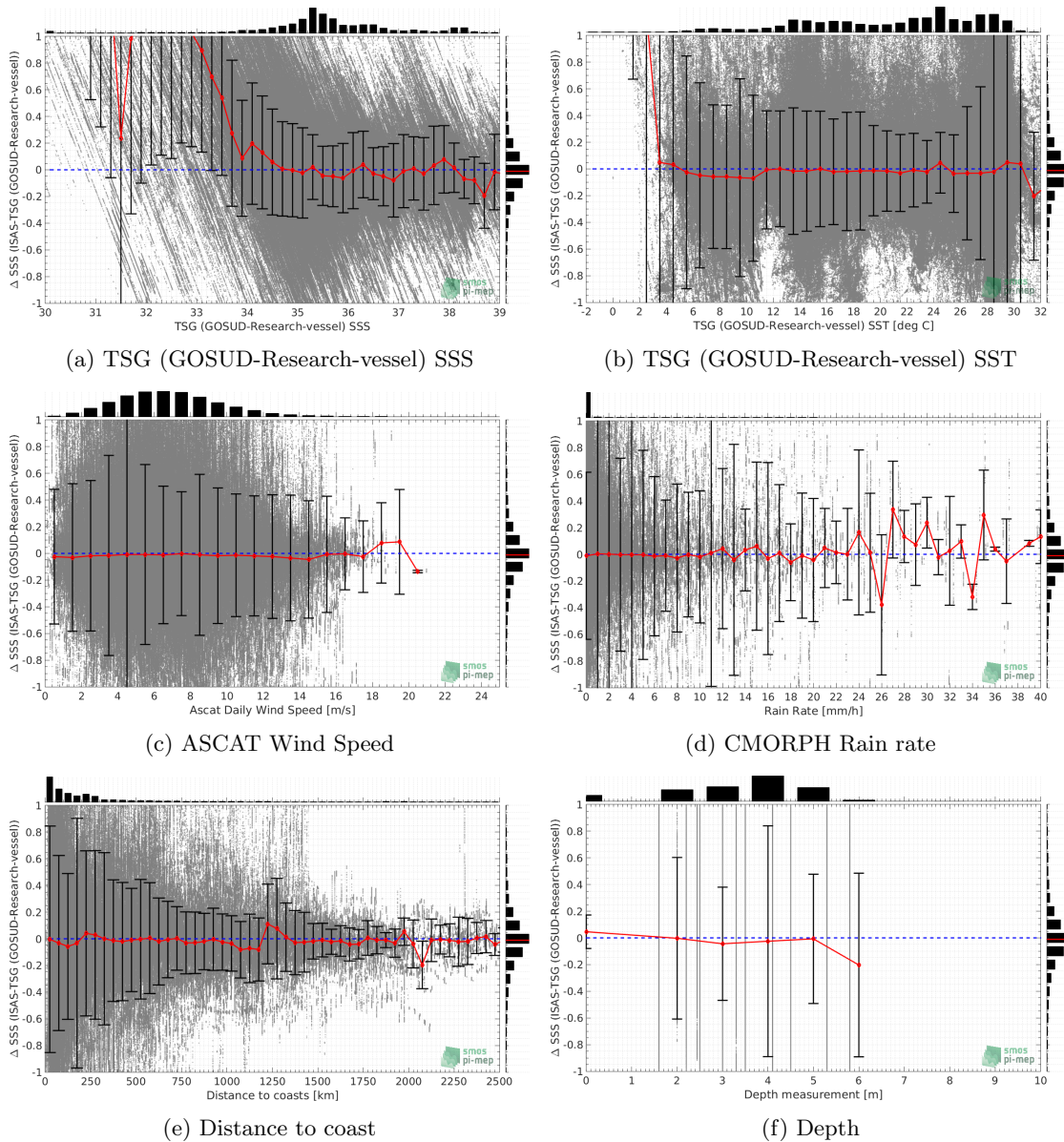


Figure 70: ΔSSS (ISAS - TSG (GOSUD-Research-vessel)) sorted as geophysical conditions: TSG (GOSUD-Research-vessel) SSS a), TSG (GOSUD-Research-vessel) SST b), ASCAT Wind speed c), CMORPH rain rate d), distance to coast (e) and depth measurements (f).

6.2.12 ΔSSS maps and statistics for different geophysical conditions

In Figures 71 and 72, we focus on sub-datasets of the match-up differences ΔSSS (*ISAS - in situ*) for the following specific geophysical conditions:

- **C1:** if the local value at *in situ* location of estimated rain rate is zero, mean daily wind is in the range [3, 12] m/s, the SST is $> 5^\circ\text{C}$ and distance to coast is > 800 km.
- **C2:** if the local value at *in situ* location of estimated rain rate is zero, mean daily wind is

in the range [3, 12] m/s.

- **C3:** if the local value at *in situ* location of estimated rain rate is high (ie. $> 1 \text{ mm/h}$) and mean daily wind is low (ie. $< 4 \text{ m/s}$).
- **C5:** if the *in situ* data is located where the climatological SSS standard deviation is low (ie. above < 0.2).
- **C6:** if the *in situ* data is located where the climatological SSS standard deviation is high (ie. above > 0.2).

For each of these conditions, the temporal mean (gridded over spatial boxes of size $1^\circ \times 1^\circ$) and the histogram of the difference ΔSSS (ISAS - *in situ*) are presented.

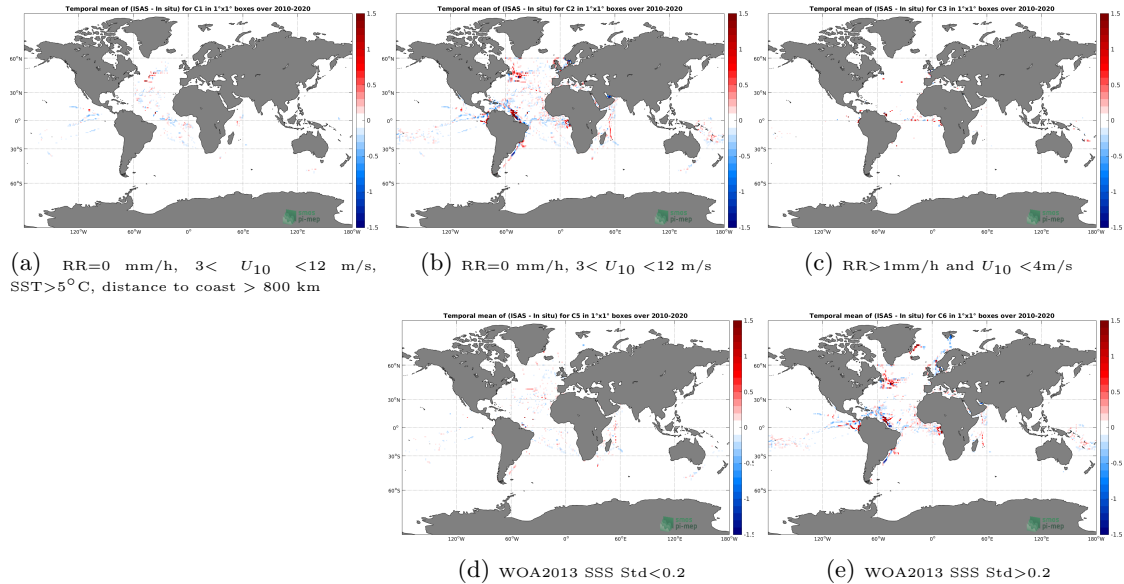


Figure 71: Temporal mean gridded over spatial boxes of size $1^\circ \times 1^\circ$ of ΔSSS (ISAS - TSG (GOSUD-Research-vessel)) for 5 different subdatasets corresponding to: RR=0 mm/h, $3 < U_{10} < 12 \text{ m/s}$, SST > 5°C , distance to coast > 800 km (a), RR=0 mm/h, $3 < U_{10} < 12 \text{ m/s}$ (b), RR > 1 mm/h and $U_{10} < 4 \text{ m/s}$ (c), WOA2013 SSS Std < 0.2 (d), WOA2013 SSS Std > 0.2 (e).

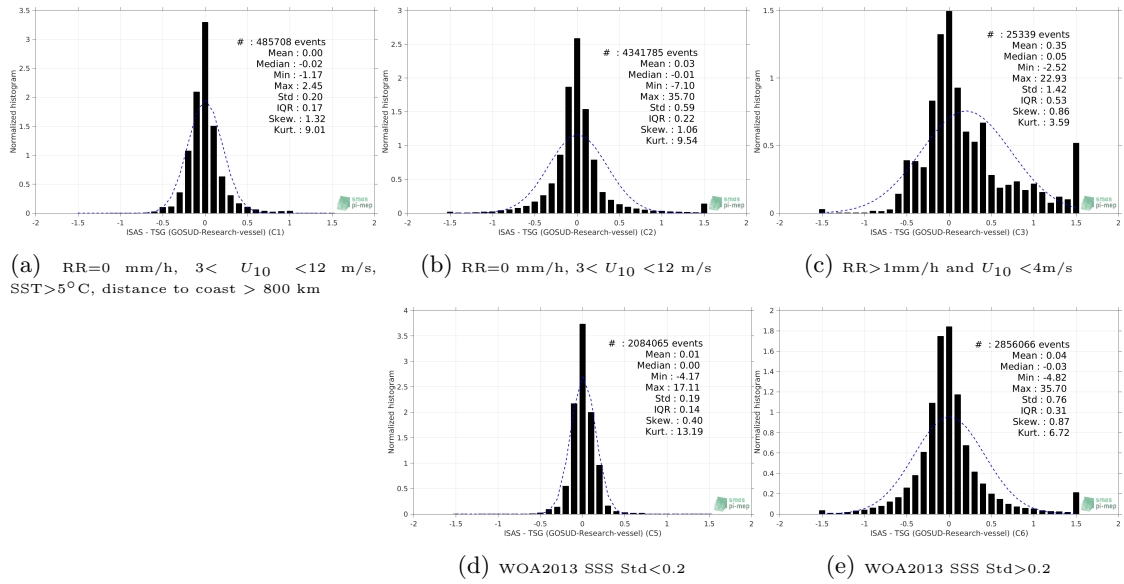


Figure 72: Normalized histogram of ΔSSS (ISAS - TSG (GOSUD-Research-vessel)) for 5 different subdatasets corresponding to: RR=0 mm/h, $3 < U_{10} < 12$ m/s, SST > 5°C, distance to coast > 800 km (a), RR=0 mm/h, $3 < U_{10} < 12$ m/s (b), RR > 1 mm/h and $U_{10} < 4$ m/s (c), WOA2013 SSS Std < 0.2 (d), WOA2013 SSS Std > 0.2 (e).

6.2.13 Summary

Table 1 shows the mean, median, standard deviation (Std), root mean square (RMS), interquartile range (IQR), correlation coefficient (r^2) and robust standard deviation (Std^*) of the match-up differences ΔSSS (ISAS - TSG (GOSUD-Research-vessel)) for the following conditions:

- all: All the match-up pairs satellite/in situ SSS values are used to derive the statistics
- C1: only pairs where RR=0 mm/h, $3 < U_{10} < 12$ m/s, SST > 5°C, distance to coast > 800 km
- C2: only pairs where RR=0 mm/h, $3 < U_{10} < 12$ m/s
- C3: only pairs where RR > 1 mm/h and $U_{10} < 4$ m/s
- C5: only pairs where WOA2013 SSS Std < 0.2
- C6: only pairs where WOA2013 SSS Std > 0.2
- C7a: only pairs with a distance to coast < 150 km.
- C7b: only pairs with a distance to coast in the range [150, 800] km.
- C7c: only pairs with a distance to coast > 800 km.
- C8a: only pairs where SST is < 5°C.
- C8b: only pairs where SST is in the range [5, 15]°C.
- C8c: only pairs where SST is > 15°C.

- C9a: only pairs where SSS is < 33.
- C9b: only pairs where SSS is in the range [33, 37].
- C9c: only pairs where SSS is > 37.

Table 1: Statistics of Δ SSS (ISAS - TSG (GOSUD-Research-vessel))

Condition	#	Median	Mean	Std	RMS	IQR	r^2	Std*
all	5707378	-0.01	0.04	0.66	0.66	0.23	0.888	0.17
C1	485708	-0.02	0.00	0.20	0.20	0.17	0.959	0.13
C2	4341785	-0.01	0.03	0.59	0.59	0.22	0.908	0.17
C3	25339	0.05	0.35	1.42	1.47	0.53	0.655	0.36
C5	2084065	0.00	0.01	0.19	0.19	0.14	0.960	0.11
C6	2856066	-0.03	0.04	0.76	0.76	0.31	0.893	0.23
C7a	2869194	-0.03	0.04	0.75	0.75	0.28	0.909	0.21
C7b	2214243	0.01	0.05	0.63	0.63	0.20	0.774	0.15
C7c	623089	-0.02	0.00	0.22	0.22	0.18	0.953	0.13
C8a	27431	0.13	0.51	1.47	1.56	1.54	0.918	1.17
C8b	1135698	-0.02	0.01	0.53	0.53	0.22	0.850	0.16
C8c	4267025	-0.01	0.04	0.69	0.70	0.23	0.890	0.17
C9a	183963	1.06	1.55	2.89	3.28	2.39	0.773	1.78
C9b	4615639	-0.01	0.00	0.32	0.32	0.23	0.813	0.17
C9c	907776	-0.03	-0.04	0.25	0.25	0.19	0.859	0.14

Table 1 numerical values can be downloaded as a csv file [here](#).

6.3 TSG (GOSUD-Sailing-ship)

6.3.1 Introduction

The TSG (GOSUD-Sailing-ship) dataset corresponds to observations of sea surface salinity obtained from voluntary sailing ships using medium or small size sensors. They complement the networks installed on research vessels or commercial ships. This delayed mode dataset ([Reynaud et al. \(2021\)](#)) is updated annually as a contribution to GOSUD (<http://www.gosud.org>) and freely available [here](#). Adjusted values when available and only collected TSG data that exhibit quality flags=1 and 2 were used.

6.3.2 Number of SSS data as a function of time and distance to coast

Figure 73 shows the time (a) and distance to coast (b) distributions of the TSG (GOSUD-Sailing-ship) *in situ* dataset.

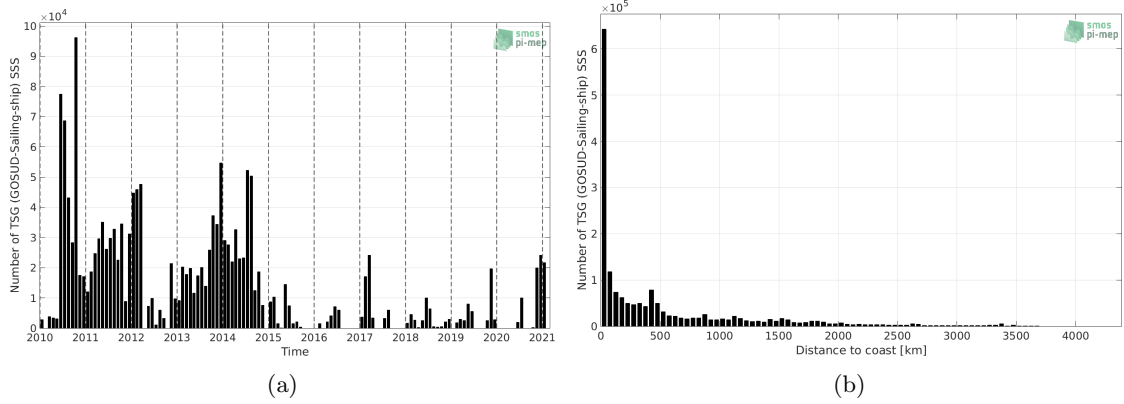


Figure 73: Number of SSS from TSG (GOSUD-Sailing-ship) as a function of time (a) and distance to coast (b).

6.3.3 Histograms of SSS

Figure 74 shows the SSS distribution of the TSG (GOSUD-Sailing-ship) (a) and colocalized ISAS (b) dataset.

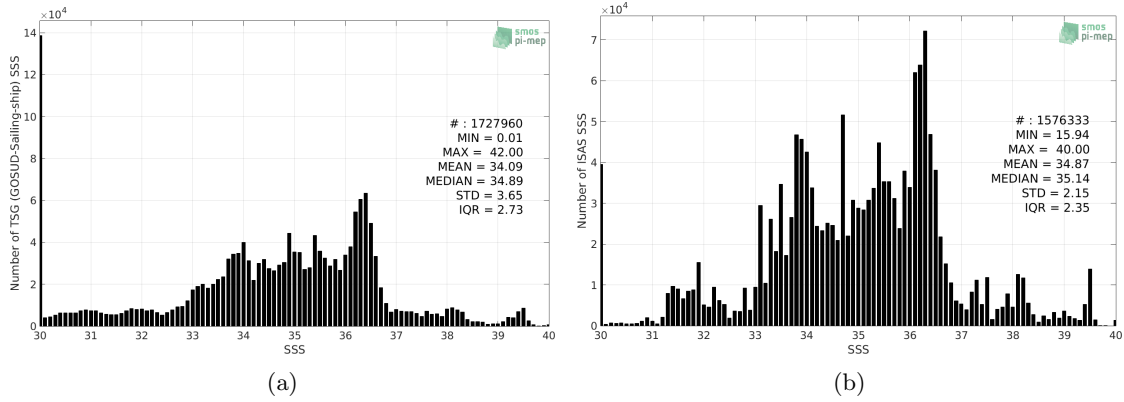


Figure 74: Histograms of SSS from TSG (GOSUD-Sailing-ship) (a) and ISAS (b) per bins of 0.1.

6.3.4 Distribution of *in situ* SSS depth measurements

In Figure 75, we show the depth distribution of the *in situ* salinity dataset (a) and the spatial distribution of the depth temporal mean in $1^\circ \times 1^\circ$ boxes and considering the full *in situ* dataset period (b).

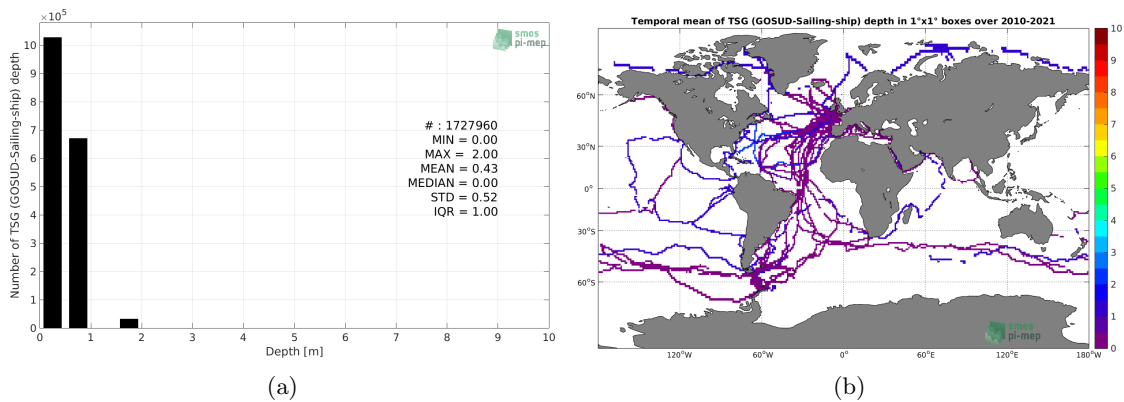


Figure 75: Depth distribution of the upper level SSS measurements from TSG (GOSUD-Sailing-ship) (a) and spatial distribution of the *in situ* SSS depth measurements showing the mean value in $1^\circ \times 1^\circ$ boxes and considering the full *in situ* dataset period (b).

6.3.5 Spatial distribution of SSS

In Figure 76, the number of TSG (GOSUD-Sailing-ship) SSS measurements in $1^\circ \times 1^\circ$ boxes is shown.

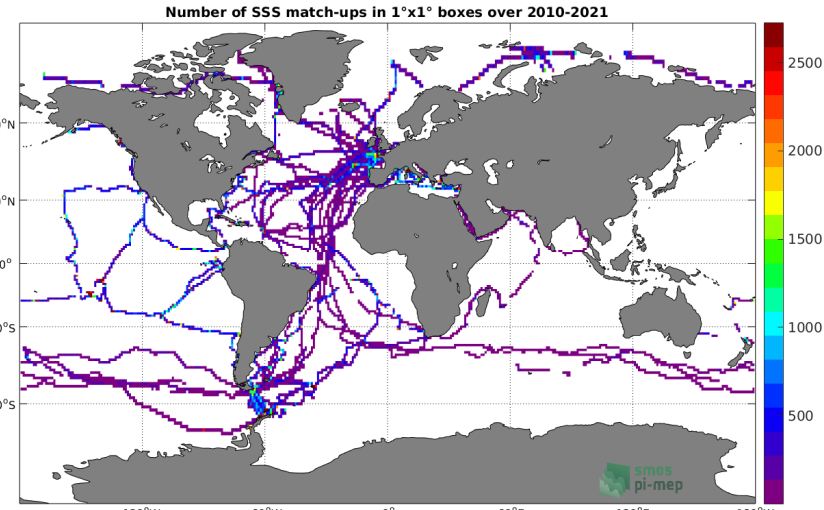


Figure 76: Number of SSS from TSG (GOSUD-Sailing-ship) in $1^\circ \times 1^\circ$ boxes.

6.3.6 Spatial Maps of the Temporal mean and Std of *in situ* and ISAS SSS and of the difference (Δ SSS)

In Figure 77, maps of temporal mean (left) and standard deviation (right) of ISAS (top), TSG (GOSUD-Sailing-ship) *in situ* dataset (middle) and the difference Δ SSS(ISAS -TSG (GOSUD-Sailing-ship)) (bottom) are shown. The temporal mean and std are calculated using all match-up pairs falling in spatial boxes of size $1^\circ \times 1^\circ$ over the full TSG (GOSUD-Sailing-ship) dataset period.

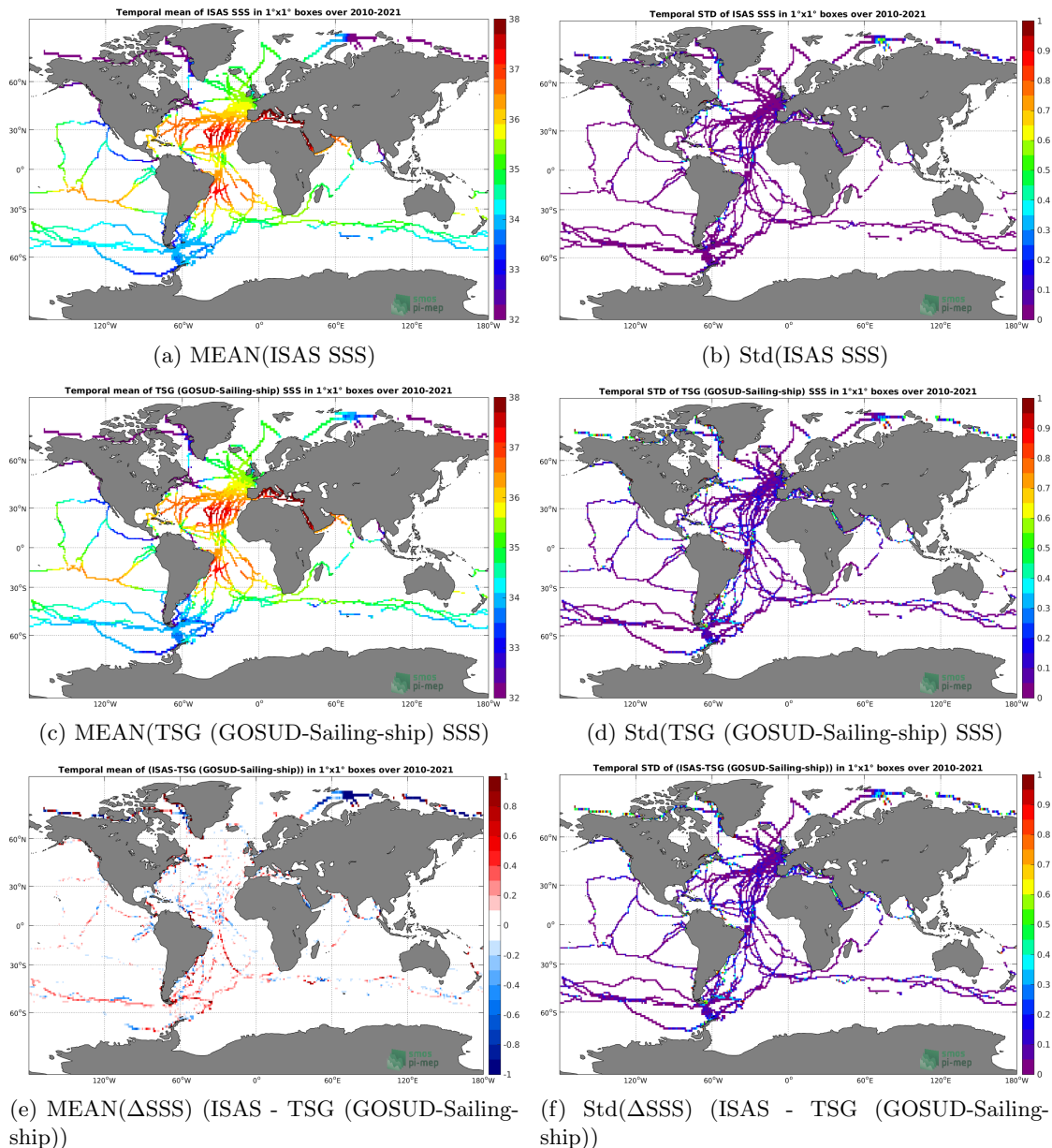


Figure 77: Temporal mean (left) and Std (right) of SSS from ISAS (top), TSG (GOSUD-Sailing-ship) (middle), and of Δ SSS (ISAS - TSG (GOSUD-Sailing-ship)). Only match-up pairs are used to generate these maps.

6.3.7 Time series of the monthly median and Std of *in situ* and ISAS SSS and of the difference (Δ SSS)

In the top panel of Figure 78, we show the time series of the monthly median SSS estimated for both ISAS SSS product (in black) and the TSG (GOSUD-Sailing-ship) *in situ* dataset (in blue) at the collected Pi-MEP match-up pairs.

In the middle panel of Figure 78, we show the time series of the monthly median of Δ SSS

(ISAS - TSG (GOSUD-Sailing-ship)) for the collected Pi-MEP match-up pairs.

In the bottom panel of Figure 78, we show the time series of the monthly standard deviation of the Δ SSS (ISAS - TSG (GOSUD-Sailing-ship)) for the collected Pi-MEP match-up pairs.

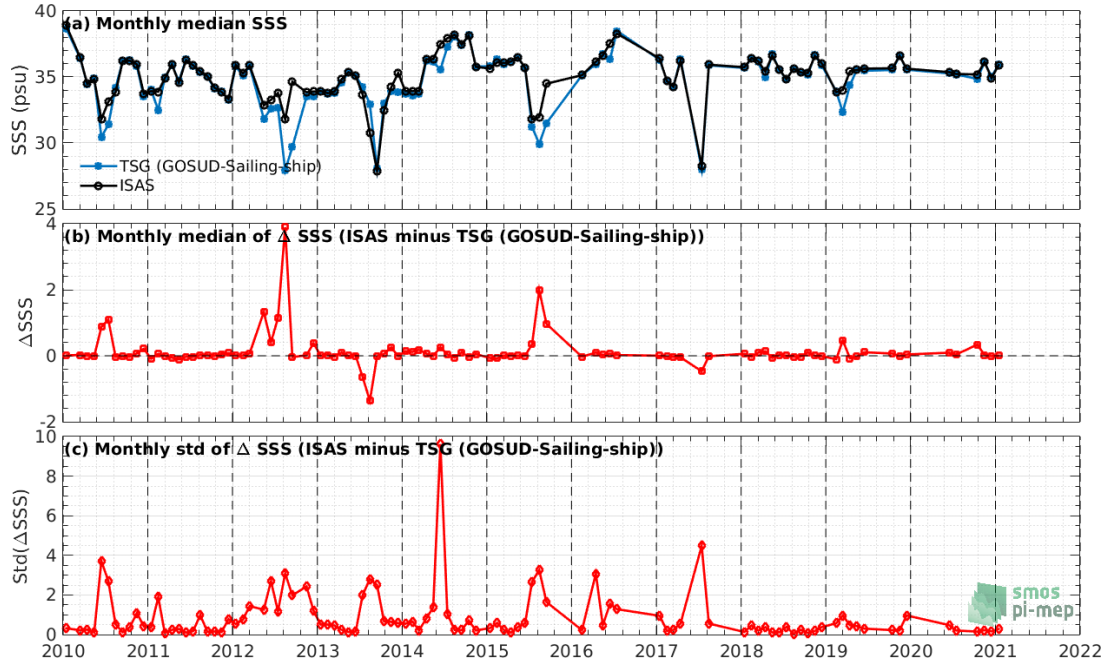


Figure 78: Time series of the monthly median SSS (top), median of Δ SSS (ISAS - TSG (GOSUD-Sailing-ship)) and Std of Δ SSS (ISAS - TSG (GOSUD-Sailing-ship)) considering all match-ups collected by the Pi-MEP.

6.3.8 Zonal mean and Std of *in situ* and ISAS SSS and of the difference Δ SSS

In Figure 79 left panel, we show the zonal mean SSS considering all Pi-MEP match-up pairs for both ISAS SSS product (in black) and the TSG (GOSUD-Sailing-ship) *in situ* dataset (in blue). The full *in situ* dataset period is used to derive the mean.

In the right panel of Figure 79, we show the zonal mean of Δ SSS (ISAS - TSG (GOSUD-Sailing-ship)) for all the collected Pi-MEP match-up pairs estimated over the full *in situ* dataset period.

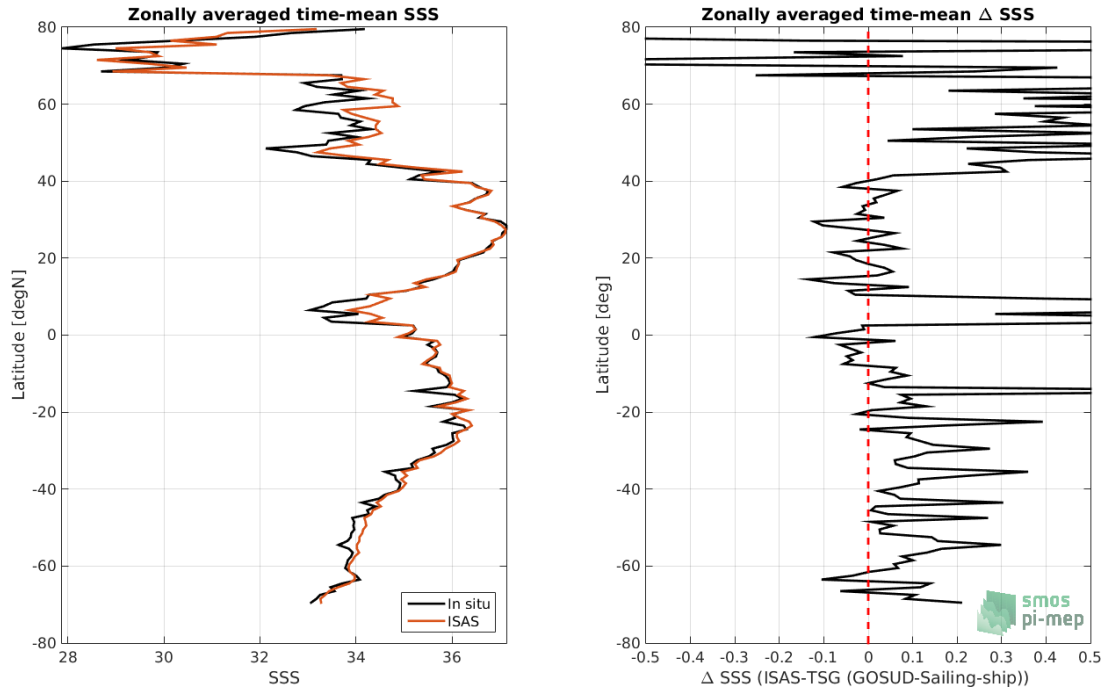


Figure 79: Left panel: Zonal mean SSS from ISAS product (black) and from TSG (GOSUD-Sailing-ship) (blue). Right panel: Zonal mean of Δ SSS (ISAS - TSG (GOSUD-Sailing-ship)) for all the collected Pi-MEP match-up pairs estimated over the full *in situ* dataset period.

6.3.9 Scatterplots of ISAS vs *in situ* SSS by latitudinal bands

In Figure 80, contour maps of the concentration of ISAS SSS (y-axis) versus TSG (GOSUD-Sailing-ship) SSS (x-axis) at match-up pairs for different latitude bands: (a) 80°S-80°N, (b) 20°S-20°N, (c) 40°S-20°S and 20°N-40°N and (d) 60°S-40°S and 40°N-60°N. For each plot, the red line shows $x=y$. The black thin and dashed lines indicate a linear fit through the data cloud and the $\pm 95\%$ confidence levels, respectively. The number match-up pairs n , the slope and R^2 coefficient of the linear fit, the root mean square (RMS) and the mean bias between ISAS and *in situ* data are indicated for each latitude band in each plots.

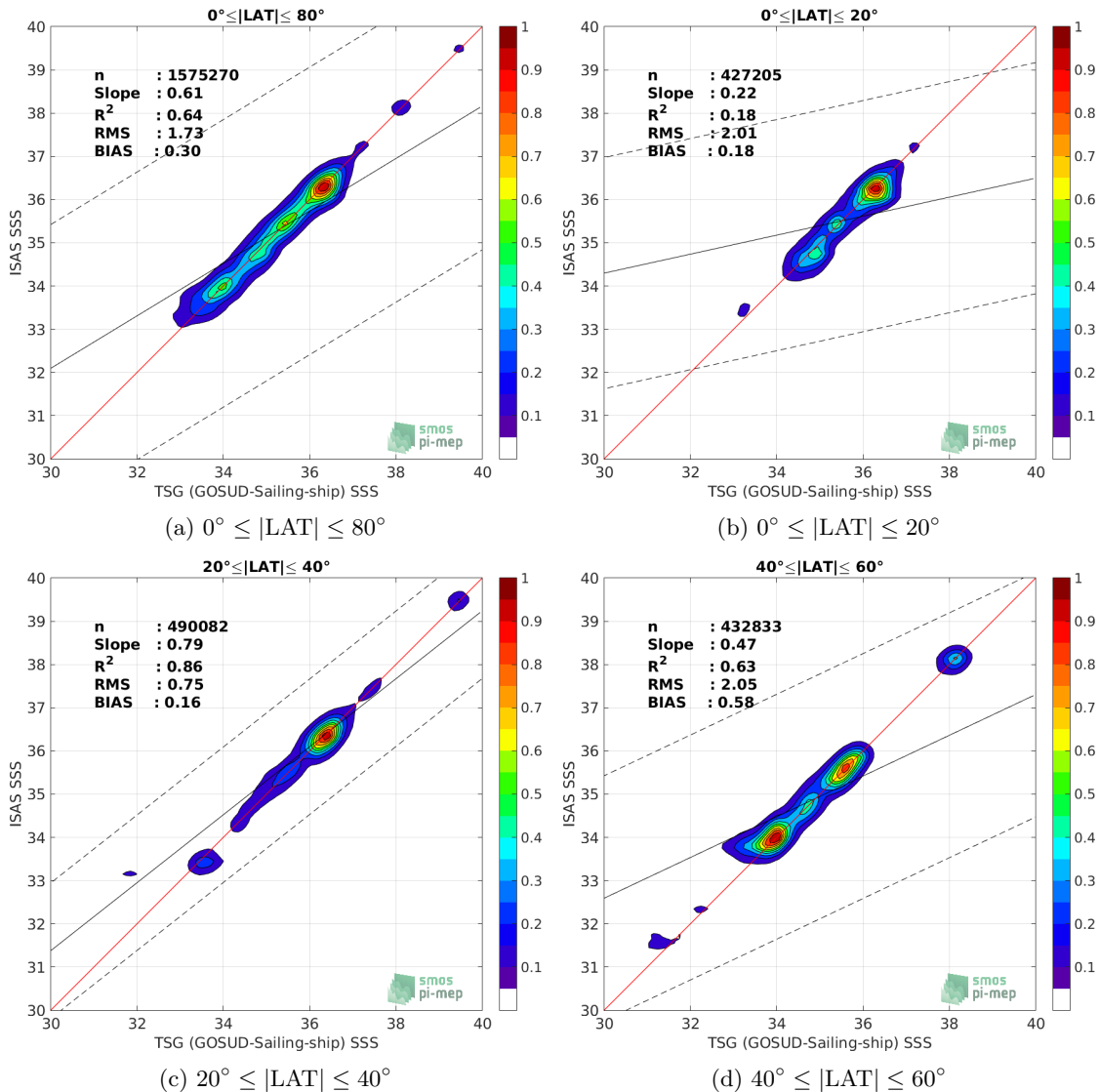


Figure 80: Contour maps of the concentration of ISAS SSS (y-axis) versus TSG (GOSUD-Sailing-ship) SSS (x-axis) at match-up pairs for different latitude bands. For each plot, the red line shows $x=y$. The black thin and dashed lines indicate a linear fit through the data cloud and the $\pm 95\%$ confidence levels, respectively. The number match-up pairs n , the slope and R^2 coefficient of the linear fit, the root mean square (RMS) and the mean bias between ISAS and *in situ* data are indicated for each latitude band in each plots.

6.3.10 Time series of the monthly median and Std of the difference ΔSSS sorted by latitudinal bands

In Figure 81, time series of the monthly median (red curves) of ΔSSS (ISAS - TSG (GOSUD-Sailing-ship)) and ± 1 Std (black vertical thick bars) as function of time for all the collected Pi-MEP match-up pairs estimated for the full *in situ* dataset period are shown for different latitude bands: (a) $80^\circ\text{S}-80^\circ\text{N}$, (b) $20^\circ\text{S}-20^\circ\text{N}$, (c) $40^\circ\text{S}-20^\circ\text{S}$ and $20^\circ\text{N}-40^\circ\text{N}$ and (d) $60^\circ\text{S}-40^\circ\text{S}$

and 40°N-60°N.

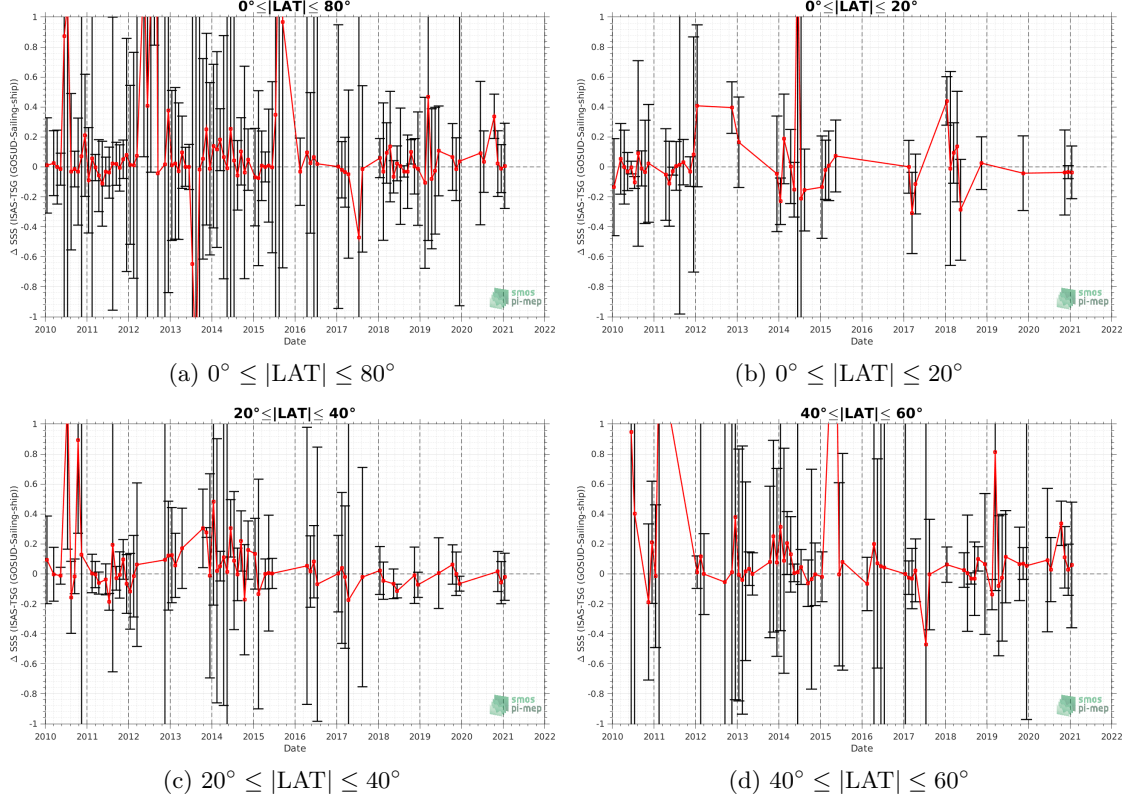


Figure 81: Monthly median (red curves) of Δ_{SSS} (ISAS - TSG (GOSUD-Sailing-ship)) and ± 1 Std (black vertical thick bars) as function of time for all the collected Pi-MEP match-up pairs for the full *in situ* dataset period are shown for different latitude bands: (a) $80^\circ\text{S}-80^\circ\text{N}$, (b) $20^\circ\text{S}-20^\circ\text{N}$, (c) $40^\circ\text{S}-20^\circ\text{S}$ and $20^\circ\text{N}-40^\circ\text{N}$ and (d) $60^\circ\text{S}-40^\circ\text{S}$ and $40^\circ\text{N}-60^\circ\text{N}$.

6.3.11 Δ_{SSS} sorted as geophysical conditions

In Figure 82, we classify the match-up differences Δ_{SSS} (ISAS - *in situ*) as function of the geophysical conditions at match-up points. The mean and std of Δ_{SSS} (ISAS - TSG (GOSUD-Sailing-ship)) is thus evaluated as function of the

- *in situ* SSS values per bins of width 0.2,
- *in situ* SST values per bins of width 1°C ,
- ASCAT daily wind values per bins of width 1 m/s,
- CMORPH 3-hourly rain rates per bins of width 1 mm/h, and,
- distance to coasts per bins of width 50 km,
- *in situ* measurement depth (if relevant).

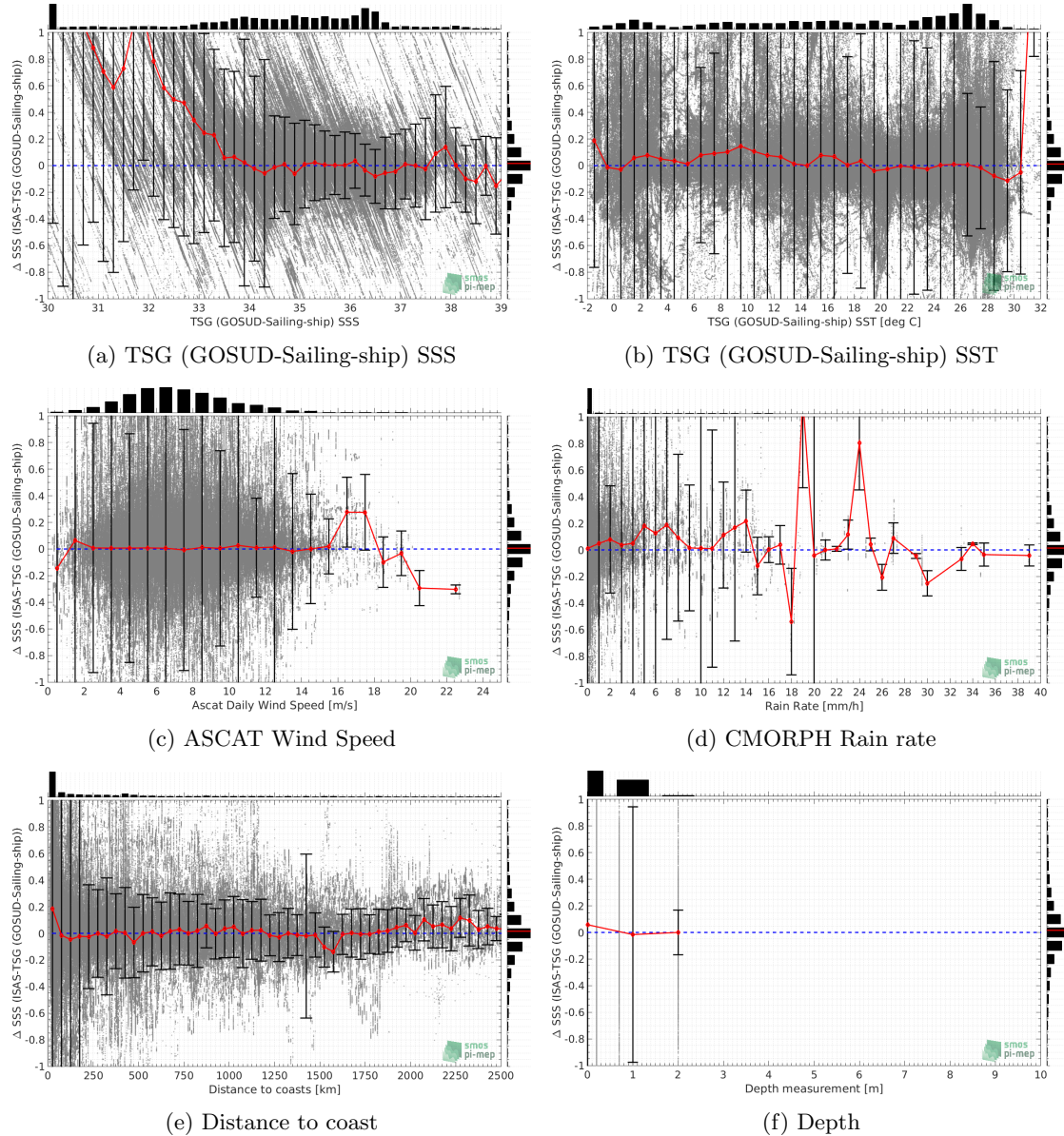


Figure 82: ΔSSS (ISAS - TSG (GOSUD-Sailing-ship)) sorted as geophysical conditions: TSG (GOSUD-Sailing-ship) SSS a), TSG (GOSUD-Sailing-ship) SST b), ASCAT Wind speed c), CMORPH rain rate d), distance to coast (e) and depth measurements (f).

6.3.12 ΔSSS maps and statistics for different geophysical conditions

In Figures 83 and 84, we focus on sub-datasets of the match-up differences ΔSSS (ISAS - *in situ*) for the following specific geophysical conditions:

- **C1:** if the local value at *in situ* location of estimated rain rate is zero, mean daily wind is in the range [3, 12] m/s, the SST is $> 5^{\circ}\text{C}$ and distance to coast is > 800 km.
- **C2:** if the local value at *in situ* location of estimated rain rate is zero, mean daily wind is

in the range [3, 12] m/s.

- **C3:** if the local value at *in situ* location of estimated rain rate is high (ie. $> 1 \text{ mm/h}$) and mean daily wind is low (ie. $< 4 \text{ m/s}$).
- **C5:** if the *in situ* data is located where the climatological SSS standard deviation is low (ie. above < 0.2).
- **C6:** if the *in situ* data is located where the climatological SSS standard deviation is high (ie. above > 0.2).

For each of these conditions, the temporal mean (gridded over spatial boxes of size $1^\circ \times 1^\circ$) and the histogram of the difference ΔSSS (ISAS - *in situ*) are presented.

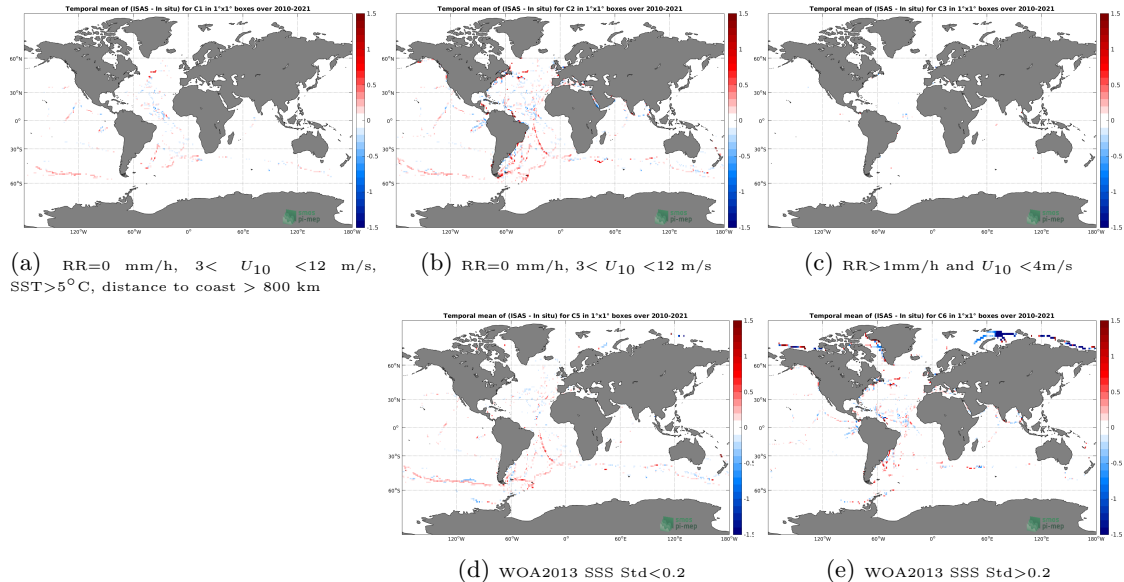


Figure 83: Temporal mean gridded over spatial boxes of size $1^\circ \times 1^\circ$ of ΔSSS (ISAS - TSG (GOSUD-Sailing-ship)) for 5 different subdatasets corresponding to: RR=0 mm/h, $3 < U_{10} < 12 \text{ m/s}$, SST > 5°C , distance to coast > 800 km (a), RR=0 mm/h, $3 < U_{10} < 12 \text{ m/s}$ (b), RR > 1mm/h and $U_{10} < 4 \text{ m/s}$ (c), WOA2013 SSS Std < 0.2 (d), WOA2013 SSS Std > 0.2 (e).

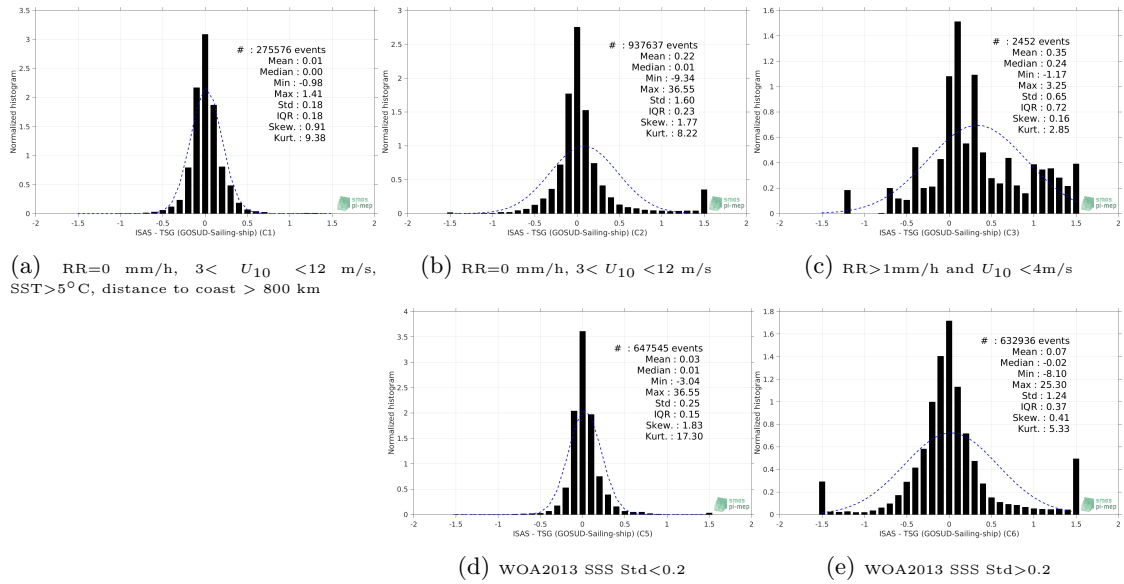


Figure 84: Normalized histogram of ΔSSS (ISAS - TSG (GOSUD-Sailing-ship)) for 5 different subdatasets corresponding to: RR=0 mm/h, $3 < U_{10} < 12$ m/s, SST> 5°C , distance to coast > 800 km (a), RR=0 mm/h, $3 < U_{10} < 12$ m/s (b), RR>1mm/h and $U_{10} < 4$ m/s (c), WOA2013 SSS Std<0.2 (d), WOA2013 SSS Std>0.2 (e).

6.3.13 Summary

Table 1 shows the mean, median, standard deviation (Std), root mean square (RMS), interquartile range (IQR), correlation coefficient (r^2) and robust standard deviation (Std^*) of the match-up differences ΔSSS (ISAS - TSG (GOSUD-Sailing-ship)) for the following conditions:

- all: All the match-up pairs satellite/in situ SSS values are used to derive the statistics
- C1: only pairs where RR=0 mm/h, $3 < U_{10} < 12$ m/s, SST> 5°C , distance to coast > 800 km
- C2: only pairs where RR=0 mm/h, $3 < U_{10} < 12$ m/s
- C3: only pairs where RR>1mm/h and $U_{10} < 4$ m/s
- C5: only pairs where WOA2013 SSS Std<0.2
- C6: only pairs where WOA2013 SSS Std>0.2
- C7a: only pairs with a distance to coast < 150 km.
- C7b: only pairs with a distance to coast in the range [150, 800] km.
- C7c: only pairs with a distance to coast > 800 km.
- C8a: only pairs where SST is < 5°C .
- C8b: only pairs where SST is in the range [$5, 15$] $^{\circ}\text{C}$.
- C8c: only pairs where SST is > 15°C .

- C9a: only pairs where SSS is < 33.
- C9b: only pairs where SSS is in the range [33, 37].
- C9c: only pairs where SSS is > 37.

Table 1: Statistics of ΔSSS (ISAS - TSG (GOSUD-Sailing-ship))

Condition	#	Median	Mean	Std	RMS	IQR	r^2	Std*
all	1576333	0.02	0.30	1.79	1.81	0.30	0.614	0.21
C1	275576	0.00	0.01	0.18	0.18	0.18	0.971	0.13
C2	937637	0.01	0.22	1.60	1.61	0.23	0.563	0.16
C3	2452	0.24	0.35	0.65	0.74	0.72	0.940	0.44
C5	647545	0.01	0.03	0.25	0.26	0.15	0.961	0.11
C6	632936	-0.02	0.07	1.24	1.24	0.37	0.793	0.27
C7a	682646	0.08	0.71	2.62	2.71	0.78	0.536	0.41
C7b	506386	-0.01	-0.02	0.54	0.54	0.20	0.900	0.15
C7c	387171	0.00	0.02	0.22	0.22	0.18	0.960	0.13
C8a	218628	0.05	-0.02	1.47	1.47	0.60	0.721	0.44
C8b	322858	0.05	0.58	1.85	1.94	0.38	0.643	0.22
C8c	983777	0.00	0.21	1.76	1.77	0.23	0.457	0.17
C9a	242798	1.00	1.97	4.04	4.49	2.22	0.123	1.44
C9b	1201251	0.00	0.00	0.48	0.48	0.22	0.819	0.17
C9c	132284	0.00	0.01	0.33	0.33	0.21	0.850	0.16

Table 1 numerical values can be downloaded as a csv file [here](#).

6.4 TSG (SAMOS)

6.4.1 Introduction

The TSG (SAMOS) dataset corresponds to "Research" quality data from the US Shipboard Automated Meteorological and Oceanographic System (SAMOS) initiative ([Smith et al. \(2009\)](#)). Data are available at <http://samos.coaps.fsu.edu/html/>. Adjusted values when available and only collected TSG data that exhibit quality flags=1 and 2 were used. After visual inspection, data from the NANCY FOSTER (ID="WTER", IMO="008993227") with date 2011/03/21 and all data from the ATLANTIS (ID="KAQP", IMO="009105798") for year 2010 have been removed from this dataset. For years, 2013 to 2022, RV Laurence Gould And Nathaniel Palmer data are coming from the "Intermediate" repository.

6.4.2 Number of SSS data as a function of time and distance to coast

Figure 85 shows the time (a) and distance to coast (b) distributions of the TSG (SAMOS) *in situ* dataset.

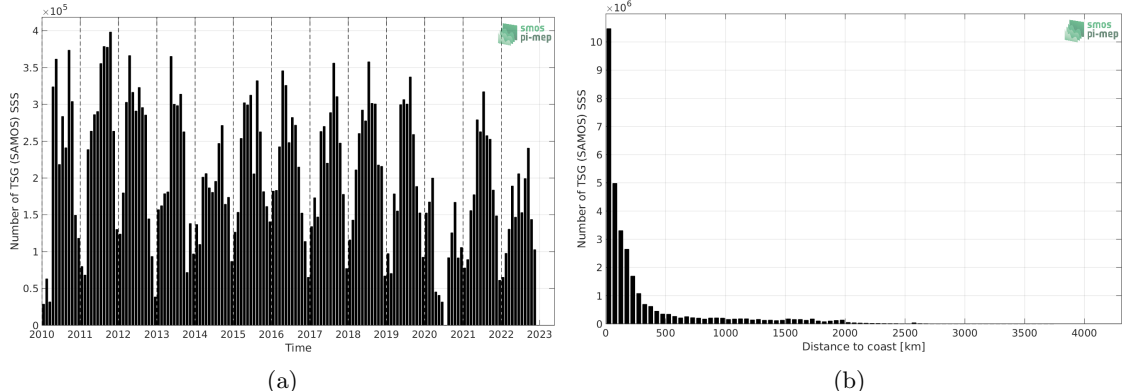


Figure 85: Number of SSS from TSG (SAMOS) as a function of time (a) and distance to coast (b).

6.4.3 Histograms of SSS

Figure 86 shows the SSS distribution of the TSG (SAMOS) (a) and colocalized ISAS (b) dataset.

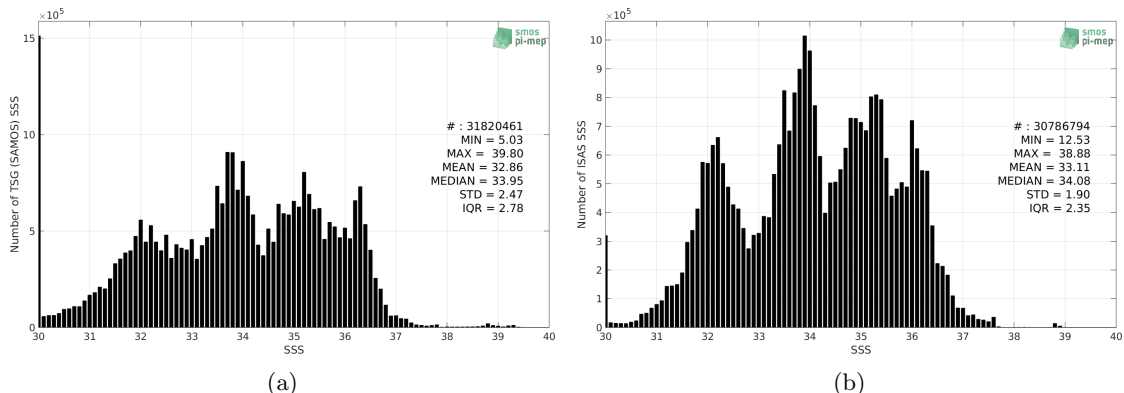


Figure 86: Histograms of SSS from TSG (SAMOS) (a) and ISAS (b) per bins of 0.1.

6.4.4 Distribution of *in situ* SSS depth measurements

In Figure 87, we show the depth distribution of the *in situ* salinity dataset (a) and the spatial distribution of the depth temporal mean in $1^\circ \times 1^\circ$ boxes and considering the full *in situ* dataset period (b).

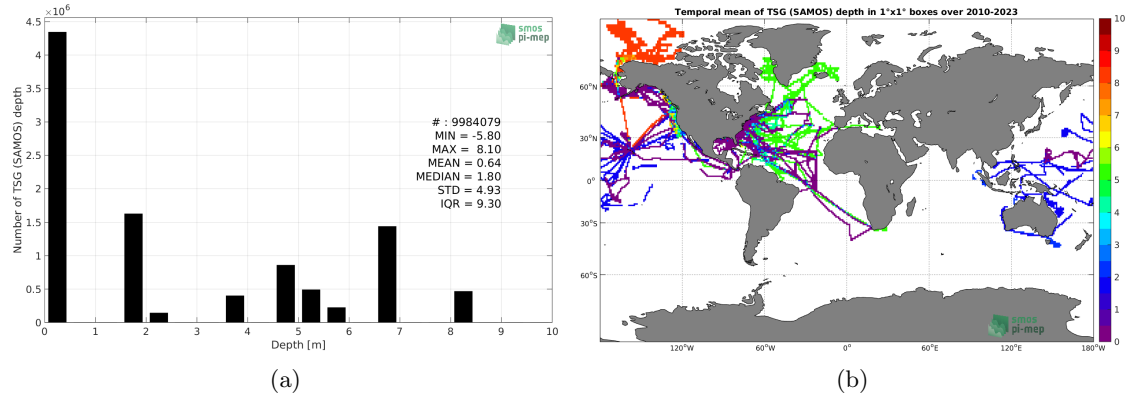


Figure 87: Depth distribution of the upper level SSS measurements from TSG (SAMOS) (a) and spatial distribution of the *in situ* SSS depth measurements showing the mean value in $1^\circ \times 1^\circ$ boxes and considering the full *in situ* dataset period (b).

6.4.5 Spatial distribution of SSS

In Figure 88, the number of TSG (SAMOS) SSS measurements in $1^\circ \times 1^\circ$ boxes is shown.

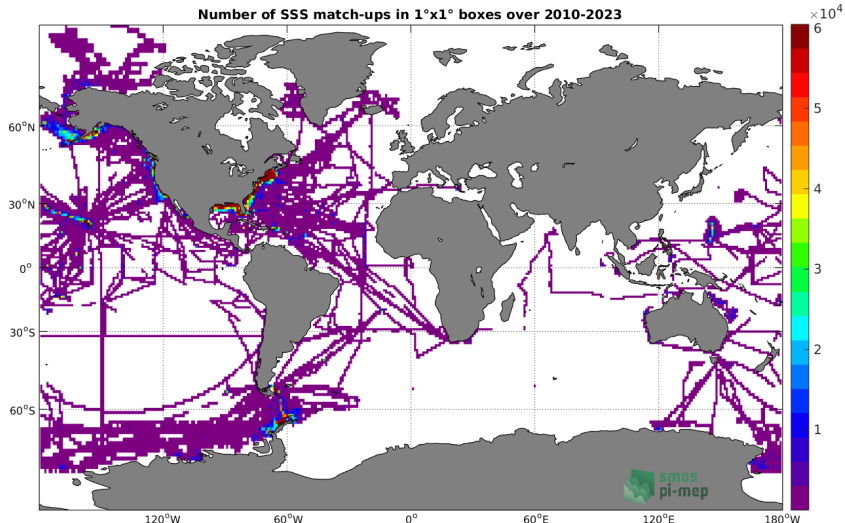


Figure 88: Number of SSS from TSG (SAMOS) in $1^\circ \times 1^\circ$ boxes.

6.4.6 Spatial Maps of the Temporal mean and Std of *in situ* and ISAS SSS and of the difference (Δ SSS)

In Figure 89, maps of temporal mean (left) and standard deviation (right) of ISAS (top), TSG (SAMOS) *in situ* dataset (middle) and the difference Δ SSS(ISAS -TSG (SAMOS)) (bottom) are shown. The temporal mean and std are calculated using all match-up pairs falling in spatial boxes of size $1^\circ \times 1^\circ$ over the full TSG (SAMOS) dataset period.

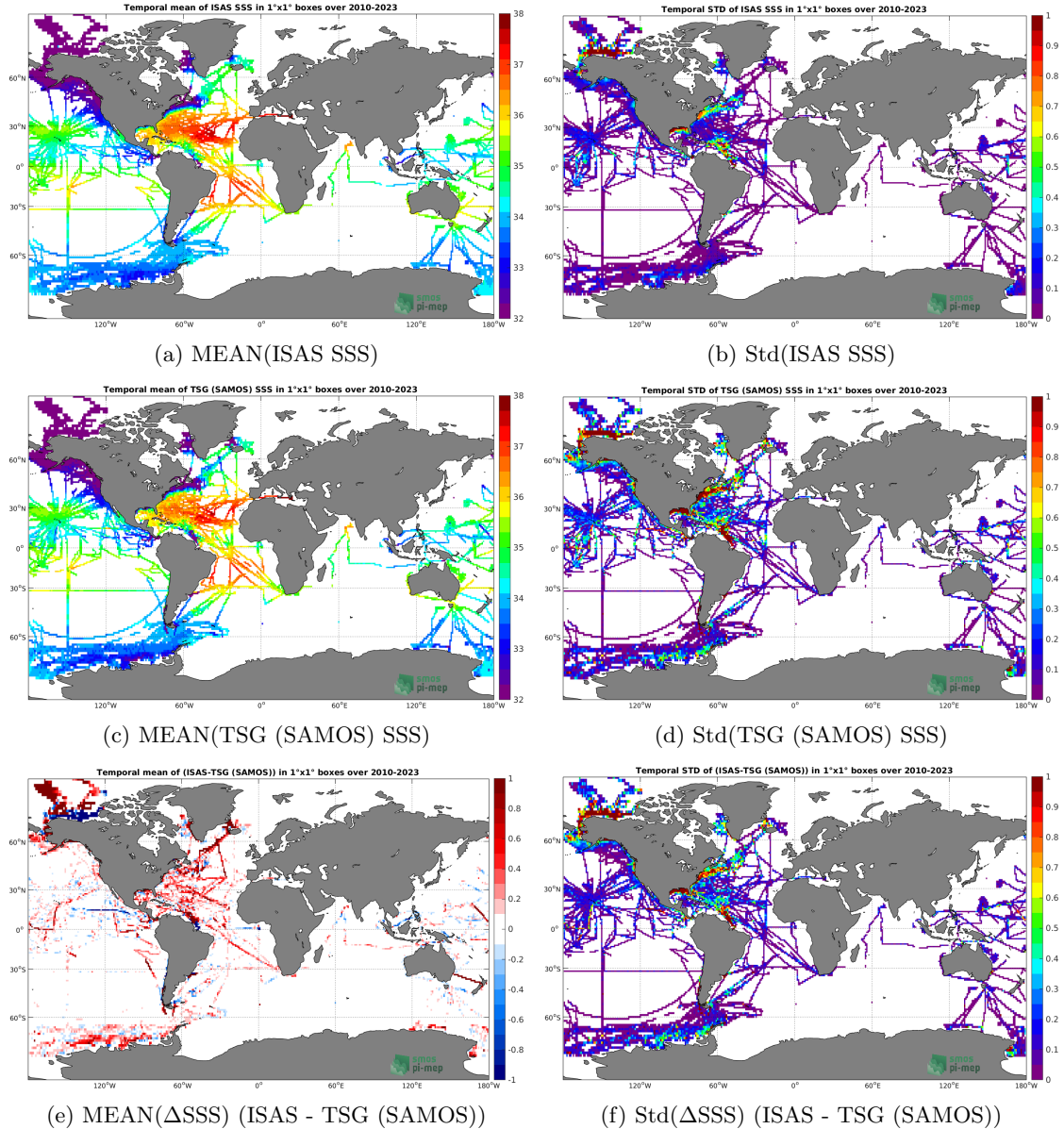


Figure 89: Temporal mean (left) and Std (right) of SSS from ISAS (top), TSG (SAMOS) (middle), and of Δ SSS (ISAS - TSG (SAMOS)). Only match-up pairs are used to generate these maps.

6.4.7 Time series of the monthly median and Std of *in situ* and ISAS SSS and of the difference (Δ SSS)

In the top panel of Figure 90, we show the time series of the monthly median SSS estimated for both ISAS SSS product (in black) and the TSG (SAMOS) *in situ* dataset (in blue) at the collected Pi-MEP match-up pairs.

In the middle panel of Figure 90, we show the time series of the monthly median of Δ SSS

(ISAS - TSG (SAMOS)) for the collected Pi-MEP match-up pairs.

In the bottom panel of Figure 90, we show the time series of the monthly standard deviation of the Δ SSS (ISAS - TSG (SAMOS)) for the collected Pi-MEP match-up pairs.

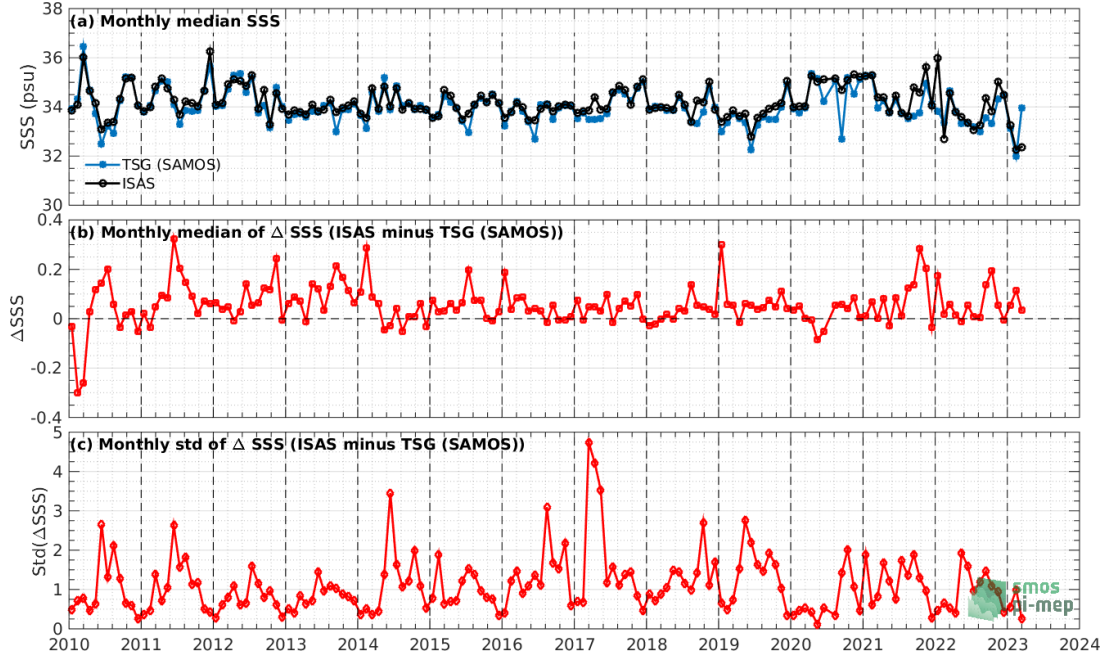


Figure 90: Time series of the monthly median SSS (top), median of Δ SSS (ISAS - TSG (SAMOS)) and Std of Δ SSS (ISAS - TSG (SAMOS)) considering all match-ups collected by the Pi-MEP.

6.4.8 Zonal mean and Std of *in situ* and ISAS SSS and of the difference Δ SSS

In Figure 91 left panel, we show the zonal mean SSS considering all Pi-MEP match-up pairs for both ISAS SSS product (in black) and the TSG (SAMOS) *in situ* dataset (in blue). The full *in situ* dataset period is used to derive the mean.

In the right panel of Figure 91, we show the zonal mean of Δ SSS (ISAS - TSG (SAMOS)) for all the collected Pi-MEP match-up pairs estimated over the full *in situ* dataset period.

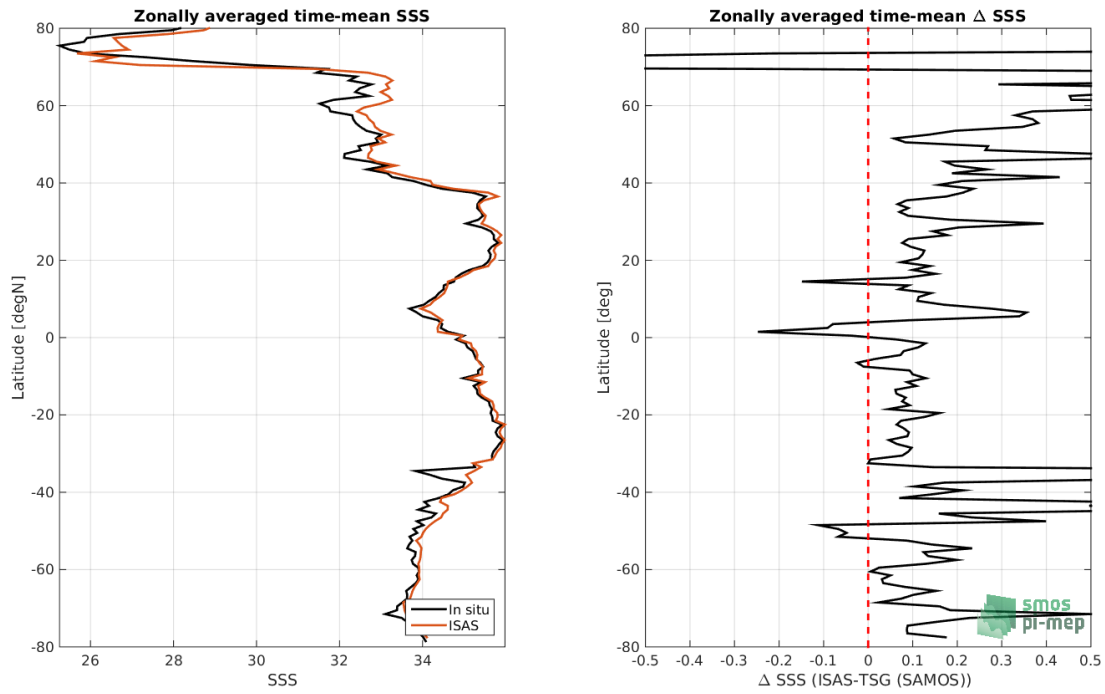


Figure 91: Left panel: Zonal mean SSS from ISAS product (black) and from TSG (SAMOS) (blue). Right panel: Zonal mean of Δ SSS (ISAS - TSG (SAMOS)) for all the collected Pi-MEP match-up pairs estimated over the full *in situ* dataset period.

6.4.9 Scatterplots of ISAS vs *in situ* SSS by latitudinal bands

In Figure 92, contour maps of the concentration of ISAS SSS (y-axis) versus TSG (SAMOS) SSS (x-axis) at match-up pairs for different latitude bands: (a) 80°S-80°N, (b) 20°S-20°N, (c) 40°S-20°S and 20°N-40°N and (d) 60°S-40°S and 40°N-60°N. For each plot, the red line shows $x=y$. The black thin and dashed lines indicate a linear fit through the data cloud and the $\pm 95\%$ confidence levels, respectively. The number match-up pairs n , the slope and R^2 coefficient of the linear fit, the root mean square (RMS) and the mean bias between ISAS and *in situ* data are indicated for each latitude band in each plots.

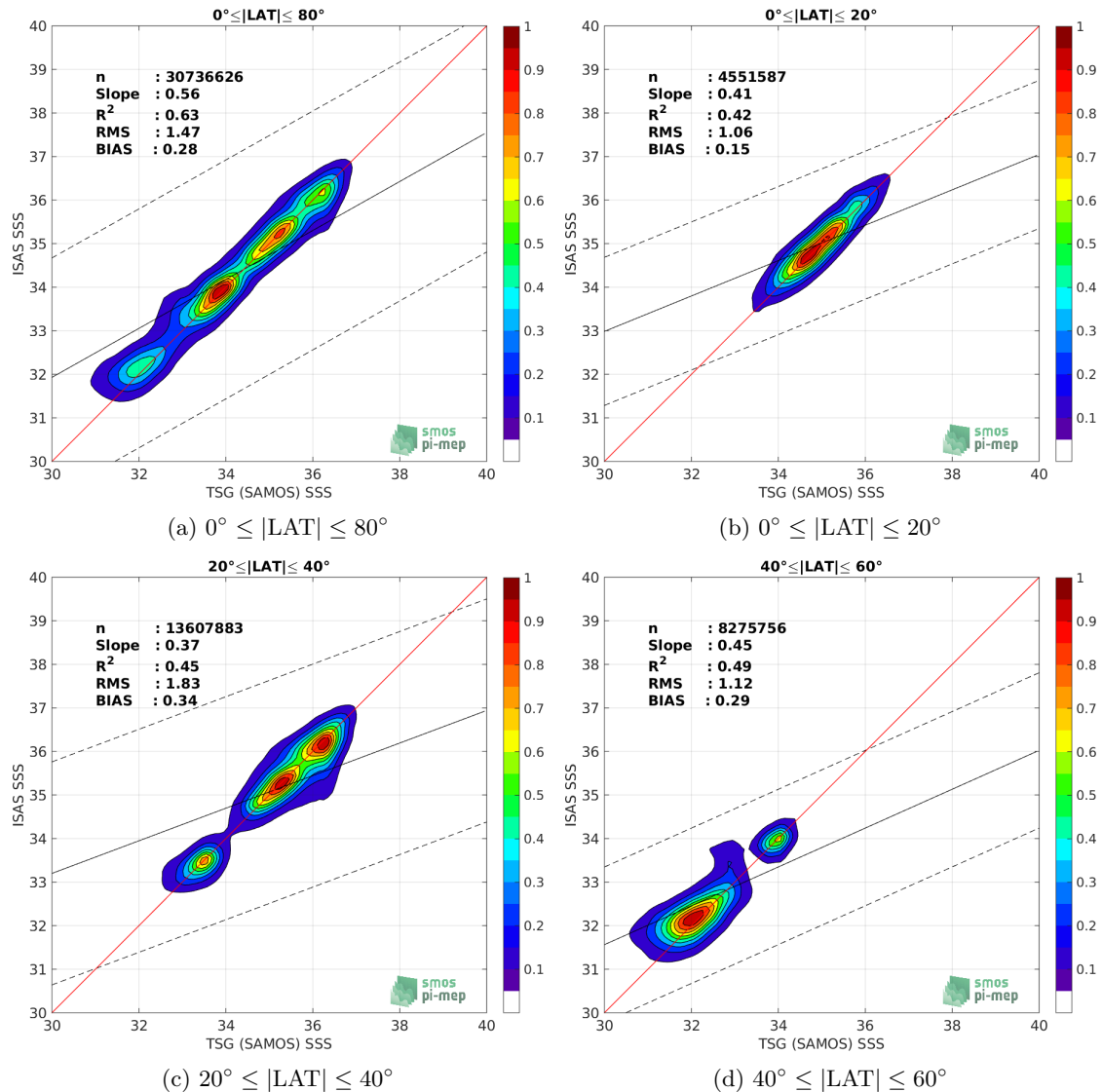


Figure 92: Contour maps of the concentration of ISAS SSS (y-axis) versus TSG (SAMOS) SSS (x-axis) at match-up pairs for different latitude bands. For each plot, the red line shows $x=y$. The black thin and dashed lines indicate a linear fit through the data cloud and the $\pm 95\%$ confidence levels, respectively. The number match-up pairs n , the slope and R^2 coefficient of the linear fit, the root mean square (RMS) and the mean bias between ISAS and *in situ* data are indicated for each latitude band in each plots.

6.4.10 Time series of the monthly median and Std of the difference ΔSSS sorted by latitudinal bands

In Figure 93, time series of the monthly median (red curves) of ΔSSS (ISAS - TSG (SAMOS)) and ± 1 Std (black vertical thick bars) as function of time for all the collected Pi-MEP match-up pairs estimated for the full *in situ* dataset period are shown for different latitude bands: (a) $80^\circ\text{S}-80^\circ\text{N}$, (b) $20^\circ\text{S}-20^\circ\text{N}$, (c) $40^\circ\text{S}-20^\circ\text{S}$ and $20^\circ\text{N}-40^\circ\text{N}$ and (d) $60^\circ\text{S}-40^\circ\text{S}$ and $40^\circ\text{N}-60^\circ\text{N}$.

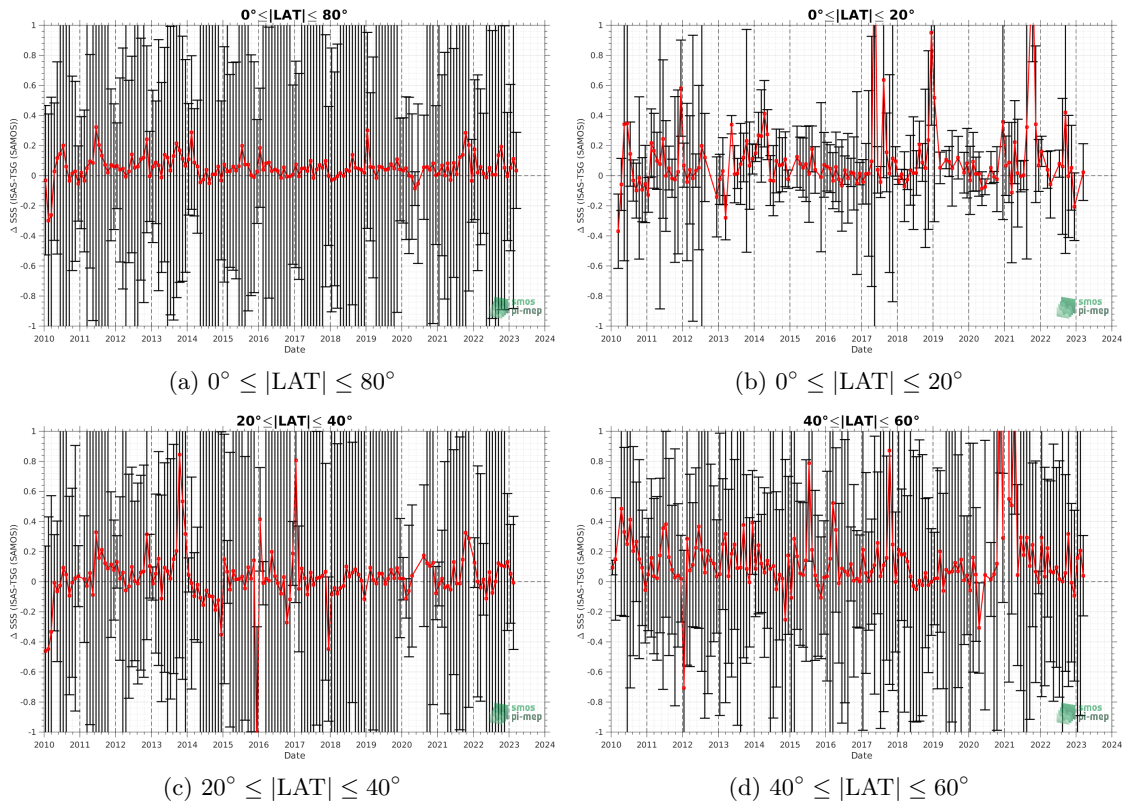


Figure 93: Monthly median (red curves) of ΔSSS (ISAS - TSG (SAMOS)) and $\pm 1 \text{ Std}$ (black vertical thick bars) as function of time for all the collected Pi-MEP match-up pairs for the full *in situ* dataset period are shown for different latitude bands: (a) $80^\circ\text{S}-80^\circ\text{N}$, (b) $20^\circ\text{S}-20^\circ\text{N}$, (c) $40^\circ\text{S}-20^\circ\text{S}$ and $20^\circ\text{N}-40^\circ\text{N}$ and (d) $60^\circ\text{S}-40^\circ\text{N}$ and $40^\circ\text{N}-60^\circ\text{N}$.

6.4.11 ΔSSS sorted as geophysical conditions

In Figure 94, we classify the match-up differences ΔSSS (ISAS - *in situ*) as function of the geophysical conditions at match-up points. The mean and std of ΔSSS (ISAS - TSG (SAMOS)) is thus evaluated as function of the

- *in situ* SSS values per bins of width 0.2,
- *in situ* SST values per bins of width 1°C ,
- ASCAT daily wind values per bins of width 1 m/s,
- CMORPH 3-hourly rain rates per bins of width 1 mm/h, and,
- distance to coasts per bins of width 50 km,
- *in situ* measurement depth (if relevant).

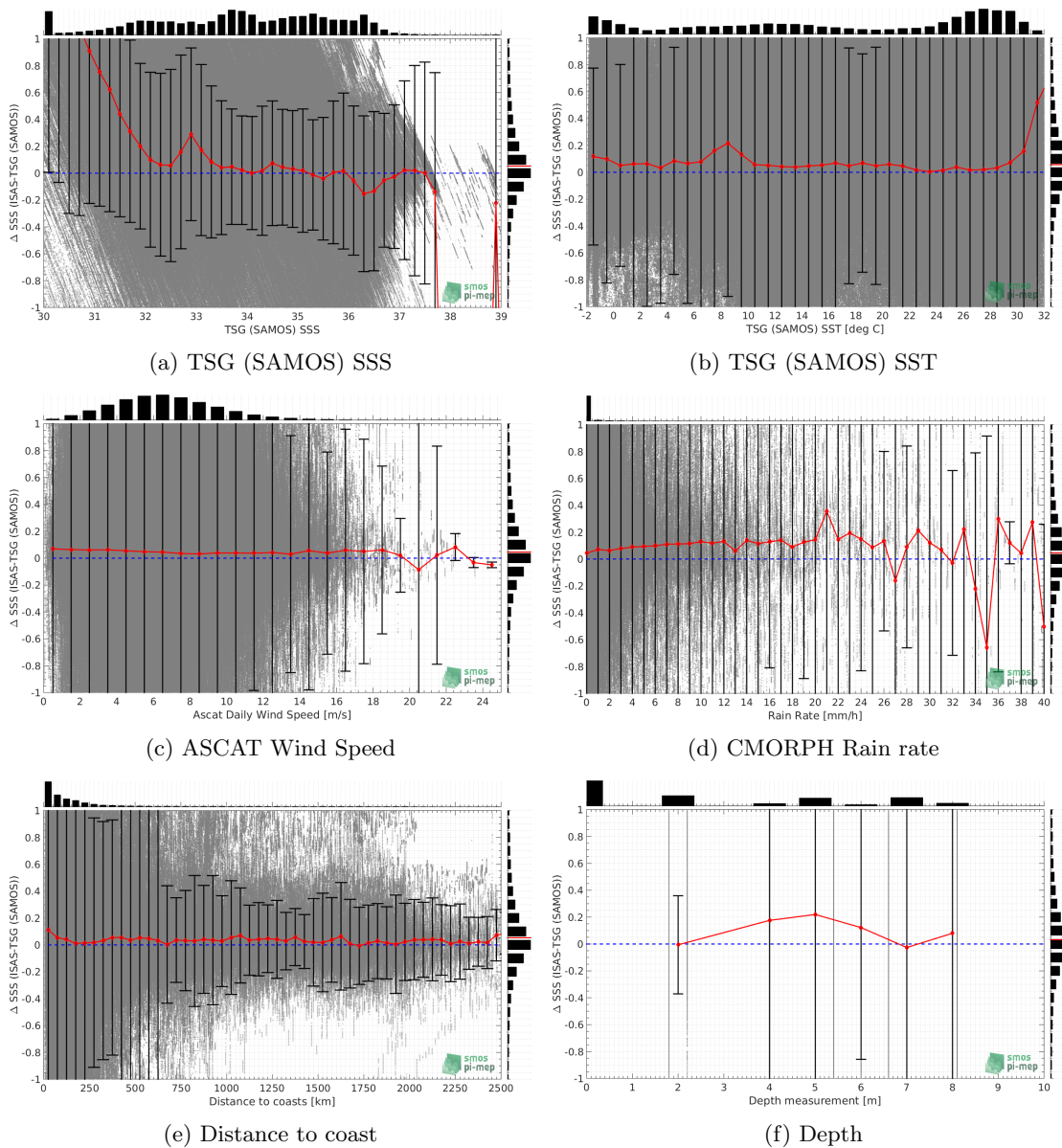


Figure 94: ΔSSS (ISAS - TSG (SAMOS)) sorted as geophysical conditions: TSG (SAMOS) SSS a), TSG (SAMOS) SST b), ASCAT Wind speed c), CMORPH rain rate d), distance to coast e) and depth measurements f).

6.4.12 ΔSSS maps and statistics for different geophysical conditions

In Figures 95 and 96, we focus on sub-datasets of the match-up differences ΔSSS (*ISAS - in situ*) for the following specific geophysical conditions:

- **C1:** if the local value at *in situ* location of estimated rain rate is zero, mean daily wind is in the range [3, 12] m/s, the SST is $> 5^\circ\text{C}$ and distance to coast is > 800 km.
- **C2:** if the local value at *in situ* location of estimated rain rate is zero, mean daily wind is

in the range [3, 12] m/s.

- **C3:** if the local value at *in situ* location of estimated rain rate is high (ie. $> 1 \text{ mm/h}$) and mean daily wind is low (ie. $< 4 \text{ m/s}$).
- **C5:** if the *in situ* data is located where the climatological SSS standard deviation is low (ie. above < 0.2).
- **C6:** if the *in situ* data is located where the climatological SSS standard deviation is high (ie. above > 0.2).

For each of these conditions, the temporal mean (gridded over spatial boxes of size $1^\circ \times 1^\circ$) and the histogram of the difference ΔSSS (ISAS - *in situ*) are presented.

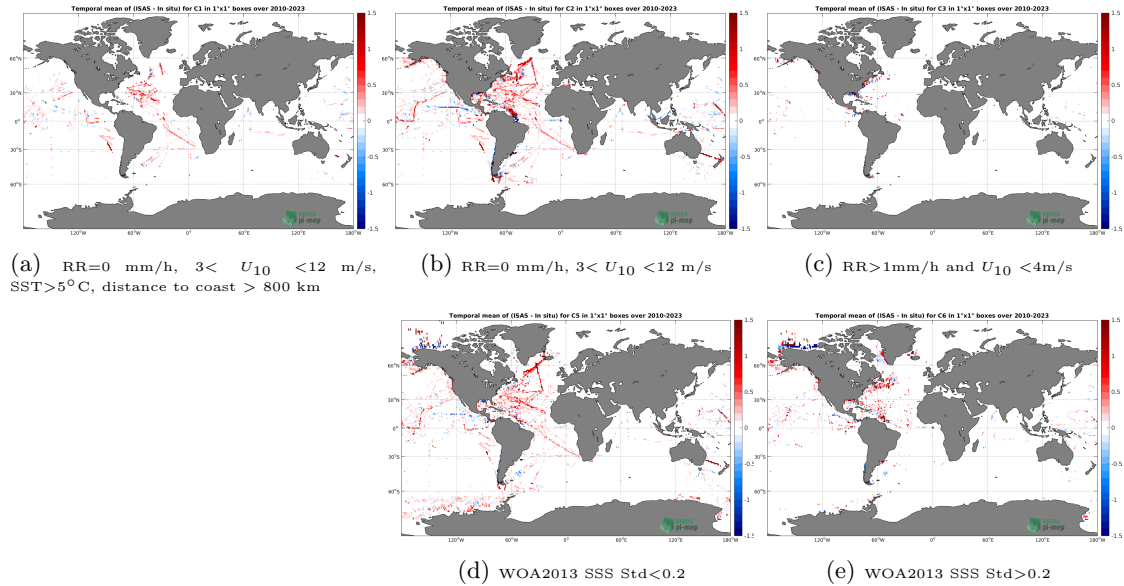


Figure 95: Temporal mean gridded over spatial boxes of size $1^\circ \times 1^\circ$ of ΔSSS (ISAS - TSG (SAMOS)) for 5 different subdatasets corresponding to: $\text{RR}=0 \text{ mm/h}, 3 < U_{10} < 12 \text{ m/s}, \text{SST} > 5^\circ\text{C}, \text{distance to coast} > 800 \text{ km}$ (a), $\text{RR}=0 \text{ mm/h}, 3 < U_{10} < 12 \text{ m/s}$ (b), $\text{RR} > 1\text{mm/h} \text{ and } U_{10} < 4\text{m/s}$ (c), WOA2013 SSS Std < 0.2 (d), WOA2013 SSS Std > 0.2 (e).

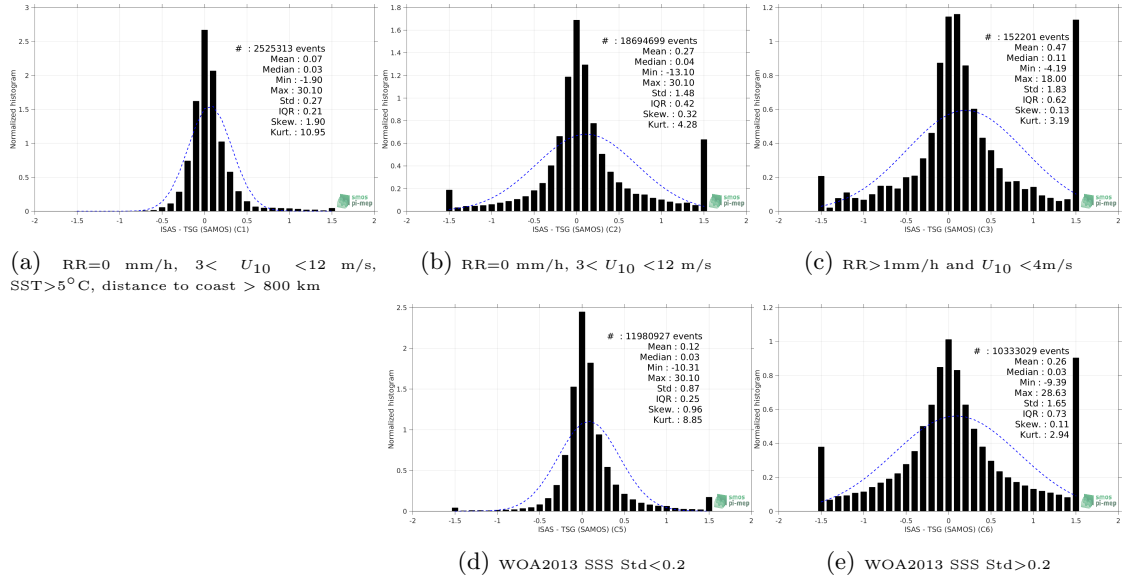


Figure 96: Normalized histogram of ΔSSS (ISAS - TSG (SAMOS)) for 5 different subdatasets corresponding to: RR=0 mm/h, $3 < U_{10} < 12$ m/s, SST > 5°C, distance to coast > 800 km (a), RR=0 mm/h, $3 < U_{10} < 12$ m/s (b), RR > 1mm/h and $U_{10} < 4$ m/s (c), WOA2013 SSS Std < 0.2 (d), WOA2013 SSS Std > 0.2 (e).

6.4.13 Summary

Table 1 shows the mean, median, standard deviation (Std), root mean square (RMS), interquartile range (IQR), correlation coefficient (r^2) and robust standard deviation (Std*) of the match-up differences ΔSSS (ISAS - TSG (SAMOS)) for the following conditions:

- all: All the match-up pairs satellite/in situ SSS values are used to derive the statistics
- C1: only pairs where RR=0 mm/h, $3 < U_{10} < 12$ m/s, SST > 5°C, distance to coast > 800 km
- C2: only pairs where RR=0 mm/h, $3 < U_{10} < 12$ m/s
- C3: only pairs where RR > 1mm/h and $U_{10} < 4$ m/s
- C5: only pairs where WOA2013 SSS Std < 0.2
- C6: only pairs where WOA2013 SSS Std > 0.2
- C7a: only pairs with a distance to coast < 150 km.
- C7b: only pairs with a distance to coast in the range [150, 800] km.
- C7c: only pairs with a distance to coast > 800 km.
- C8a: only pairs where SST is < 5°C.
- C8b: only pairs where SST is in the range [5, 15]°C.
- C8c: only pairs where SST is > 15°C.

- C9a: only pairs where SSS is < 33.
- C9b: only pairs where SSS is in the range [33, 37].
- C9c: only pairs where SSS is > 37.

Table 1: Statistics of Δ SSS (ISAS - TSG (SAMOS))

Condition	#	Median	Mean	Std	RMS	IQR	r^2	Std*
all	30786794	0.05	0.28	1.44	1.47	0.44	0.630	0.31
C1	2525313	0.03	0.07	0.27	0.28	0.21	0.916	0.16
C2	18694699	0.04	0.27	1.48	1.51	0.42	0.576	0.30
C3	152201	0.11	0.47	1.83	1.89	0.62	0.493	0.43
C5	11980927	0.03	0.12	0.87	0.88	0.25	0.741	0.18
C6	10333029	0.03	0.26	1.65	1.67	0.73	0.502	0.54
C7a	17834915	0.08	0.39	1.67	1.72	0.58	0.495	0.40
C7b	8953395	0.03	0.13	1.21	1.21	0.35	0.638	0.26
C7c	3969498	0.03	0.09	0.33	0.35	0.22	0.919	0.16
C8a	5167845	0.08	0.16	0.86	0.88	0.36	0.709	0.25
C8b	7195006	0.08	0.29	1.30	1.33	0.59	0.401	0.41
C8c	16703261	0.04	0.32	1.63	1.66	0.41	0.512	0.29
C9a	9410604	0.37	0.98	2.33	2.52	1.05	0.061	0.67
C9b	21085018	0.01	-0.02	0.51	0.52	0.30	0.831	0.22
C9c	291172	-0.07	-1.02	1.57	1.87	2.82	0.074	0.33

Table 1 numerical values can be downloaded as a csv file [here](#).

6.5 TSG (CSIC-UTM)

6.5.1 Introduction

The TSG (CSIC-UTM) dataset contains sea surface temperature and salinity data collected from 2010 to 2022 mainly in the Atlantic Ocean, Mediterranean Sea and the Southern Ocean from 3 CSIC-UTM research vessels (B/O Sarmiento de Gamboa, R/V Hespérides and R/V García del Cid). Measurements have been obtained through thermosalinograph (TSG) during more than 100 cruises. On-board TSG devices have been regularly calibrated and continuously monitored in-between cruises. The data has been gathered through the <http://data.utm.csic.es/portal/> data portal.

6.5.2 Number of SSS data as a function of time and distance to coast

Figure 97 shows the time (a) and distance to coast (b) distributions of the TSG (CSIC-UTM) *in situ* dataset.

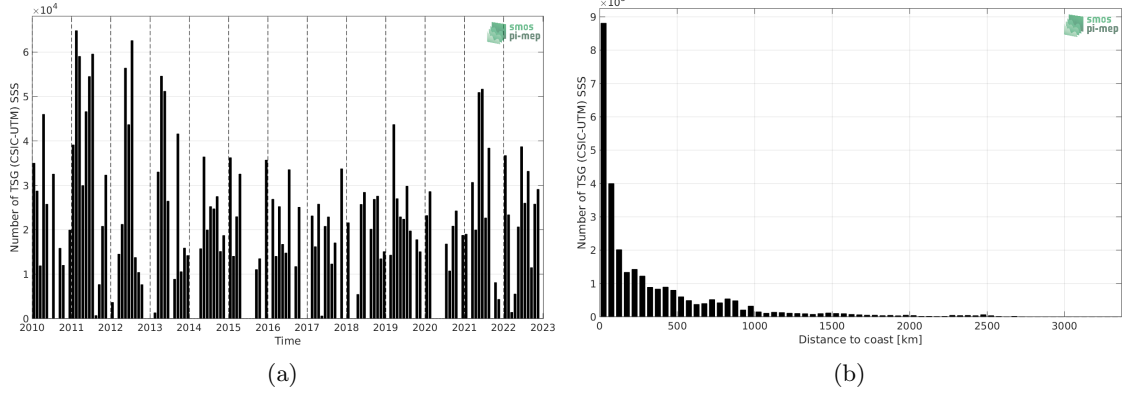


Figure 97: Number of SSS from TSG (CSIC-UTM) as a function of time (a) and distance to coast (b).

6.5.3 Histograms of SSS

Figure 98 shows the SSS distribution of the TSG (CSIC-UTM) (a) and colocalized ISAS (b) dataset.

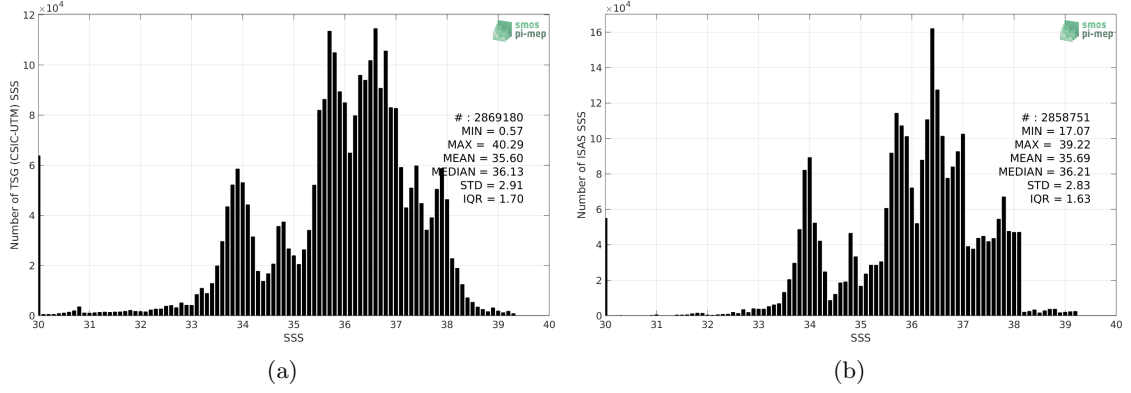


Figure 98: Histograms of SSS from TSG (CSIC-UTM) (a) and ISAS (b) per bins of 0.1.

6.5.4 Distribution of *in situ* SSS depth measurements

In Figure 99, we show the depth distribution of the *in situ* salinity dataset (a) and the spatial distribution of the depth temporal mean in $1^\circ \times 1^\circ$ boxes and considering the full *in situ* dataset period (b).

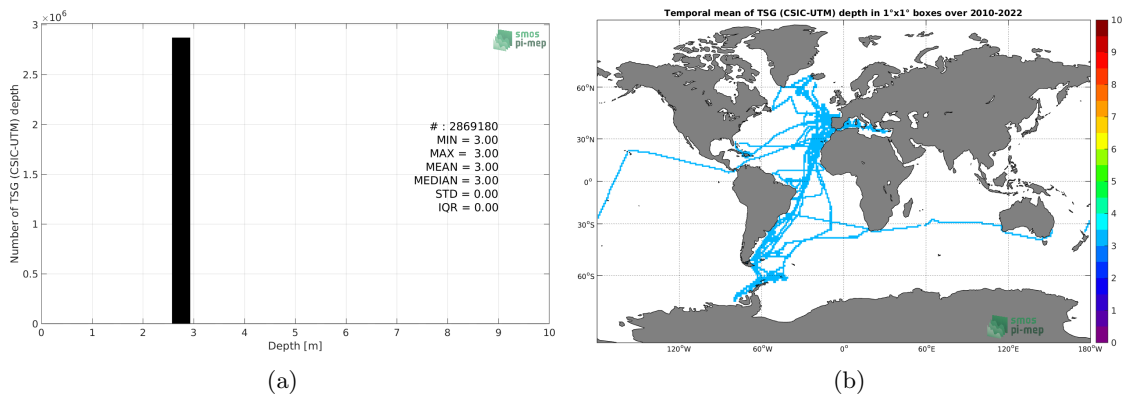


Figure 99: Depth distribution of the upper level SSS measurements from TSG (CSIC-UTM) (a) and spatial distribution of the *in situ* SSS depth measurements showing the mean value in $1^\circ \times 1^\circ$ boxes and considering the full *in situ* dataset period (b).

6.5.5 Spatial distribution of SSS

In Figure 100, the number of TSG (CSIC-UTM) SSS measurements in $1^\circ \times 1^\circ$ boxes is shown.

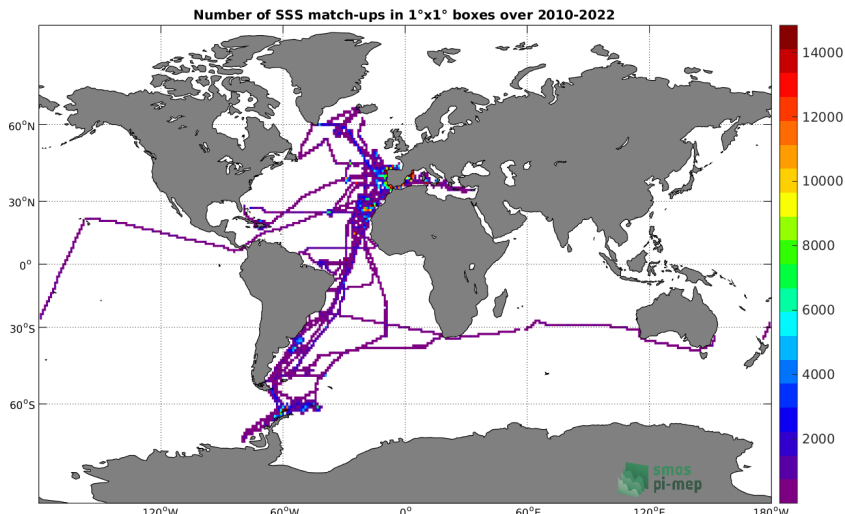


Figure 100: Number of SSS from TSG (CSIC-UTM) in $1^\circ \times 1^\circ$ boxes.

6.5.6 Spatial Maps of the Temporal mean and Std of *in situ* and ISAS SSS and of the difference (Δ SSS)

In Figure 101, maps of temporal mean (left) and standard deviation (right) of ISAS (top), TSG (CSIC-UTM) *in situ* dataset (middle) and the difference Δ SSS(ISAS -TSG (CSIC-UTM)) (bottom) are shown. The temporal mean and std are calculated using all match-up pairs falling in spatial boxes of size $1^\circ \times 1^\circ$ over the full TSG (CSIC-UTM) dataset period.

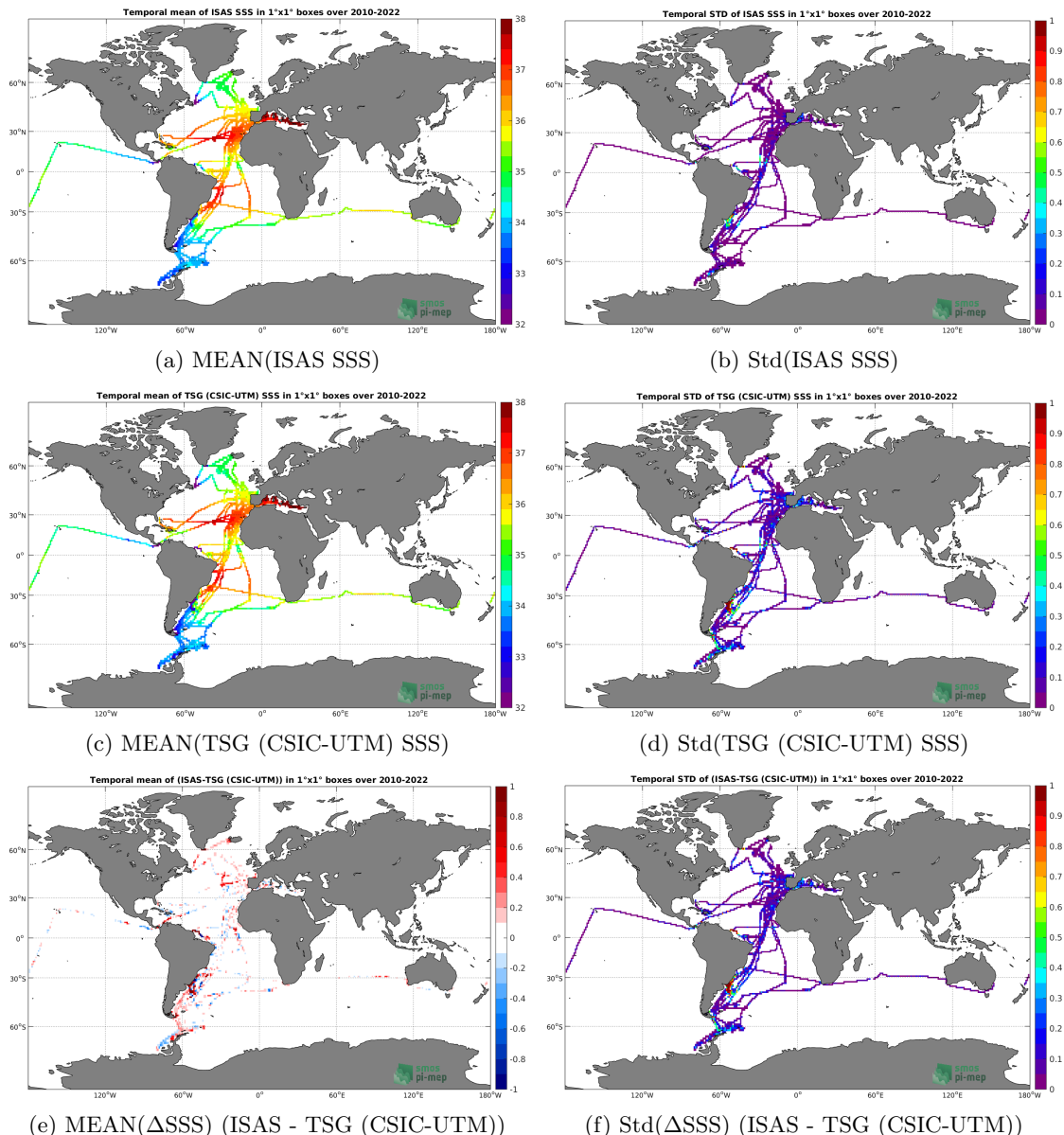


Figure 101: Temporal mean (left) and Std (right) of SSS from ISAS (top), TSG (CSIC-UTM) (middle), and of Δ SSS (ISAS - TSG (CSIC-UTM)). Only match-up pairs are used to generate these maps.

6.5.7 Time series of the monthly median and Std of *in situ* and ISAS SSS and of the difference (Δ SSS)

In the top panel of Figure 102, we show the time series of the monthly median SSS estimated for both ISAS SSS product (in black) and the TSG (CSIC-UTM) *in situ* dataset (in blue) at the collected Pi-MEP match-up pairs.

In the middle panel of Figure 102, we show the time series of the monthly median of Δ SSS

(ISAS - TSG (CSIC-UTM)) for the collected Pi-MEP match-up pairs.

In the bottom panel of Figure 102, we show the time series of the monthly standard deviation of the Δ SSS (ISAS - TSG (CSIC-UTM)) for the collected Pi-MEP match-up pairs.

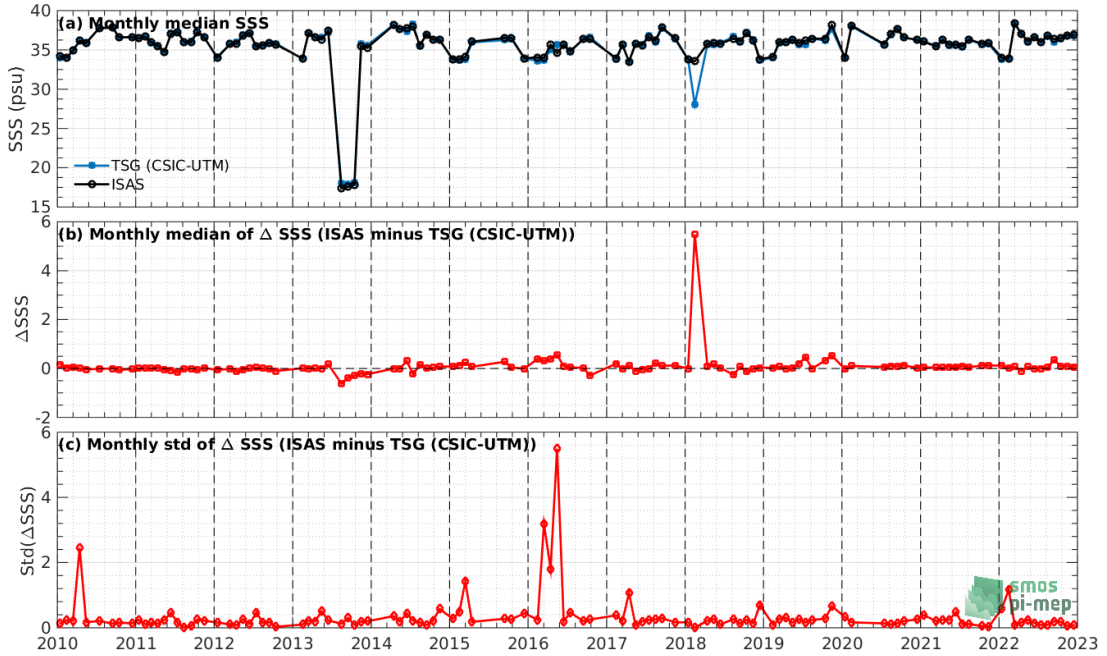


Figure 102: Time series of the monthly median SSS (top), median of Δ SSS (ISAS - TSG (CSIC-UTM)) and Std of Δ SSS (ISAS - TSG (CSIC-UTM)) considering all match-ups collected by the Pi-MEP.

6.5.8 Zonal mean and Std of *in situ* and ISAS SSS and of the difference Δ SSS

In Figure 103 left panel, we show the zonal mean SSS considering all Pi-MEP match-up pairs for both ISAS SSS product (in black) and the TSG (CSIC-UTM) *in situ* dataset (in blue). The full *in situ* dataset period is used to derive the mean.

In the right panel of Figure 103, we show the zonal mean of Δ SSS (ISAS - TSG (CSIC-UTM)) for all the collected Pi-MEP match-up pairs estimated over the full *in situ* dataset period.

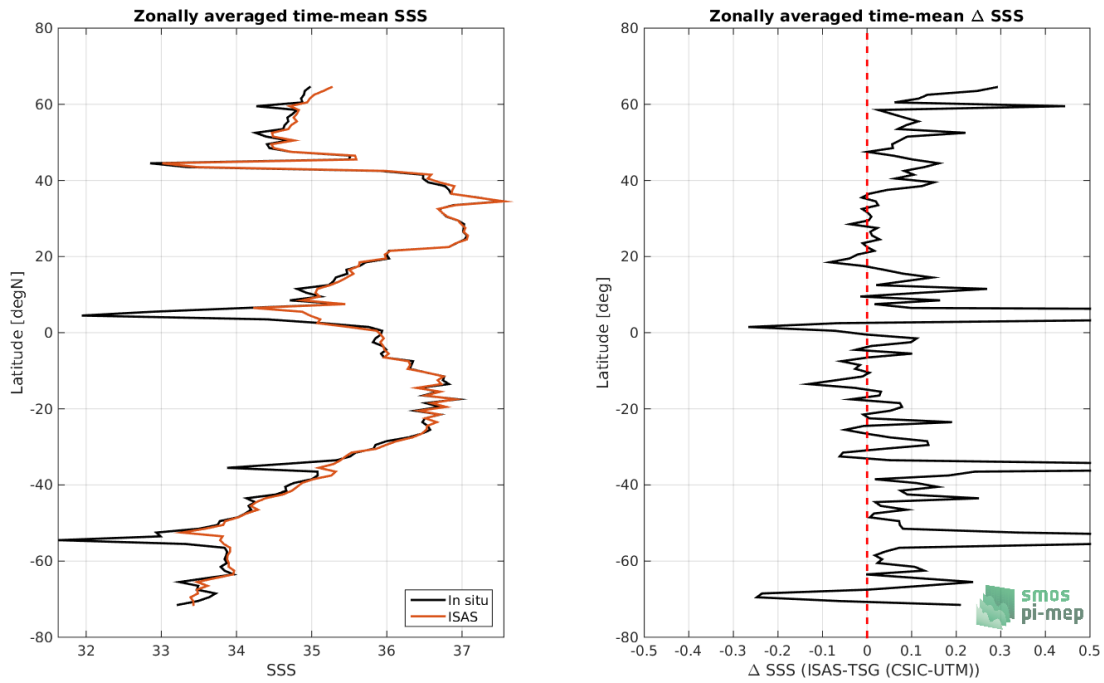


Figure 103: Left panel: Zonal mean SSS from ISAS product (black) and from TSG (CSIC-UTM) (blue). Right panel: Zonal mean of ΔSSS (ISAS - TSG (CSIC-UTM)) for all the collected Pi-MEP match-up pairs estimated over the full *in situ* dataset period.

6.5.9 Scatterplots of ISAS vs *in situ* SSS by latitudinal bands

In Figure 104, contour maps of the concentration of ISAS SSS (y-axis) versus TSG (CSIC-UTM) SSS (x-axis) at match-up pairs for different latitude bands: (a) 80°S-80°N, (b) 20°S-20°N, (c) 40°S-20°S and 20°N-40°N and (d) 60°S-40°S and 40°N-60°N. For each plot, the red line shows $x=y$. The black thin and dashed lines indicate a linear fit through the data cloud and the $\pm 95\%$ confidence levels, respectively. The number match-up pairs n , the slope and R^2 coefficient of the linear fit, the root mean square (RMS) and the mean bias between ISAS and *in situ* data are indicated for each latitude band in each plots.

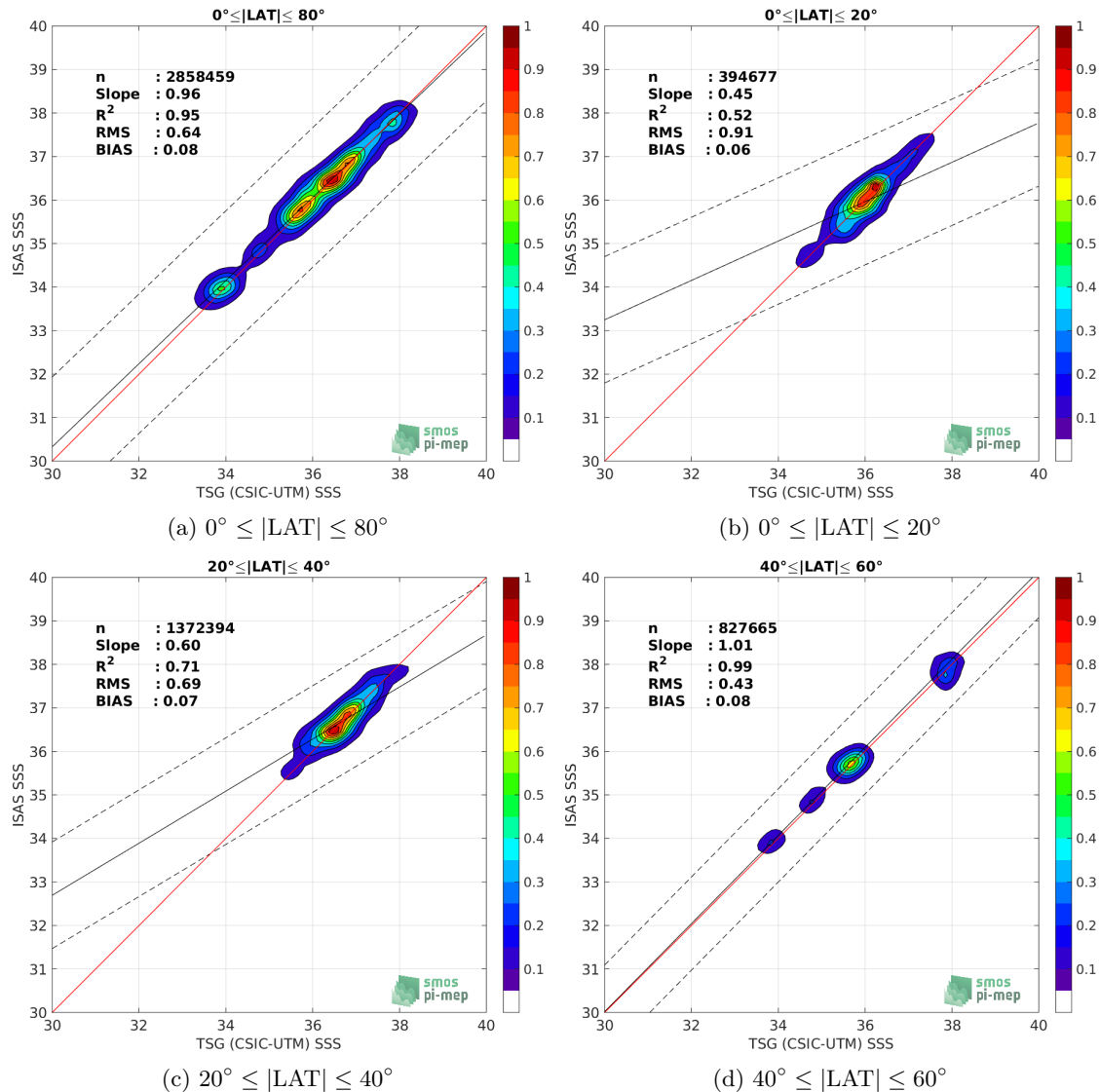


Figure 104: Contour maps of the concentration of ISAS SSS (y-axis) versus TSG (CSIC-UTM) SSS (x-axis) at match-up pairs for different latitude bands. For each plot, the red line shows $x=y$. The black thin and dashed lines indicate a linear fit through the data cloud and the $\pm 95\%$ confidence levels, respectively. The number match-up pairs n , the slope and R^2 coefficient of the linear fit, the root mean square (RMS) and the mean bias between ISAS and *in situ* data are indicated for each latitude band in each plots.

6.5.10 Time series of the monthly median and Std of the difference ΔSSS sorted by latitudinal bands

In Figure 105, time series of the monthly median (red curves) of ΔSSS (ISAS - TSG (CSIC-UTM)) and ± 1 Std (black vertical thick bars) as function of time for all the collected Pi-MEP match-up pairs estimated for the full *in situ* dataset period are shown for different latitude bands: (a) $80^\circ\text{S}-80^\circ\text{N}$, (b) $20^\circ\text{S}-20^\circ\text{N}$, (c) $40^\circ\text{S}-20^\circ\text{S}$ and $20^\circ\text{N}-40^\circ\text{N}$ and (d) $60^\circ\text{S}-40^\circ\text{S}$ and $40^\circ\text{N}-60^\circ\text{N}$.

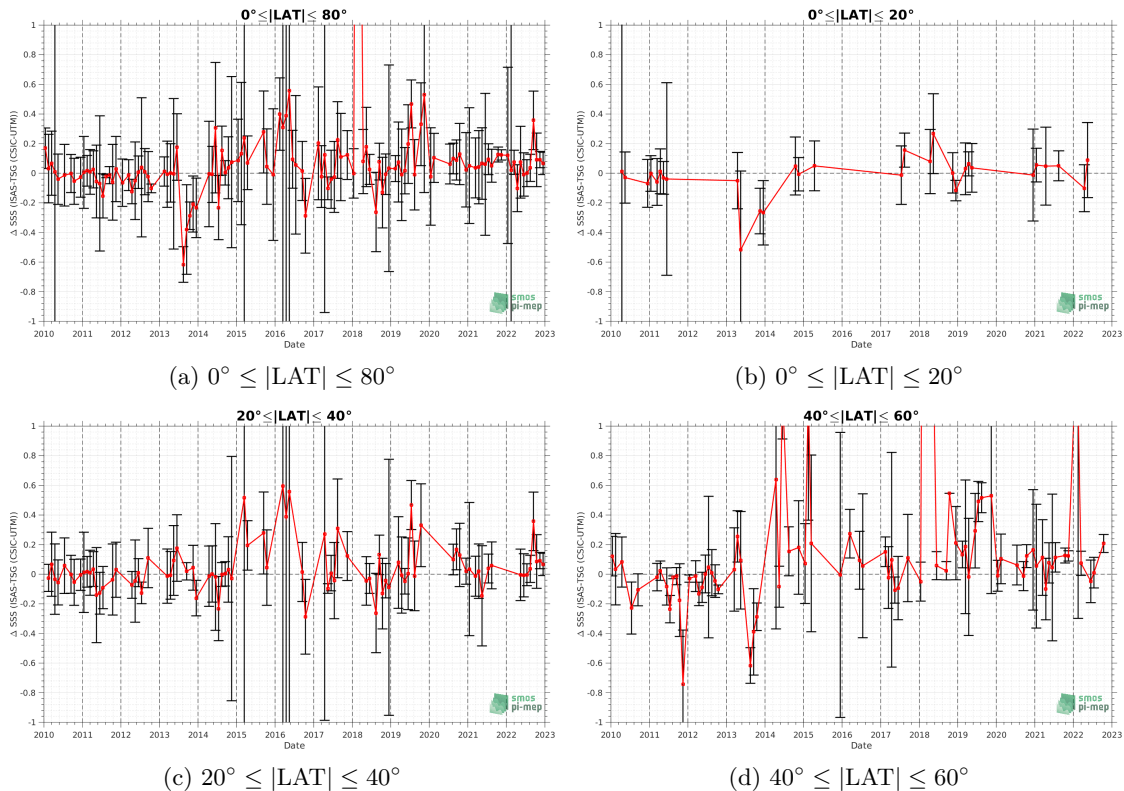


Figure 105: Monthly median (red curves) of ΔSSS (ISAS - TSG (CSIC-UTM)) and ± 1 Std (black vertical thick bars) as function of time for all the collected Pi-MEP match-up pairs for the full *in situ* dataset period are shown for different latitude bands: (a) $80^\circ\text{S}-80^\circ\text{N}$, (b) $20^\circ\text{S}-20^\circ\text{N}$, (c) $40^\circ\text{S}-20^\circ\text{S}$ and $20^\circ\text{N}-40^\circ\text{N}$ and (d) $60^\circ\text{S}-40^\circ\text{S}$ and $40^\circ\text{N}-60^\circ\text{N}$.

6.5.11 ΔSSS sorted as geophysical conditions

In Figure 106, we classify the match-up differences ΔSSS (ISAS - *in situ*) as function of the geophysical conditions at match-up points. The mean and std of ΔSSS (ISAS - TSG (CSIC-UTM)) is thus evaluated as function of the

- *in situ* SSS values per bins of width 0.2,
- *in situ* SST values per bins of width 1°C ,
- ASCAT daily wind values per bins of width 1 m/s,
- CMORPH 3-hourly rain rates per bins of width 1 mm/h, and,
- distance to coasts per bins of width 50 km,
- *in situ* measurement depth (if relevant).

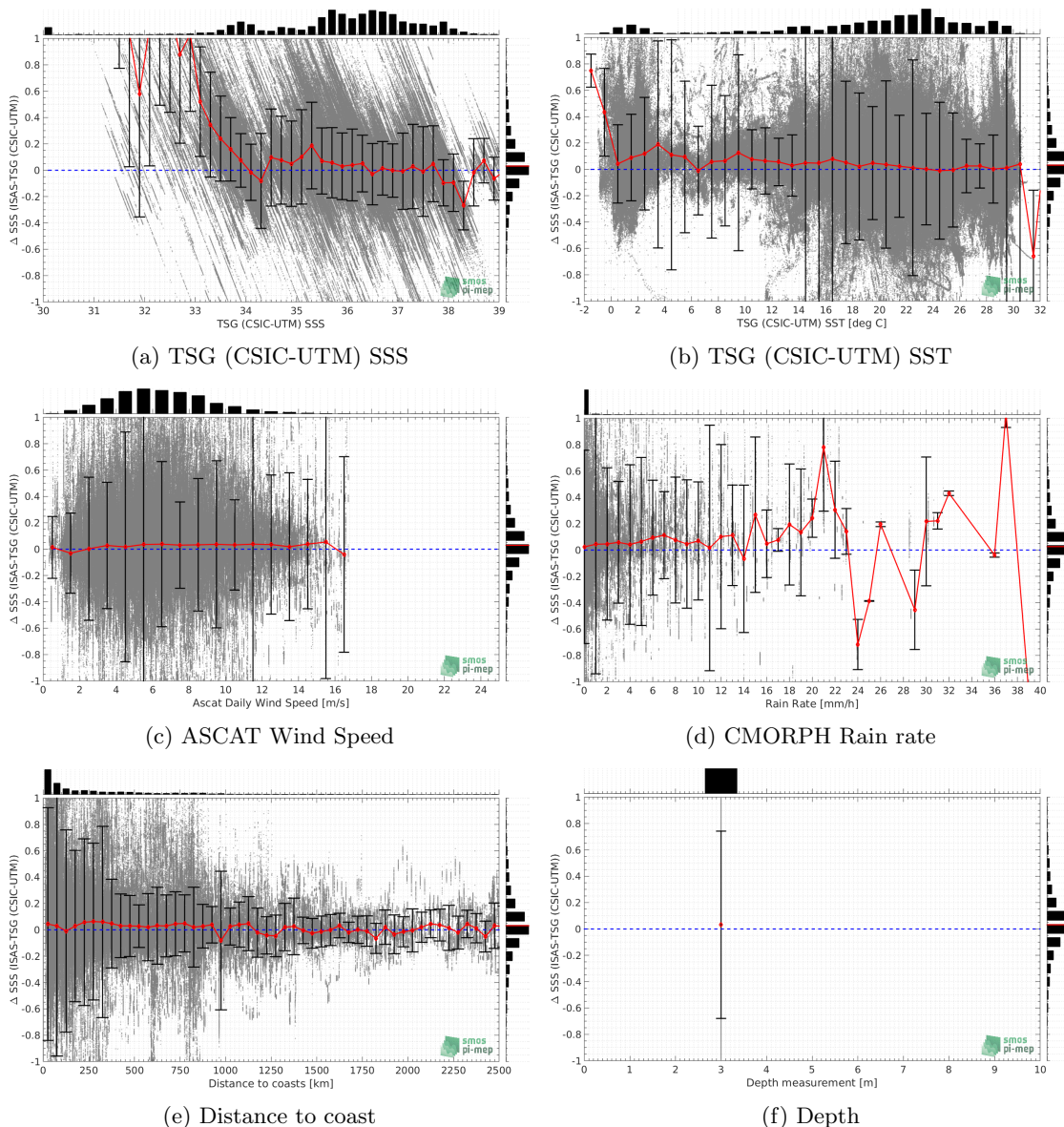


Figure 106: ΔSSS (ISAS - TSG (CSIC-UTM)) sorted as geophysical conditions: TSG (CSIC-UTM) SSS a), TSG (CSIC-UTM) SST b), ASCAT Wind speed c), CMORPH rain rate d), distance to coast (e) and depth measurements (f).

6.5.12 ΔSSS maps and statistics for different geophysical conditions

In Figures 107 and 108, we focus on sub-datasets of the match-up differences ΔSSS (ISAS - *in situ*) for the following specific geophysical conditions:

- **C1:** if the local value at *in situ* location of estimated rain rate is zero, mean daily wind is in the range [3, 12] m/s, the SST is $> 5^\circ\text{C}$ and distance to coast is > 800 km.
- **C2:** if the local value at *in situ* location of estimated rain rate is zero, mean daily wind is

in the range [3, 12] m/s.

- **C3:** if the local value at *in situ* location of estimated rain rate is high (ie. $> 1 \text{ mm/h}$) and mean daily wind is low (ie. $< 4 \text{ m/s}$).
- **C5:** if the *in situ* data is located where the climatological SSS standard deviation is low (ie. above < 0.2).
- **C6:** if the *in situ* data is located where the climatological SSS standard deviation is high (ie. above > 0.2).

For each of these conditions, the temporal mean (gridded over spatial boxes of size $1^\circ \times 1^\circ$) and the histogram of the difference ΔSSS (ISAS - *in situ*) are presented.

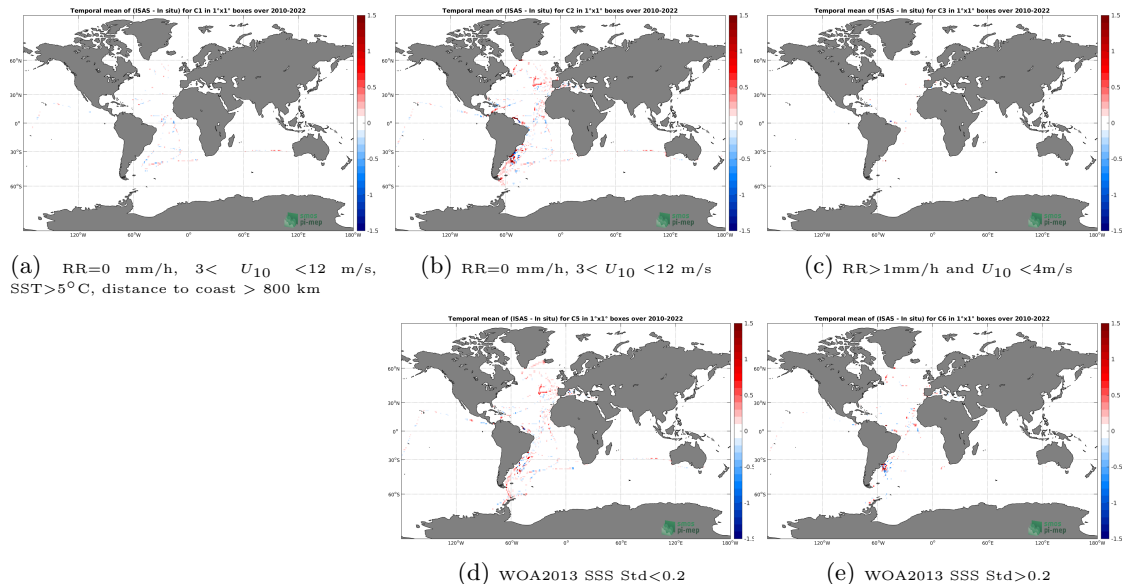


Figure 107: Temporal mean gridded over spatial boxes of size $1^\circ \times 1^\circ$ of ΔSSS (ISAS - TSG (CSIC-UTM)) for 5 different subdatasets corresponding to: RR=0 mm/h, $3 < U_{10} < 12 \text{ m/s}$, SST $>5^\circ\text{C}$, distance to coast $> 800 \text{ km}$ (a), RR=0 mm/h, $3 < U_{10} < 12 \text{ m/s}$ (b), RR $>1\text{mm/h}$ and $U_{10} < 4\text{m/s}$ (c), WOA2013 SSS Std <0.2 (d), WOA2013 SSS Std >0.2 (e).

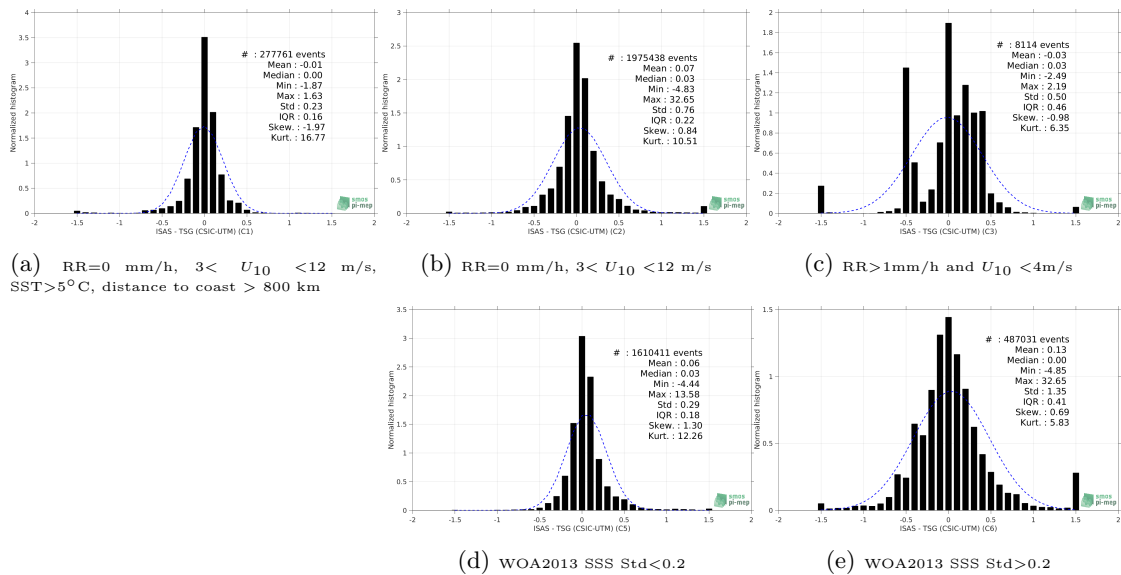


Figure 108: Normalized histogram of ΔSSS (ISAS - TSG (CSIC-UTM)) for 5 different sub-datasets corresponding to: $RR=0 \text{ mm/h}, 3 < U_{10} < 12 \text{ m/s}, SST > 5^\circ\text{C}, \text{distance to coast} > 800 \text{ km}$ (a), $RR=0 \text{ mm/h}, 3 < U_{10} < 12 \text{ m/s}$ (b), $RR > 1 \text{ mm/h and } U_{10} < 4 \text{ m/s}$ (c), WOA2013 SSS Std < 0.2 (d), WOA2013 SSS Std > 0.2 (e).

6.5.13 Summary

Table 1 shows the mean, median, standard deviation (Std), root mean square (RMS), interquartile range (IQR), correlation coefficient (r^2) and robust standard deviation (Std*) of the match-up differences ΔSSS (ISAS - TSG (CSIC-UTM)) for the following conditions:

- all: All the match-up pairs satellite/in situ SSS values are used to derive the statistics
- C1: only pairs where $RR=0 \text{ mm/h}, 3 < U_{10} < 12 \text{ m/s}, SST > 5^\circ\text{C}, \text{distance to coast} > 800 \text{ km}$
- C2: only pairs where $RR=0 \text{ mm/h}, 3 < U_{10} < 12 \text{ m/s}$
- C3: only pairs where $RR > 1 \text{ mm/h and } U_{10} < 4 \text{ m/s}$
- C5: only pairs where WOA2013 SSS Std < 0.2
- C6: only pairs where WOA2013 SSS Std > 0.2
- C7a: only pairs with a distance to coast < 150 km.
- C7b: only pairs with a distance to coast in the range [150, 800] km.
- C7c: only pairs with a distance to coast > 800 km.
- C8a: only pairs where SST is < 5°C .
- C8b: only pairs where SST is in the range $[5, 15]^\circ\text{C}$.
- C8c: only pairs where SST is > 15°C .

- C9a: only pairs where SSS is < 33.
- C9b: only pairs where SSS is in the range [33, 37].
- C9c: only pairs where SSS is > 37.

Table 1: Statistics of Δ SSS (ISAS - TSG (CSIC-UTM))

Condition	#	Median	Mean	Std	RMS	IQR	r^2	Std*
all	2858751	0.03	0.08	0.71	0.72	0.23	0.940	0.17
C1	277761	0.00	-0.01	0.23	0.23	0.16	0.939	0.12
C2	1975438	0.03	0.07	0.76	0.76	0.22	0.934	0.16
C3	8114	0.03	-0.03	0.50	0.50	0.46	0.757	0.32
C5	1610411	0.03	0.06	0.29	0.30	0.18	0.968	0.13
C6	487031	0.00	0.13	1.35	1.35	0.41	0.945	0.31
C7a	1471655	0.03	0.11	0.90	0.91	0.31	0.946	0.23
C7b	1019618	0.04	0.08	0.47	0.48	0.18	0.863	0.14
C7c	367305	0.00	-0.02	0.25	0.25	0.16	0.928	0.12
C8a	284249	0.09	0.18	0.42	0.46	0.30	0.206	0.22
C8b	350036	0.06	0.14	0.99	1.00	0.18	0.910	0.13
C8c	2224448	0.02	0.06	0.69	0.69	0.24	0.944	0.18
C9a	117479	0.07	1.12	3.06	3.26	1.92	0.851	0.92
C9b	2138546	0.04	0.06	0.27	0.28	0.22	0.931	0.16
C9c	602726	-0.02	-0.04	0.28	0.29	0.25	0.650	0.18

Table 1 numerical values can be downloaded as a csv file [here](#).

6.6 TSG (Polarstern)

6.6.1 Introduction

The TSG (Polarstern) dataset has been gathered through the <https://www.pangaea.de/> data warehouse utility using the following criteria: basis:”Polarstern”, device:”Underway cruise track measurements (CT)”, time coverage form 2010/01/01 to present. The result of the query is a collection of 79 different datasets with the following identification numbers: 736345, 742729, 753224, 753225, 753226, 753227, 758080, 760120, 760121, 761277, 770034, 770035, 770828, 776596, 776597, 780004, 802809, 802810, 802811, 802812, 803431, 808835, 808836, 808838, 809727, 810678, 816055, 819831, 823259, 839406, 839407, 839408, 848615, 858879, 858880, 858881, 858882, 858883, 858884, 858885, 863228, 863229, 863230, 863231, 863232, 863234, 873145, 873147, 873151, 873153, 873155, 873156, 873158, 887767, 889444, 889513, 889515, 889516, 889517, 889535, 889542, 889548, 895578, 895579, 895581, 898225, 898233, 898266, 905555, 905562, 905608, 905610, 905734, 930022, 930023, 930024, 930026, 930027, 930028.

6.6.2 Number of SSS data as a function of time and distance to coast

Figure 109 shows the time (a) and distance to coast (b) distributions of the TSG (Polarstern) *in situ* dataset.

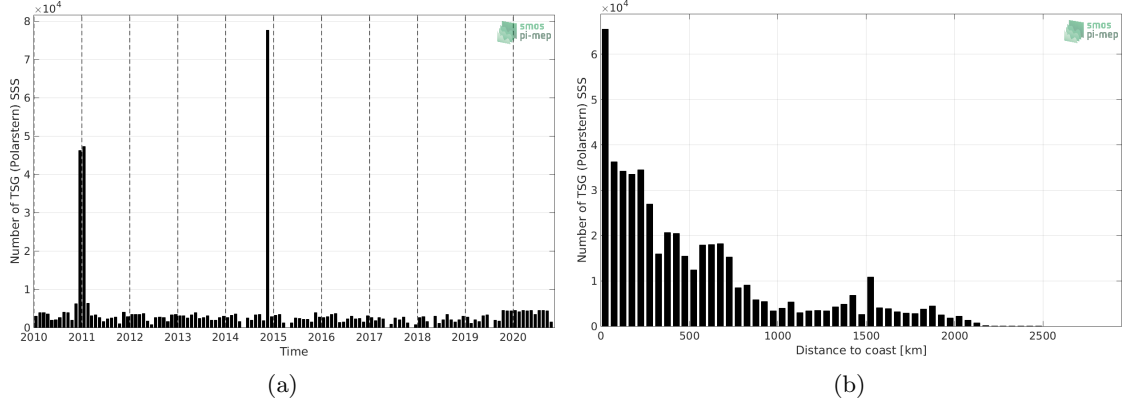


Figure 109: Number of SSS from TSG (Polarstern) as a function of time (a) and distance to coast (b).

6.6.3 Histograms of SSS

Figure 110 shows the SSS distribution of the TSG (Polarstern) (a) and colocalized ISAS (b) dataset.

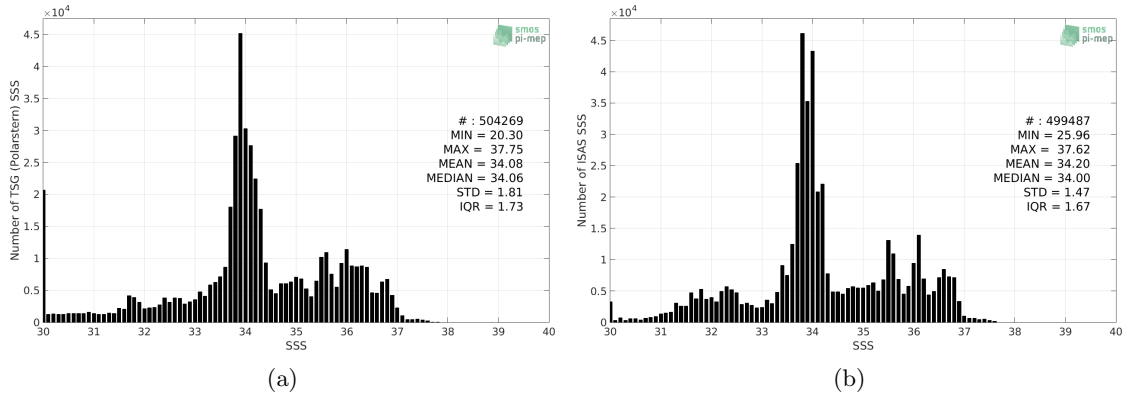


Figure 110: Histograms of SSS from TSG (Polarstern) (a) and ISAS (b) per bins of 0.1.

6.6.4 Distribution of *in situ* SSS depth measurements

In Figure 111, we show the depth distribution of the *in situ* salinity dataset (a) and the spatial distribution of the depth temporal mean in $1^\circ \times 1^\circ$ boxes and considering the full *in situ* dataset period (b).

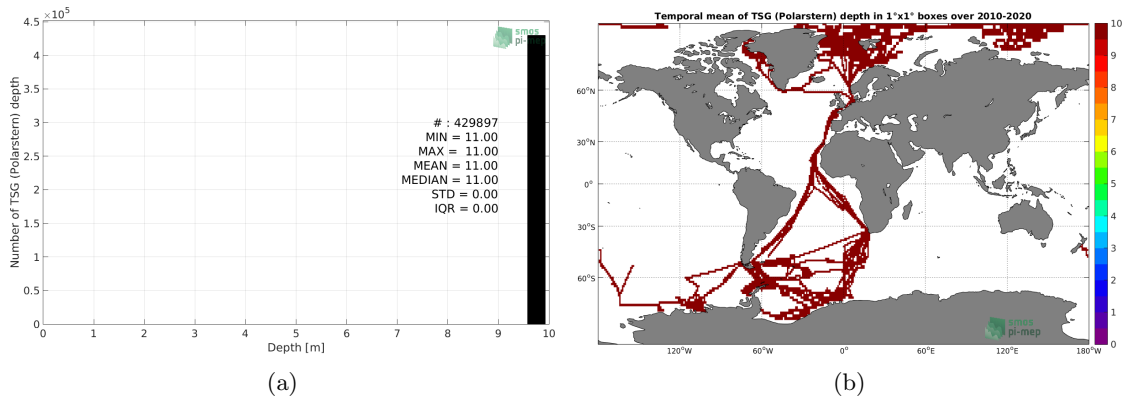


Figure 111: Depth distribution of the upper level SSS measurements from TSG (Polarstern) (a) and spatial distribution of the *in situ* SSS depth measurements showing the mean value in 1°x1° boxes and considering the full *in situ* dataset period (b).

6.6.5 Spatial distribution of SSS

In Figure 112, the number of TSG (Polarstern) SSS measurements in 1°x1° boxes is shown.

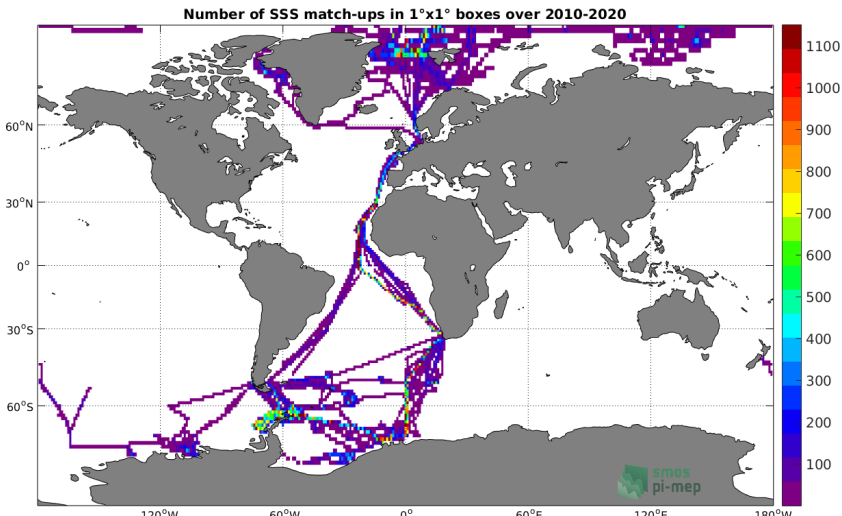


Figure 112: Number of SSS from TSG (Polarstern) in 1°x1° boxes.

6.6.6 Spatial Maps of the Temporal mean and Std of *in situ* and ISAS SSS and of the difference (Δ SSS)

In Figure 113, maps of temporal mean (left) and standard deviation (right) of ISAS (top), TSG (Polarstern) *in situ* dataset (middle) and the difference Δ SSS(ISAS - TSG (Polarstern)) (bottom) are shown. The temporal mean and std are calculated using all match-up pairs falling in spatial boxes of size 1°x1° over the full TSG (Polarstern) dataset period.

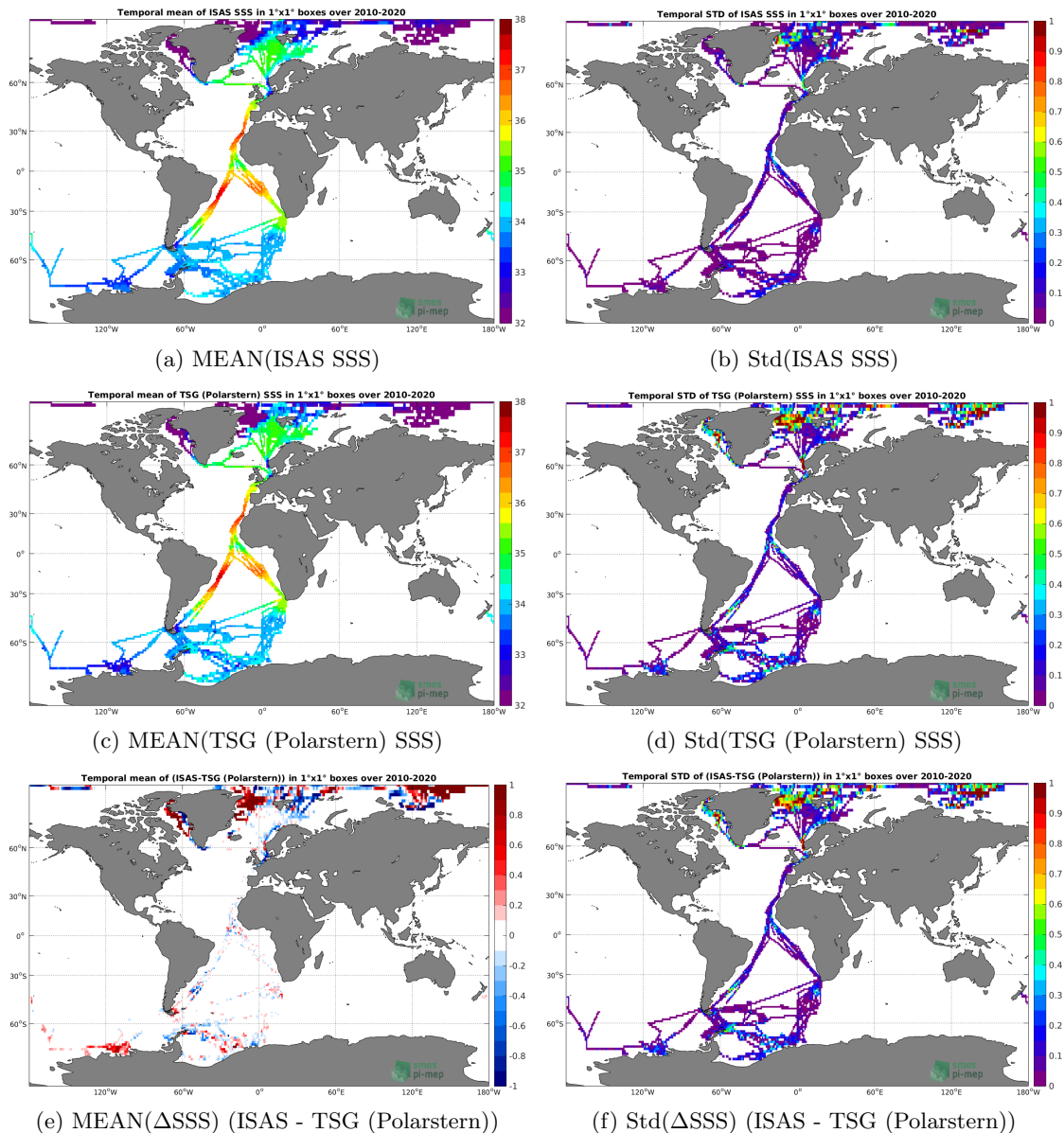


Figure 113: Temporal mean (left) and Std (right) of SSS from ISAS (top), TSG (Polarstern) (middle), and of Δ SSS (ISAS - TSG (Polarstern)). Only match-up pairs are used to generate these maps.

6.6.7 Time series of the monthly median and Std of *in situ* and ISAS SSS and of the difference (Δ SSS)

In the top panel of Figure 114, we show the time series of the monthly median SSS estimated for both ISAS SSS product (in black) and the TSG (Polarstern) *in situ* dataset (in blue) at the collected Pi-MEP match-up pairs.

In the middle panel of Figure 114, we show the time series of the monthly median of Δ SSS (ISAS - TSG (Polarstern)) for the collected Pi-MEP match-up pairs.

In the bottom panel of Figure 114, we show the time series of the monthly standard deviation of the Δ SSS (ISAS - TSG (Polarstern)) for the collected Pi-MEP match-up pairs.

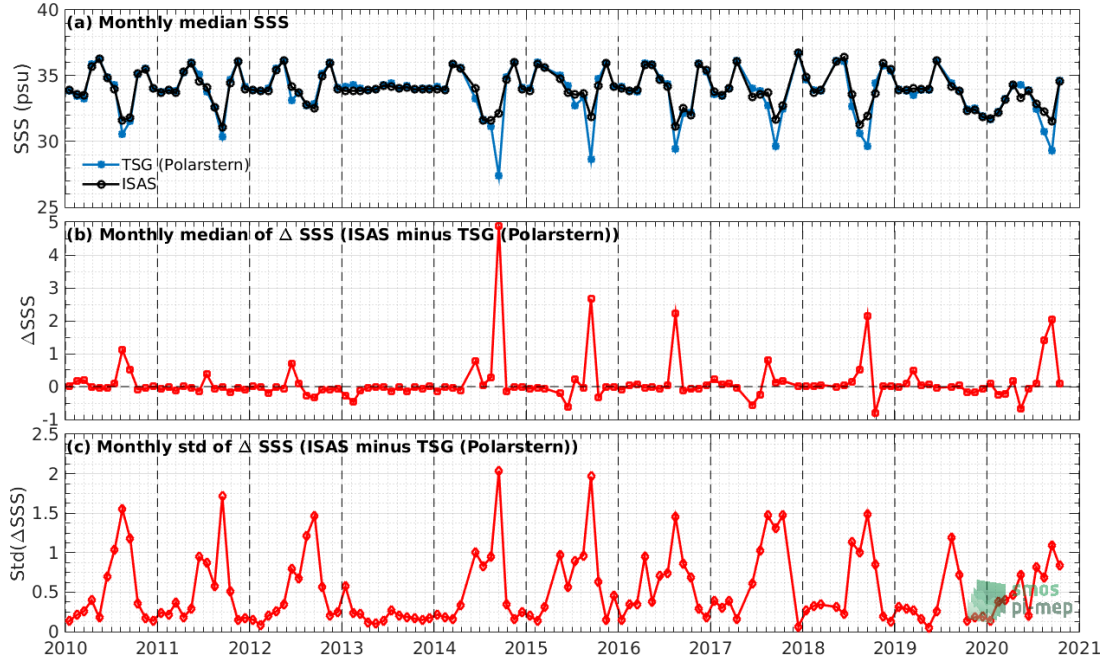


Figure 114: Time series of the monthly median SSS (top), median of Δ SSS (ISAS - TSG (Polarstern)) and Std of Δ SSS (ISAS - TSG (Polarstern)) considering all match-ups collected by the Pi-MEP.

6.6.8 Zonal mean and Std of *in situ* and ISAS SSS and of the difference Δ SSS

In Figure 115 left panel, we show the zonal mean SSS considering all Pi-MEP match-up pairs for both ISAS SSS product (in black) and the TSG (Polarstern) *in situ* dataset (in blue). The full *in situ* dataset period is used to derive the mean.

In the right panel of Figure 115, we show the zonal mean of Δ SSS (ISAS - TSG (Polarstern)) for all the collected Pi-MEP match-up pairs estimated over the full *in situ* dataset period.

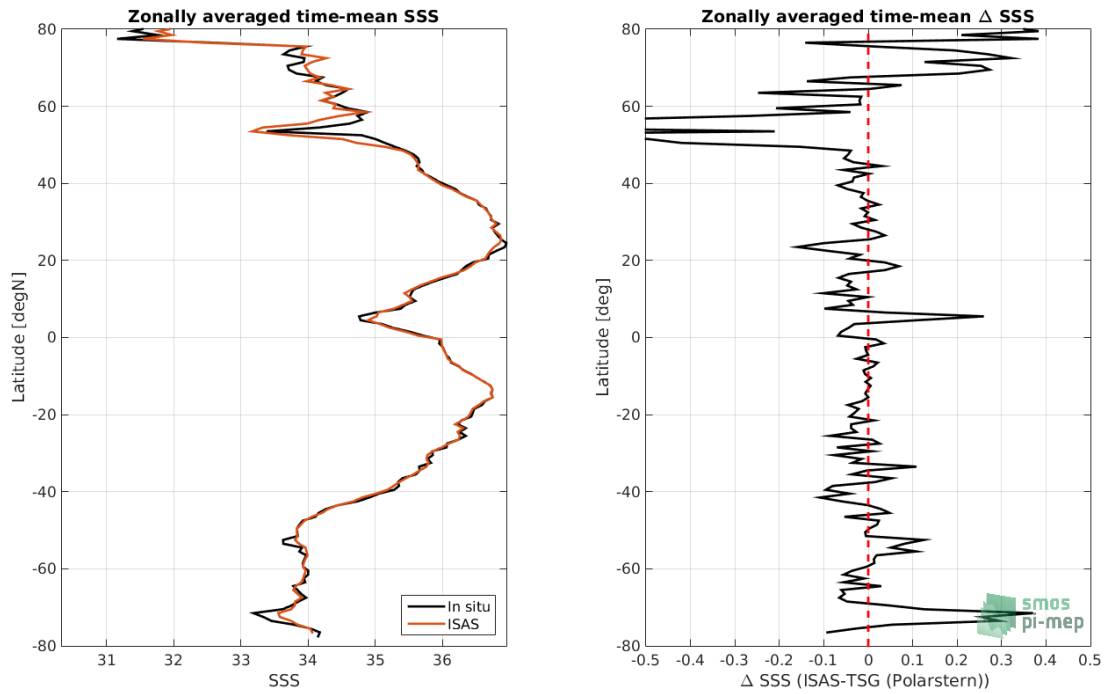


Figure 115: Left panel: Zonal mean SSS from ISAS product (black) and from TSG (Polarstern) (blue). Right panel: Zonal mean of Δ SSS (ISAS - TSG (Polarstern)) for all the collected Pi-MEP match-up pairs estimated over the full *in situ* dataset period.

6.6.9 Scatterplots of ISAS vs *in situ* SSS by latitudinal bands

In Figure 116, contour maps of the concentration of ISAS SSS (y-axis) versus TSG (Polarstern) SSS (x-axis) at match-up pairs for different latitude bands: (a) 80°S-80°N, (b) 20°S-20°N, (c) 40°S-20°S and 20°N-40°N and (d) 60°S-40°S and 40°N-60°N. For each plot, the red line shows $x=y$. The black thin and dashed lines indicate a linear fit through the data cloud and the $\pm 95\%$ confidence levels, respectively. The number match-up pairs n , the slope and R^2 coefficient of the linear fit, the root mean square (RMS) and the mean bias between ISAS and *in situ* data are indicated for each latitude band in each plots.

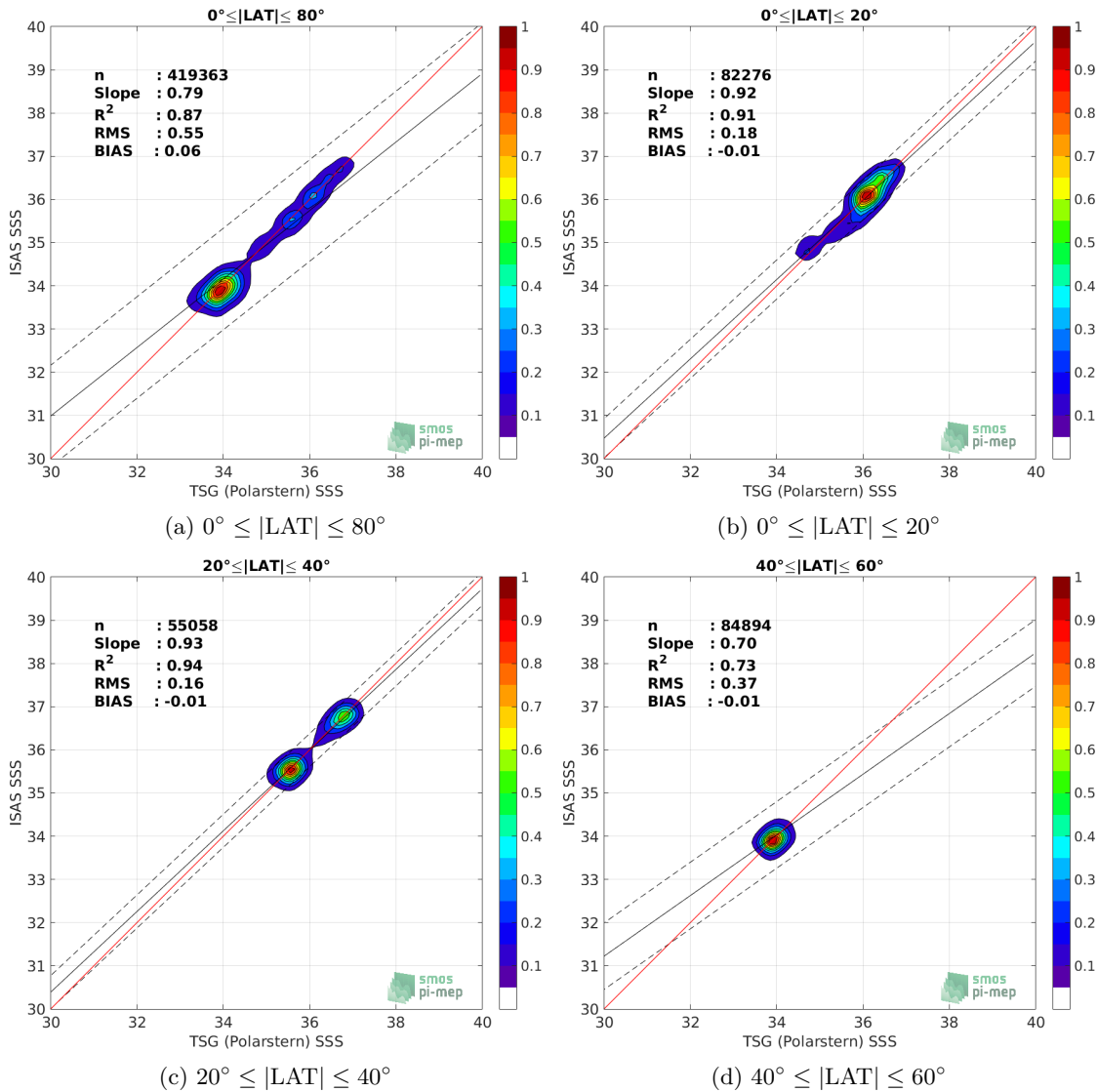


Figure 116: Contour maps of the concentration of ISAS SSS (y-axis) versus TSG (Polarstern) SSS (x-axis) at match-up pairs for different latitude bands. For each plot, the red line shows $x=y$. The black thin and dashed lines indicate a linear fit through the data cloud and the $\pm 95\%$ confidence levels, respectively. The number match-up pairs n , the slope and R^2 coefficient of the linear fit, the root mean square (RMS) and the mean bias between ISAS and *in situ* data are indicated for each latitude band in each plots.

6.6.10 Time series of the monthly median and Std of the difference ΔSSS sorted by latitudinal bands

In Figure 117, time series of the monthly median (red curves) of ΔSSS (ISAS - TSG (Polarstern)) and ± 1 Std (black vertical thick bars) as function of time for all the collected Pi-MEP match-up pairs estimated for the full *in situ* dataset period are shown for different latitude bands: (a) $80^\circ\text{S}-80^\circ\text{N}$, (b) $20^\circ\text{S}-20^\circ\text{N}$, (c) $40^\circ\text{S}-20^\circ\text{S}$ and $20^\circ\text{N}-40^\circ\text{N}$ and (d) $60^\circ\text{S}-40^\circ\text{S}$ and $40^\circ\text{N}-60^\circ\text{N}$.

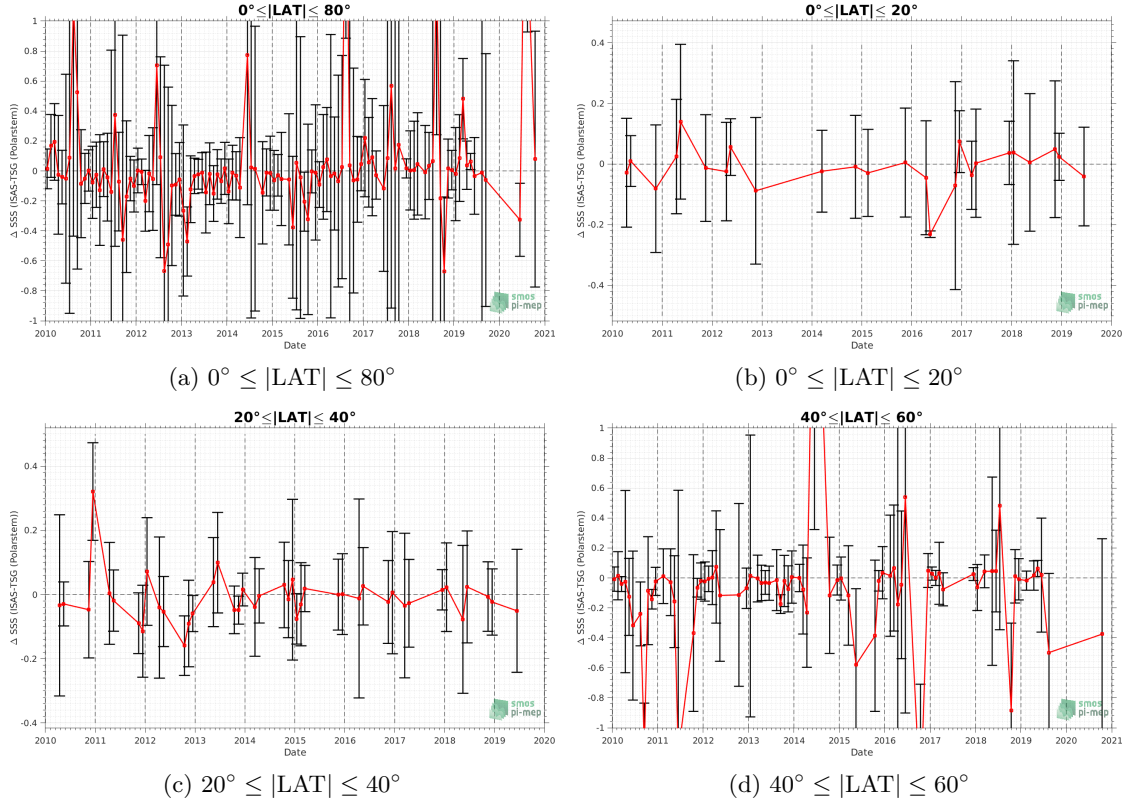


Figure 117: Monthly median (red curves) of ΔSSS (ISAS - TSG (Polarstern)) and ± 1 Std (black vertical thick bars) as function of time for all the collected Pi-MEP match-up pairs for the full *in situ* dataset period are shown for different latitude bands: (a) $80^\circ\text{S}-80^\circ\text{N}$, (b) $20^\circ\text{S}-20^\circ\text{N}$, (c) $40^\circ\text{S}-20^\circ\text{S}$ and $20^\circ\text{N}-40^\circ\text{N}$ and (d) $60^\circ\text{S}-40^\circ\text{S}$ and $40^\circ\text{N}-60^\circ\text{N}$.

6.6.11 ΔSSS sorted as geophysical conditions

In Figure 118, we classify the match-up differences ΔSSS (ISAS - *in situ*) as function of the geophysical conditions at match-up points. The mean and std of ΔSSS (ISAS - TSG (Polarstern)) is thus evaluated as function of the

- *in situ* SSS values per bins of width 0.2,
- *in situ* SST values per bins of width 1°C ,
- ASCAT daily wind values per bins of width 1 m/s,
- CMORPH 3-hourly rain rates per bins of width 1 mm/h, and,
- distance to coasts per bins of width 50 km,
- *in situ* measurement depth (if relevant).

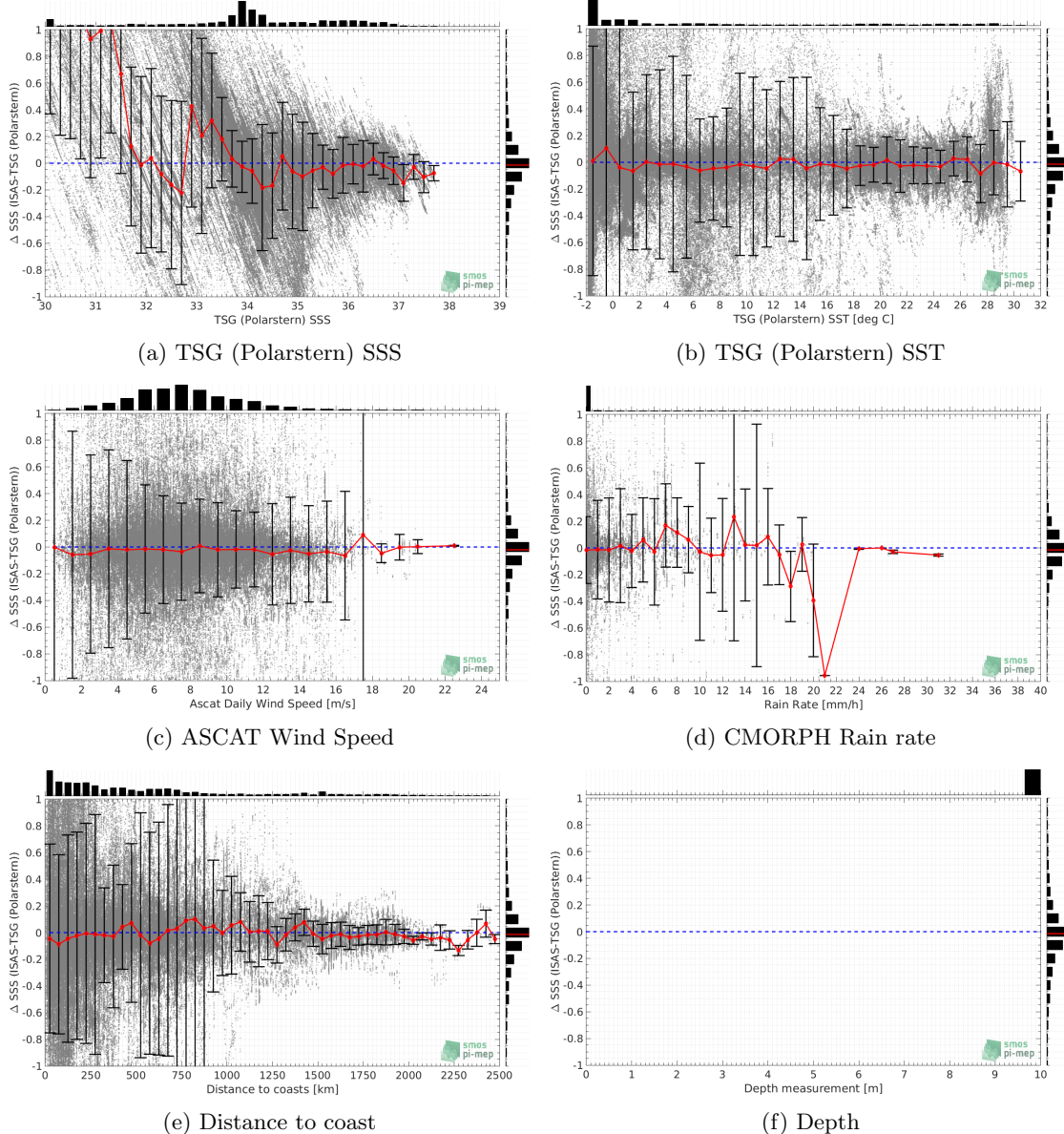


Figure 118: ΔSSS (ISAS - TSG (Polarstern)) sorted as geophysical conditions: TSG (Polarstern) SSS a), TSG (Polarstern) SST b), ASCAT Wind speed c), CMORPH rain rate d), distance to coast (e) and depth measurements (f).

6.6.12 ΔSSS maps and statistics for different geophysical conditions

In Figures 119 and 120, we focus on sub-datasets of the match-up differences ΔSSS (ISAS - *in situ*) for the following specific geophysical conditions:

- **C1:** if the local value at *in situ* location of estimated rain rate is zero, mean daily wind is in the range [3, 12] m/s, the SST is $> 5^\circ\text{C}$ and distance to coast is > 800 km.
- **C2:** if the local value at *in situ* location of estimated rain rate is zero, mean daily wind is

in the range [3, 12] m/s.

- **C3:** if the local value at *in situ* location of estimated rain rate is high (ie. $> 1 \text{ mm/h}$) and mean daily wind is low (ie. $< 4 \text{ m/s}$).
- **C5:** if the *in situ* data is located where the climatological SSS standard deviation is low (ie. above < 0.2).
- **C6:** if the *in situ* data is located where the climatological SSS standard deviation is high (ie. above > 0.2).

For each of these conditions, the temporal mean (gridded over spatial boxes of size $1^\circ \times 1^\circ$) and the histogram of the difference ΔSSS (ISAS - *in situ*) are presented.

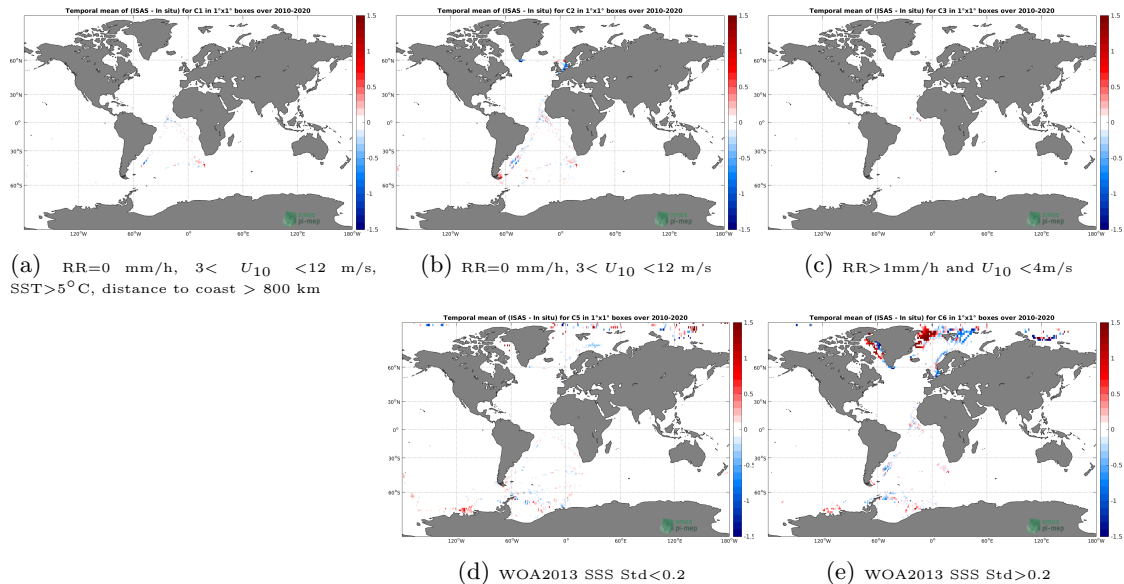


Figure 119: Temporal mean gridded over spatial boxes of size $1^\circ \times 1^\circ$ of ΔSSS (ISAS - TSG (Polarstern)) for 5 different subdatasets corresponding to: RR = 0 mm/h, $3 < U_{10} < 12 \text{ m/s}$, SST $> 5^\circ\text{C}$, distance to coast $> 800 \text{ km}$ (a), RR = 0 mm/h, $3 < U_{10} < 12 \text{ m/s}$ (b), RR $> 1\text{mm/h}$ and $U_{10} < 4\text{m/s}$ (c), WOA2013 SSS Std < 0.2 (d), WOA2013 SSS Std > 0.2 (e).

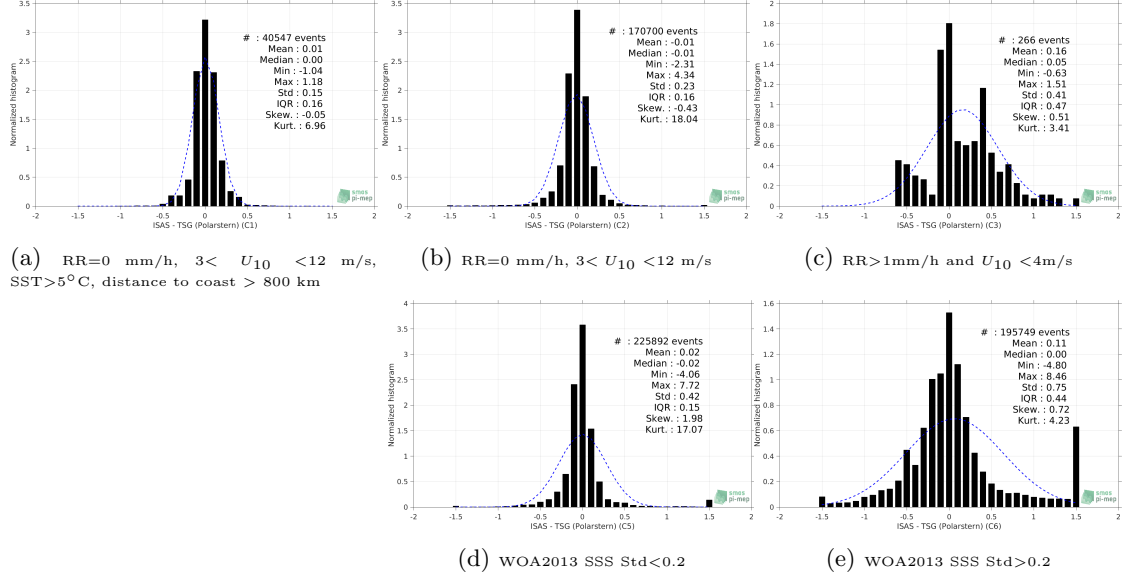


Figure 120: Normalized histogram of ΔSSS (ISAS - TSG (Polarstern)) for 5 different subdatasets corresponding to: RR=0 mm/h, $3 < U_{10} < 12$ m/s, SST> 5°C , distance to coast > 800 km (a), RR=0 mm/h, $3 < U_{10} < 12$ m/s (b), RR>1mm/h and $U_{10} < 4$ m/s (c), WOA2013 SSS Std<0.2 (d), WOA2013 SSS Std>0.2 (e).

6.6.13 Summary

Table 1 shows the mean, median, standard deviation (Std), root mean square (RMS), interquartile range (IQR), correlation coefficient (r^2) and robust standard deviation (Std*) of the match-up differences ΔSSS (ISAS - TSG (Polarstern)) for the following conditions:

- all: All the match-up pairs satellite/in situ SSS values are used to derive the statistics
- C1: only pairs where RR=0 mm/h, $3 < U_{10} < 12$ m/s, SST> 5°C , distance to coast > 800 km
- C2: only pairs where RR=0 mm/h, $3 < U_{10} < 12$ m/s
- C3: only pairs where RR>1mm/h and $U_{10} < 4$ m/s
- C5: only pairs where WOA2013 SSS Std<0.2
- C6: only pairs where WOA2013 SSS Std>0.2
- C7a: only pairs with a distance to coast < 150 km.
- C7b: only pairs with a distance to coast in the range [150, 800] km.
- C7c: only pairs with a distance to coast > 800 km.
- C8a: only pairs where SST is < 5°C .
- C8b: only pairs where SST is in the range [5, 15] $^{\circ}\text{C}$.
- C8c: only pairs where SST is > 15 $^{\circ}\text{C}$.

- C9a: only pairs where SSS is < 33.
- C9b: only pairs where SSS is in the range [33, 37].
- C9c: only pairs where SSS is > 37.

Table 1: Statistics of Δ SSS (ISAS - TSG (Polarstern))

Condition	#	Median	Mean	Std	RMS	IQR	r^2	Std*
all	499487	-0.01	0.11	0.77	0.77	0.27	0.830	0.20
C1	40547	0.00	0.01	0.15	0.15	0.16	0.973	0.12
C2	170700	-0.01	-0.01	0.23	0.23	0.16	0.956	0.12
C3	266	0.05	0.16	0.41	0.44	0.47	0.878	0.37
C5	225892	-0.02	0.02	0.42	0.42	0.15	0.912	0.11
C6	195749	0.00	0.11	0.75	0.76	0.44	0.826	0.33
C7a	131773	-0.05	0.03	0.72	0.72	0.40	0.809	0.31
C7b	257674	0.00	0.16	0.85	0.86	0.30	0.809	0.22
C7c	110003	-0.01	0.08	0.59	0.59	0.16	0.882	0.12
C8a	288338	0.00	0.21	0.95	0.97	0.40	0.662	0.28
C8b	69242	-0.04	-0.05	0.56	0.57	0.26	0.687	0.19
C8c	105979	-0.02	-0.02	0.21	0.21	0.18	0.904	0.13
C9a	85630	0.59	0.94	1.45	1.73	1.85	0.244	1.19
C9b	409548	-0.03	-0.06	0.31	0.32	0.22	0.914	0.16
C9c	4309	-0.09	-0.11	0.13	0.17	0.20	0.744	0.15

Table 1 numerical values can be downloaded as a csv file [here](#).

6.7 TSG (NCEI-0170743)

6.7.1 Introduction

The TSG (NCEI-0170743) dataset ([Aulicino et al. \(2018\)](#)) contains sea surface temperature and salinity data collected from 2010 to 2017 in the South Atlantic Ocean and Southern Ocean from S.A. Agulhas and Agulhas-II research vessels, in the framework of South African National Antarctic Programme ([SANAP](#)), South African Department of Environmental Affairs ([DEA](#)) and Italian National Antarctic Research Programme ([PNRA](#)) scientific activities. Measurements have been obtained through thermosalinograph (TSG) during several cruises to both Antarctica and sub-Antarctic islands. On-board TSG devices have been regularly calibrated and continuously monitored in-between cruises; no appreciable sensor drift emerged. Independent water samples taken along the cruises have been used to validate the data; salinity measurement error was a few hundredths of a unit on the practical salinity scale. A careful quality control allowed to discard bad data for each single campaign.

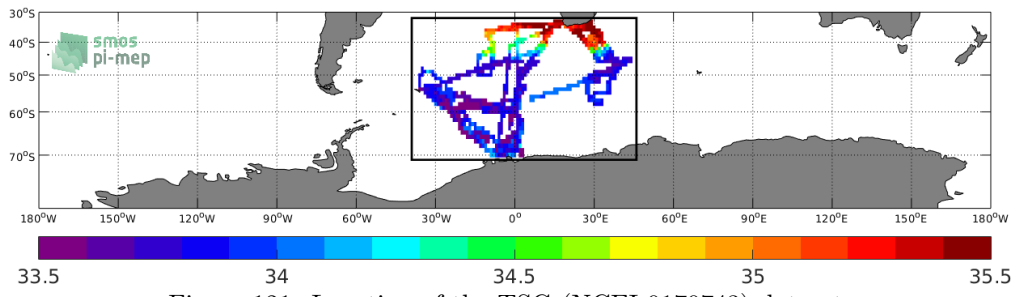


Figure 121: Location of the TSG (NCEI-0170743) dataset.

6.7.2 Number of SSS data as a function of time and distance to coast

Figure 122 shows the time (a) and distance to coast (b) distributions of the TSG (NCEI-0170743) *in situ* dataset.

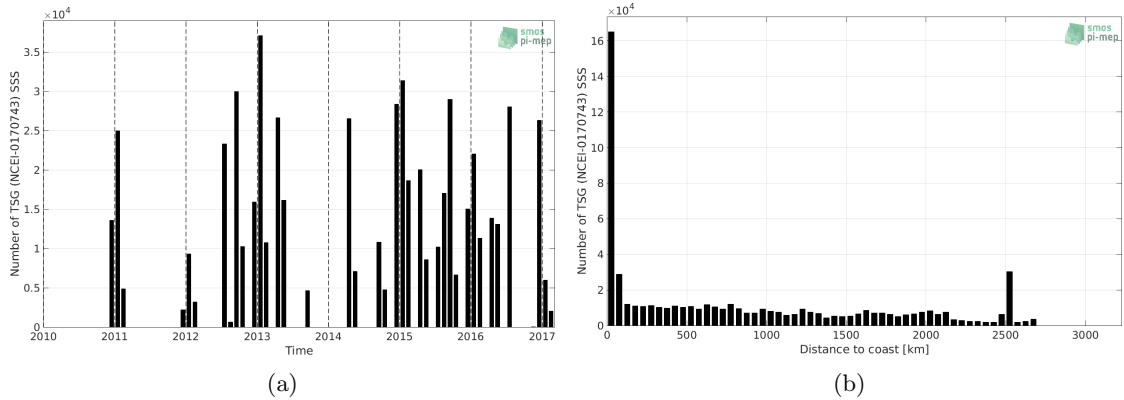


Figure 122: Number of SSS from TSG (NCEI-0170743) as a function of time (a) and distance to coast (b).

6.7.3 Histograms of SSS

Figure 123 shows the SSS distribution of the TSG (NCEI-0170743) (a) and colocalized ISAS (b) dataset.

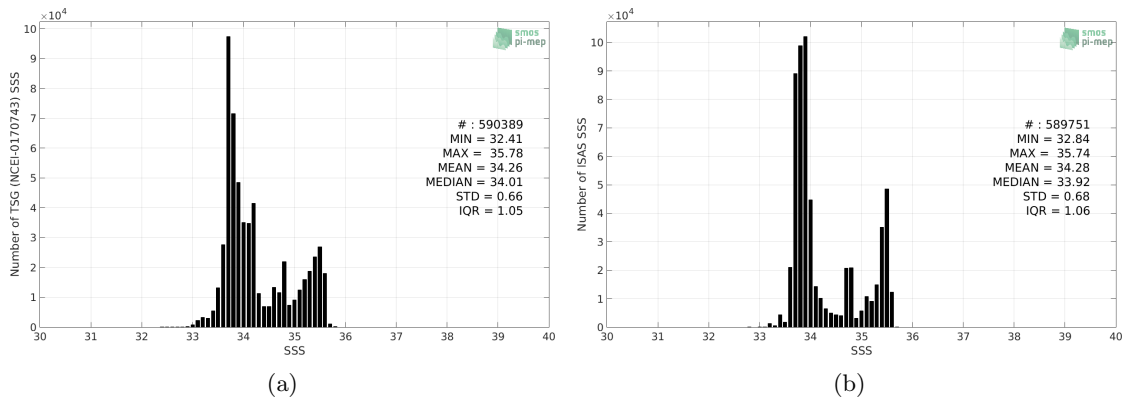


Figure 123: Histograms of SSS from TSG (NCEI-0170743) (a) and ISAS (b) per bins of 0.1.

6.7.4 Distribution of *in situ* SSS depth measurements

In Figure 124, we show the depth distribution of the *in situ* salinity dataset (a) and the spatial distribution of the depth temporal mean in $1^\circ \times 1^\circ$ boxes and considering the full *in situ* dataset period (b).

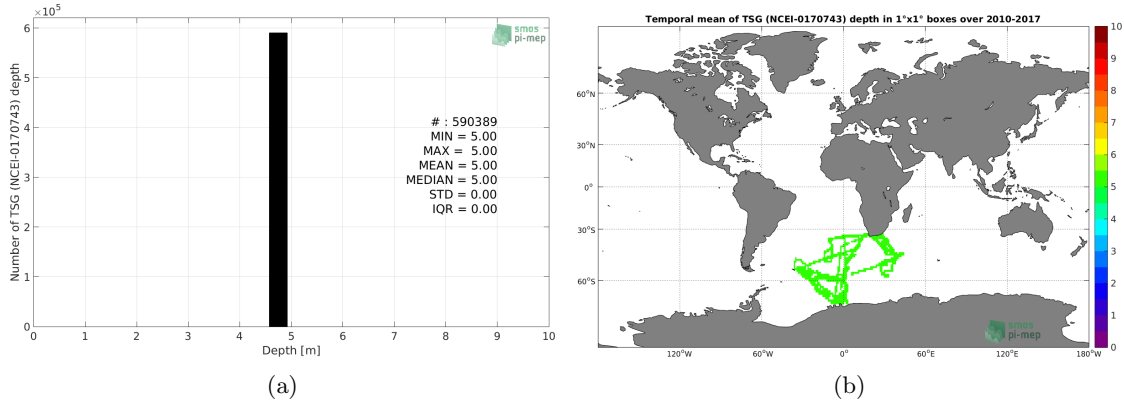


Figure 124: Depth distribution of the upper level SSS measurements from TSG (NCEI-0170743) (a) and spatial distribution of the *in situ* SSS depth measurements showing the mean value in $1^\circ \times 1^\circ$ boxes and considering the full *in situ* dataset period (b).

6.7.5 Spatial distribution of SSS

In Figure 125, the number of TSG (NCEI-0170743) SSS measurements in $1^\circ \times 1^\circ$ boxes is shown.

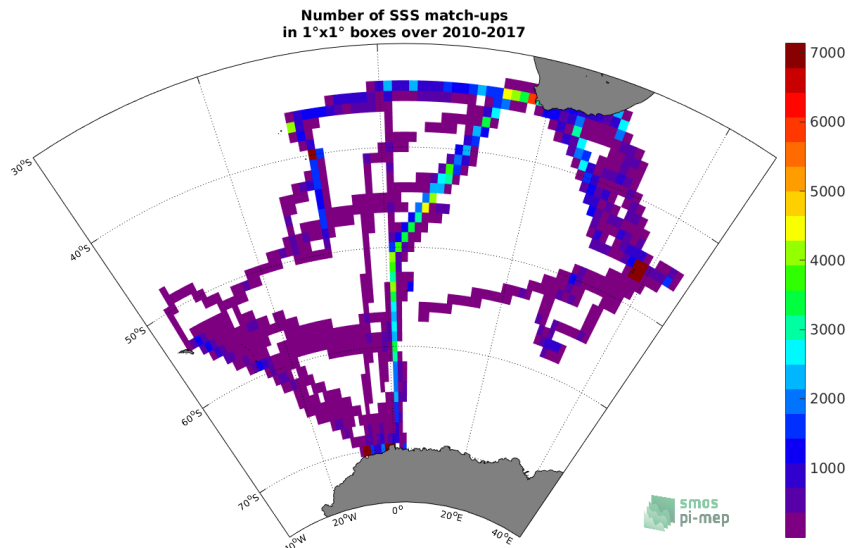


Figure 125: Number of SSS from TSG (NCEI-0170743) in $1^\circ \times 1^\circ$ boxes.

6.7.6 Spatial Maps of the Temporal mean and Std of *in situ* and ISAS SSS and of the difference (Δ SSS)

In Figure 126, maps of temporal mean (left) and standard deviation (right) of ISAS (top), TSG (NCEI-0170743) *in situ* dataset (middle) and the difference Δ SSS(ISAS -TSG (NCEI-0170743)) (bottom) are shown. The temporal mean and std are calculated using all match-up pairs falling in spatial boxes of size $1^\circ \times 1^\circ$ over the full TSG (NCEI-0170743) dataset period.

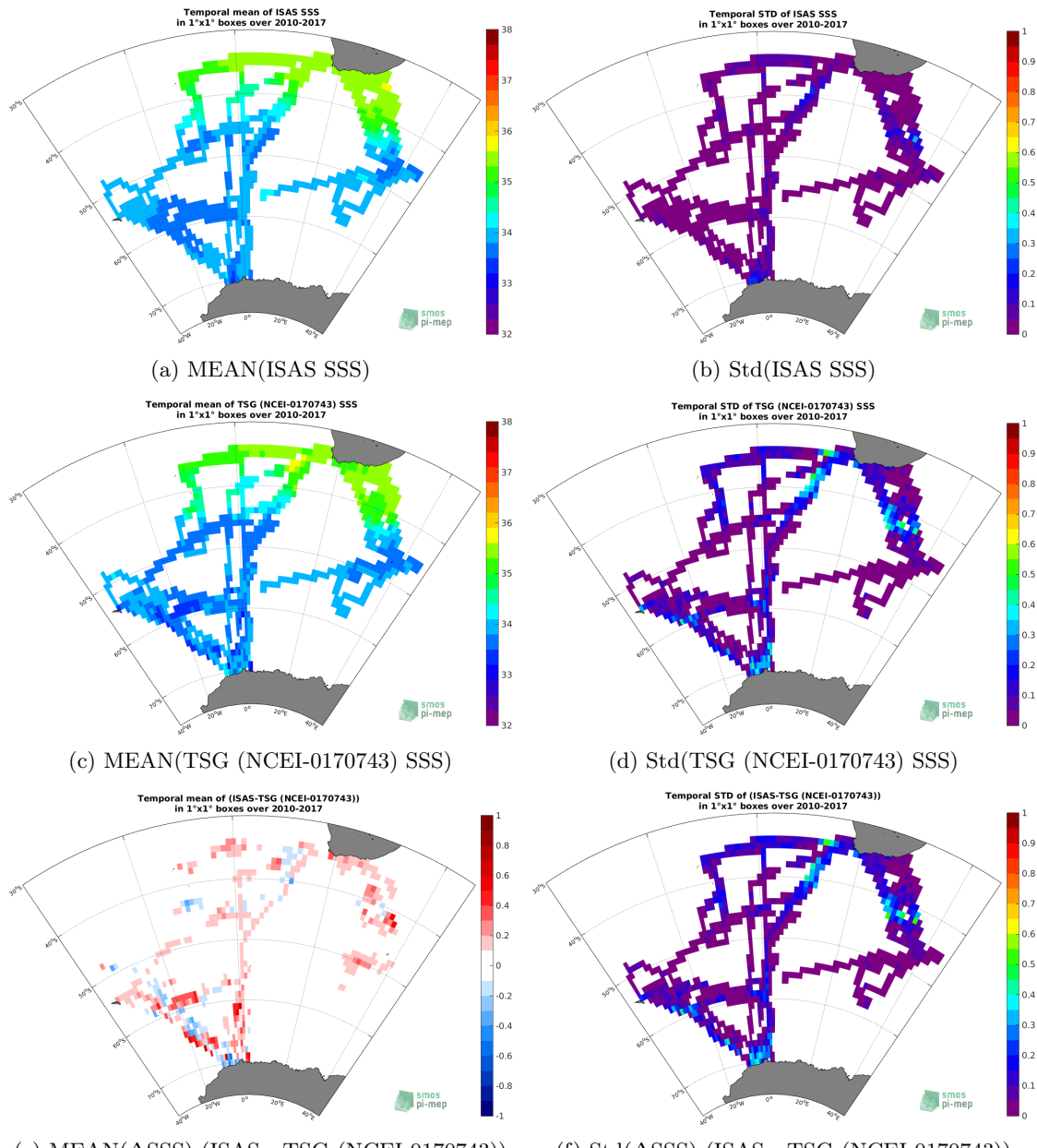


Figure 126: Temporal mean (left) and Std (right) of SSS from ISAS (top), TSG (NCEI-0170743) (middle), and of Δ SSS (ISAS - TSG (NCEI-0170743)). Only match-up pairs are used to generate these maps.

6.7.7 Time series of the monthly median and Std of *in situ* and ISAS SSS and of the difference (Δ SSS)

In the top panel of Figure 127, we show the time series of the monthly median SSS estimated for both ISAS SSS product (in black) and the TSG (NCEI-0170743) *in situ* dataset (in blue) at the collected Pi-MEP match-up pairs.

In the middle panel of Figure 127, we show the time series of the monthly median of ΔSSS (ISAS - TSG (NCEI-0170743)) for the collected Pi-MEP match-up pairs.

In the bottom panel of Figure 127, we show the time series of the monthly standard deviation of the ΔSSS (ISAS - TSG (NCEI-0170743)) for the collected Pi-MEP match-up pairs.

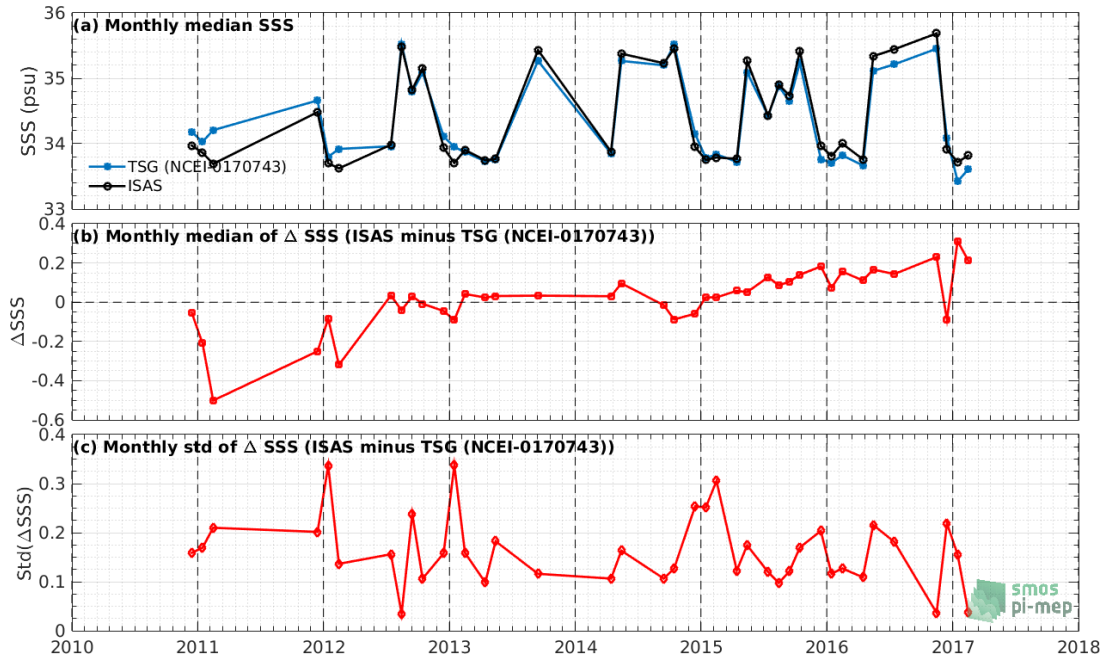


Figure 127: Time series of the monthly median SSS (top), median of ΔSSS (ISAS - TSG (NCEI-0170743)) and Std of ΔSSS (ISAS - TSG (NCEI-0170743)) considering all match-ups collected by the Pi-MEP.

6.7.8 Zonal mean and Std of *in situ* and ISAS SSS and of the difference ΔSSS

In Figure 128 left panel, we show the zonal mean SSS considering all Pi-MEP match-up pairs for both ISAS SSS product (in black) and the TSG (NCEI-0170743) *in situ* dataset (in blue). The full *in situ* dataset period is used to derive the mean.

In the right panel of Figure 128, we show the zonal mean of ΔSSS (ISAS - TSG (NCEI-0170743)) for all the collected Pi-MEP match-up pairs estimated over the full *in situ* dataset period.

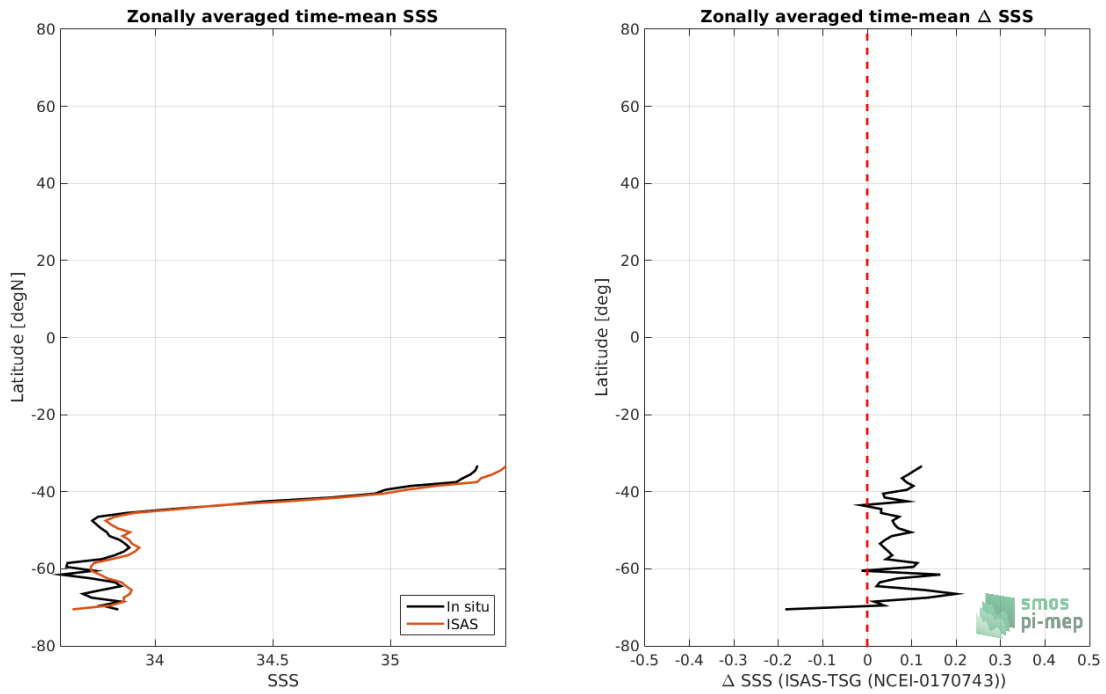


Figure 128: Left panel: Zonal mean SSS from ISAS product (black) and from TSG (NCEI-0170743) (blue). Right panel: Zonal mean of Δ SSS (ISAS - TSG (NCEI-0170743)) for all the collected Pi-MEP match-up pairs estimated over the full *in situ* dataset period.

6.7.9 Scatterplots of ISAS vs *in situ* SSS by latitudinal bands

In Figure 129, contour maps of the concentration of ISAS SSS (y-axis) versus TSG (NCEI-0170743) SSS (x-axis) at match-up pairs for different latitude bands: (a) 80°S-80°N, (b) 20°S-20°N, (c) 40°S-20°S and 20°N-40°N and (d) 60°S-40°S and 40°N-60°N. For each plot, the red line shows $x=y$. The black thin and dashed lines indicate a linear fit through the data cloud and the $\pm 95\%$ confidence levels, respectively. The number match-up pairs n , the slope and R^2 coefficient of the linear fit, the root mean square (RMS) and the mean bias between ISAS and *in situ* data are indicated for each latitude band in each plots.

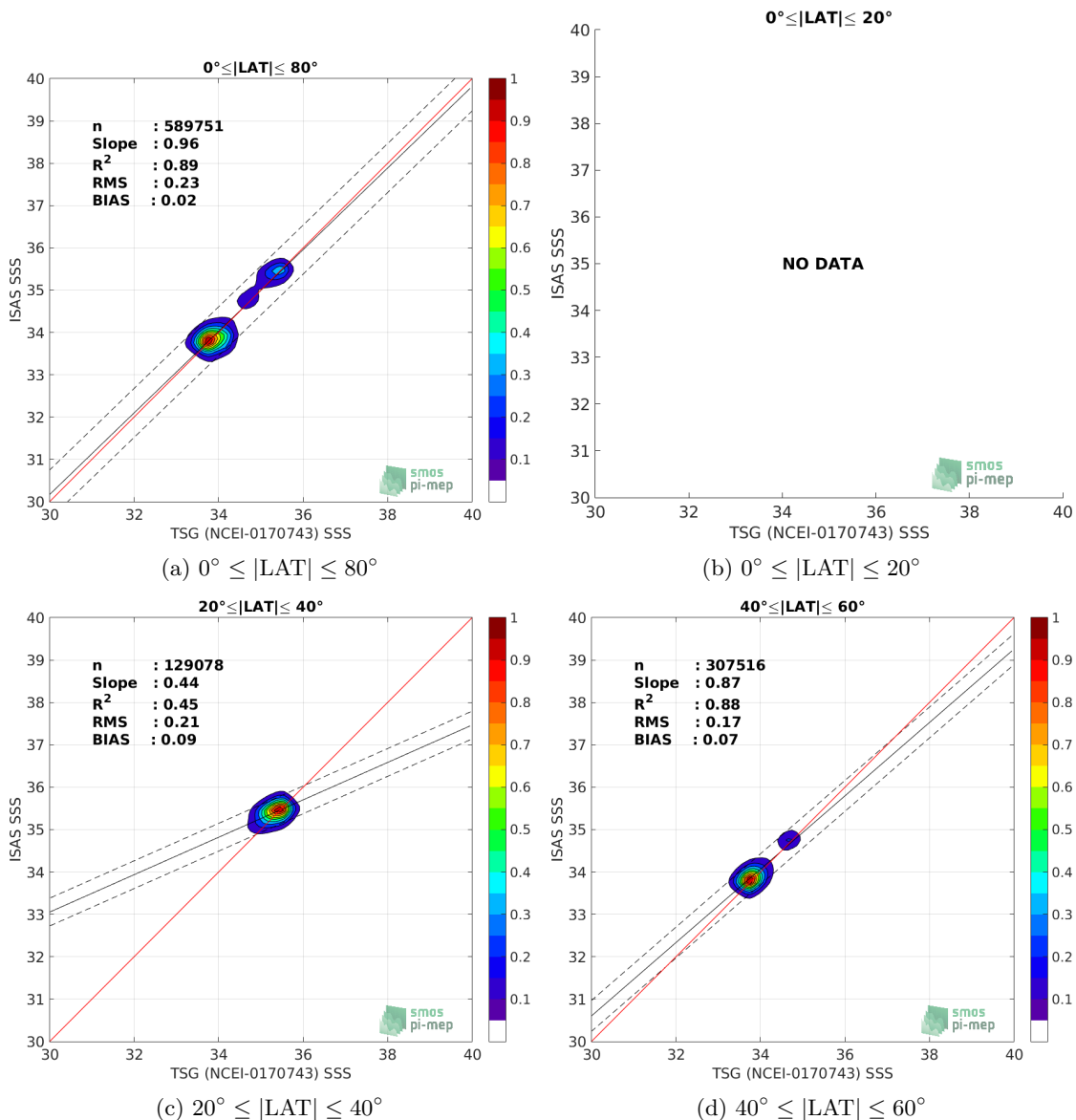


Figure 129: Contour maps of the concentration of ISAS SSS (y-axis) versus TSG (NCEI-0170743) SSS (x-axis) at match-up pairs for different latitude bands. For each plot, the red line shows $x=y$. The black thin and dashed lines indicate a linear fit through the data cloud and the $\pm 95\%$ confidence levels, respectively. The number match-up pairs n , the slope and R^2 coefficient of the linear fit, the root mean square (RMS) and the mean bias between ISAS and *in situ* data are indicated for each latitude band in each plots.

6.7.10 Time series of the monthly median and Std of the difference ΔSSS sorted by latitudinal bands

In Figure 130, time series of the monthly median (red curves) of ΔSSS (ISAS - TSG (NCEI-0170743)) and ± 1 Std (black vertical thick bars) as function of time for all the collected Pi-MEP

match-up pairs estimated for the full *in situ* dataset period are shown for different latitude bands: (a) 80°S-80°N, (b) 20°S-20°N, (c) 40°S-20°S and 20°N-40°N and (d) 60°S-40°S and 40°N-60°N.

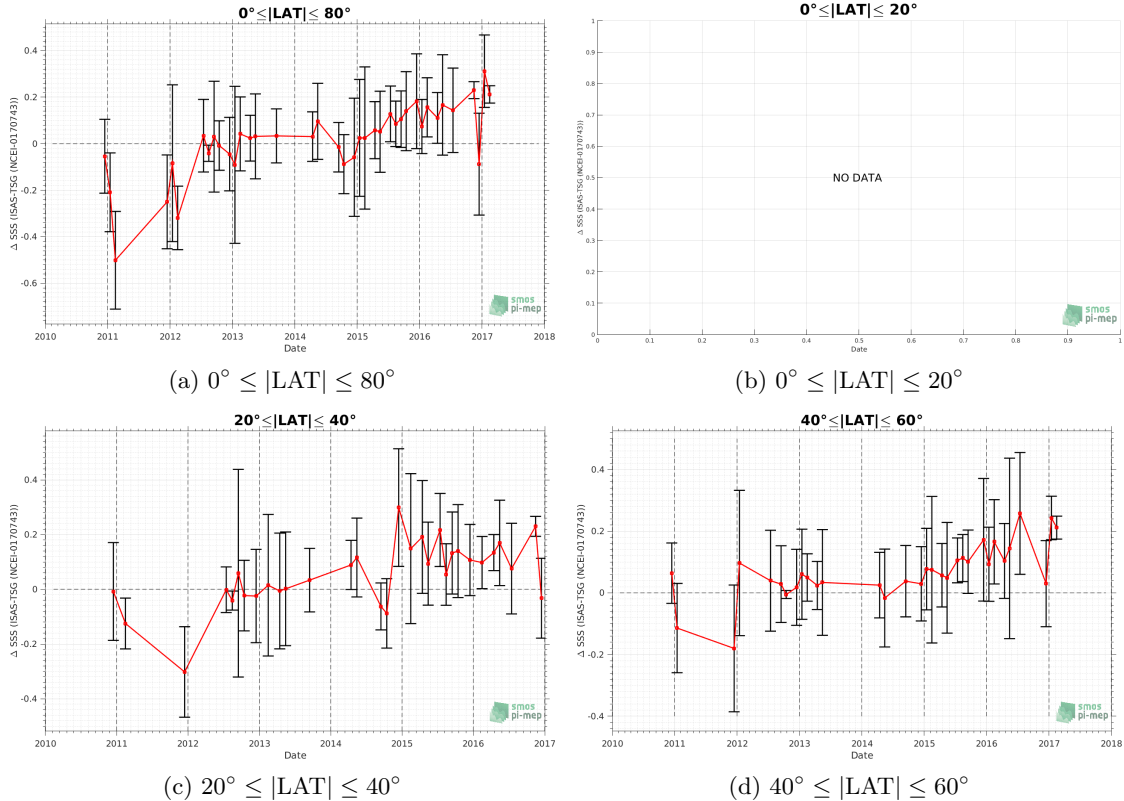


Figure 130: Monthly median (red curves) of ΔSSS (ISAS - TSG (NCEI-0170743)) and ± 1 Std (black vertical thick bars) as function of time for all the collected Pi-MEP match-up pairs for the full *in situ* dataset period are shown for different latitude bands: (a) 80°S-80°N, (b) 20°S-20°N, (c) 40°S-20°S and 20°N-40°N and (d) 60°S-40°S and 40°N-60°N.

6.7.11 ΔSSS sorted as geophysical conditions

In Figure 131, we classify the match-up differences ΔSSS (ISAS - *in situ*) as function of the geophysical conditions at match-up points. The mean and std of ΔSSS (ISAS - TSG (NCEI-0170743)) is thus evaluated as function of the

- *in situ* SSS values per bins of width 0.2,
- *in situ* SST values per bins of width 1°C,
- ASCAT daily wind values per bins of width 1 m/s,
- CMORPH 3-hourly rain rates per bins of width 1 mm/h, and,
- distance to coasts per bins of width 50 km,
- *in situ* measurement depth (if relevant).

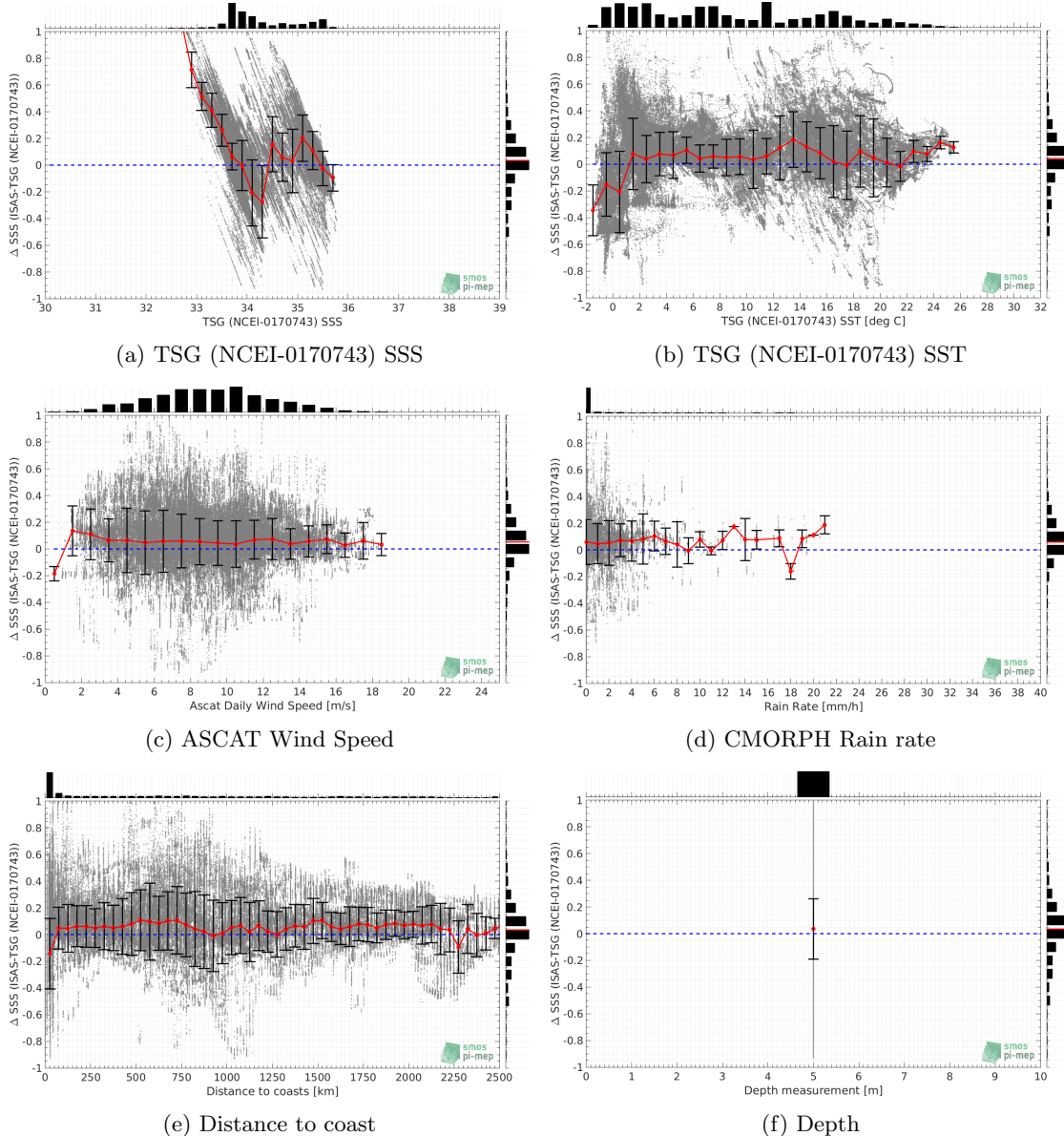


Figure 131: ΔSSS (ISAS - TSG (NCEI-0170743)) sorted as geophysical conditions: TSG (NCEI-0170743) SSS a), TSG (NCEI-0170743) SST b), ASCAT Wind speed c), CMORPH rain rate d), distance to coast (e) and depth measurements (f).

6.7.12 ΔSSS maps and statistics for different geophysical conditions

In Figures 132 and 133, we focus on sub-datasets of the match-up differences ΔSSS (*ISAS - in situ*) for the following specific geophysical conditions:

- **C1:** if the local value at *in situ* location of estimated rain rate is zero, mean daily wind is in the range [3, 12] m/s, the SST is $> 5^\circ\text{C}$ and distance to coast is > 800 km.
- **C2:** if the local value at *in situ* location of estimated rain rate is zero, mean daily wind is

in the range [3, 12] m/s.

- **C3:** if the local value at *in situ* location of estimated rain rate is high (ie. > 1 mm/h) and mean daily wind is low (ie. < 4 m/s).
- **C5:** if the *in situ* data is located where the climatological SSS standard deviation is low (ie. above < 0.2).
- **C6:** if the *in situ* data is located where the climatological SSS standard deviation is high (ie. above > 0.2).

For each of these conditions, the temporal mean (gridded over spatial boxes of size $1^\circ \times 1^\circ$) and the histogram of the difference ΔSSS (ISAS - *in situ*) are presented.

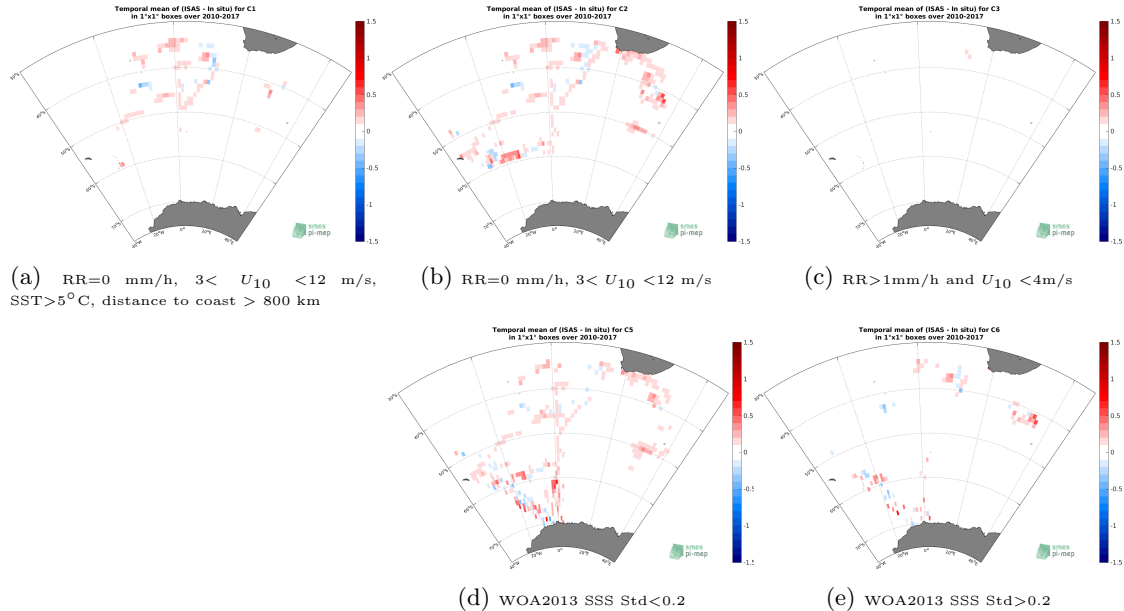


Figure 132: Temporal mean gridded over spatial boxes of size $1^\circ \times 1^\circ$ of ΔSSS (ISAS - TSG (NCEI-0170743)) for 5 different subdatasets corresponding to: RR=0 mm/h, $3 < U_{10} < 12$ m/s, SST> 5°C , distance to coast > 800 km (a), RR=0 mm/h, $3 < U_{10} < 12$ m/s (b), RR>1mm/h and $U_{10} < 4$ m/s (c), WOA2013 SSS Std<0.2 (d), WOA2013 SSS Std>0.2 (e).

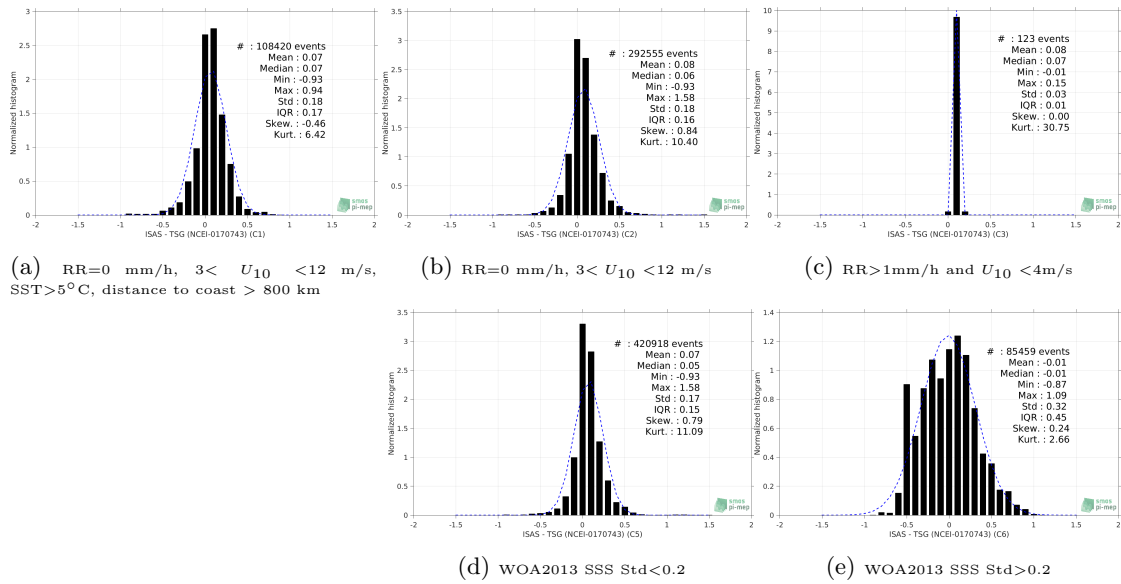


Figure 133: Normalized histogram of ΔSSS (ISAS - TSG (NCEI-0170743)) for 5 different sub-datasets corresponding to: RR=0 mm/h, $3 < U_{10} < 12$ m/s, SST>5°C, distance to coast > 800 km (a), RR=0 mm/h, $3 < U_{10} < 12$ m/s (b), RR>1mm/h and $U_{10} < 4$ m/s (c), WOA2013 SSS Std<0.2 (d), WOA2013 SSS Std>0.2 (e).

6.7.13 Summary

Table 1 shows the mean, median, standard deviation (Std), root mean square (RMS), interquartile range (IQR), correlation coefficient (r^2) and robust standard deviation (Std*) of the match-up differences ΔSSS (ISAS - TSG (NCEI-0170743)) for the following conditions:

- all: All the match-up pairs satellite/in situ SSS values are used to derive the statistics
- C1: only pairs where RR=0 mm/h, $3 < U_{10} < 12$ m/s, SST>5°C, distance to coast > 800 km
- C2: only pairs where RR=0 mm/h, $3 < U_{10} < 12$ m/s
- C3: only pairs where RR>1mm/h and $U_{10} < 4$ m/s
- C5: only pairs where WOA2013 SSS Std<0.2
- C6: only pairs where WOA2013 SSS Std>0.2
- C7a: only pairs with a distance to coast < 150 km.
- C7b: only pairs with a distance to coast in the range [150, 800] km.
- C7c: only pairs with a distance to coast > 800 km.
- C8a: only pairs where SST is < 5°C.
- C8b: only pairs where SST is in the range [5, 15]°C.
- C8c: only pairs where SST is > 15°C.

- C9a: only pairs where SSS is < 33.
- C9b: only pairs where SSS is in the range [33, 37].
- C9c: only pairs where SSS is > 37.

Table 1: Statistics of Δ SSS (ISAS - TSG (NCEI-0170743))

Condition	#	Median	Mean	Std	RMS	IQR	r^2	Std*
all	589751	0.03	0.02	0.23	0.23	0.21	0.890	0.16
C1	108420	0.07	0.07	0.18	0.19	0.17	0.906	0.13
C2	292555	0.06	0.08	0.18	0.19	0.16	0.941	0.12
C3	123	0.07	0.08	0.03	0.09	0.01	1.000	0.01
C5	420918	0.05	0.07	0.17	0.18	0.15	0.943	0.11
C6	85459	-0.01	-0.01	0.32	0.32	0.45	0.792	0.34
C7a	205194	-0.01	-0.08	0.26	0.27	0.35	0.793	0.25
C7b	138113	0.07	0.09	0.21	0.23	0.22	0.932	0.16
C7c	246444	0.06	0.07	0.17	0.18	0.16	0.925	0.12
C8a	194461	0.00	-0.03	0.26	0.26	0.35	0.044	0.24
C8b	219434	0.06	0.08	0.15	0.17	0.13	0.919	0.09
C8c	124692	0.04	0.06	0.23	0.23	0.22	0.776	0.16
C9a	940	0.87	0.86	0.20	0.88	0.31	0.202	0.27
C9b	588811	0.03	0.02	0.22	0.22	0.21	0.892	0.15
C9c	0	NaN	NaN	NaN	NaN	NaN	NaN	NaN

Table 1 numerical values can be downloaded as a csv file [here](#).

6.8 TSG (LEGOS-Survostral)

6.8.1 Introduction

The TSG (LEGOS-Survostral) dataset corresponds to delayed mode regional data from TSG installed on the Astrolabe vessel (IPEV) during the round trips between Hobart (Tasmania) and the French Antarctic base at Dumont d'Urville ([Morrow and Kestenare \(2014\)](#)). It is provided by the [Survostral project](#) and available [here](#). Adjusted values when available and only collected TSG data that exhibit quality flags=1 and 2 were used.

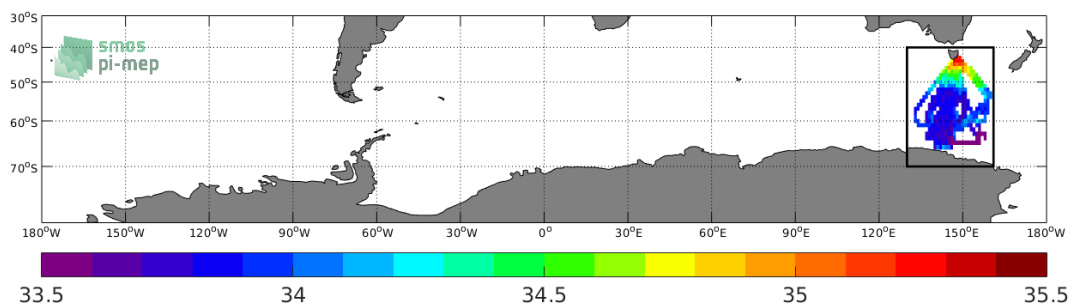


Figure 134: Location of the TSG (LEGOS-Survostral) dataset.

6.8.2 Number of SSS data as a function of time and distance to coast

Figure 135 shows the time (a) and distance to coast (b) distributions of the TSG (LEGOS-Survostral) *in situ* dataset.

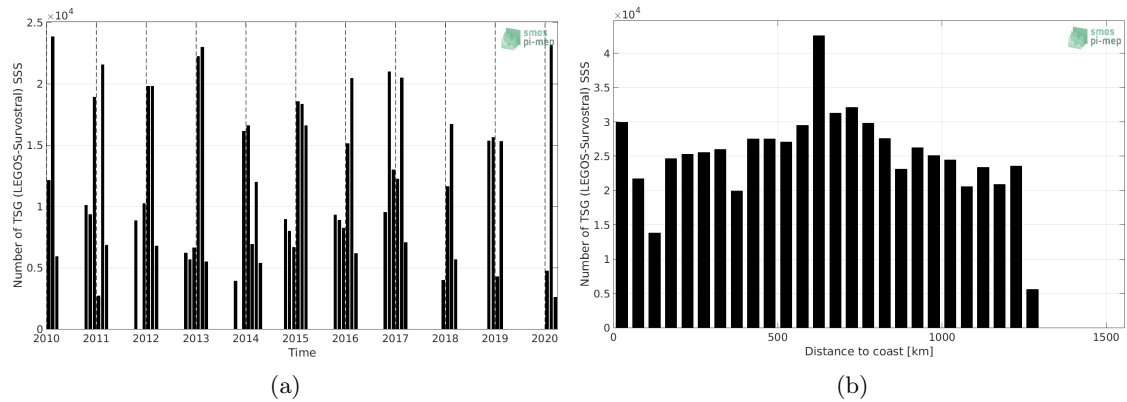


Figure 135: Number of SSS from TSG (LEGOS-Survostral) as a function of time (a) and distance to coast (b).

6.8.3 Histograms of SSS

Figure 136 shows the SSS distribution of the TSG (LEGOS-Survostral) (a) and colocalized ISAS (b) dataset.

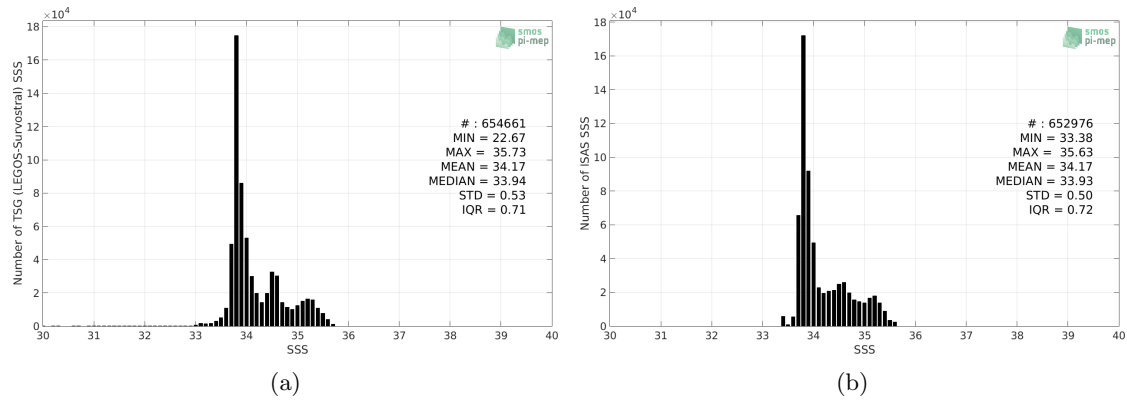


Figure 136: Histograms of SSS from TSG (LEGOS-Survostral) (a) and ISAS (b) per bins of 0.1.

6.8.4 Distribution of *in situ* SSS depth measurements

In Figure 137, we show the depth distribution of the *in situ* salinity dataset (a) and the spatial distribution of the depth temporal mean in $1^\circ \times 1^\circ$ boxes and considering the full *in situ* dataset period (b).

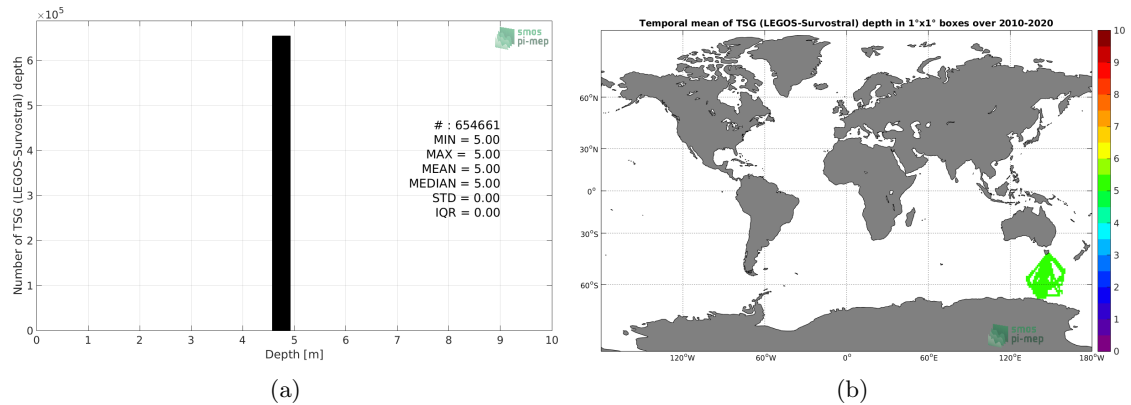


Figure 137: Depth distribution of the upper level SSS measurements from TSG (LEGOS-Survostral) (a) and spatial distribution of the *in situ* SSS depth measurements showing the mean value in $1^\circ \times 1^\circ$ boxes and considering the full *in situ* dataset period (b).

6.8.5 Spatial distribution of SSS

In Figure 138, the number of TSG (LEGOS-Survostral) SSS measurements in $1^\circ \times 1^\circ$ boxes is shown.

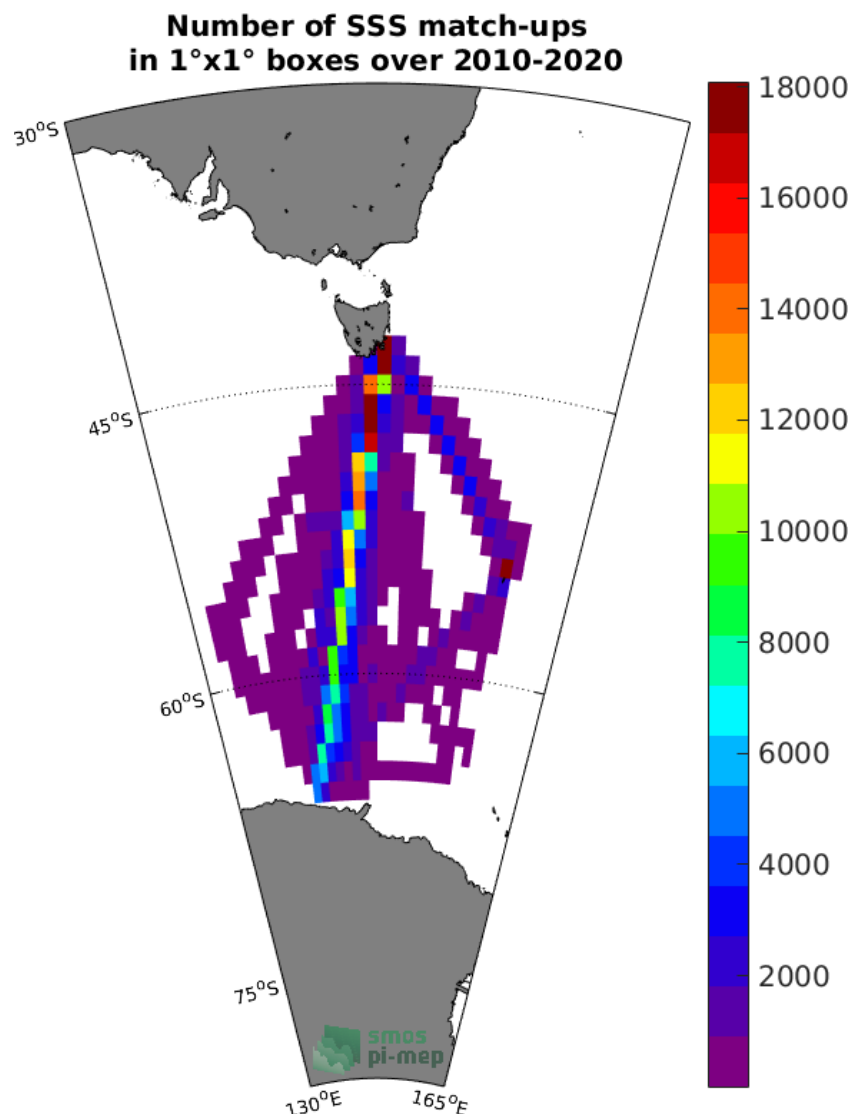


Figure 138: Number of SSS from TSG (LEGOS-Survostral) in $1^{\circ} \times 1^{\circ}$ boxes.

6.8.6 Spatial Maps of the Temporal mean and Std of *in situ* and ISAS SSS and of the difference (Δ SSS)

In Figure 139, maps of temporal mean (left) and standard deviation (right) of ISAS (top), TSG (LEGOS-Survostral) *in situ* dataset (middle) and the difference Δ SSS(ISAS -TSG (LEGOS-Survostral)) (bottom) are shown. The temporal mean and std are calculated using all match-up pairs falling in spatial boxes of size $1^{\circ} \times 1^{\circ}$ over the full TSG (LEGOS-Survostral) dataset period.

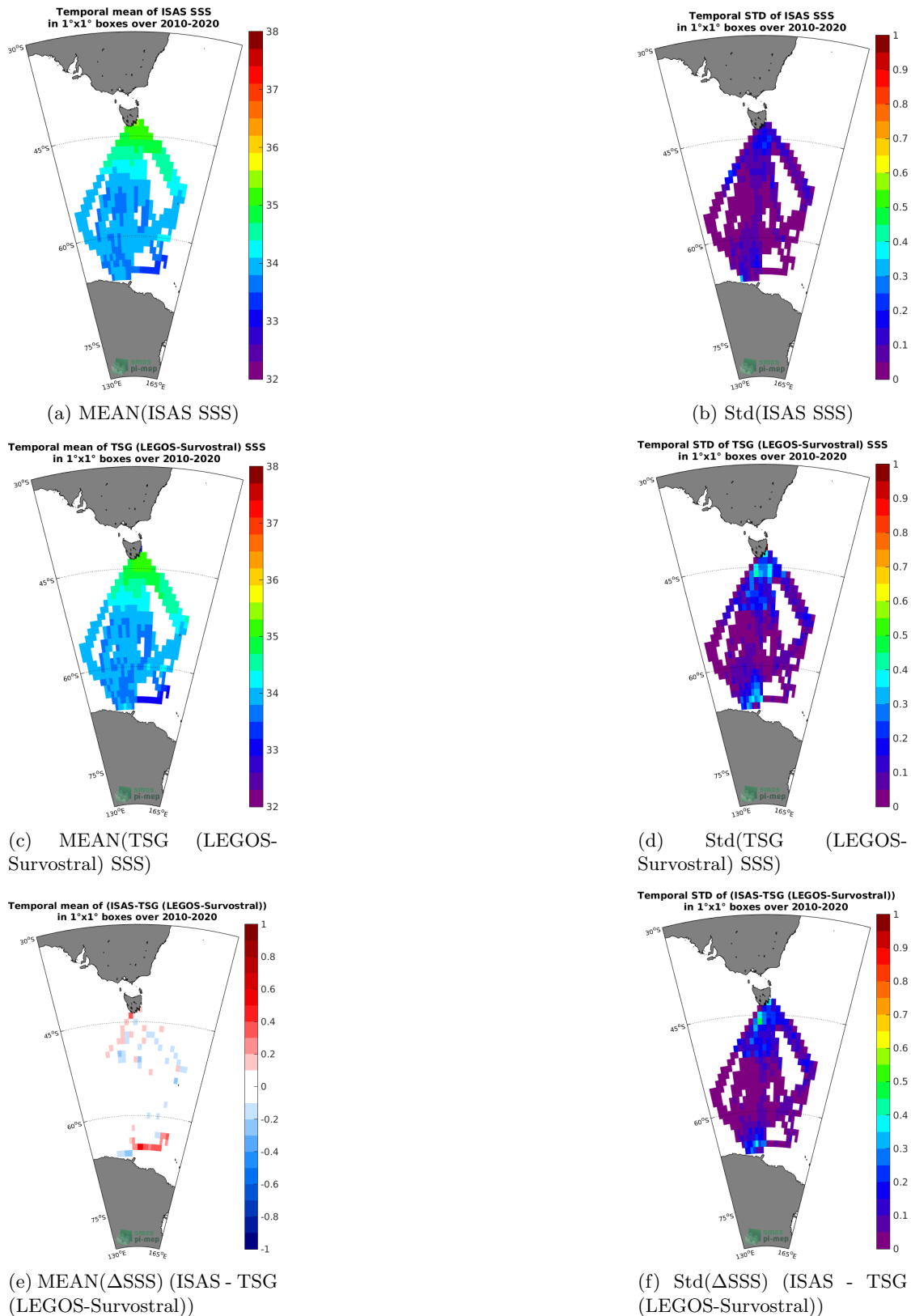


Figure 139: Temporal mean (left) and Std (right) of SSS from ISAS (top), TSG (LEGOS-Survostral) (middle), and of Δ SSS (ISAS - TSG (LEGOS-Survostral)). Only match-up pairs are used to generate these maps.

6.8.7 Time series of the monthly median and Std of *in situ* and ISAS SSS and of the difference (Δ SSS)

In the top panel of Figure 140, we show the time series of the monthly median SSS estimated for both ISAS SSS product (in black) and the TSG (LEGOS-Survostral) *in situ* dataset (in blue) at the collected Pi-MEP match-up pairs.

In the middle panel of Figure 140, we show the time series of the monthly median of Δ SSS (ISAS - TSG (LEGOS-Survostral)) for the collected Pi-MEP match-up pairs.

In the bottom panel of Figure 140, we show the time series of the monthly standard deviation of the Δ SSS (ISAS - TSG (LEGOS-Survostral)) for the collected Pi-MEP match-up pairs.

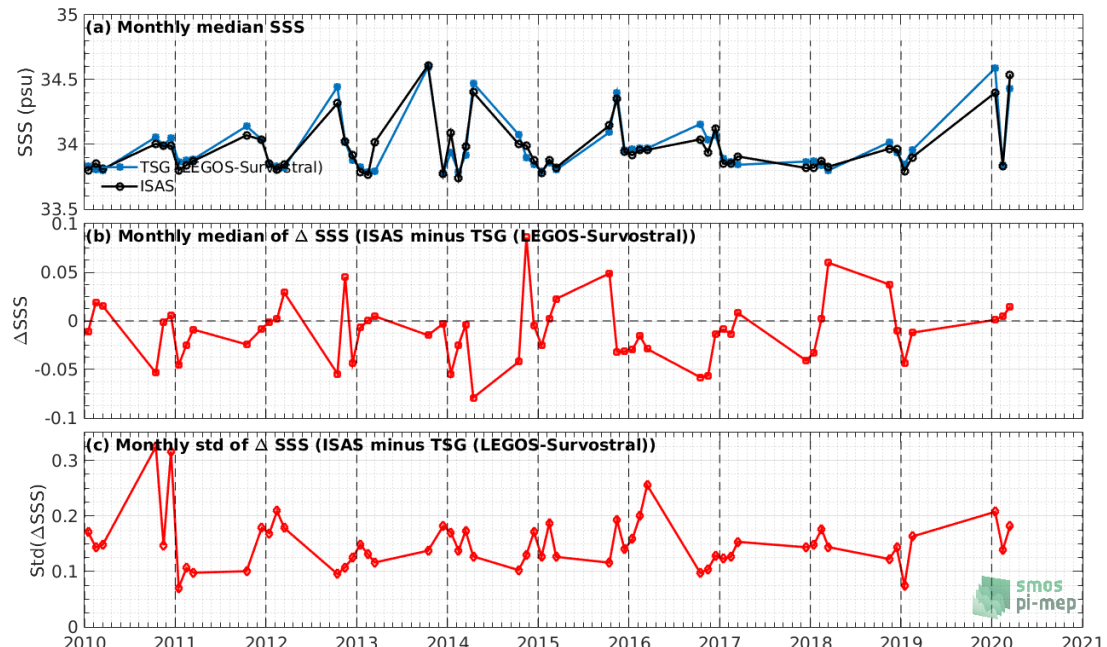


Figure 140: Time series of the monthly median SSS (top), median of Δ SSS (ISAS - TSG (LEGOS-Survostral)) and Std of Δ SSS (ISAS - TSG (LEGOS-Survostral)) considering all match-ups collected by the Pi-MEP.

6.8.8 Zonal mean and Std of *in situ* and ISAS SSS and of the difference Δ SSS

In Figure 141 left panel, we show the zonal mean SSS considering all Pi-MEP match-up pairs for both ISAS SSS product (in black) and the TSG (LEGOS-Survostral) *in situ* dataset (in blue). The full *in situ* dataset period is used to derive the mean.

In the right panel of Figure 141, we show the zonal mean of Δ SSS (ISAS - TSG (LEGOS-Survostral)) for all the collected Pi-MEP match-up pairs estimated over the full *in situ* dataset period.

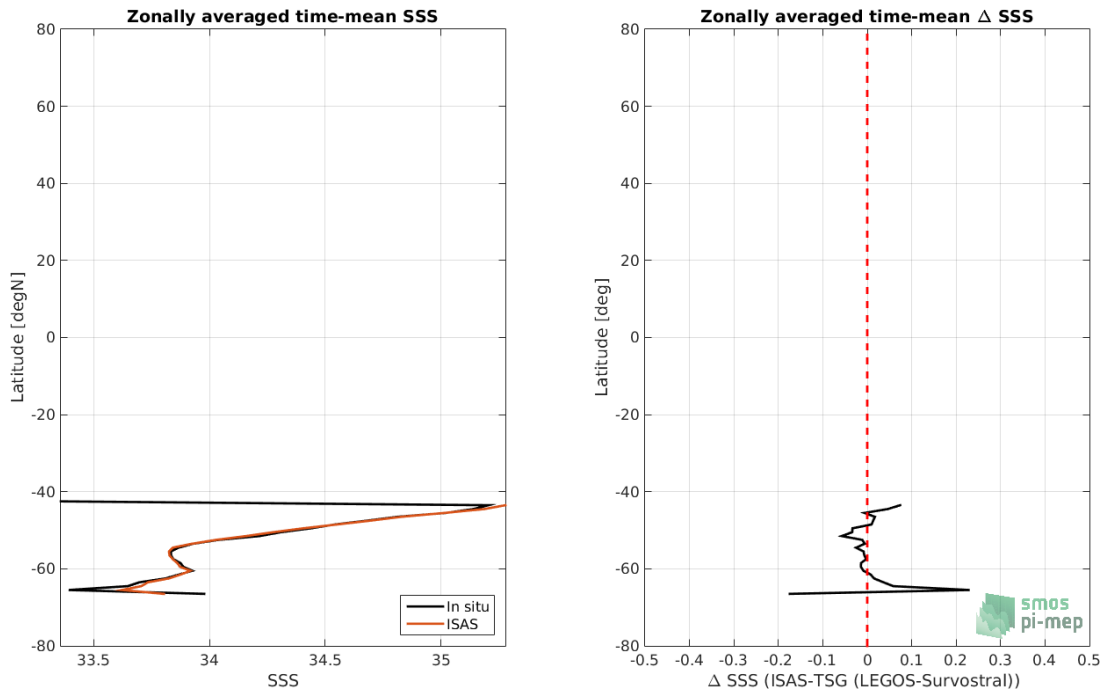


Figure 141: Left panel: Zonal mean SSS from ISAS product (black) and from TSG (LEGO-Survostral) (blue). Right panel: Zonal mean of Δ SSS (ISAS - TSG (LEGO-Survostral)) for all the collected Pi-MEP match-up pairs estimated over the full *in situ* dataset period.

6.8.9 Scatterplots of ISAS vs *in situ* SSS by latitudinal bands

In Figure 142, contour maps of the concentration of ISAS SSS (y-axis) versus TSG (LEGO-Survostral) SSS (x-axis) at match-up pairs for different latitude bands: (a) 80°S-80°N, (b) 20°S-20°N, (c) 40°S-20°S and 20°N-40°N and (d) 60°S-40°S and 40°N-60°N. For each plot, the red line shows $x=y$. The black thin and dashed lines indicate a linear fit through the data cloud and the $\pm 95\%$ confidence levels, respectively. The number match-up pairs n , the slope and R^2 coefficient of the linear fit, the root mean square (RMS) and the mean bias between ISAS and *in situ* data are indicated for each latitude band in each plots.

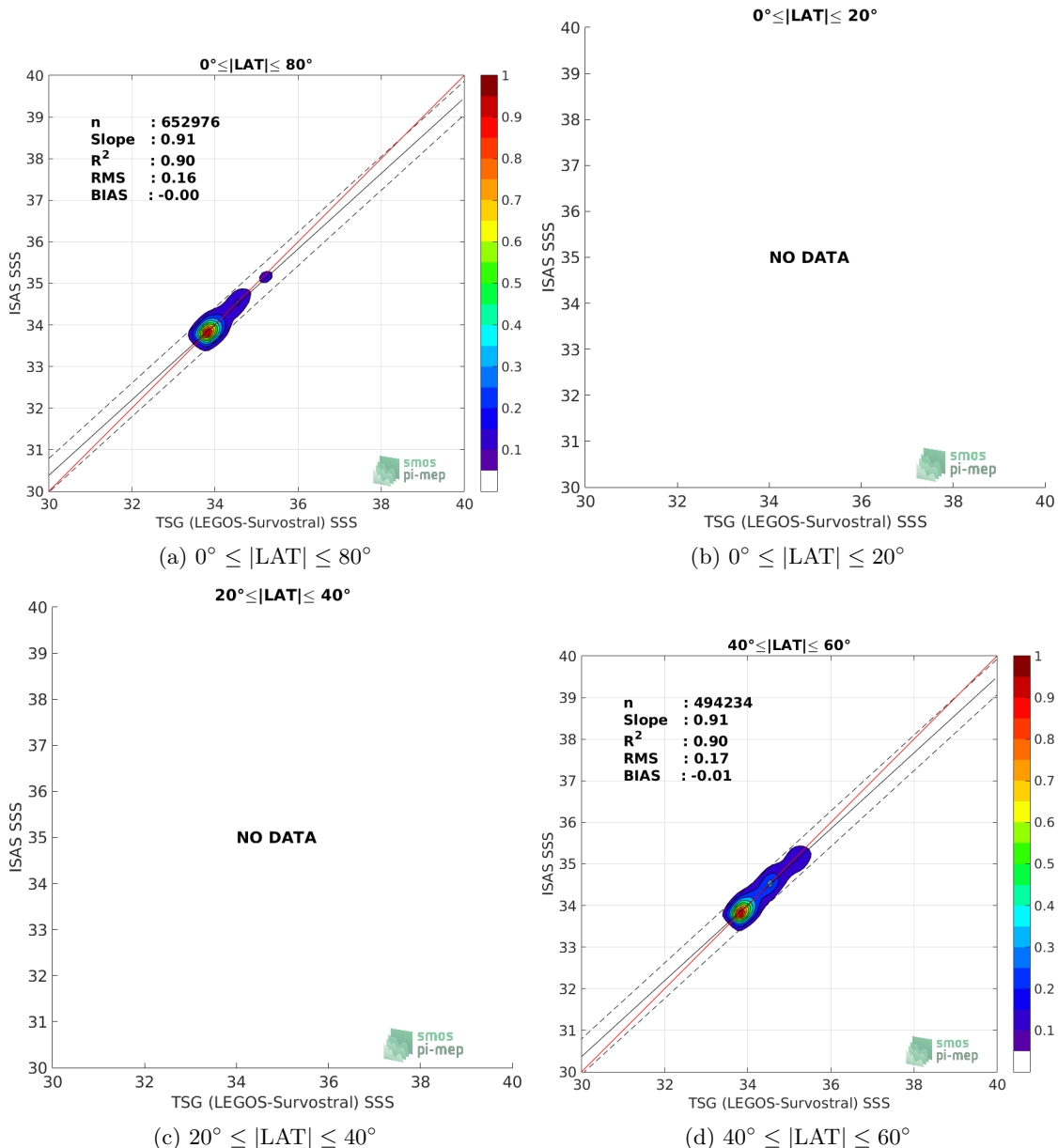


Figure 142: Contour maps of the concentration of ISAS SSS (y-axis) versus TSG (LEGOS-Survostral) SSS (x-axis) at match-up pairs for different latitude bands. For each plot, the red line shows $x=y$. The black thin and dashed lines indicate a linear fit through the data cloud and the $\pm 95\%$ confidence levels, respectively. The number match-up pairs n , the slope and R^2 coefficient of the linear fit, the root mean square (RMS) and the mean bias between ISAS and *in situ* data are indicated for each latitude band in each plots.

6.8.10 Time series of the monthly median and Std of the difference ΔSSS sorted by latitudinal bands

In Figure 143, time series of the monthly median (red curves) of ΔSSS (ISAS - TSG (LEGOS-Survostral)) and ± 1 Std (black vertical thick bars) as function of time for all the collected Pi-MEP match-up pairs estimated for the full *in situ* dataset period are shown for different latitude bands: (a) $80^\circ\text{S}-80^\circ\text{N}$, (b) $20^\circ\text{S}-20^\circ\text{N}$, (c) $40^\circ\text{S}-20^\circ\text{S}$ and $20^\circ\text{N}-40^\circ\text{N}$ and (d) $60^\circ\text{S}-40^\circ\text{S}$ and $40^\circ\text{N}-60^\circ\text{N}$.

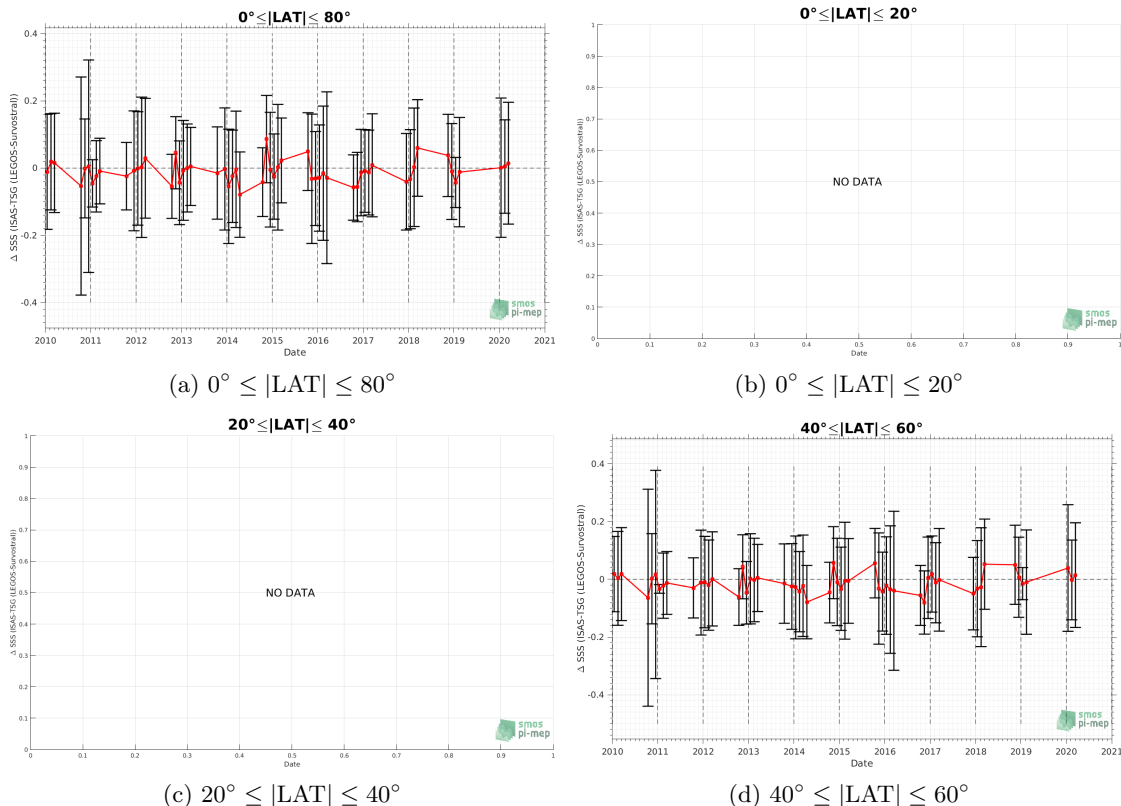


Figure 143: Monthly median (red curves) of ΔSSS (ISAS - TSG (LEGOS-Survostral)) and ± 1 Std (black vertical thick bars) as function of time for all the collected Pi-MEP match-up pairs for the full *in situ* dataset period are shown for different latitude bands: (a) $80^\circ\text{S}-80^\circ\text{N}$, (b) $20^\circ\text{S}-20^\circ\text{N}$, (c) $40^\circ\text{S}-20^\circ\text{S}$ and $20^\circ\text{N}-40^\circ\text{N}$, (d) $60^\circ\text{S}-40^\circ\text{S}$ and $40^\circ\text{N}-60^\circ\text{N}$.

6.8.11 ΔSSS sorted as geophysical conditions

In Figure 144, we classify the match-up differences ΔSSS (ISAS - *in situ*) as function of the geophysical conditions at match-up points. The mean and std of ΔSSS (ISAS - TSG (LEGOS-Survostral)) is thus evaluated as function of the

- *in situ* SSS values per bins of width 0.2,
- *in situ* SST values per bins of width 1°C ,
- ASCAT daily wind values per bins of width 1 m/s,

- CMORPH 3-hourly rain rates per bins of width 1 mm/h, and,
- distance to coasts per bins of width 50 km,
- *in situ* measurement depth (if relevant).

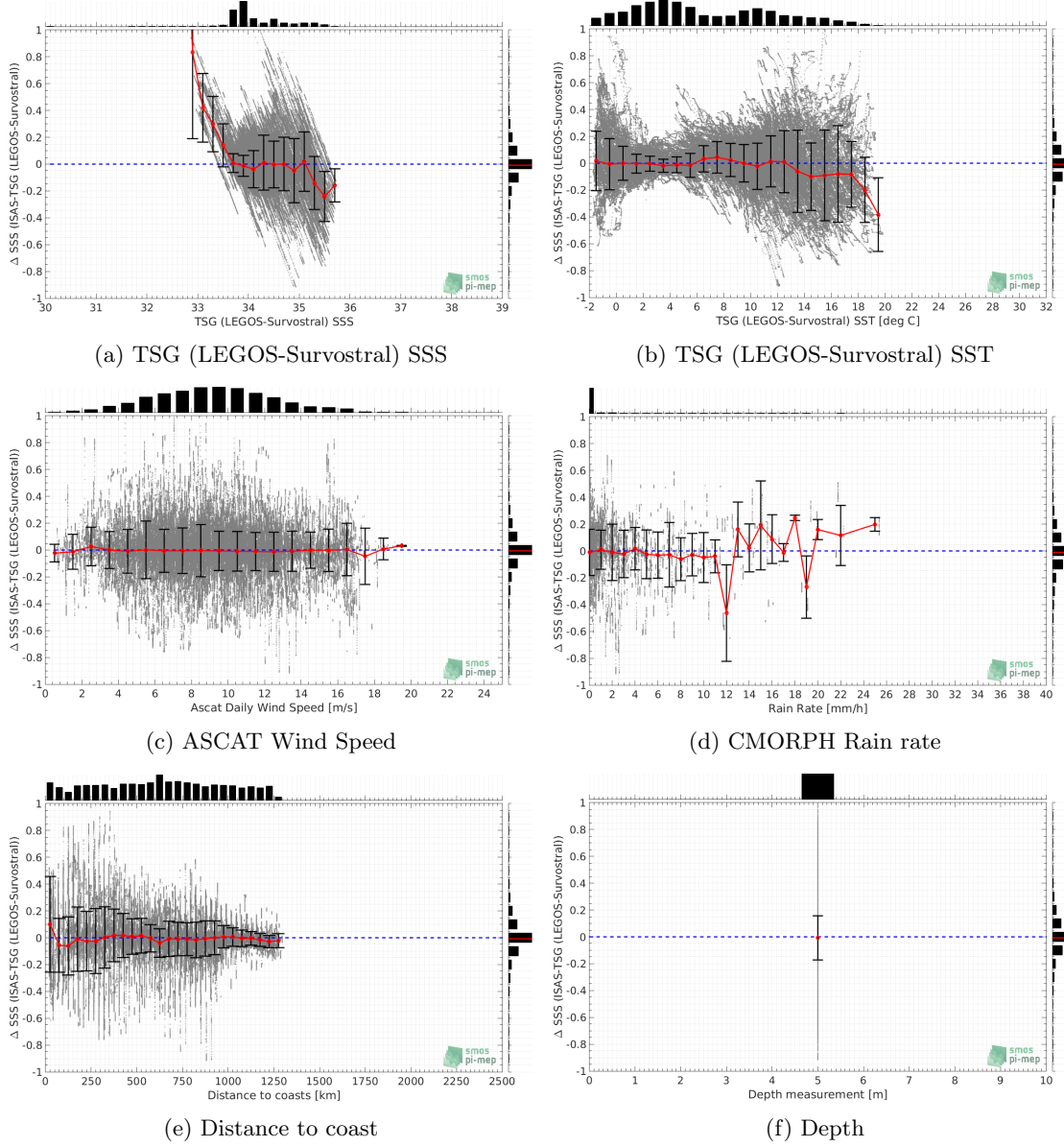


Figure 144: ΔSSS (ISAS - TSG (LEGOS-Survostral)) sorted as geophysical conditions: TSG (LEGOS-Survostral) SSS a), TSG (LEGOS-Survostral) SST b), ASCAT Wind speed c), CMORPH rain rate d), distance to coast (e) and depth measurements (f).

6.8.12 Δ SSS maps and statistics for different geophysical conditions

In Figures 145 and 146, we focus on sub-datasets of the match-up differences Δ SSS (ISAS - *in situ*) for the following specific geophysical conditions:

- **C1:**if the local value at *in situ* location of estimated rain rate is zero, mean daily wind is in the range [3, 12] m/s, the SST is $> 5^{\circ}\text{C}$ and distance to coast is > 800 km.
- **C2:**if the local value at *in situ* location of estimated rain rate is zero, mean daily wind is in the range [3, 12] m/s.
- **C3:**if the local value at *in situ* location of estimated rain rate is high (ie. > 1 mm/h) and mean daily wind is low (ie. < 4 m/s).
- **C5:**if the *in situ* data is located where the climatological SSS standard deviation is low (ie. above < 0.2).
- **C6:**if the *in situ* data is located where the climatological SSS standard deviation is high (ie. above > 0.2).

For each of these conditions, the temporal mean (gridded over spatial boxes of size $1^{\circ} \times 1^{\circ}$) and the histogram of the difference Δ SSS (ISAS - *in situ*) are presented.

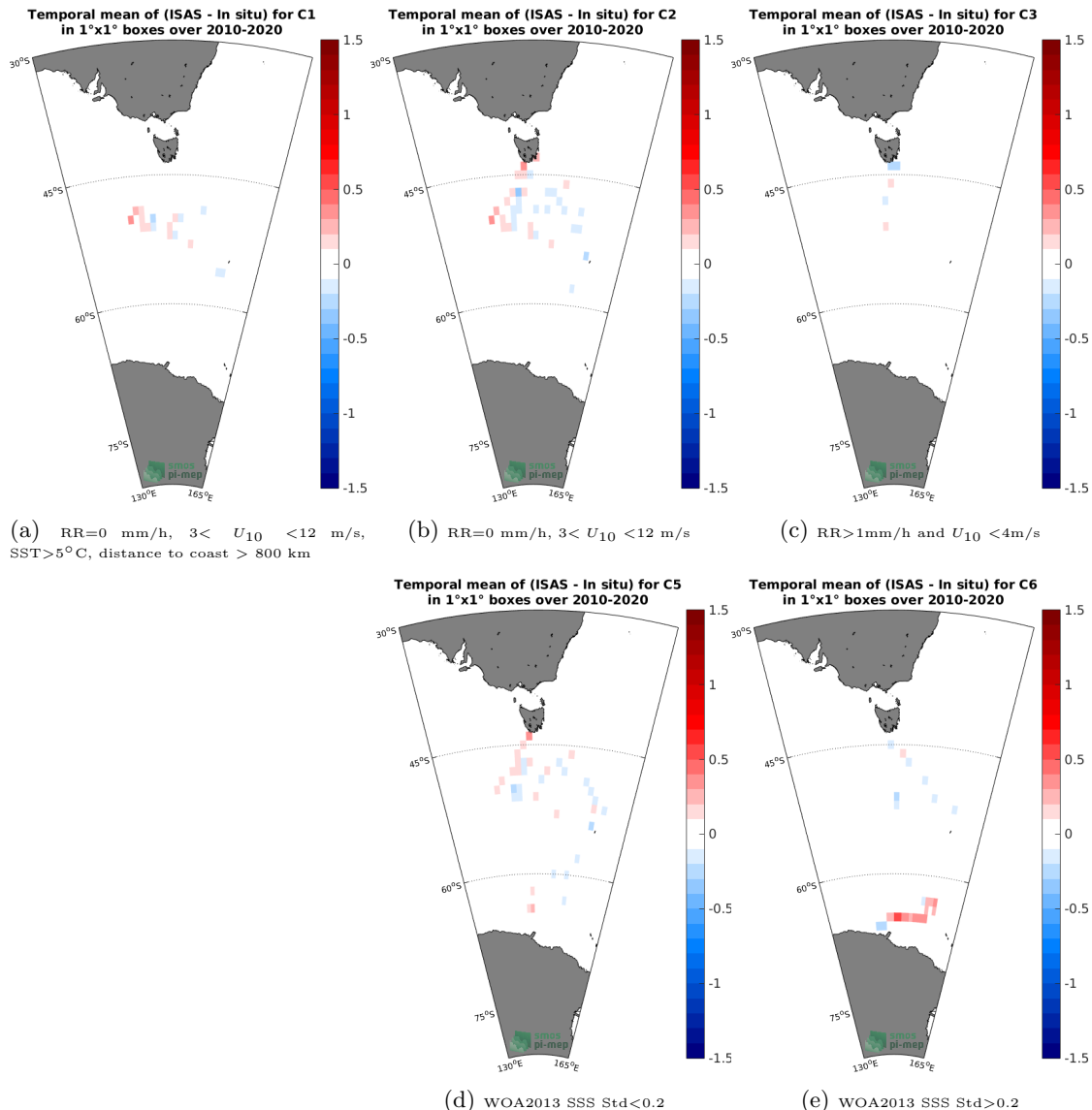


Figure 145: Temporal mean gridded over spatial boxes of size $1^\circ \times 1^\circ$ of ΔSSS (ISAS - TSG (LEGOS-Survostral)) for 5 different subdatasets corresponding to: $\text{RR}=0 \text{ mm/h}$, $3 < U_{10} < 12 \text{ m/s}$, $\text{SST} > 5^\circ\text{C}$, distance to coast > 800 km (a), $\text{RR}=0 \text{ mm/h}$, $3 < U_{10} < 12 \text{ m/s}$ (b), $\text{RR} > 1 \text{ mm/h}$ and $U_{10} < 4 \text{ m/s}$ (c), WOA2013 SSS Std < 0.2 (d), WOA2013 SSS Std > 0.2 (e).

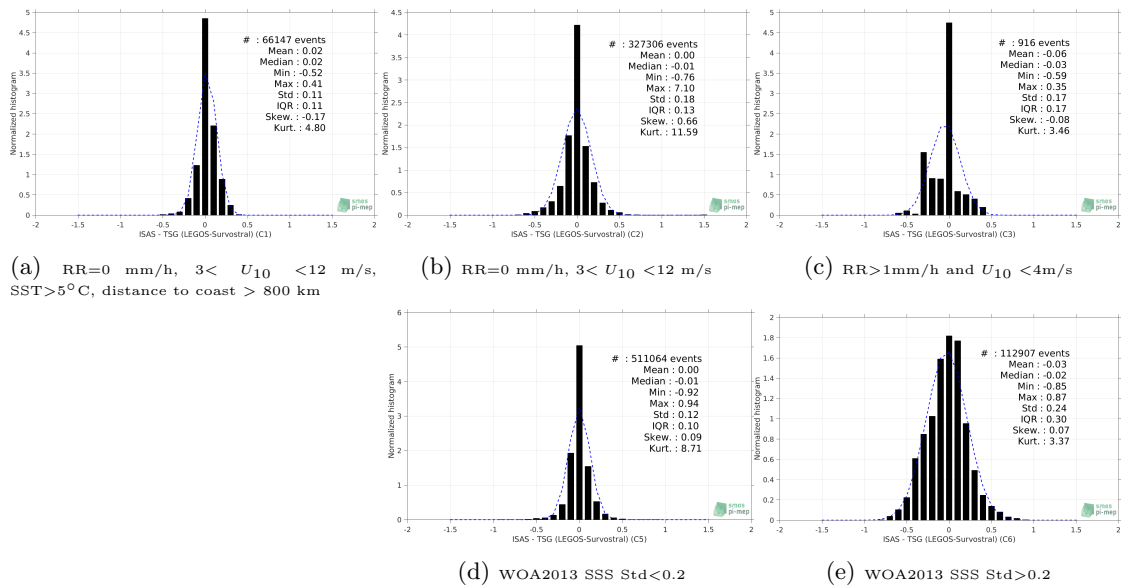


Figure 146: Normalized histogram of ΔSSS (ISAS - TSG (LEGOS-Survostral)) for 5 different subdatasets corresponding to: RR=0 mm/h, $3 < U_{10} < 12 \text{ m/s}$, SST>5°C, distance to coast > 800 km (a), RR=0 mm/h, $3 < U_{10} < 12 \text{ m/s}$ (b), RR>1mm/h and $U_{10} < 4 \text{ m/s}$ (c), WOA2013 SSS Std<0.2 (d), WOA2013 SSS Std>0.2 (e).

6.8.13 Summary

Table 1 shows the mean, median, standard deviation (Std), root mean square (RMS), interquartile range (IQR), correlation coefficient (r^2) and robust standard deviation (Std*) of the match-up differences ΔSSS (ISAS - TSG (LEGOS-Survostral)) for the following conditions:

- all: All the match-up pairs satellite/in situ SSS values are used to derive the statistics
- C1: only pairs where RR=0 mm/h, $3 < U_{10} < 12 \text{ m/s}$, SST>5°C, distance to coast > 800 km
- C2: only pairs where RR=0 mm/h, $3 < U_{10} < 12 \text{ m/s}$
- C3: only pairs where RR>1mm/h and $U_{10} < 4 \text{ m/s}$
- C5: only pairs where WOA2013 SSS Std<0.2
- C6: only pairs where WOA2013 SSS Std>0.2
- C7a: only pairs with a distance to coast < 150 km.
- C7b: only pairs with a distance to coast in the range [150, 800] km.
- C7c: only pairs with a distance to coast > 800 km.
- C8a: only pairs where SST is < 5°C.
- C8b: only pairs where SST is in the range [5, 15]°C.
- C8c: only pairs where SST is > 15°C.

- C9a: only pairs where SSS is < 33.
- C9b: only pairs where SSS is in the range [33, 37].
- C9c: only pairs where SSS is > 37.

Table 1: Statistics of ΔSSS (ISAS - TSG (LEGOS-Survostral))

Condition	#	Median	Mean	Std	RMS	IQR	r^2	Std*
all	652976	-0.01	0.00	0.16	0.16	0.12	0.902	0.09
C1	66147	0.02	0.02	0.11	0.11	0.11	0.743	0.08
C2	327306	-0.01	0.00	0.18	0.18	0.13	0.897	0.09
C3	916	-0.03	-0.06	0.17	0.18	0.17	0.917	0.08
C5	511064	-0.01	0.00	0.12	0.12	0.10	0.923	0.07
C6	112907	-0.02	-0.03	0.24	0.24	0.30	0.855	0.22
C7a	63782	0.00	0.03	0.29	0.29	0.31	0.847	0.23
C7b	368723	-0.01	-0.01	0.17	0.17	0.15	0.898	0.11
C7c	220471	-0.01	0.00	0.09	0.09	0.08	0.738	0.06
C8a	308616	-0.01	0.00	0.10	0.10	0.08	0.520	0.06
C8b	295347	0.00	0.00	0.18	0.18	0.19	0.845	0.14
C8c	42997	-0.10	-0.07	0.32	0.33	0.38	0.004	0.28
C9a	400	0.92	1.73	1.27	2.15	1.77	0.155	0.76
C9b	652576	-0.01	0.00	0.16	0.16	0.12	0.912	0.09
C9c	0	NaN	NaN	NaN	NaN	NaN	NaN	NaN

Table 1 numerical values can be downloaded as a csv file [here](#).

6.9 TSG (LEGOS-Survostral-Adelie)

6.9.1 Introduction

The TSG (LEGOS-Survostral-Adelie) dataset corresponds to delayed mode regional dataset along the Adelie coast provided by the [Survostral project](#) and available via [here](#). Adjusted values when available and only collected TSG data that exhibit quality flags=1 and 2 were used.

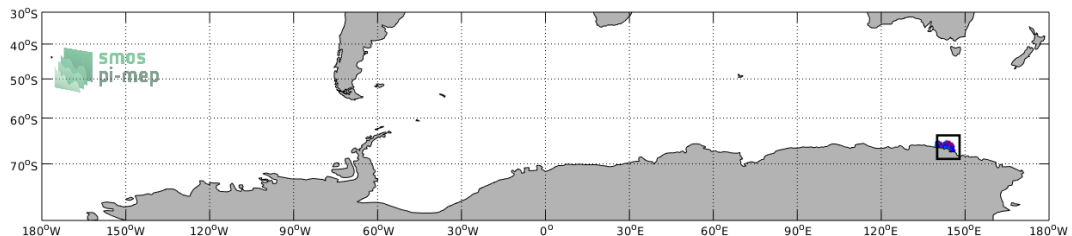


Figure 147: Location of the TSG (LEGOS-Survostral-Adélie) dataset.

6.9.2 Number of SSS data as a function of time and distance to coast

Figure 148 shows the time (a) and distance to coast (b) distributions of the TSG (LEGOS-Survostral-Adélie) *in situ* dataset.

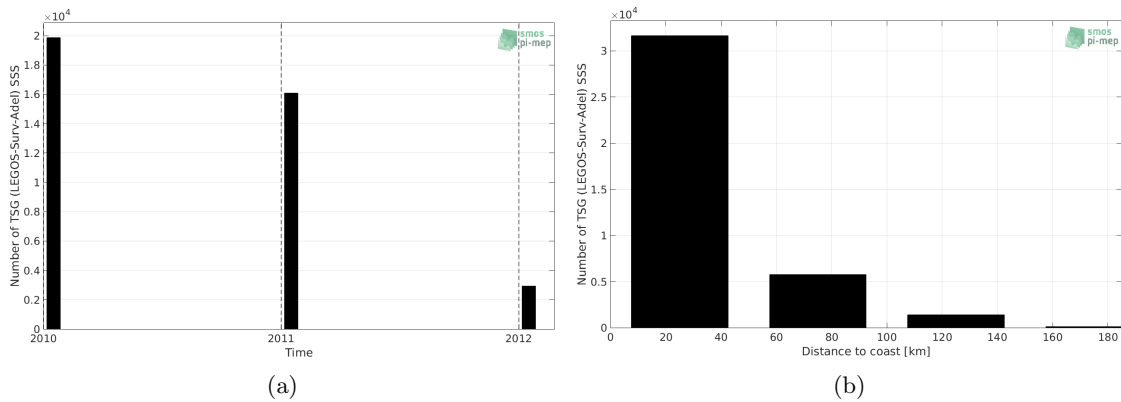


Figure 148: Number of SSS from TSG (LEGOS-Survostral-Adélie) as a function of time (a) and distance to coast (b).

6.9.3 Histograms of SSS

Figure 149 shows the SSS distribution of the TSG (LEGOS-Survostral-Adélie) (a) and colocalized ISAS (b) dataset.

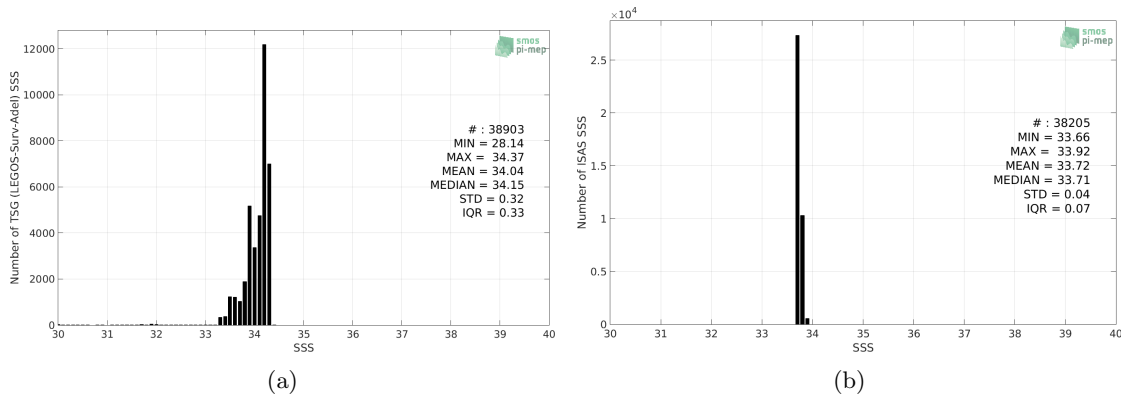


Figure 149: Histograms of SSS from TSG (LEGOS-Survostral-Adélie) (a) and ISAS (b) per bins of 0.1.

6.9.4 Distribution of *in situ* SSS depth measurements

In Figure 150, we show the depth distribution of the *in situ* salinity dataset (a) and the spatial distribution of the depth temporal mean in $1^\circ \times 1^\circ$ boxes and considering the full *in situ* dataset period (b).

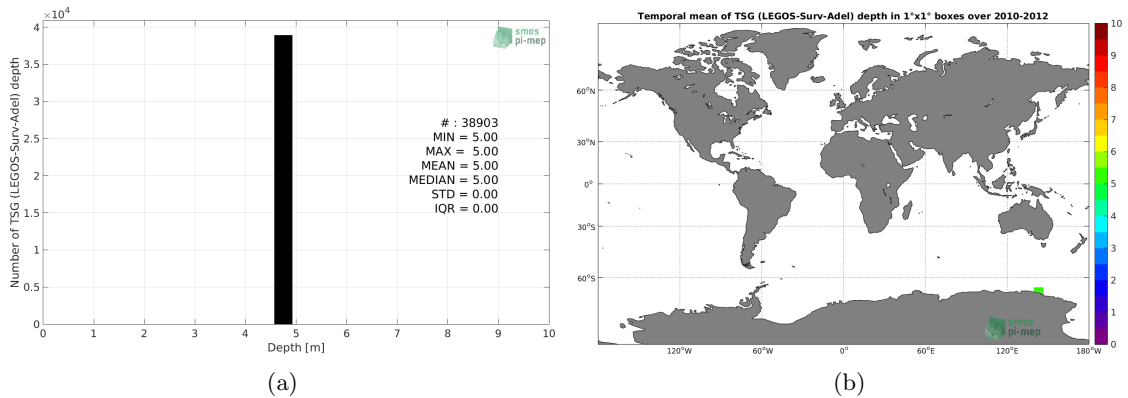


Figure 150: Depth distribution of the upper level SSS measurements from TSG (LEGOS-Survostral-Adélie) (a) and spatial distribution of the *in situ* SSS depth measurements showing the mean value in $1^\circ \times 1^\circ$ boxes and considering the full *in situ* dataset period (b).

6.9.5 Spatial distribution of SSS

In Figure 151, the number of TSG (LEGOS-Survostral-Adélie) SSS measurements in $1^\circ \times 1^\circ$ boxes is shown.

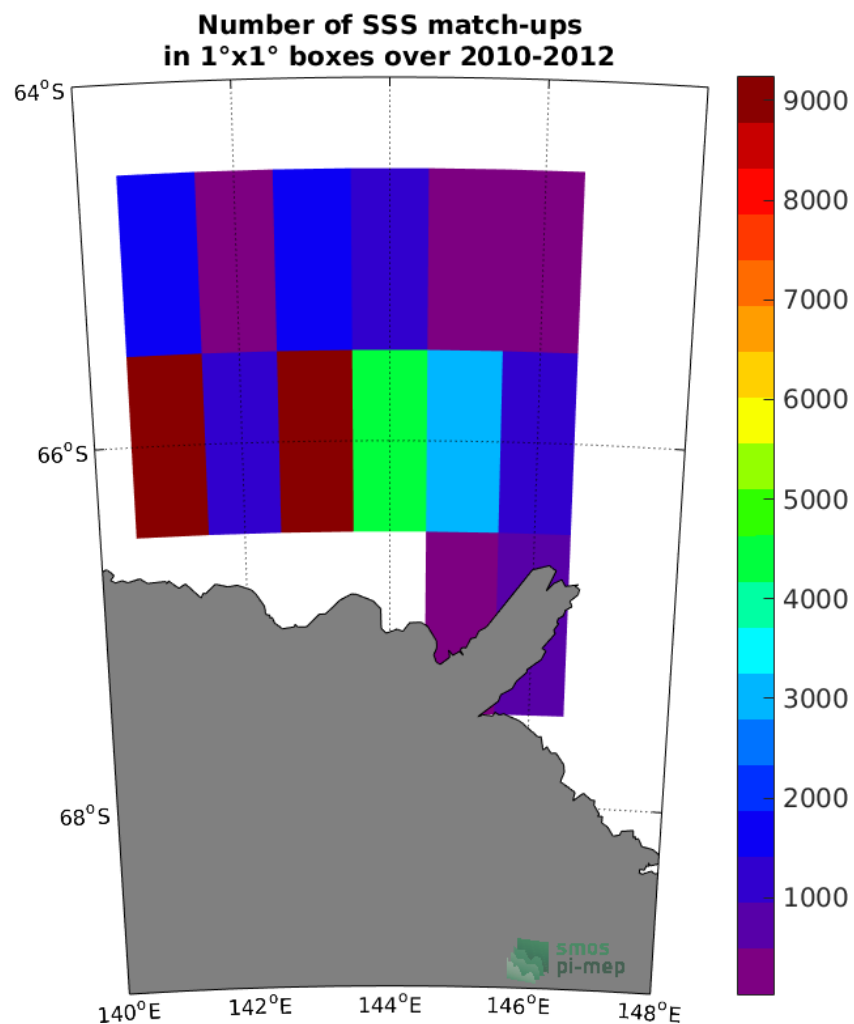


Figure 151: Number of SSS from TSG (LEGOS-Survostral-Adélie) in $1^\circ \times 1^\circ$ boxes.

6.9.6 Spatial Maps of the Temporal mean and Std of *in situ* and ISAS SSS and of the difference (Δ SSS)

In Figure 152, maps of temporal mean (left) and standard deviation (right) of ISAS (top), TSG (LEGOS-Survostral-Adélie) *in situ* dataset (middle) and the difference Δ SSS(ISAS -TSG (LEGOS-Survostral-Adélie)) (bottom) are shown. The temporal mean and std are calculated using all match-up pairs falling in spatial boxes of size $1^\circ \times 1^\circ$ over the full TSG (LEGOS-Survostral-Adélie) dataset period.

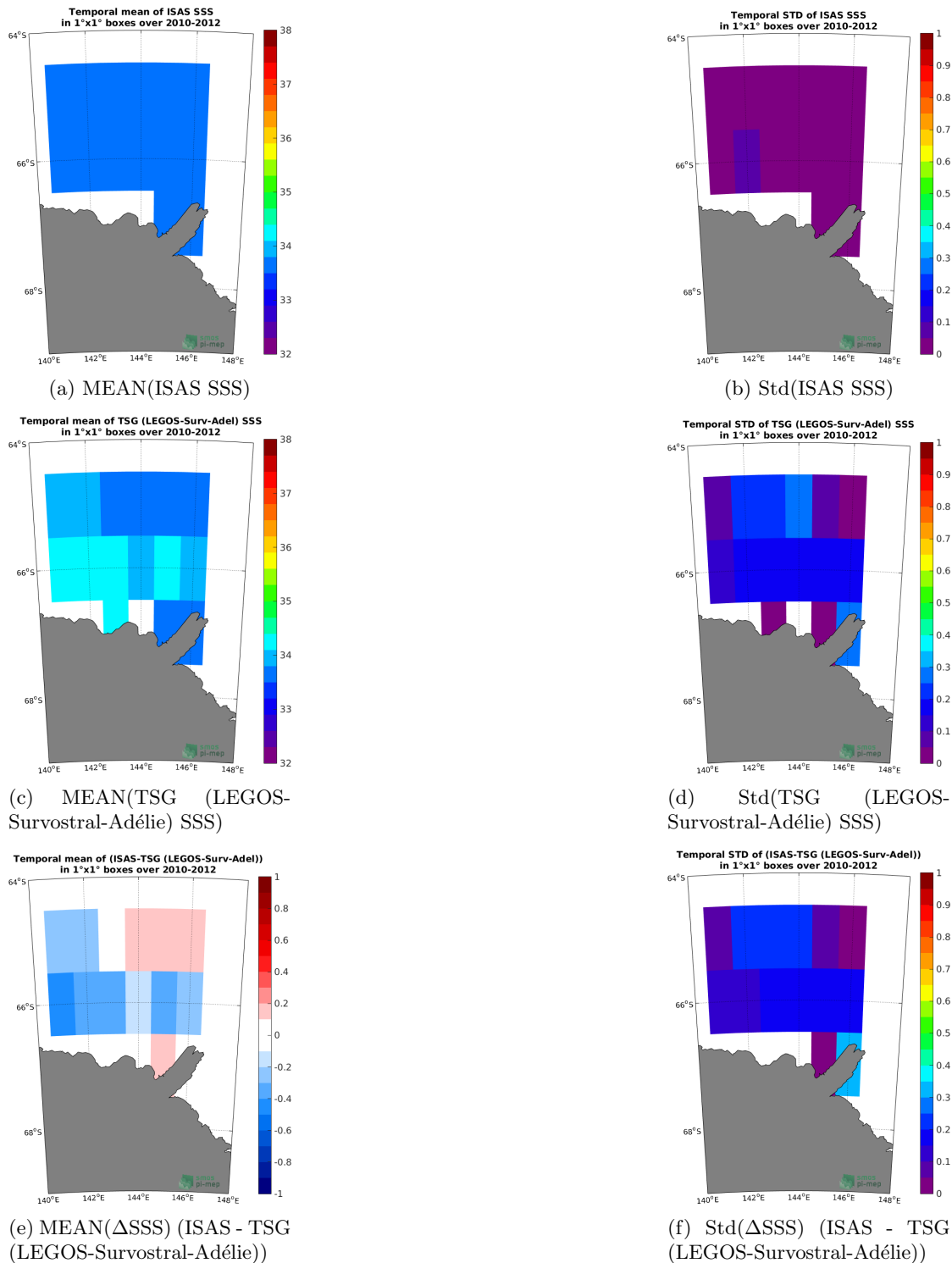


Figure 152: Temporal mean (left) and Std (right) of SSS from ISAS (top), TSG (LEGOS-Survostral-Adélie) (middle), and of Δ SSS (ISAS - TSG (LEGOS-Survostral-Adélie)). Only match-up pairs are used to generate these maps.

6.9.7 Time series of the monthly median and Std of *in situ* and ISAS SSS and of the difference (Δ SSS)

In the top panel of Figure 153, we show the time series of the monthly median SSS estimated for both ISAS SSS product (in black) and the TSG (LEGOS-Survostral-Adélie) *in situ* dataset (in blue) at the collected Pi-MEP match-up pairs.

In the middle panel of Figure 153, we show the time series of the monthly median of Δ SSS (ISAS - TSG (LEGOS-Survostral-Adélie)) for the collected Pi-MEP match-up pairs.

In the bottom panel of Figure 153, we show the time series of the monthly standard deviation of the Δ SSS (ISAS - TSG (LEGOS-Survostral-Adélie)) for the collected Pi-MEP match-up pairs.

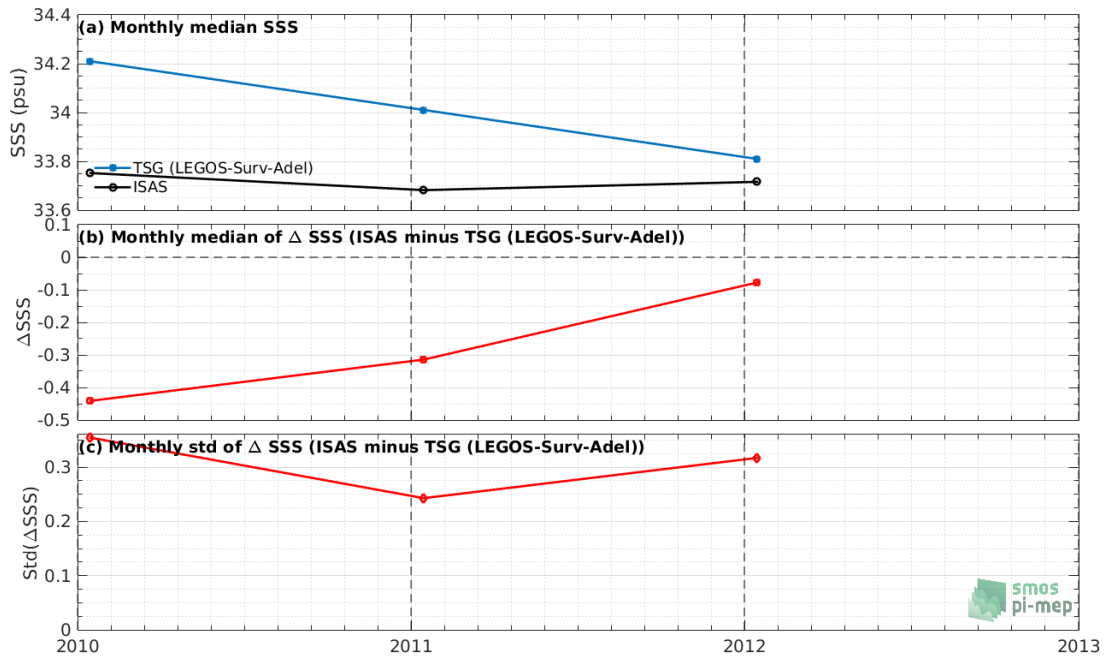


Figure 153: Time series of the monthly median SSS (top), median of Δ SSS (ISAS - TSG (LEGOS-Survostral-Adélie)) and Std of Δ SSS (ISAS - TSG (LEGOS-Survostral-Adélie)) considering all match-ups collected by the Pi-MEP.

6.9.8 Zonal mean and Std of *in situ* and ISAS SSS and of the difference Δ SSS

In Figure 154 left panel, we show the zonal mean SSS considering all Pi-MEP match-up pairs for both ISAS SSS product (in black) and the TSG (LEGOS-Survostral-Adélie) *in situ* dataset (in blue). The full *in situ* dataset period is used to derive the mean.

In the right panel of Figure 154, we show the zonal mean of Δ SSS (ISAS - TSG (LEGOS-Survostral-Adélie)) for all the collected Pi-MEP match-up pairs estimated over the full *in situ* dataset period.

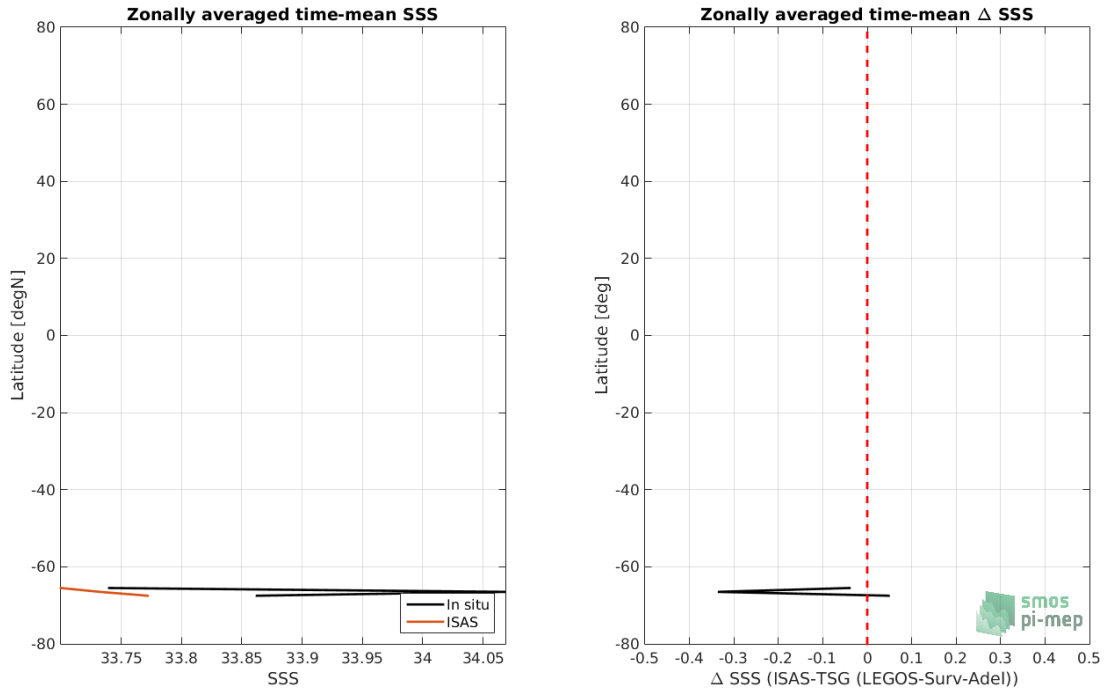


Figure 154: Left panel: Zonal mean SSS from ISAS product (black) and from TSG (LEGOS-Survostral-Adélie) (blue). Right panel: Zonal mean of Δ SSS (ISAS - TSG (LEGOS-Survostral-Adélie)) for all the collected Pi-MEP match-up pairs estimated over the full *in situ* dataset period.

6.9.9 Scatterplots of ISAS vs *in situ* SSS by latitudinal bands

In Figure 155, contour maps of the concentration of ISAS SSS (y-axis) versus TSG (LEGOS-Survostral-Adélie) SSS (x-axis) at match-up pairs for different latitude bands: (a) 80°S-80°N, (b) 20°S-20°N, (c) 40°S-20°S and 20°N-40°N and (d) 60°S-40°S and 40°N-60°N. For each plot, the red line shows $x=y$. The black thin and dashed lines indicate a linear fit through the data cloud and the $\pm 95\%$ confidence levels, respectively. The number match-up pairs n , the slope and R^2 coefficient of the linear fit, the root mean square (RMS) and the mean bias between ISAS and *in situ* data are indicated for each latitude band in each plots.

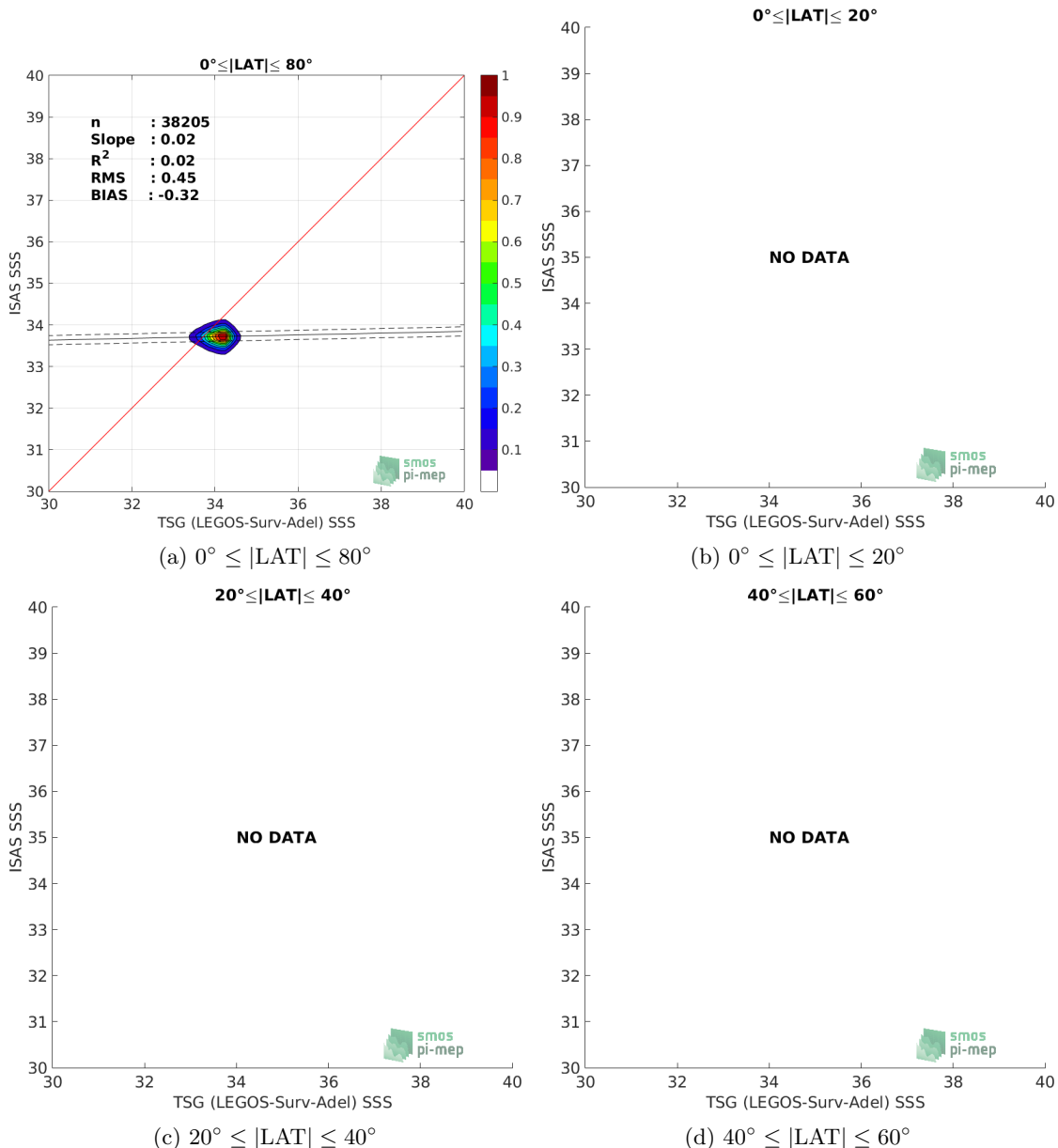


Figure 155: Contour maps of the concentration of ISAS SSS (y-axis) versus TSG (LEGOS-Survostral-Adélie) SSS (x-axis) at match-up pairs for different latitude bands. For each plot, the red line shows $x=y$. The black thin and dashed lines indicate a linear fit through the data cloud and the $\pm 95\%$ confidence levels, respectively. The number match-up pairs n , the slope and R^2 coefficient of the linear fit, the root mean square (RMS) and the mean bias between ISAS and *in situ* data are indicated for each latitude band in each plots.

6.9.10 Time series of the monthly median and Std of the difference ΔSSS sorted by latitudinal bands

In Figure 156, time series of the monthly median (red curves) of ΔSSS (ISAS - TSG (LEGOS-Survostral-Adélie)) and ± 1 Std (black vertical thick bars) as function of time for all the collected Pi-MEP match-up pairs estimated for the full *in situ* dataset period are shown for different latitude bands: (a) $80^\circ\text{S}-80^\circ\text{N}$, (b) $20^\circ\text{S}-20^\circ\text{N}$, (c) $40^\circ\text{S}-20^\circ\text{S}$ and $20^\circ\text{N}-40^\circ\text{N}$ and (d) $60^\circ\text{S}-40^\circ\text{S}$ and $40^\circ\text{N}-60^\circ\text{N}$.

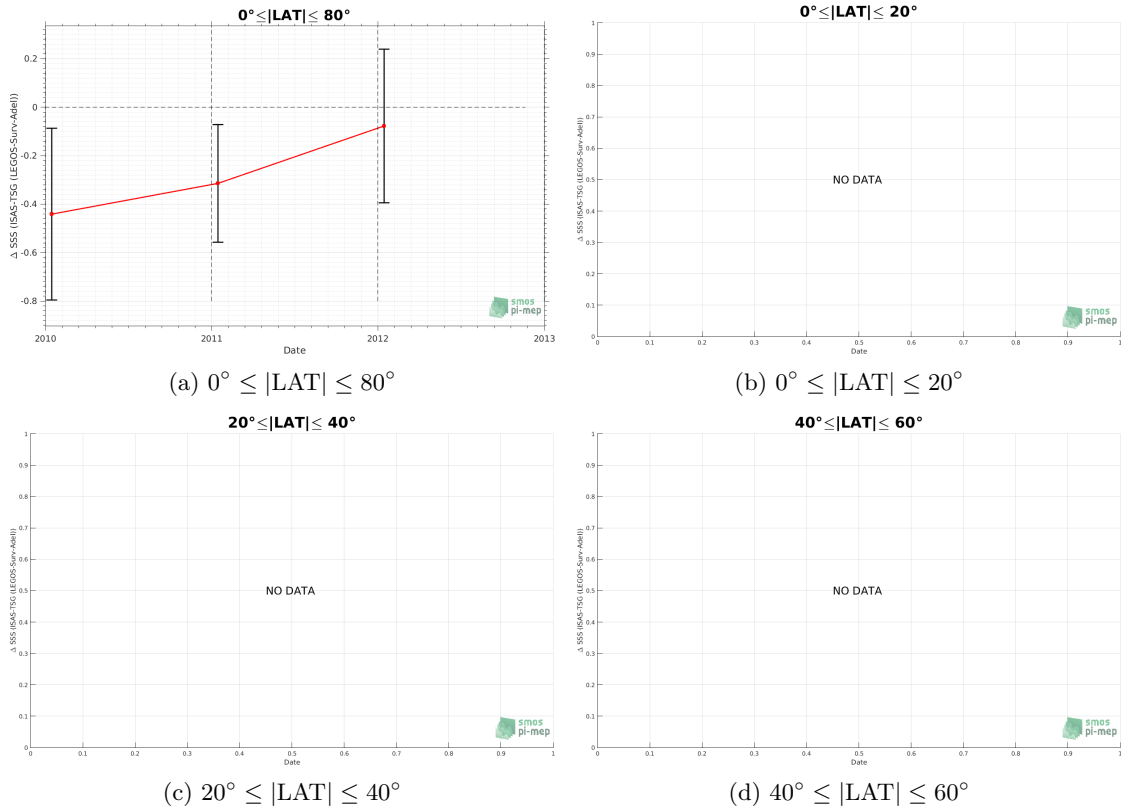


Figure 156: Monthly median (red curves) of ΔSSS (ISAS - TSG (LEGOS-Survostral-Adélie)) and ± 1 Std (black vertical thick bars) as function of time for all the collected Pi-MEP match-up pairs for the full *in situ* dataset period are shown for different latitude bands: (a) $80^\circ\text{S}-80^\circ\text{N}$, (b) $20^\circ\text{S}-20^\circ\text{N}$, (c) $40^\circ\text{S}-20^\circ\text{S}$ and $20^\circ\text{N}-40^\circ\text{N}$ and (d) $60^\circ\text{S}-40^\circ\text{S}$ and $40^\circ\text{N}-60^\circ\text{N}$.

6.9.11 ΔSSS sorted as geophysical conditions

In Figure 157, we classify the match-up differences ΔSSS (ISAS - *in situ*) as function of the geophysical conditions at match-up points. The mean and std of ΔSSS (ISAS - TSG (LEGOS-Survostral-Adélie)) is thus evaluated as function of the

- *in situ* SSS values per bins of width 0.2,
- *in situ* SST values per bins of width 1°C ,
- ASCAT daily wind values per bins of width 1 m/s,

- CMORPH 3-hourly rain rates per bins of width 1 mm/h, and,
- distance to coasts per bins of width 50 km,
- *in situ* measurement depth (if relevant).

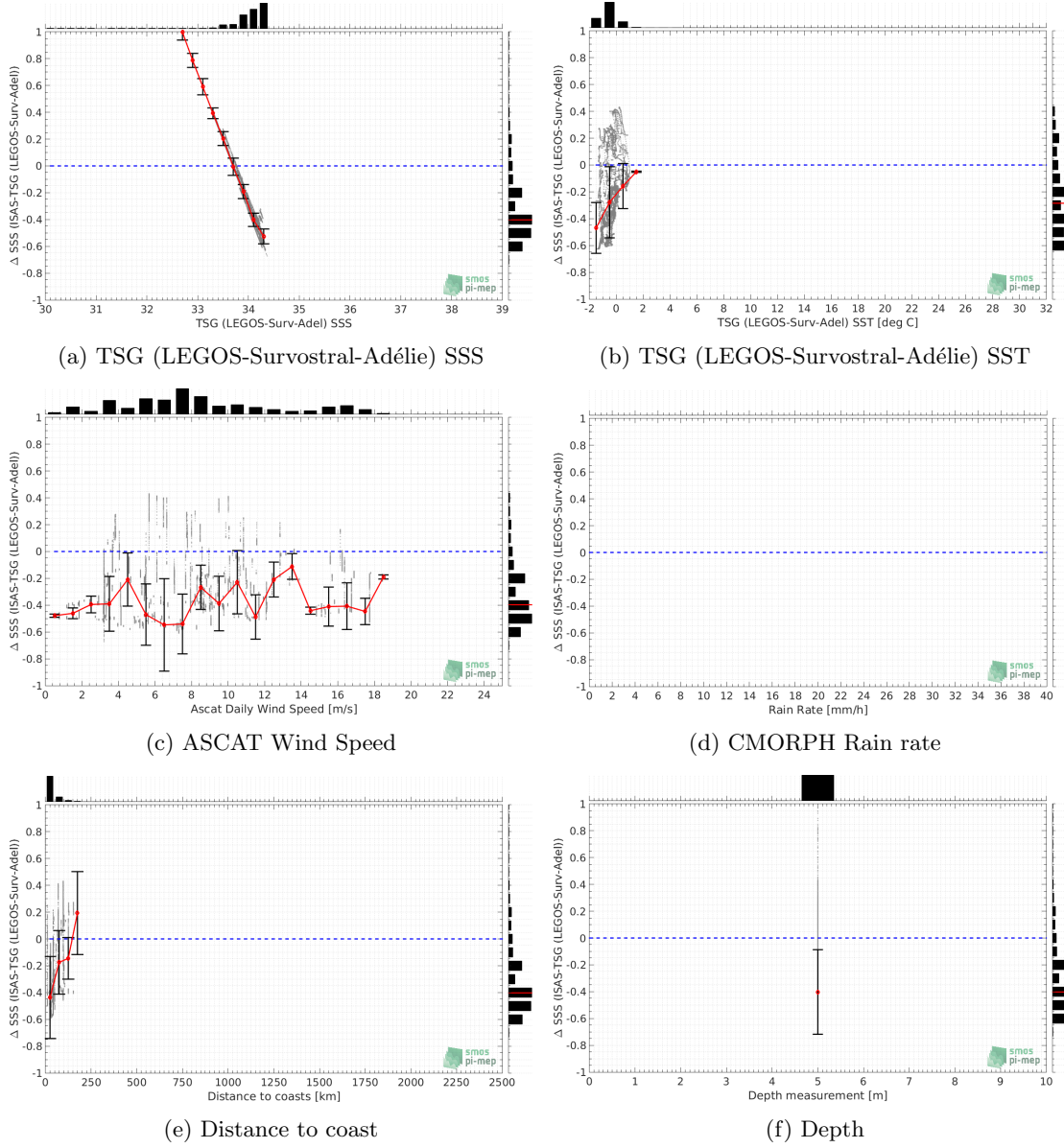


Figure 157: Δ SSS (ISAS - TSG (LEGOS-Survostral-Adélie)) sorted as geophysical conditions: TSG (LEGOS-Survostral-Adélie) SSS a), TSG (LEGOS-Survostral-Adélie) SST b), ASCAT Wind speed c), CMORPH rain rate d), distance to coast (e) and depth measurements (f).

6.9.12 Δ SSS maps and statistics for different geophysical conditions

In Figures 158 and 159, we focus on sub-datasets of the match-up differences Δ SSS (ISAS - *in situ*) for the following specific geophysical conditions:

- **C1:**if the local value at *in situ* location of estimated rain rate is zero, mean daily wind is in the range [3, 12] m/s, the SST is $> 5^{\circ}\text{C}$ and distance to coast is > 800 km.
- **C2:**if the local value at *in situ* location of estimated rain rate is zero, mean daily wind is in the range [3, 12] m/s.
- **C3:**if the local value at *in situ* location of estimated rain rate is high (ie. > 1 mm/h) and mean daily wind is low (ie. < 4 m/s).
- **C5:**if the *in situ* data is located where the climatological SSS standard deviation is low (ie. above < 0.2).
- **C6:**if the *in situ* data is located where the climatological SSS standard deviation is high (ie. above > 0.2).

For each of these conditions, the temporal mean (gridded over spatial boxes of size $1^{\circ} \times 1^{\circ}$) and the histogram of the difference Δ SSS (ISAS - *in situ*) are presented.

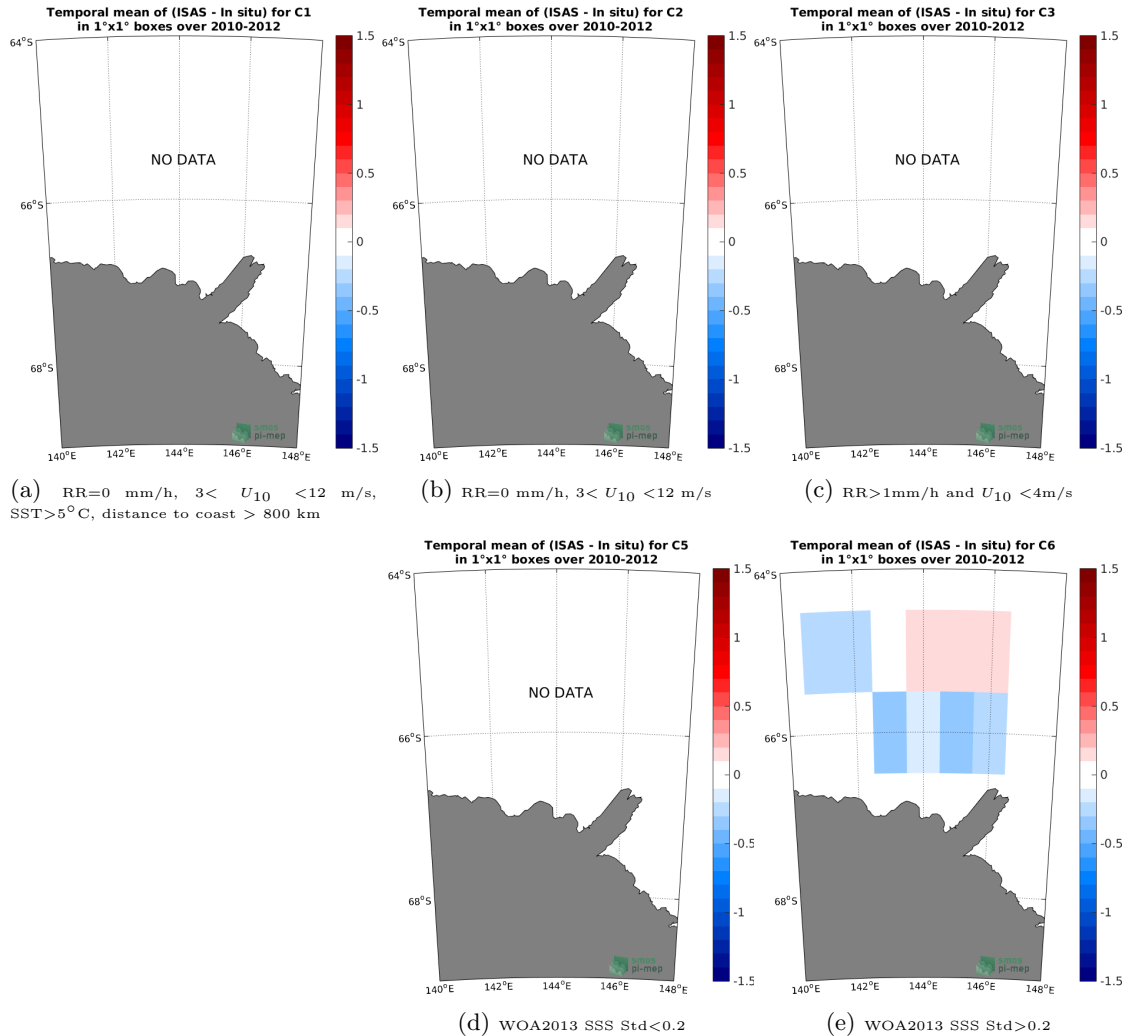


Figure 158: Temporal mean gridded over spatial boxes of size $1^\circ \times 1^\circ$ of ΔSSS (ISAS - TSG (LEGOS-Survostral-Adélie)) for 5 different subdatasets corresponding to: RR=0 mm/h, $3 < U_{10} < 12 \text{ m/s}$, SST > 5°C, distance to coast > 800 km (a), RR=0 mm/h, $3 < U_{10} < 12 \text{ m/s}$ (b), RR > 1 mm/h and $U_{10} < 4 \text{ m/s}$ (c), WOA2013 SSS Std < 0.2 (d), WOA2013 SSS Std > 0.2 (e).

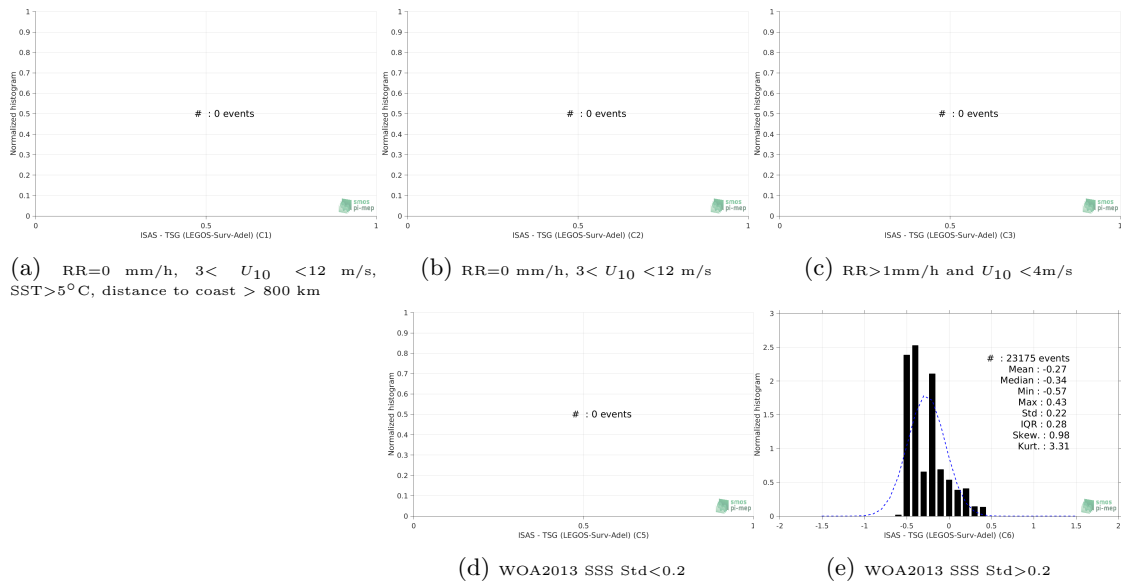


Figure 159: Normalized histogram of ΔSSS (ISAS - TSG (LEGOS-Survostral-Adélie)) for 5 different subdatasets corresponding to: RR=0 mm/h, 3 < U_{10} < 12 m/s, SST > 5°C, distance to coast > 800 km (a), RR=0 mm/h, 3 < U_{10} < 12 m/s (b), RR > 1 mm/h and $U_{10} < 4 \text{ m/s}$ (c), WOA2013 SSS Std < 0.2 (d), WOA2013 SSS Std > 0.2 (e).

6.9.13 Summary

Table 1 shows the mean, median, standard deviation (Std), root mean square (RMS), interquartile range (IQR), correlation coefficient (r^2) and robust standard deviation (Std^*) of the match-up differences ΔSSS (ISAS - TSG (LEGOS-Survostral-Adélie)) for the following conditions:

- all: All the match-up pairs satellite/in situ SSS values are used to derive the statistics
- C1: only pairs where RR=0 mm/h, 3 < U_{10} < 12 m/s, SST > 5°C, distance to coast > 800 km
- C2: only pairs where RR=0 mm/h, 3 < U_{10} < 12 m/s
- C3: only pairs where RR > 1 mm/h and $U_{10} < 4 \text{ m/s}$
- C5: only pairs where WOA2013 SSS Std < 0.2
- C6: only pairs where WOA2013 SSS Std > 0.2
- C7a: only pairs with a distance to coast < 150 km.
- C7b: only pairs with a distance to coast in the range [150, 800] km.
- C7c: only pairs with a distance to coast > 800 km.
- C8a: only pairs where SST is < 5°C.
- C8b: only pairs where SST is in the range [5, 15]°C.
- C8c: only pairs where SST is > 15°C.

- C9a: only pairs where SSS is < 33.
- C9b: only pairs where SSS is in the range [33, 37].
- C9c: only pairs where SSS is > 37.

Table 1: Statistics of ΔSSS (ISAS - TSG (LEGOS-Survostral-Adélie))

Condition	#	Median	Mean	Std	RMS	IQR	r^2	Std*
all	38205	-0.40	-0.32	0.32	0.45	0.30	0.024	0.20
C1	0	NaN	NaN	NaN	NaN	NaN	NaN	NaN
C2	0	NaN	NaN	NaN	NaN	NaN	NaN	NaN
C3	0	NaN	NaN	NaN	NaN	NaN	NaN	NaN
C5	0	NaN	NaN	NaN	NaN	NaN	NaN	NaN
C6	23175	-0.34	-0.27	0.22	0.35	0.28	0.405	0.21
C7a	38109	-0.40	-0.32	0.32	0.45	0.30	0.023	0.20
C7b	96	0.19	0.00	0.31	0.31	0.65	0.991	0.12
C7c	0	NaN	NaN	NaN	NaN	NaN	NaN	NaN
C8a	18615	-0.29	-0.27	0.26	0.37	0.34	0.218	0.26
C8b	0	NaN	NaN	NaN	NaN	NaN	NaN	NaN
C8c	0	NaN	NaN	NaN	NaN	NaN	NaN	NaN
C9a	270	1.76	2.09	1.16	2.39	0.93	0.000	0.59
C9b	37935	-0.40	-0.34	0.22	0.40	0.30	0.031	0.20
C9c	0	NaN	NaN	NaN	NaN	NaN	NaN	NaN

Table 1 numerical values can be downloaded as a csv file [here](#).

7 Moorings

7.1 Introduction

The Pi-MEP collects data from the Global Tropical Moored Buoy Array (**GTMBA**), a multi-national effort to provide data in real-time for climate research and forecasting. Major components include the TAO/TRITON array in the Pacific, PIRATA in the Atlantic, and RAMA in the Indian Ocean. Data collected within TAO/TRITON, PIRATA and RAMA come primarily from ATLAS and TRITON moorings. These two mooring systems are functionally equivalent in terms of sensors, sample rates, and data quality. The data are directly downloaded from [ftp.pmel.noaa.gov](ftp://pmel.noaa.gov) every day and stored in the Pi-MEP. Only salinity data measured at 1 or 1.5 meter depth with standard (pre-deployment calibration applied) and highest quality (pre/post calibration in agreement) are considered. A careful filtering of suspiciously erroneous mooring salinity data when compared with all satellite data has also been performed (cf. [presentation](#)). The Pi-MEP project acknowledges the GTMBA Project Office of NOAA/PMEL for providing the data. Data from the Ocean Station **PAPA** are also added to the Pi-MEP *in situ* database.

From the **Upper Ocean Processes Group** at Woods Hole Oceanographic Institution (**WHOI**), several moorings data are also included in the Pi-MEP. Namely, delayed mode surface mooring salinity records under the stratus cloud deck in the eastern tropical Pacific (**Stratus**), in the trade wind region of the northwest tropical Atlantic (**NTAS**), 100 km north of Oahu at the WHOI Hawaii Ocean Time-series Site (**WHOTS**), in the salinity maximum region of the subtropical North Atlantic (**SPURS-1**) and in the Pacific intertropical convergence zone (**SPURS-2**).

7.2 Number of SSS data as a function of time and distance to coast

Figure 160 shows the time (a) and distance to coast (b) distributions of the Moorings *in situ* dataset.

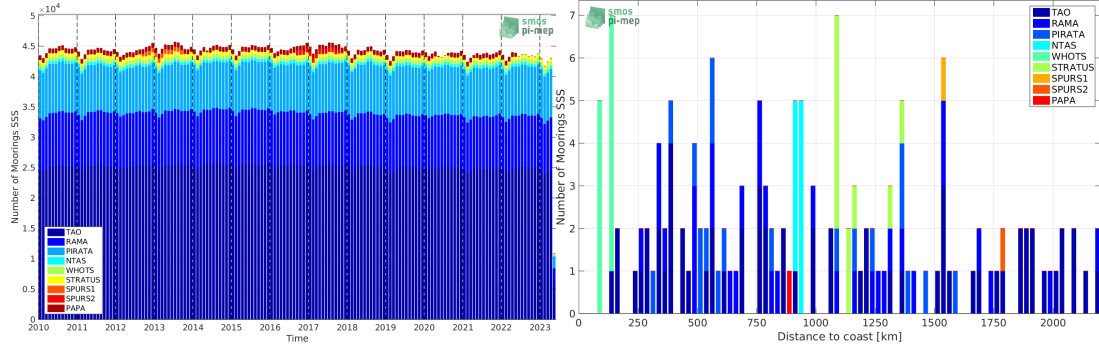


Figure 160: Number of SSS from Moorings as a function of time (left) and distance to coast (right).

7.3 Histogram of SSS

Figure 161 shows the SSS distribution of the Moorings.

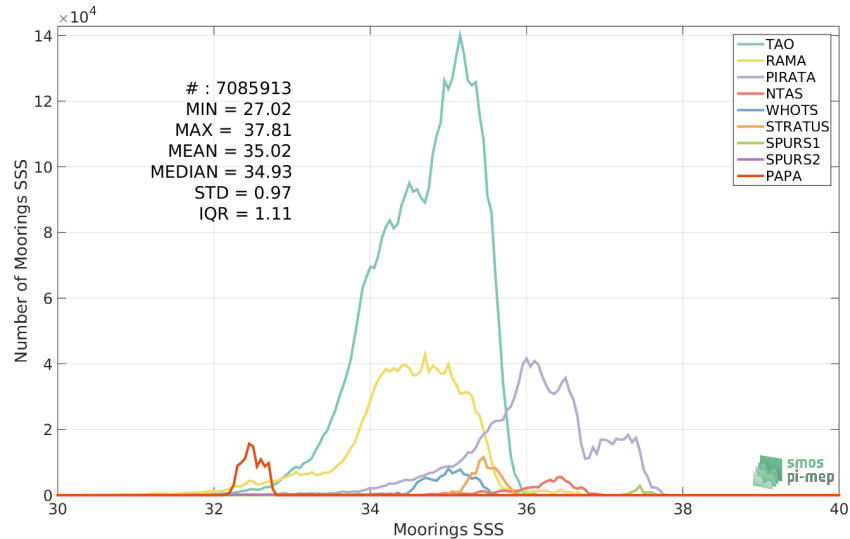


Figure 161: Distribution of SSS from Moorings per bins of 0.1.

7.4 Temporal mean of shallowest salinity

Figure 162 show a map of the mooring locations and the color of each circle indicates the temporal mean calculated using the full time series from 2010 to now of each mooring.

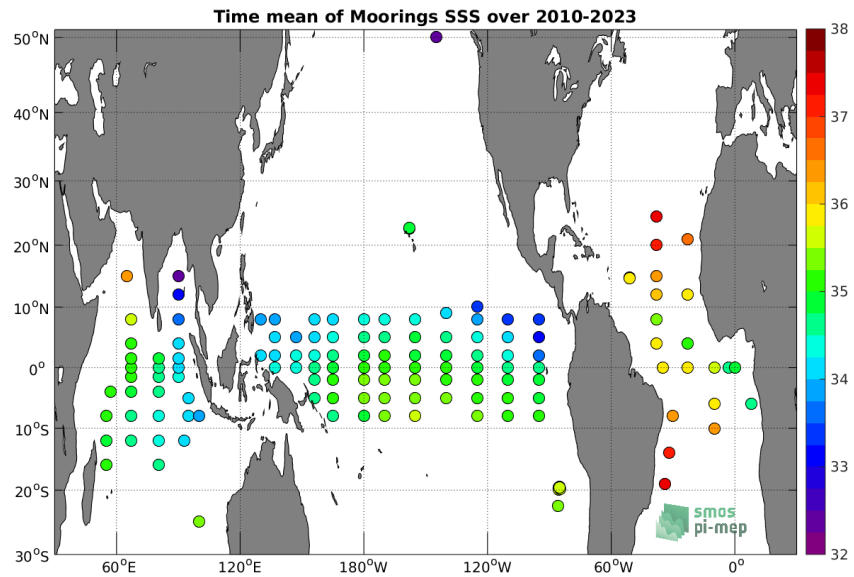


Figure 162: Temporal mean SSS from Moorings.

7.5 Temporal Std of shallowest salinity

Figure 163 show maps of the mooring locations and the color of each circle indicates the temporal standard deviation calculated using the full time series from 2010 to now of each mooring.

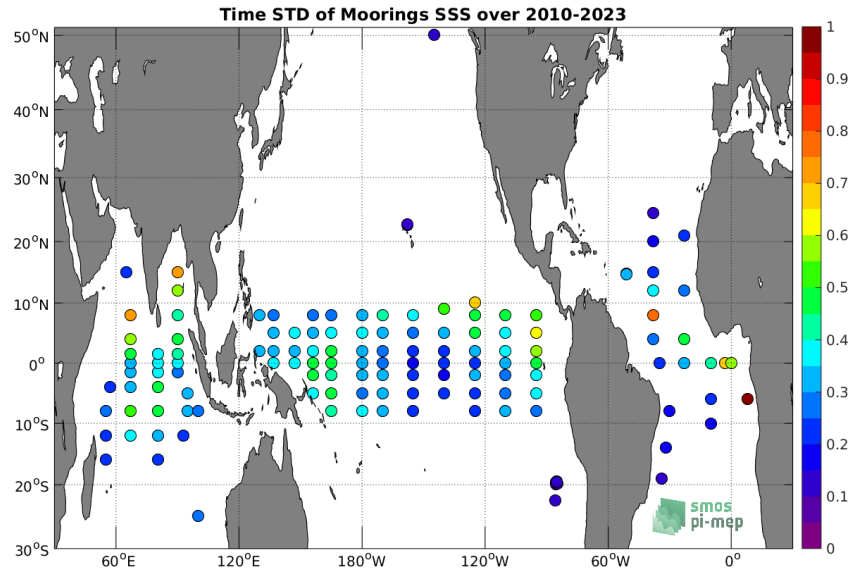


Figure 163: Temporal Std of SSS from Moorings.

7.6 Number of shallowest salinity

Figure 164 show maps of the mooring locations and the color of each circle indicates the number of SSS data measured by each mooring from 2010 to now.

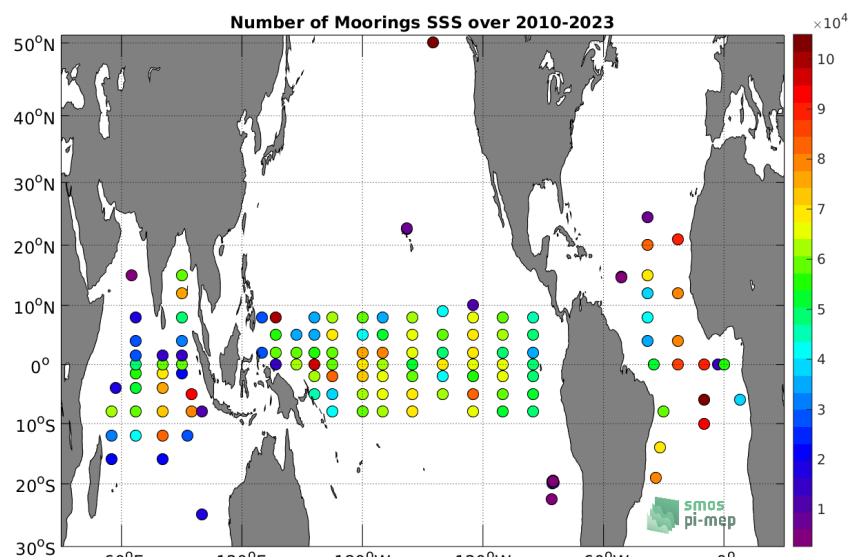


Figure 164: Number of SSS from Moorings.

7.7 Time series of shallowest salinity

The following figures (165) show time series of shallowest salinity for each mooring. To switch from a mooring to another, you can play with the arrows between the plot and the caption.

Figure 165: Time series of mooring shallowest salinity

8 SPURS-2

The SPURS-2 dataset is subdivided into 4 subdatasets following sensor type subdivisions.

- [Salinity snake](#)
- [Saildrone](#)
- [Waveglider](#)
- [Seaglider](#)

8.1 Salinity Snake

8.1.1 Introduction

The Salinity Snake (SS) measures sea surface salinity in the top 1 - 2 cm of the water column, which is the radiometric depth of L-Band satellite radiometers such as on Aquarius/SAC-D, SMAP and SMOS satellites that measure salinity remotely. The SS consists of four key components: a 10m boom mast, a hose, which is deployed from this boom, a powerful self-priming peristaltic pump which transports a constant stream of a seawater/air emulsion, and a shipboard apparatus, which filters, de-bubbles, sterilizes and analyses the salinity of the water. The SS (<https://doi.org/10.5067/SPUR2-SNAKE>) was deployed during both SPURS-2 Reveille cruises in August 2016 and October 2017. Focused around a central mooring located near 10°N,125°W, the objective of SPURS-2 (NASA-funded oceanographic process study) was to study the dynamics of the rainfall-dominated surface ocean at the western edge of the eastern Pacific fresh pool subject to high seasonal variability and strong zonal flows associated with the North Equatorial Current and Countercurrent.

8.1.2 Number of SSS data as a function of time and distance to coast

Figure 166 shows the time (a) and distance to coast (b) distributions of the Salinity snake *in situ* dataset.

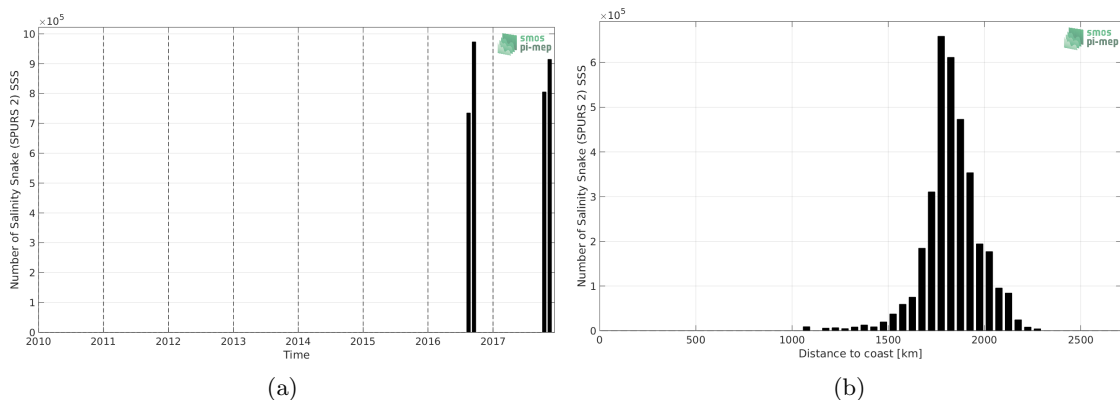


Figure 166: Number of SSS from Salinity snake as a function of time (a) and distance to coast (b).

8.1.3 Histograms of SSS

Figure 167 shows the SSS distribution of the Salinity snake (a) and colocalized ISAS (b) dataset.

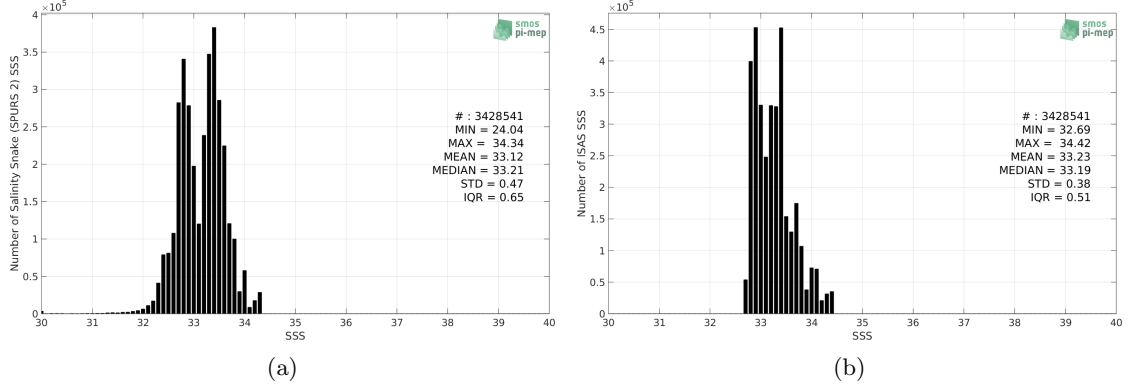


Figure 167: Histograms of SSS from Salinity snake (a) and ISAS (b) per bins of 0.1.

8.1.4 Distribution of *in situ* SSS depth measurements

In Figure 168, we show the depth distribution of the *in situ* salinity dataset (a) and the spatial distribution of the depth temporal mean in $1^\circ \times 1^\circ$ boxes and considering the full *in situ* dataset period (b).

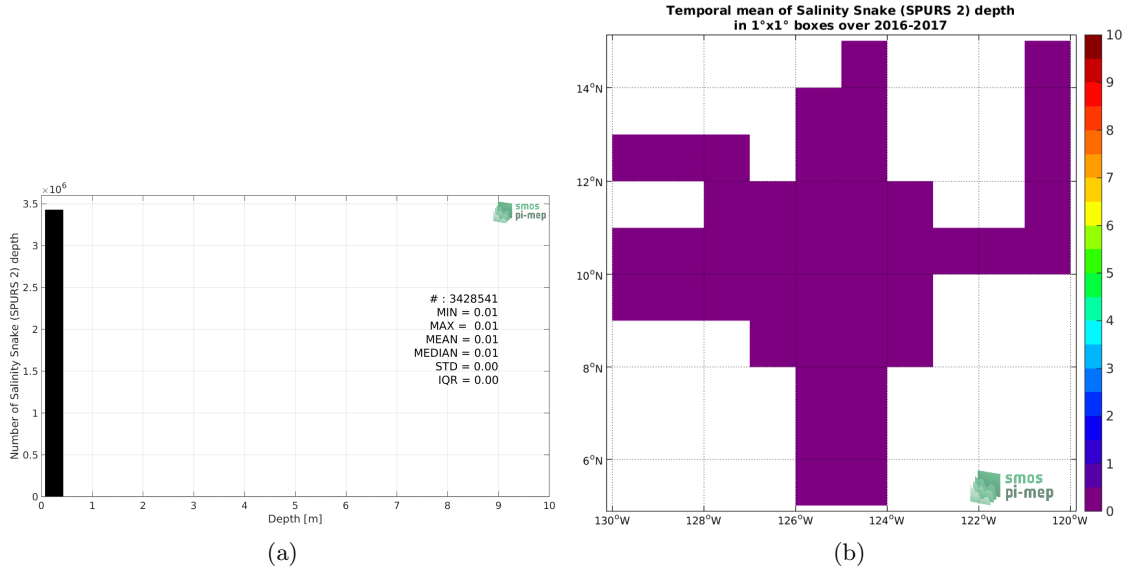


Figure 168: Depth distribution of the upper level SSS measurements from Salinity snake (a) and spatial distribution of the *in situ* SSS depth measurements showing the mean value in $1^\circ \times 1^\circ$ boxes and considering the full *in situ* dataset period (b).

8.1.5 Spatial distribution of SSS

In Figure 169, the number of Salinity snake SSS measurements in $1^\circ \times 1^\circ$ boxes is shown.

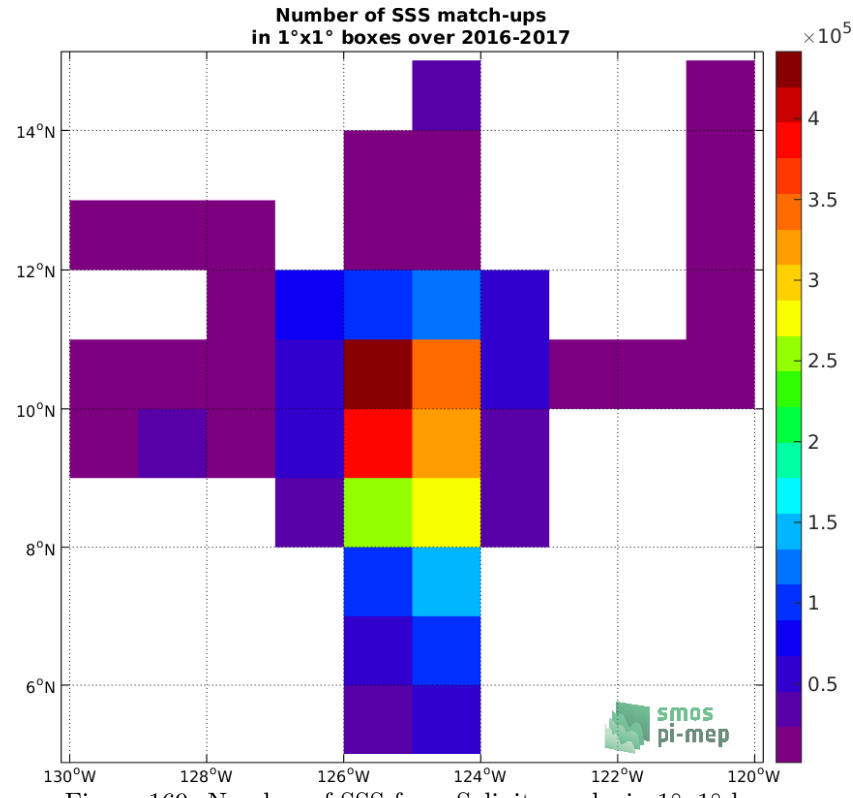


Figure 169: Number of SSS from Salinity snake in $1^{\circ} \times 1^{\circ}$ boxes.

8.1.6 Spatial Maps of the Temporal mean and Std of *in situ* and ISAS SSS and of the difference (Δ SSS)

In Figure 170, maps of temporal mean (left) and standard deviation (right) of ISAS (top), Salinity snake *in situ* dataset (middle) and the difference Δ SSS(ISAS -Salinity snake) (bottom) are shown. The temporal mean and std are calculated using all match-up pairs falling in spatial boxes of size $1^{\circ} \times 1^{\circ}$ over the full Salinity snake dataset period.

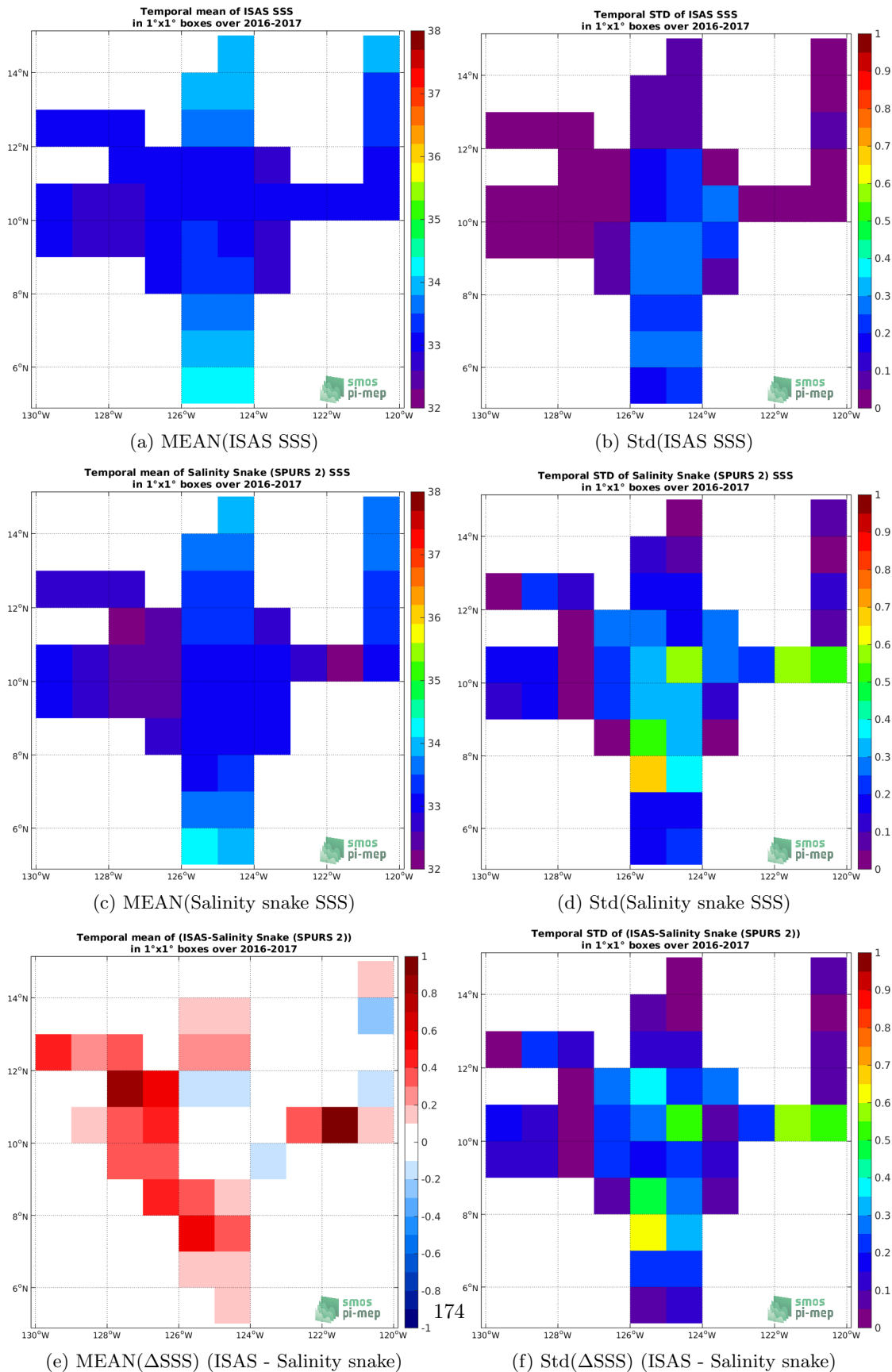


Figure 170: Temporal mean (left) and Std (right) of SSS from ISAS (top), Salinity snake (middle), and of Δ SSS (ISAS - Salinity snake). Only match-up pairs are used to generate these maps.

8.1.7 Time series of the monthly median and Std of *in situ* and ISAS SSS and of the difference (Δ SSS)

In the top panel of Figure 171, we show the time series of the monthly median SSS estimated for both ISAS SSS product (in black) and the Salinity snake *in situ* dataset (in blue) at the collected Pi-MEP match-up pairs.

In the middle panel of Figure 171, we show the time series of the monthly median of Δ SSS (ISAS - Salinity snake) for the collected Pi-MEP match-up pairs.

In the bottom panel of Figure 171, we show the time series of the monthly standard deviation of the Δ SSS (ISAS - Salinity snake) for the collected Pi-MEP match-up pairs.

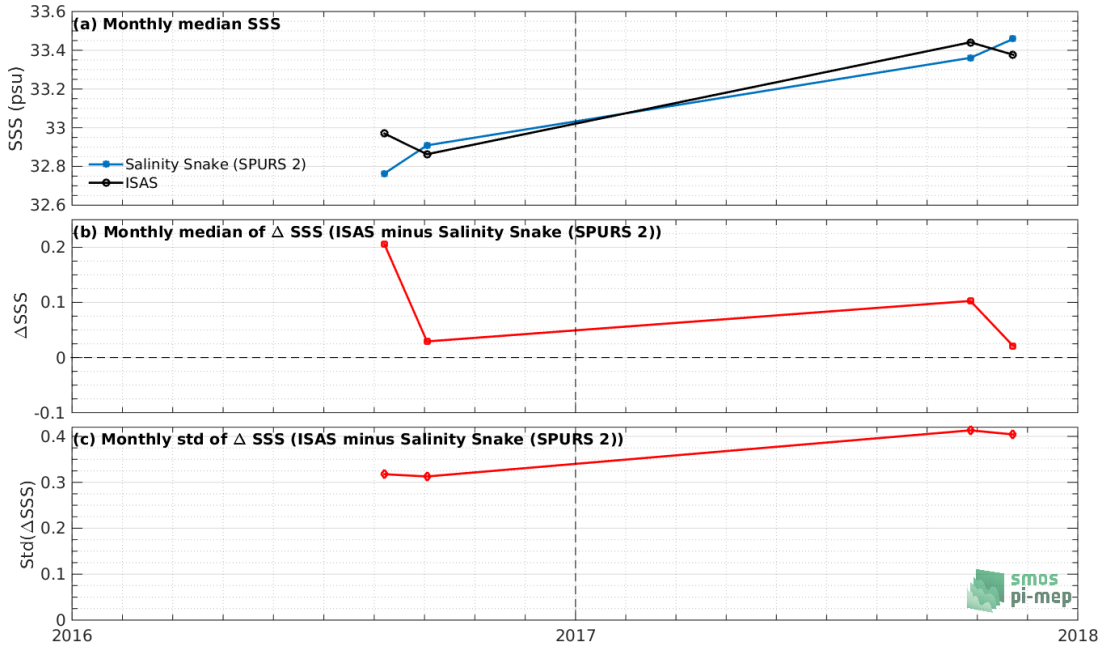


Figure 171: Time series of the monthly median SSS (top), median of Δ SSS (ISAS - Salinity snake) and Std of Δ SSS (ISAS - Salinity snake) considering all match-ups collected by the Pi-MEP.

8.1.8 Zonal mean and Std of *in situ* and ISAS SSS and of the difference Δ SSS

In Figure 172 left panel, we show the zonal mean SSS considering all Pi-MEP match-up pairs for both ISAS SSS product (in black) and the Salinity snake *in situ* dataset (in blue). The full *in situ* dataset period is used to derive the mean.

In the right panel of Figure 172, we show the zonal mean of Δ SSS (ISAS - Salinity snake) for all the collected Pi-MEP match-up pairs estimated over the full *in situ* dataset period.

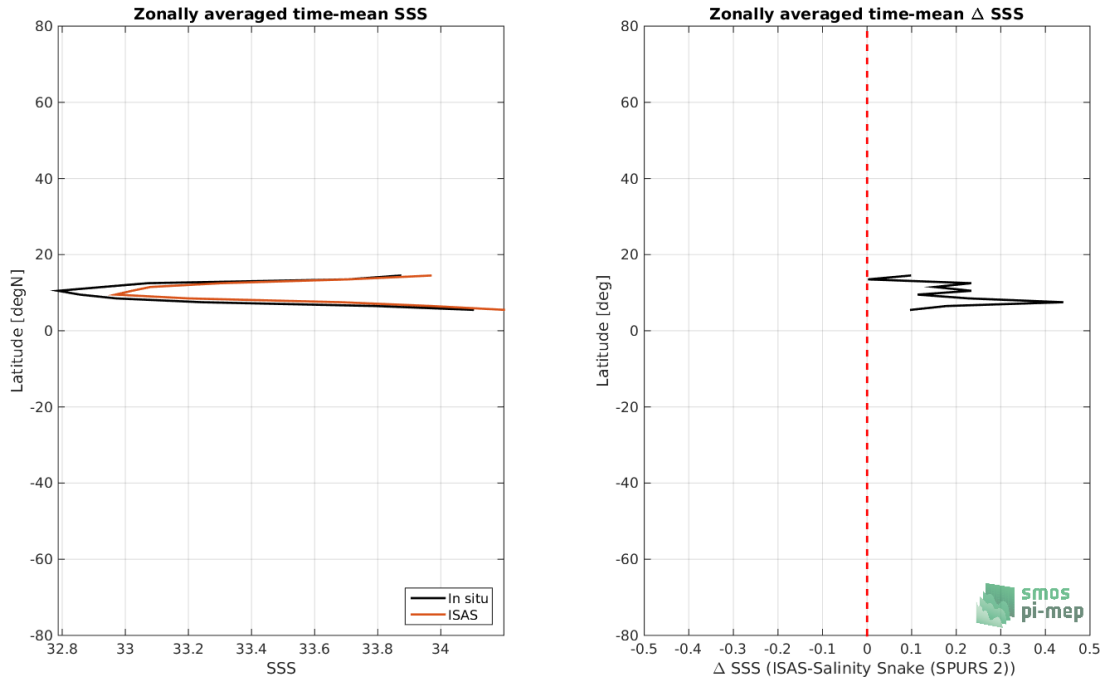


Figure 172: Left panel: Zonal mean SSS from ISAS product (black) and from Salinity snake (blue). Right panel: Zonal mean of Δ SSS (ISAS - Salinity snake) for all the collected Pi-MEP match-up pairs estimated over the full *in situ* dataset period.

8.1.9 Scatterplots of ISAS vs *in situ* SSS by latitudinal bands

In Figure 173, contour maps of the concentration of ISAS SSS (y-axis) versus Salinity snake SSS (x-axis) at match-up pairs for different latitude bands: (a) 80°S-80°N, (b) 20°S-20°N, (c) 40°S-20°S and 20°N-40°N and (d) 60°S-40°S and 40°N-60°N. For each plot, the red line shows $x=y$. The black thin and dashed lines indicate a linear fit through the data cloud and the $\pm 95\%$ confidence levels, respectively. The number match-up pairs n , the slope and R^2 coefficient of the linear fit, the root mean square (RMS) and the mean bias between ISAS and *in situ* data are indicated for each latitude band in each plots.

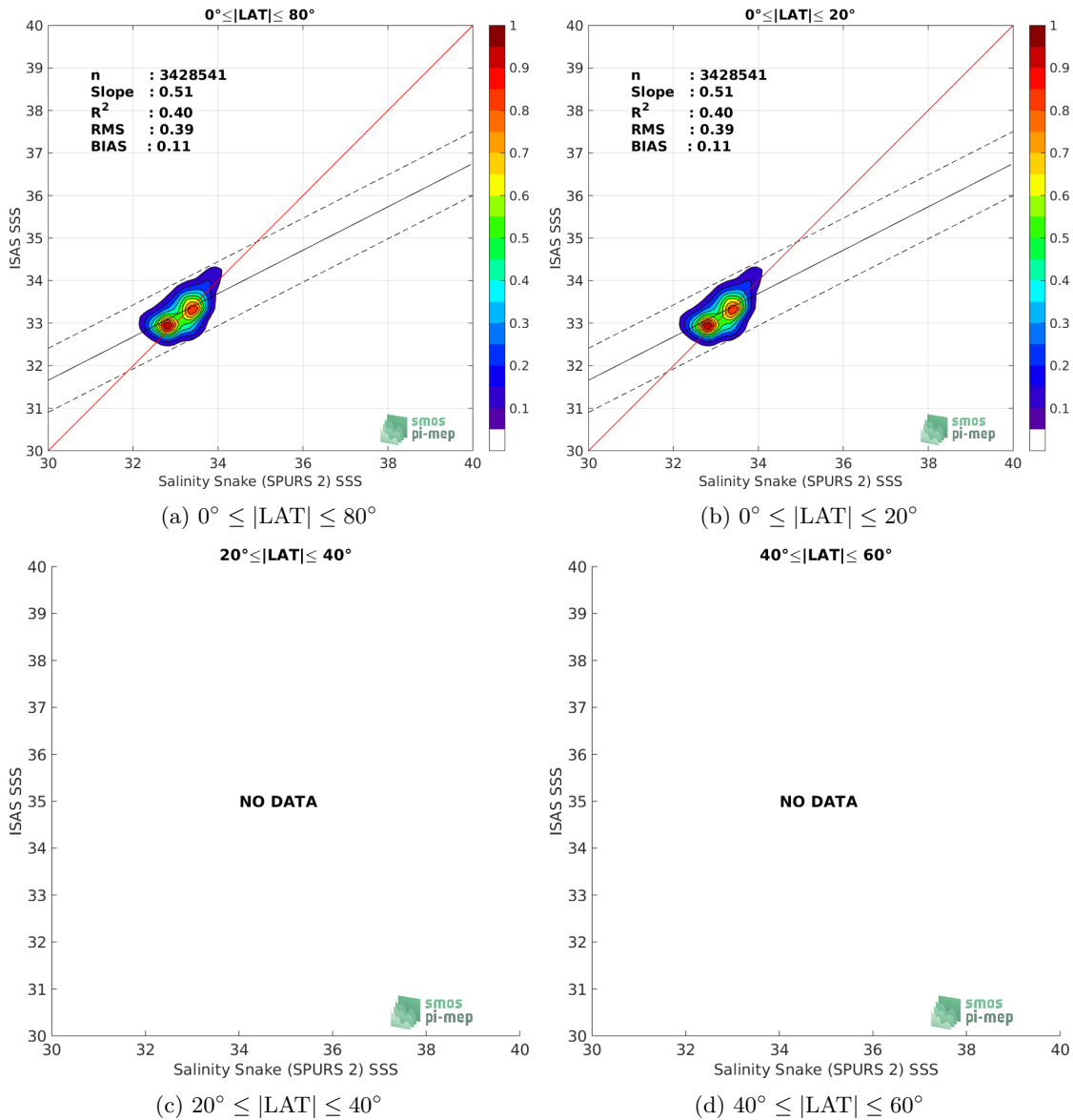


Figure 173: Contour maps of the concentration of ISAS SSS (y-axis) versus Salinity snake SSS (x-axis) at match-up pairs for different latitude bands. For each plot, the red line shows $x=y$. The black thin and dashed lines indicate a linear fit through the data cloud and the $\pm 95\%$ confidence levels, respectively. The number match-up pairs n , the slope and R^2 coefficient of the linear fit, the root mean square (RMS) and the mean bias between ISAS and *in situ* data are indicated for each latitude band in each plots.

8.1.10 Time series of the monthly median and Std of the difference ΔSSS sorted by latitudinal bands

In Figure 174, time series of the monthly median (red curves) of ΔSSS (ISAS - Salinity snake) and ± 1 Std (black vertical thick bars) as function of time for all the collected Pi-MEP match-up

pairs estimated for the full *in situ* dataset period are shown for different latitude bands: (a) 80°S-80°N, (b) 20°S-20°N, (c) 40°S-20°S and 20°N-40°N and (d) 60°S-40°S and 40°N-60°N.

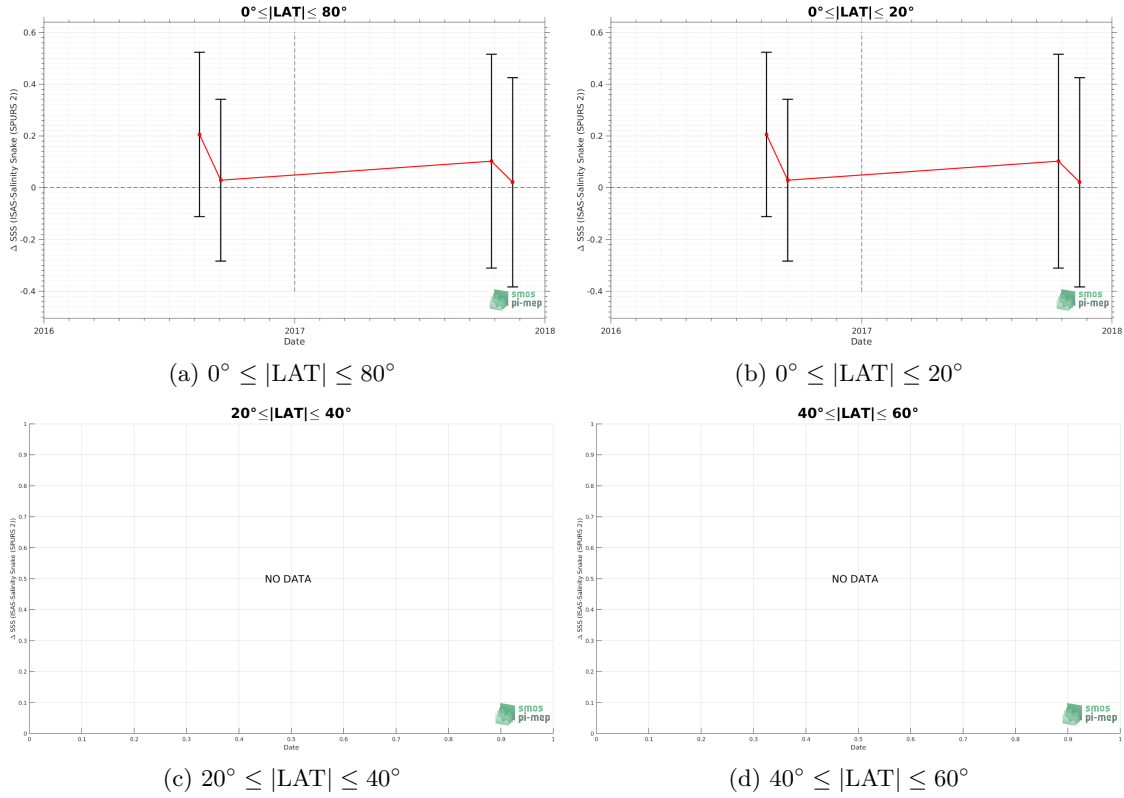


Figure 174: Monthly median (red curves) of ΔSSS (ISAS - Salinity snake) and ± 1 Std (black vertical thick bars) as function of time for all the collected Pi-MEP match-up pairs for the full *in situ* dataset period are shown for different latitude bands: (a) 80°S-80°N, (b) 20°S-20°N, (c) 40°S-20°S and 20°N-40°N and (d) 60°S-40°S and 40°N-60°N.

8.1.11 ΔSSS sorted as geophysical conditions

In Figure 175, we classify the match-up differences ΔSSS (ISAS - *in situ*) as function of the geophysical conditions at match-up points. The mean and std of ΔSSS (ISAS - Salinity snake) is thus evaluated as function of the

- *in situ* SSS values per bins of width 0.2,
- *in situ* SST values per bins of width 1°C,
- ASCAT daily wind values per bins of width 1 m/s,
- CMORPH 3-hourly rain rates per bins of width 1 mm/h, and,
- distance to coasts per bins of width 50 km,
- *in situ* measurement depth (if relevant).

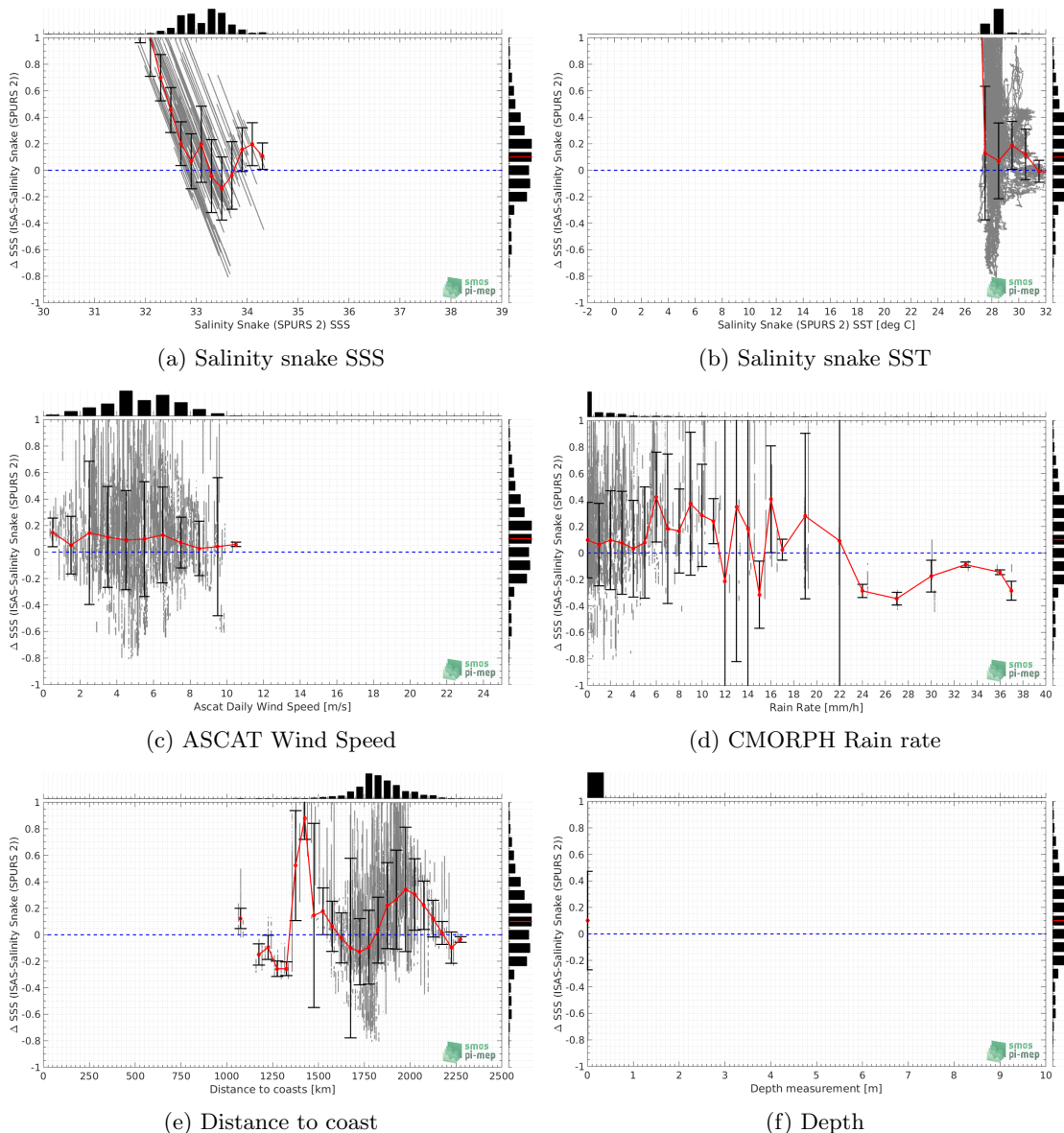


Figure 175: Δ SSS (ISAS - Salinity snake) sorted as geophysical conditions: Salinity snake SSS a), Salinity snake SST b), ASCAT Wind speed c), CMORPH rain rate d), distance to coast (e) and depth measurements (f).

8.1.12 Δ SSS maps and statistics for different geophysical conditions

In Figures 176 and 177, we focus on sub-datasets of the match-up differences Δ SSS (*ISAS - in situ*) for the following specific geophysical conditions:

- **C1:** if the local value at *in situ* location of estimated rain rate is zero, mean daily wind is in the range [3, 12] m/s, the SST is $> 5^{\circ}\text{C}$ and distance to coast is > 800 km.
- **C2:** if the local value at *in situ* location of estimated rain rate is zero, mean daily wind is

in the range [3, 12] m/s.

- **C3:** if the local value at *in situ* location of estimated rain rate is high (ie. > 1 mm/h) and mean daily wind is low (ie. < 4 m/s).
- **C5:** if the *in situ* data is located where the climatological SSS standard deviation is low (ie. above < 0.2).
- **C6:** if the *in situ* data is located where the climatological SSS standard deviation is high (ie. above > 0.2).

For each of these conditions, the temporal mean (gridded over spatial boxes of size $1^\circ \times 1^\circ$) and the histogram of the difference ΔSSS (ISAS - *in situ*) are presented.

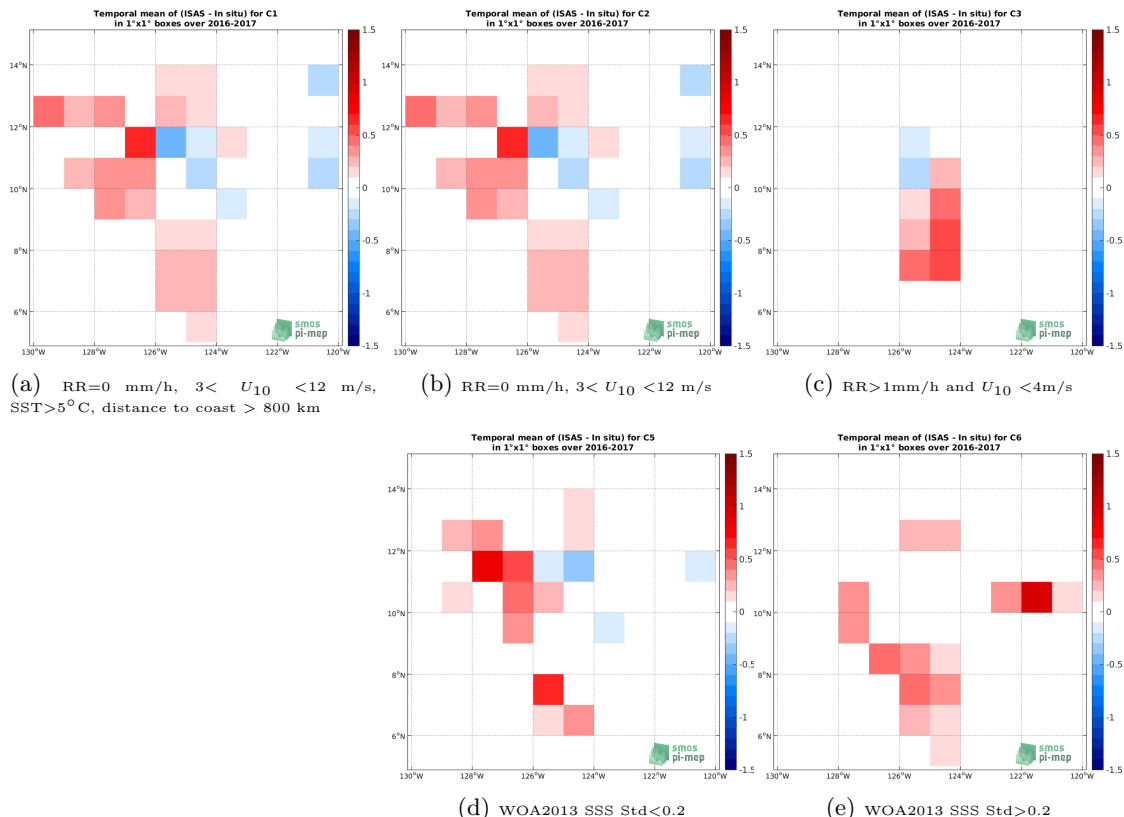


Figure 176: Temporal mean gridded over spatial boxes of size $1^\circ \times 1^\circ$ of ΔSSS (ISAS - Salinity snake) for 5 different subdatasets corresponding to: RR=0 mm/h, $3 < U_{10} < 12$ m/s, SST $>5^\circ\text{C}$, distance to coast > 800 km (a), RR=0 mm/h, $3 < U_{10} < 12$ m/s (b), RR>1mm/h and $U_{10} < 4$ m/s (c), WOA2013 SSS Std<0.2 (d), WOA2013 SSS Std>0.2 (e).

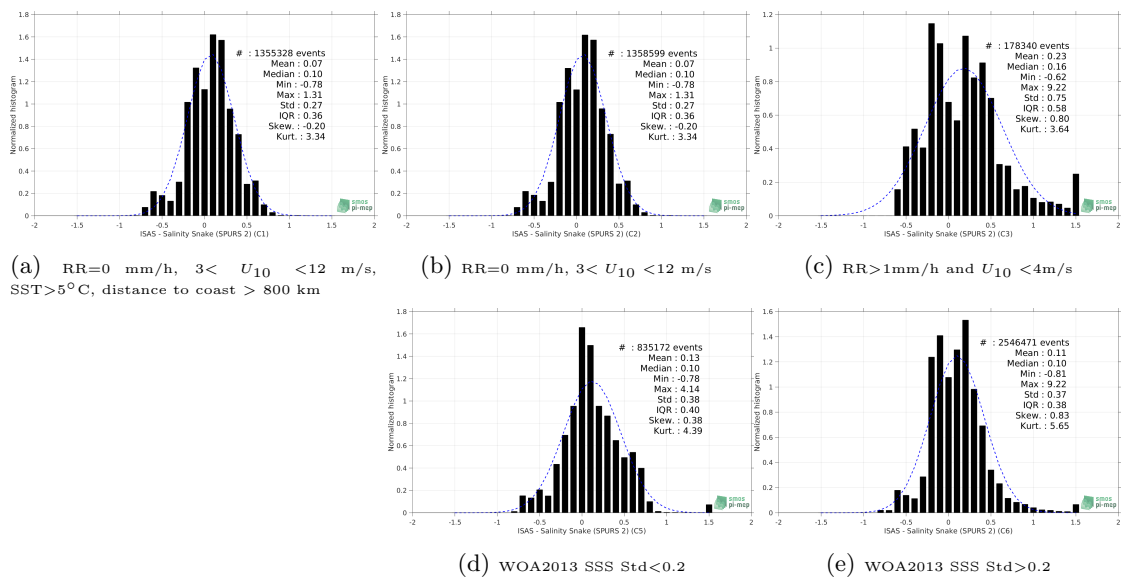


Figure 177: Normalized histogram of ΔSSS (ISAS - Salinity snake) for 5 different subdatasets corresponding to: $RR=0 \text{ mm/h}$, $3 < U_{10} < 12 \text{ m/s}$, $SST > 5^\circ\text{C}$, distance to coast > 800 km (a), $RR=0 \text{ mm/h}$, $3 < U_{10} < 12 \text{ m/s}$ (b), $RR > 1 \text{ mm/h}$ and $U_{10} < 4 \text{ m/s}$ (c), WOA2013 SSS Std < 0.2 (d), WOA2013 SSS Std > 0.2 (e).

8.1.13 Summary

Table 1 shows the mean, median, standard deviation (Std), root mean square (RMS), interquartile range (IQR), correlation coefficient (r^2) and robust standard deviation (Std*) of the match-up differences ΔSSS (ISAS - Salinity snake) for the following conditions:

- all: All the match-up pairs satellite/in situ SSS values are used to derive the statistics
- C1: only pairs where $RR=0 \text{ mm/h}$, $3 < U_{10} < 12 \text{ m/s}$, $SST > 5^\circ\text{C}$, distance to coast > 800 km
- C2: only pairs where $RR=0 \text{ mm/h}$, $3 < U_{10} < 12 \text{ m/s}$
- C3: only pairs where $RR > 1 \text{ mm/h}$ and $U_{10} < 4 \text{ m/s}$
- C5: only pairs where WOA2013 SSS Std < 0.2
- C6: only pairs where WOA2013 SSS Std > 0.2
- C7a: only pairs with a distance to coast < 150 km.
- C7b: only pairs with a distance to coast in the range [150, 800] km.
- C7c: only pairs with a distance to coast > 800 km.
- C8a: only pairs where SST is < 5°C .
- C8b: only pairs where SST is in the range $[5, 15]^\circ\text{C}$.
- C8c: only pairs where SST is > 15°C .

- C9a: only pairs where SSS is < 33.
- C9b: only pairs where SSS is in the range [33, 37].
- C9c: only pairs where SSS is > 37.

Table 1: Statistics of ΔSSS (ISAS - Salinity snake)

Condition	#	Median	Mean	Std	RMS	IQR	r^2	Std*
all	3428541	0.10	0.11	0.37	0.39	0.39	0.403	0.29
C1	1355328	0.10	0.07	0.27	0.28	0.36	0.681	0.27
C2	1358599	0.10	0.07	0.27	0.28	0.36	0.681	0.27
C3	178340	0.16	0.23	0.75	0.78	0.58	0.003	0.45
C5	835172	0.10	0.13	0.38	0.40	0.40	0.405	0.30
C6	2546471	0.10	0.11	0.37	0.38	0.38	0.374	0.29
C7a	0	NaN	NaN	NaN	NaN	NaN	NaN	NaN
C7b	0	NaN	NaN	NaN	NaN	NaN	NaN	NaN
C7c	3428541	0.10	0.11	0.37	0.39	0.39	0.403	0.29
C8a	0	NaN	NaN	NaN	NaN	NaN	NaN	NaN
C8b	0	NaN	NaN	NaN	NaN	NaN	NaN	NaN
C8c	3402834	0.10	0.11	0.37	0.39	0.39	0.400	0.30
C9a	1385563	0.20	0.29	0.42	0.51	0.36	0.041	0.26
C9b	2042978	-0.03	-0.01	0.27	0.27	0.37	0.427	0.26
C9c	0	NaN	NaN	NaN	NaN	NaN	NaN	NaN

Table 1 numerical values can be downloaded as a csv file [here](#).

8.2 Saildrone

8.2.1 Introduction

Saildrone is a state-of-the-art, remotely guided, wind and solar powered unmanned surface vehicle (USV) capable of long distance deployments lasting up to 12 months. It is equipped with a suite of instruments and sensors providing high quality, georeferenced, near real-time, multi-parameter surface ocean and atmospheric observations while transiting at typical speeds of 3-5 knots. Two saildrones (<https://doi.org/10.5067/SPUR2-SDRON>) were deployed over a month period during the second SPURS-2 R/V Revelle cruise in 2017. The SPURS-2 campaign involved two month-long cruises by the R/V Revelle in August 2016 and October 2017 combined with complementary sampling on a more continuous basis over this period by the schooner Lady Amber. Focused around a central mooring located near 10°N, 125°W, the objective of **SPURS-2** (NASA-funded oceanographic process study) was to study the dynamics of the rainfall-dominated surface ocean at the western edge of the eastern Pacific fresh pool subject to high seasonal variability and strong zonal flows associated with the North Equatorial Current and Countercurrent.

8.2.2 Number of SSS data as a function of time and distance to coast

Figure 178 shows the time (a) and distance to coast (b) distributions of the Saildrone *in situ* dataset.

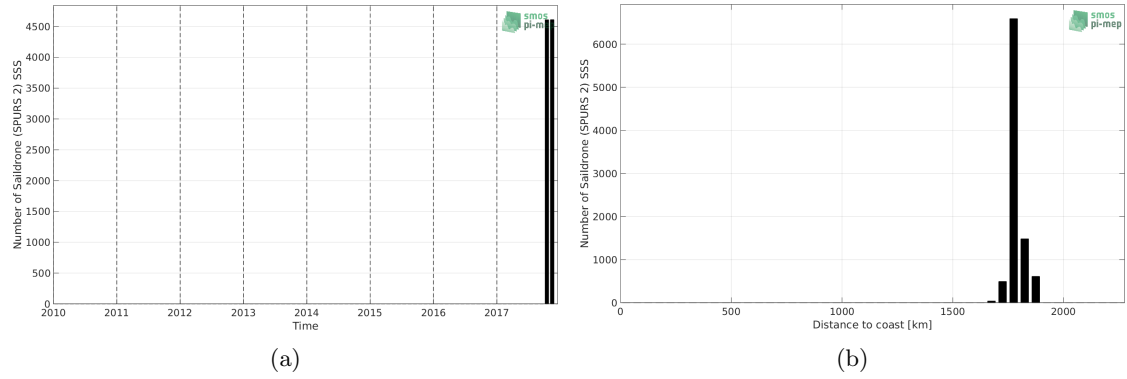


Figure 178: Number of SSS from Saildrone as a function of time (a) and distance to coast (b).

8.2.3 Histograms of SSS

Figure 179 shows the SSS distribution of the Saildrone (a) and colocalized ISAS (b) dataset.

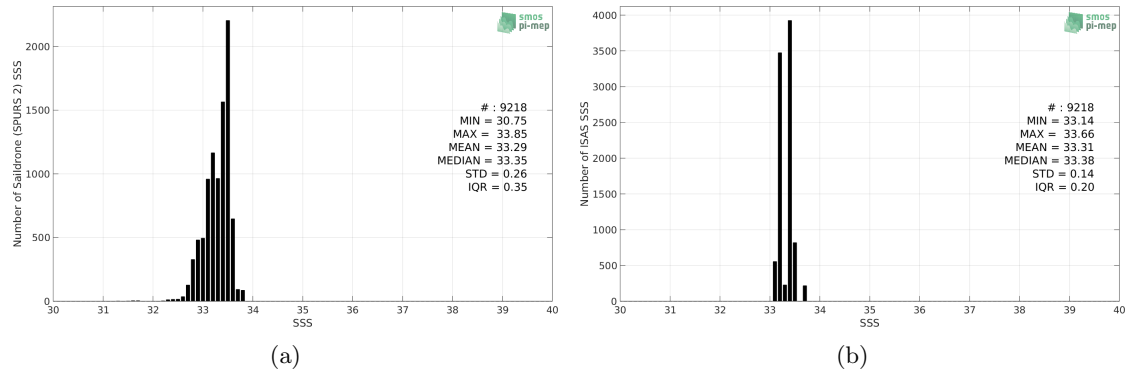


Figure 179: Histograms of SSS from Saildrone (a) and ISAS (b) per bins of 0.1.

8.2.4 Distribution of *in situ* SSS depth measurements

In Figure 180, we show the depth distribution of the *in situ* salinity dataset (a) and the spatial distribution of the depth temporal mean in $1^\circ \times 1^\circ$ boxes and considering the full *in situ* dataset period (b).

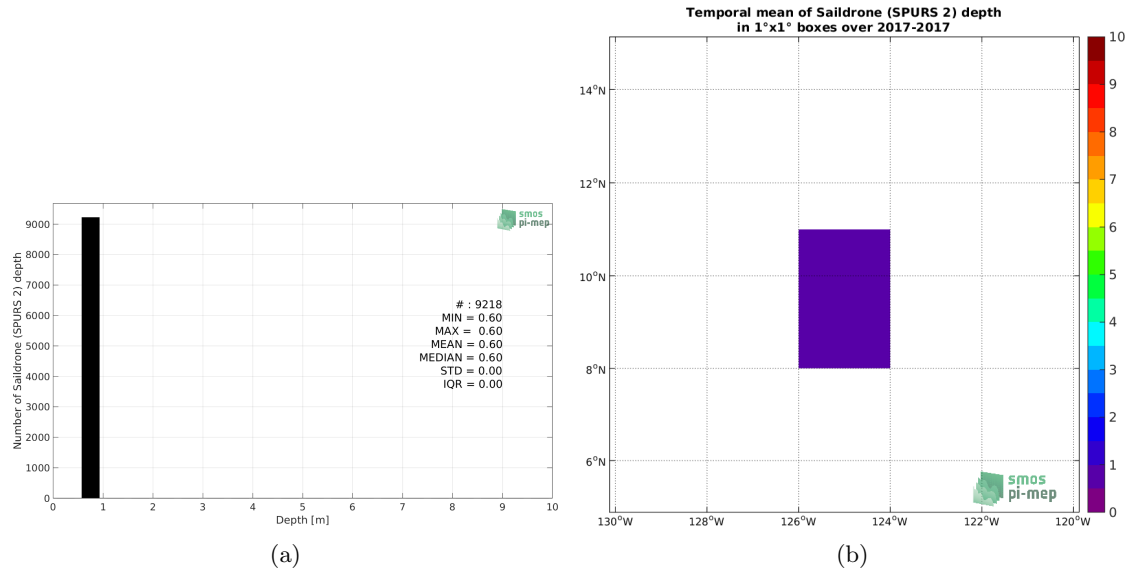
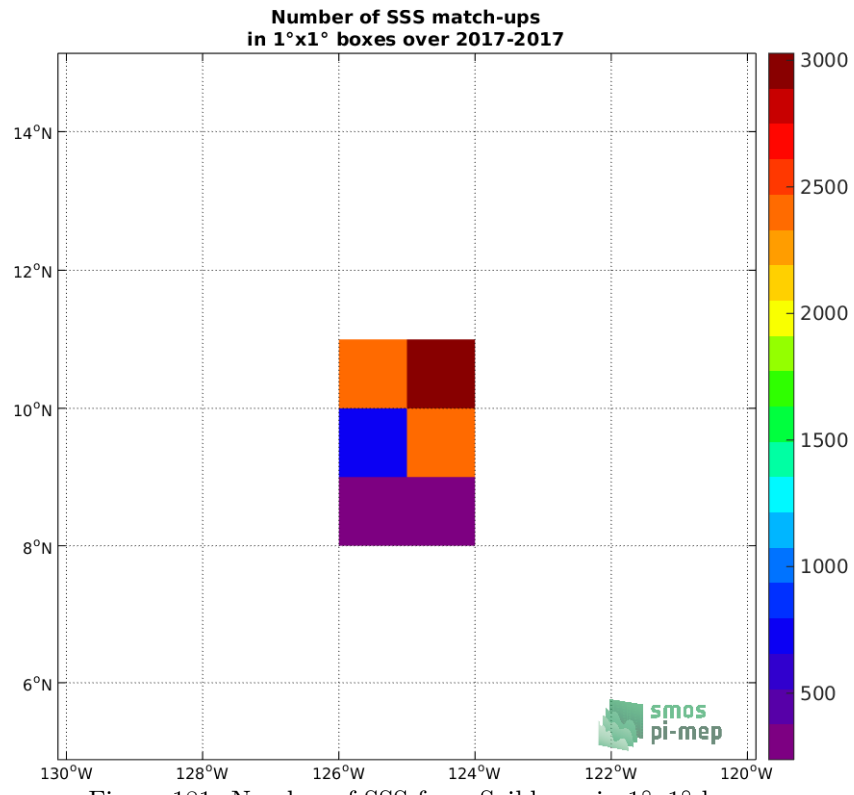


Figure 180: Depth distribution of the upper level SSS measurements from Saildrone (a) and spatial distribution of the *in situ* SSS depth measurements showing the mean value in 1°x1° boxes and considering the full *in situ* dataset period (b).

8.2.5 Spatial distribution of SSS

In Figure 181, the number of Saildrone SSS measurements in 1°x1° boxes is shown.



8.2.6 Spatial Maps of the Temporal mean and Std of *in situ* and ISAS SSS and of the difference (Δ SSS)

In Figure 182, maps of temporal mean (left) and standard deviation (right) of ISAS (top), Saildrone *in situ* dataset (middle) and the difference Δ SSS(ISAS -Saildrone) (bottom) are shown. The temporal mean and std are calculated using all match-up pairs falling in spatial boxes of size $1^{\circ} \times 1^{\circ}$ over the full Saildrone dataset period.

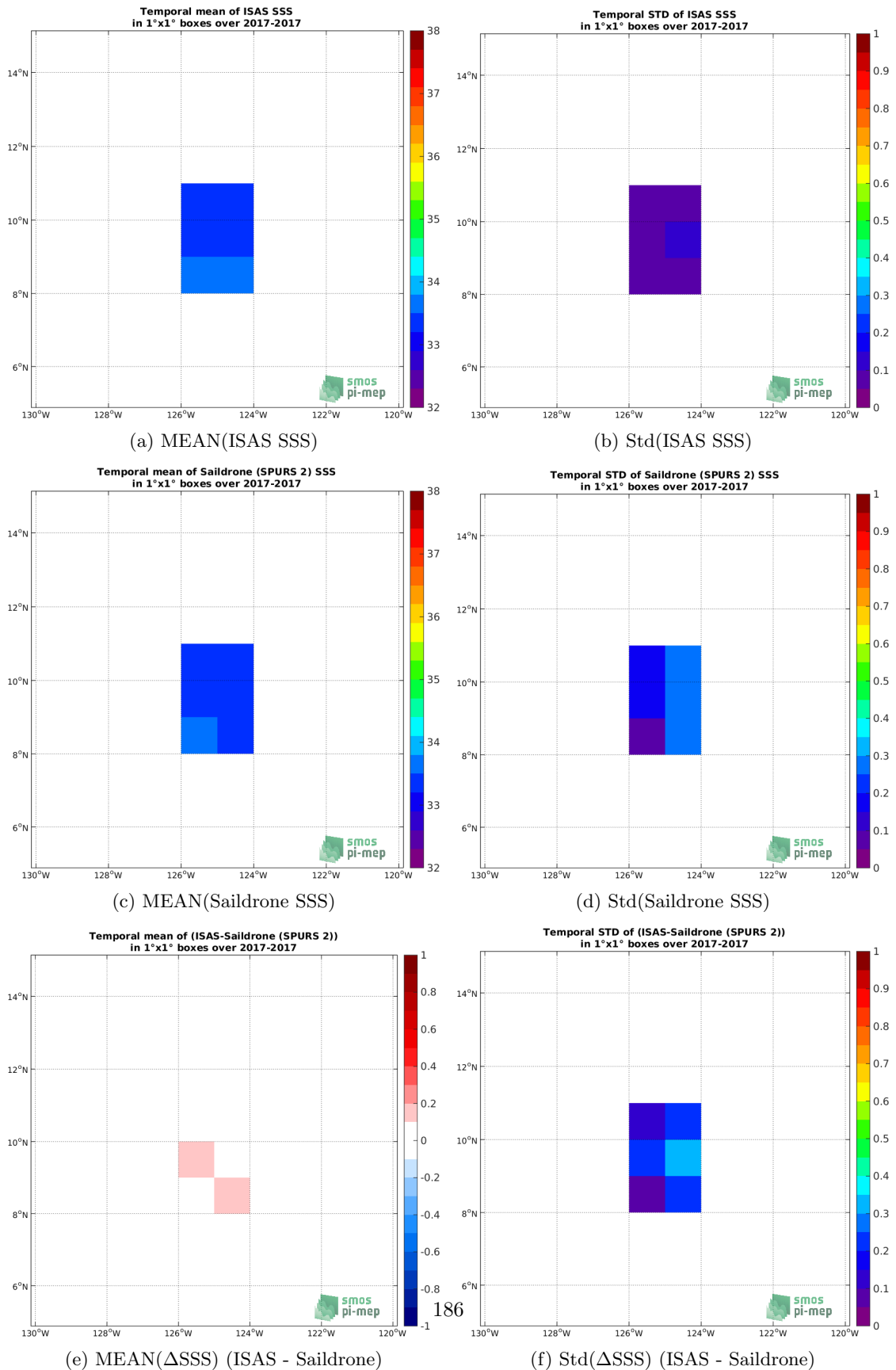


Figure 182: Temporal mean (left) and Std (right) of SSS from ISAS (top), Saildrone (middle), and of Δ SSS (ISAS - Saildrone). Only match-up pairs are used to generate these maps.

8.2.7 Time series of the monthly median and Std of *in situ* and ISAS SSS and of the difference (Δ SSS)

In the top panel of Figure 183, we show the time series of the monthly median SSS estimated for both ISAS SSS product (in black) and the Saildrone *in situ* dataset (in blue) at the collected Pi-MEP match-up pairs.

In the middle panel of Figure 183, we show the time series of the monthly median of Δ SSS (ISAS - Saildrone) for the collected Pi-MEP match-up pairs.

In the bottom panel of Figure 183, we show the time series of the monthly standard deviation of the Δ SSS (ISAS - Saildrone) for the collected Pi-MEP match-up pairs.

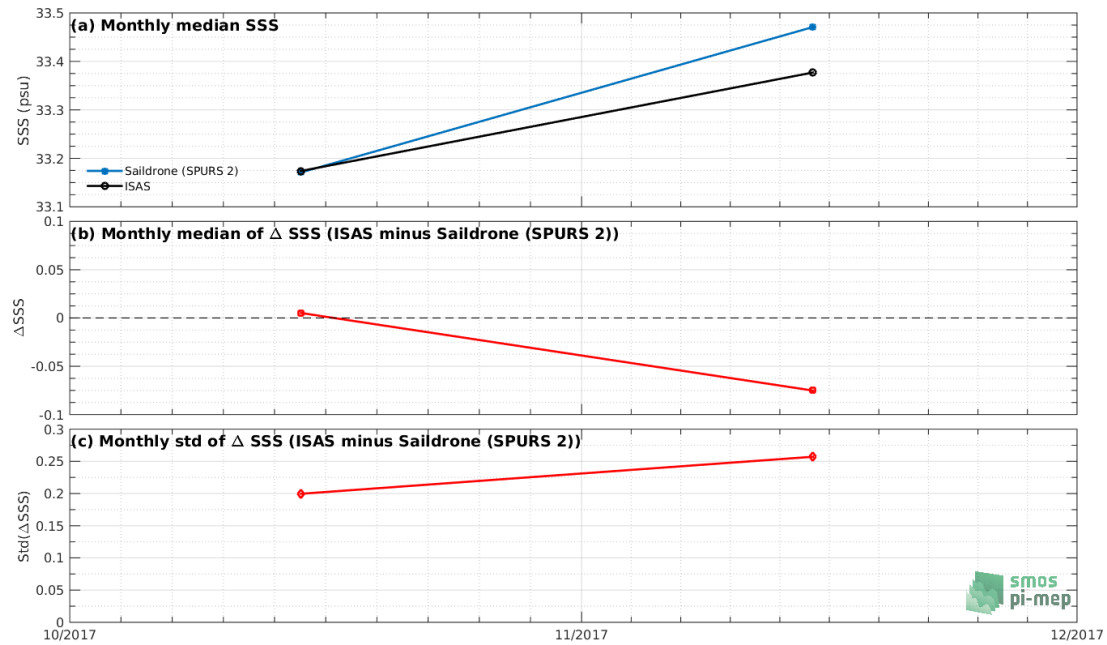


Figure 183: Time series of the monthly median SSS (top), median of Δ SSS (ISAS - Saildrone) and Std of Δ SSS (ISAS - Saildrone) considering all match-ups collected by the Pi-MEP.

8.2.8 Zonal mean and Std of *in situ* and ISAS SSS and of the difference Δ SSS

In Figure 184 left panel, we show the zonal mean SSS considering all Pi-MEP match-up pairs for both ISAS SSS product (in black) and the Saildrone *in situ* dataset (in blue). The full *in situ* dataset period is used to derive the mean.

In the right panel of Figure 184, we show the zonal mean of Δ SSS (ISAS - Saildrone) for all the collected Pi-MEP match-up pairs estimated over the full *in situ* dataset period.

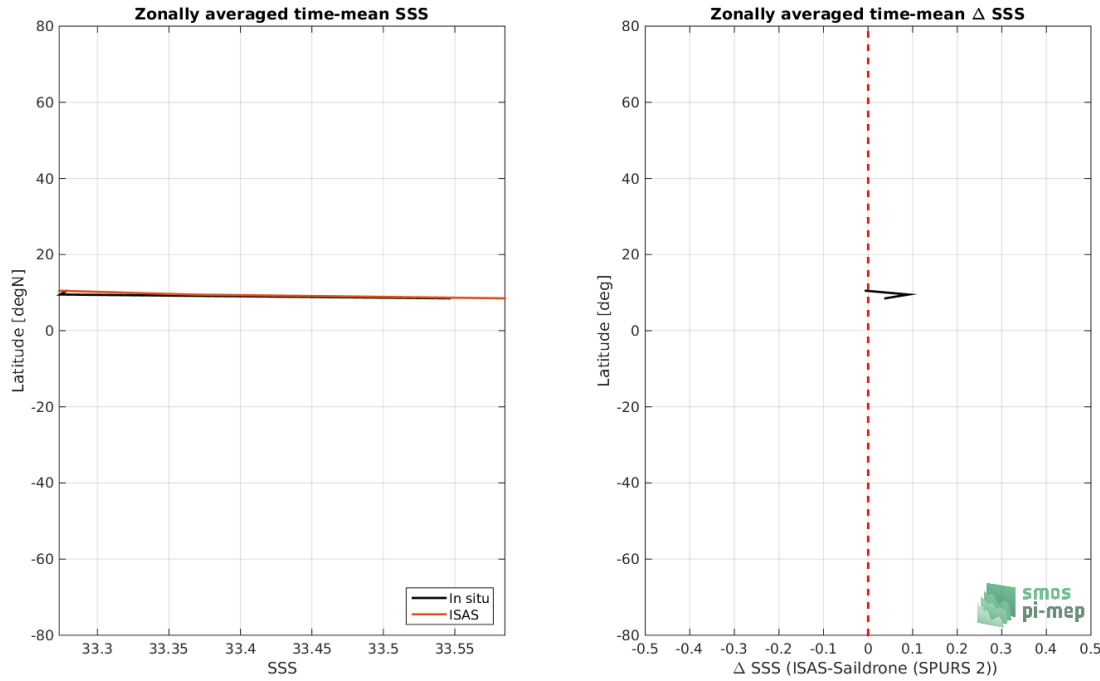


Figure 184: Left panel: Zonal mean SSS from ISAS product (black) and from Saildrone (blue). Right panel: Zonal mean of ΔSSS (ISAS - Saildrone) for all the collected Pi-MEP match-up pairs estimated over the full *in situ* dataset period.

8.2.9 Scatterplots of ISAS vs *in situ* SSS by latitudinal bands

In Figure 185, contour maps of the concentration of ISAS SSS (y-axis) versus Saildrone SSS (x-axis) at match-up pairs for different latitude bands: (a) 80°S-80°N, (b) 20°S-20°N, (c) 40°S-20°S and 20°N-40°N and (d) 60°S-40°S and 40°N-60°N. For each plot, the red line shows $x=y$. The black thin and dashed lines indicate a linear fit through the data cloud and the $\pm 95\%$ confidence levels, respectively. The number match-up pairs n , the slope and R^2 coefficient of the linear fit, the root mean square (RMS) and the mean bias between ISAS and *in situ* data are indicated for each latitude band in each plots.

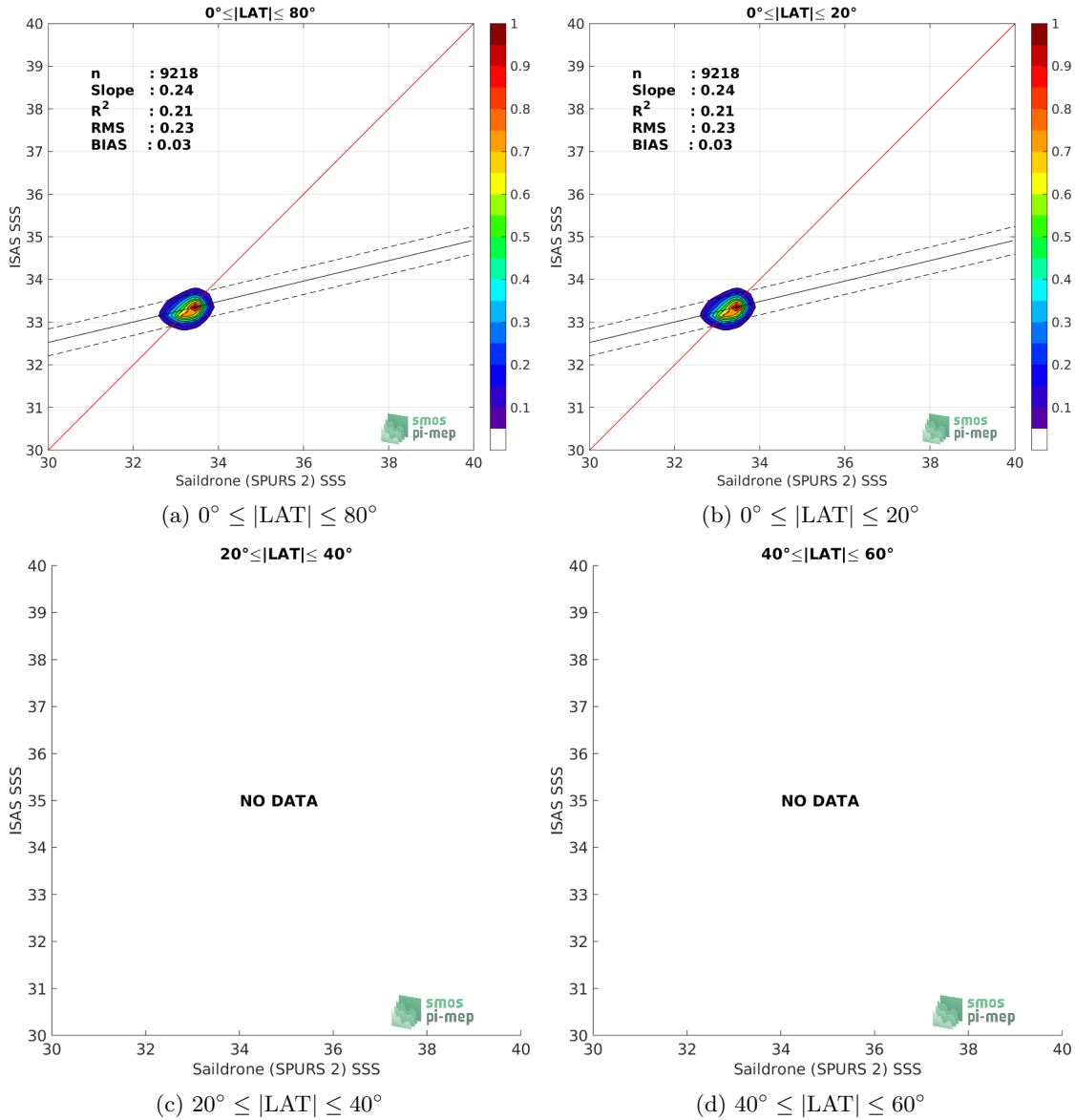


Figure 185: Contour maps of the concentration of ISAS SSS (y-axis) versus Saildrone SSS (x-axis) at match-up pairs for different latitude bands. For each plot, the red line shows $x=y$. The black thin and dashed lines indicate a linear fit through the data cloud and the $\pm 95\%$ confidence levels, respectively. The number match-up pairs n , the slope and R^2 coefficient of the linear fit, the root mean square (RMS) and the mean bias between ISAS and *in situ* data are indicated for each latitude band in each plots.

8.2.10 Time series of the monthly median and Std of the difference ΔSSS sorted by latitudinal bands

In Figure 186, time series of the monthly median (red curves) of ΔSSS (ISAS - Saildrone) and ± 1 Std (black vertical thick bars) as function of time for all the collected Pi-MEP match-up

pairs estimated for the full *in situ* dataset period are shown for different latitude bands: (a) 80°S-80°N, (b) 20°S-20°N, (c) 40°S-20°S and 20°N-40°N and (d) 60°S-40°S and 40°N-60°N.

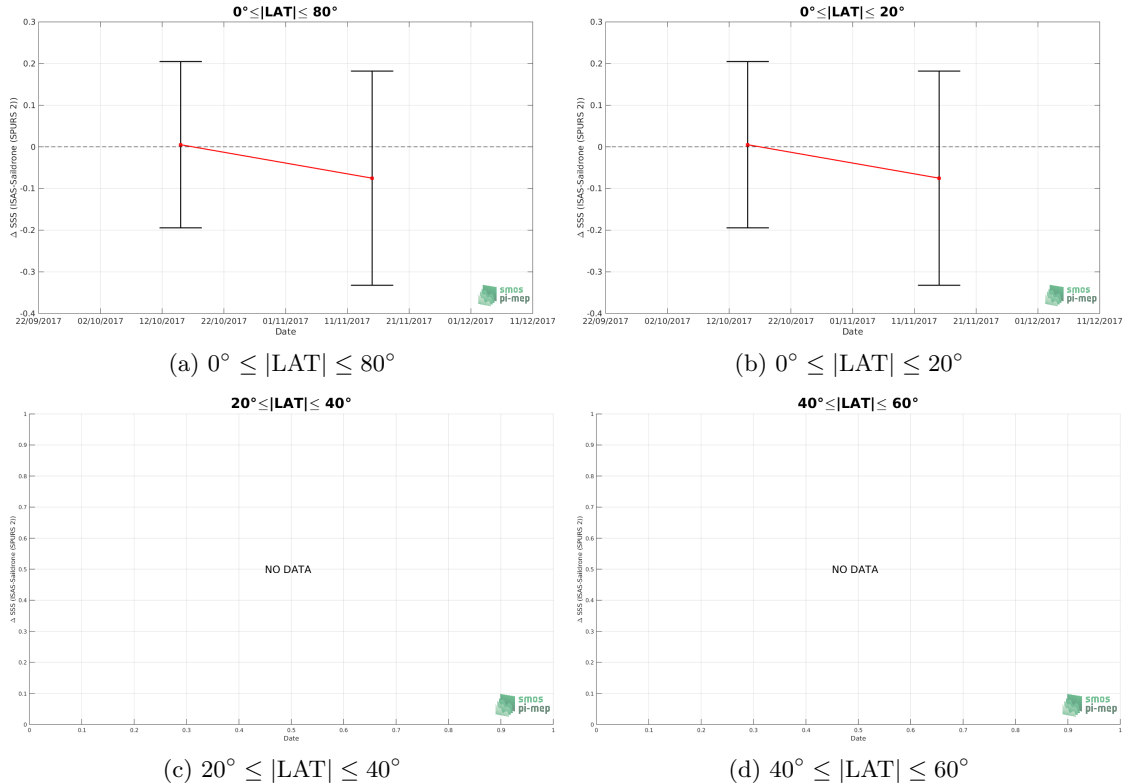


Figure 186: Monthly median (red curves) of ΔSSS (ISAS - Saildrone) and ± 1 Std (black vertical thick bars) as function of time for all the collected Pi-MEP match-up pairs for the full *in situ* dataset period are shown for different latitude bands: (a) 80°S-80°N, (b) 20°S-20°N, (c) 40°S-20°S and 20°N-40°N and (d) 60°S-40°S and 40°N-60°N.

8.2.11 ΔSSS sorted as geophysical conditions

In Figure 187, we classify the match-up differences ΔSSS (ISAS - *in situ*) as function of the geophysical conditions at match-up points. The mean and std of ΔSSS (ISAS - Saildrone) is thus evaluated as function of the

- *in situ* SSS values per bins of width 0.2,
- *in situ* SST values per bins of width 1°C,
- ASCAT daily wind values per bins of width 1 m/s,
- CMORPH 3-hourly rain rates per bins of width 1 mm/h, and,
- distance to coasts per bins of width 50 km,
- *in situ* measurement depth (if relevant).

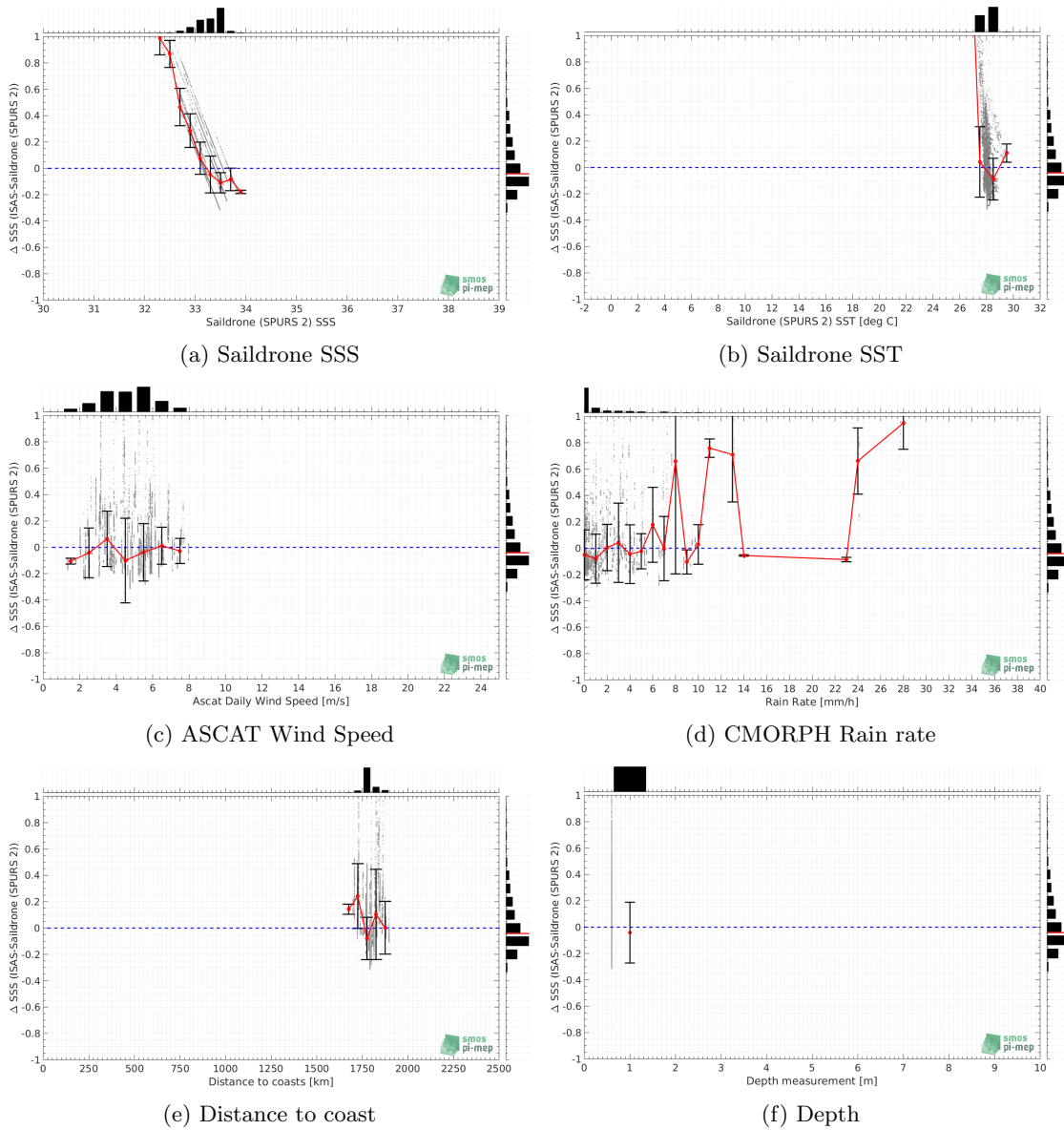


Figure 187: ΔSSS (ISAS - Saildrone) sorted as geophysical conditions: Saildrone SSS a), Saildrone SST b), ASCAT Wind speed c), CMORPH rain rate d), distance to coast (e) and depth measurements (f).

8.2.12 ΔSSS maps and statistics for different geophysical conditions

In Figures 188 and 189, we focus on sub-datasets of the match-up differences ΔSSS (ISAS - *in situ*) for the following specific geophysical conditions:

- **C1:** if the local value at *in situ* location of estimated rain rate is zero, mean daily wind is in the range [3, 12] m/s, the SST is $> 5^\circ\text{C}$ and distance to coast is > 800 km.
- **C2:** if the local value at *in situ* location of estimated rain rate is zero, mean daily wind is

in the range [3, 12] m/s.

- **C3:** if the local value at *in situ* location of estimated rain rate is high (ie. $> 1 \text{ mm/h}$) and mean daily wind is low (ie. $< 4 \text{ m/s}$).
- **C5:** if the *in situ* data is located where the climatological SSS standard deviation is low (ie. above < 0.2).
- **C6:** if the *in situ* data is located where the climatological SSS standard deviation is high (ie. above > 0.2).

For each of these conditions, the temporal mean (gridded over spatial boxes of size $1^\circ \times 1^\circ$) and the histogram of the difference ΔSSS (ISAS - *in situ*) are presented.

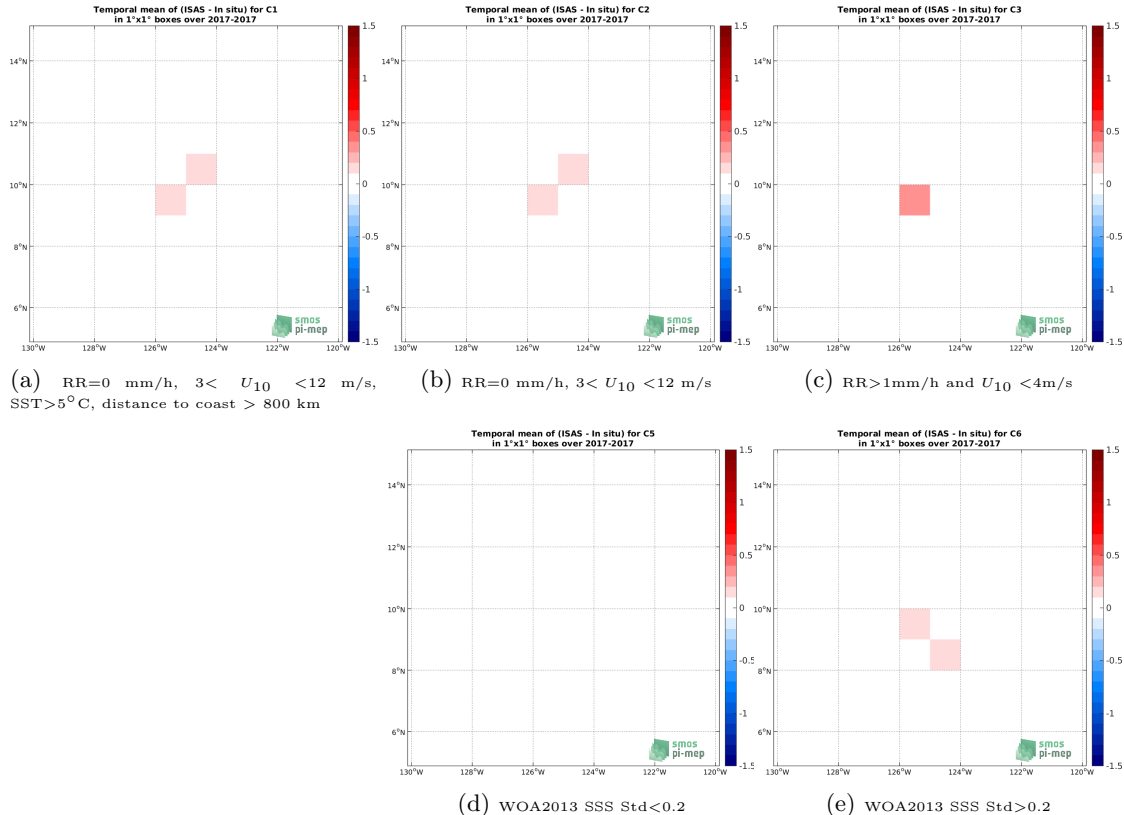


Figure 188: Temporal mean gridded over spatial boxes of size $1^\circ \times 1^\circ$ of ΔSSS (ISAS - Saildrone) for 5 different subdatasets corresponding to: RR=0 mm/h, $3 < U_{10} < 12 \text{ m/s}$, SST $>5^\circ\text{C}$, distance to coast $> 800 \text{ km}$ (a), RR=0 mm/h, $3 < U_{10} < 12 \text{ m/s}$ (b), RR $>1\text{mm/h}$ and $U_{10} < 4\text{m/s}$ (c), WOA2013 SSS Std <0.2 (d), WOA2013 SSS Std >0.2 (e).

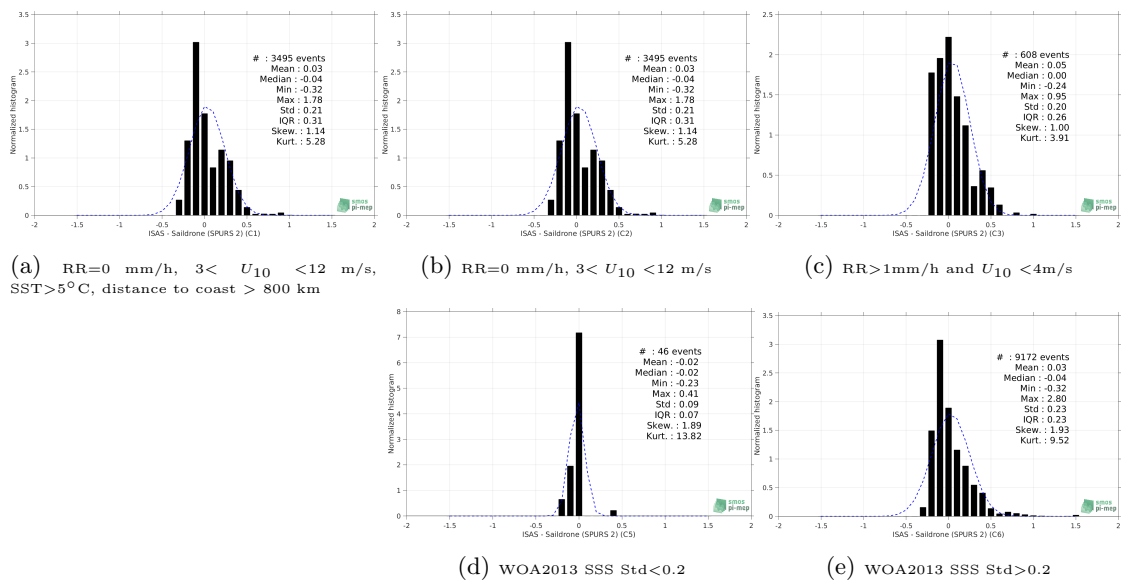


Figure 189: Normalized histogram of ΔSSS (ISAS - Saildrone) for 5 different subdatasets corresponding to: $RR=0 \text{ mm/h}, 3 < U_{10} < 12 \text{ m/s}, SST > 5^\circ\text{C}, \text{distance to coast} > 800 \text{ km}$ (a), $RR=0 \text{ mm/h}, 3 < U_{10} < 12 \text{ m/s}$ (b), $RR > 1 \text{ mm/h} \text{ and } U_{10} < 4 \text{ m/s}$ (c), WOA2013 SSS Std < 0.2 (d), WOA2013 SSS Std > 0.2 (e).

8.2.13 Summary

Table 1 shows the mean, median, standard deviation (Std), root mean square (RMS), interquartile range (IQR), correlation coefficient (r^2) and robust standard deviation (Std*) of the match-up differences ΔSSS (ISAS - Saildrone) for the following conditions:

- all: All the match-up pairs satellite/in situ SSS values are used to derive the statistics
- C1: only pairs where $RR=0 \text{ mm/h}, 3 < U_{10} < 12 \text{ m/s}, SST > 5^\circ\text{C}, \text{distance to coast} > 800 \text{ km}$
- C2: only pairs where $RR=0 \text{ mm/h}, 3 < U_{10} < 12 \text{ m/s}$
- C3: only pairs where $RR > 1 \text{ mm/h} \text{ and } U_{10} < 4 \text{ m/s}$
- C5: only pairs where WOA2013 SSS Std < 0.2
- C6: only pairs where WOA2013 SSS Std > 0.2
- C7a: only pairs with a distance to coast < 150 km.
- C7b: only pairs with a distance to coast in the range [150, 800] km.
- C7c: only pairs with a distance to coast > 800 km.
- C8a: only pairs where SST is < 5°C .
- C8b: only pairs where SST is in the range $[5, 15]^\circ\text{C}$.
- C8c: only pairs where SST is > 15°C .

- C9a: only pairs where SSS is < 33.
- C9b: only pairs where SSS is in the range [33, 37].
- C9c: only pairs where SSS is > 37.

Table 1: Statistics of ΔSSS (ISAS - Saildrone)

Condition	#	Median	Mean	Std	RMS	IQR	r^2	Std*
all	9218	-0.04	0.03	0.23	0.23	0.23	0.207	0.15
C1	3495	-0.04	0.03	0.21	0.21	0.31	0.362	0.17
C2	3495	-0.04	0.03	0.21	0.21	0.31	0.362	0.17
C3	608	0.00	0.05	0.20	0.21	0.26	0.294	0.19
C5	46	-0.02	-0.02	0.09	0.09	0.07	0.000	0.05
C6	9172	-0.04	0.03	0.23	0.23	0.23	0.206	0.15
C7a	0	NaN	NaN	NaN	NaN	NaN	NaN	NaN
C7b	0	NaN	NaN	NaN	NaN	NaN	NaN	NaN
C7c	9218	-0.04	0.03	0.23	0.23	0.23	0.207	0.15
C8a	0	NaN	NaN	NaN	NaN	NaN	NaN	NaN
C8b	0	NaN	NaN	NaN	NaN	NaN	NaN	NaN
C8c	9218	-0.04	0.03	0.23	0.23	0.23	0.207	0.15
C9a	1210	0.35	0.43	0.30	0.52	0.23	0.175	0.15
C9b	8008	-0.06	-0.04	0.14	0.14	0.17	0.382	0.12
C9c	0	NaN	NaN	NaN	NaN	NaN	NaN	NaN

Table 1 numerical values can be downloaded as a csv file [here](#).

8.3 Waveglider

8.3.1 Introduction

A Waveglider is an autonomous platform propelled by the conversion of ocean wave energy into forward thrust and employing solar panels to power instrumentation. For SPURS-2, sensors included a CTD at the near-surface and another at 6 m depth, providing continuous salinity and temperature observations plus air temperature and wind measurements. Three wavegliders (<https://doi.org/10.5067/SPUR2-GLID3>) were deployed from the Reveille in August 2016 and again in November 2017 before final retrieval at the conclusion on the second cruise. Waveglider trajectories followed a 20x20km square loop around the moorings and a butterfly pattern around the neutrally-buoyant float. Focused around a central mooring located near 10°N,125°W, the objective of SPURS-2 (NASA-funded oceanographic process study) was to study the dynamics of the rainfall-dominated surface ocean at the western edge of the eastern Pacific fresh pool subject to high seasonal variability and strong zonal flows associated with the North Equatorial Current and Countercurrent.

8.3.2 Number of SSS data as a function of time and distance to coast

Figure 190 shows the time (a) and distance to coast (b) distributions of the Waveglider *in situ* dataset.

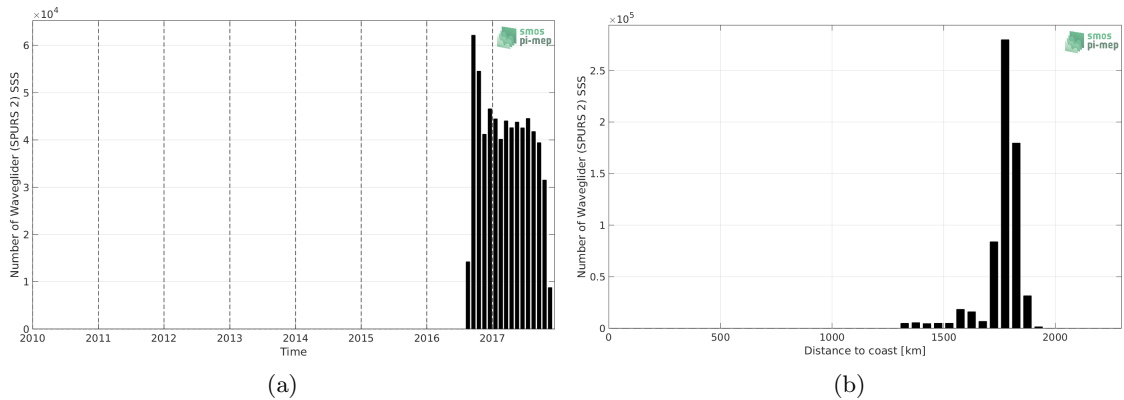


Figure 190: Number of SSS from Waveglider as a function of time (a) and distance to coast (b).

8.3.3 Histograms of SSS

Figure 191 shows the SSS distribution of the Waveglider (a) and colocalized ISAS (b) dataset.

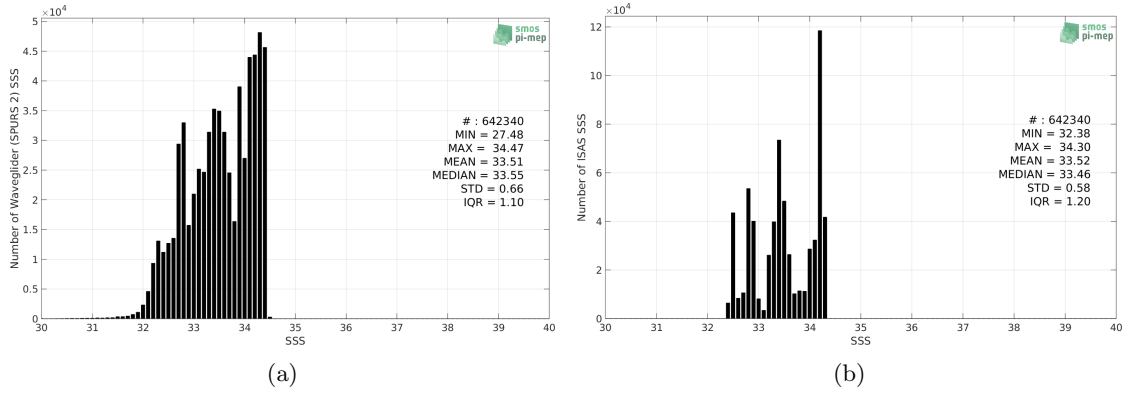


Figure 191: Histograms of SSS from Waveglider (a) and ISAS (b) per bins of 0.1.

8.3.4 Distribution of *in situ* SSS depth measurements

In Figure 192, we show the depth distribution of the *in situ* salinity dataset (a) and the spatial distribution of the depth temporal mean in $1^\circ \times 1^\circ$ boxes and considering the full *in situ* dataset period (b).

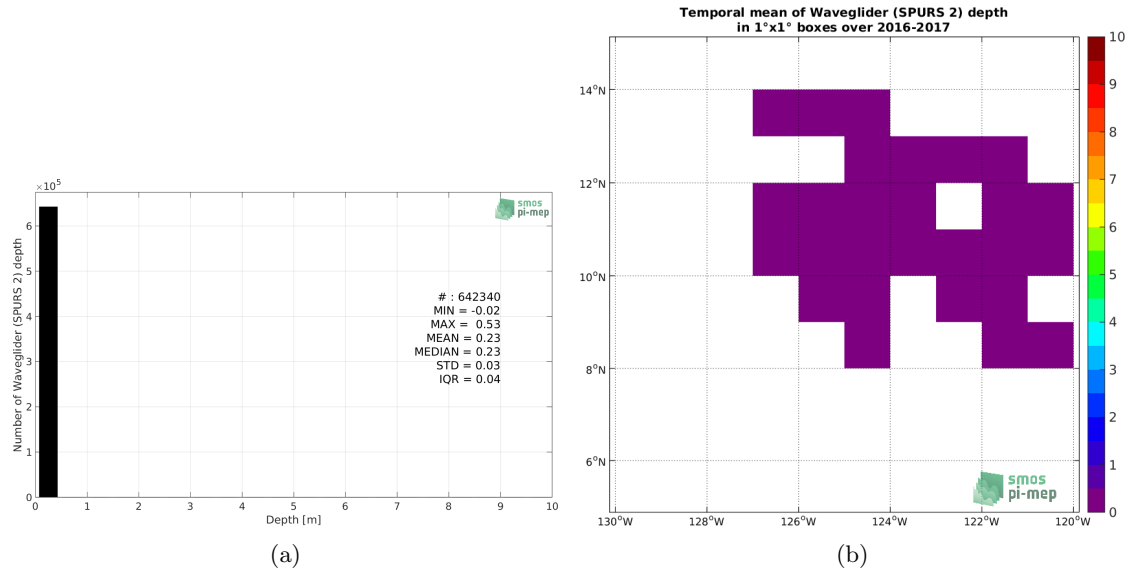
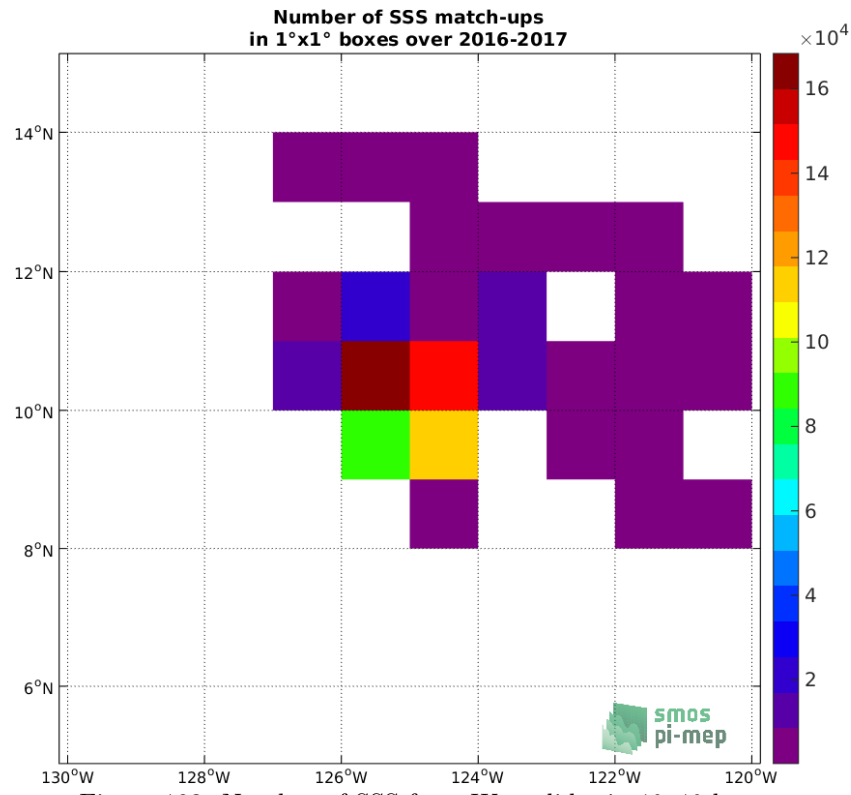


Figure 192: Depth distribution of the upper level SSS measurements from Waveglider (a) and spatial distribution of the *in situ* SSS depth measurements showing the mean value in $1^\circ \times 1^\circ$ boxes and considering the full *in situ* dataset period (b).

8.3.5 Spatial distribution of SSS

In Figure 193, the number of Waveglider SSS measurements in $1^\circ \times 1^\circ$ boxes is shown.


 Figure 193: Number of SSS from Waveglider in $1^\circ \times 1^\circ$ boxes.

8.3.6 Spatial Maps of the Temporal mean and Std of *in situ* and ISAS SSS and of the difference (Δ SSS)

In Figure 194, maps of temporal mean (left) and standard deviation (right) of ISAS (top), Waveglider *in situ* dataset (middle) and the difference Δ SSS(ISAS -Waveglider) (bottom) are shown. The temporal mean and std are calculated using all match-up pairs falling in spatial boxes of size $1^\circ \times 1^\circ$ over the full Waveglider dataset period.

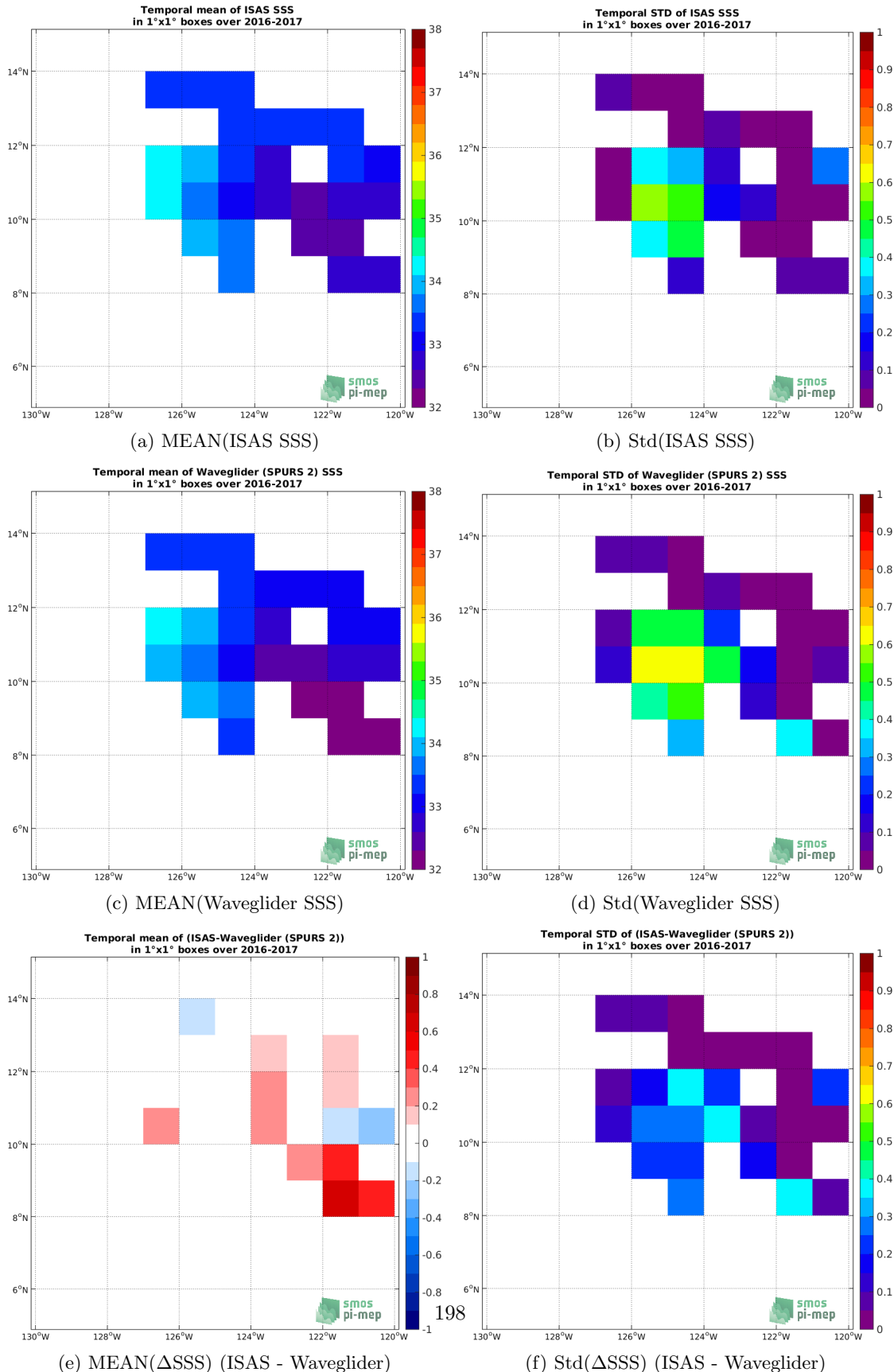


Figure 194: Temporal mean (left) and Std (right) of SSS from ISAS (top), Waveglider (middle), and of Δ SSS (ISAS - Waveglider). Only match-up pairs are used to generate these maps.

8.3.7 Time series of the monthly median and Std of *in situ* and ISAS SSS and of the difference (Δ SSS)

In the top panel of Figure 195, we show the time series of the monthly median SSS estimated for both ISAS SSS product (in black) and the Waveglider *in situ* dataset (in blue) at the collected Pi-MEP match-up pairs.

In the middle panel of Figure 195, we show the time series of the monthly median of Δ SSS (ISAS - Waveglider) for the collected Pi-MEP match-up pairs.

In the bottom panel of Figure 195, we show the time series of the monthly standard deviation of the Δ SSS (ISAS - Waveglider) for the collected Pi-MEP match-up pairs.

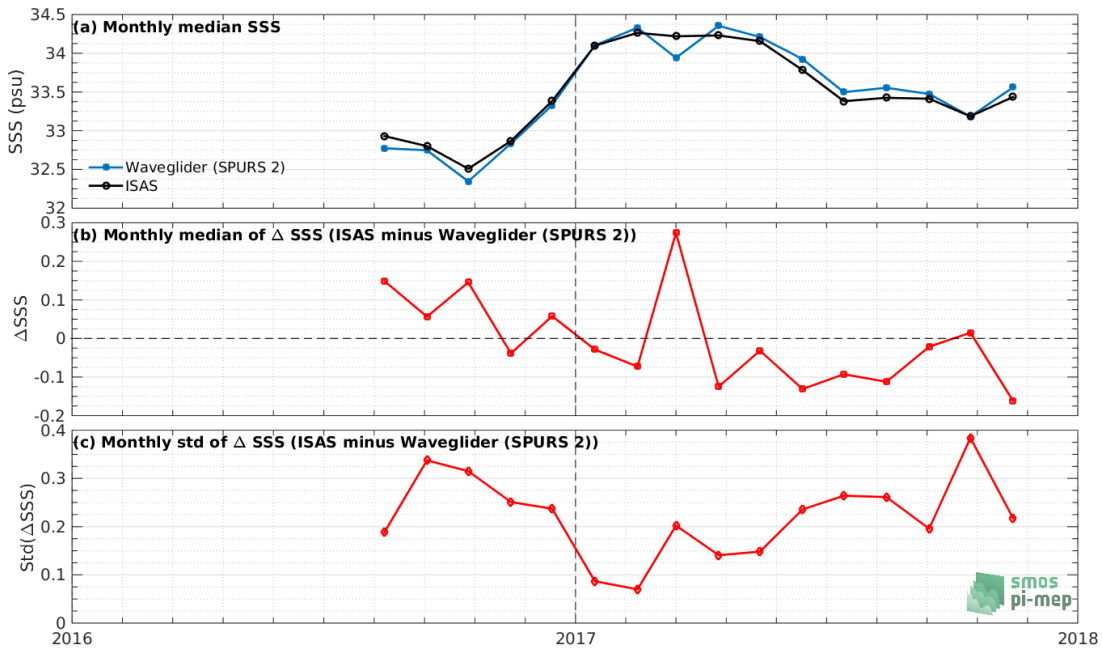


Figure 195: Time series of the monthly median SSS (top), median of Δ SSS (ISAS - Waveglider) and Std of Δ SSS (ISAS - Waveglider) considering all match-ups collected by the Pi-MEP.

8.3.8 Zonal mean and Std of *in situ* and ISAS SSS and of the difference Δ SSS

In Figure 196 left panel, we show the zonal mean SSS considering all Pi-MEP match-up pairs for both ISAS SSS product (in black) and the Waveglider *in situ* dataset (in blue). The full *in situ* dataset period is used to derive the mean.

In the right panel of Figure 196, we show the zonal mean of Δ SSS (ISAS - Waveglider) for all the collected Pi-MEP match-up pairs estimated over the full *in situ* dataset period.

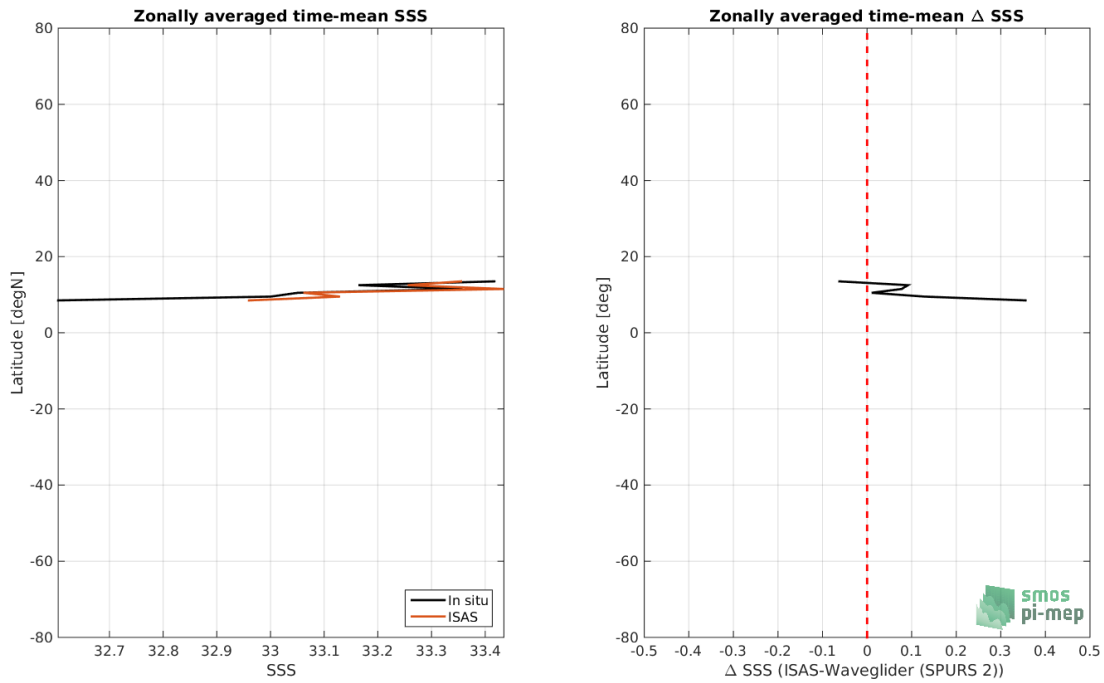


Figure 196: Left panel: Zonal mean SSS from ISAS product (black) and from Waveglider (blue). Right panel: Zonal mean of ΔSSS (ISAS - Waveglider) for all the collected Pi-MEP match-up pairs estimated over the full *in situ* dataset period.

8.3.9 Scatterplots of ISAS vs *in situ* SSS by latitudinal bands

In Figure 197, contour maps of the concentration of ISAS SSS (y-axis) versus Waveglider SSS (x-axis) at match-up pairs for different latitude bands: (a) 80°S-80°N, (b) 20°S-20°N, (c) 40°S-20°S and 20°N-40°N and (d) 60°S-40°S and 40°N-60°N. For each plot, the red line shows $x=y$. The black thin and dashed lines indicate a linear fit through the data cloud and the $\pm 95\%$ confidence levels, respectively. The number match-up pairs n , the slope and R^2 coefficient of the linear fit, the root mean square (RMS) and the mean bias between ISAS and *in situ* data are indicated for each latitude band in each plots.

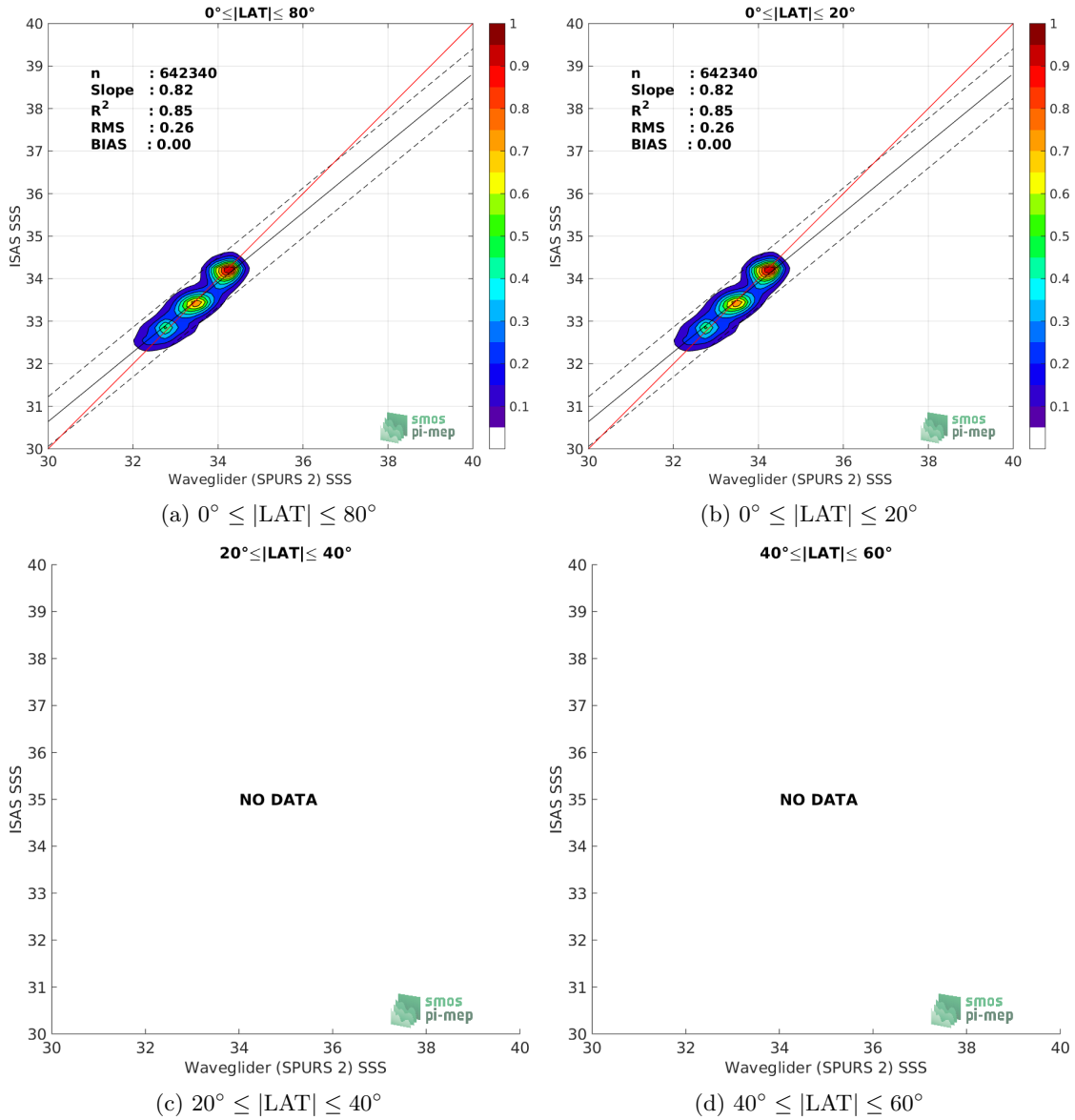


Figure 197: Contour maps of the concentration of ISAS SSS (y-axis) versus Waveglider SSS (x-axis) at match-up pairs for different latitude bands. For each plot, the red line shows $x=y$. The black thin and dashed lines indicate a linear fit through the data cloud and the $\pm 95\%$ confidence levels. The number match-up pairs n , the slope and R^2 coefficient of the linear fit, the root mean square (RMS) and the mean bias between ISAS and *in situ* data are indicated for each latitude band in each plots.

8.3.10 Time series of the monthly median and Std of the difference ΔSSS sorted by latitudinal bands

In Figure 198, time series of the monthly median (red curves) of ΔSSS (ISAS - Waveglider) and ± 1 Std (black vertical thick bars) as function of time for all the collected Pi-MEP match-up

pairs estimated for the full *in situ* dataset period are shown for different latitude bands: (a) 80°S-80°N, (b) 20°S-20°N, (c) 40°S-20°S and 20°N-40°N and (d) 60°S-40°S and 40°N-60°N.

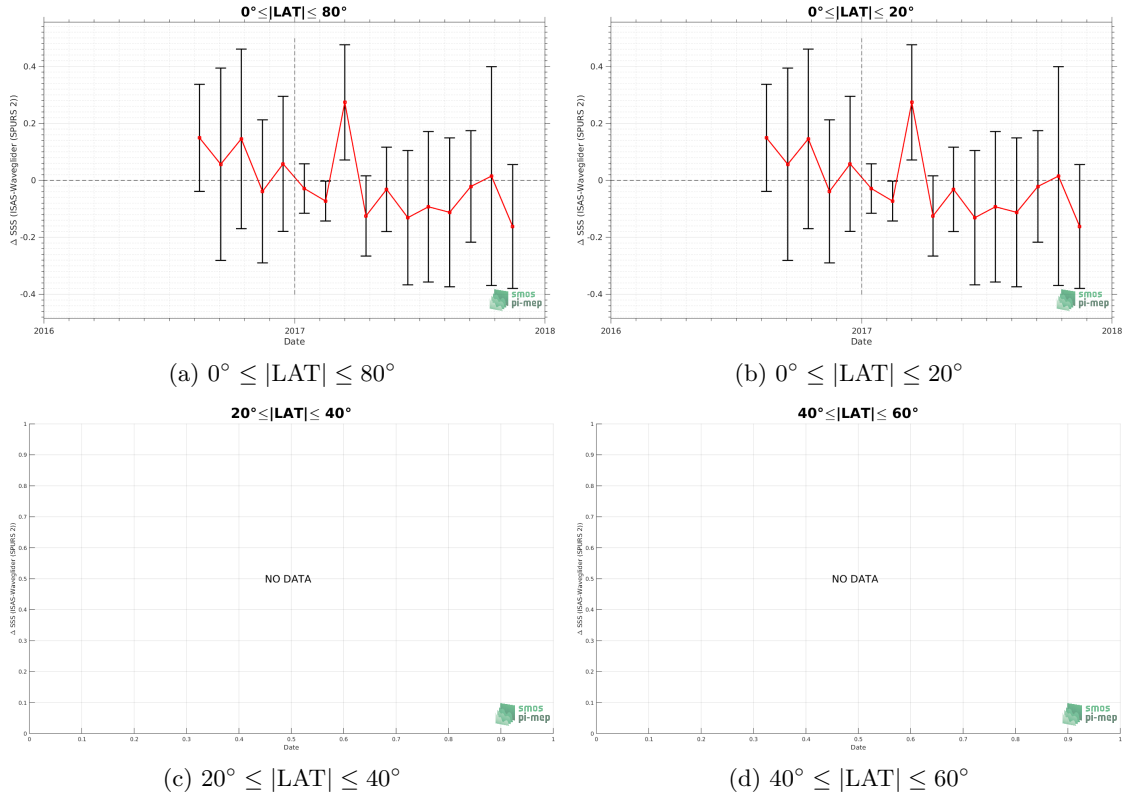


Figure 198: Monthly median (red curves) of ΔSSS (ISAS - Waveglider) and ± 1 Std (black vertical thick bars) as function of time for all the collected Pi-MEP match-up pairs for the full *in situ* dataset period are shown for different latitude bands: (a) 80°S-80°N, (b) 20°S-20°N, (c) 40°S-20°S and 20°N-40°N and (d) 60°S-40°S and 40°N-60°N.

8.3.11 ΔSSS sorted as geophysical conditions

In Figure 199, we classify the match-up differences ΔSSS (ISAS - *in situ*) as function of the geophysical conditions at match-up points. The mean and std of ΔSSS (ISAS - Waveglider) is thus evaluated as function of the

- *in situ* SSS values per bins of width 0.2,
- *in situ* SST values per bins of width 1°C,
- ASCAT daily wind values per bins of width 1 m/s,
- CMORPH 3-hourly rain rates per bins of width 1 mm/h, and,
- distance to coasts per bins of width 50 km,
- *in situ* measurement depth (if relevant).

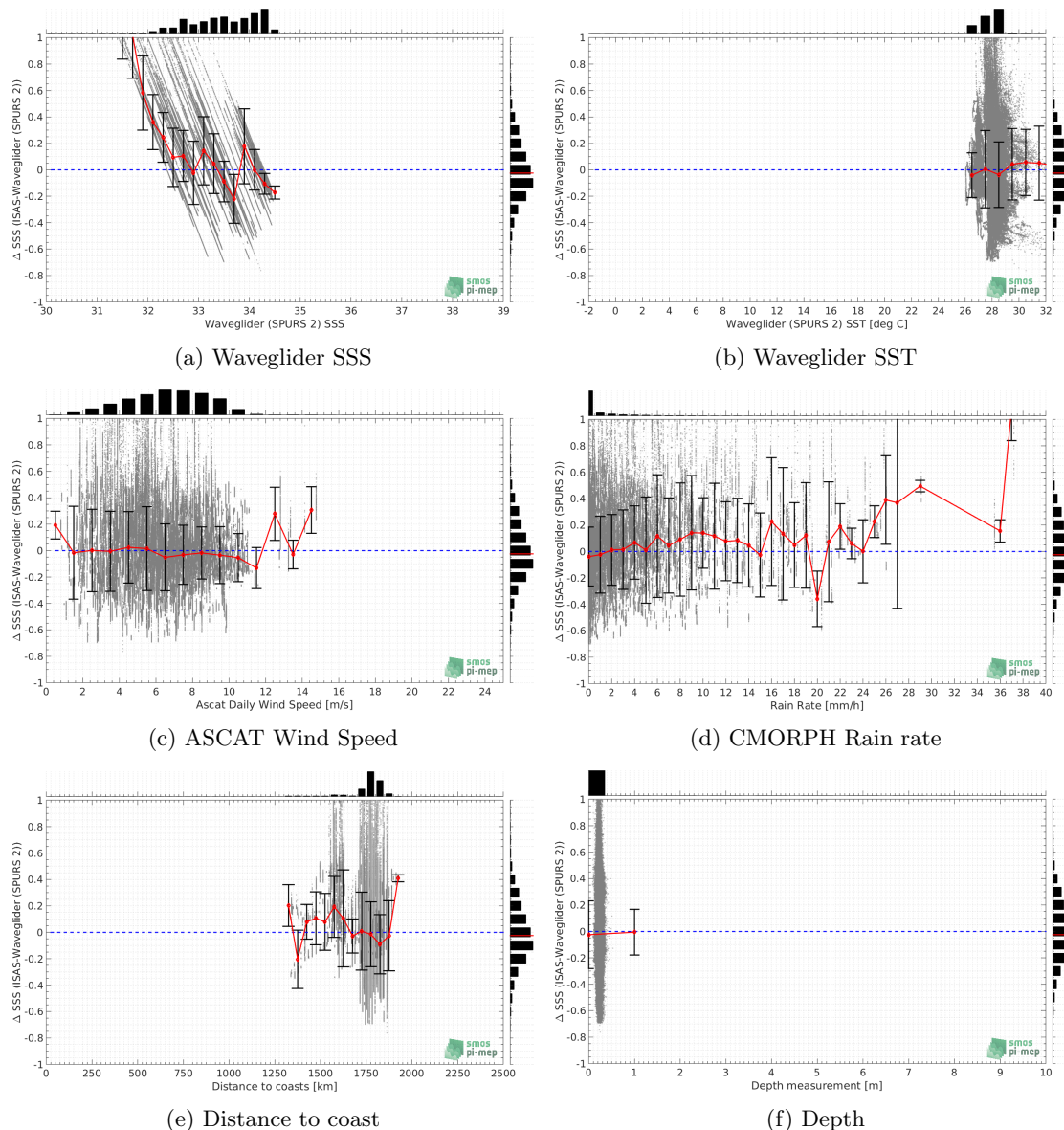


Figure 199: ΔSSS (ISAS - Waveglider) sorted as geophysical conditions: Waveglider SSS a), Waveglider SST b), ASCAT Wind speed c), CMORPH rain rate d), distance to coast (e) and depth measurements (f).

8.3.12 ΔSSS maps and statistics for different geophysical conditions

In Figures 200 and 201, we focus on sub-datasets of the match-up differences ΔSSS (ISAS - *in situ*) for the following specific geophysical conditions:

- **C1:** if the local value at *in situ* location of estimated rain rate is zero, mean daily wind is in the range [3, 12] m/s, the SST is $> 5^\circ\text{C}$ and distance to coast is > 800 km.
- **C2:** if the local value at *in situ* location of estimated rain rate is zero, mean daily wind is

in the range [3, 12] m/s.

- **C3:** if the local value at *in situ* location of estimated rain rate is high (ie. > 1 mm/h) and mean daily wind is low (ie. < 4 m/s).
- **C5:** if the *in situ* data is located where the climatological SSS standard deviation is low (ie. above < 0.2).
- **C6:** if the *in situ* data is located where the climatological SSS standard deviation is high (ie. above > 0.2).

For each of these conditions, the temporal mean (gridded over spatial boxes of size $1^\circ \times 1^\circ$) and the histogram of the difference ΔSSS (ISAS - *in situ*) are presented.

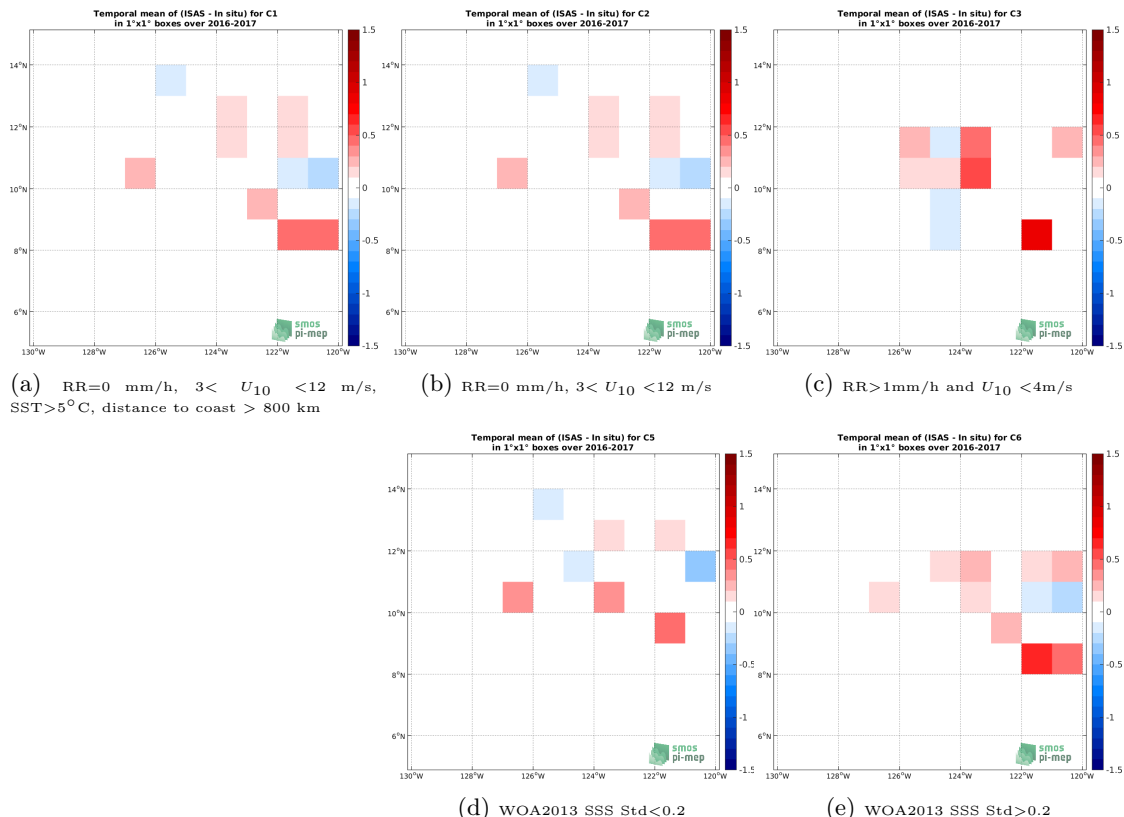


Figure 200: Temporal mean gridded over spatial boxes of size $1^\circ \times 1^\circ$ of ΔSSS (ISAS - Waveglider) for 5 different subdatasets corresponding to: RR=0 mm/h, $3 < U_{10} < 12$ m/s, SST > 5°C, distance to coast > 800 km (a), RR=0 mm/h, $3 < U_{10} < 12$ m/s (b), RR > 1 mm/h and $U_{10} < 4$ m/s (c), WOA2013 SSS Std < 0.2 (d), WOA2013 SSS Std > 0.2 (e).

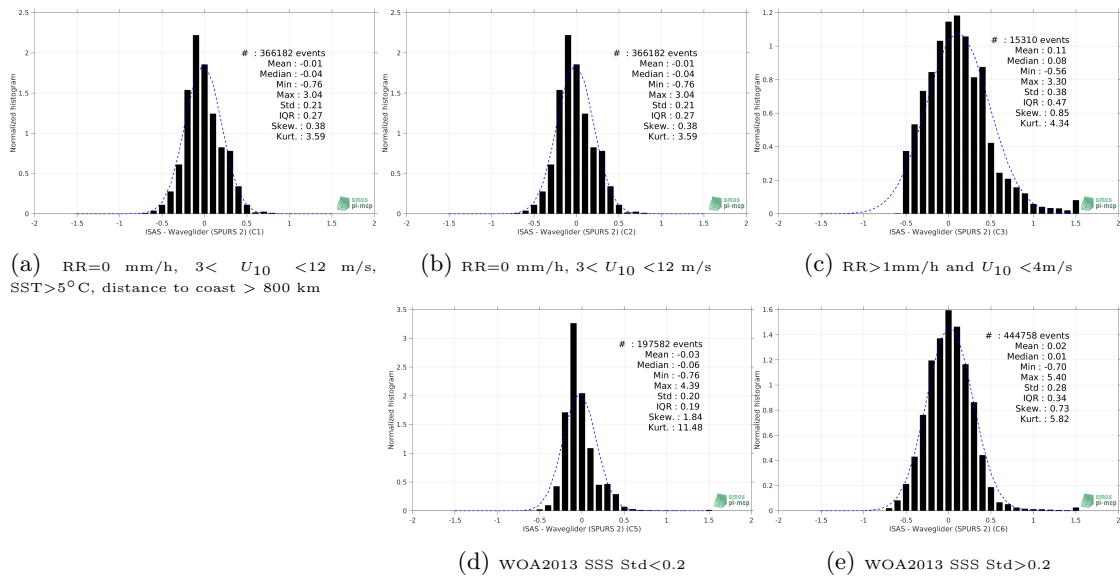


Figure 201: Normalized histogram of ΔSSS (ISAS - Waveglider) for 5 different subdatasets corresponding to: RR=0 mm/h, $3 < U_{10} < 12 \text{ m/s}$, SST > 5°C, distance to coast > 800 km (a), RR=0 mm/h, $3 < U_{10} < 12 \text{ m/s}$ (b), RR > 1 mm/h and $U_{10} < 4 \text{ m/s}$ (c), WOA2013 SSS Std < 0.2 (d), WOA2013 SSS Std > 0.2 (e).

8.3.13 Summary

Table 1 shows the mean, median, standard deviation (Std), root mean square (RMS), interquartile range (IQR), correlation coefficient (r^2) and robust standard deviation (Std*) of the match-up differences ΔSSS (ISAS - Waveglider) for the following conditions:

- all: All the match-up pairs satellite/in situ SSS values are used to derive the statistics
- C1: only pairs where RR=0 mm/h, $3 < U_{10} < 12 \text{ m/s}$, SST > 5°C, distance to coast > 800 km
- C2: only pairs where RR=0 mm/h, $3 < U_{10} < 12 \text{ m/s}$
- C3: only pairs where RR > 1 mm/h and $U_{10} < 4 \text{ m/s}$
- C5: only pairs where WOA2013 SSS Std < 0.2
- C6: only pairs where WOA2013 SSS Std > 0.2
- C7a: only pairs with a distance to coast < 150 km.
- C7b: only pairs with a distance to coast in the range [150, 800] km.
- C7c: only pairs with a distance to coast > 800 km.
- C8a: only pairs where SST is < 5°C.
- C8b: only pairs where SST is in the range [5, 15]°C.
- C8c: only pairs where SST is > 15°C.

- C9a: only pairs where SSS is < 33.
- C9b: only pairs where SSS is in the range [33, 37].
- C9c: only pairs where SSS is > 37.

Table 1: Statistics of Δ SSS (ISAS - Waveglider)

Condition	#	Median	Mean	Std	RMS	IQR	r^2	Std*
all	642340	-0.02	0.00	0.26	0.26	0.30	0.850	0.21
C1	366182	-0.04	-0.01	0.21	0.21	0.27	0.883	0.19
C2	366182	-0.04	-0.01	0.21	0.21	0.27	0.883	0.19
C3	15310	0.08	0.11	0.38	0.40	0.47	0.605	0.35
C5	197582	-0.06	-0.03	0.20	0.20	0.19	0.854	0.13
C6	444758	0.01	0.02	0.28	0.28	0.34	0.809	0.26
C7a	0	NaN	NaN	NaN	NaN	NaN	NaN	NaN
C7b	0	NaN	NaN	NaN	NaN	NaN	NaN	NaN
C7c	642340	-0.02	0.00	0.26	0.26	0.30	0.850	0.21
C8a	0	NaN	NaN	NaN	NaN	NaN	NaN	NaN
C8b	0	NaN	NaN	NaN	NaN	NaN	NaN	NaN
C8c	642340	-0.02	0.00	0.26	0.26	0.30	0.850	0.21
C9a	158669	0.14	0.17	0.31	0.36	0.32	0.144	0.24
C9b	483671	-0.07	-0.05	0.21	0.21	0.25	0.789	0.18
C9c	0	NaN	NaN	NaN	NaN	NaN	NaN	NaN

Table 1 numerical values can be downloaded as a csv file [here](#).

8.4 Seaglider

8.4.1 Introduction

The Seaglider is an autonomous profiler measuring salinity and temperature. A total of five Seagliders (<https://doi.org/10.5067/SPUR2-GLID1>) were deployed over the two SPURS2 cruises. Three Seagliders were deployed on the first Revelle cruise in August 2016, recovered by the Lady Amber after 7 months and redeployed, to be retrieved finally during the second cruise in November 2017. One of the Seagliders was deployed alongside and tracked the Lagrangian array across the study region, diving to depths of 1000m. Focused around a central mooring located near 10°N,125°W, the objective of SPURS-2 (NASA-funded oceanographic process study) was to study the dynamics of the rainfall-dominated surface ocean at the western edge of the eastern Pacific fresh pool subject to high seasonal variability and strong zonal flows associated with the North Equatorial Current and Countercurrent.

8.4.2 Number of SSS data as a function of time and distance to coast

Figure 202 shows the time (a) and distance to coast (b) distributions of the Seaglider *in situ* dataset.

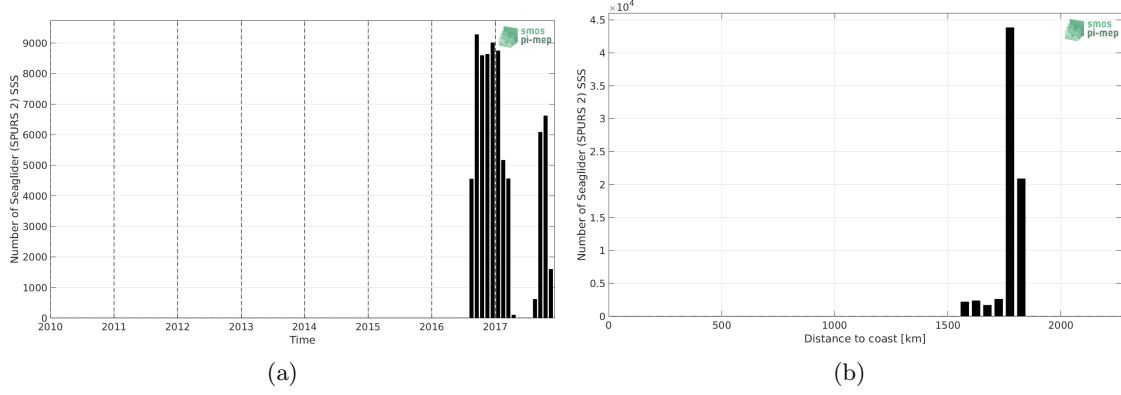


Figure 202: Number of SSS from Seaglider as a function of time (a) and distance to coast (b).

8.4.3 Histograms of SSS

Figure 203 shows the SSS distribution of the Seaglider (a) and colocalized ISAS (b) dataset.

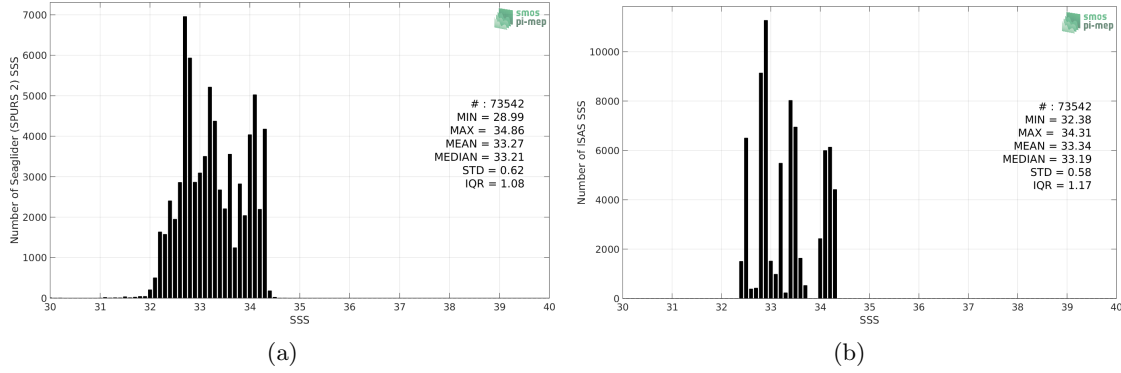


Figure 203: Histograms of SSS from Seaglider (a) and ISAS (b) per bins of 0.1.

8.4.4 Distribution of *in situ* SSS depth measurements

In Figure 204, we show the depth distribution of the *in situ* salinity dataset (a) and the spatial distribution of the depth temporal mean in $1^\circ \times 1^\circ$ boxes and considering the full *in situ* dataset period (b).

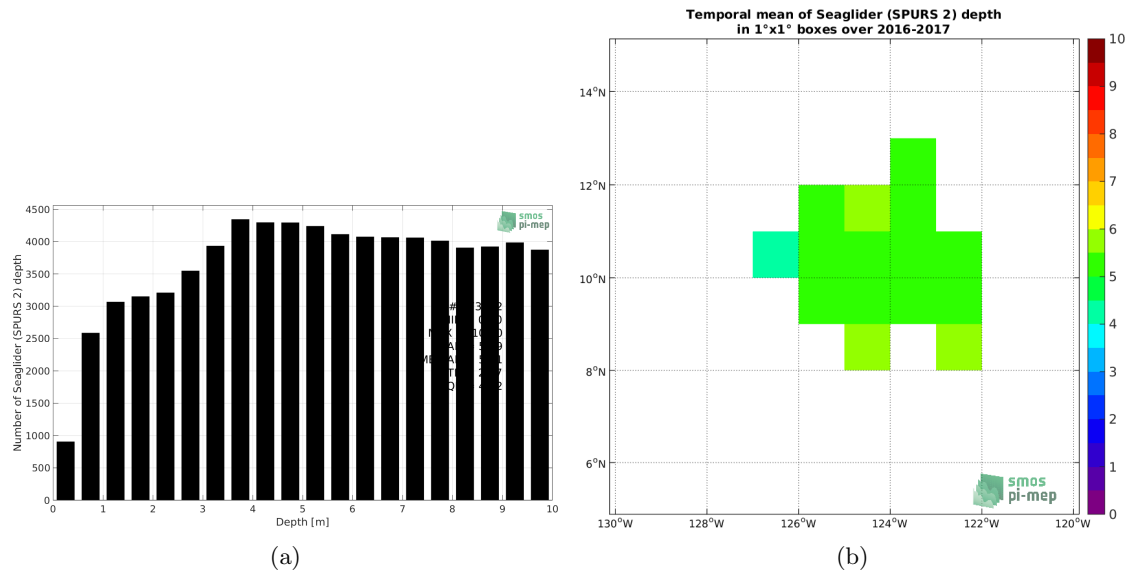
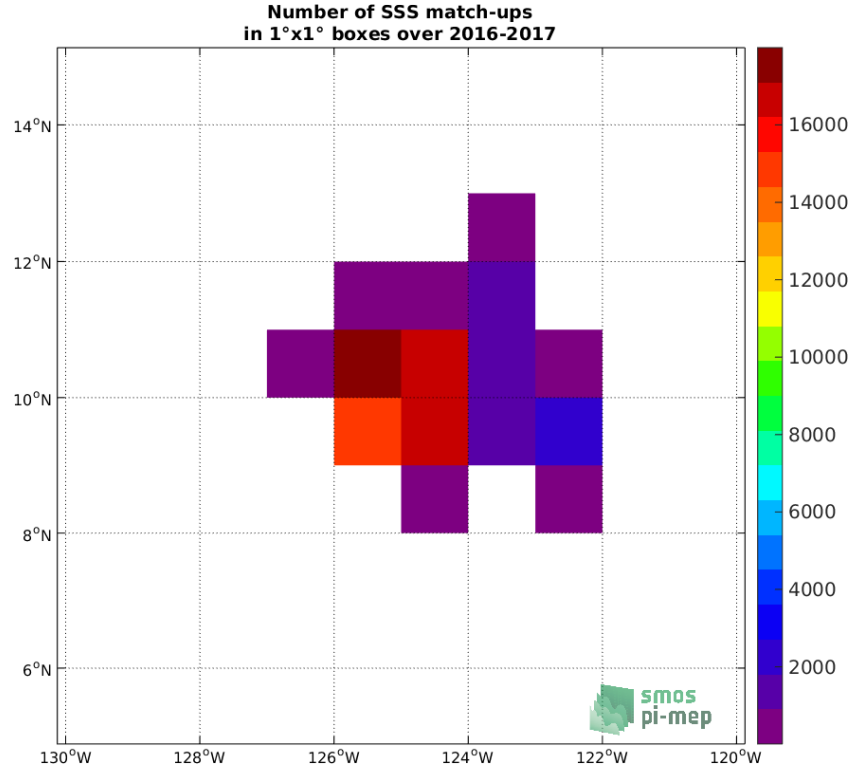


Figure 204: Depth distribution of the upper level SSS measurements from Seaglider (a) and spatial distribution of the *in situ* SSS depth measurements showing the mean value in $1^{\circ} \times 1^{\circ}$ boxes and considering the full *in situ* dataset period (b).

8.4.5 Spatial distribution of SSS

In Figure 205, the number of Seaglider SSS measurements in $1^{\circ} \times 1^{\circ}$ boxes is shown.


 Figure 205: Number of SSS from Seaglider in $1^{\circ} \times 1^{\circ}$ boxes.

8.4.6 Spatial Maps of the Temporal mean and Std of *in situ* and ISAS SSS and of the difference (Δ SSS)

In Figure 206, maps of temporal mean (left) and standard deviation (right) of ISAS (top), Seaglider *in situ* dataset (middle) and the difference Δ SSS (ISAS - Seaglider) (bottom) are shown. The temporal mean and std are calculated using all match-up pairs falling in spatial boxes of size $1^{\circ} \times 1^{\circ}$ over the full Seaglider dataset period.

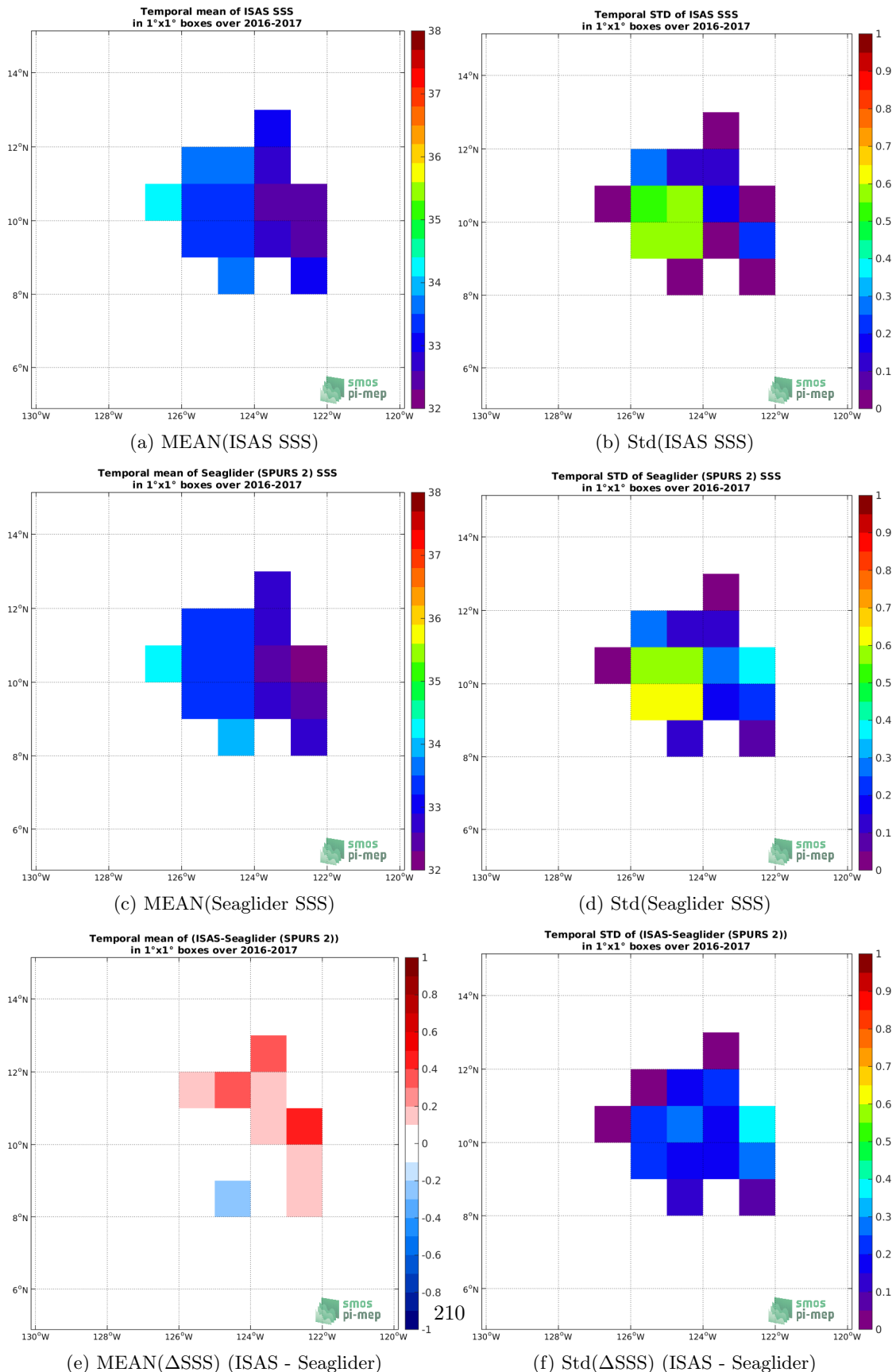


Figure 206: Temporal mean (left) and Std (right) of SSS from ISAS (top), Seaglider (middle), and of Δ SSS (ISAS - Seaglider). Only match-up pairs are used to generate these maps.

8.4.7 Time series of the monthly median and Std of *in situ* and ISAS SSS and of the difference (Δ SSS)

In the top panel of Figure 207, we show the time series of the monthly median SSS estimated for both ISAS SSS product (in black) and the Seaglider *in situ* dataset (in blue) at the collected Pi-MEP match-up pairs.

In the middle panel of Figure 207, we show the time series of the monthly median of Δ SSS (ISAS - Seaglider) for the collected Pi-MEP match-up pairs.

In the bottom panel of Figure 207, we show the time series of the monthly standard deviation of the Δ SSS (ISAS - Seaglider) for the collected Pi-MEP match-up pairs.

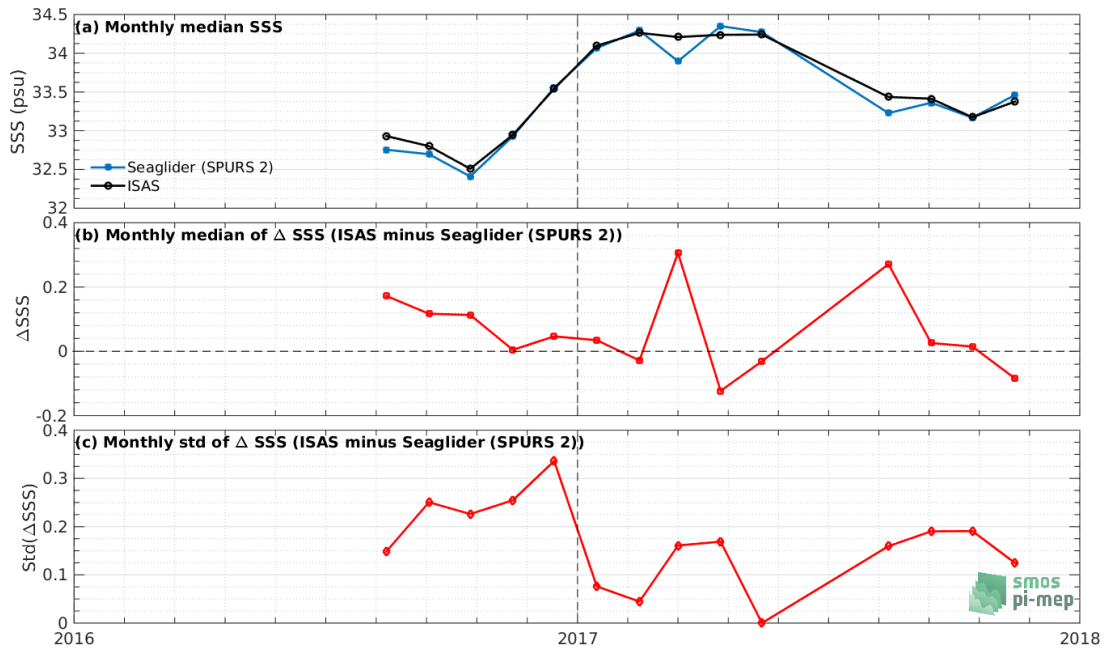


Figure 207: Time series of the monthly median SSS (top), median of Δ SSS (ISAS - Seaglider) and Std of Δ SSS (ISAS - Seaglider) considering all match-ups collected by the Pi-MEP.

8.4.8 Zonal mean and Std of *in situ* and ISAS SSS and of the difference Δ SSS

In Figure 208 left panel, we show the zonal mean SSS considering all Pi-MEP match-up pairs for both ISAS SSS product (in black) and the Seaglider *in situ* dataset (in blue). The full *in situ* dataset period is used to derive the mean.

In the right panel of Figure 208, we show the zonal mean of Δ SSS (ISAS - Seaglider) for all the collected Pi-MEP match-up pairs estimated over the full *in situ* dataset period.

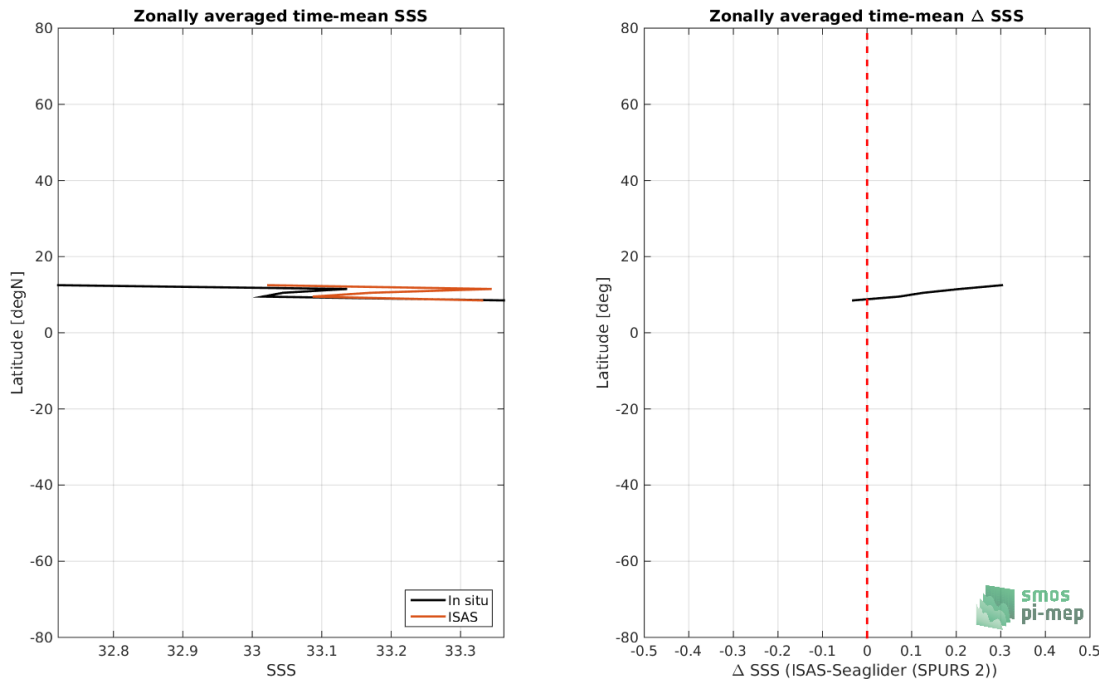


Figure 208: Left panel: Zonal mean SSS from ISAS product (black) and from Seaglider (blue). Right panel: Zonal mean of Δ SSS (ISAS - Seaglider) for all the collected Pi-MEP match-up pairs estimated over the full *in situ* dataset period.

8.4.9 Scatterplots of ISAS vs *in situ* SSS by latitudinal bands

In Figure 209, contour maps of the concentration of ISAS SSS (y-axis) versus Seaglider SSS (x-axis) at match-up pairs for different latitude bands: (a) 80°S-80°N, (b) 20°S-20°N, (c) 40°S-20°S and 20°N-40°N and (d) 60°S-40°S and 40°N-60°N. For each plot, the red line shows $x=y$. The black thin and dashed lines indicate a linear fit through the data cloud and the $\pm 95\%$ confidence levels, respectively. The number match-up pairs n , the slope and R^2 coefficient of the linear fit, the root mean square (RMS) and the mean bias between ISAS and *in situ* data are indicated for each latitude band in each plots.

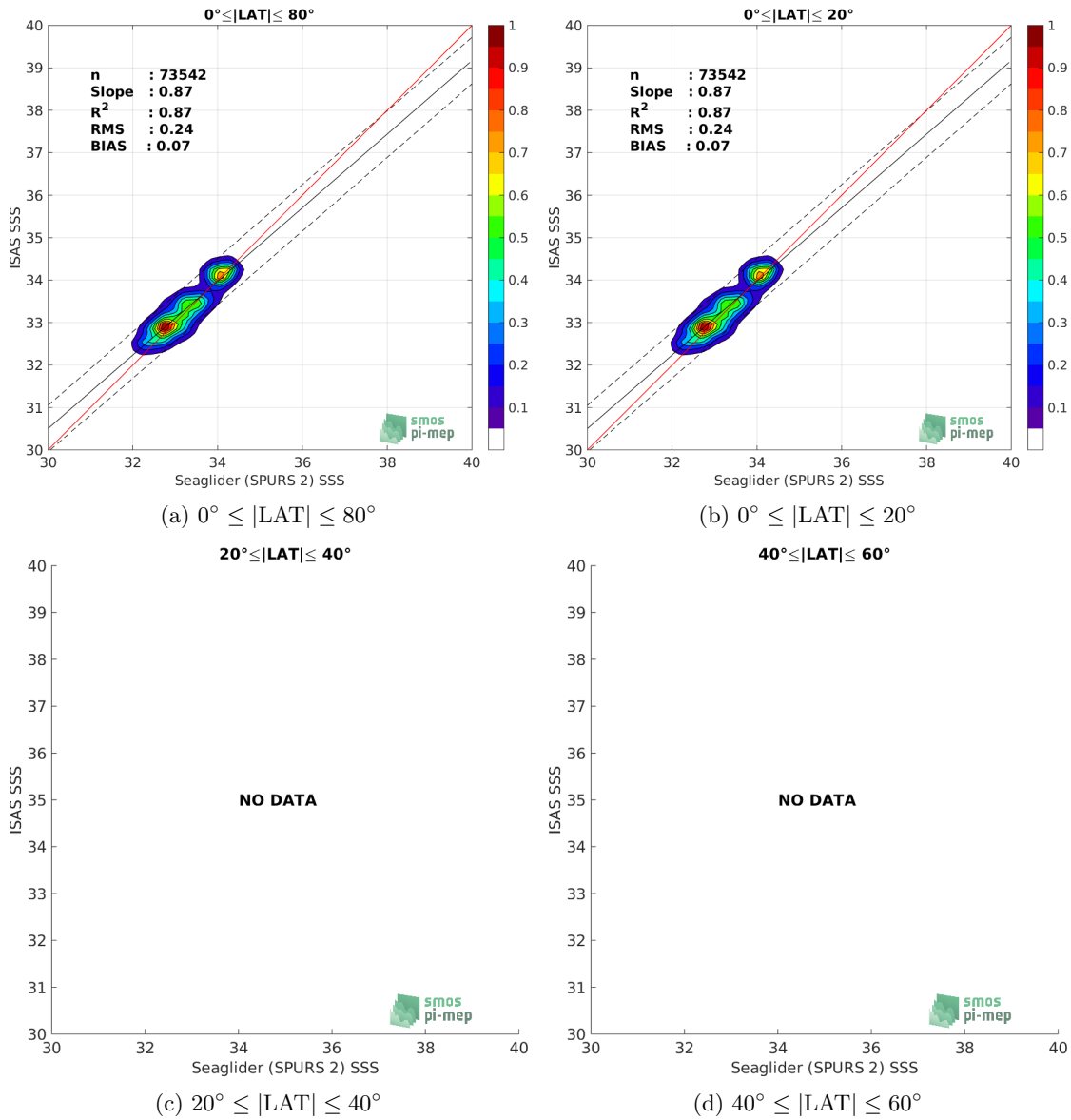


Figure 209: Contour maps of the concentration of ISAS SSS (y-axis) versus Seaglider SSS (x-axis) at match-up pairs for different latitude bands. For each plot, the red line shows $x=y$. The black thin and dashed lines indicate a linear fit through the data cloud and the $\pm 95\%$ confidence levels. The number match-up pairs n , the slope and R^2 coefficient of the linear fit, the root mean square (RMS) and the mean bias between ISAS and *in situ* data are indicated for each latitude band in each plots.

8.4.10 Time series of the monthly median and Std of the difference ΔSSS sorted by latitudinal bands

In Figure 210, time series of the monthly median (red curves) of ΔSSS (ISAS - Seaglider) and ± 1 Std (black vertical thick bars) as function of time for all the collected Pi-MEP match-up

pairs estimated for the full *in situ* dataset period are shown for different latitude bands: (a) 80°S - 80°N , (b) 20°S - 20°N , (c) 40°S - 20°S and 20°N - 40°N and (d) 60°S - 40°S and 40°N - 60°N .

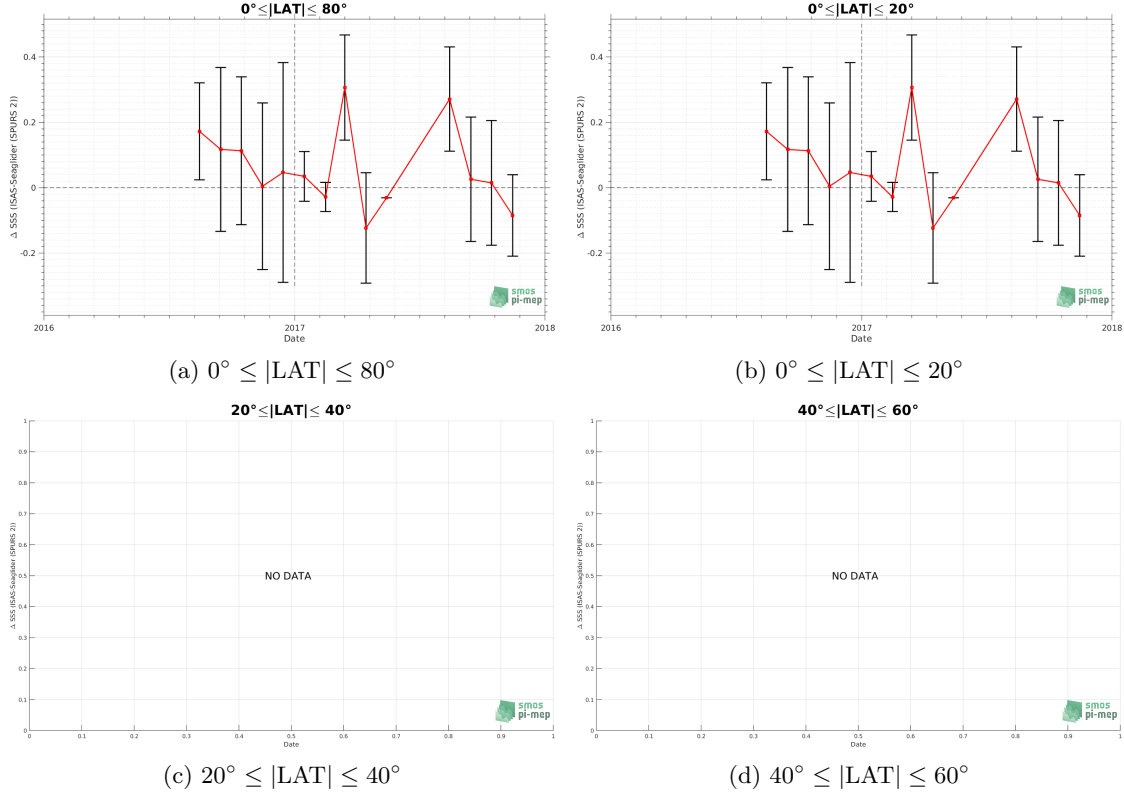


Figure 210: Monthly median (red curves) of ΔSSS (ISAS - Seaglider) and ± 1 Std (black vertical thick bars) as function of time for all the collected Pi-MEP match-up pairs for the full *in situ* dataset period are shown for different latitude bands: (a) 80°S - 80°N , (b) 20°S - 20°N , (c) 40°S - 20°S and 20°N - 40°N and (d) 60°S - 40°S and 40°N - 60°N .

8.4.11 ΔSSS sorted as geophysical conditions

In Figure 211, we classify the match-up differences ΔSSS (ISAS - *in situ*) as function of the geophysical conditions at match-up points. The mean and std of ΔSSS (ISAS - Seaglider) is thus evaluated as function of the

- *in situ* SSS values per bins of width 0.2,
- *in situ* SST values per bins of width 1°C ,
- ASCAT daily wind values per bins of width 1 m/s,
- CMORPH 3-hourly rain rates per bins of width 1 mm/h, and,
- distance to coasts per bins of width 50 km,
- *in situ* measurement depth (if relevant).

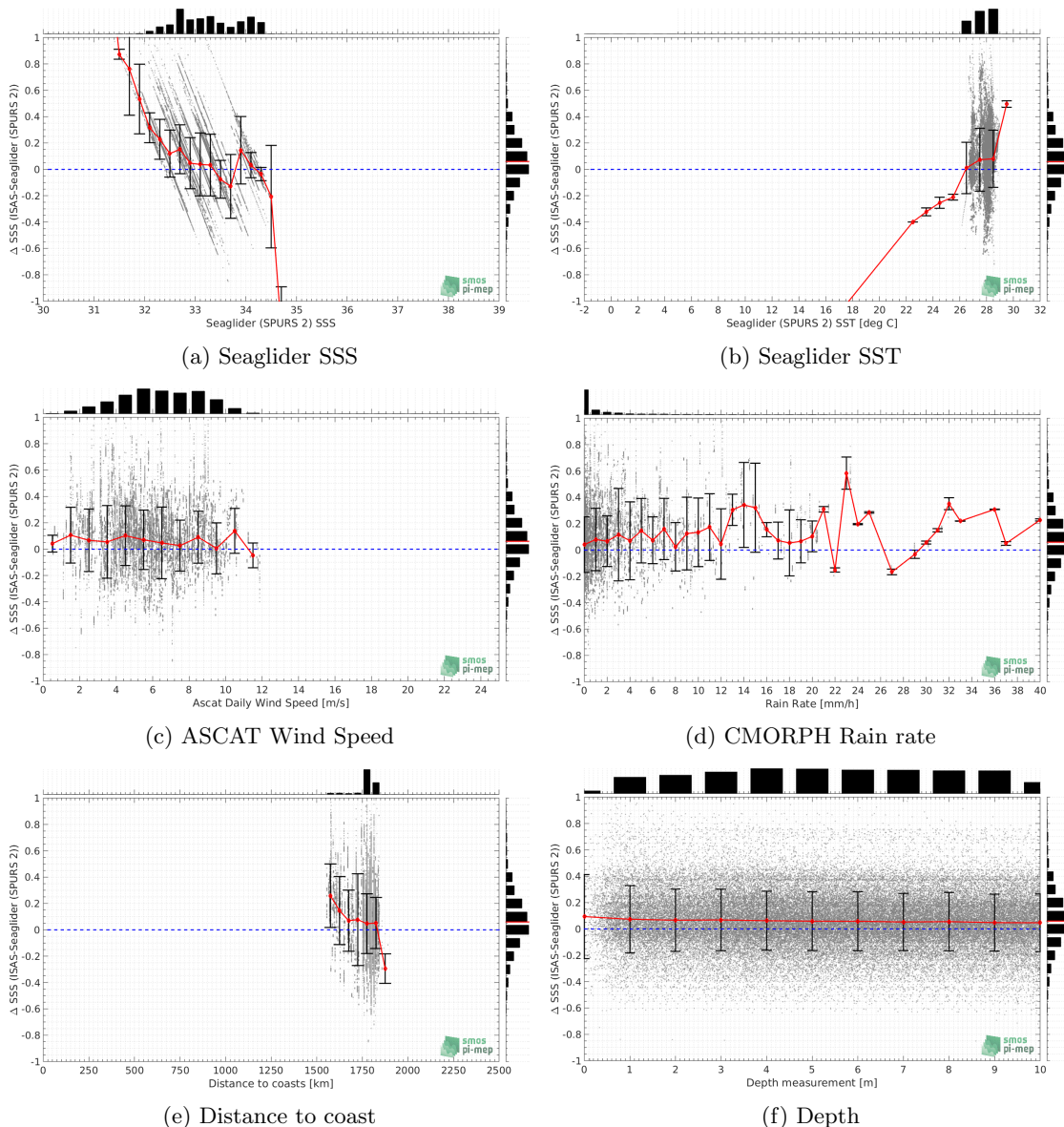


Figure 211: Δ SSS (ISAS - Seaglider) sorted as geophysical conditions: Seaglider SSS a), Seaglider SST b), ASCAT Wind speed c), CMORPH rain rate d), distance to coast (e) and depth measurements (f).

8.4.12 Δ SSS maps and statistics for different geophysical conditions

In Figures 212 and 213, we focus on sub-datasets of the match-up differences Δ SSS (*ISAS - in situ*) for the following specific geophysical conditions:

- **C1:** if the local value at *in situ* location of estimated rain rate is zero, mean daily wind is in the range [3, 12] m/s, the SST is $> 5^{\circ}\text{C}$ and distance to coast is > 800 km.
- **C2:** if the local value at *in situ* location of estimated rain rate is zero, mean daily wind is

in the range [3, 12] m/s.

- **C3:** if the local value at *in situ* location of estimated rain rate is high (ie. > 1 mm/h) and mean daily wind is low (ie. < 4 m/s).
- **C5:** if the *in situ* data is located where the climatological SSS standard deviation is low (ie. above < 0.2).
- **C6:** if the *in situ* data is located where the climatological SSS standard deviation is high (ie. above > 0.2).

For each of these conditions, the temporal mean (gridded over spatial boxes of size $1^\circ \times 1^\circ$) and the histogram of the difference ΔSSS (ISAS - *in situ*) are presented.

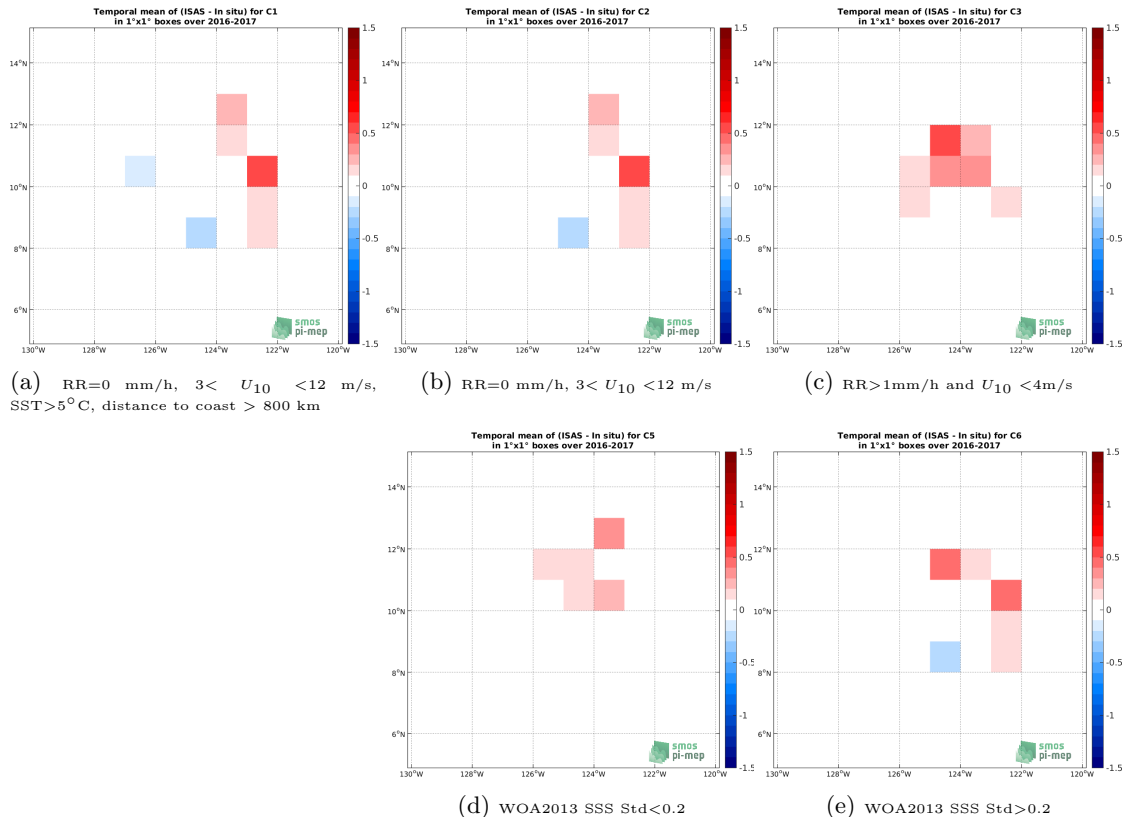


Figure 212: Temporal mean gridded over spatial boxes of size $1^\circ \times 1^\circ$ of ΔSSS (ISAS - Seaglider) for 5 different subdatasets corresponding to: RR=0 mm/h, $3 < U_{10} < 12$ m/s, SST $>5^\circ\text{C}$, distance to coast > 800 km (a), RR=0 mm/h, $3 < U_{10} < 12$ m/s (b), RR>1mm/h and $U_{10} < 4$ m/s (c), WOA2013 SSS Std<0.2 (d), WOA2013 SSS Std>0.2 (e).

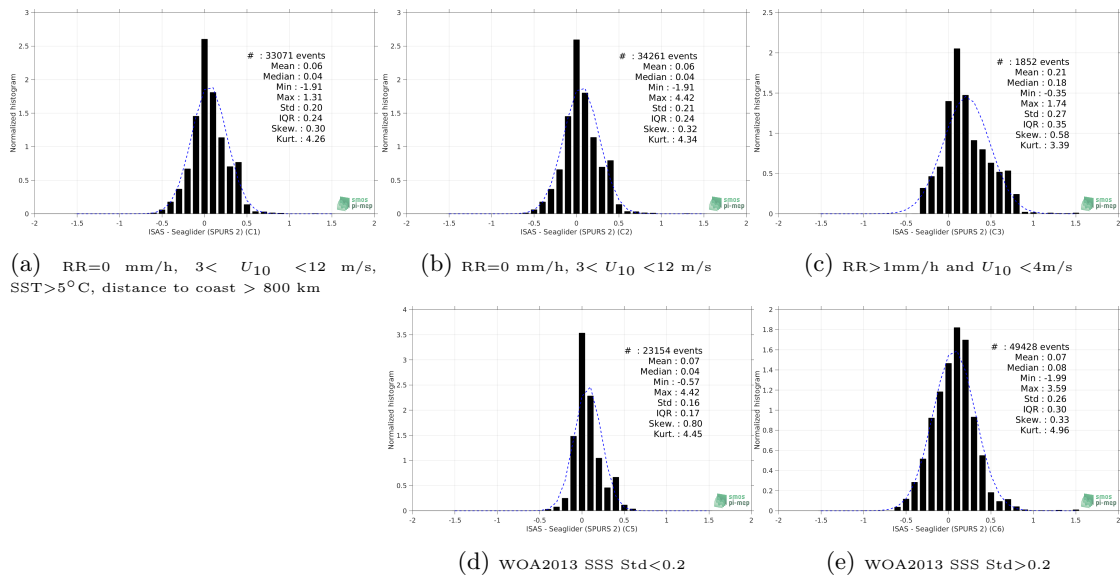


Figure 213: Normalized histogram of ΔSSS (ISAS - Seaglider) for 5 different subdatasets corresponding to: $RR=0 \text{ mm/h}$, $3 < U_{10} < 12 \text{ m/s}$, $SST > 5^\circ\text{C}$, distance to coast $> 800 \text{ km}$ (a), $RR=0 \text{ mm/h}$, $3 < U_{10} < 12 \text{ m/s}$ (b), $RR > 1 \text{ mm/h}$ and $U_{10} < 4 \text{ m/s}$ (c), WOA2013 SSS Std < 0.2 (d), WOA2013 SSS Std > 0.2 (e).

8.4.13 Summary

Table 1 shows the mean, median, standard deviation (Std), root mean square (RMS), interquartile range (IQR), correlation coefficient (r^2) and robust standard deviation (Std*) of the match-up differences ΔSSS (ISAS - Seaglider) for the following conditions:

- all: All the match-up pairs satellite/in situ SSS values are used to derive the statistics
- C1: only pairs where $RR=0 \text{ mm/h}$, $3 < U_{10} < 12 \text{ m/s}$, $SST > 5^\circ\text{C}$, distance to coast $> 800 \text{ km}$
- C2: only pairs where $RR=0 \text{ mm/h}$, $3 < U_{10} < 12 \text{ m/s}$
- C3: only pairs where $RR > 1 \text{ mm/h}$ and $U_{10} < 4 \text{ m/s}$
- C5: only pairs where WOA2013 SSS Std < 0.2
- C6: only pairs where WOA2013 SSS Std > 0.2
- C7a: only pairs with a distance to coast $< 150 \text{ km}$.
- C7b: only pairs with a distance to coast in the range $[150, 800] \text{ km}$.
- C7c: only pairs with a distance to coast $> 800 \text{ km}$.
- C8a: only pairs where SST is $< 5^\circ\text{C}$.
- C8b: only pairs where SST is in the range $[5, 15]^\circ\text{C}$.
- C8c: only pairs where SST is $> 15^\circ\text{C}$.

- C9a: only pairs where SSS is < 33.
- C9b: only pairs where SSS is in the range [33, 37].
- C9c: only pairs where SSS is > 37.

Table 1: Statistics of ΔSSS (ISAS - Seaglider)

Condition	#	Median	Mean	Std	RMS	IQR	r^2	Std*
all	73542	0.06	0.07	0.23	0.24	0.25	0.865	0.19
C1	33071	0.04	0.06	0.20	0.21	0.24	0.903	0.17
C2	34261	0.04	0.06	0.21	0.22	0.24	0.900	0.17
C3	1852	0.18	0.21	0.27	0.35	0.35	0.504	0.26
C5	23154	0.04	0.07	0.16	0.17	0.17	0.947	0.12
C6	49428	0.08	0.07	0.26	0.26	0.30	0.747	0.23
C7a	0	NaN	NaN	NaN	NaN	NaN	NaN	NaN
C7b	0	NaN	NaN	NaN	NaN	NaN	NaN	NaN
C7c	73542	0.06	0.07	0.23	0.24	0.25	0.865	0.19
C8a	0	NaN	NaN	NaN	NaN	NaN	NaN	NaN
C8b	3	-1.97	-1.96	0.04	1.96	0.04	0.977	0.02
C8c	70905	0.06	0.07	0.22	0.23	0.25	0.871	0.19
C9a	28790	0.15	0.16	0.23	0.28	0.20	0.326	0.15
C9b	44752	0.00	0.01	0.21	0.21	0.22	0.801	0.17
C9c	0	NaN	NaN	NaN	NaN	NaN	NaN	NaN

Table 1 numerical values can be downloaded as a csv file [here](#).

9 EUREC4A

9.1 Introduction

The field campaign, **EUREC⁴A**, is an international initiative in support of the World Climate Research Programme's Grand Science Challenge on Clouds, Circulation and Climate Sensitivity ([Bony et al. \(2017\)](#)). EUREC⁴A took place between January and March 2020 with operations based out of Barbados. The EUREC⁴A Pi-MEP in situ dataset is composed of upper ocean salinity and temperature measurements recorded between 0 m and 10 m depth coming from the following platforms:

- 4 research vessels: R/V L'Atalante, R/V Maria S. Merian, R/V Meteor and R/V Ron Brown,
- 3 Autonomous Saildrone vehicles (<https://www.saildrone.com/>),
- 4 ocean gliders,
- 24 Argo floats (around 470 profiles),
- 9 SVP drifters provided by NOAA/AOML under the ATOMIC program.

All the data are freely available [here](#).

9.2 Number of SSS data as a function of time and distance to coast

Figure 214 shows the time (a) and distance to coast (b) distributions of the EUREC4A *in situ* dataset.

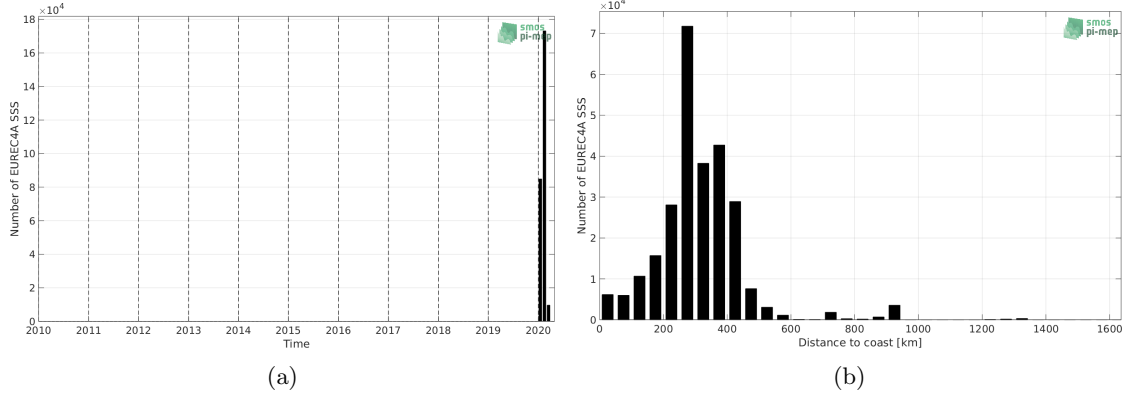


Figure 214: Number of SSS from EUREC4A as a function of time (a) and distance to coast (b).

9.3 Histograms of SSS

Figure 215 shows the SSS distribution of the EUREC4A (a) and colocalized ISAS (b) dataset.

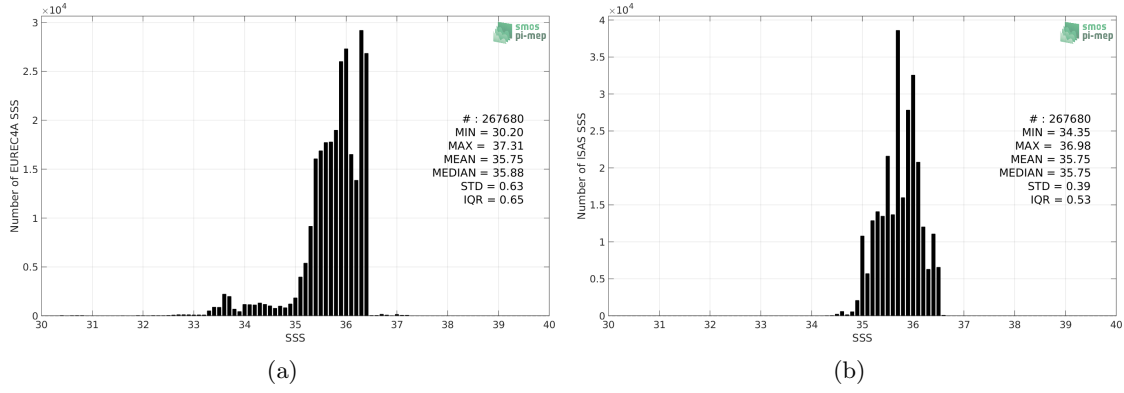


Figure 215: Histograms of SSS from EUREC4A (a) and ISAS (b) per bins of 0.1.

9.4 Distribution of *in situ* SSS depth measurements

In Figure 216, we show the depth distribution of the *in situ* salinity dataset (a) and the spatial distribution of the depth temporal mean in $1^\circ \times 1^\circ$ boxes and considering the full *in situ* dataset period (b).

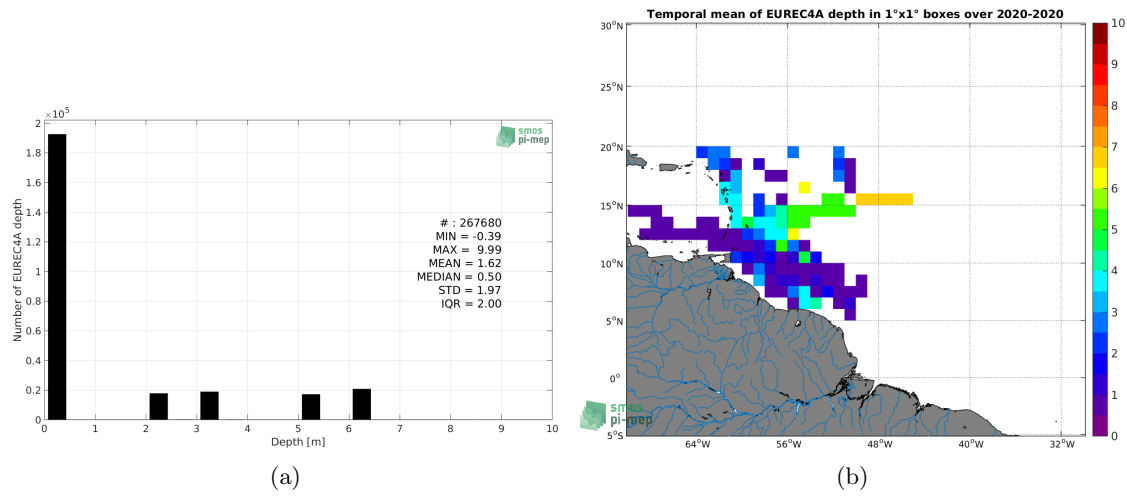


Figure 216: Depth distribution of the upper level SSS measurements from EUREC4A (a) and spatial distribution of the *in situ* SSS depth measurements showing the mean value in 1°x1° boxes and considering the full *in situ* dataset period (b).

9.5 Spatial distribution of SSS

In Figure 217, the number of EUREC4A SSS measurements in 1°x1° boxes is shown.

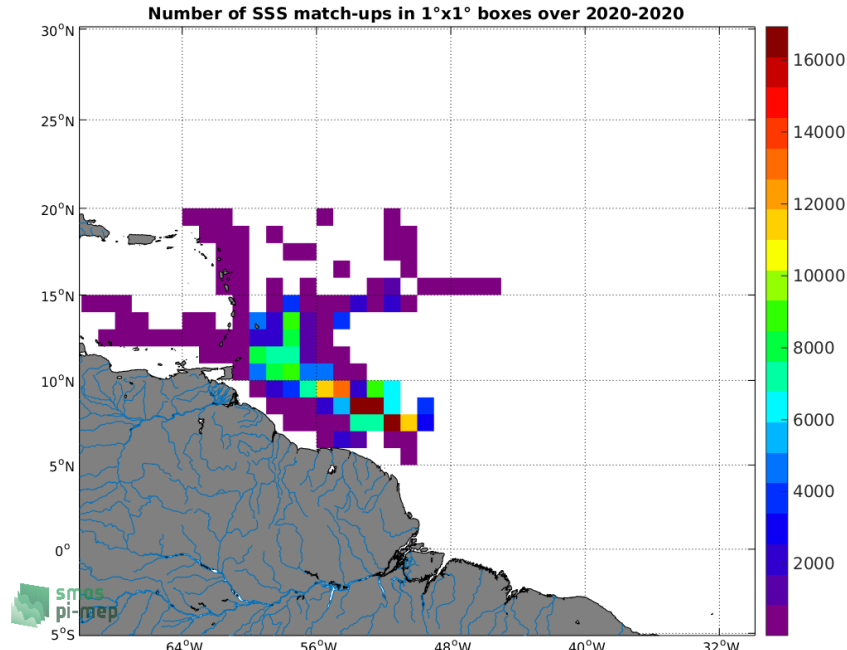


Figure 217: Number of SSS from EUREC4A in 1°x1° boxes.

9.6 Spatial Maps of the Temporal mean and Std of *in situ* and ISAS SSS and of the difference (Δ SSS)

In Figure 218, maps of temporal mean (left) and standard deviation (right) of ISAS (top), EUREC4A *in situ* dataset (middle) and the difference Δ SSS(ISAS -EUREC4A) (bottom) are shown. The temporal mean and std are calculated using all match-up pairs falling in spatial boxes of size $1^\circ \times 1^\circ$ over the full EUREC4A dataset period.

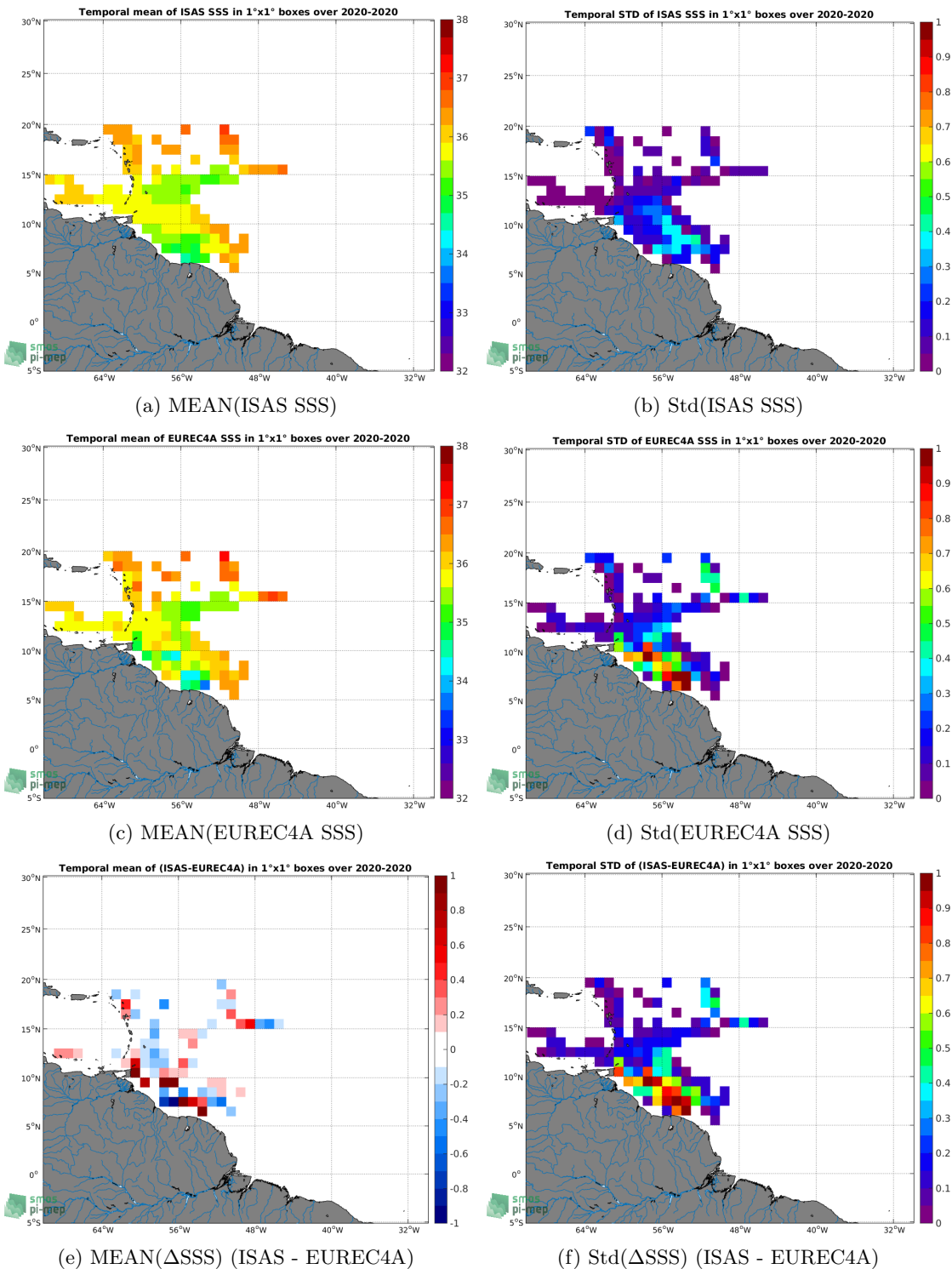


Figure 218: Temporal mean (left) and Std (right) of SSS from ISAS (top), EUREC4A (middle), and of Δ SSS (ISAS - EUREC4A). Only match-up pairs are used to generate these maps.

9.7 Time series of the monthly median and Std of *in situ* and ISAS SSS and of the difference (Δ SSS)

In the top panel of Figure 219, we show the time series of the monthly median SSS estimated for both ISAS SSS product (in black) and the EUREC4A *in situ* dataset (in blue) at the collected Pi-MEP match-up pairs.

In the middle panel of Figure 219, we show the time series of the monthly median of Δ SSS (ISAS - EUREC4A) for the collected Pi-MEP match-up pairs.

In the bottom panel of Figure 219, we show the time series of the monthly standard deviation of the Δ SSS (ISAS - EUREC4A) for the collected Pi-MEP match-up pairs.

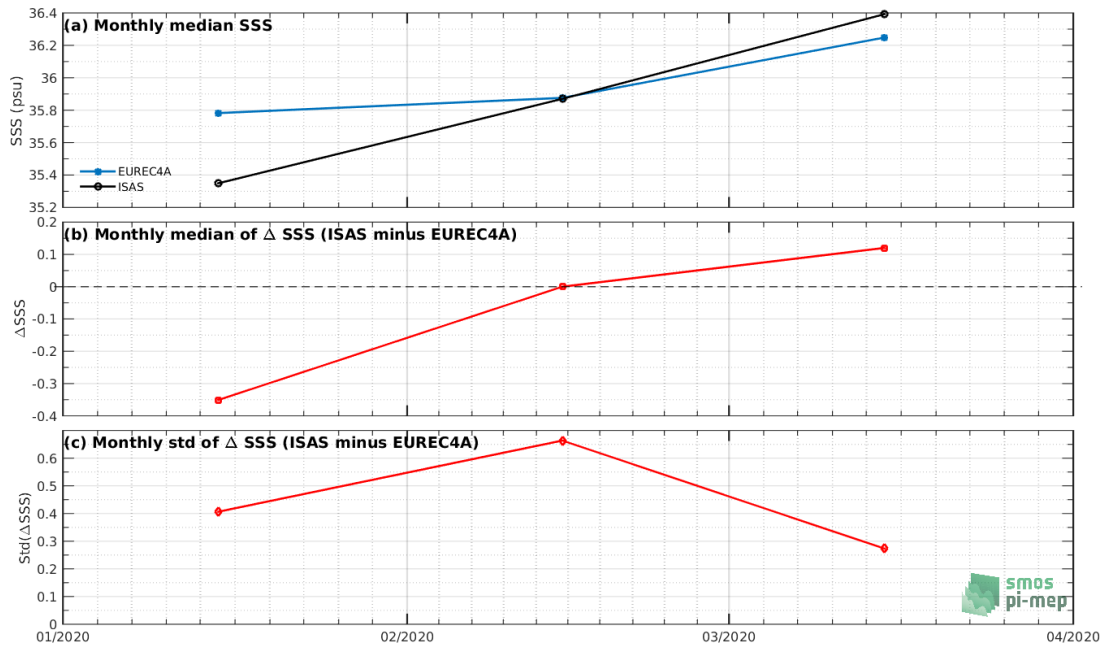


Figure 219: Time series of the monthly median SSS (top), median of Δ SSS (ISAS - EUREC4A) and Std of Δ SSS (ISAS - EUREC4A) considering all match-ups collected by the Pi-MEP.

9.8 Zonal mean and Std of *in situ* and ISAS SSS and of the difference Δ SSS

In Figure 220 left panel, we show the zonal mean SSS considering all Pi-MEP match-up pairs for both ISAS SSS product (in black) and the EUREC4A *in situ* dataset (in blue). The full *in situ* dataset period is used to derive the mean.

In the right panel of Figure 220, we show the zonal mean of Δ SSS (ISAS - EUREC4A) for all the collected Pi-MEP match-up pairs estimated over the full *in situ* dataset period.

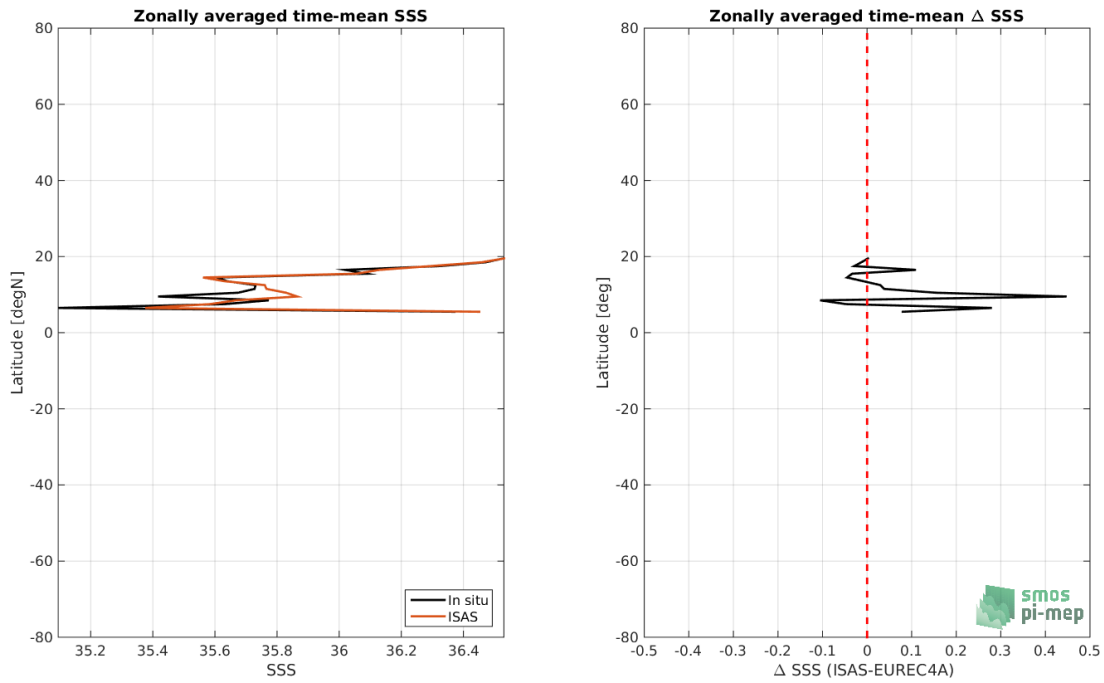


Figure 220: Left panel: Zonal mean SSS from ISAS product (black) and from EUREC4A (blue). Right panel: Zonal mean of Δ SSS (ISAS - EUREC4A) for all the collected Pi-MEP match-up pairs estimated over the full *in situ* dataset period.

9.9 Scatterplots of ISAS vs *in situ* SSS by latitudinal bands

In Figure 221, contour maps of the concentration of ISAS SSS (y-axis) versus EUREC4A SSS (x-axis) at match-up pairs for different latitude bands: (a) 80°S-80°N, (b) 20°S-20°N, (c) 40°S-20°S and 20°N-40°N and (d) 60°S-40°S and 40°N-60°N. For each plot, the red line shows $x=y$. The black thin and dashed lines indicate a linear fit through the data cloud and the $\pm 95\%$ confidence levels, respectively. The number match-up pairs n , the slope and R^2 coefficient of the linear fit, the root mean square (RMS) and the mean bias between ISAS and *in situ* data are indicated for each latitude band in each plots.

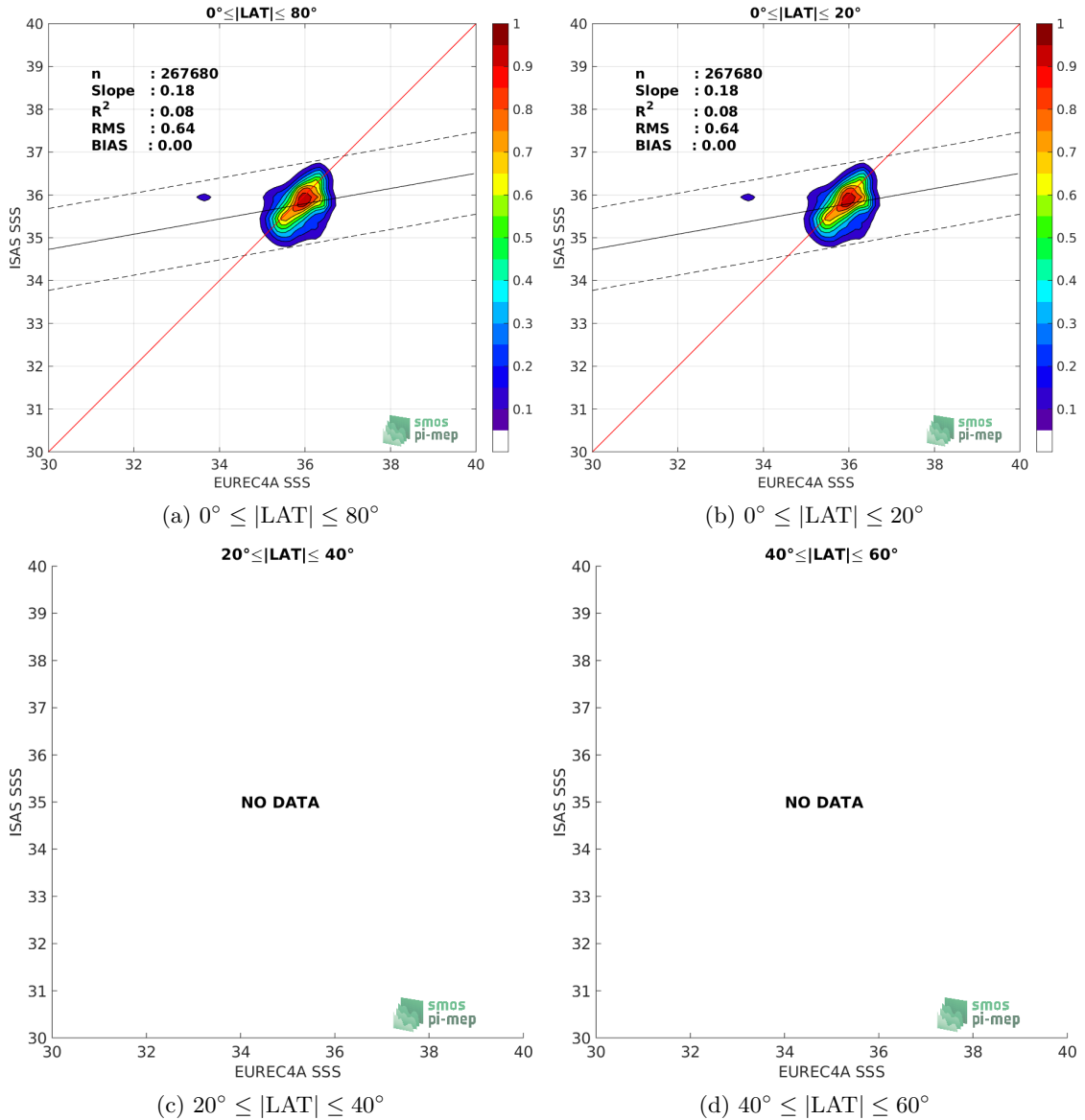


Figure 221: Contour maps of the concentration of ISAS SSS (y-axis) versus EUREC4A SSS (x-axis) at match-up pairs for different latitude bands. For each plot, the red line shows $x=y$. The black thin and dashed lines indicate a linear fit through the data cloud and the $\pm 95\%$ confidence levels, respectively. The number match-up pairs n , the slope and R^2 coefficient of the linear fit, the root mean square (RMS) and the mean bias between ISAS and *in situ* data are indicated for each latitude band in each plots.

9.10 Time series of the monthly median and Std of the difference ΔSSS sorted by latitudinal bands

In Figure 222, time series of the monthly median (red curves) of ΔSSS (ISAS - EUREC4A) and ± 1 Std (black vertical thick bars) as function of time for all the collected Pi-MEP match-up

pairs estimated for the full *in situ* dataset period are shown for different latitude bands: (a) 80°S-80°N, (b) 20°S-20°N, (c) 40°S-20°S and 20°N-40°N and (d) 60°S-40°S and 40°N-60°N.

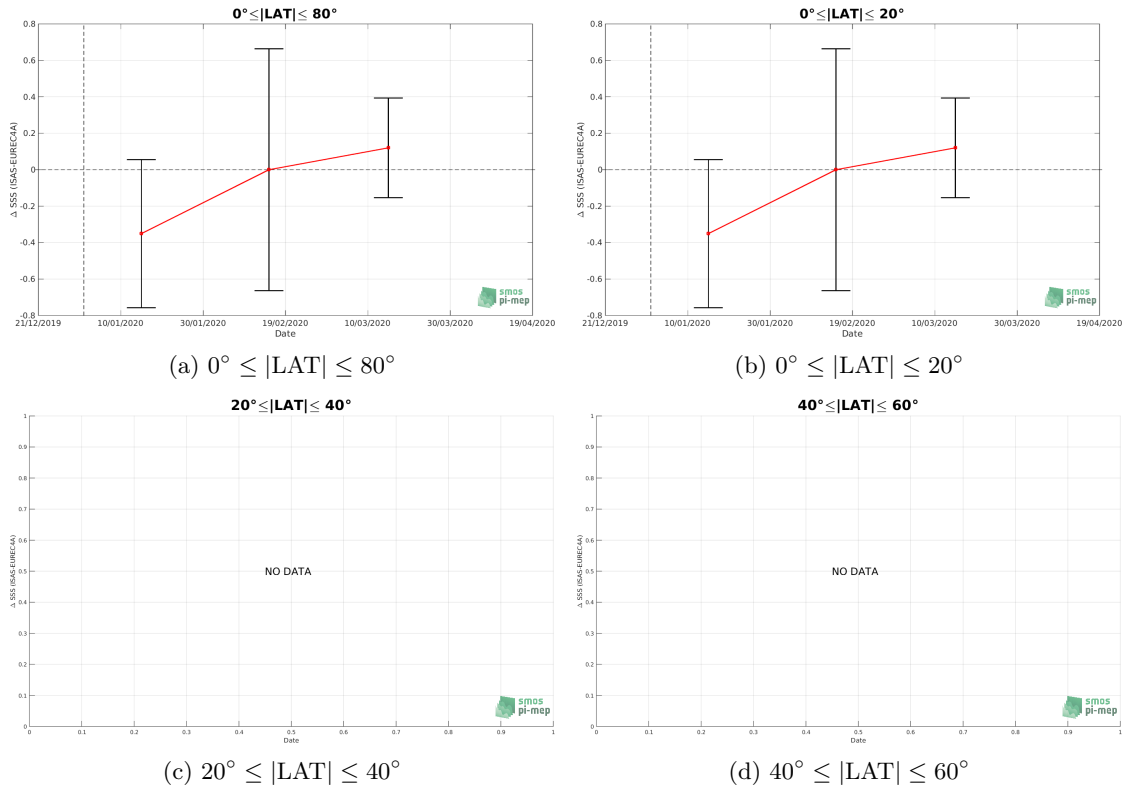


Figure 222: Monthly median (red curves) of ΔSSS (ISAS - EUREC4A) and ± 1 Std (black vertical thick bars) as function of time for all the collected Pi-MEP match-up pairs for the full *in situ* dataset period are shown for different latitude bands: (a) 80°S-80°N, (b) 20°S-20°N, (c) 40°S-20°S and 20°N-40°N and (d) 60°S-40°S and 40°N-60°N.

9.11 ΔSSS sorted as geophysical conditions

In Figure 223, we classify the match-up differences ΔSSS (ISAS - *in situ*) as function of the geophysical conditions at match-up points. The mean and std of ΔSSS (ISAS - EUREC4A) is thus evaluated as function of the

- *in situ* SSS values per bins of width 0.2,
- *in situ* SST values per bins of width 1°C,
- ASCAT daily wind values per bins of width 1 m/s,
- CMORPH 3-hourly rain rates per bins of width 1 mm/h, and,
- distance to coasts per bins of width 50 km,
- *in situ* measurement depth (if relevant).

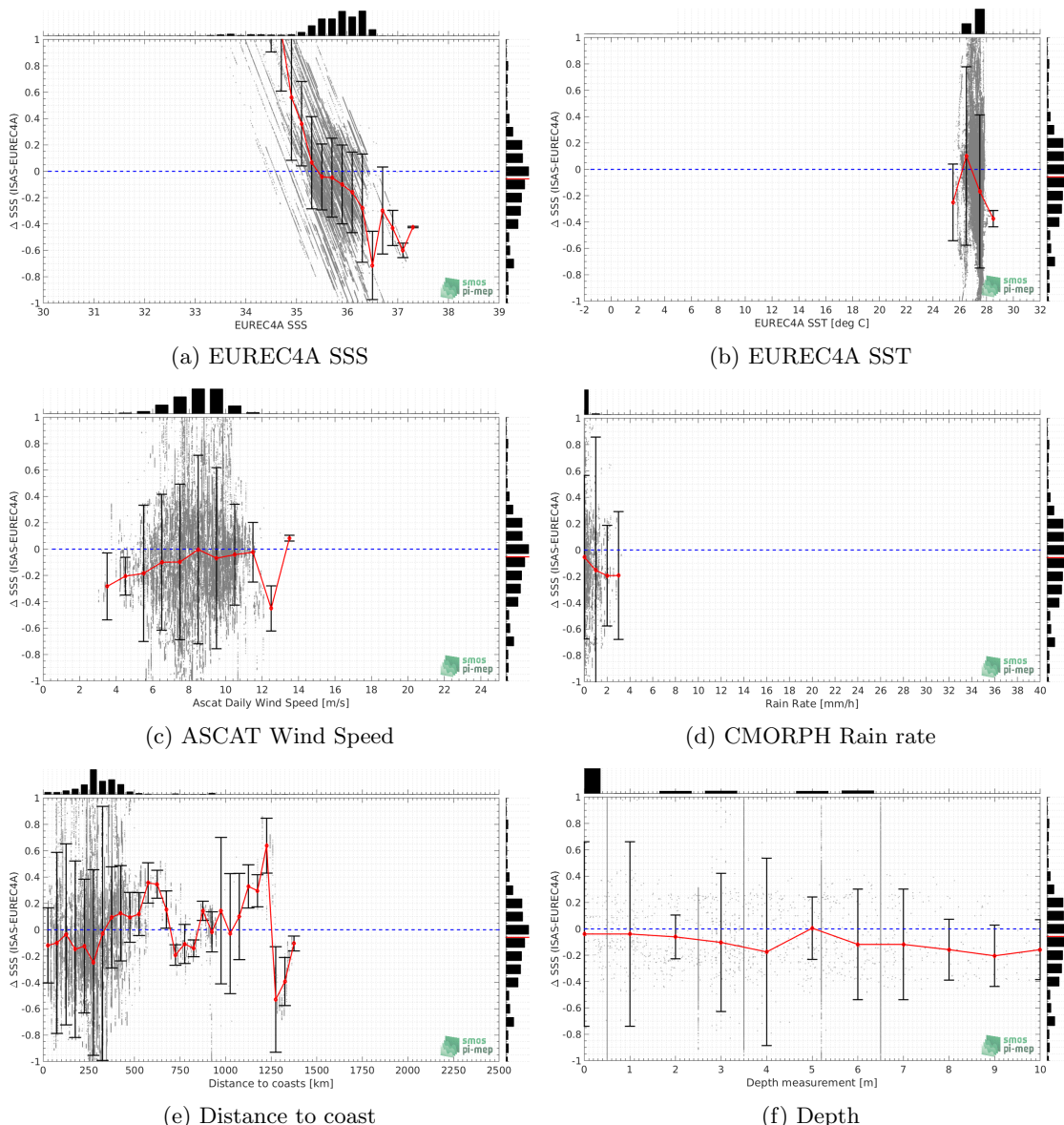


Figure 223: Δ SSS (ISAS - EUREC4A) sorted as geophysical conditions: EUREC4A SSS a), EUREC4A SST b), ASCAT Wind speed c), CMORPH rain rate d), distance to coast (e) and depth measurements (f).

9.12 Δ SSS maps and statistics for different geophysical conditions

In Figures 224 and 225, we focus on sub-datasets of the match-up differences Δ SSS (ISAS - *in situ*) for the following specific geophysical conditions:

- **C1:** if the local value at *in situ* location of estimated rain rate is zero, mean daily wind is in the range [3, 12] m/s, the SST is $> 5^{\circ}\text{C}$ and distance to coast is > 800 km.
- **C2:** if the local value at *in situ* location of estimated rain rate is zero, mean daily wind is

in the range [3, 12] m/s.

- **C3:** if the local value at *in situ* location of estimated rain rate is high (ie. > 1 mm/h) and mean daily wind is low (ie. < 4 m/s).
- **C5:** if the *in situ* data is located where the climatological SSS standard deviation is low (ie. above < 0.2).
- **C6:** if the *in situ* data is located where the climatological SSS standard deviation is high (ie. above > 0.2).

For each of these conditions, the temporal mean (gridded over spatial boxes of size $1^\circ \times 1^\circ$) and the histogram of the difference ΔSSS (ISAS - *in situ*) are presented.

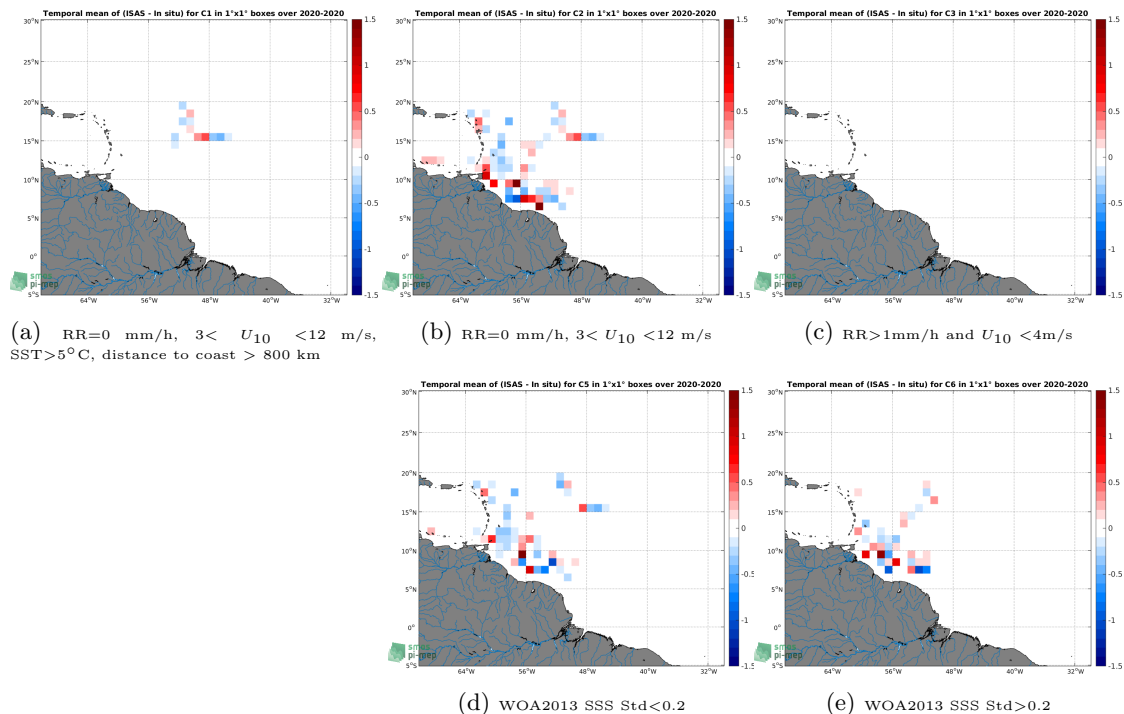


Figure 224: Temporal mean gridded over spatial boxes of size $1^\circ \times 1^\circ$ of ΔSSS (ISAS - EUREC4A) for 5 different subdatasets corresponding to: $\text{RR}=0 \text{ mm/h}$, $3 < U_{10} < 12 \text{ m/s}$, $\text{SST} > 5^\circ\text{C}$, distance to coast $> 800 \text{ km}$ (a), $\text{RR}=0 \text{ mm/h}$, $3 < U_{10} < 12 \text{ m/s}$ (b), $\text{RR} > 1 \text{ mm/h and } U_{10} < 4 \text{ m/s}$ (c), WOA2013 SSS Std < 0.2 (d), WOA2013 SSS Std > 0.2 (e).

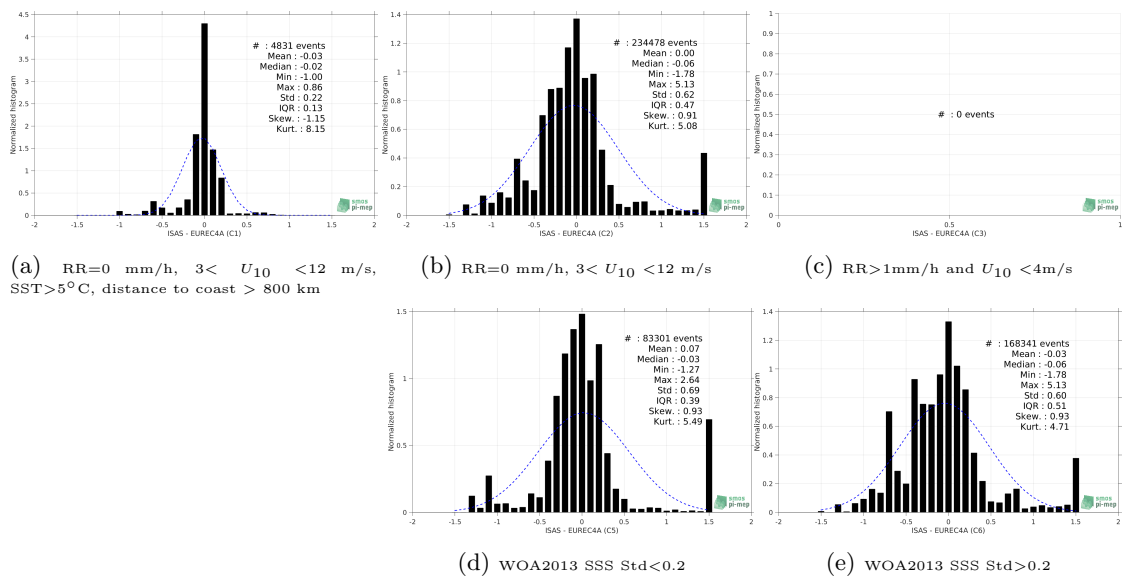


Figure 225: Normalized histogram of ΔSSS (ISAS - EUREC4A) for 5 different subdatasets corresponding to: $RR=0 \text{ mm/h}$, $3 < U_{10} < 12 \text{ m/s}$, $SST > 5^\circ\text{C}$, $\text{distance to coast} > 800 \text{ km}$ (a), $RR=0 \text{ mm/h}$, $3 < U_{10} < 12 \text{ m/s}$ (b), $RR > 1 \text{ mm/h}$ and $U_{10} < 4 \text{ m/s}$ (c), WOA2013 SSS Std < 0.2 (d), WOA2013 SSS Std > 0.2 (e).

9.13 Summary

Table 1 shows the mean, median, standard deviation (Std), root mean square (RMS), interquartile range (IQR), correlation coefficient (r^2) and robust standard deviation (Std*) of the match-up differences ΔSSS (ISAS - EUREC4A) for the following conditions:

- all: All the match-up pairs satellite/in situ SSS values are used to derive the statistics
- C1: only pairs where $RR=0 \text{ mm/h}$, $3 < U_{10} < 12 \text{ m/s}$, $SST > 5^\circ\text{C}$, $\text{distance to coast} > 800 \text{ km}$
- C2: only pairs where $RR=0 \text{ mm/h}$, $3 < U_{10} < 12 \text{ m/s}$
- C3: only pairs where $RR > 1 \text{ mm/h}$ and $U_{10} < 4 \text{ m/s}$
- C5: only pairs where WOA2013 SSS Std < 0.2
- C6: only pairs where WOA2013 SSS Std > 0.2
- C7a: only pairs with a distance to coast $< 150 \text{ km}$.
- C7b: only pairs with a distance to coast in the range $[150, 800] \text{ km}$.
- C7c: only pairs with a distance to coast $> 800 \text{ km}$.
- C8a: only pairs where SST is $< 5^\circ\text{C}$.
- C8b: only pairs where SST is in the range $[5, 15]^\circ\text{C}$.
- C8c: only pairs where SST is $> 15^\circ\text{C}$.

- C9a: only pairs where SSS is < 33.
- C9b: only pairs where SSS is in the range [33, 37].
- C9c: only pairs where SSS is > 37.

Table 1: Statistics of ΔSSS (ISAS - EUREC4A)

Condition	#	Median	Mean	Std	RMS	IQR	r^2	Std*
all	267680	-0.06	0.00	0.64	0.64	0.47	0.085	0.35
C1	4831	-0.02	-0.03	0.22	0.23	0.13	0.787	0.09
C2	234478	-0.06	0.00	0.62	0.62	0.47	0.107	0.35
C3	0	NaN	NaN	NaN	NaN	NaN	NaN	NaN
C5	83301	-0.03	0.07	0.69	0.69	0.39	0.100	0.30
C6	168341	-0.06	-0.03	0.60	0.60	0.51	0.046	0.40
C7a	22855	-0.05	0.03	0.61	0.61	0.29	0.280	0.22
C7b	239671	-0.07	0.00	0.65	0.65	0.50	0.060	0.37
C7c	5154	-0.02	-0.03	0.22	0.23	0.14	0.794	0.09
C8a	0	NaN	NaN	NaN	NaN	NaN	NaN	NaN
C8b	0	NaN	NaN	NaN	NaN	NaN	NaN	NaN
C8c	267680	-0.06	0.00	0.64	0.64	0.47	0.085	0.35
C9a	984	2.84	3.11	0.91	3.24	1.37	0.000	0.64
C9b	266474	-0.06	-0.01	0.61	0.61	0.47	0.078	0.35
C9c	222	-0.60	-0.59	0.06	0.60	0.08	0.264	0.05

Table 1 numerical values can be downloaded as a csv file [here](#).

10 ICES

10.1 Introduction

The International Council for the Exploration of the Sea (ICES) oceanographic database holds a wealth of oceanographic data from 1877 to present ([ice](#)). All data are quality controlled according to [documented](#) guidelines and visually inspected by experienced staff to further improve the quality of the data. The ICES Pi-MEP in situ dataset is a collection of the Surface data, Pump data and High resolution CTD data freely available via the following link <https://data.ices.dk/view-map?theme=201809>.

10.2 Number of SSS data as a function of time and distance to coast

Figure 226 shows the time (a) and distance to coast (b) distributions of the ICES *in situ* dataset.

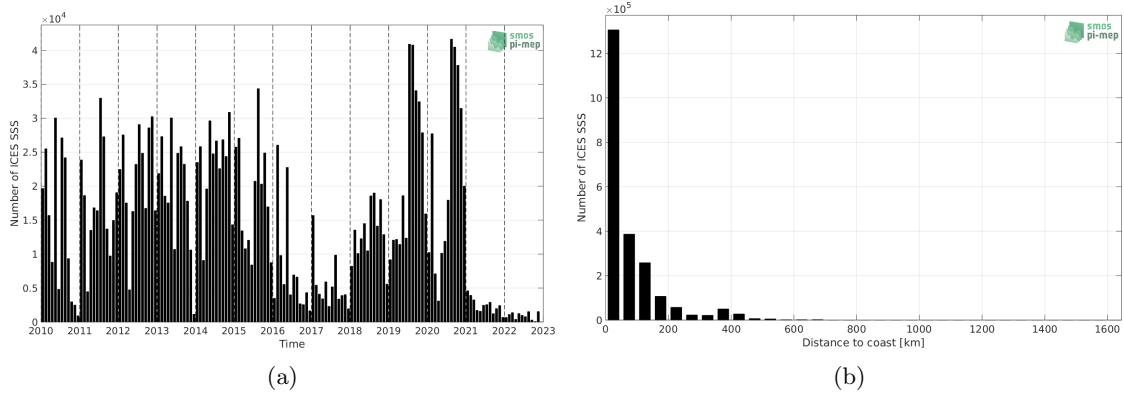


Figure 226: Number of SSS from ICES as a function of time (a) and distance to coast (b).

10.3 Histograms of SSS

Figure 227 shows the SSS distribution of the ICES (a) and colocalized ISAS (b) dataset.

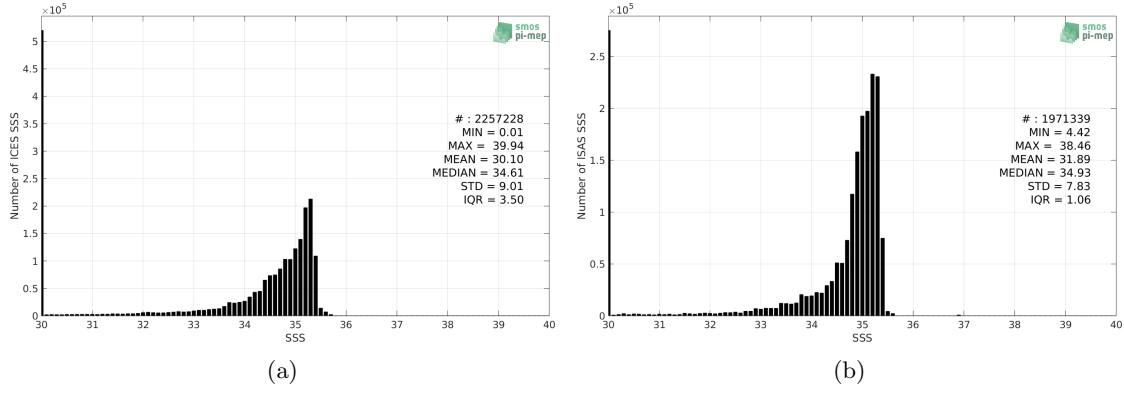


Figure 227: Histograms of SSS from ICES (a) and ISAS (b) per bins of 0.1.

10.4 Distribution of *in situ* SSS depth measurements

In Figure 228, we show the depth distribution of the *in situ* salinity dataset (a) and the spatial distribution of the depth temporal mean in $1^\circ \times 1^\circ$ boxes and considering the full *in situ* dataset period (b).

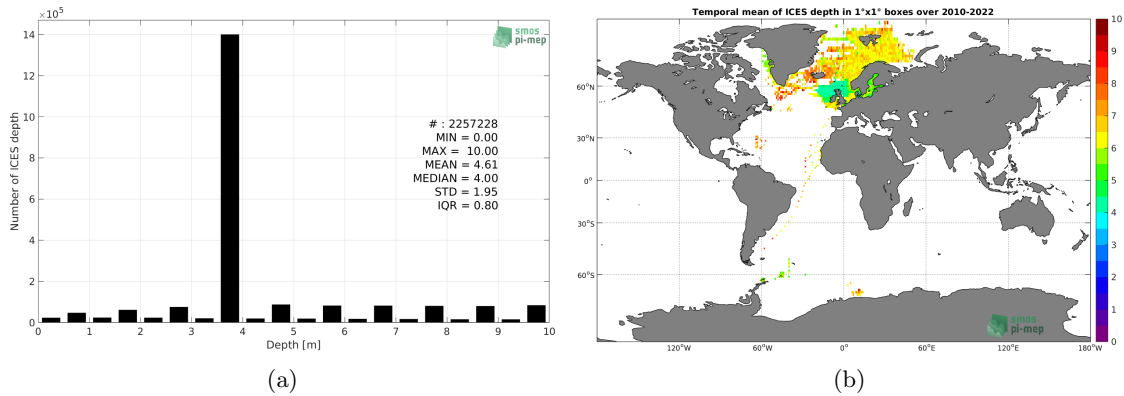


Figure 228: Depth distribution of the upper level SSS measurements from ICES (a) and spatial distribution of the *in situ* SSS depth measurements showing the mean value in 1°x1° boxes and considering the full *in situ* dataset period (b).

10.5 Spatial distribution of SSS

In Figure 229, the number of ICES SSS measurements in 1°x1° boxes is shown.

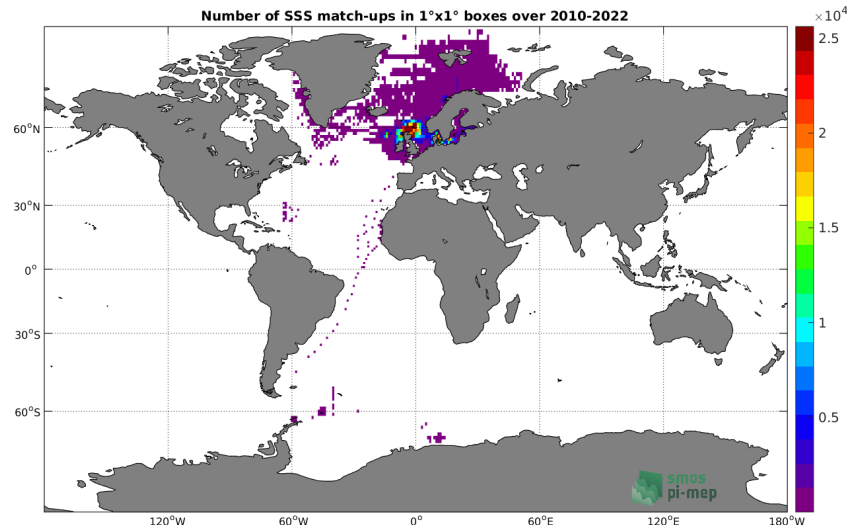


Figure 229: Number of SSS from ICES in 1°x1° boxes.

10.6 Spatial Maps of the Temporal mean and Std of *in situ* and ISAS SSS and of the difference (Δ SSS)

In Figure 230, maps of temporal mean (left) and standard deviation (right) of ISAS (top), ICES *in situ* dataset (middle) and the difference Δ SSS(ISAS -ICES) (bottom) are shown. The temporal mean and std are calculated using all match-up pairs falling in spatial boxes of size 1°x1° over the full ICES dataset period.

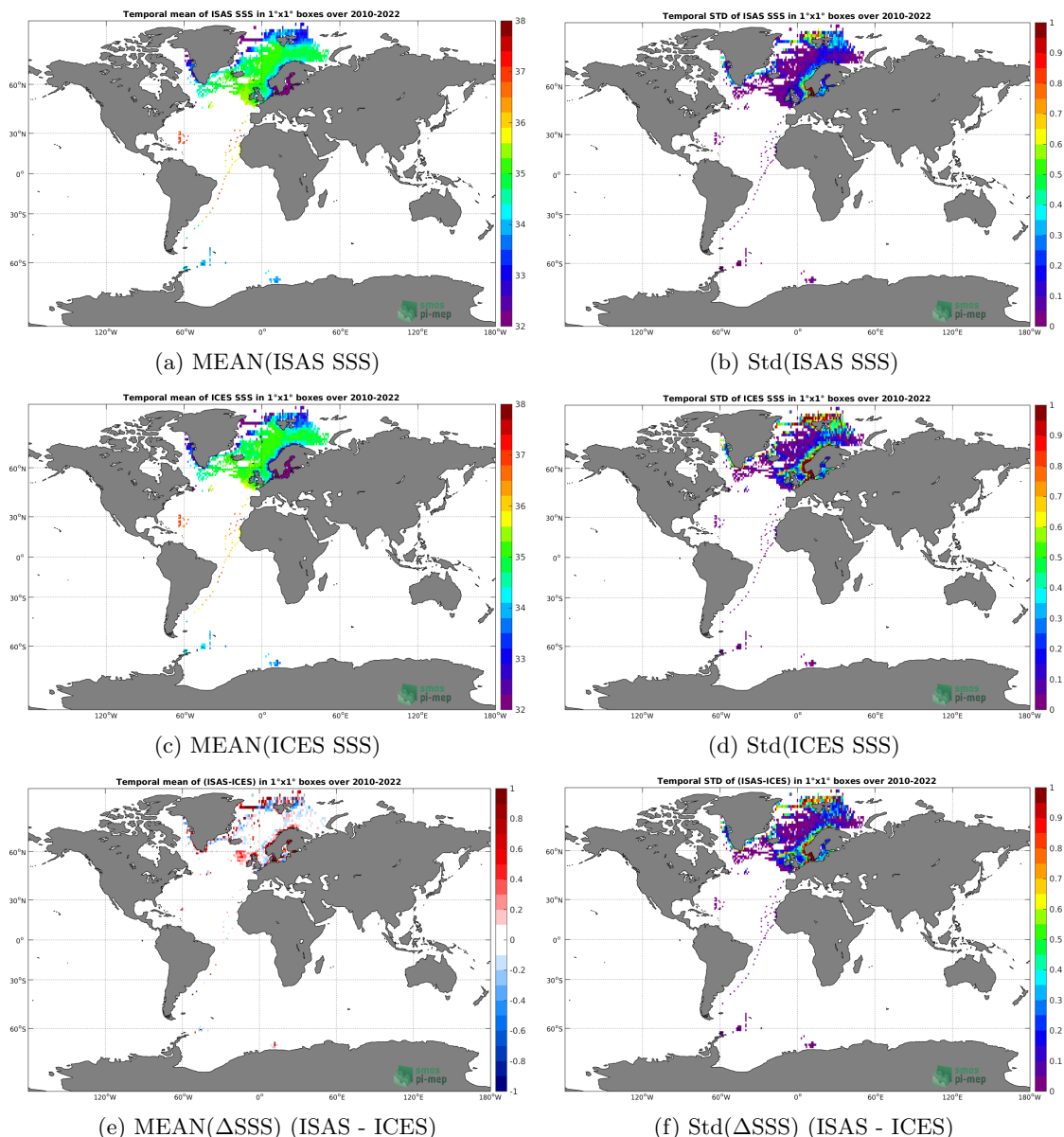


Figure 230: Temporal mean (left) and Std (right) of SSS from ISAS (top), ICES (middle), and of Δ SSS (ISAS - ICES). Only match-up pairs are used to generate these maps.

10.7 Time series of the monthly median and Std of *in situ* and ISAS SSS and of the difference (Δ SSS)

In the top panel of Figure 231, we show the time series of the monthly median SSS estimated for both ISAS SSS product (in black) and the ICES *in situ* dataset (in blue) at the collected Pi-MEP match-up pairs.

In the middle panel of Figure 231, we show the time series of the monthly median of Δ SSS (ISAS - ICES) for the collected Pi-MEP match-up pairs.

In the bottom panel of Figure 231, we show the time series of the monthly standard deviation of the Δ SSS (ISAS - ICES) for the collected Pi-MEP match-up pairs.

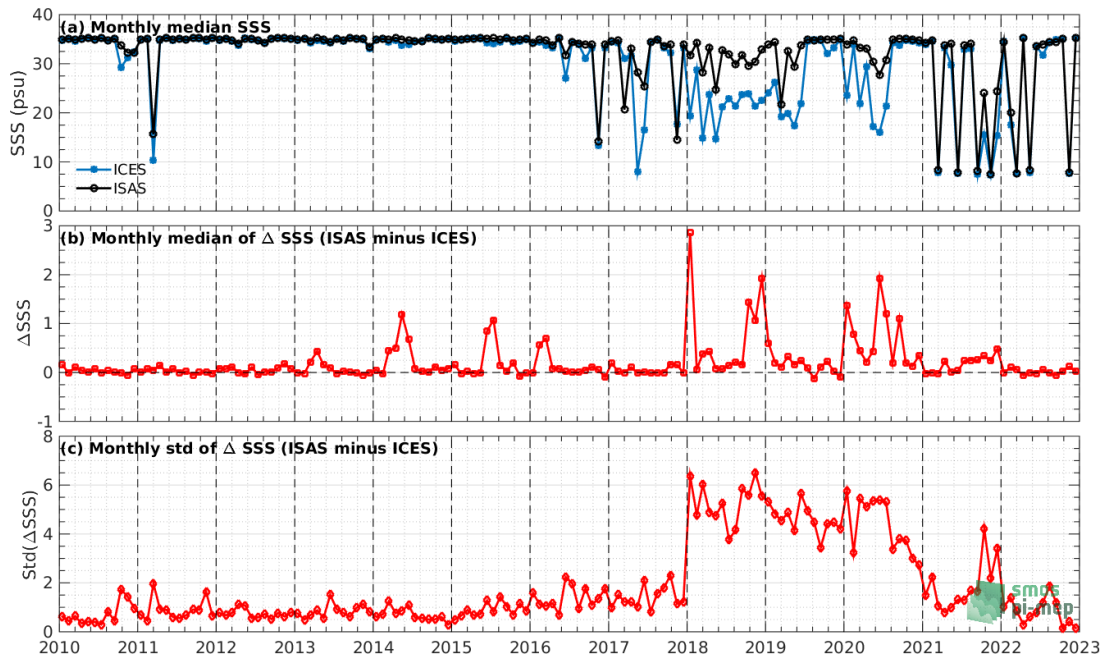


Figure 231: Time series of the monthly median SSS (top), median of Δ SSS (ISAS - ICES) and Std of Δ SSS (ISAS - ICES) considering all match-ups collected by the Pi-MEP.

10.8 Zonal mean and Std of *in situ* and ISAS SSS and of the difference Δ SSS

In Figure 232 left panel, we show the zonal mean SSS considering all Pi-MEP match-up pairs for both ISAS SSS product (in black) and the ICES *in situ* dataset (in blue). The full *in situ* dataset period is used to derive the mean.

In the right panel of Figure 232, we show the zonal mean of Δ SSS (ISAS - ICES) for all the collected Pi-MEP match-up pairs estimated over the full *in situ* dataset period.

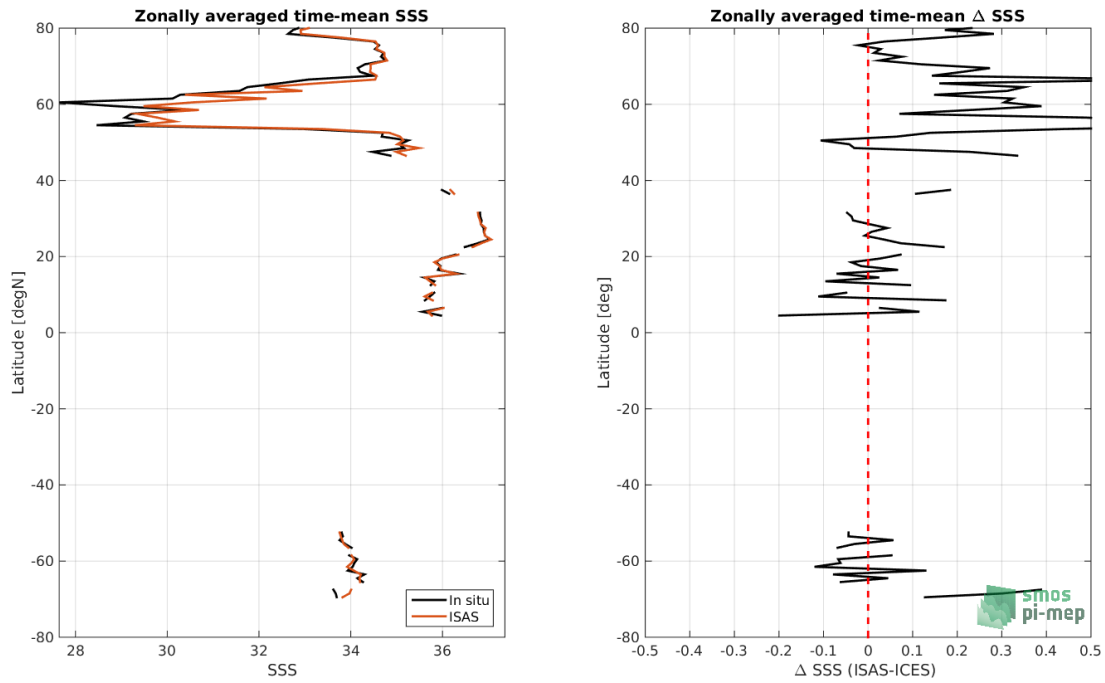


Figure 232: Left panel: Zonal mean SSS from ISAS product (black) and from ICES (blue). Right panel: Zonal mean of Δ SSS (ISAS - ICES) for all the collected Pi-MEP match-up pairs estimated over the full *in situ* dataset period.

10.9 Scatterplots of ISAS vs *in situ* SSS by latitudinal bands

In Figure 233, contour maps of the concentration of ISAS SSS (y-axis) versus ICES SSS (x-axis) at match-up pairs for different latitude bands: (a) 80°S-80°N, (b) 20°S-20°N, (c) 40°S-20°S and 20°N-40°N and (d) 60°S-40°S and 40°N-60°N. For each plot, the red line shows $x=y$. The black thin and dashed lines indicate a linear fit through the data cloud and the $\pm 95\%$ confidence levels, respectively. The number match-up pairs n , the slope and R^2 coefficient of the linear fit, the root mean square (RMS) and the mean bias between ISAS and *in situ* data are indicated for each latitude band in each plots.

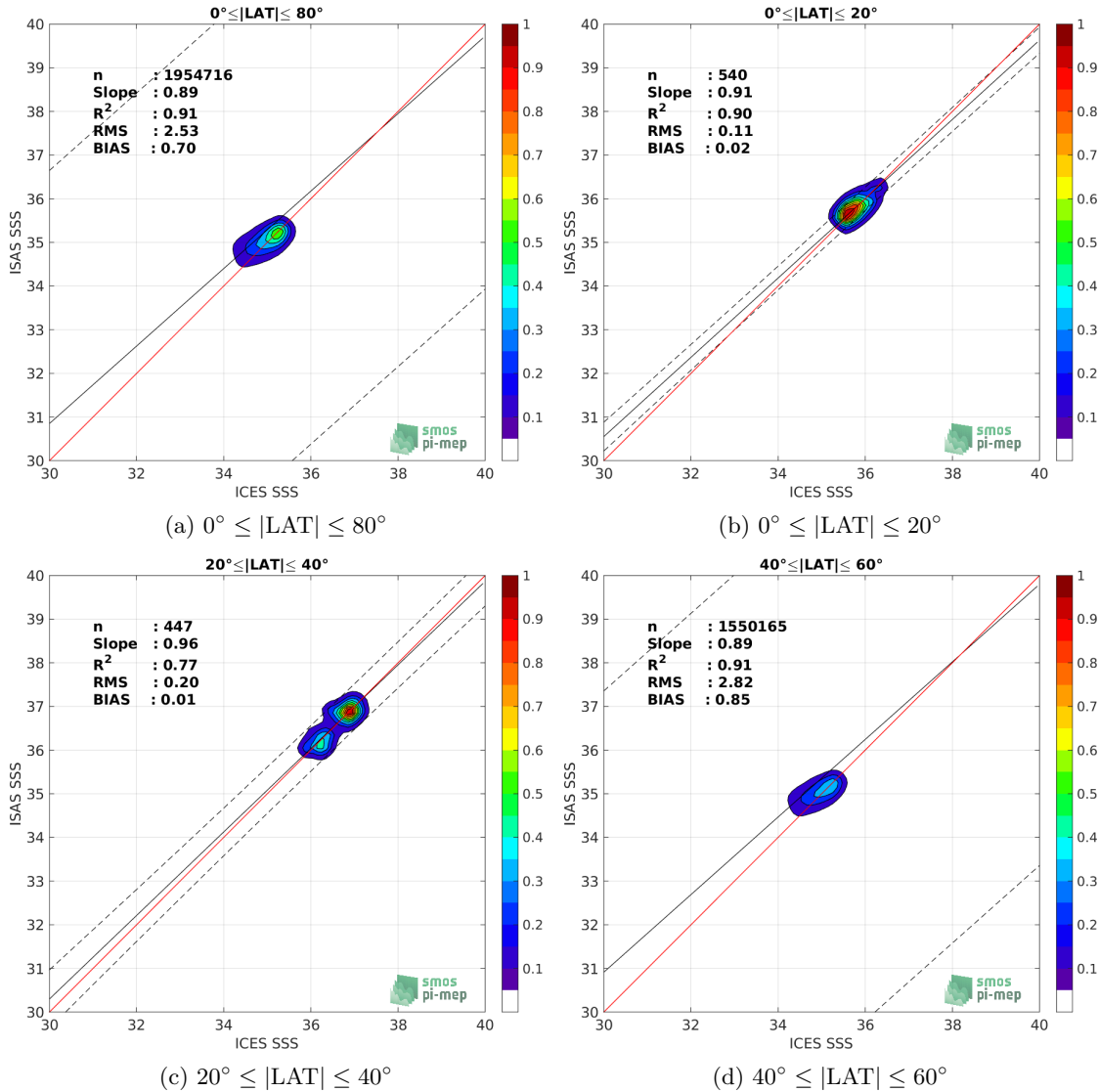


Figure 233: Contour maps of the concentration of ISAS SSS (y-axis) versus ICES SSS (x-axis) at match-up pairs for different latitude bands. For each plot, the red line shows $x=y$. The black thin and dashed lines indicate a linear fit through the data cloud and the $\pm 95\%$ confidence levels, respectively. The number match-up pairs n , the slope and R^2 coefficient of the linear fit, the root mean square (RMS) and the mean bias between ISAS and *in situ* data are indicated for each latitude band in each plots.

10.10 Time series of the monthly median and Std of the difference ΔSSS sorted by latitudinal bands

In Figure 234, time series of the monthly median (red curves) of ΔSSS (ISAS - ICES) and ± 1 Std (black vertical thick bars) as function of time for all the collected Pi-MEP match-up pairs estimated for the full *in situ* dataset period are shown for different latitude bands: (a) $80^\circ\text{S}-80^\circ\text{N}$, (b) $20^\circ\text{S}-20^\circ\text{N}$, (c) $40^\circ\text{S}-20^\circ\text{N}$ and $20^\circ\text{N}-40^\circ\text{N}$ and (d) $60^\circ\text{S}-40^\circ\text{S}$ and $40^\circ\text{N}-60^\circ\text{N}$.

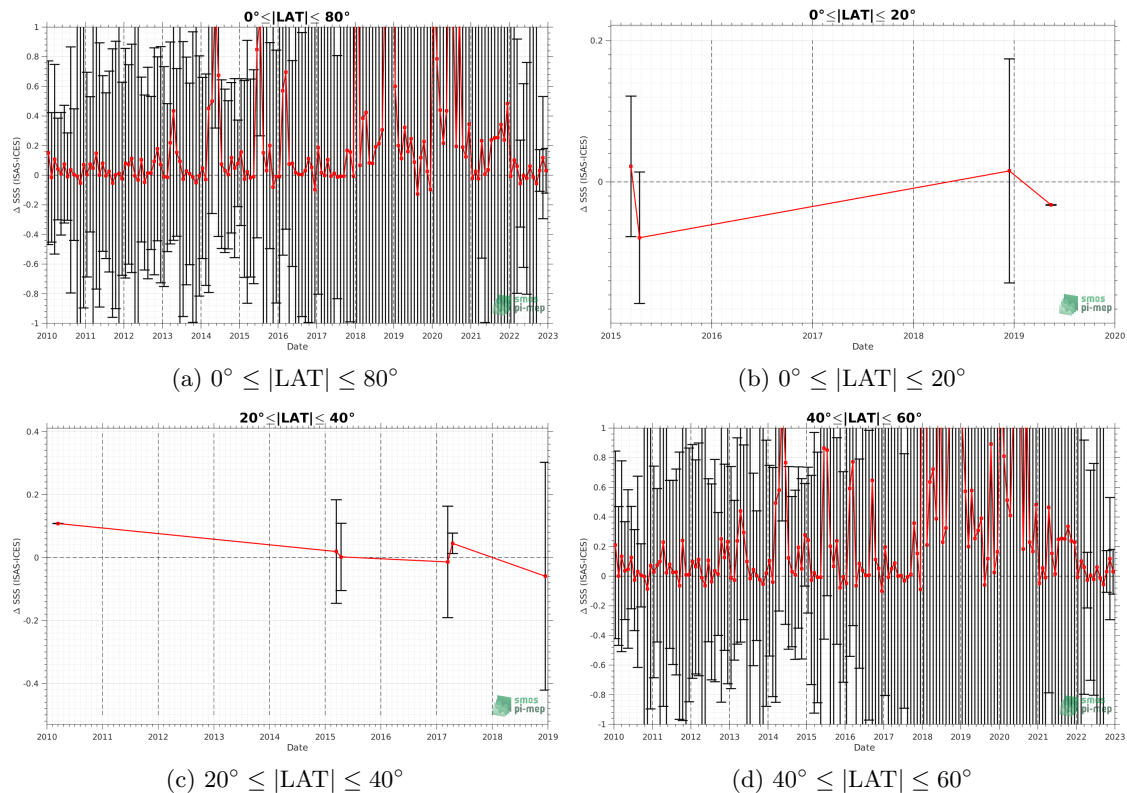


Figure 234: Monthly median (red curves) of ΔSSS (ISAS - ICES) and ± 1 Std (black vertical thick bars) as function of time for all the collected Pi-MEP match-up pairs for the full *in situ* dataset period are shown for different latitude bands: (a) $80^\circ\text{S}-80^\circ\text{N}$, (b) $20^\circ\text{S}-20^\circ\text{N}$, (c) $40^\circ\text{S}-20^\circ\text{S}$ and $20^\circ\text{N}-40^\circ\text{N}$ and (d) $60^\circ\text{S}-40^\circ\text{S}$ and $40^\circ\text{N}-60^\circ\text{N}$.

10.11 ΔSSS sorted as geophysical conditions

In Figure 235, we classify the match-up differences ΔSSS (ISAS - *in situ*) as function of the geophysical conditions at match-up points. The mean and std of ΔSSS (ISAS - ICES) is thus evaluated as function of the

- *in situ* SSS values per bins of width 0.2,
- *in situ* SST values per bins of width 1°C ,
- ASCAT daily wind values per bins of width 1 m/s,
- CMORPH 3-hourly rain rates per bins of width 1 mm/h, and,
- distance to coasts per bins of width 50 km,
- *in situ* measurement depth (if relevant).

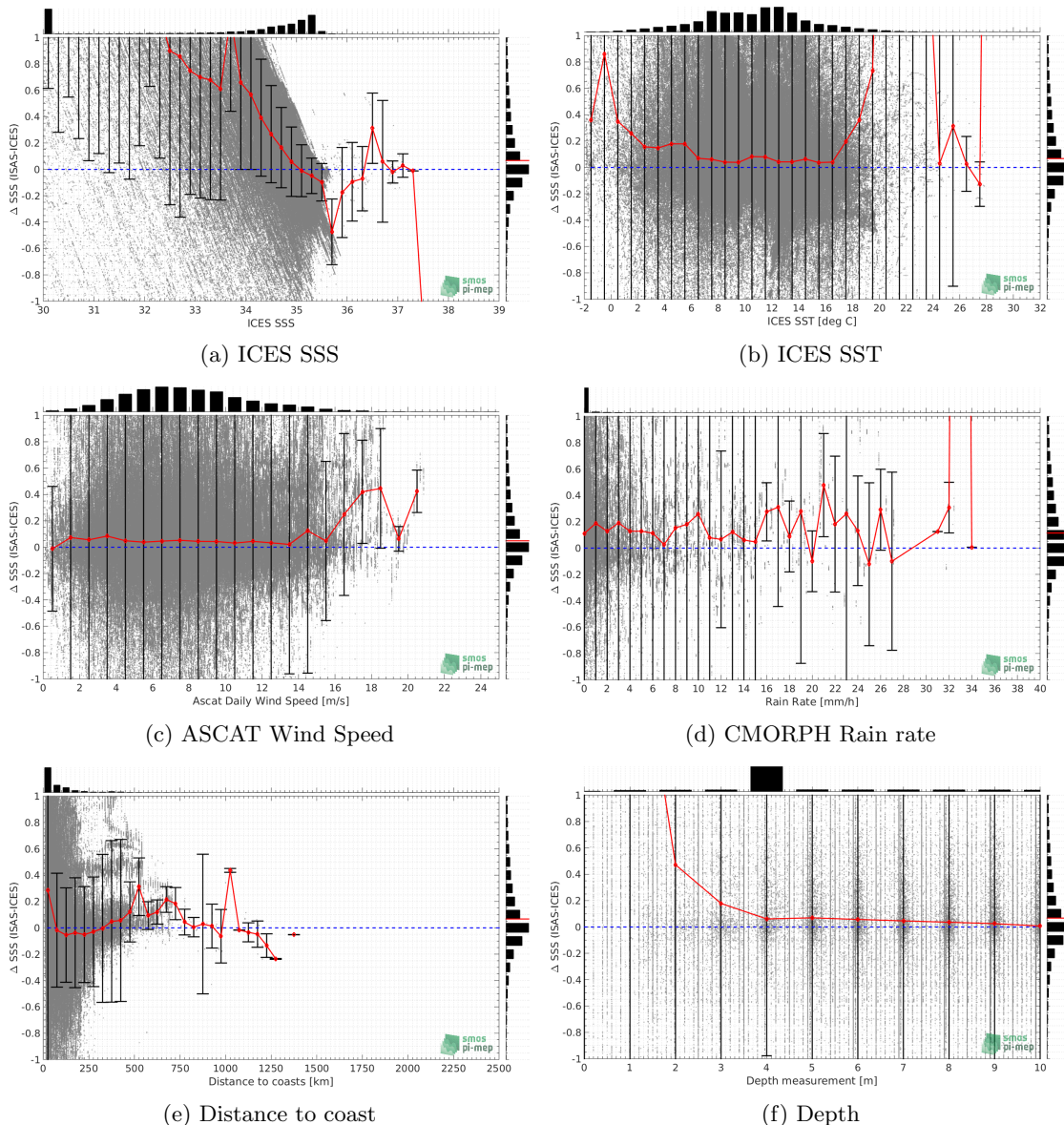


Figure 235: Δ SSS (ISAS - ICES) sorted as geophysical conditions: ICES SSS a), ICES SST b), ASCAT Wind speed c), CMORPH rain rate d), distance to coast (e) and depth measurements (f).

10.12 Δ SSS maps and statistics for different geophysical conditions

In Figures 236 and 237, we focus on sub-datasets of the match-up differences Δ SSS (ISAS - *in situ*) for the following specific geophysical conditions:

- **C1:** if the local value at *in situ* location of estimated rain rate is zero, mean daily wind is in the range [3, 12] m/s, the SST is $> 5^{\circ}\text{C}$ and distance to coast is > 800 km.
- **C2:** if the local value at *in situ* location of estimated rain rate is zero, mean daily wind is

in the range [3, 12] m/s.

- **C3:** if the local value at *in situ* location of estimated rain rate is high (ie. $> 1 \text{ mm/h}$) and mean daily wind is low (ie. $< 4 \text{ m/s}$).
- **C5:** if the *in situ* data is located where the climatological SSS standard deviation is low (ie. above < 0.2).
- **C6:** if the *in situ* data is located where the climatological SSS standard deviation is high (ie. above > 0.2).

For each of these conditions, the temporal mean (gridded over spatial boxes of size $1^\circ \times 1^\circ$) and the histogram of the difference ΔSSS (ISAS - *in situ*) are presented.

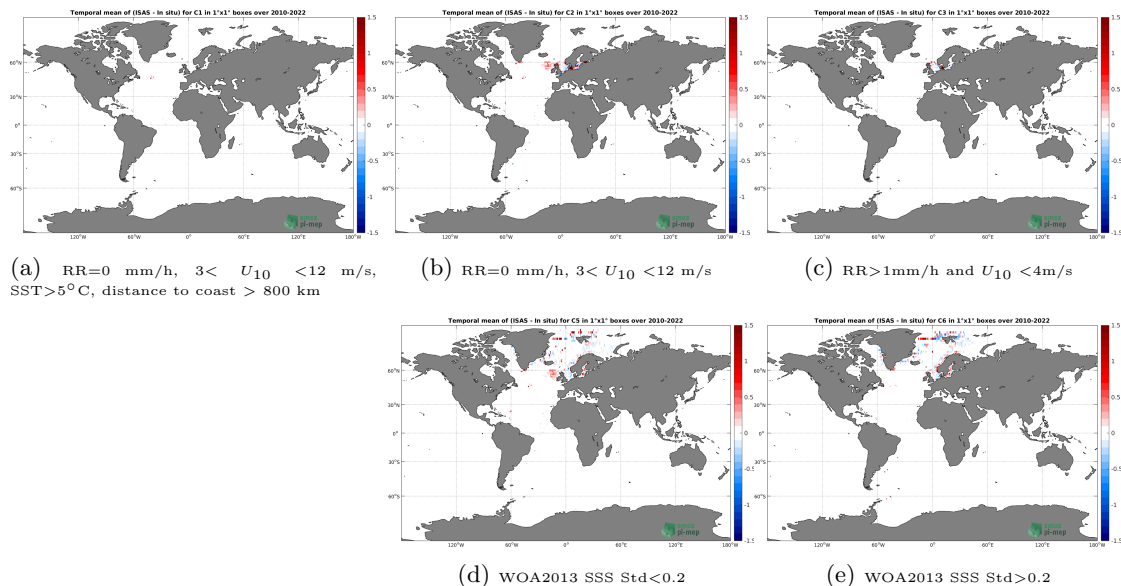


Figure 236: Temporal mean gridded over spatial boxes of size $1^\circ \times 1^\circ$ of ΔSSS (ISAS - ICES) for 5 different subdatasets corresponding to: RR = 0 mm/h, $3 < U_{10} < 12 \text{ m/s}$, SST $> 5^\circ\text{C}$, distance to coast $> 800 \text{ km}$ (a), RR = 0 mm/h, $3 < U_{10} < 12 \text{ m/s}$ (b), RR $> 1\text{mm/h}$ and $U_{10} < 4\text{m/s}$ (c), WOA2013 SSS Std < 0.2 (d), WOA2013 SSS Std > 0.2 (e).

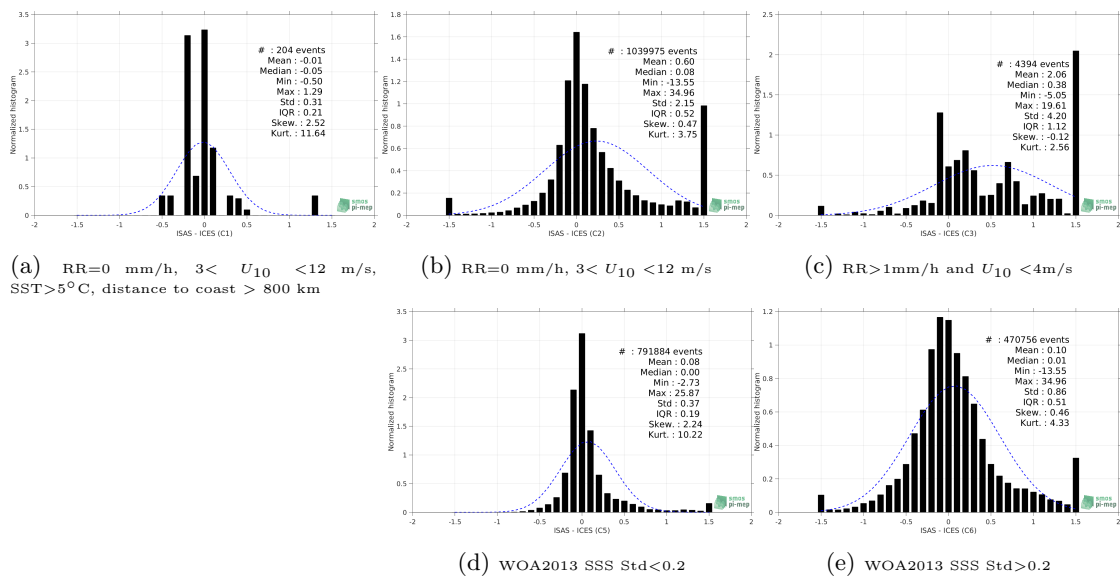


Figure 237: Normalized histogram of ΔSSS (ISAS - ICES) for 5 different subdatasets corresponding to: $RR=0 \text{ mm/h}$, $3 < U_{10} < 12 \text{ m/s}$, $SST > 5^\circ\text{C}$, $\text{distance to coast} > 800 \text{ km}$ (a), $RR=0 \text{ mm/h}$, $3 < U_{10} < 12 \text{ m/s}$ (b), $RR > 1 \text{ mm/h}$ and $U_{10} < 4 \text{ m/s}$ (c), WOA2013 SSS Std < 0.2 (d), WOA2013 SSS Std > 0.2 (e).

10.13 Summary

Table 1 shows the mean, median, standard deviation (Std), root mean square (RMS), interquartile range (IQR), correlation coefficient (r^2) and robust standard deviation (Std*) of the match-up differences ΔSSS (ISAS - ICES) for the following conditions:

- all: All the match-up pairs satellite/in situ SSS values are used to derive the statistics
- C1: only pairs where $RR=0 \text{ mm/h}$, $3 < U_{10} < 12 \text{ m/s}$, $SST > 5^\circ\text{C}$, $\text{distance to coast} > 800 \text{ km}$
- C2: only pairs where $RR=0 \text{ mm/h}$, $3 < U_{10} < 12 \text{ m/s}$
- C3: only pairs where $RR > 1 \text{ mm/h}$ and $U_{10} < 4 \text{ m/s}$
- C5: only pairs where WOA2013 SSS Std < 0.2
- C6: only pairs where WOA2013 SSS Std > 0.2
- C7a: only pairs with a distance to coast $< 150 \text{ km}$.
- C7b: only pairs with a distance to coast in the range $[150, 800] \text{ km}$.
- C7c: only pairs with a distance to coast $> 800 \text{ km}$.
- C8a: only pairs where SST is $< 5^\circ\text{C}$.
- C8b: only pairs where SST is in the range $[5, 15]^\circ\text{C}$.
- C8c: only pairs where SST is $> 15^\circ\text{C}$.

- C9a: only pairs where SSS is < 33 .
- C9b: only pairs where SSS is in the range [33, 37].
- C9c: only pairs where SSS is > 37 .

Table 1: Statistics of Δ SSS (ISAS - ICES)

Condition	#	Median	Mean	Std	RMS	IQR	r^2	Std*
all	1971339	0.07	0.73	2.55	2.65	0.53	0.909	0.31
C1	204	-0.05	-0.01	0.31	0.31	0.21	0.826	0.17
C2	1039975	0.08	0.60	2.15	2.23	0.52	0.946	0.33
C3	4394	0.38	2.06	4.20	4.68	1.12	0.843	0.70
C5	791884	0.00	0.08	0.37	0.38	0.19	0.993	0.14
C6	470756	0.01	0.10	0.86	0.86	0.51	0.992	0.37
C7a	1664688	0.09	0.84	2.76	2.88	0.59	0.907	0.35
C7b	306323	0.01	0.11	0.49	0.51	0.23	0.297	0.16
C7c	328	-0.01	-0.01	0.26	0.26	0.19	0.908	0.10
C8a	143777	0.20	1.44	3.57	3.85	1.31	0.916	0.63
C8b	1615818	0.06	0.48	1.93	1.99	0.45	0.920	0.27
C8c	210759	0.11	2.10	4.59	5.04	2.28	0.817	0.64
C9a	424732	1.05	2.94	4.83	5.66	4.29	0.821	1.90
C9b	1546566	0.03	0.12	0.44	0.45	0.34	0.410	0.23
C9c	41	0.02	-0.46	1.44	1.50	0.20	0.772	0.06

Table 1 numerical values can be downloaded as a csv file [here](#).

11 Summary

In the following summary section, some of the plots presented in the previous sections corresponding to the time distribution [11.1], SSS distribution [11.2], temporal mean [11.3] and std [11.4], and spatial density [11.5], are combined to emphasize similarities/differences between each *in situ* datasets. Some characteristics of each *in situ* datasets for each Pi-MEP region are also presented in 11.6.

11.1 Number of SSS data as a function of time

Figures 238 show the time distribution of the different *in situ* datasets.

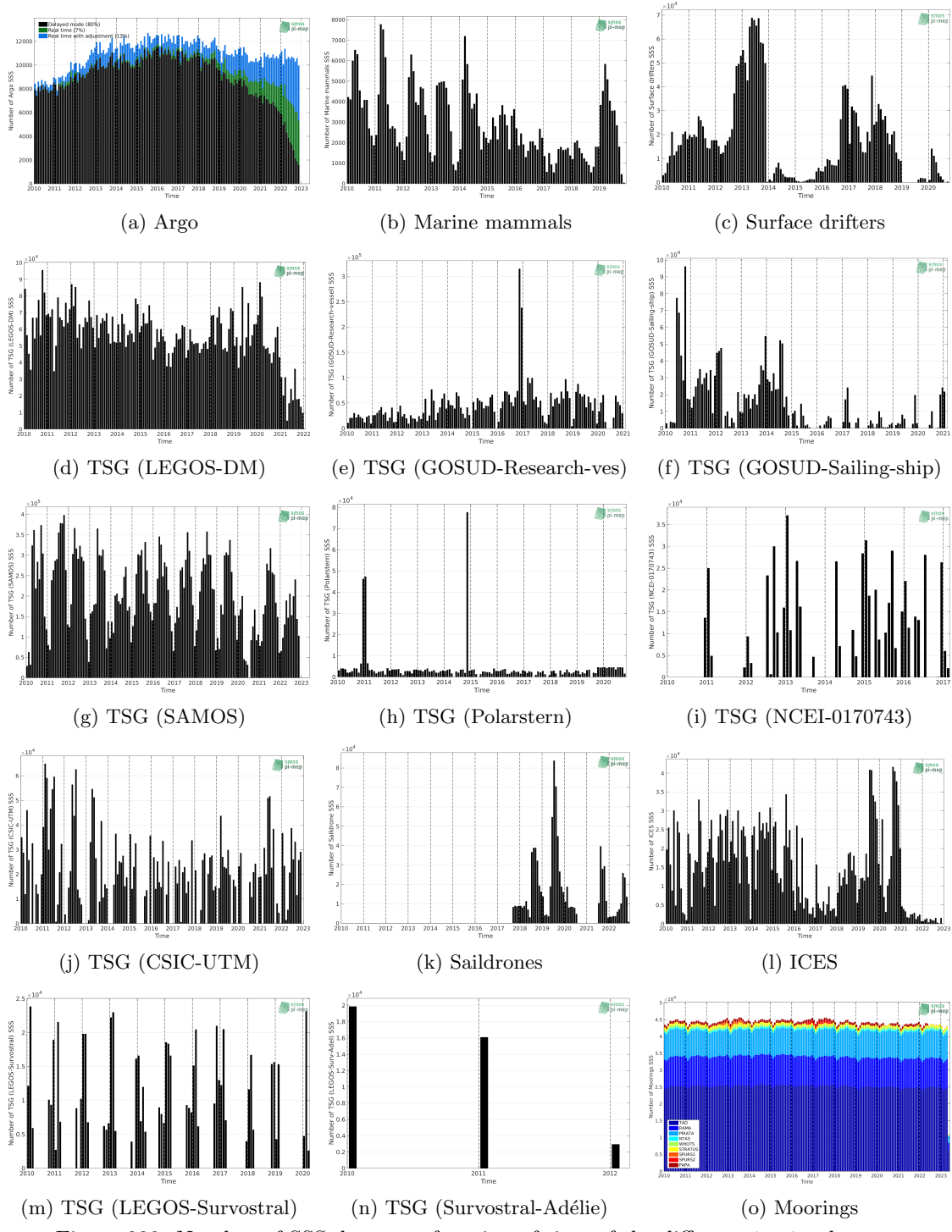
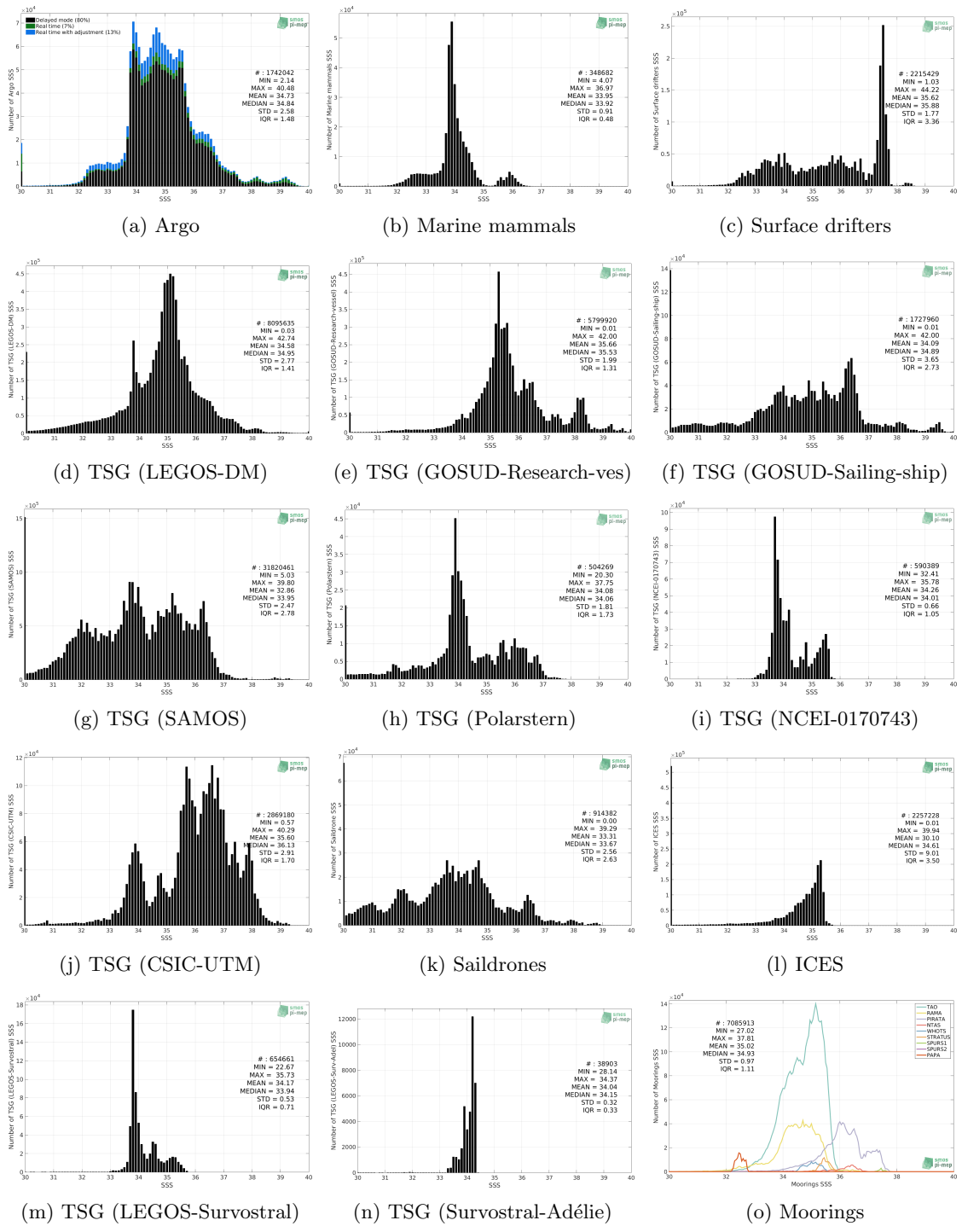


Figure 238: Number of SSS data as a function of time of the different *in situ* datasets

11.2 Histogram of SSS

Figures 239 show the SSS distribution of the different *in situ* datasets.


Figure 239: Distribution of SSS per bins of 0.1 of the different *in situ* datasets.

11.3 Temporal mean of SSS

Figures 240 show the temporal mean gridded over spatial boxes of size $1^\circ \times 1^\circ$ using the full period of each *in situ* datasets.

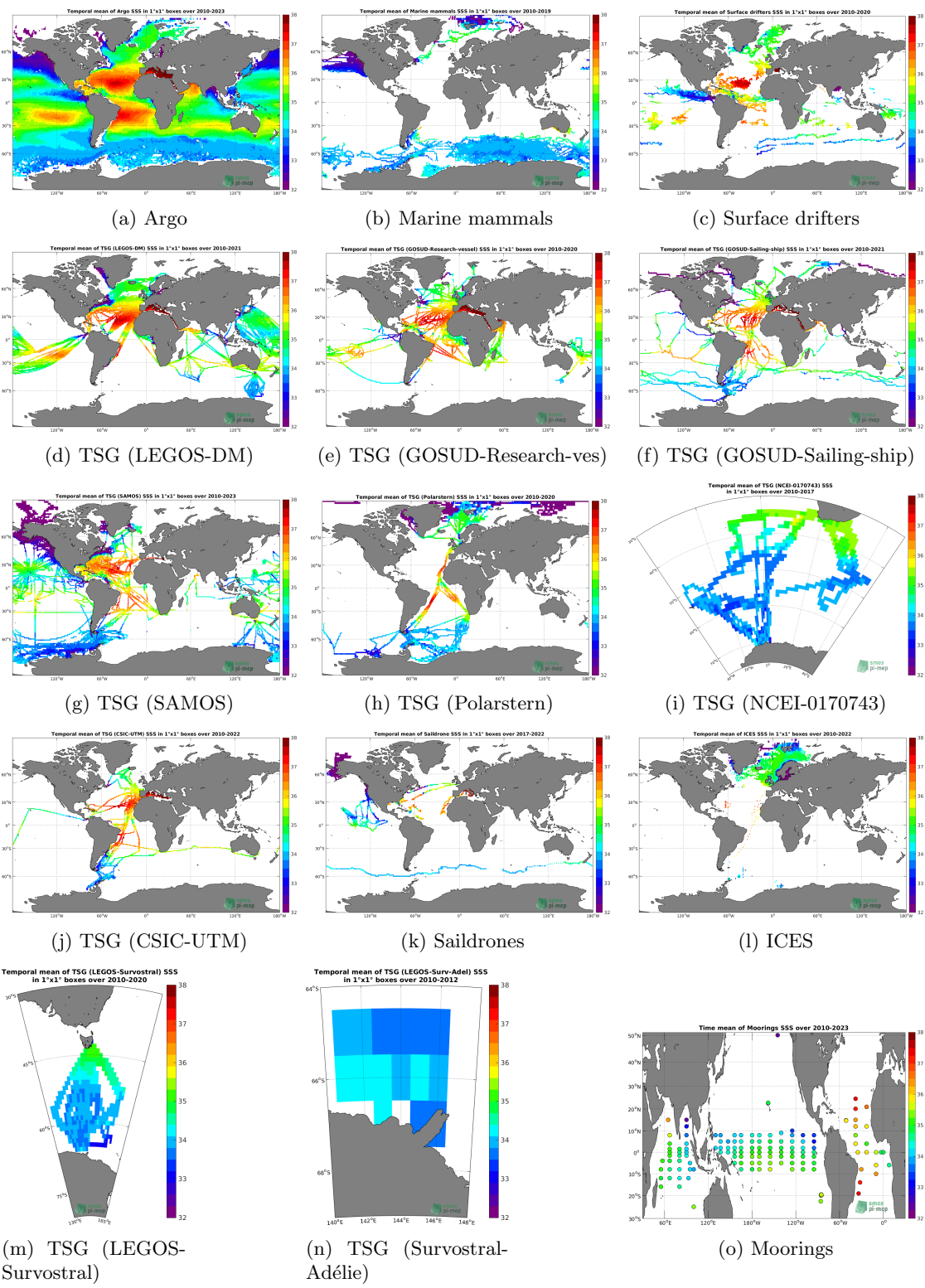
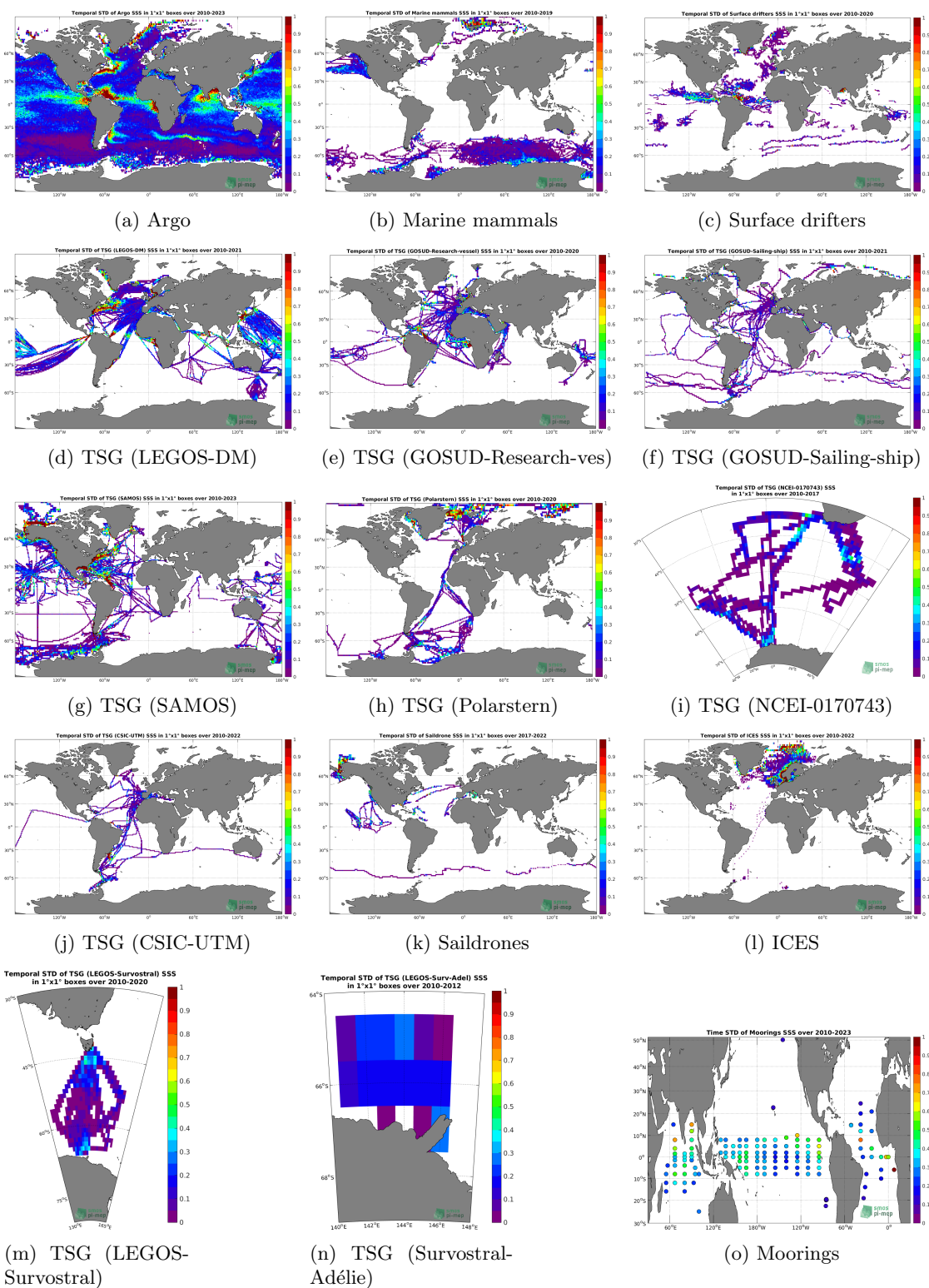


Figure 240: Temporal mean of SSS in $1^\circ \times 1^\circ$ boxes.

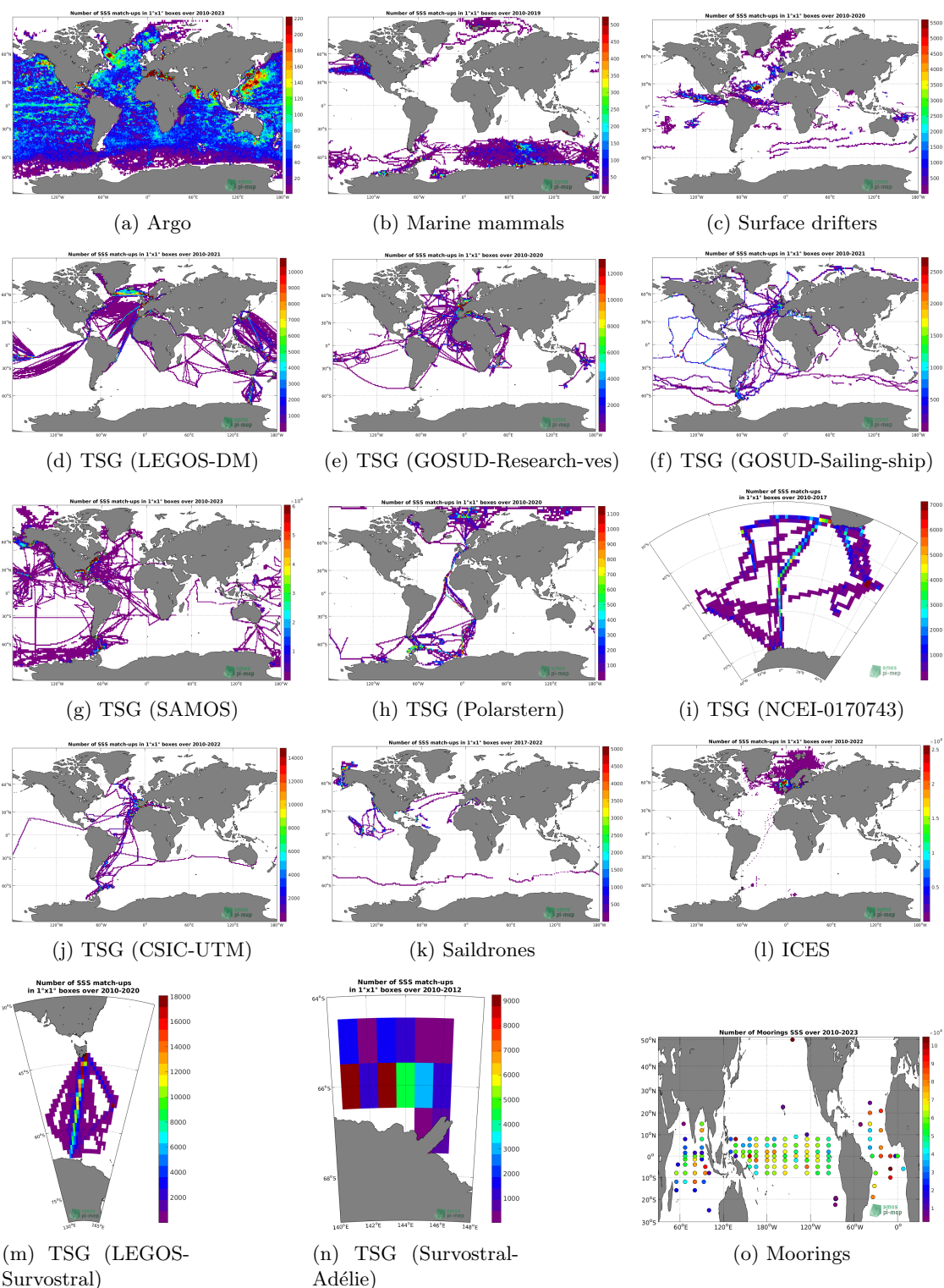
11.4 Temporal Std of SSS

Figures 241 show the temporal standard deviation (std) gridded over spatial boxes of size $1^{\circ} \times 1^{\circ}$ using the full period of each *in situ* datasets.


Figure 241: Temporal Std of SSS in $1^\circ \times 1^\circ$ boxes.

11.5 Spatial density of SSS

Figures 242 show the spatial distribution of SSS gridded over spatial boxes of size $1^{\circ} \times 1^{\circ}$ using the full period of each *in situ* datasets.


Figure 242: Number of SSS in $1^\circ \times 1^\circ$ boxes.

11.6 Characteristics for each Pi-MEP region

The following tables show some characteristics of each *in situ* dataset after applying the different Pi-MEP region masks described [here](#). To switch from a region to another, you can play with the arrows between the plot and the caption.

References

- Ices data portal, dataset on ocean hydrochemistry, extracted february 14, 2023. ices, copenhagen.
- Gaël Alory, T. Delcroix, P. Téchiné, D. Diverrès, D. Varillon, S. Cravatte, Y. Gouriou, J. Grelet, S. Jacquin, E. Kestenare, and et al. The French contribution to the voluntary observing ships network of sea surface salinity. *Deep-Sea Res. Pt. I*, 105:1–18, November 2015. ISSN 0967-0637. doi: [10.1016/j.dsr.2015.08.005](https://doi.org/10.1016/j.dsr.2015.08.005).
- Argo. Argo float data and metadata from Global Data Assembly Centre (Argo GDAC), 2023. doi: [10.17882/42182](https://doi.org/10.17882/42182).
- Giuseppe Aulicino, Yuri Cotroneo, Isabelle Ansorge, and Marcel Van Den Berg. Sea surface temperature and salinity collected aboard the S.A. AGULHAS II and S.A. AGULHAS in the South Atlantic Ocean and Southern Ocean from 2010-12-08 to 2017-02-02 (NCEI Accession 0170743), 2018. doi: [10.7289/v56m3545](https://doi.org/10.7289/v56m3545).

Abderrahim Bentamy and Denis Croize Fillon. Gridded surface wind fields from Metop/ASCAT measurements. *Int. J. Remote Sens.*, 33(6):1729–1754, March 2012. ISSN 1366-5901. doi: [10.1080/01431161.2011.600348](https://doi.org/10.1080/01431161.2011.600348).

Abderrahim Bentamy, Semyon A. Grodsky, James A. Carton, Denis Croizé-Fillon, and Bertrand Chapron. Matching ASCAT and QuikSCAT winds. *J. Geophys. Res.*, 117(C2), February 2012. ISSN 0148-0227. doi: [10.1029/2011JC007479](https://doi.org/10.1029/2011JC007479).

Sandrine Bony, Bjorn Stevens, Felix Ament, Sébastien Bigorre, Patrick Chazette, Susanne Crewell, Julien Delanoë, Kerry Emanuel, David Farrell, Cyrille Flamant, Silke Gross, Lutz Hirsch, Johannes Karstensen, Bernhard Mayer, Louise Nuijens, James H. Ruppert, Irina Sandu, Pier Siebesma, Sabrina Speich, Frédéric Szczap, Julien Totems, Raphaela Vogel, Manfred Wendisch, and Martin Wirth. EUREC⁴A: A Field Campaign to Elucidate the Couplings Between Clouds, Convection and Circulation. *Surveys in Geophysics*, 38(6):1529–1568, sep 2017. doi: [10.1007/s10712-017-9428-0](https://doi.org/10.1007/s10712-017-9428-0).

Jacqueline Boutin, Y. Chao, W. E. Asher, T. Delcroix, R. Drucker, K. Drushka, N. Kolodziejczyk, T. Lee, N. Reul, G. Reverdin, J. Schanze, A. Soloviev, L. Yu, J. Anderson, L. Brucker, E. Dinnat, A. S. Garcia, W. L. Jones, C. Maes, T. Meissner, W. Tang, N. Vinogradova, and B. Ward. Satellite and In Situ Salinity: Understanding Near-Surface Stratification and Sub-footprint Variability. *Bull. Am. Meterol. Soc.*, 97(8):1391–1407, 2016. ISSN 1520-0477. doi: [10.1175/bams-d-15-00032.1](https://doi.org/10.1175/bams-d-15-00032.1).

Ralph R. Ferraro. SSM/I derived global rainfall estimates for climatological applications. *J. Geophys. Res.*, 102(D14):16715–16736, 07 1997. doi: [10.1029/97JD01210](https://doi.org/10.1029/97JD01210).

Ralph R. Ferraro, Fuzhong Weng, Norman C. Grody, and Limin Zhao. Precipitation characteristics over land from the NOAA-15 AMSU sensor. *Geophys. Res. Lett.*, 27(17):2669–2672, 2000. doi: [10.1029/2000GL011665](https://doi.org/10.1029/2000GL011665).

Fabienne Gaillard, Thierry Reynaud, Virginie Thierry, Nicolas Kolodziejczyk, and Karina von Schuckmann. In Situ-Based Reanalysis of the Global Ocean Temperature and Salinity with ISAS: Variability of the Heat Content and Steric Height. *J. Clim.*, 29(4):1305–1323, February 2016. ISSN 1520-0442. doi: [10.1175/jcli-d-15-0028.1](https://doi.org/10.1175/jcli-d-15-0028.1).

Robert J. Joyce, John E. Janowiak, Phillip A. Arkin, and Pingping Xie. CMORPH: A Method that Produces Global Precipitation Estimates from Passive Microwave and Infrared Data at High Spatial and Temporal Resolution. *J. Hydrometeorol.*, 5(3):487–503, June 2004. doi: [10.1175/1525-7541\(2004\)005<0487:camtpg>2.0.co;2](https://doi.org/10.1175/1525-7541(2004)005<0487:camtpg>2.0.co;2).

Nicolas Kolodziejczyk, Gilles Reverdin, and Alban Lazar. Interannual Variability of the Mixed Layer Winter Convection and Spice Injection in the Eastern Subtropical North Atlantic. *J. Phys. Oceanogr.*, 45(2):504–525, Feb 2015. ISSN 1520-0485. doi: [10.1175/jpo-d-14-0042.1](https://doi.org/10.1175/jpo-d-14-0042.1).

Nicolas Kolodziejczyk, Mathieu Hamon, Jacqueline Boutin, Jean-Luc Vergely, Gilles Reverdin, Alexandre Supply, and Nicolas Reul. Objective analysis of SMOS and SMAP sea surface salinity to reduce large-scale and time-dependent biases from low to high latitudes. *Journal of Atmospheric and Oceanic Technology*, 38(3):405–421, mar 2021. doi: [10.1175/jtech-d-20-0093.1](https://doi.org/10.1175/jtech-d-20-0093.1).

Christian Kummerow, Y. Hong, W. S. Olson, S. Yang, R. F. Adler, J. McCollum, R. Ferraro, G. Petty, D-B. Shin, and T. T. Wilheit. The Evolution of the Goddard Profiling Algorithm (GPROF) for Rainfall Estimation from Passive Microwave Sensors. *J. Appl. Meteorol.*, 40(11):1801–1820, 2001. doi: [10.1175/1520-0450\(2001\)040<1801:TEOTGP>2.0.CO;2](https://doi.org/10.1175/1520-0450(2001)040<1801:TEOTGP>2.0.CO;2).

Rosemary Morrow and Elodie Kestenare. Nineteen-year changes in surface salinity in the southern ocean south of australia. *J. Mar. Sys.*, 129:472–483, January 2014. doi: [10.1016/j.jmarsys.2013.09.011](https://doi.org/10.1016/j.jmarsys.2013.09.011).

Thierry Reynaud, Nicolas Kolodziejczyk, Christophe Maes, Fabienne Gaillard, Gilles Reverdin, Floriane Despres De Gesincourt, and Hervé Le Goff. Sea surface salinity from sailing ships : Delayed mode dataset, annual release, 2021. doi: <https://doi.org/10.17882/39476>.

Fabien Roquet, Christophe Guinet, Jean-Benoit Charrassin, Daniel P. Costa, Kit M Kovacs, Christian Lydersen, Horst Bornemann, Marthan N. Bester, Monica C. Muelbert, Mark A. Hindell, Clive R. McMahon, Rob Harcourt, Lars Boehme, and Mike A. Fedak. MEOP-CTD in-situ data collection: a Southern ocean Marine-mammals calibrated sea water temperatures and salinities observations, 2021. doi: [10.17882/45461](https://doi.org/10.17882/45461).

Shawn R. Smith, Jeremy J. Rolph, Kristen Briggs, and Mark A. Bourassa. Quality-Controlled Underway Oceanographic and Meteorological Data from the Center for Ocean-Atmospheric Predictions Center (COAPS) - Shipboard Automated Meteorological and Oceanographic System (SAMOS), 2009. doi: [10.7289/v5qj7f8r](https://doi.org/10.7289/v5qj7f8r).

Anne Treasure, Fabien Roquet, Isabelle Ansorge, Marthán Bester, Lars Boehme, Horst Bornemann, Jean-Benoît Charrassin, Damien Chevallier, Daniel Costa, Mike Fedak, Christophe Guinet, Mike Hammill, Robert Harcourt, Mark Hindell, Kit Kovacs, Mary-Anne Lea, Phil Lovell, Andrew Lowther, Christian Lydersen, Trevor McIntyre, Clive McMahon, Mônica Muelbert, Keith Nicholls, Baptiste Picard, Gilles Reverdin, Andrew Trites, Guy Williams, and P.J. Nico de Bruyn. Marine Mammals Exploring the Oceans Pole to Pole: A Review of the MEOP Consortium. *Oceanography*, 30(2):132–138, jun 2017. doi: [10.5670/oceanog.2017.234](https://doi.org/10.5670/oceanog.2017.234).